AD NUMBER
AD001531
LIMITATION CHANGES

TO:

Approved for public release; distribution is unlimited.

FROM:

Distribution authorized to U.S. Gov't. agencies and their contractors; Administrative/Operational Use; 30 SEP 1951. Other requests shall be referred to Ballistic Research Laboratory, Aberdeen Proving Ground, MD 21005.

AUTHORITY

DCSL D/A notice dtd 18 Jun 1980

UNCLASSIFIED

AD 00153/
Statement A (Tab 80-

BALLISTIC RESEARCH LABORATORIES

UNCLASSIFIED

Regraded:

By Authority of: DIR BRL 2 Oct 72

S/ HH LAMBERT, SO.

By: L.C. Henry, STINFO

HIRAM E. LAMBERT
Chief, Security & Services Division
Ballistic Research Laboratories
2 Nov 76

REPORT NO. 837

0009

Regraded
Authority; letter from BRL, APG
dtd. 4 Dec 53 (actg)

Transactions of Symposium on

Shaped Charges

Held at the

Ballistic Research Laboratories
Aberdeen Proving Ground
Maryland

GROUP 1
EXCLUDED FROM AUTOMATIC DOWNGRADING
AND DECLASSIFICATION

November 13—16, 1951

ABERDEEN PROVING GROUND, MARYLAND

FOREWORD

This symposium was the outcome of a meeting at the Naval Ordnance Laboratory in July 1951 between representatives of The Naval Ordnance Laboratory, Carnegie Institute of Technology, New York University, and The Ballistic Research Laboratories (Army Ordnance).

Mr. Louis Zernow, Ballistic Research Laboratories, was appointed chairman of a committee consisting of Mr. Anson W. Solem, Naval Ordnance Laboratory, and Mr. Robert Eichelberger, Carnegie Institute of Technology. The technical program was arranged by this committee.

The local arrangements committee at the Ballistic Research Laboratories consisted of Mr. Louis Zernow, Mr. John L. Squier, Mr. Joseph M. Regan, Mr. Irving Lieberman, Lt. John C. Rhodes, Lt. John C. Whitmore, and Mr. Robert W. Foster, with the assistance of Mr. W. D. Dickinson and his staff.

Project No. TB3-0134 for Research and
Development Division, Ordnance Corps

iii

TABLE OF CONTENTS

TABLE OF CONTENTS - Continued

Sessions 3 and 4. INSTRUMENTATION

TABLE OF CONTENTS - Continued

Sessions 5 and 6. WEAPONS

TABLE OF CONTENTS - Continued

Session 7. ROTATION

Session 8. EFFECTIVENESS OF, AND DEFENSE AGAINST
SHAPED CHARGES

WELCOME BY

MAJOR GENERAL E. E. MacMORLAND
Commanding General
Aberdeen Proving Ground

I would like to extend a cordial welcome to all of you assembled here
for this important conference. The problems you are going to discuss are
both pressing and fundamental. I expect that you will all be in a better
position to improve our shaped charge weapons as a result of this discussion.
I would therefore like to express my hope that you meeting will be both
fruitful and enjoyable.

INTRODUCTORY REMARKS

by

COLONEL ALDEN P. TABER

Director

Ballistic Research Laboratories

The Ballistic Research Laboratories have a great interest in the shaped charge program. Although the shaped charge type of munition is only one of several different means to defeat heavy armor or fortifications, it has certain distinct advantages over other types of weapons. Generally, the shaped charge round is more efficient than others of the same calibre; and often the launching weapon may be lighter. In the hands of an enemy, the shaped charge munition presents us with a very difficult defensive problem. In fact, a defense against this type of attack may never be solved to the satisfaction of our field forces.

Our efforts in the shaped charge program in the BRL are directed toward three principal objectives, as follows:

1. Increasing the efficiency of penetration of a round.

2. Compensating for the spin of a round fired from a conventional cannon.

3. Providing a satisfactory defensive material or design against enemy shaped charge munitions.

I should like to comment briefly on these objectives.

An increase of 100% in the efficiency of penetration of shaped charge munitions would result in lighter and more potent weapons in the hands of our soldiers. The present bazooka could be smaller and more effective. Our light tanks with their relatively small calibre guns would be capable of defeating anything encountered on the battlefield.

Compensating for the spin of a shaped charge round fired from a conventional cannon would eliminate special weapons and increase greatly the effectiveness of this type of artillery ammunition.

As mentioned before, the defense against shaped charge type munitions is a difficult problem. A suitable material or materials for this purpose may never be found. The problem may resolve itself into one of design only.

In order to accomplish the objectives, that I have mentioned, one requires a better understanding of what actually happens in jet formation, the behavior of the jet in its travel in the air and in the target material, and the behavior of the target material. A great deal of basic and applied research is necessary to determine and evaluate the many variables involved. For example: Why is a copper cone better than a steel cone? What are the effects of different changes in the geometry of a cone? How important are hardness heat treatment, micro-structure or atomic structure of cones? Why does glass offer more resistance to penetration than other target materials of comparable density? There are tens or perhaps hundreds of other similar questions that need and are undergoing investigation. The answers to these questions must come from research. A great deal of research on this subject is in progress. As an end result, it is hoped that a suitable theory or rational explanation of observed facts will be attained.

Once a suitable theory is obtained and the fundamentals on the mechanism of jet formation and its behavior through different media are understood, a great step will have been taken toward solution of present objectives.

REMARKS ON SOME FUNDAMENTAL FEATURES OF DETONATION

S. J. Jacobs

U. S. Naval Ordnance Laboratory, White Oak, Silver Spring, Maryland

ABSTRACT

Computations for the shaped charge effect require that one know the state of detonation product gases and the isentropic relation for expansion to a reasonable degree of precision. These functions have been or can be derived from basic data for a number of compounds and mixtures using more or less approximate equations of state. Experimental checks indicate that the important parameters for calculations of boundary motions are capable of being predicted with reasonable precision, say 5 or 10%. Though this does not mean that all is well in our state of knowledge in this field, the new worker should not be required to share the pessimism which often is voiced when the subject is discussed from the viewpoint of equation of state. The discussion will present some useful approximations to aid in computations.

Mr. Chairman, Ladies and Gentlemen: It is, indeed, a privilege to be given the first opportunity to speak at this symposium on shaped charges. The reason for opening the discussion with some comments on detonation is, I believe, due to the realization that progress in extending our knowledge toward improving shaped charge weapons requires, among other things, that we understand the detonation process and use this knowledge as a tool in improving our understanding of the shaped charge effect. I shall endeavor, in the limited time I have, to mention the results of important elements of progress which have occurred in the past decade.

Detonation may be defined as the decomposition of an energy-rich explosive compound; that decomposition being effected by a shock wave in which initiation occurs such as to complete the energy release in a short time. The unit of time for such a process is the microsecond. The shock velocity for solid explosives, as most of you know, ranges from about 4000 to 9000 meters per second depending on the specific energy and the loading density. The prediction of detonation velocity from thermodynamic and hydrodynamic conservation laws using thermo chemical data has been worked out to give satisfactory answers for most of the explosives of interest to this group. The calculations are made through the use of steady-state assumptions. The results predict the pressure, sound speed, mass velocity and temperature in addition to the propagation rate of the wave. The fundamental way in which calculations are made and the numerous assumptions required to obtain the answers has led many to distrust the results obtained. It is usually considered that relative values are rather good for pressure, etc. but that absolute values may be in large error. A paper by H. Jones presented at the 1948 Symposium on Combustion, etc. is of great help in this regard in that it places a figure of precision on the absolute magnitudes of pressure and particle velocity. I shall return to this paper in a few minutes.

The present view of the shape of the reaction region leading to the postulate of an initiation "spike", was presented by von Neumann in this country and by Zeldovich in Russia. A first statement of a non-steady state detonation in which a rarefaction wave follows the reaction shock was presented by Sir Geoffrey Taylor. This is a step in the direction toward obtaining the flow pattern for the detonation products for general boundary conditions and general explosive configuration. Some work has been published on gas rarefaction in two dimension steady flow by Doring and Burkhardt. This trend of studying flow behind detonations should be followed more diligently for it is here where the external effect of an explosion is coupled to the nature of the explosion products and the energy release. The data that is needed from the detonation is the pressure and the adiabatic p-v relation for the gas expansion.

The basic piston in a cylinder of gas model most commonly used to develop one dimensional shock theory is a most illustrative way to show the equations of steady detonation and the effect of rarefaction. (Figure 1) If the "gas" is considered to be a solid explosive which has been started to detonate at $t = 0$; $x = 0$ with both the piston and the end of the reaction, (2) starting to move from $x = 0$, and if (1) refers to the state ahead of the propagating wave, (2) to the state immediately behind the end of reaction (dotted line) and (3) to the state at the piston we can easily write the conservation laws for mass, momentum and energy when $u_3 = u_2$ for then the entire gas between (3) and (2) will be of uniform state and moving with velocity u_2. Referring to ρ as density, p as pressure, D as shock velocity, us as "gas" velocity, c as local sound speed and E as internal energy (including chemical); the following equations can be deduced without difficulty:

$$D \rho_1 = (D - u)\rho_2$$

$$p_2 - p_1 = D \rho_1 u$$

$$E_2 - E_1 = 1/2 (p_2 + p_1) (\frac{1}{\rho_1} - \frac{1}{\rho_2})$$

It can be shown that u_3 can only equal u_2 when:

$$u_3 + c_3 = u_2 + c_2 \gtrless D.$$

Equality to D implies the Chapman-Jouquet condition; inequality implies an over boostered detonation. An interesting problem was brought up at NOL the other day which, I think, has important bearing on the proof of the Chapman-Jouquet condition. This is to consider what would happen if the piston, initially moving at a uniform velocity $u_3 = D - c_3$, were suddenly stopped at a time $T > 0$. According to the Riemann theory a rarefaction wave would move from the piston (now at rest) with its head moving at a velocity $u_2 + c_2 = D$. But the detonation is also moving at velocity, D, so that a region of constant velocity, u_2, having a constant length $(D - u_2) T$ will be following the detonation. The detonation is not distrubed. If now the time of stopping the piston is reduced to an infinitesimally small value greater than zero, we would end up with a detonation propagating without being affected by a simple wave which is attached to it. This is the problem solved first by G. I. Taylor and leads to a picture of a propagating wave as shown in Figure 2.

6
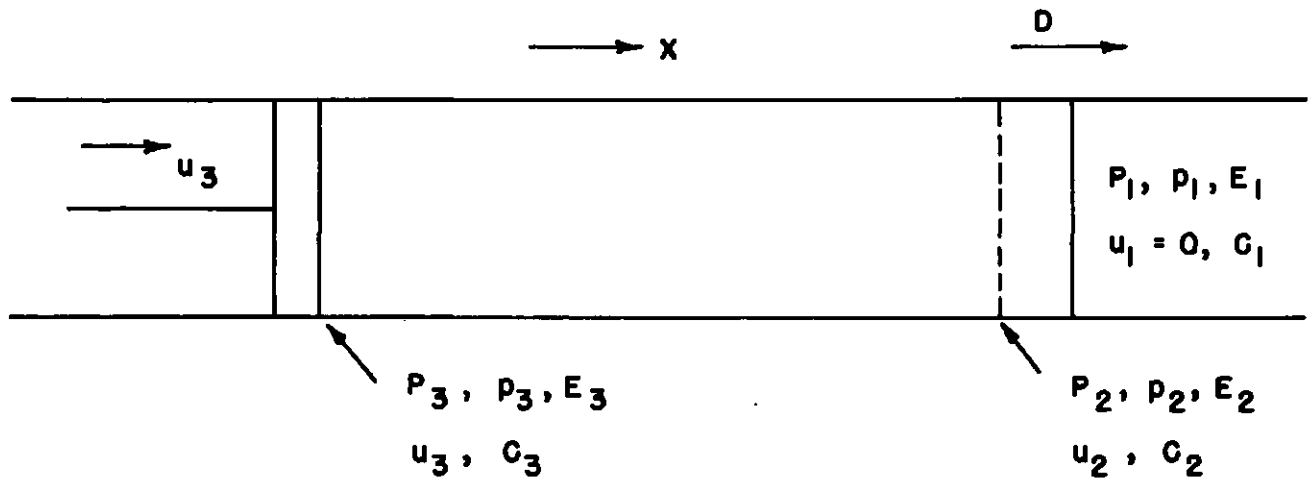
Figure 1—Piston in a cylinder model for presenting conservation laws.
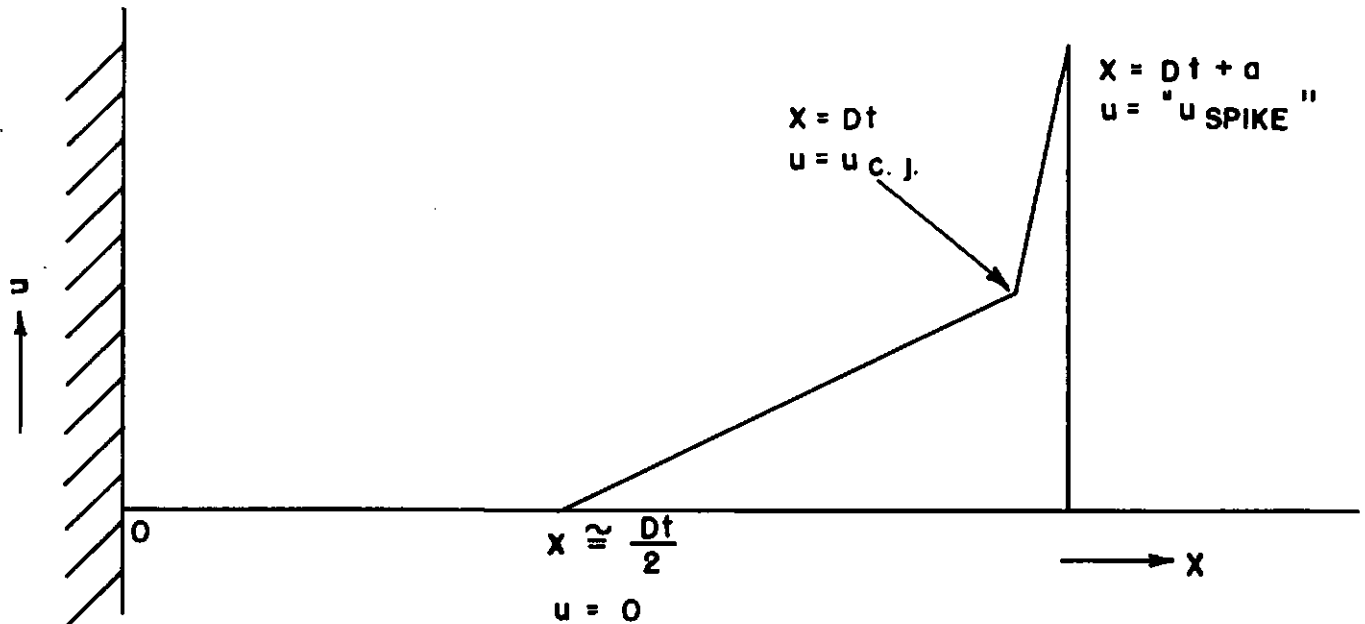
Figure 2—Detonation in closed tube with back boundary at rest.

The existence in gaseous detonation of the rest point shown in Figure 2 has been pointed out by Patterson in a photograph taken by Bone and Fraser. Time does not permit my saying anything about the effect of expansion to the sides of a finite charge such as a cylinder. I do believe that the problem is one which can be tackled by the use of characteristics in steady-two dimensional flow. The one solution which exists to my knowledge applies to an ideal gas case. We need to generalize it to the case for the imperfect gases from solid explosives.

Returning now to calculations of pressures, particle velocity, sound speed and density at the Chapman-Jouquet plane for dense explosives, there are two useful approximations for quick answers. One is the assumption that particle velocity is 1/4 of detonation velocity. For cast or high density pressed explosives, this is probably better than ± 20%. The other is the use of H. Jones equation which may be written:

$$\frac{D}{u} = (2 + \alpha)\left(1 + \frac{\rho_1}{D}\frac{dD}{d\rho_1}\right)$$

where α is a thermodynamic quantity shown to be positive and of magnitude of about 0.25. $\frac{dD}{d\rho_1}$ is the slope of the detonation velocity vs. density curve at density, ρ_1.

Thus detonation data can give an estimate for $\frac{D}{u}$ from which other detonation data can be derived with an estimated accuracy of 5-10% based on an assumed error of 50% in α. One other result, not too familiar in this country is the use of a polytropic equation of state for the adiabatic expansion after detonation. This is of the form:

$$p = A(s)\rho^{\kappa}$$ (s referring to entropy constant), and is a useful approxi-

mation for computing other functions such as the Riemann function $\int \frac{c}{\rho} d\rho$ with

$$c^2 = \left(\frac{dp}{d\rho}\right)_s = \kappa A \rho^{\kappa-1}$$

The usefulness of this equation is partly due to the relation between κ and $\frac{D}{u}$ which can easily be shown to be:

$$\kappa + 1 = \frac{D}{u}.$$

Thus, much of the data needed for determining the effect of an explosive in detonation can be obtained from the measured detonation velocity. A table is included to show a comparison of parameters so calculated with (a) calculations made by Snay using the Kistiakowsky-Wilson equation of state and least squared co-volume data, and (b) results calculated from measurements on velocities set up in Aluminum targets when they are impacted normally by a plane detonation.

In conclusion, I would like to emphasize that there seems to be no reason to believe that the calculations one makes on detonation parameters lead to any less accurate data than similar calculations for low pressure phenomena. The conservation of momentum and mass plays such an important role in these shock effects that the equation of state is relegated to a secondary role. If velocities, pressures and densities are the required functions from detonation data, these can be obtained with accuracy satisfactory for our present needs. If equilibrium or temperature are wanted, then the picture is different. This for us is fortunately not the immediate need.

TABLE I

Explosive and Method of Calculation	ρ_1	D	p	p	u	κ	ρ_2
Comp B (60/40)	1.68	7790	3085				
u = D/4 assumption				255	1950	3	2.24
Jones equation				272	2085	2.76	2.295
Snay's calculation				243	1780	3.38	2.18
Al Target exp.				275	2115	2.69	2.30
TNT	1.58	6880	3225				
u = D/4 assumption				187	1720	3	2.10
Jones equation				191	1760	2.91	2.12
Snay's calculations				166	1530	3.49	2.04
Al Target exp.				184	1690	3.07	2.10

Note: pressure in kilobars (1 k.bar $\cong 10^3$ atm.) velocities in meters/second.

REFERENCES

1. J. von Neuman, "On the Theory of Stationary Detonation Waves," OSRD 1140 (1942), (or see Reference 11, Page 227).

2. Y. B. Zeldovich, "On the Theory of the Propagation of Detonation in Gaseous Systems", Translated in NACA, Technical Memorandum 1261 (1950). (Originally published in Russian in 1940.)

3. H. Jones, "Third Symposium on Combustion, Flame and Explosion Phenomena", page 590 - 594, Williams and Wilkins Company, Baltimore, Maryland (1949).

4. Brinkley, S. and Wilson, E. B., "Revised Method of Predicting the Detonation Velocity in Solids", OSRD 905, (1942), also OSRD 1707 (1943).

5. Stewart, Patterson, "The Hydrodynamic Theory of Detonation", Part II, Research, 1, 5, (1948) Page 221-234.

6. G. B. Kistiakowsky and E. B. Wilson, "Final Report on the Hydrodynamic Theory of Detonation and Shock Waves", OSRD 114 (1941).

7. E. A. Christian and H. G. Snays, "Analysis of Experimental Data on Detonation Velocities", NavOrd Report No. 1508 (1951).

8. H. Snay and I. Stegun, "Auxilliary Functions for Thermodynamic Calculations Based on the K-W Equation of State", NavOrd Report No. 1732, (1951).

9

9. Sir Geoffrey Taylor, "The Dynamics of the Combustion Products Behind Plane and Spherical Detonation Fronts in Explosives", Proc. Roy. Soc. A. <u>200</u>, 1061, page 235-247 (1950).

10. S. Patterson, "One-dimensional Flow Behind a Steady Plane Detonation," Research <u>3</u>, page 99, (1950).

11. R. H. Cole, "Underwater Explosions", Princeton University Press; Princeton, New Jersey (1948).

12. R. Courant and K. O. Friedricks, "Supersonic Flow and Shock Waves", Interscience Publishers, New York, (1948).

13. W. Doring and G. Burkhardt, "Contributions to the Theory of Detonation", (Translated by Brown University). Technical Report No. F-TS-1227-IA (GDAM A9 - T - 46) Air Material Command, Wright-Patterson AFB, Dayton, Ohio (1949).

14. R. W. Goranson, H. D. Mallory and S. J. Jacobs, "Detonation Pressures in Solid Explosives by the Measurement of Shock and Surface Velocities Induced in Metal Targets", NavOrd 1883, (in preparation).

15. A series of papers on a Symposium on Detonation held in Great Britain appears in Proc. Royal Society, A, <u>204</u>, 1-30, (November 1950).

Note: Abstracts on Detonation generally appear in Physics Abstracts, Sec. A under the class numbers 541.11 or 541.12. (Physical Chemistry, Chemical Reactions.)

THEORY OF LINED HOLLOW CHARGES

Emerson M. Pugh

Department of Physics, Carnegie Institute of Technology, Pittsburgh, Pennsylvania

ABSTRACT

An extension of the theory of cone collapse and jet formation published in the Journal of Applied Physics[1] is presented. By assuming a time gradient in the velocity of collapse of the cone walls, the long rear end of the jet is explained[18] without recourse to a slug extrusion theory. Experiments[18] verifying this theory are discussed. The theory of penetration[1] is reviewed to see how well it explains the experimental results obtained with liners of different materials and with targets of different materials. A release wave hypothesis, based upon characteristic surfaces of Courant and Friedrichs[23], is briefly mentioned. Though manifestly inadequate, it provides a very rough correlation between the performances of explosives of quite different shape.

In discussing the present state of the theory of lined hollow charges with you, I will presume that you have all read the article published in the Journal of Applied Physics[1]. While this was as good a summary as could be declassified for publication at the time, much was necessarily omitted. Individuals cleared for access to the original sources should most certainly consult these sources. They contain much valuable material that could not be repeated in any summary of reasonable length. A bibliography of reports important to the development of the theory, together with some brief historical notes is being prepared to aid investigators in this field. A first draft is being distributed here in the hope that you will call our attention to reports that have been missed* and help us to make it a more complete and useful document.

The theory of lined cavity charges will be presented in what may appear to be a backwards order; namely, target penetration first, jet formation second and the interaction of the explosive with the liner third. This order seems most natural to me, since it is the order in which I learned the subject.

---

1   Journ. Appl. Phys. Vol. 19, 6 pp. 563-582, June 1948.

*   It has been noted, since this list was made, that much has been missed by lumping the duPont reports into one item. Several of these are of outstanding importance and will be listed separately. One glaring flaw is the omission, in this summary, of the development of the theory, of important papers by M. A. Cook.

PENETRATION

Early researches by MacDougall[2] and his collaborators established that conical steel liners produced long, small diameter jets of steel fragments having velocities up to 10,000 meters per second at the front and little more than 1,000 meters per second at the rear. Perforation of a target plate by one of these jets used up the front of the jet but the rear of the jet passed through the hole unaffected by the plate. The volumes of the holes made in targets were shown to be roughly proportional to the kinetic energy of the jet used up and dependent upon the strength properties of the target material. Qualitative reasoning suggested that the improved penetration with standoff was due to the jet lengthening as it traveled. By considering the momentum transfer from this stream of high speed particles to the target (whose strength was assumed to be negligible for these high velocity particles), they derived the relation, $\rho_j V_j (V_j - U) = \rho U^2/2$, between jet velocity V_j and penetration velocity U, where ρ_j and ρ were the jet and target densities respectively. Their drum camera measurements established that the ratio V_j/U was dependent upon the density in rough agreement with predictions of this equation. These researches paved the way for the more complete theory[3] of penetration given by the author in May, 1944.

Reconsideration of the momentum transfer relations convinced the author[3] that the relationship between the velocities should be of the form, $1/2\ \rho_j A_j (V_j - U)^2 = \rho A U^2/2$, where[4] $A/A_j = 1$ for perfectly made charges and greater than one for imperfect charges. This relationship leads immediately to $V_j/U = 1 + \text{const.}\sqrt{\rho}$, which was beautifully verified by the experimental data of G. H. Messerly and D. P. MacDougall, and to $P = \int \frac{\sqrt{\rho_j} A_j}{\sqrt{\rho}\ A}$ which immediately suggested why penetration P increased with standoff. The length ℓ of the jet increased because of its large gradient in velocity, and therefore, its penetration increased with increasing standoff. Because the jet density ρ_j was inversely proportional to ℓ, penetration for this particle jet could increase only as $\sqrt{\ell}$ and therefore as $\sqrt{S}$. Carefully determined P vs. S curves showed that with reasonable constants $\sqrt{S}$ could not possibly increase fast enough to account for the rapid increase in P at low standoffs. It was, therefore, postulated that ρ_j remained constant during the early stages of jet travel (i.e. within the cone and just beyond its base) and that the jet later broke up into particles. Thus penetration (for good charges in which $A/A_j = 1$) started proportional to ℓ or S and after break-up became proportional to $\sqrt{\ell}$ or $\sqrt{S}$. This made it possible to fit the P vs. S curves very well and a whole series of quantitative correlations[3] followed.

---

2   G. B. Kistiakowsky, MacDougall and Messerly, "The Mechanism of Action of Cavity Charges," O.S.R.D. 1338, April 1943.

3   E. M. Pugh, "A Theory of Target Penetration by Jets," O.S.R.D. 3752, May 1944.

4   The relationship between jet area A_j and effective area of impact on the target was suggested by the fact the unpublished radiographs of J. C. Clark and L. B. Seely generally showed misaligned jets. See BRL Rpt. 368.

Hill, Mott and Pack[5] independently derived the relations $\frac{\lambda \rho_j}{2} (V_j - U)^2 = \frac{\rho U^2}{2} + \sigma$ and $P = \ell \sqrt{\lambda \rho_j / \rho}$ when $\sigma \ll \lambda \rho_j V_j^2 / 2$. The strength of the target material is represented by σ. They used conservation of momentum and energy relations to obtain the velocity equation with particle jets and Bernoulli's equation to obtain this equation for fluid jets. They were able to combine the two into one equation where $\lambda = 1$ for fluid jets and $\lambda = 2$ for particle jets. They assumed that low melting point metals formed fluid jets while high melting point metals formed particle jets. While this point of view was not too successful in explaining the different penetrating powers of different metals as liners, it did point out an error in the author's original formulation of the velocity equation for the continuous jets. It also introduced a term to take account of target strength. A term σ proportional to ultimate target strength was added. Since the H-M-P formulation of the velocity equation was the most rigorous, it was adopted generally. While their basic velocity equations strictly applied to steady-state conditions only, experimental evidence indicated that the predictions obtained from their application to the non-steady conditions in these jets agreed with the experiments.

In the author's treatment continuous jets[6], whether fluid or solid, are assumed to follow the Bernoulli equation ($\lambda = 1$). Particle jets require $\lambda \cong 2$, since they cannot support internal pressures. The correction required by the H-M-P formulation was included into the original theory[3] by introducing what might be called a pseudo density $J = \lambda \rho_j A_j / A$. For perfectly symmetrical charges $J = \lambda \rho_j$. The velocity equation is then $J (V_j - U)^2 = \rho U^2 + 2\sigma$ and the penetration due to each jet element (when σ is small) is given by $dP = d\ell \sqrt{J/\rho}$. As in the original theory, the penetration of each jet element is proportional to $d\ell$ when J is constant as in ductile drawing (λ and ρ_j both const.) and proportional to $\sqrt{d\ell}$ after the jet is fully broken up and ρ_j becomes proportional to $1/d\ell$. The only effect of these changes in the original penetration theory[3] was to make invalid the original estimates of where the jets broke up. All of the correlations but one of the original theory were still valid. Immediately after break-up λ starts to increase and ρ_j starts to decrease. Thus $J = \lambda \rho_j$ remains nearly constant for a time after the break-up. This means that the break-up must take place somewhere along the linear[7] portion of the P vs. S curve,

---

5   R. Hill, N. F. Mott and D. C. Pack, "Penetration by Munroe Jets," Armament
     Research Dept., AC Rpt. No. 5756, Feb. 1944.

6   For simplicity, solid and fluid metals are assumed to be incompressible.

7   Integrated values of $P = \int d\ell \sqrt{J/\rho}$ are not quite linear, since the elements
     break up at different points in space and also may have different alignments.

instead of at the point where the curve becomes parabolic, as was originally believed. While the original correlations were obtained by the use of average values instead of by actual integration, they were later confirmed when Fireman[8] integrated the equation $P = \int d\ell \sqrt{J/\rho}$ and reached essentially these same conclusions.

The corrections indicated above were introduced into the penetration theory at a Symposium[9] on Shaped Charges in May 1945. At the same time it was postulated that the remarkably large penetrations produced at long standoff by charges having copper or aluminum liners, were due to the high ductility of these materials under these conditions. Figure 1 is taken directly from an old duPont report[10]. The P vs. S curves for conical liners of copper, aluminum and steel are typical of the many curves that have been obtained with these metals. At low standoffs the penetrations made by cones of copper and steel are pretty much the same but penetrations made by cones of aluminum are smaller because of its lower density. Copper and aluminum penetrations rise continuously with standoff whereas steel penetrations fall off at rather low standoffs. The explanation proposed[9] was that these copper and aluminum jets remained continuous longer than the more brittle steel jets. This prediction made in 1945 has been verified recently in the pictures taken by R. Heine-Geldern and E. Mutschler. Figure 2 shows photographs of jets from two M9A1 size charges, identical except that the one on the left had a steel liner and the one on the right had a copper liner. Taken at the instant when each had traveled about 12 in. beyond the base of their liner, the steel jet is broken up while the copper jet is still continuous. Figure 3 shows a copper jet from the same kind of charge after it had traveled 30 in. beyond the base of its liner. At this stage the copper jet has finally broken up into particles[11]. Kerr cell photographs have also been obtained of aluminum and brass liners. The aluminum jets remain continuous to long standoffs whereas the brass jets breakup at low standoff, as should be expected from their penetration vs. standoff characteristics. The straightness of the 30 in. long copper jet is worthy of note. The copper jet shows little evidence of radial spreading at 20 diameters standoff. Steel jets spread more quickly than copper, but with well made charges there is little evidence of spreading of steel jets within 10 diam. standoff. Thus any reduction in the average penetration at standoffs less than 10 diam. must be attributed to lack of symmetry in the charge assembly rather than to unavoidable radial spreading of the jet. Figure 4 shows a penetration vs. standoff curve for apparently identical charges lined with steel cones made to the early manufacturing tolerances. The wide spread in the penetrations due to different asymmetries is clearly seen. When charges are as well made as they can be today, average penetrations at these low standoffs do not fall off as shown in this figure. For simplicity the remainder of my remarks will be limited to perfectly made charges where these asymmetries would not exist.

---

8   E. Fireman and Emerson M. Pugh, "Fundamentals of Penetration by Jets," OSRD 4829b, March 1945. These calculations were necessarily based upon certain assumptions. It is possible that these assumptions could be altered to allow steel jets to break up before reaching the liner's base; i.e. at negative S.

9   Emerson M. Pugh, "Theories of Penetration," pp 79-101, in OSRD 5754, May 9, 1945.

10 C. O. Davis and W. R. Burke, "Cavity Effect with Cones of Various Pure Metals," E. I. duPont de Nemours report for March 1943.

11 After this paper was presented orally, Louis Zernow presented some beautiful flash radiographs that showed more clearly than these Kerr Cell pictures that steel liners break up at low standoff whereas copper liners remain continuous much longer and only break up at long standoff.
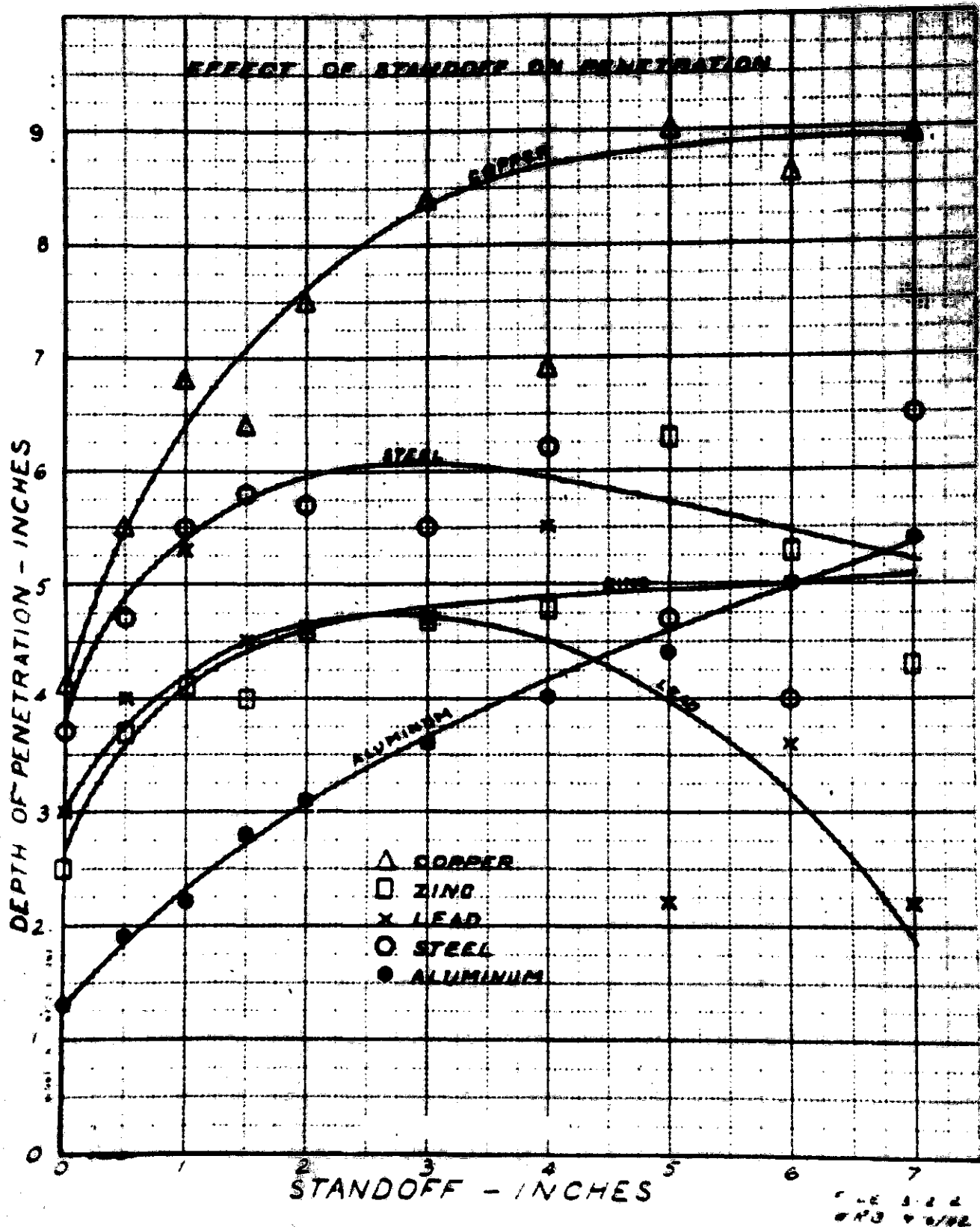
Figure 1—Penetration vs. standoff curves for liners of various pure metals
from duPont report for March 1943.
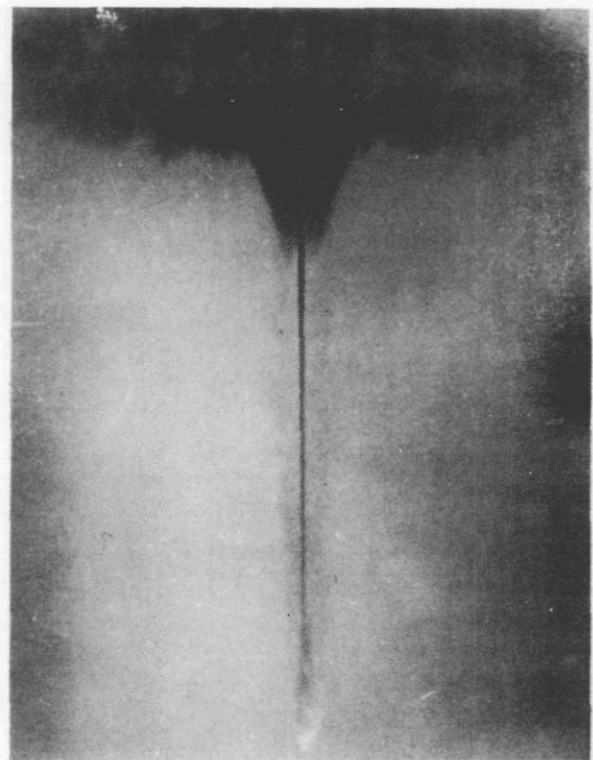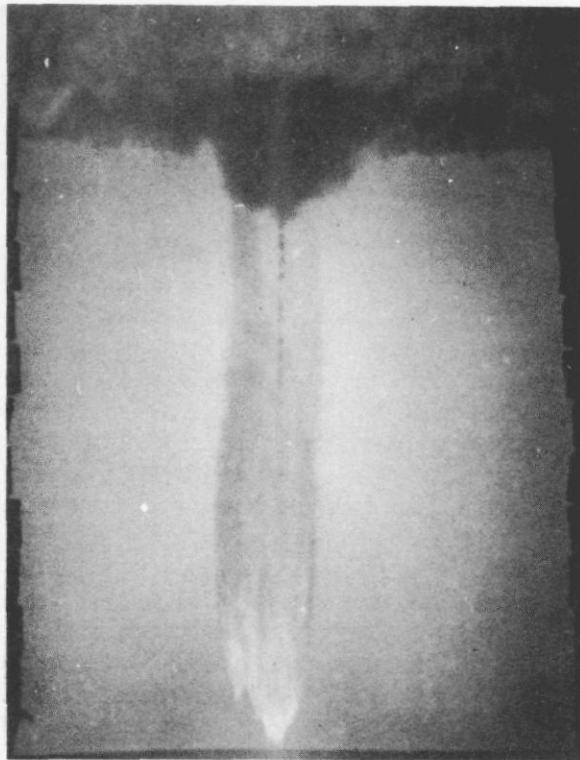
Figure 2—Kerr cell photographs of 12 in. long jets from a steel cone (left)
and a copper cone (right). The steel jet is broken up
whereas the copper is still continuous.
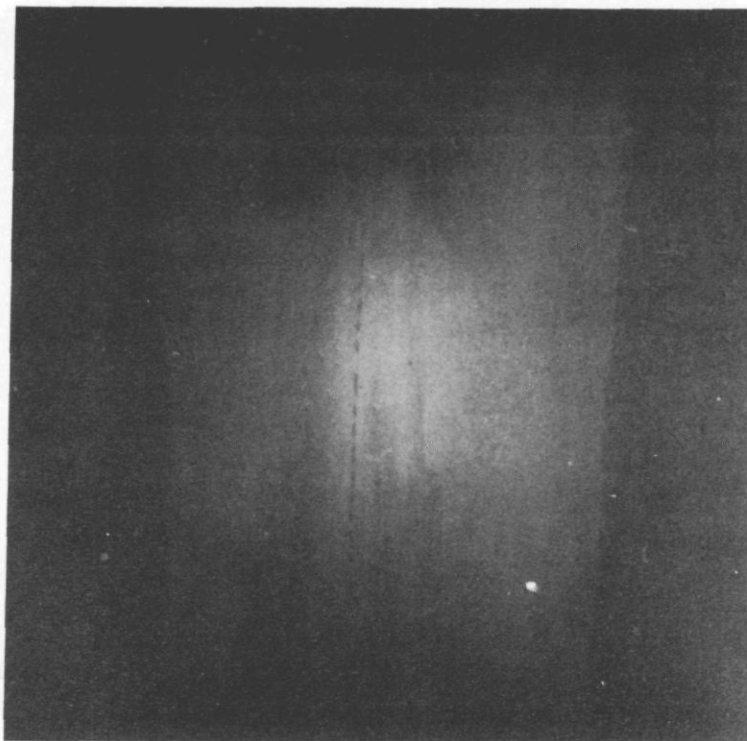
Figure 3—Kerr cell photograph of a 30 in. long copper jet. At this long standoff
the copper jet is finally broken into particles.

16

AVERAGE, MAXIMUM AND MINIMUM PENETRATIONS VERSUS STANDOFF

| C.I.T. CHARGE | CONE DIAM. | 1.63 IN. |
| 50/50 PENTOLITE | WT. CHARGE | 115 GRAMS |
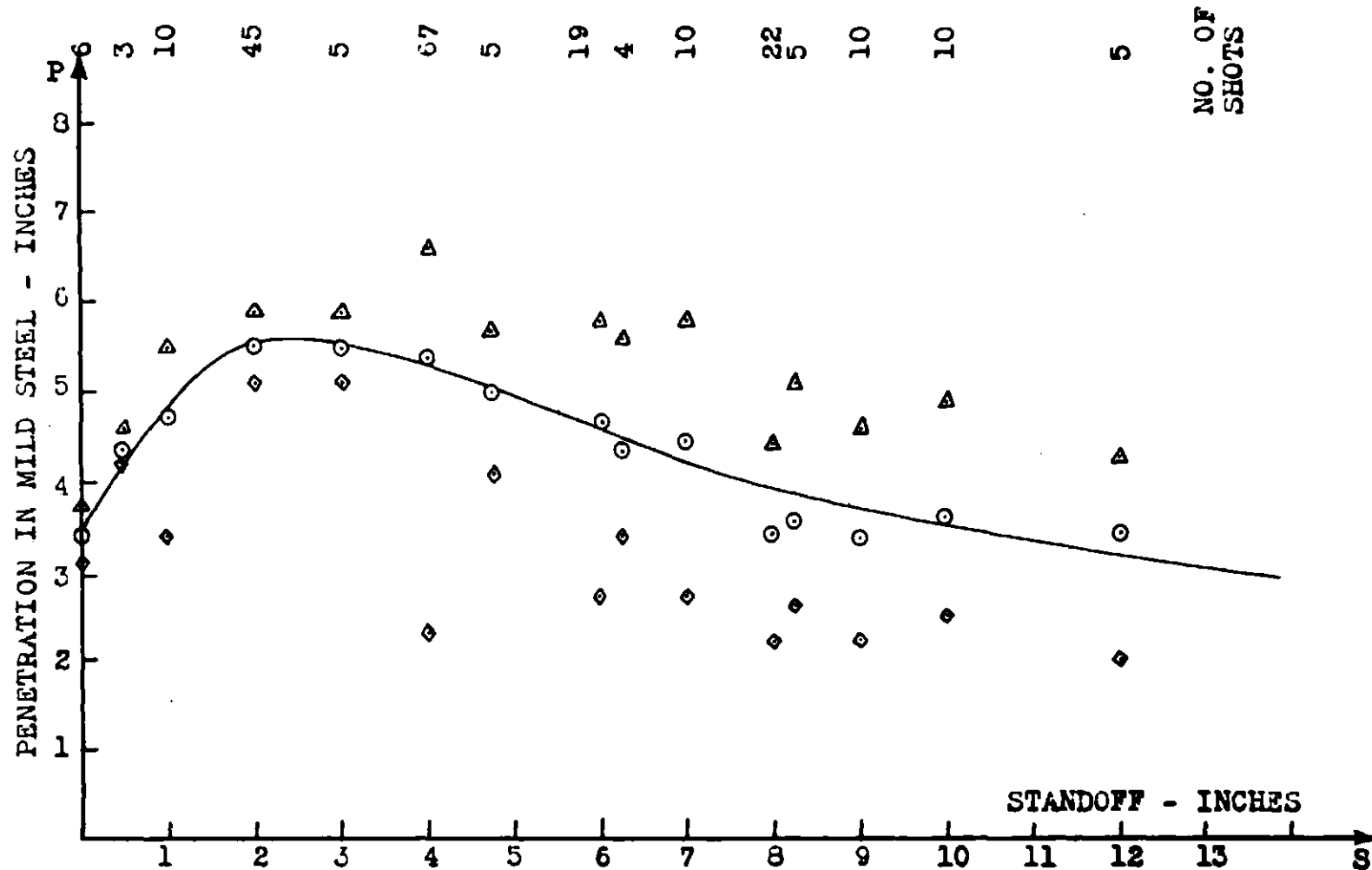
Figure 4—Penetration vs. standoff curve for CIT standard charges made with early manufacturing techniques. The average penetration is small at long standoff because of lack of symmetry in the charges. Occasional charges performed well at long standoffs.

TIME IS MEASURED FROM WHEN THE
DETONATION WAVE WAS AT THE CONE

20 μ sec.

33.5 μ sec.

105.6 μ sec.

INCHES ⟶
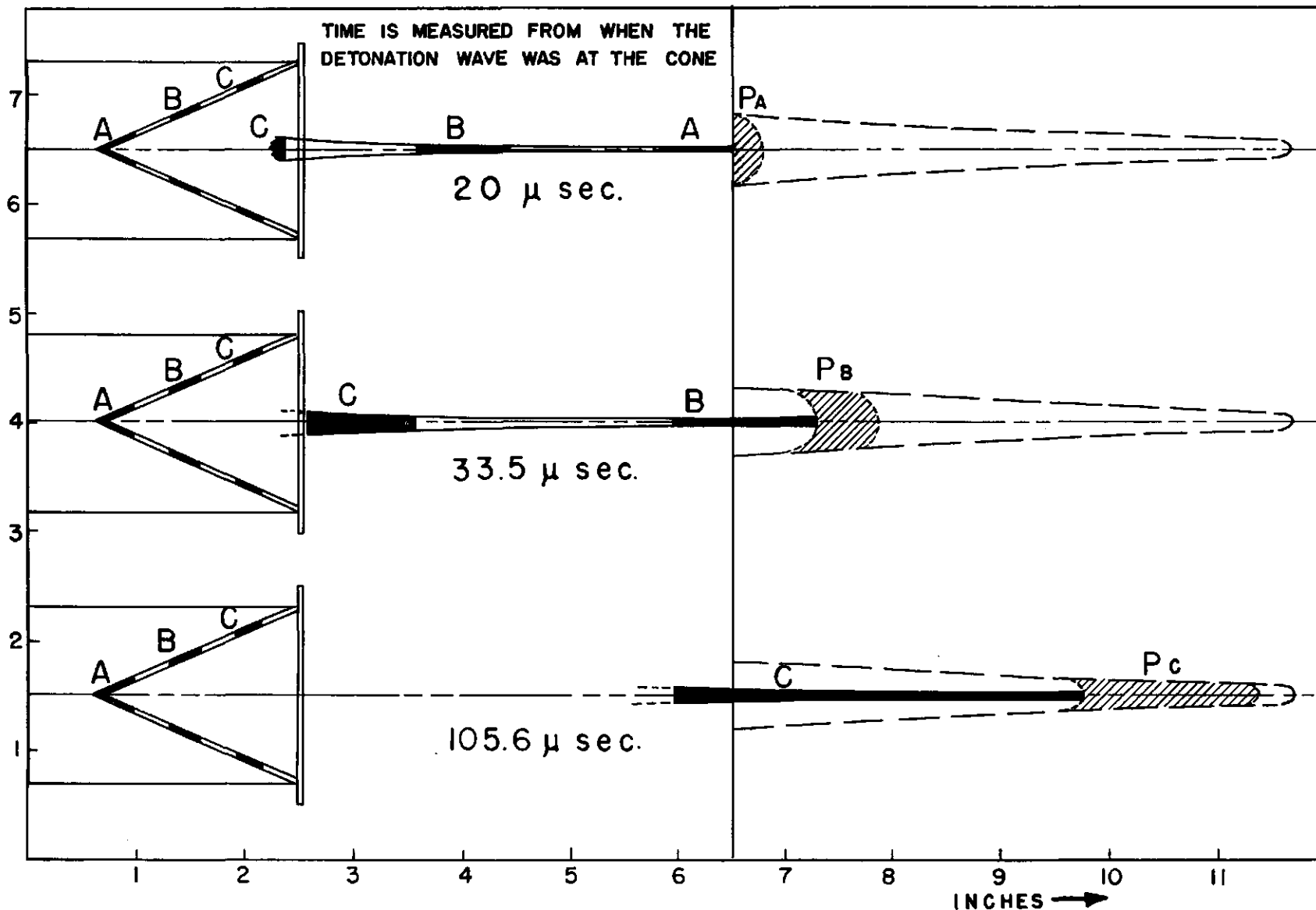
SEVERAL STAGES OF PENETRATION OF A MILD STEEL TARGET BY A STANDARD

CHARGE CONTAINING A M9AI STEEL CONE

Figure 5—Diagram illustrating penetration of mild steel targets by jets from CIT
standard charges. The contributions to the jet, of three equal length zonal elements
of the liner, are shown at three instants of time during their travel to the target.
The lengthening of these elements with travel is due to their velocity gradients.
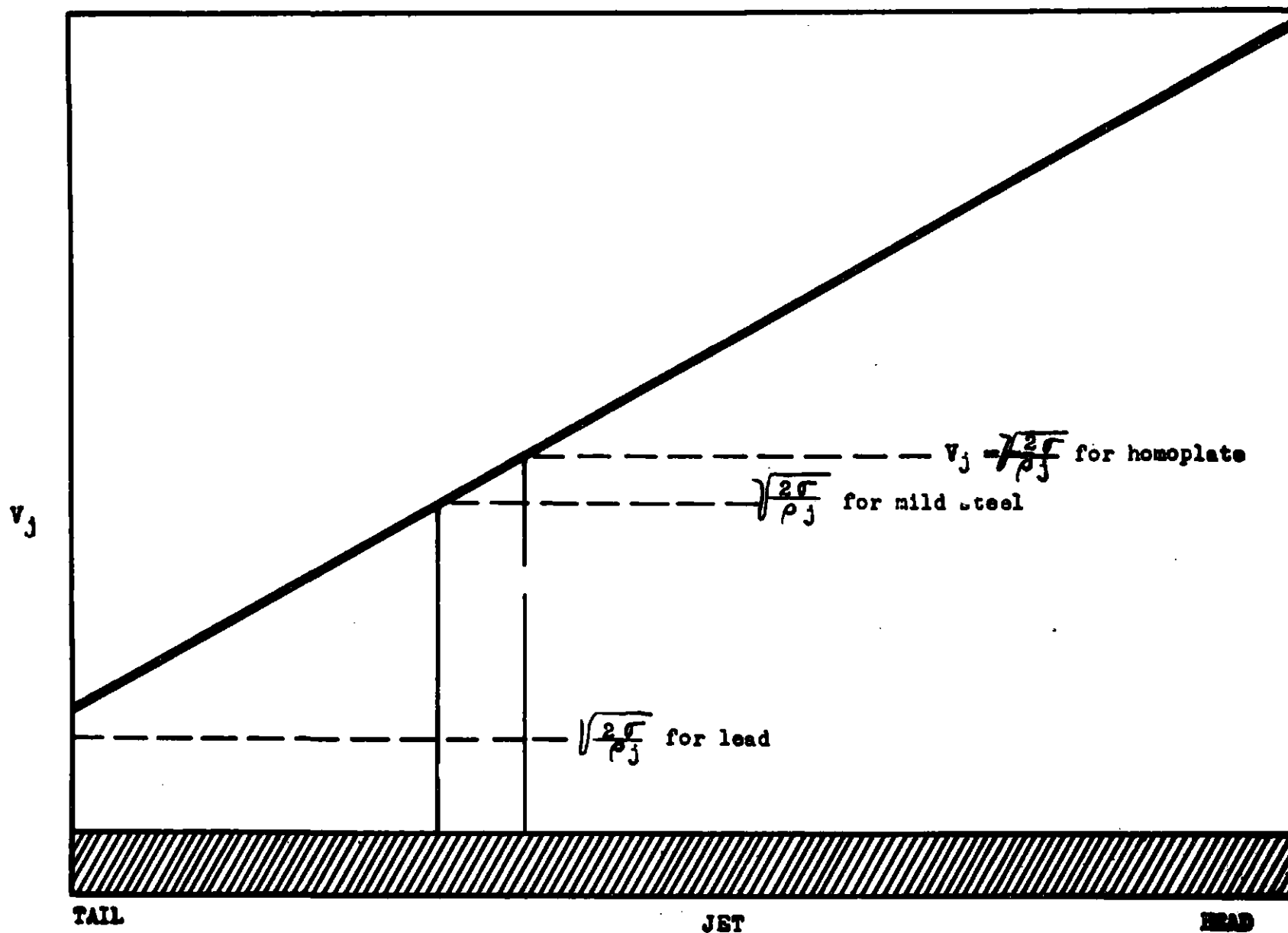
Figure 6—Diagram showing how the effective jet length depends upon the target.
The low velocity rear elements cannot penetrate strong targets.
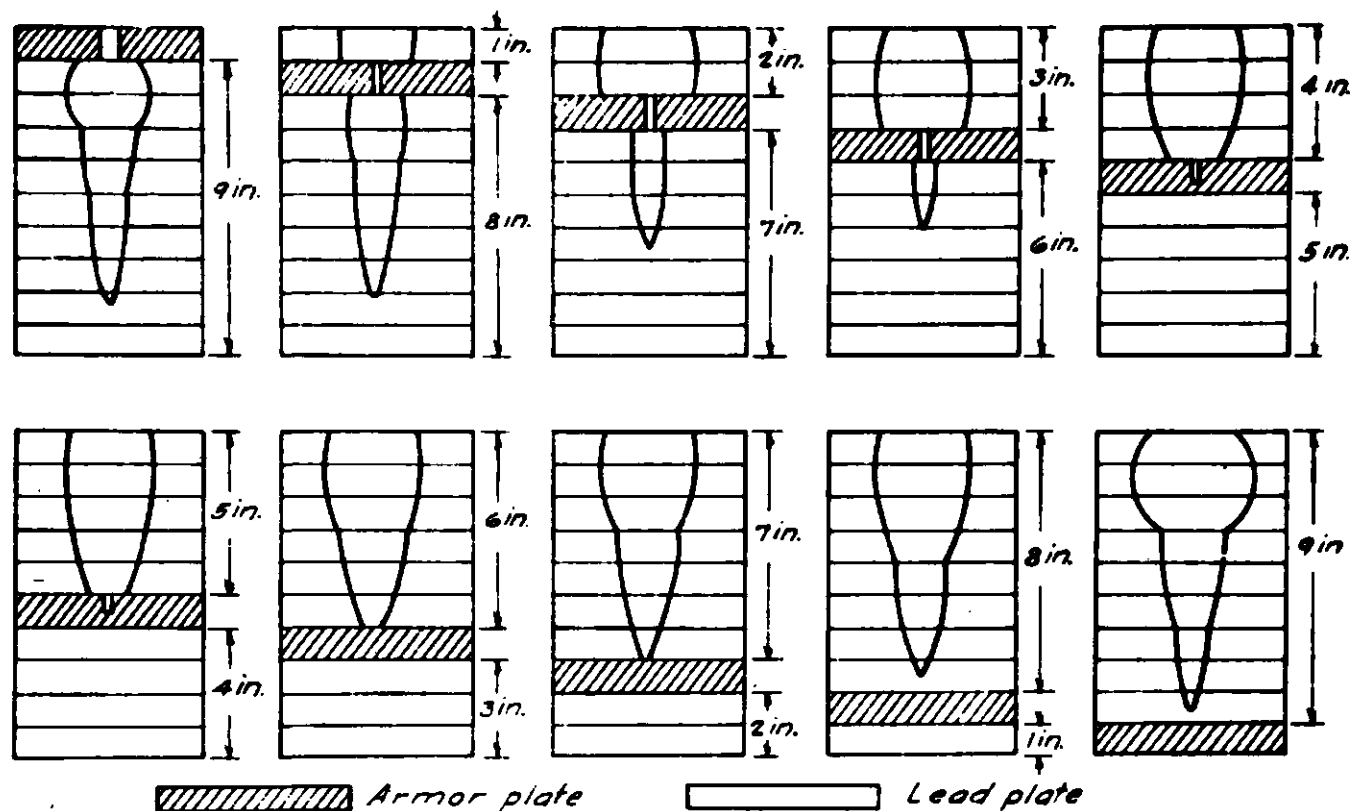
Fig. 7. Hole profiles in combination lead-plate, armor-plate targets. The distance from the top of the pile to the top of the armor plate is designated A in the discussion.

Carnegie Institute of Technology

Figure 7—Eichelberger experiment. Illustrates the stopping of slow
rear elements of jet by hard homoplate.

If perfectly made charges were shot through vacuum, the penetrations into steel should stop increasing with standoff when the particles of the jet are spread so far apart longitudinally that the penetration due to one particle is completed before the next particle arrives. This means that with perfectly made charges, the penetration (produced by any given element of the jet) should; first rise linearly with S, second rise linearly with $\sqrt{S}$ and later become constant. Penetrations at small standoffs are in excellent agreement with this theory. Here air resistance is of little importance. At long standoffs the situation is quite different. Air resistance must cause radial spreading and may completely stop most of the finer particles. For long standoff penetrations the effects of asymmetries become exaggerated.

In Figure 5 three zonal elements A, B and C of a cone liner are shown. The jet elements from these three cone elements are shown at three different times in their travel to a target. At 20 μ sec. jet element C is not yet formed and the front of jet element A has just reached the target. The shaded portion shows the part of the hole in the target that is made by jet element A. At 33.5 μ sec. jet element C is completely formed, the tip of B has just reached the target and A is used up. The shaded portion shows the part of the hole made by jet element B. At 105.6 μ sec. the tip of C has just reached the target and A and B are used up. Notice that both A and B lengthen while they travel but that the increase in length is much the greatest for C. While this Figure 5 has been drawn from calculations made with the theory, the results have been verified with jet velocity and penetration vs. time measurements.

Several thousand shots through some 50 to 100 different materials have shown that, with the exception of one class of materials[12], all target materials are penetrated by the high velocity front end of these jets in accordance with the two relations $dP = d\left(\sqrt{J/\rho}\right)$ and $J(V_j - U)^2 = \rho U^2$. The first of these relations will be taken up by R. J. Eichelberger in his paper on protection under "Residual Penetration Theory." For the slower moving elements at the rear of the jets the situation is different. As one passes from the fast moving front elements toward the slower moving rear elements to the region where V_j approaches the value $\sqrt{2\sigma/J}$, the simple relations break down. When $V_j = \sqrt{2\sigma/J}$, penetration stops and the remainder of the jet has no effect upon the target. The effective length of the jet then depends upon the strength of the target material. This accounts for the total penetration into armor plate being just a little less than in mild steel.

This fact was first stated qualitatively by MacDougall. The effective shortening of the jet length is illustrated in Figure 6. A jet (at a given instant of time) is drawn along the axis of abscissa and the velocity of the various elements is plotted as ordinates. Dotted horizontal lines illustrate the locations of $V_j = \sqrt{2\sigma/J}$ for targets of homoplate, mild steel and lead. The vertical dotted lines show the point in the jet where penetration in the particular target will be stopped. The effective length of the jet is that portion of the whole jet lying between the front tip (at the right) and the vertical dotted line corresponding to the particular target material.

12　Glasses and rocks containing high percentages of quartzite are the only materials that have been found to date that provide significantly different resistance to the front of these jets than is predicted by these relations. These materials provide much better than the theoretical protection when used in large blocks. In finely divided form they are ineffective for in this form they too follow the "density law."

The truth of these statements is strikingly illustrated by an experiment devised by Eichelberger[13] and illustrated in Figure 7. One in. thick homoplate was moved down through stacks of 1 in. lead plates from top to bottom. At the top of the stack the effect of armor plate was little different than the effect of an equivalent thickness of lead. As the armor plate was moved down through the lead stack its effect became more and more noticeable. When it reached the point where it intercepted only those parts of the jet where V_j was no longer large compared to $\sqrt{2\sigma/J}$ for armor plate,

the remainder of the jet was stopped in this plate. Here the total penetration was less than in a stack of armor plate. As the armor was moved below this position the slow moving jet particles penetrated the soft lead and still reached the armor plate. The fact that the average penetration in the last stack was greater than in the one before, even though the jet did not reach the armor in either case, may have been due to one of two causes. First the averages are unreliable because only two shots per stack were made, and second the armor may support the lead and contribute some strength properties to it.

JET FORMATION

Theories of target penetration developed rather logically from the researches of the Explosives Research Laboratory group starting in late 1941 under MacDougall to the formulation in 1945 of the modern version by the author.

On the other hand, attempts to formulate theories for the formation of these jets met with little success until the spring of 1943. During this period J. L. Tuck[14] in England and independently J. C. Clark and L. B. Seely[15] at the Aberdeen Proving Ground obtained flash radiographs of collapsing conical liners. With the information obtained from these radiographs, Sir Geoffrey Taylor[16] and independently Garrett Birkhoff[17] obtained their well known hydrodynamic theory of jet formation. This theory was very successful in explaining the appearances of the radiographs in the early stages of jet formation. It was based upon the assumption that steady-state conditions existed in a moving frame of reference. The radiographs seemed to justify these assumptions, since the collapse angles appeared to be nearly constant and the slug and jet appeared to be the same length "throughout the collapse process." However, the jet appeared "to be issuing from the slug long after the collapse process was completed," and the jet was found to have a gradient in the velocity of its elements that caused it to stretch out to great lengths. No satisfactory theory was available to explain these facts, nor to explain the fact that more of the liner mass near the base of the cone went into forming the jet than was predicted by the steady-state

13 R. J. Eichelberger, "Fundamental Principles of Jet Penetration" Carnegie Tech Project AN-1, Monthly Rpt., Sept. 15, 1944 or "Protection Against Shaped Charges," Final Rpt. O.S.R.D. 6384, Nov. 10, 1945.

14 J. L. Tuck, "Studies of Shaped Charges by Flash Radiography I. Preliminary," AC 3654, March 15, 1943.

15 Sir Geoffrey Taylor, "A Formulation of Mr. Tuck's Conception of Munroe Jets," AC 3724, May 27, 1943.

16 L. B. Seely and J. C. Clark, "High Speed Radiographic Studies of Controlled Fragmentation. I. The Collapse of Steel Cavity Liners," BRL Rpt. 368, June 16, 1943.

17 Garrett Birkhoff, "Mathematical Jet Theory of Lined Hollow Charges" BRL Rpt. 370, June 18, 1943.

theory. The possibility that these discrepancies could be explained, if the process of collapse of the liner was not truly steady-state, was considered by many. It was thought, however, that this possibility was ruled out by the radiographic evidence quoted above.

Several facts were overlooked in the above interpretation of the radiographic negatives. While the collapse angle appears roughly constant during the time when the detonation wave is sweeping the liner, it is far from constant during the period in the collapse process that follows. The zonal elements of the cone near the base are projected inward at a much lower velocity than are those near the apex, the complete collapse of the liner requires many times as long as the time required for the detonation wave to sweep the liner. The observation that "the jet appears to be issuing from the slug long after the collapse process is completed" means only that the last jet and slug element that are formed travel forward at the same speed. The remainder of the jet stretches out rapidly because of the large velocity gradient. The radiographs show that the collapsing liner is never perfectly conical and deviations from the conical shape increase toward the end of the process.

By introducing into the Taylor-Birkhoff theory of jet formation the assumption that the collapse velocity decreases from apex to base of the cone, it has been possible to derive a theory[18] that accounts for all of these discrepancies. This theory accounts for the mass distribution in the whole jet, for its velocity gradient, for the appearance of the radiographs throughout the process of jet formation. In the first attempt at formulating this theory the additional assumption was made that the detonation velocity also decreased as it swept across the cone from apex to base. Subsequent measurements have shown, however, that this detonation velocity changes less than a fraction of a percent. Calculations then showed that the theory agreed better with experiment when the detonation velocity was assumed constant and the collapse velocity was assumed variable than when both were assumed variable.

A number of the relations in the steady-state theory of jet formation can be carried over directly to the non-steady theory. As in the steady-state theory it is assumed that the liner acts like a perfect fluid. It is further considered that this perfect fluid assumption means that adjacent elements move independently so that the laws of conservation of mass, momentum and energy may by applied to each element separately. The difference between the steady-state and the non-steady theories is illustrated in Figure 8. Consider a zonal element of liner originally at P. In either theory the detonation wave has moved from P to Q in unit time, hence the distance $PQ = U = U_D \cos \alpha$, where U_D is the detonation velocity. In the same unit time the liner element has moved with a velocity V_o from P to J. In the steady-state V_o is the same for each element and P_1 would have moved to D_1. Thus in the steady-state the contour of the collapsing liner is a true cone indicated by the dotted line JD_1Q. In the non-steady case V_o is less for the element P_1 than for P and hence P_1

18 Emerson M. Pugh, R. J. Eichelberger and Norman Rostoker, "Theory of the Formation of Jets by Charges with Lined Conical Cavities," CIT-ORD 21, June 30, 1949 and CIT-ORD 31, Feb. 28, 1951.
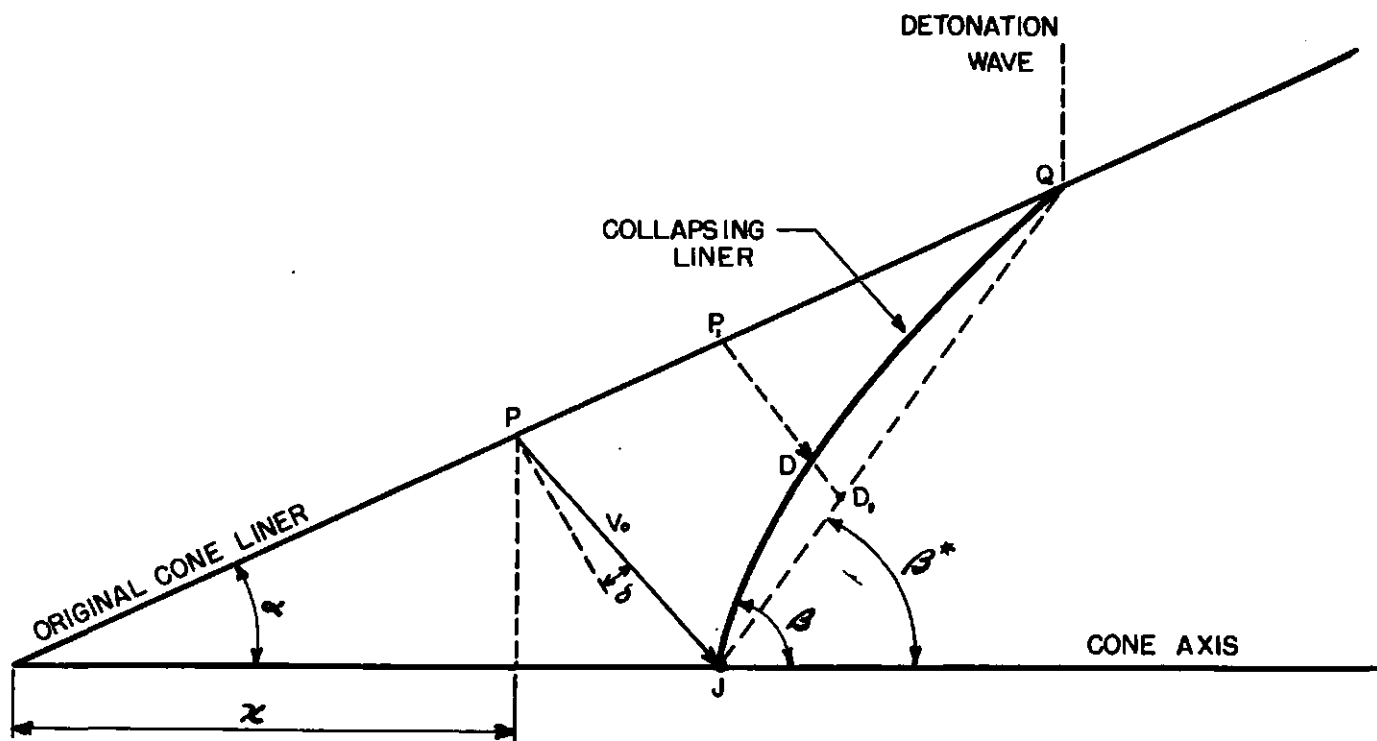
Figure 8—Liner collapse and jet formation.   Dotted line shows the contour of the
collapsing liner on the steady-state theory and the solid line
shows this contour on the non-steady theory.

Unknowns
$$\beta, V_0, \delta$$

$$\underline{1)} \quad \sin \delta = V_0 / 2U$$

$$\underline{10)} \quad \cos^2 \beta/2 = dm_s / dm$$

$$\underline{7)} \quad V_j = V_0 \csc \beta/2 \cos(\alpha - \beta/2 + \delta)$$

$$\underline{18)} \quad \tan \beta = \frac{\sin \beta^* - x \sin \alpha (1 - \tan A \tan \delta) V_0' / V_0}{\cos \beta^* + x \sin \alpha (\tan A + \tan \delta) V_0' / V_0}$$

$$\beta^* \equiv 2\delta + \alpha \qquad 2A \equiv \beta^* + \alpha \qquad V_j = V_j (m_j)$$

$$\text{but} \quad m_j = m_j (x)$$

Figure 9—Important equations of the
non-steady theory of jet formation.

24

has moved only to D. The collapsing liner is not conical but curved as shown by the line JDQ. The important equations of the non-steady theory are shown in Figure 9 (numbered as in the papers[18] on this theory). All of the variable properties of the elements of the liner, slug and jet, are expressed in terms of x, the coordinate determining the location of the element in the original liner. The first two equations, (1) and (10) are identical with those of the steady-state theory. The angle between the axis and the collapsing liner element is β^+ in the steady-state theory and β in the non-steady theory. In accordance with a theorem given by Sir Geoffrey Taylor, the collapse velocity V_o makes an angle δ with the normal to the original liner, which is equal to half the angle PQJ of the isoceles triangle PQJ; hence Eq. (1) follows from simple trigonometry. In this non-steady theory the division of the liner mass between jet and slug expressed by Eq. (10), and the jet velocity expressed by Eq. (7), depend upon β instead of upon β^+ as in the steady-state theory. The angle β is given by Eq. (18), where $2A = \beta^+ + \alpha$ and $V_o' = dV_o/dx$.

Under certain conditions the predictions of the non-steady theory may differ radically from those of the steady-state theory. This is due to the fact that the mass and the velocity of the jet elements depend so critically upon the collapse angles and to the fact that these collapse angles β and β^+ may differ so greatly. For example, either in the CIT standard charge or in the charge used by Seely and Clark[19] in their flash radiographs, the elements of the liner near the base may have relatively small values of V_o and relatively large negative values of V_o'.

Consider the case where $V_o \ll 2U$ and $V_o \ll xV_o'$, which are true for the basal elements of the liner in most charge designs. Here β approaches $90^\circ + \alpha$, while β^+ approaches α. Putting the values into Eq. (7) and into the equation for V_S (Eq. (8), footnote 18) gives $V_j = V_S$ and the elements of jet and slug travel along the axis together at the same velocity.

At this stage nearly two-thirds of the mass of this rather massive liner element may be going into the jet. Since the front of the jet travels at many times this velocity, the radiographs create the illusion that the jet is being extruded from the slug. This phenomenon, which is clearly observed in flash radiographs, gave rise to the oft quoted statement[1] "an 'after jet' continues to be emitted (from the slug)

---

19   L. B. Seely and J. C. Clark, "High Speed Radiographic Studies of Controlled
     Fragmentation. I. Collapse of Steel Cavity Charge liners," BRL Rpt. 368,
     June 16, 1943.

long after the walls have completely collapsed." [20]

The four equations in Fig. 9 have been used to obtain an experimental verification of the non-steady theory. They contain just three unknowns (β, V_o and δ ; all functions of x) that cannot be determined by experiment. Eqs. (1) and (7) can be used to eliminate V_o and δ from (18), leaving two independent Eqs. (10) and (18) in the single unknown, β. Figure 10 shows the result of solving these two equations for β. The circled points were obtained by solving Eq. (18) graphically and the solid line is obtained from Eq. (10) using slug recovery data. The values in Figure 10 were obtained with a CIT standard charge of pentolite, lined with an M9Al steel cone. Similar results have been obtained with other charges. The close agreement between the two sets of values for β provides strong support for the non-steady theory of cone collapse and jet formation. During the early stages of cone collapse β does not change very rapidly. This helped to justify the original steady-state theory. The angle β, however, increases very rapidly for elements near the base of the cone. This is clearly shown in the series of flash radiographs published by Clark[21]. The second radiograph (the first of the collapsing liner) shows a β near 40° whereas the third radiograph shows β more than 80°. The interpretation of the last is uncertain though it appears to me to show a β greater than 90°.

---

20   On the basis of the radiographic evidence that appeared to show jet issuing from the slug, at least two slug extrusion theories have been presented.

Birkhoff visualized the slug as having a nearly fluid core, which was squirted out by the application of a residual gas pressure converging on the slug. A mathematical analysis showed that the core of the slug would be much hotter than the outer layers.

M. A. Cook, "Investigation of Cavity Effect" E. I. duPont de Nemours Co., Contract W-670-ORD-4331, Apr. 15, 1944, devised an ingenious theory in which the core of the slug contained a quasi-fluid of fine metal particles. The pressure required for the extrusion came from residual inward kinetic energy of the slug walls. The gradient in the jet was produced by friction of the outer layers of the extruding jet along the inner walls of the slug.

Recent slug recovery experiments, together with other evidence, appear to rule out both of these theories. It would be difficult for either of these theories to explain the slug recovery results obtained with charges having large belts of explosive around the base of the cone, which are discussed in the closing paragraphs of this paper.

21   J. C. Clark "Flash Radiography Applied to Ordnance Problems," Journal of Applied Physics, Vol. 20, No. 4, April 1949, Figure 11.
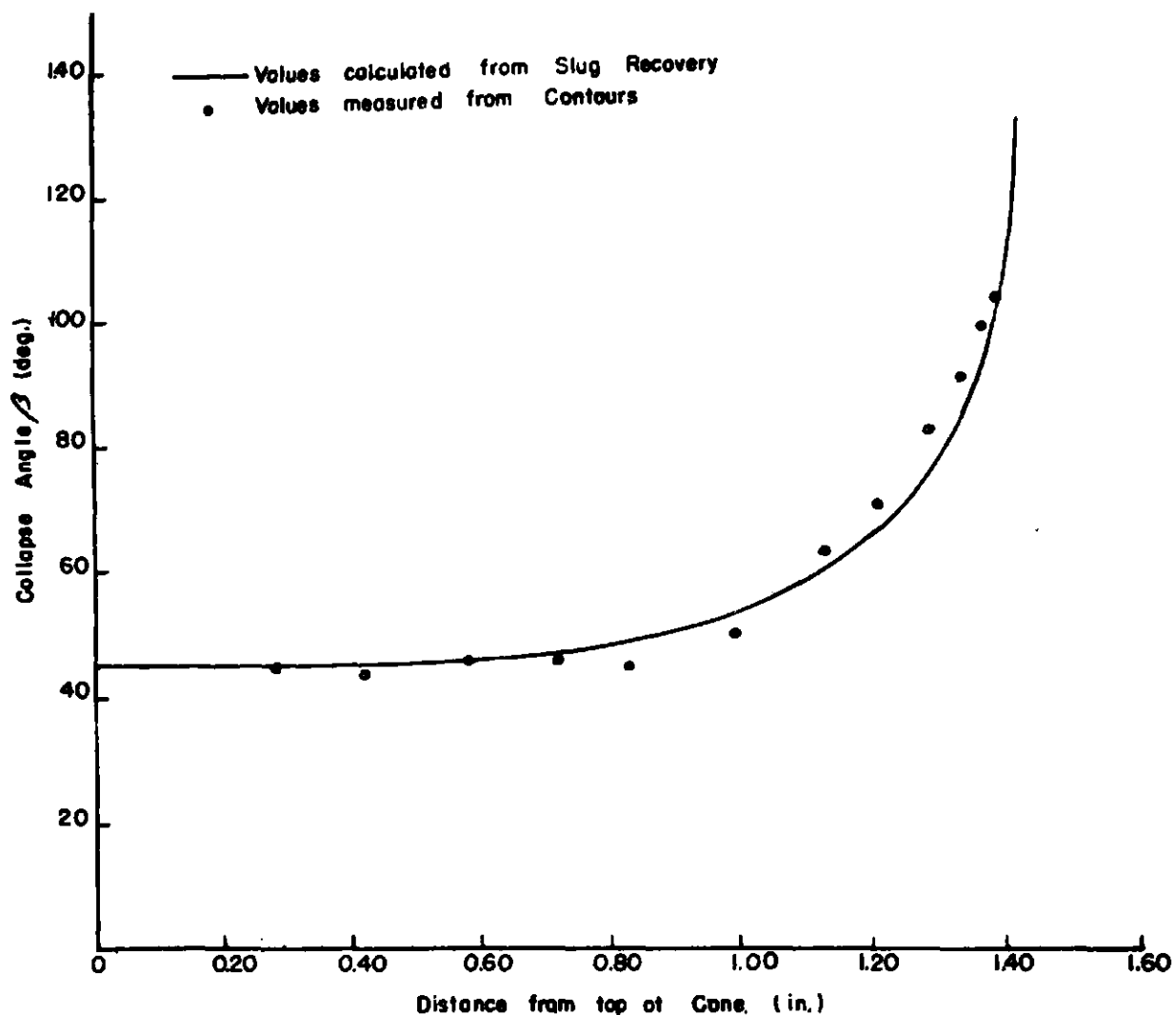
Figure 10—Independent determinations of the collapse angle β. The agreement
between the solid line and the circled points provides a verification
of the non-steady extension of the theory.
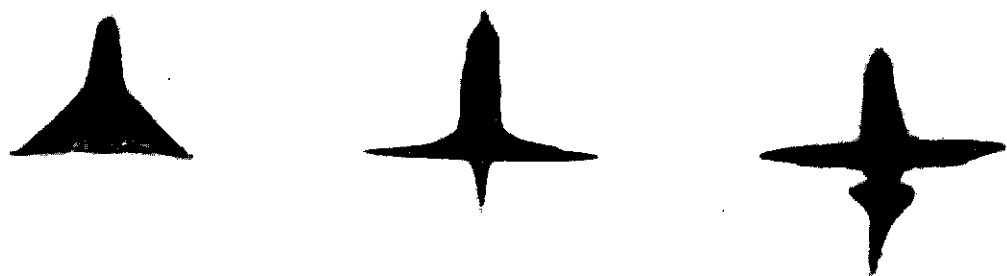
Figure 11—Flash radiographs by J. C. Clark showing three stages of liner collapse and
jet formation. These collapse angles agree qualitatively with the values
determined in Figure 10.

27

Values of U for Eq. (1) were obtained with a rotating mirror camera. Values of V_j for Eq. (7) were also obtained with the rotating mirror camera. However, to obtain these velocities at various points along the jet, it was necessary to pass these jets through target plates to knock off the desired portion of the forward jet elements. The mass of the remaining elements were determined by collecting and weighing the portion of the jet that passed through. Thus a curve of V_j vs. m_j was determined. To identify these velocities with the original cone element from which they came, it was necessary to use slug recovery data. Slug sections have less mass than the cone section from which they came. The difference is the mass forced into the jet, $m_j = m - m_s$. Thus m_j was determined as a function of x and, since V_j vs. m_j was known, V_j versus x was determined. The slug recovery data also determined dm_s/dm for use in Eq. (10). For slug recovery experiments[22], the charge liners were made in two parts, divided along a plane perpendicular to the axis. When these charges were shot into water or other recovery medium, two slugs were recovered. The weight of these compared to the weight of the original cone sections provided a point on the m_s vs. m curve shown in Figure 12. This curve then was differentiated to obtain dm_s/dm.

V_o vs. x can be calculated from the preceding information. The values for the CIT standard charge are shown in Figure 13. It is desirable to be able to calculate $V_o(x)$ directly from the properties of the explosive and the goemetry of the charge assembly. A semi-empirical release wave procedure is now being developed for this purpose.

The release wave theory is being developed by Eichelberger, Linder and Dreesen. It employs ideas gleaned from the much more exact treatment of Courant and Friedrichs with a treatment of a special case given by Gurney and Sterne. The aim is to develop a simplified procedure for analyzing the effects produced by different explosive geometries. Several effects must be neglected. An empirical approach is used to determine which effects may be safely ignored. Briefly the theory visualizes a high pressure zone in the gases behind a detonation wave that is cut off by release waves initiated at any free surface touched by the detonation wave.

In its present unfinished state this procedure has successfully predicted liner velocities for several charge geometries. Charges having conical cavities lined with metal present a difficult problem. Nevertheless, predictions of $V_o(x)$ have been made for two radically different charge geometries (with lined conical cavities) that agree qualitatively with the results obtained from slug recovery and jet velocity measurements.

These two charges are illustrated in Figure 14. Charge S is the standard CIT charge while charge C has belts of explosive around the liner of uniform thickness from apex to base.

22   This type of experimental analysis was originally devised by D. P. MacDougall and M. A. Paul. The technique has been modified by R. J. Eichelberger to produce precision results.

23   R. Courant and K. O. Friedrichs, "Supersonic Flow and Shock Waves," Interscience Publishers, 1948.
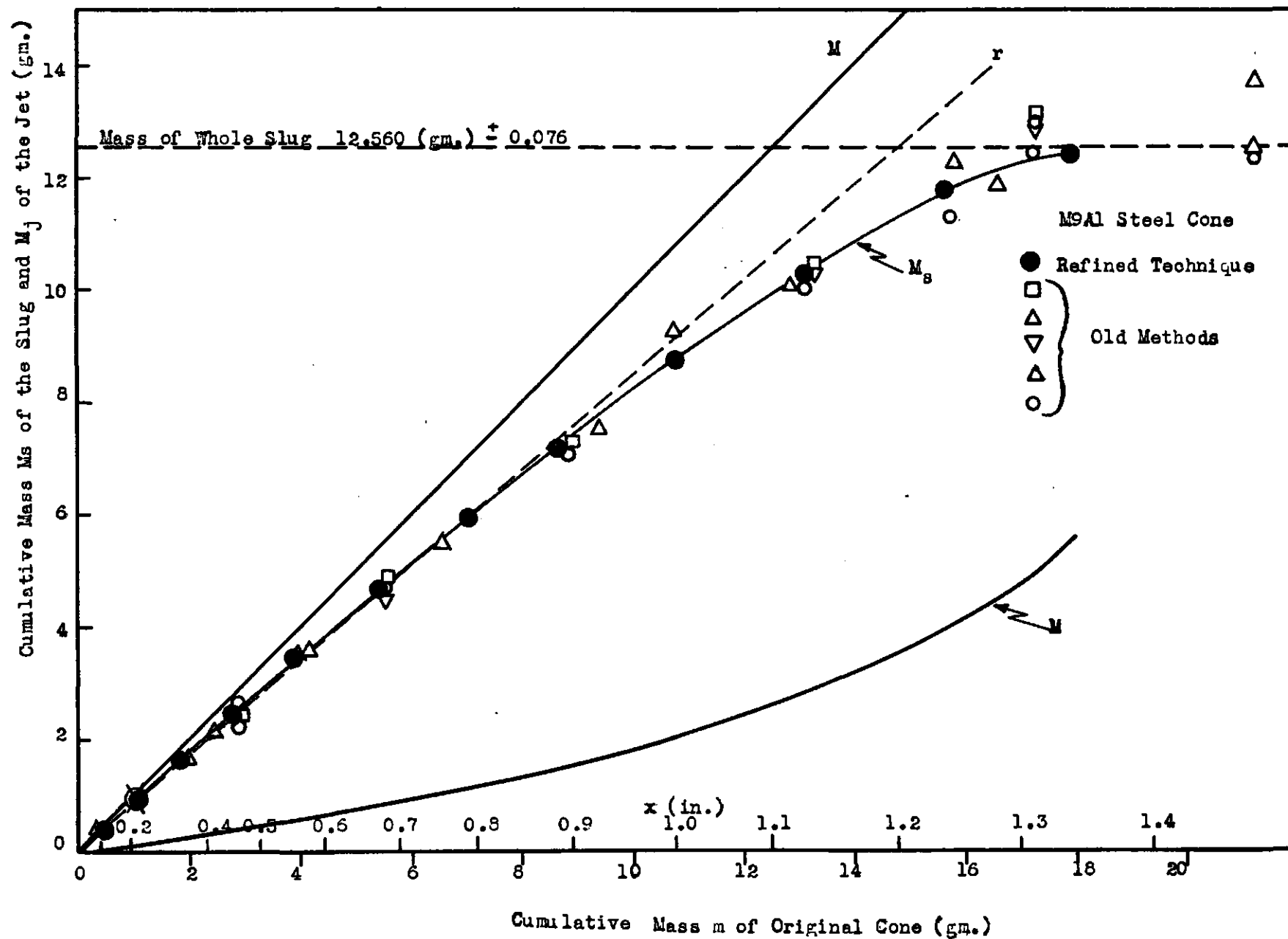
Figure 12—Division of steel cone between jet and slug. Results obtained by
recovering slugs from sectioned cones; using CIT standard charges.
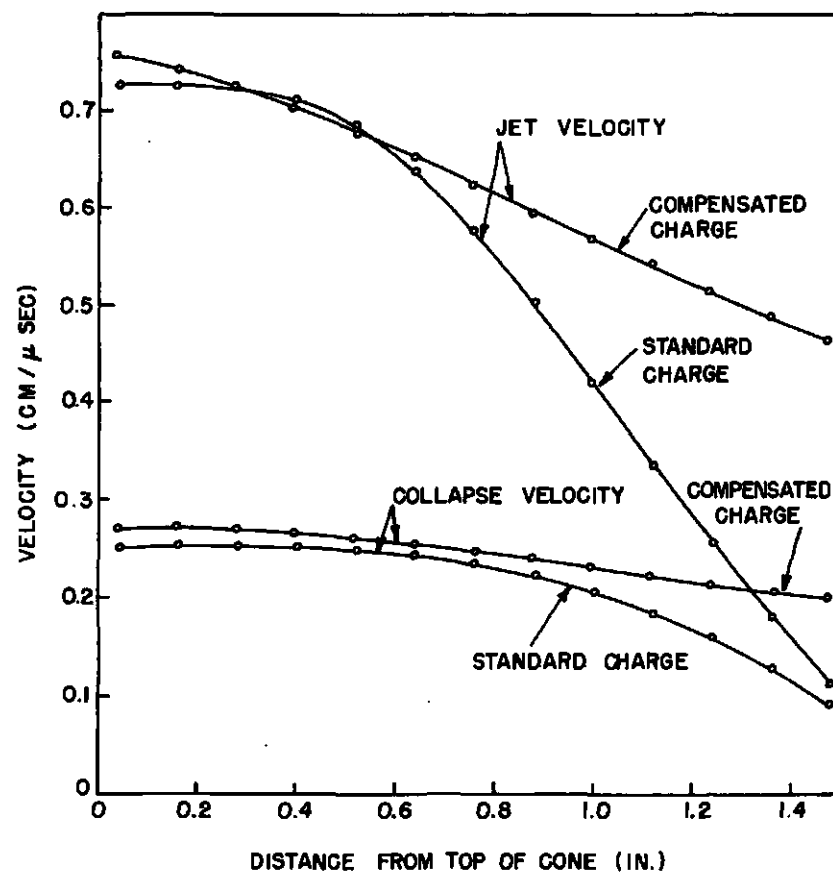
Figure 13—Jet velocities and liner collapse
velocities for the S and C type charges
shown in Figure 14.

$$\frac{dm_d}{dm} = 1 - \frac{dm_s}{dm}$$

	P in.	V cc
S	7.9	11.8
C	4.5	19.0
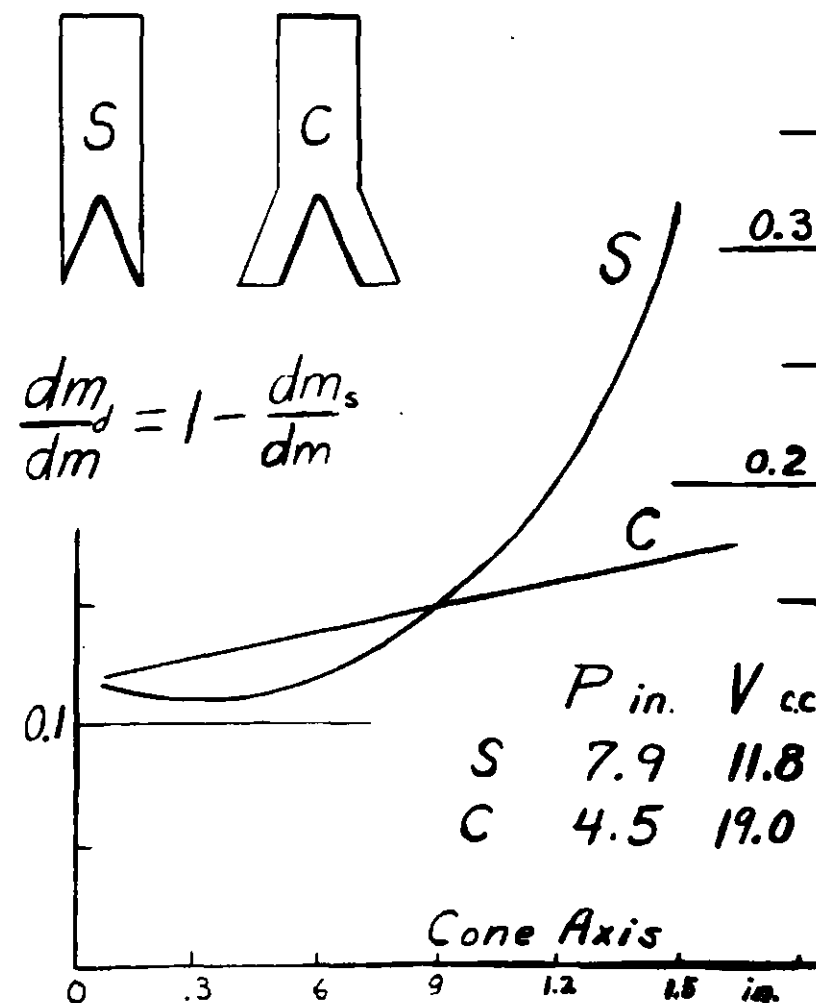
Figure 14—Percent of cone liner going into
jet formation vs. the distance of the original
zonal element from the apex; for the S and
C type charges pictured.

The values of $V_j(x)$ and $V_o(x)$ for these two charges are shown in Figure 13. These are in rough qualitative agreement with the predictions of the incomplete release wave theory. The average penetrations with the S- charge were 7.9 in. and with the C- charge were only 4.5 in. The large value of V_o' in the S- charge resulted in a long jet, which therefore penetrated deeply. The large belt of explosive around the base in the C- charge made the value of V_o large and V_o' small at the base. The resulting short jet did not penetrate deeply, though it did make a bigger hole (19.0 cc against 11.8 for the S- charge) because of its greater energy. The slug recovery results shown in Figure 14 are most instructive. Towards the base of the cone, the percentage of the mass of the liner going into the jet, increases rapidly for the S-charge (up to 31%) but very slowly for the C-charge (to only 17%). From Eq. (18) β was large for the basal elements in the S- charge but small for those in the C- charge. Then from Eq. (10) dm_s/dm became small for the S- but almost constant for the C-charge.

On the other hand, it appears to be practically impossible to justify this result on the basis of any slug extrusion theory. Before slug recovery results were available on charges having large belts of explosive around the base of the cone, it was generally believed that the reduced penetrating power was caused by the exploded gases breaking out around the liner base to disrupt the rear of the jet. This analyses appeared to be supported by radiographic evidence, which showed that the connection between the jet and slug, commonly observed with other charges, was missing.

The obvious explanation with the non-steady theory is that V_o is not much smaller than xV_o' and, therefore, $V_j \neq V_s$ but $V_j > V_s$. Thus the rear of the jet separates from the slug and the radiographs do not show jet in contact with the slug.

CONCLUSION

The present non-steady hydrodynamic theories of jet formation and target penetration appear to be capable of interpreting the experimental results obtained with conical metallic liners, provided their thicknesses are not too far from the optimum and their apex angles lie between $30°$ and $90°$. Undoubtedly these theories would also apply to cones with angles outside these limits, provided the liners are sufficiently thin.

MULTIPLE-FRAGMENT-IMPACT EFFECTS IN SHAPED CHARGE PENETRATION

John S. Rinehart

Michelson Laboratory

U. S. Naval Ordnance Test Station, Inyokern, China Lake, California

ABSTRACT

It is assumed that a shaped charge jet contains a relatively small group of discrete hypervelocity solid fragments. The probable cumulative effects of the successive impacts of the several fragments are predicted from known facts concerning the impacts of very high velocity fragments. The predictions are compared with experimental observations on the interactions between targets and shaped charge jets. The conclusion reached is that the cumulative effects of multiple impacts appear, in some cases, to play an important role in the mechanics of shaped charge penetration. It is urged that further theoretical and experimental studies be pursued in order to establish the relative place that these multiple-fragment-impact effects must occupy in a complete treatment of shaped charge penetration.

INTRODUCTION

It has been well established that a shaped charge jet usually contains as an important component, a relatively small group of discrete hypervelocity solid fragments. The total number of fragments that will be found within a particular jet will depend upon the size of the charge, cone angle, liner thickness, liner material, and many other factors. The masses of the fragments and their respective velocities will be governed by the same variables. Observations on jet-target interactions suggest that the cumulative effects of the multiple impacts of the fragments of the group could and probably do play an important role in the mechanics of shaped charge penetration. The primary purpose of this paper is to present a type of approach that appears to offer much promise toward establishing the relative place that multiple-fragment-impact effects must occupy in a complete treatment of shaped charge penetration. Known facts concerning the effects produced on a target by the impact of a single hypervelocity fragment are used to predict the cumulative effect of several successive impacts. It is assumed that the masses of the fragments with which we are concerned lie between a few hundredths of a gram and a few grams and that their velocities lie in the range from 10,000 to 30,000 feet per second.

EFFECT OF SINGLE FRAGMENT IMPACT

When a fragment strikes a target, the most characteristic thing that it does is to produce a hole or crater. The shape and size of the crater will depend upon the shape, mass, and velocity of the fragment and upon the physical properties of the target. The general character of the variation of shape of crater with impacting velocity is illustrated in Figure 1. At low velocity (below about 4,000 feet per second for a steel target) the crater is simply a straight-sided hole whose cross-section is similar to that

LOW VELOCITY <4000 ft/sec

HIGH VELOCITY 4000 - 10,000 ft/sec

HYPERVELOCITY >10,000 ft/sec
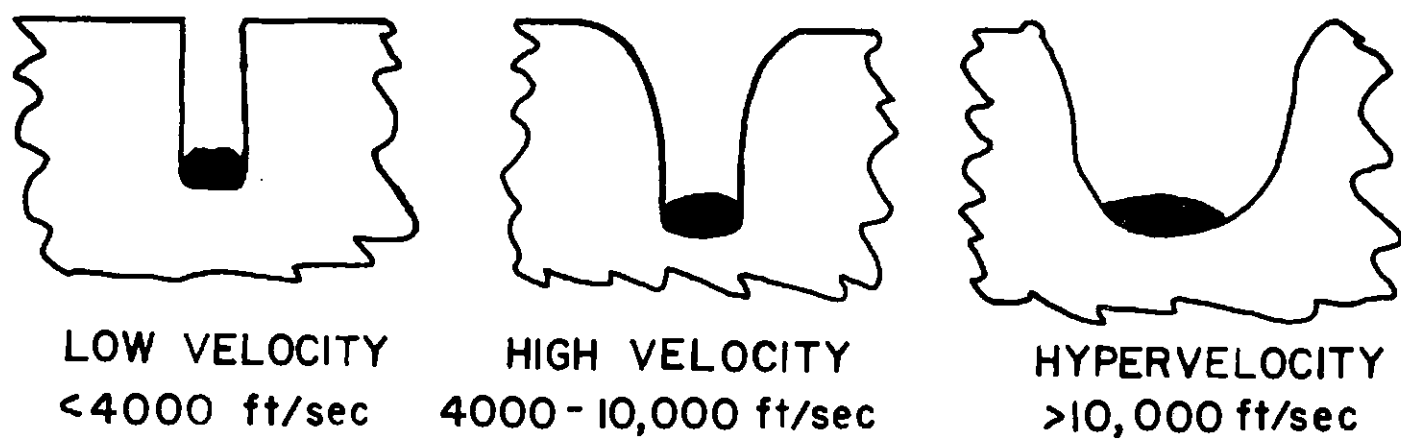
Figure 1—Variation of shape of crater with impacting velocity.

SURFACE OF FAILURE
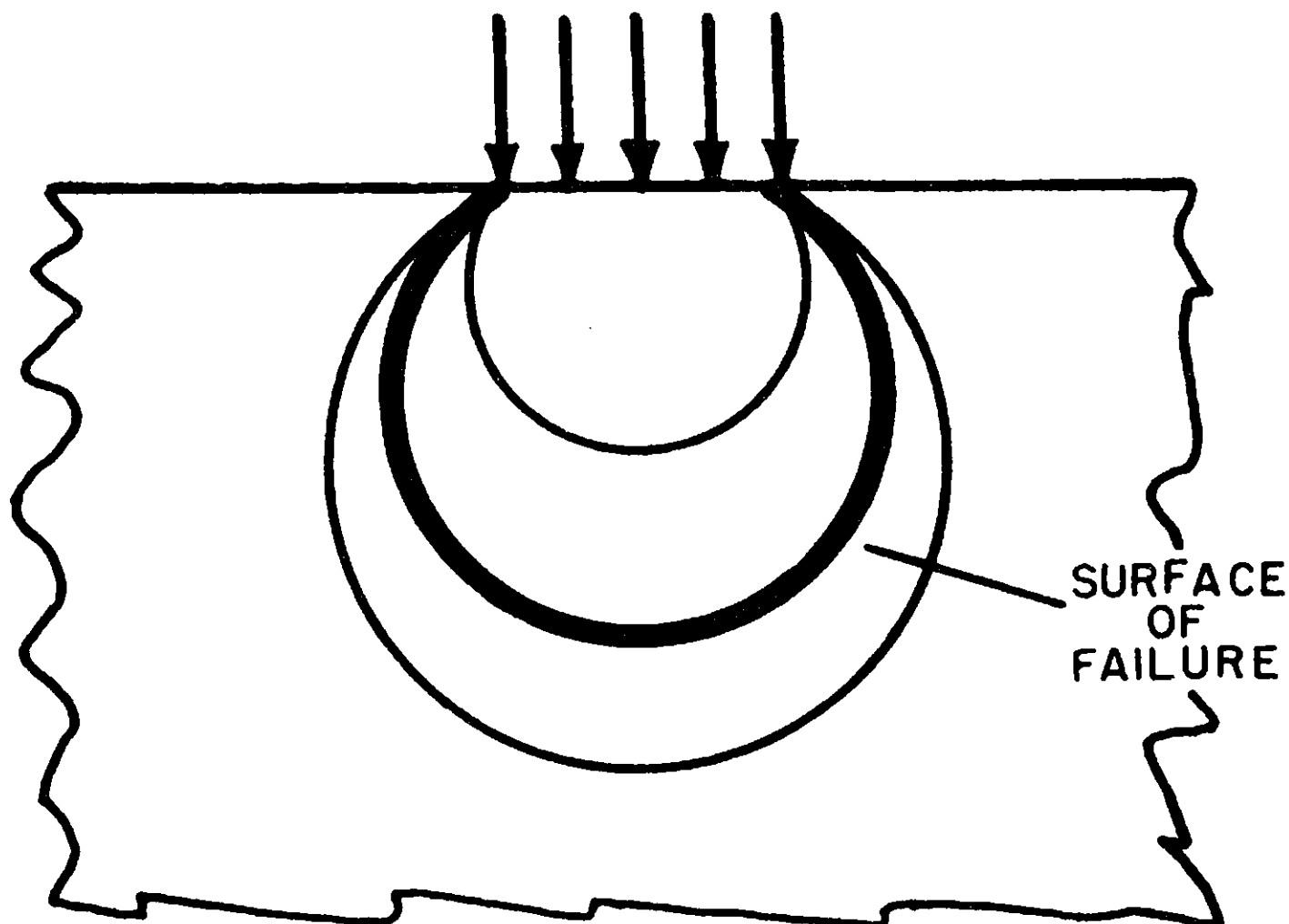
Figure 2—Distribution of shearing stress produced by application of load over small area.

34

The mechanisms involved in crater formation at the very high velocities are still
somewhat obscure. A most profitable way of looking at the problem is to suppose that
the size and shape of a crater will depend primarily upon the stress-distribution ex-
isting in the target during and immediately following deceleration of the fragment.
Stresses that are undoubtedly much higher than the plastic limit for steel must exist
during this time in the region close to the area of impact. The probable shape of the
crater is arrived at by assuming (a) that the fragment is stopped in a negligibly short
distance, (b) that the force of the impact distributes itself within the target in
accordance with the same geometry as the stresses produced by a static load, and (c)
that the target material will fail within a region in which the shearing stress exceeds
a certain critical value.

When a semi-infinite solid body is subjected to a static load over a small area,
the distribution of shearing stress is approximately that shown in Figure 2. Each of
the circles in the figure corresponds to the intercept of a surface of constant shearing
stress with the plane of the figure. As one moves away from the area of application of
force the magnitude of the shearing stress decreases and eventually becomes less than
that required to cause the material to fail. There will exist a surface of failure
that corresponds to a critical limiting shearing stress. Such an assumed surface has
been drawn as a heavier line in the figure. We might expect that the crater would have
approximately the shape of this limiting surface of failure with the exception that ma-
terial near the free surface of the block would be pushed upward and outward since it
is under little restraint.

The profiles of craters produced by hypervelocity pellets are in substantial
agreement with the above predictions. Tracings of the profiles of two craters produced
in a lead target are shown in Figure 3. The crater on the left was made by a 8,000
feet per second, 2 gram, steel pellet and that on the right by a 15,000 feet per second,
2/3 gram, aluminum pellet. The profile of the crater made by the aluminum pellet has
been superimposed onto a stress distribution of the type discussed above in Figure 4.
The latter drawing lends considerable support to the concept of a surface of failure
that corresponds to a critical limiting shearing stress. More precisely, we should
probably use here the von Mises criterion of failure. To the accuracy needed the
critical shearing stress criterion seems to be adequate. Although craters in lead
targets have been used here for illustrative purposes, it is well known that the crater
made by a shaped charge fragment striking a steel target has essentially the same shape.

It has been recognized for many years that the volume of the crater produced by
an impacting missile or fragment is directly proportional to the kinetic energy of the
missile or fragment. The depth of penetration of a fragment of specified mass and
velocity can be computed if this observation is used and, if in addition, the shape of
the crater is specified.

A first approximation to the shape of the crater made by a hypervelocity fragment
is a sphere that is tangent to the point of impact. For this shape of crater, the
depth, p, to which an impacting fragment will cause the material to fail is given by

1 in.
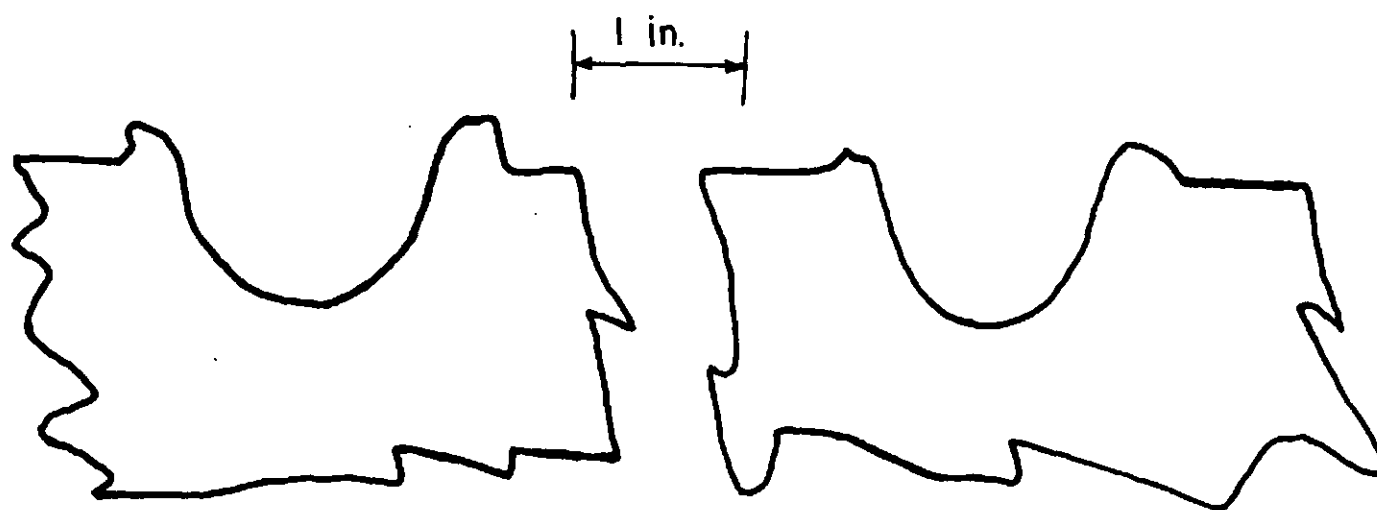
TARGET: LEAD

STEEL PELLET
   DIAMETER: ~0.5 in.
   MASS: 2.0 gm.
   VELOCITY: 8,000 ft/sec
   VOLUME OF CRATER: 14 cc.

ALUMINUM PELLET
   DIAMETER: ~0.5 in.
   MASS: 0.7 gm.
   VELOCITY: 15,000 ft/sec
   VOLUME OF CRATER: 17 cc.

K.E. OF AL./K.E. OF STEEL = 1.2

Figure 3—Tracings of profiles of craters made in lead by hypervelocity pellets
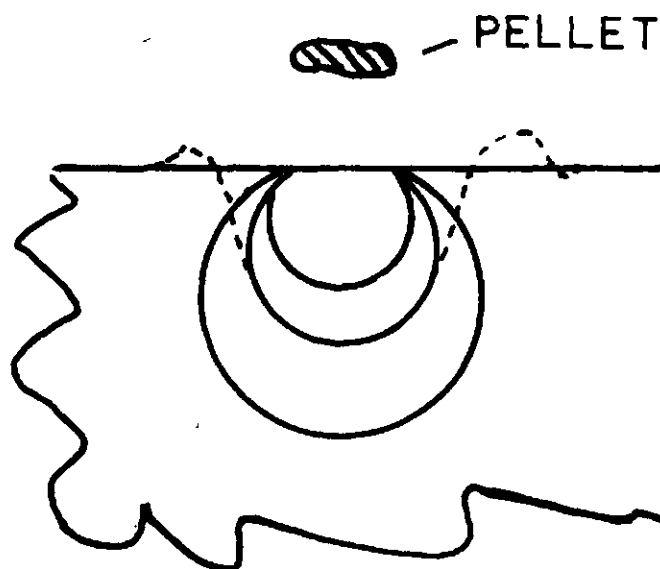
— PELLET

Figure 4—Superposition of crater profile
and probable shearing stress distribution.
Crater made in lead target by 15,000 ft/sec,
0.7 gm, aluminum pellet.

36

$$p = (\frac{6V}{\pi})^{1/3} \tag{1}$$

where V is the volume of the crater. Now the volume in terms of the kinetic energy of the fragment will be given by

$$V = c_1 \cdot \frac{1}{2} mv^2 \tag{2}$$

where c_1 is a constant that depends upon the target material and m and v are the mass and velocity, respectively, of the fragment. Substitution of the value of the volume V given by Eq. (2) into Eq. (1) gives

$$p = c_2 m^{1/3} v^{2/3} \tag{3}$$

where

$$c_2 = (\frac{3c_1}{\pi})^{1/3} \tag{4}$$

It is evident from Eq. (3) that the penetration of a very high velocity fragment is proportional to the one-third power of its mass and the two-thirds power of its velocity. At low impacting velocities penetration is proportional to the square of the velocity.

The constant c_1 of Eq. (2) is the volume of target material displaced per unit of kinetic energy of the impacting fragment. Its value and, hence, the value of c_2 of Eq. (3), depends upon the target material. Experimentally determined values of c_1 and computed values of relative penetration are listed for several target materials in Table I. Steel has been taken as unity. It is significant that the penetration varies as the cube root of c_1. Although the volume of the crater formed by a particular hypervelocity fragment will be nearly ten times as great in lead as in steel, the depth to which it will penetrate will only be 2.3 times as great.

CUMULATIVE EFFECT OF MULTIPLE IMPACTS

The effect of multiple impacts on a target can be readily arrived at. Consider first the situation shown in Figure 5. Several fragments of respective masses, m_1, m_2, . . . and velocities v_1, v_2, . . . separated in space, are all traveling in the same straight line toward a target. When the first strikes the target, it produces a crater of depth, p_1, equal to $c_2 m_1^{1/3} v_1^{2/3}$. The next fragment then strikes and produces another crater. The result at this instant is shown in Figure 5b. This process continues until all of the fragments have struck (Figure 5c). The total depth of penetration, P, will be given by

(A)   **(B)**   **(C)**
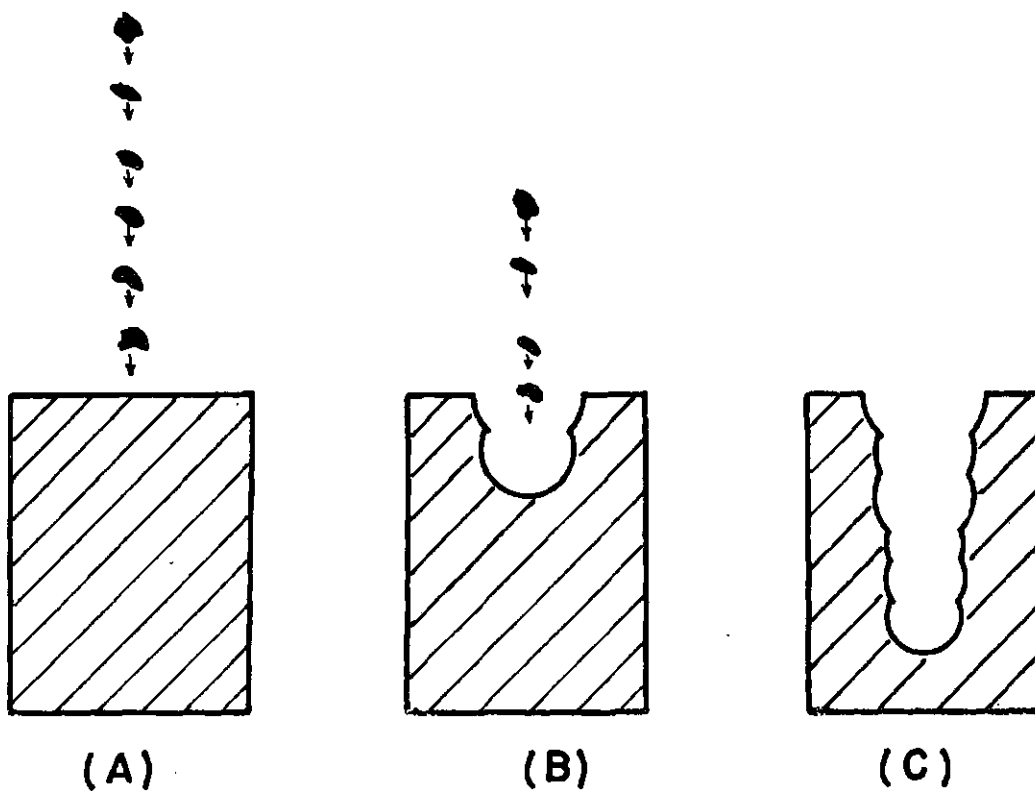
Figure 5—Diagrams that show effect of multiple impacts on target (a) just before impact, (b) after two particles have struck, and (c) total effect of all six particles.
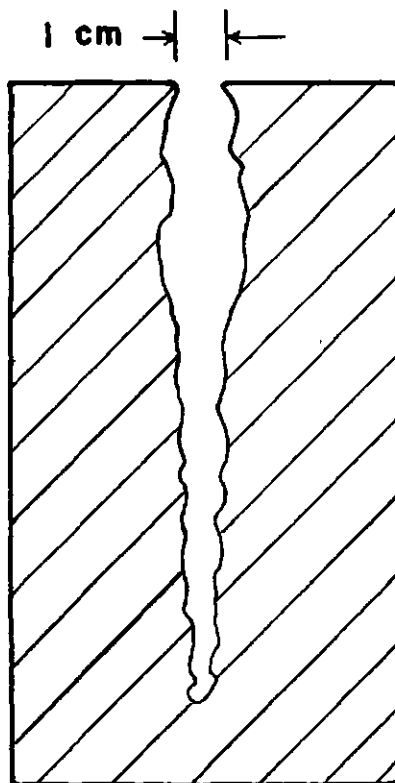
Figure 6—Trace of outline of hole produced by steel lined Mk. 1 shaped charge.

38

$$P = \sum_{i=1}^{n} p_i = c_2 \sum_{i=1}^{n} m_i^{1/3} v_i^{2/3} \tag{5}$$

The contour of the hole will be the envelope of the several craters and should have a general sausage-like shape.

It is interesting to consider at this point the relative penetrations produced by a single fragment of mass, m, and velocity, v, and by the same mass broken up into n equal parts, all of which have the same velocity but strike one after the other. The penetration, p, of the single fragment will be

$$p = c_2 m^{1/3} v^{2/3} \tag{6}$$

The penetration, P, of the n fragments will be

$$P = c_2 v^{2/3} n \left(\frac{m}{n}\right)^{1/3} \tag{7}$$

The relative penetrations will be given by

$$\frac{P}{p} = n^{2/3} \tag{8}$$

It can be shown mathematically that division into n equal parts yields the maximum relative penetration.

EXPERIMENTAL OBSERVATION

In this section the above concepts will be related to available experimental data on shaped charge penetration. The following two experimental facts are well established. First, the depth of penetration produced by most lined shaped charges increases as the distance between the charge and the target is increased from zero to some optimum distance that is of the order of several charge diameters. At greater than optimum stand-off, depths of penetration are likely to be erratic. Charges which are presumably well aligned will sometimes give depths equal to those obtained at optimum standoff. Second, the volume of the hole remains substantially constant as standoff is increased to the optimum for depth of penetration. Beyond the optimum, the average hole volume decreases with increasing standoff.

A third observation is that the contours of the holes made by shaped charge jets exhibit a characteristic irregularity. This irregularity is characterized by a quite noticeable pattern of swellings and constrictions. The contour of a typical crater made by a steel lined Mk. 1 cone in a steel target has been traced in Figure 6. The same type of irregularity is also observable in most of the photographs of cavities that have been published.

Qualitatively, the concept that the cumulative effect of the impacts of a group of discrete fragments is an important aspect in the penetration of a shaped charge jet, fits the experimental observations well.
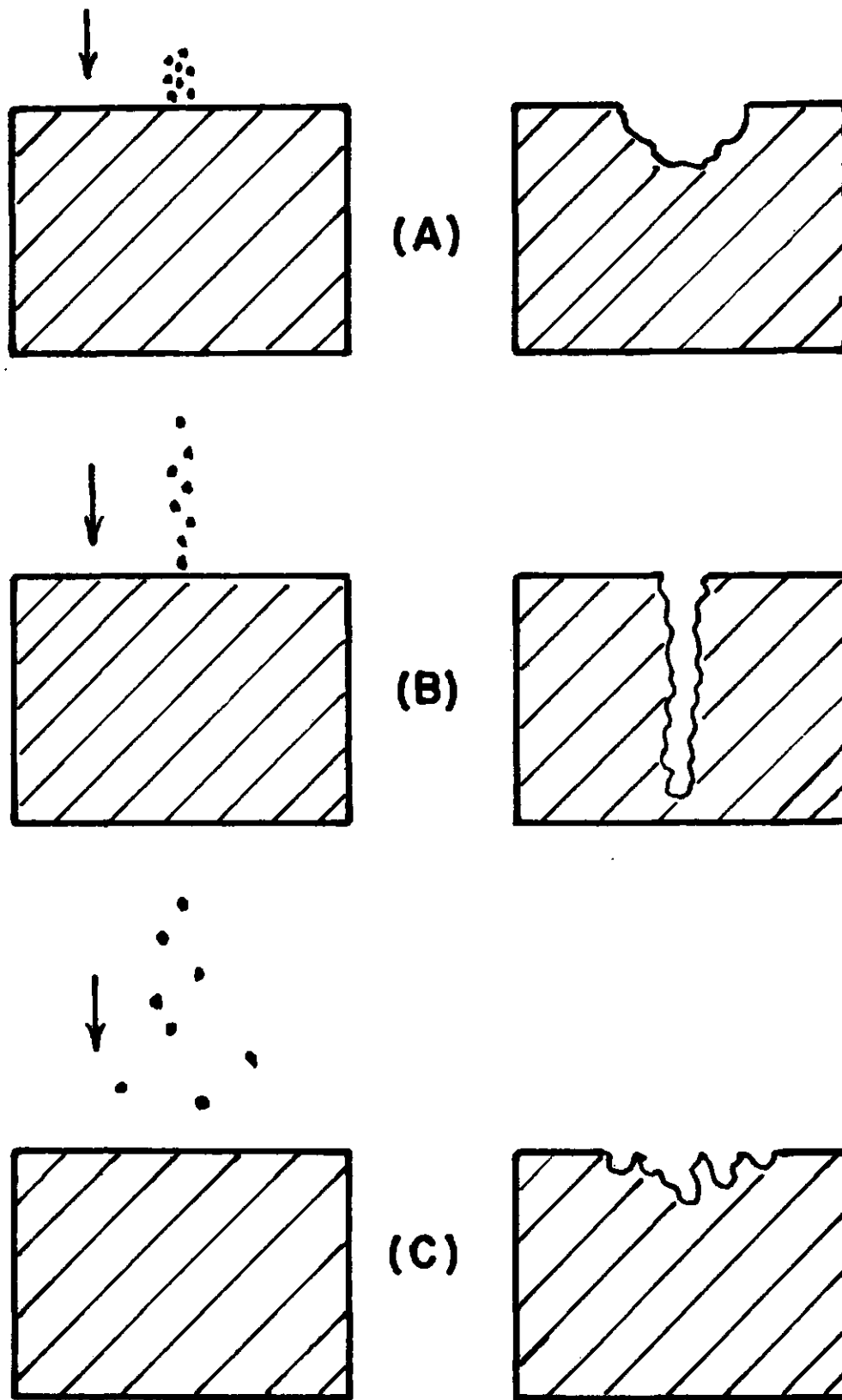
Figure 7—Diagrams that show change in penetration with standoff
(a) close standoff, (b) optimum standoff, and (c) long standoff.

First, over short distances, the fragments will lose little velocity so that the total volume of the cavity, since it depends upon the total energy of all of the fragments, ought to remain practically constant. At longer distances, it ought to decrease somewhat because of retardation of the fragments.

Second, an optimum standoff is to be expected. This optimum will occur at a distance from the charge such that the fragments are separated just enough to produce essentially individual craters, all of which lie very nearly along the same line. Beyond this optimum standoff, the fragments may be poorly collimated so that their individual penetrations will not be additive. As noted above, however, very good penetrations are sometimes observed at long standoff. This probably occurs in those rare cases in which the jet remains well collimated. The three situations, close standoff, optimum standoff, and long standoff, are illustrated schematically in Figure 7.

The fairly regular pattern of swellings and constrictions described above, and evident in Figure 6, may be explained by assuming that each bulge corresponds to the impact of an individual fragment. If this were strictly true, the bulging would be very regular; however, it is not. The non-uniformity of the bulging undoubtedly arises from the simultaneous, or near simultaneous of two or more fragments; the skewness, from fragments striking slightly off axis.

The number of bulges ought to correspond roughly to the number of fragments. Photographs of Mk 1 shaped charge jets taken with a streak camera usually exhibit some 15 to 25 traces, each one of which corresponds to a discrete fragment of appreciable size. Experiments have been carried out in which the shaped charge was moving laterally at the time of firing. Under such conditions the jet fragments produced some 15 or 20 individual small craters in a steel plate placed a short distance from the charge. The hole in Figure 6 ought, therefore, to contain some 15 to 25 bulges. Even though the hole is irregular and an accurate count is not possible, the number of observable bulges appears to be in agreement with the number expected.

The diameter of the crater that will be made by a hypervelocity fragment can be computed directly from Eq. (3) since for the shape of crater assumed the diameter and depth are numerically equal. Taking a value for c_1 of 0.29×10^{-4} in^3/ft-lb, we find that a 20,000 feet per second, 0.1 gram, steel fragment, the very approximate velocity and mass, respectively, of Mk 1 shaped charge fragments would produce a crater about 1 cm in diameter. The diameter of the crater profile, drawn in Figure 6, ranges from a minimum of 0.4 cm to a maximum of 1.7 cm. It is not unreasonable to expect that it could have been excavated by successive impacts of several fragments of the above mass and velocity.

SUMMARY

The several foregoing rather general observations suggest strongly that the cumulative effects of multiple impacts of hypervelocity fragments may play an important role in the mechanics of shaped charge penetration. The data and observations are still too meager to establish unambiguously the relative place that these multiple-fragment-impact effects must occupy in a complete treatment of shaped charge penetration. It is felt that the general method of approach is most promising and should be pursued vigorously.

TABLE I

Experimentally Determined Values of Material Displaced Per Unit of Energy.

Material	Volume displaced per unit of energy c_1 $(in^3/ft\text{-}lb \times 10^4)$	Relative penetration (Steel taken as reference)
Steel	0.23 to 0.29	1
Lead	3.31	2.3
Copper	0.55	1.3
24ST Al.	0.45	1.2

GENERAL BIBLIOGRAPHY

1. G. Birkhoff, D. P. MacDougall, E. M. Pugh and G. I. Taylor, "Explosives with Lined Cavities", J. Appl. Phys., 19 563 (1948).

2. J. S. Rinehart, "Some Observations on High Speed Impact", Pop. Astron. LVIII 458 (1950).

3. J. S. Rinehart and W. C. White, "Shapes of Craters Formed in Plaster of Paris Targets by Ultra-Speed Pellets", American J. of Phys. (In Press).

4. Felix Helie, "Traite de balistique experimentale", Dumaine, Paris (1840).

5. W. M. Evans and A. R. Ubbelohde, "Formation of Munroe Jets and Their Action on Massive Targets", Research 331 (1950).

6. W. M. Evans and A. R. Ubbelohde, "Some Kinematic Properties of Munroe Jets", Research 376 (1950).

7. R. Hill, "An Analysis of R.R.L. Experiments on Cavitation in Mild Steel", Armament Research Department Report 11/48, Theoretical Research Report 1/48, March 1948 (Confidential).

INITIAL STUDY OF THE EFFECTS OF ANNEALING   ON THE PENETRATION PERFORMANCE OF COPPER
SHAPED CHARGE LINERS

R. L. Phebus

W. O. Rassenfoss

Ordnance Engineering Laboratory, Ballistic Research Laboratories,
Aberdeen Proving Ground, Maryland

ABSTRACT

Previous studies of various metals as shaped charge liners
are summarized. The need for additional study of metallurgical
aspects of liner performance is indicated.

Copper liners of various hardness were fired to study the
effect of the variable upon stand-off-penetration curves. These
tests indicate that annealing within this recovery region or grain
growth region will improve the penetration performance of copper
liners. No improvement will be observed when copper liners are
annealed within the recrystallization region.

A proposed investigation is outlined to study the effect of
second phases and their distribution upon liner performance.

The simple hydrodynamic theory of jet formation from metal cavity liners as pro-
posed by Birkhoff, Pugh, MacDougal and Taylor (1) has considered only density as a
liner parameter. Deviations in the performance of metal cavity liners from pre-
dictions of this theory have indicated that other parameters may be involved.

The search for these other parameters has in a large measure been unsuccessful.
Other properties which have been considered are; boiling point, melting point, (2)
ductility, tensile strength, and hardness. Experiments involving studies of these
properties have not been too successful in explaining the deviations from predicted
performance.

Among the more comprehensive investigations of the performance of shaped charges
are those conducted by the DuPont Company (3)(4) using 1.63" diameter liners. These
investigations report stand-off penetration curves for liners of various cone angles
and wall thicknesses. The DuPont data will be summarized below.

Steel

Figure 1 shows the effect of various wall thicknesses on the stand-off penetration
curve for 80° drawn steel liners. These curves indicate that maximum penetration
occurs at approximately 3 to 4 diameters stand-off and that the optimum thickness for
80° drawn steel liners is approximately 0.037" - 0.048".

In Figure 2 the effect of various cone angles upon penetration is studied. These
data show that maximum penetration occurs at 2 1/2 cone diameters. Examination of
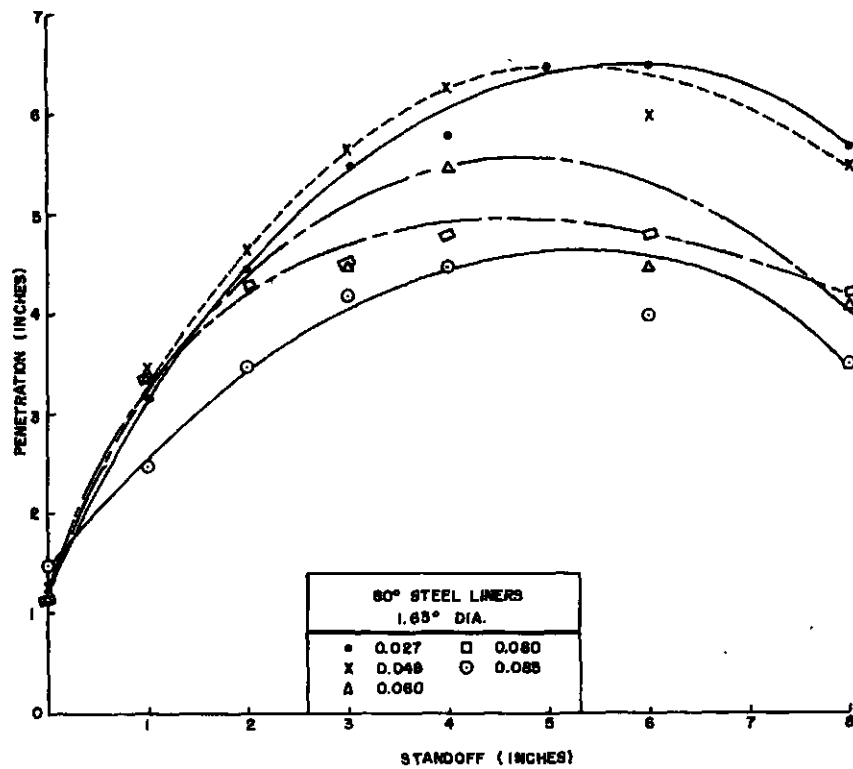
Figure 1—80° Steel liners, 1.63" dia.
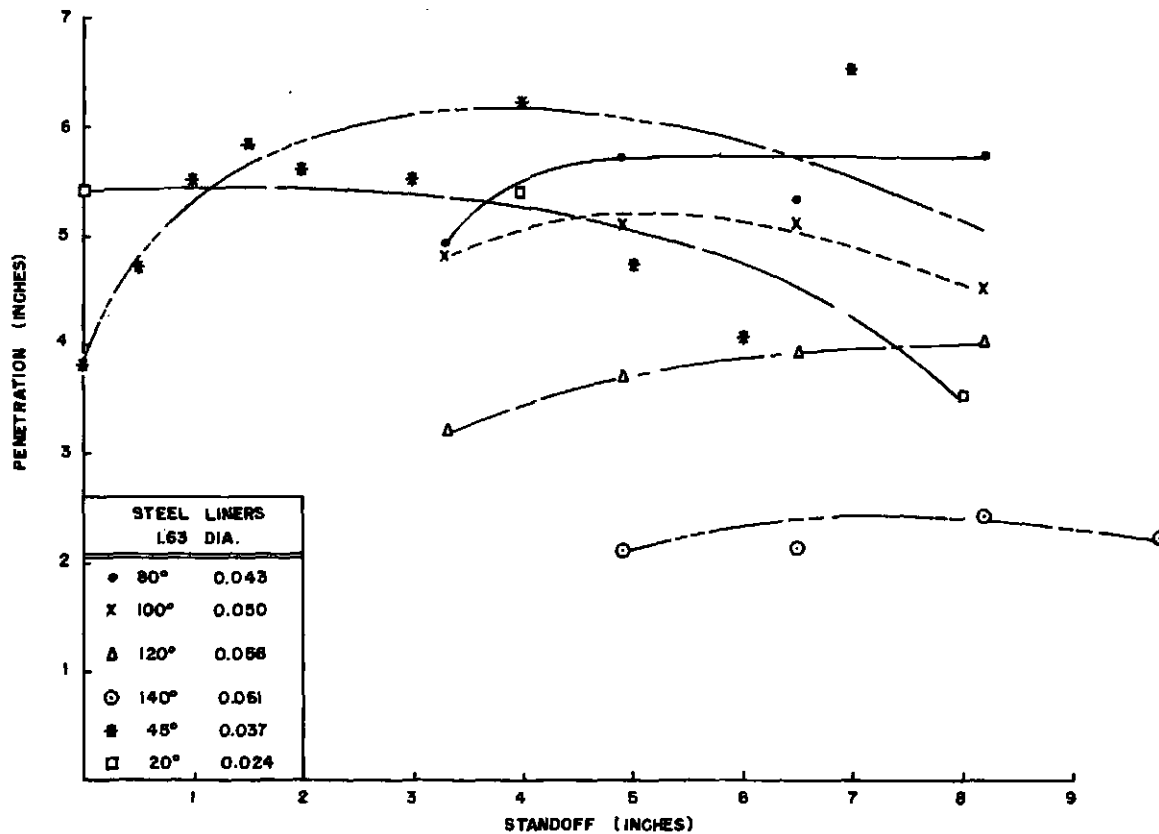
Figure 2—Steel liners, 1.63" dia.

44

these data shows that the optimum cone angle for drawn steel liners is 45°.

The curves shown in Figures 1 and 2 present the overall picture of the effects of cone angle, and wall thickness upon penetration of steel liners. However, upon closer examination these curves do not present the complete picture when observed from the standpoint of a metallurgical selection of a liner material. The first question which arises is "What steel was used"? The second question to be raised is "What is the condition of the steel?"

In answer to these questions, DuPont (4) in 1944 conducted evaluation tests of a number of deep-drawing steels used for the manufacture of metal cavity liners. Metal cavity liners, 45° cone angle, 1.63" diameter were made from various steels and tested in four conditions: as received, annealed 1000°F, annealed 1250°F, and annealed 1650°F. Liners made from Armco Irons appeared to be superior in all conditions tested. And this investigation recommended that future steel cones be equivalent of Armco Iron. These data are presented in Table I.

What is the explanation for the apparent superior performance of Armco Irons? Armco Irons are essentially single phase alloys (ferrite with iron oxide inclusions); that is, the carbon is in solution. The other materials tested are two phase alloys (ferrite and cementite); carbon is present in sufficient quantity to form the component Fe_3C which precipitates as a second phase. If the collapse of the liner, and jet formation are related to the flow characteristics of the material, then the presence of a second phase may become extremely important.

Aluminum

DuPont has investigated spun aluminum for use as 1.63" diameter liners. Figure 3 shows the effect of wall thicknesses upon the stand-off penetration curve for 45° spun aluminum liners. These data show penetration to increase with increasing stand-off, with an apparent maximum at 5 cone diameters. Also it appears that the optimum wall thickness for spun aluminum liners is approximately 0.035".

The effect of cone angle upon the stand-off penetration curve is shown in Figure 4. Examination of these data indicates that maximum penetration occurs at approximately 5 cone diameters and that the optimum cone angle for spun aluminum cones is approximately 30° - 45°.

Since aluminum is a work hardening material, it would be very interesting to study the effect of working upon the stand-off penetration curve for various cone angles and wall thicknesses. Many aluminum alloys are of the precipitation type and a study of the effect of age hardening upon penetration could also be very interesting.

Copper

These curves show that copper is superior to steel and aluminum and apparently has its maximum effect at approximately 4-1/2 cone diameters. It is interesting to note that while the penetration of aluminum continues to increase with an increase in stand-off, Figure 3 shows that even at 6 cone diameters, the maximum penetration is less than that observed for steel.

1.63" STAND-OFF 45° .025" WALL THICKNESS   TABLE I

LOT NO.	AS REC'D. AV. DEPTH (INCHES)	ANNEALED 1000° F AV. DEPTH (INCHES)	ANNEALED 1250° F AV. DEPTH (INCHES)	ANNEALED 1650° F AV. DEPTH (INCHES)	C	MN	P	S	SI	CR	NI	MATERIAL
1A	5.44	5.20	5.79	5.47	.022	.055	.003	.029	.010	.013	.029	TOCAN IRON
1B	5.60	4.82	5.42	5.49	.025	.055	.006	.027	.006	.010	.033	TOCAN IRON
2A	5.76	5.49	5.97	5.24	.081	.36	.008	.033	.011	.005	.025	RIMMED STEEL
2B	5.48	5.80	5.47	5.19	.075	.36	.008	.028	.002	.025	.024	RIMMED STEEL
4	5.38	5.57	5.45	5.81	.13	.33	.008	.034	.010	.017	.020	KILLED STEEL
5	5.85	5.94	6.10	5.20	.17	.33	.011	.036	.012	.050	.024	KILLED STEEL
6	5.93	5.85	5.72	5.63	.037	.022	.004	.026	.011	—	.025	ARMCO ENAMELING IRON
7	5.90	5.79	6.00	5.65	.030	.048	.004	.035	.010	.003	.010	ARMCO IRON
8	6.10	6.00	6.44	5.59	.038	.028	.006	.023	.022	.003	.026	ARMCO INGOT IRON
9A	6.24	5.74	5.73	5.48	.052	.46	.008	.018	—	.06	—	UNKOWN
9B	6.31	DECARBURIZED LINERS			.085	.46	.007	.018	—	.04	—	

Figure 3—45° Aluminum liners, 1.68″ dia.
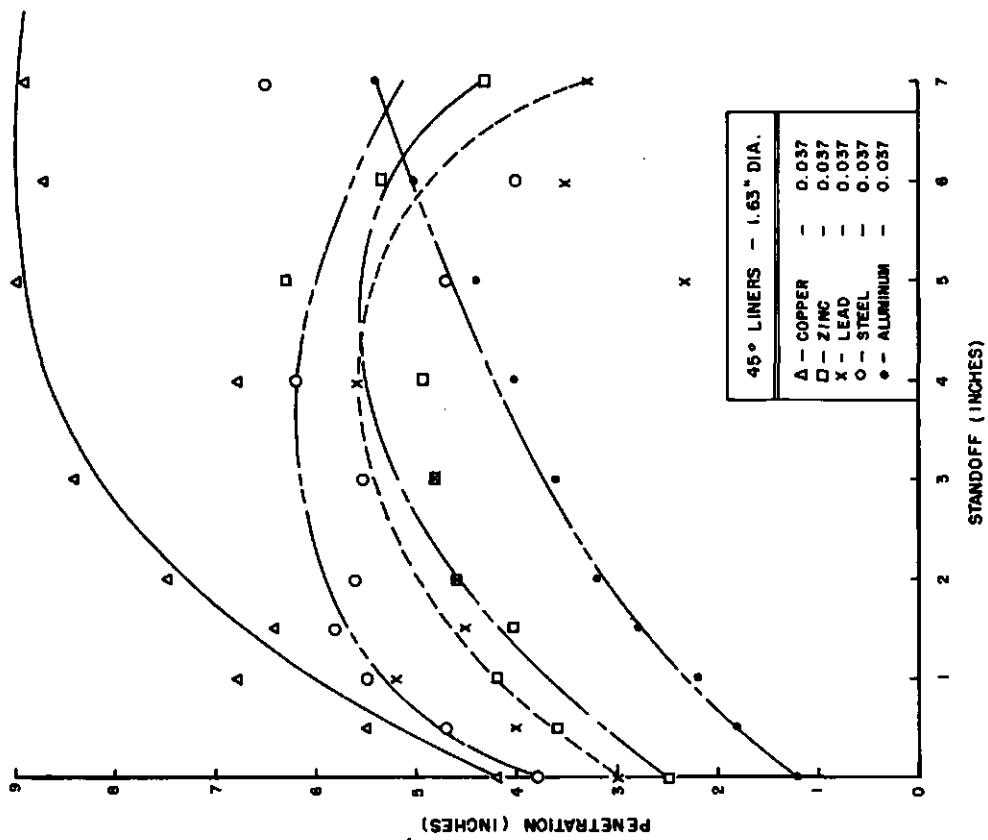
Figure 5—45° Liners, 1.63" dia.
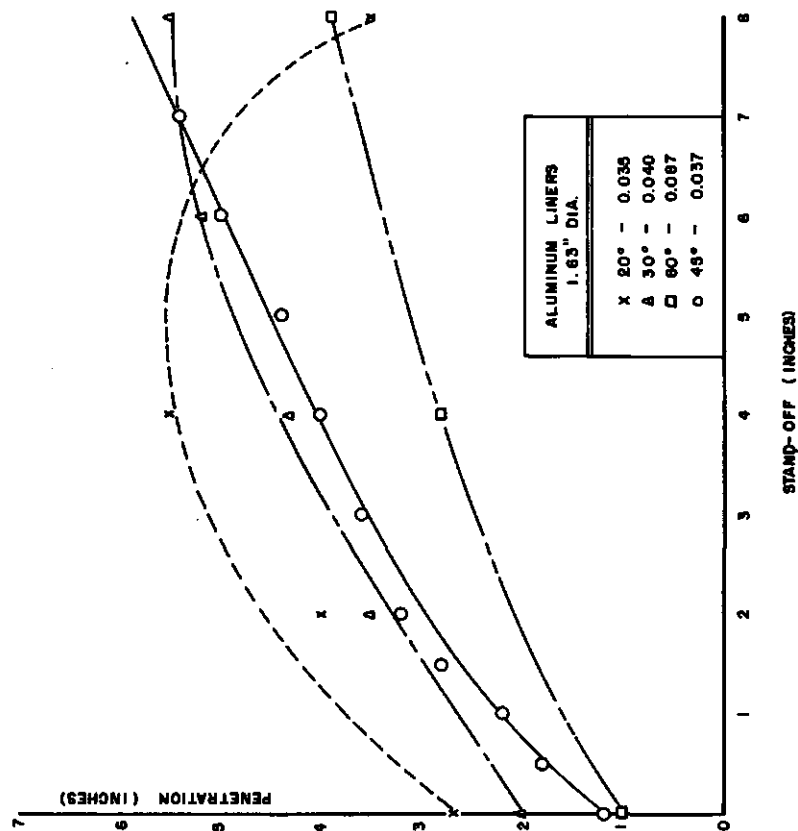
Figure 4—Aluminum liners, 1.63" dia.

TABLE II

TYPE	CONE DIA.	CONE ANGLE	WALL THICK.	STAND-OFF	PENE.	
A	2.0"	45°	0.048"	2.0"	3.90" 2.10"	TYPE A DENTAL AMALGAM
B	2.0"	45°	0.048"	2.0"	3.9" 3.8"	TYPE B 50% CD., 50% HG.

C	2.0"	45°	0.048"	2.0"	5.5"
					5.1"
						TYPE C
						    45% CD.
						    47% HG.

A	2.5"	45°	0.048"	2.0"	4.2" 4.7"	2.5% PB. 5.6% SN.
B	2.5"	45°	0.048"	2.0"	5.1" 4.9"	
C	2.5"	45°	0.048"	2.0"	4.3" 4.6"	

TABLE III

STEEL		PURE COPPER		COPPER + 0.1% AG.	
RD. #	PENETRATION MM	RD. #	PENETRATION MM	RD. #	PENETRATION MM
1	149	6	207	11	206
2	160	7	200	12	214
3	179	8	217	13	211
4	165	9	205	14	200
5	161	10	192	15	198
AV.	163		203		207

Copper is now generally accepted as the most suitable material for the manufacture of metal cavity liners. Figure 5 shows the stand-off penetration curves for various pure metals. The liners used to obtain these curves were 45" cones having a base diameter of 1.63" and a wall thickness of 0.037".

Copper, like aluminum, is a work hardening material and studies of the effects of working upon penetration may prove enlightening.

Other Material

In addition to copper, aluminum, and steel, the pure metals zinc and lead have been used as metal cavity liners. Stand-off penetration curves for these metals are shown in Figure 5. The curves for these materials show them to be inferior to copper and steel.

Various alloys have been used as liner material. Results of firing tests for these materials are recorded in Tables II and III and also in Figure 6. The penetration data for the dental amalgam and cadmium liners (5) when compared with data for the smaller diameter liners in Figure 5 show these materials to be inferior to copper and steel.

Figure 6 compares the stand-off penetration curves for copper, silver, red brass, and steel (5). Since these curves are drawn from only two points, the information presented is only qualitatively useful. It may be seen in this figure that at all stand-offs, red brass appears superior to steel, and copper and silver appear better than red brass.

Table III compares the penetration data for steel, copper, and copper - 0.1% silver (6). These data indicate that the copper-silver alloy is as good as copper. This is the first indication that alloy liners perform as well as pure metal liners. Examining the phase diagram for this system it may be shown that the solubility of silver in copper is approximately 1% at 300°C; hence, this alloy may be considered a single phase alloy. Previous tests with alloys have been conducted with compositions within the multiphase regions. Studies of alloy systems having a large solid solubility range at room temperatures should be extremely interesting. A study of such a system (copper-aluminum) is now being undertaken.

Hardness

Hardness is a variable which has been studied to see if it has an effect upon the stand-off penetration curve. In Figure 7 a portion of the stand-off penetration curves for drawn steel liners of various hardness are shown. These data show that the softer material gives deeper penetrations. Annealing of copper liners has been tried. Data have been obtained with these liners and have shown no significant improvement in penetration; however, the spread in penetration obtained appeared to be reduced when annealed liners were used.

Recently in the course of other experiments a large difference was observed between two lots of copper liners supplied by one manufacturer. These were identical in all respects with the exception of the geometry of the flange at the base. This difference
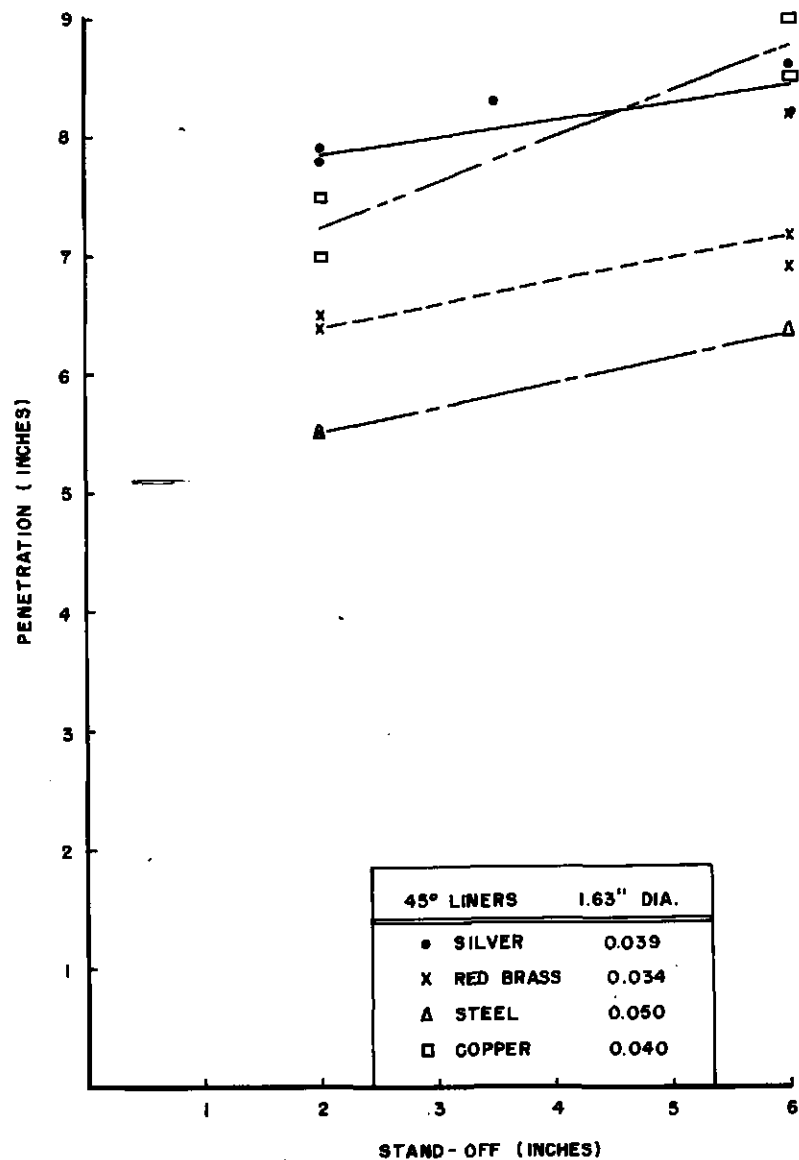
Figure 6—45° Liners, 1.63" dia.
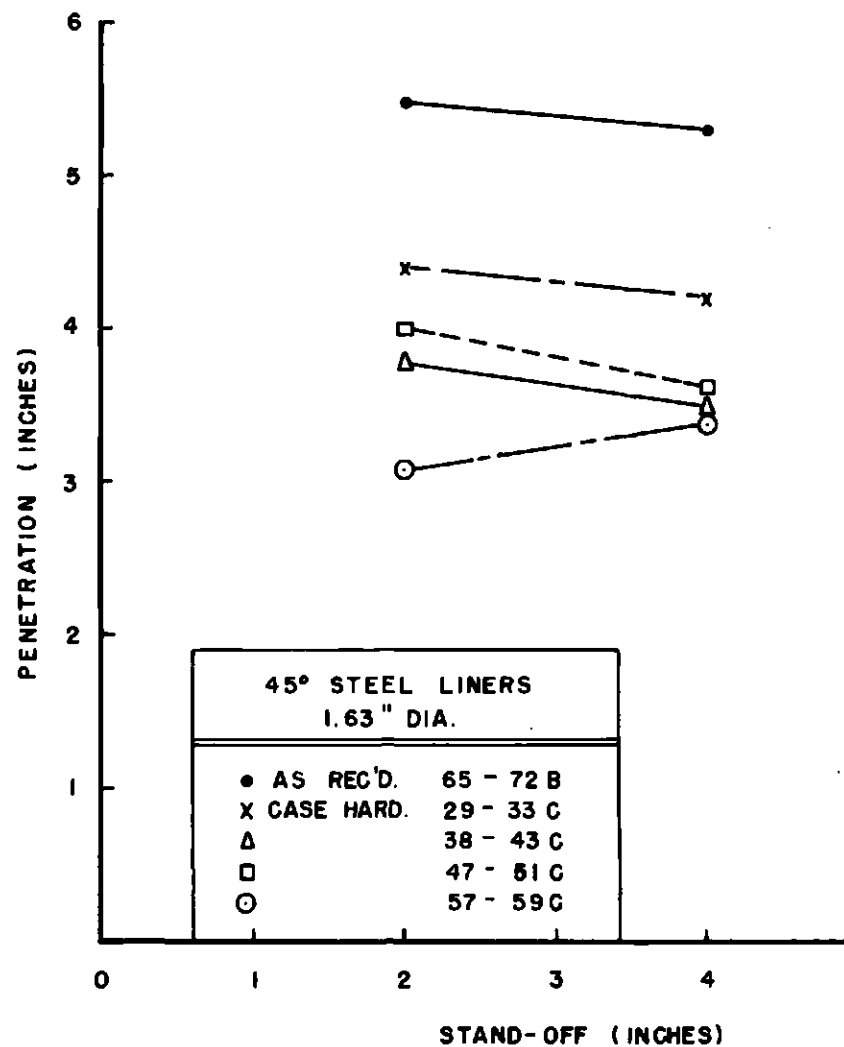
Figure 7—45° Steel liners, 1.63" dia.
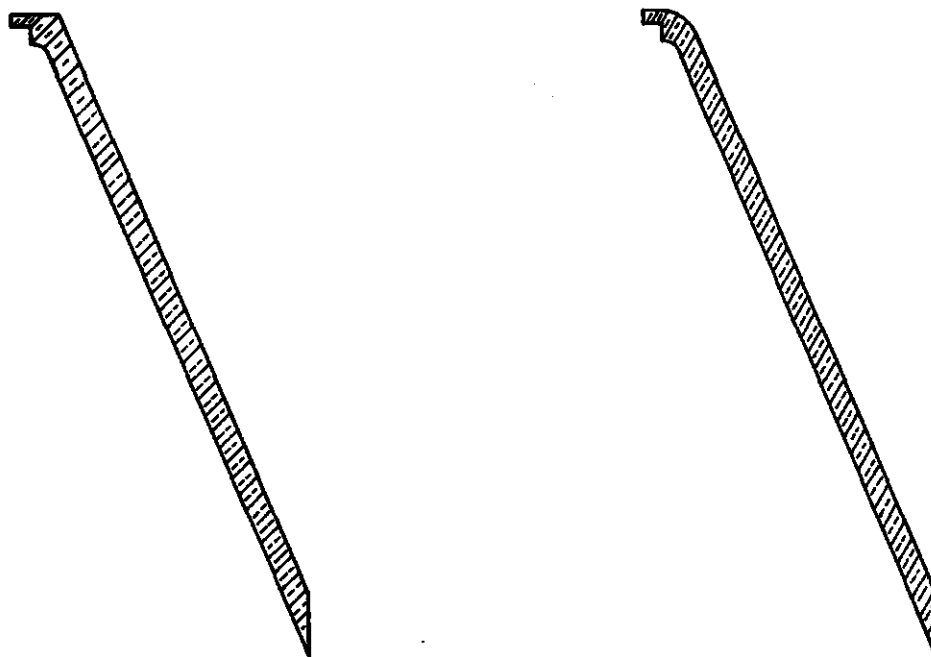
Figure 8—Sketch showing cross section of two lots of copper liners—
sharp cone shown on left—round cone on right.
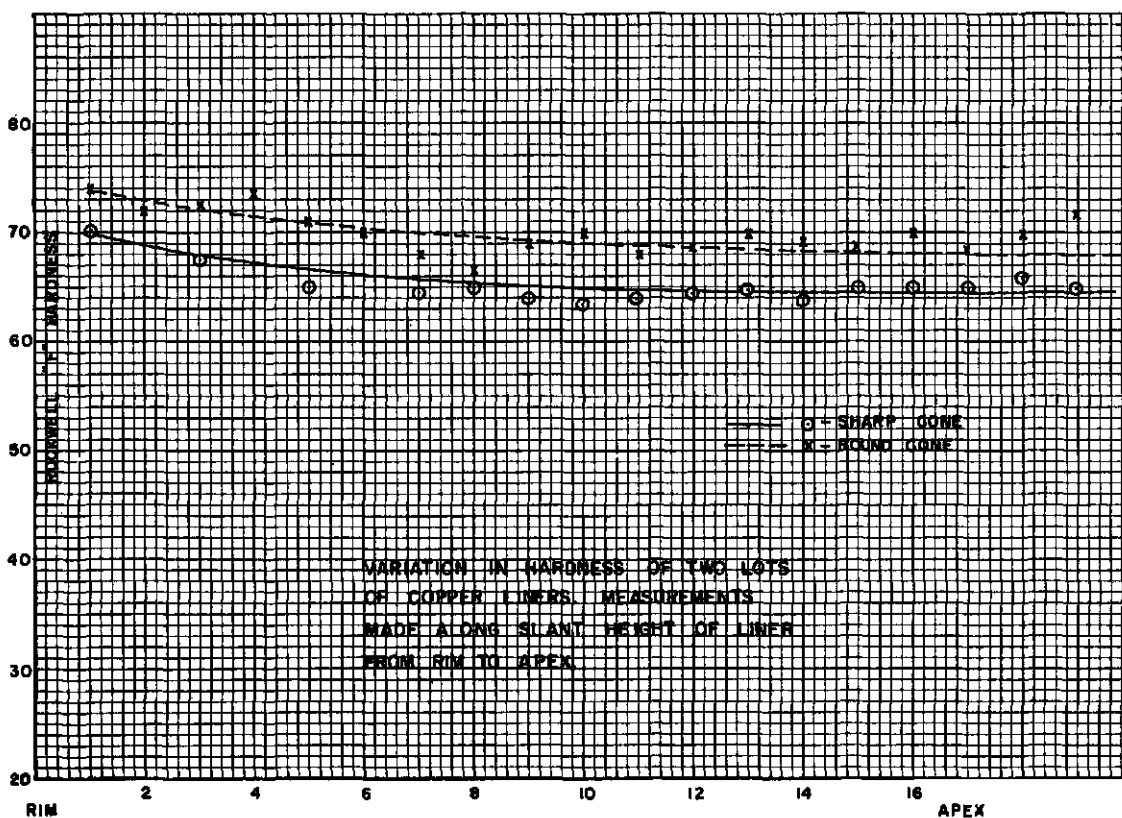
Figure 9—Variation in hardness of two lots of copper liners.   Measurements
made along slant height of liner from rim to apex.

52

in geometry is shown in Figure 8. Tests were conducted in which the geometry at the base was changed so that both lots were identical. These tests indicated that the rounding of the base could not completely account for the poorer performance.

Chemical analysis and metallographic examination revealed no outstanding differences. Standard Rockwell "F" hardness measurements revealed a five point difference in hardness between the two lots as is shown in Figure 9. While it was felt that this difference in hardness was not necessarily responsible for the large difference in performance observed, it was deemed advisable to initiate a study of the effect of hardness upon performance of copper liners.

The hardness program was conducted with 105mm 45° copper liners with spit-back tubes. In these tests, liners supplied by a contractor were heat treated to various hardness and stand-off penetration curves were determined. Figure 10 compares the softening curves for various reduction in area of cold rolled copper. Commercial cold drawn copper bar stock sufficiently large to machine 105mm liners has been subjected to approximately 10% reduction. These curves indicate that three phenomena are occurring during the annealing of copper. (1) recovery (or stress relief), (2) recrystallization and growth, and (3) grain growth. During stage 1 the working stresses are relieved with no apparent change in properties as may be shown in Figure 11. In stage 2 recrystallization occurs. In this process, the more heavily deformed grains break up into smaller new grains in a lower energy state having a somewhat preferred orientation. These newly formed grains grow at the expense of the less heavily deformed grains. During this stage, there exists a highly unstable energy state with many different orientations. This may be shown by the hardness measurements shown in Figure 12. In stage 3, migration of the grain boundaries occur as the material seeks to attain a minimum of orientations. Given the proper time and temperature conditions, it is possible to obtain a single crystal with a single preferred orientation. This uniformity of the energy condition and somewhat preferred orientation of the grains may be seen in the hardness curves of Figure 13.

By annealing at 300°F, 600°F and 900°F, liners in each of the three conditions described above were obtained.

The hardness of the liners was measured on a standard Rockwell tester using a special fixture as shown in Figure 14. Normal variation in hardness was observed in the liners heat treated at 300°F and 900°F. Erratic hardness was obtained with the liners annealed at 600°F. The explanation of this phenomenon is that during the cold drawing operation, uniform working of the bar was not accomplished. Therefore, from the curves in Figure 10 we see that in the more severely worked portion of the bar, complete recrystallization and partial grain growth have occurred, while in the less severely worked portions of the bar recovery and partial recrystallization have occurred.

Stand-off penetration curves were obtained by firing five liners from each heat treatment at each of three different stand-offs. These results were compared with data obtained with unannealed liners at the same stand-off.
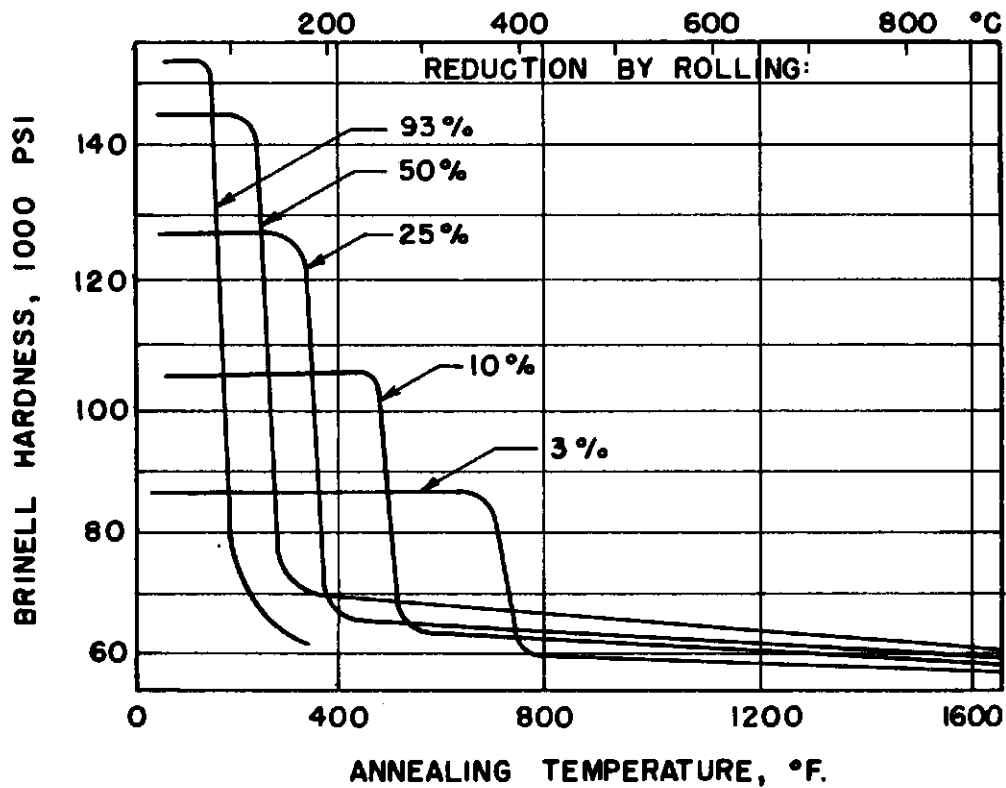
THE DECREASE IN HARDNESS PRODUCED BY THE
ANNEALING OF COPPER SHEET THAT PREVIOUSLY
RECEIVED DIFFERENT REDUCTIONS BY ROLLING.

(KOESTER)

Figure 10—The decrease in hardness produced by the annealing of copper sheet
that previously received different reductions by rolling.
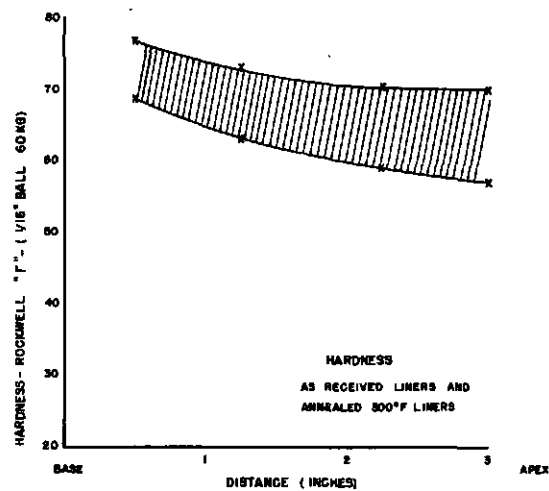
Figure 11—Hardness of as received liners
and annealed 300° F liners.
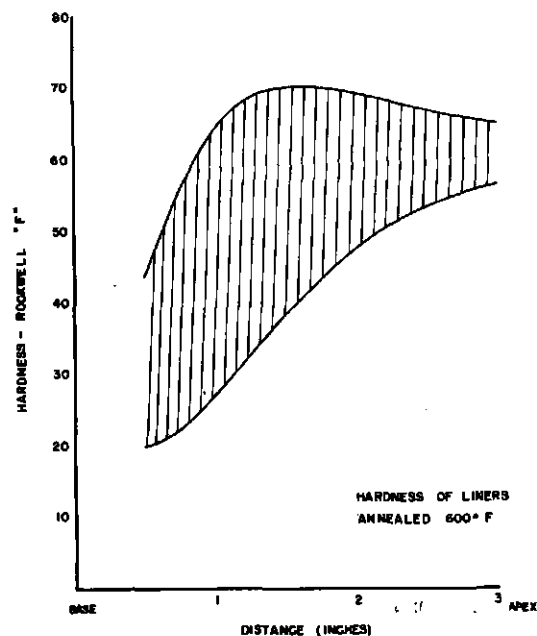
Figure 12—Hardness of liners
annealed 600° F.
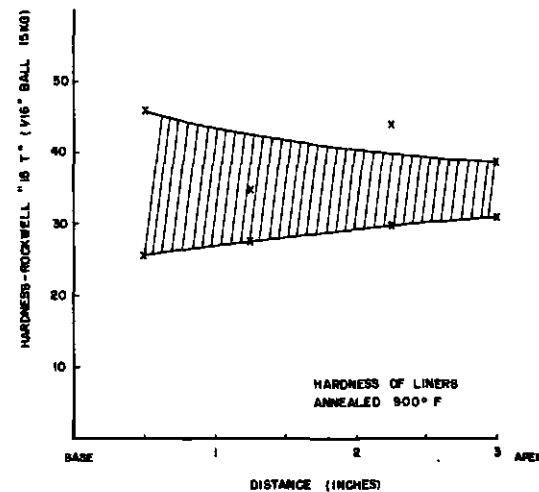
Figure 13—Hardness of liners
annealed 900° F.
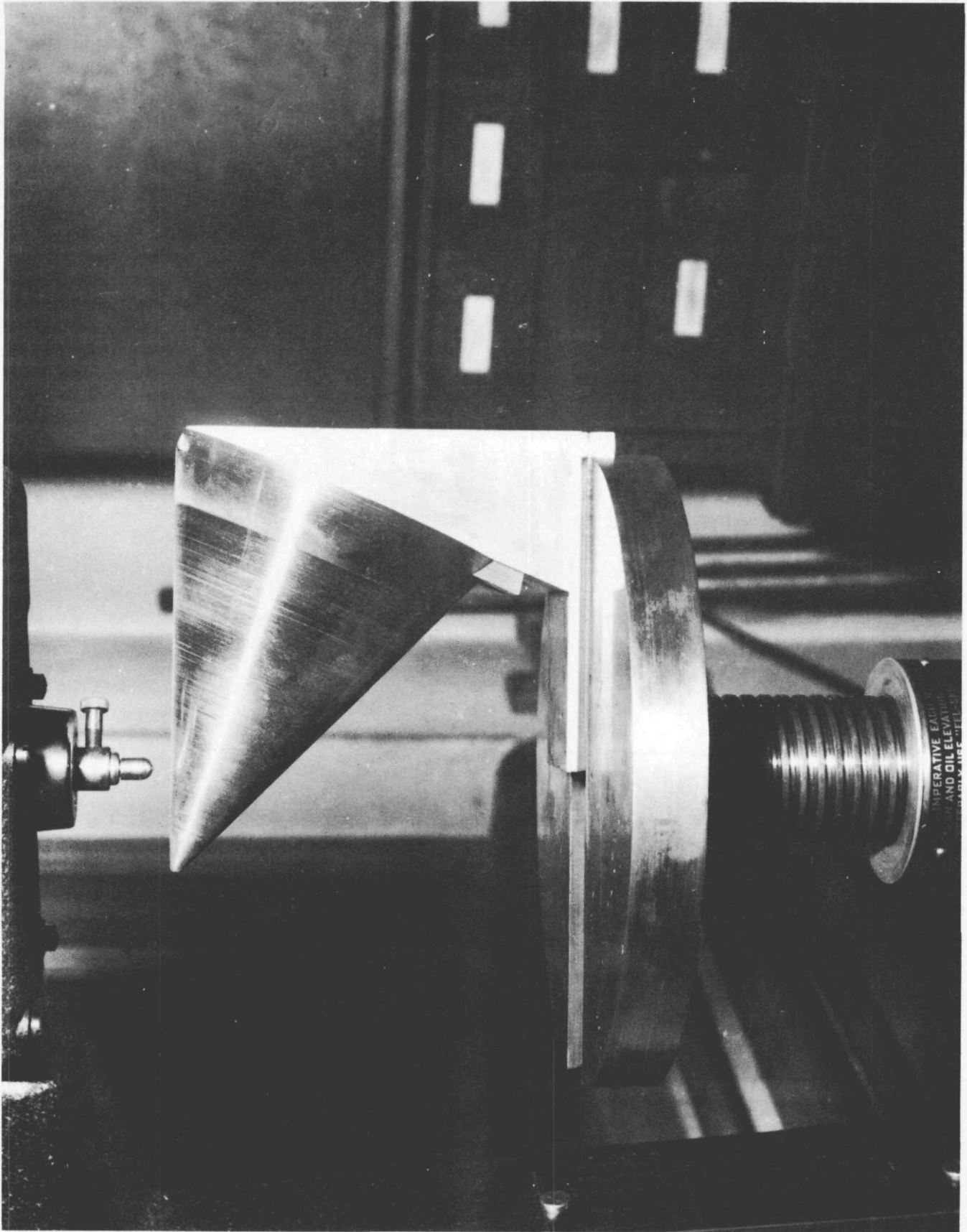
Figure 14

The results of these tests are shown in Figure 15. Here we see that when copper
is annealed either within the recovery region or the grain growth region, the stand-off
penetration curves are essentially identical. A statistical comparison of these data
with as received data reveals a significant effect of annealing. These differences in
penetration are significant at a 0.05 level, this is to say that there is only a 5%
chance that the penetration data for the annealed liners came from the same population
as the received liners.

However, we have not considered the curve for the 600°F treatment. These liners
are expected to be in some intermediate state of strain. In this region, there exists
areas of high strain which attempt to reach a lower level of strain. These nuclie cause
the original grain to break up and smaller grains are formed which grow at the expense
of the larger grains until the material has completely recrystallized after which normal
grain growth begins. The liners treated at 600°F were in this state of unbalanced
stress, and the poorer results are for the present attributed to this condition.

We cautiously conclude that if work hardened copper liners are annealed within the
recovery region or grain growth region (which for practical purposes are strain-free
regions) an improvement in penetration will be obtained. If the liners are annealed
within the recrystallization region, no improvement in penetration appears to be ob-
served. These results need further verification before they can be considered con-
clusive.

Multi-Phase Alloy

A systematic metallurgical investigation to study the effects of second phases
and their distribution upon liner performance is being conducted. The copper-aluminum
system was selected for this study. In Figure 16 is shown the copper rich side of the
copper-aluminum phase diagram. From this diagram we see that with a few compositions
it is possible to study several single phase regions and several combinations of two
phase regions. In these studies sufficient liners of each phase combination will be
obtained so that a stand-off penetration curve may be plotted.

Conclusions

It seems likely at this stage that any metalurgical investigation of material for
use as metal cavity liners should consider the following as variables; (1) Crystal
structure, inasmuch as various structures lend themselves more readily to slip or flow.
(2) The degree of cold work, since this has an effect upon the yield strength of the
metal. This is particularly true for the work hardening metals such as copper and
aluminum. Grain size might also be considered as the flow characteristics of some
metals at various temperatures are influenced by grain size. The presence of two or
more phases should be considered as it is known that the presence of a second phase
often hinders the flow properties of metals. The usual mechanical properties such as
tensile strength, hardness, and ductility are inter-related and may be varied within
limits; however, these properties themselves are dependent upon the fundamental prop-
erties; crystal structure, and the number of phases present, and they also depend on
the degree of working.

STAND-OFF (INCHES)

PENETRATION (INCHES)

ANNEALED 300° F

ANNEALED 600° F

ANNEALED 900° F

AS RECEIVED
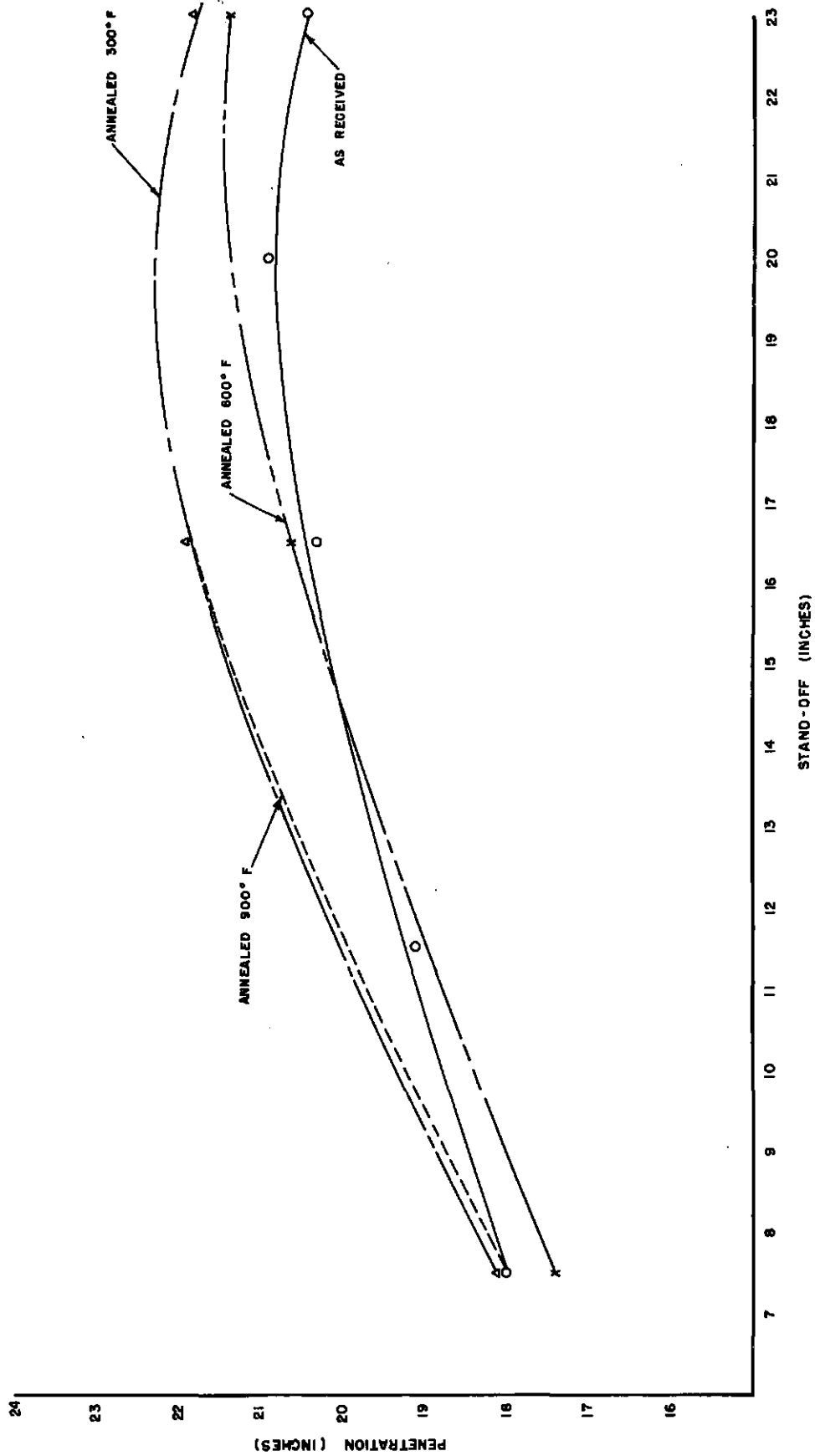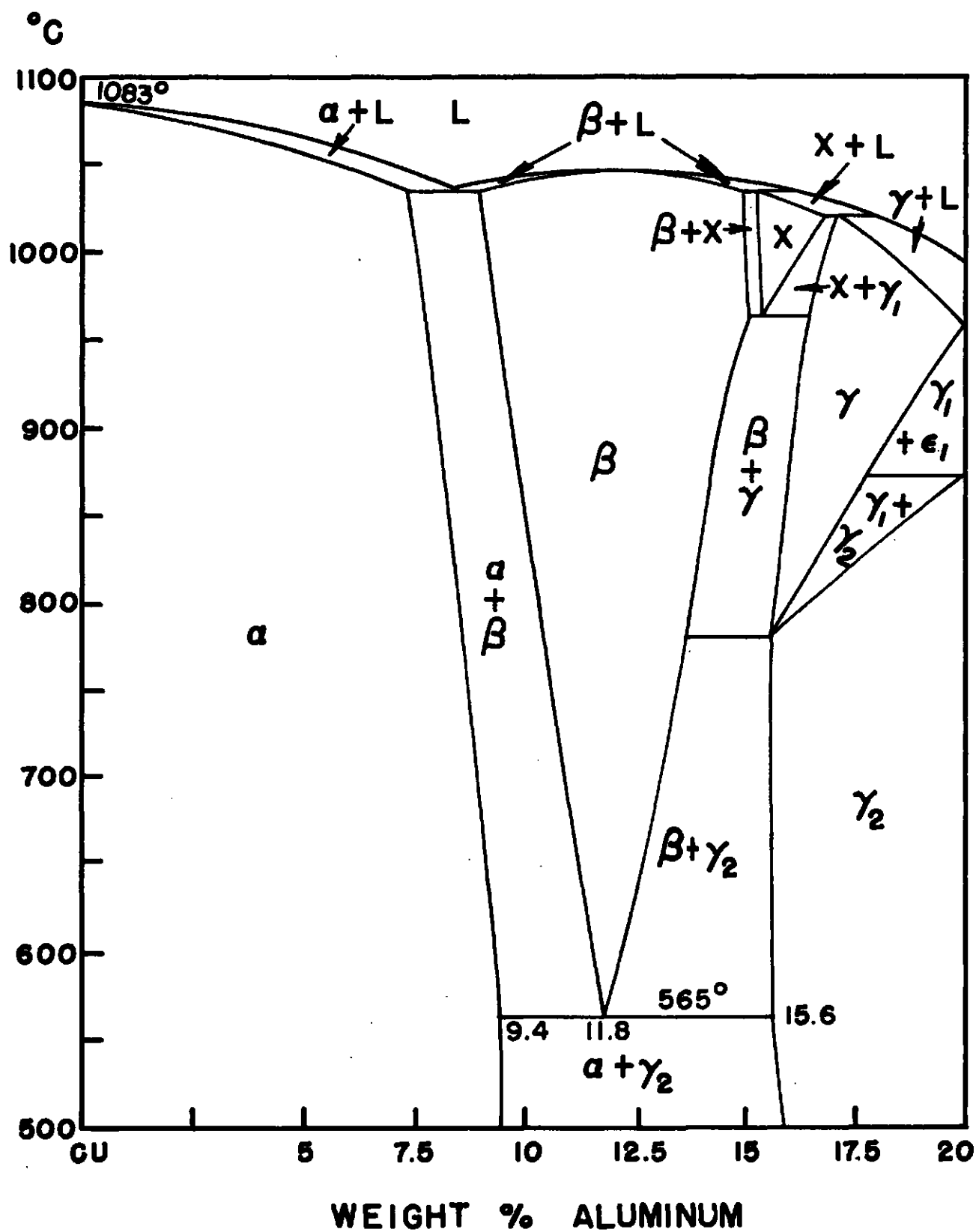
Figure 15

Figure 16

REFERENCES

1. Birkhoff, G; McDougall, D. P.; Pugh, E. M. and Taylor, G. I. - "Explosives with Liner Cavities", J. App. Phy. 19, 1948, pp 563-582.

2. Lennard-Jones, J.E.; and Devonshire, A. F. - "Some Notes on the Theory of Hollow Charges", A. C. 2934.

3. DuPont - "Investigation of Cavity Effect, Final Report", 18 Sept. 1943.

4. DuPont - "Evaluation of Deep Drawing Steels for Manufacture of Purity Charge Cones", 6 Dec. 1944.

5. National Defense Research Council - "Interim Report on Shaped Charges", 1945 NDRC/Dir. 8 SC-1-SC-21.

6. Nash, T. and Evans, W. M. - "A Comparison Between Steel, Pure Copper, and Copper/Silver Alloy Conical Liners for Hollow Charges", ARD/Expl. 406/46.

GENERALIZATIONS CONCERNING THE MOTION OF A THIN SHAPED CHARGE LINER WITH AN ARBITRARY INITIAL CONTOUR

G. E. Hudson[+]

C. Gardner

New York University, New York, N. Y.

[+]Portions of this report were presented at a Symposium on Shaped Charges at Aberdeen by G. E. Hudson; the report was written by Hudson whereas much of the mathematical background for the theoretical work herein discussed grew out of conversations between Hudson and other member of the Institute for Mathematics and Mechanics, but particularly between Hudson and Gardner.

ABSTRACT

Upon assuming a thin liner whose particles do not exert any forces on one another, and upon treating it as an incompressible fluid during its motion, general equations of motion and continuity are derived. It is shown that these are equivalent to a Schrodinger time-dependent type of equation with space and time variables interchanged. The impingement and subsequent extrusion of this liner at an arbitrarily moving and oriented surface element are investigated.

This formulation suggests several new problems, experimental, theoretical, and mathematical, as well as the importance of further investigation of some already considered. In the latter class are the problems of the interaction of simple waves of finite amplitude, and the effects of compressibility in the liner. Friedrichs, Keller and A. Lax, and then Touart have considered the possibility of rarefaction and compression shocks in the liner, and have thus justified the assumption by G. I. Taylor that the liner acts as a continuously turning stream of non-interacting incompressible fluid particles. Touart and Friedrichs have also shown that the observed mass distribution in the jet can be accounted for by the continuing pressure exerted by the burnt explosive on the liner as it collapses. In addition, Touart has shown that the probable effect of the rarefaction wave in the burnt explosive as it expands into the atmosphere is the observed decrease in velocity from head to tail of the jet. Thus the external shaping of the explosive is important in stand-off effects.

61

I. INTRODUCTION

The theories of the liner collapse and jet extrusion processes which have been presented in the past (1) (2) (3), all have the common feature of considering the processes as steady state ones when viewed from the proper frames of reference.* However, it is known that the actual processes are not steady ones -- and that the effect of the unsteadiness is paramount in determining such important phenomena as the mass distribution and velocity distribution in the jet. In this paper an attempt is made to reformulate the problem to include non-steady motions in a logical manner.

For orientation purposes, let us review briefly some of the points of view in the previous attacks on the problem.

The theory of Birkhoff et al, avoids the difficult problem of determining the pressure on the collapsing liner by means of the assumptions of an impulsive velocity for each liner particle, produced as the detonation front sweeps by, and thereafter a uniform rectilinear motion independent of the other particles, until extrusion takes place. In this way, questions of material strength are also avoided almost completely and the mathematical theory can be given a very simple form indeed. These considerations are considerably generalized by the work of Friedrichs, Keller, A. Lax, and Touart. By assuming a steady liner motion in the "detonation frame", the expansion of the gases from the burnt explosive against the collapsing liner is treated as a combination shock and simple wave problem (in two dimensions) so that estimates of the continuing pressures on the liner can be made. It is clear that the assumption of a steady motion precludes the exact treatment of the case with cylindrical symmetry, and avoids the problems connected with the interaction of the rarefaction wave, due to the expansion of the explosive into the external atmosphere, with the expansion (and compression shock) wave spreading from the liner.* In this theory, the effect of wave motion in the liner material itself is considered, and is shown to lead to a justification of G. I. Taylor's assumption that the liner particles do not interact with one another.

In the present paper we are naturally influenced strongly by the above investigations, both by their achievements as well as their shortcomings. To aid in accomplishing our purposes here; namely, to include non-steady motions, and to make a beginning in the study of the stability of shaped charge phenomena, we shall introduce certain compromises and limitations: the liner will be treated as an infinitesimally thin, continuous collection of particles, as in reference (2), whose strength properties, considered to a certain extent in reference (1), can be neglected. Thus the importance of thickness and strength of materials both in experiment and in making a proper theoretical formulation of the problem will be emphasized in a negative way. The problem of determining the pressure exerted by the burnt gases (and the atmosphere) is not considered here directly, as it is in reference (1), but the presence of such

---

* C. Touart and Friedrichs have generalized the Friedrichs theory slightly by introducing "quasi-steady state processes" but the error introduced by such a treatment has not been estimated. Pugh and Rostoker have also made similar generalizations.

continuing pressures is taken into account. The formulation presented herein is limited to a consideration of two-dimensional motions (generalized wedge-shaped charges) only; it is possible however to extend it, rather easily, to include cylindrically symmetric motion.

We have been motivated in this formulation by the desire for mathematical simplicity and by the possibility of deriving descriptions of liner motions more nearly agreeing with observations. Yet simplicity, generality, or agreement with observations are not the only motivating influences. It is felt that by pursuing the problem in the direction we have taken, important engineering questions may ultimately be answered. In this category is the question, "Given a jet having certain characteristics (e.g., a certain velocity distribution, or density distribution), how may one obtain an initial liner and charge configuration that would produce this jet?" Another important question is, "If the initial configuration is altered slightly, what will the effect be on the jet?"; in this paper we shall be much concerned with an initial exploration of this phase of the problem.

II. DERIVATION OF THE EQUATIONS OF MOTION OF A LINER SECTION

A. Coordinates and Initial Conditions

Consider a shaped-charge and liner configuration which is perfectly uniform in one direction (z). In a plane $(z = 0)$ which is perpendicular to the direction of uniformity introduce rectangular Cartesian axes (x,y). Consider a section of the liner of unit width included between the planes $z = 0$ and $z = 1$, and the motion of the plane trace of this section in the plane $z = 0$. This trace may be considered to be made up of a continuous one-dimensional array of mass particles having a linear density distribution $\gamma(x,y)$ (mass of section per unit length along the trace).

Let "a" be the Lagrange coordinate of the particles of the trace; it is defined as the mass of the section measured from one end of its trace $(a = 0)$ up to the particle in question. Then

$$a = \int \gamma \, ds \tag{1}$$

where $ds = \sqrt{dx^2 + dy^2}$ is the element of arc length, and the integral is taken from one end of the trace of the liner section to the particle in question. We shall always assume that the position of each point mass particle is completely determined by a specification of the Lagrange coordinate "a" and the time "t"; this is what we mean by stating that the liner is infinitesimally thin. If we denote the position vector to a particle of the liner by the complex number

$$\psi = x + iy, \tag{2}$$

then evidently a choice of the complex-valued function $\psi(a,t)$ completely specifies a motion of the liner trace.

It is of interest to note, as in Figure 1, that the argument, θ say, of ψ_a* specifies the angle the trace at each point makes with the x-direction, while its modulus

$$\left| \psi_a \right| = \frac{ds}{da}$$

is the specific length of the liner section (length per unit mass).

Let us suppose that a pressure difference, acts across each element of the section at time t; this pressure difference, multiplied by the unit section width in the z-direction will be denoted by p; $|p|$ is the magnitude of the force per unit length (linear pressure) acting on each arc element ds of the trace. Clearly the force acting on such a trace element is perpendicular to it; if p is > 0 when the force is in the direction specified by a counter-clockwise rotation of 90° (i.e., multiplication by i) from the direction of increasing values of a, then the force on an element may be denoted by the complex number

$$ie^{i\theta} p \, ds.$$

This must equal the mass, da, of the element times its acceleration, according to Newton. Dividing this equality by da we see that

$$\psi_{tt} = i p \, \psi_a \tag{3}$$

is the partial differential equation of motion of linear trace elements.

In this equation, p would ordinarily be determined in terms of the pressure exerted by the detonation products next to the element in question at time t; that is, we should in general regard p as a real-valued function of ψ, its derivatives, and t. It should be pointed out, in passing, that (3) has the form of Schrodinger's time dependent equation, with, however, a zero potential energy, the time and space variables interchanged, and a variable ratio of Planck's constant to the mass of the fundamental particle. As we shall see immediately, the type of initial-value problem which we consider in this report also differs fundamentally from that considered in the quantum-mechanical case.

At time t = 0, the liner has some shape and some velocity distribution specified by

$$\psi(a,0) = X(a) + iY(a)$$
$$\psi_t(a,0) = U(a) + iV(a) \tag{4}$$

Until the pressure function p is specified it is clear that the problem is not yet completely formulated. However there are certain cases of interest, some of which have been considered in the past, where we may specify p. In this way we see that the "Cauchy" problem (3) and (4) leads to very interesting results, which may be indicative of certain important practical conclusions.

---

* Subscripts indicate partial differentiation except where otherwise specified.
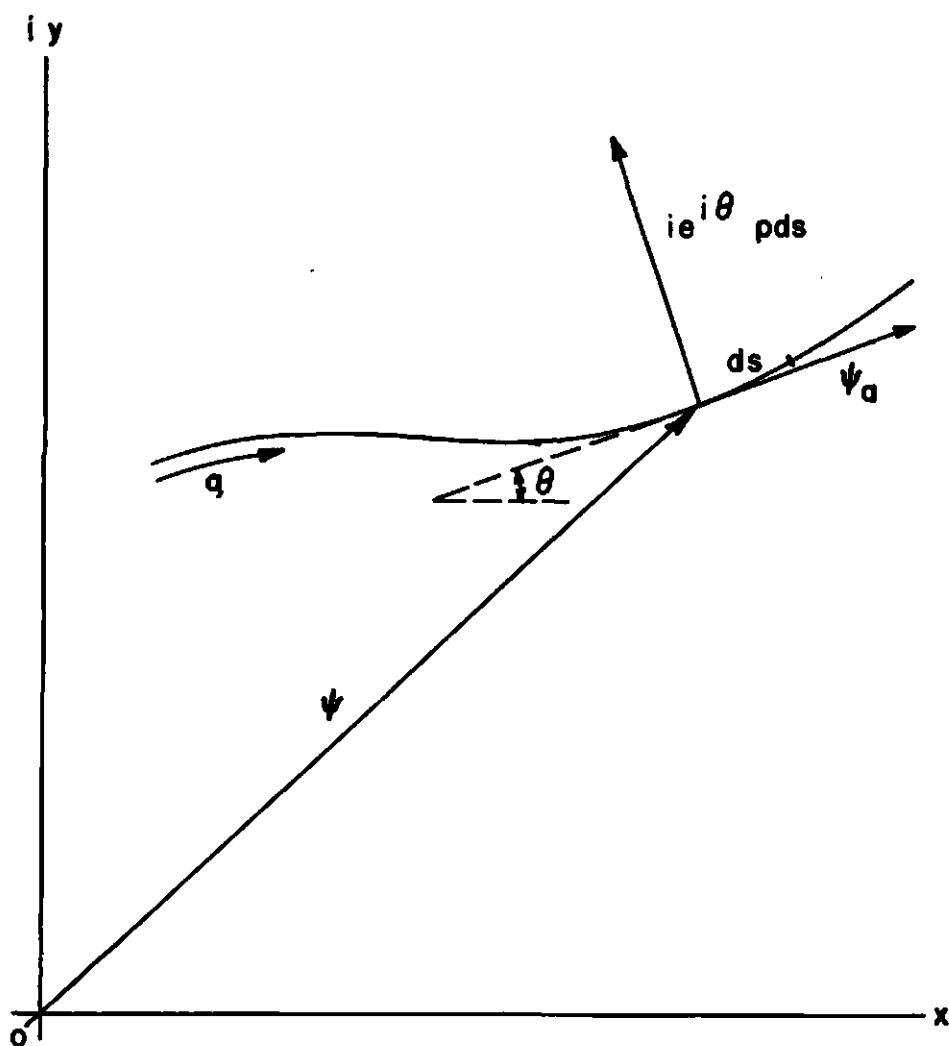
Figure 1—Representation of the motion of a liner by the motion of
its trace in a complex plane.

III. SOLUTIONS

It is possible to "cook up" a wide variety of "solutions" of the system of equations (3), (4), corresponding to various choices of the pressure function p, and the initial data. In this way one may hope to describe motions which are close to physically observable ones. We shall consider only those functions ψ to be solutions which are continuous everywhere, which have derivatives ψ_t, ψ_{tt}, and ψ_a, and satisfy equations (3) and (4) except on a denumerable set of points $\{a_i, t_i\}$.

A. Elementary Solutions

Case 1. <u>p = 0</u> (rectilinear particle motion)

In this case the solution is obviously:

$$\psi(a,t) = \psi(a,T) + \psi_t(a,T)(t - T) \tag{5}$$

where the data $\psi(a,T)$, $\psi_t(a,T)$ are considered to be supplied at time T.

Case 2. <u>p = constant</u> (central elliptic motion about the origin)

Let the initial data be

$$\begin{cases} \psi(a,0) = R e^{2\pi i \frac{a}{m}}, \quad (0 \le a \le m) \\ \psi_t(a,0) = i\omega R e^{2\pi i \frac{a}{m}} \end{cases}$$

where m is the mass of the section; hence the liner particles form a closed circle of radius R and are moving initially with uniform angular speed ω about the origin, tangentially to the circle. The solution satisfying these conditions is,

$$\psi(a,t) = R \left(\cos t \sqrt{\frac{2\pi p}{m}} + i\omega \sqrt{\frac{m}{2\pi p}} \sin t \sqrt{\frac{2\pi p}{m}}\right) e^{2\pi i \frac{a}{m}} \tag{6}$$

which represents a circle of particles whose radius oscillates from R to $R\omega\sqrt{\frac{m}{2\pi p}}$ and back with a period one half as long as the period, $\sqrt{\frac{2\pi m}{p}}$, which it takes a particle to make a complete elliptical circuit about the origin. If $\omega^2 = 2\pi\frac{p}{m}$, the solution is

$$\psi = R e^{i(\omega t + 2\pi\frac{a}{m})} \tag{6a}$$

which represents a uniformly rotating ring of particles having a constant angular velocity ω and radius R. If p is negative 2π is changed to -2π, then the order in which the particles are arranged in the circle is reversed, the pressure p which formerly was exerted inward is now outward according to our convention, and the motion is no longer periodic; this is borne out by noting that the trigonometric functions in (6) become hyperbolic.

66

Case 3. p = constant (analytic initial data)

The above solutions are particular cases of the somewhat more general one in which the initial data have derivatives of all orders, which are sufficiently bounded. Then an expansion in a power series in t yields the symbolic form

$$\psi(a,t) = (\cosh t \sqrt{ipD_a})\ \psi(a,0) + \left(\frac{\sinh t \sqrt{ipD_a}}{\sqrt{ipD_a}}\right)\ \psi_t(a,0) \tag{7}$$

involving the hyperbolic operators containing the differential operator, $D_a \equiv \frac{d}{da}$, in their arguments.

It will become evident later that, unless the initial data belong to some such special class of functions as the analytic one considered above, there actually will exist no solution for constant p values. Physically, this means that a liner with the characteristics we have assumed would almost always fly to pieces, except in certain cases which are actually in practice unrealizable. This fact emphasizes the statement that the present theory is by no means a complete one -- it must be supplemented by further investigations of the dependence of p on the time and liner position and shape, and of the strength characteristics of the liner. Nevertheless, as we shall see, the formulation may be used heuristically to generate solutions which describe motions approximating in some degree those actually observed.

Case 4. p = f(a)P (analytic initial data)

In case the pressure depends analytically on the mass parameter "a" only, and the initial data are analytic, the problem may be reduced to the previous case. For, set

$$b = \int^a \frac{da}{f(a)},\ \text{so that}\ a = a(b) \tag{8a}$$

Then we must solve

$$\psi_{tt} = iP\ \psi_b \tag{8b}$$

subject to the given initial data

$$\psi(a(b),0),\qquad \psi_t(a(b),0) \tag{8c}$$

B. One Dimensional Motion

If the velocity ψ_t and the tangent ψ_a are proportional, with a real proportionality factor $\lambda(a,t)$, then all particle trajectories coincide with a single liner trace; the motion is not necessarily stationary, although this case is included. In particular we shall see that the elementary solution given by Birkhoff, et al, appears as a special case of this kind of motion.

Roughly speaking, the specialization

$$\psi_a = \lambda(a,t)\ \psi_t \tag{9}$$

67

implies that one may have given only a limited portion of the data arbitrarily, such as the initial distribution of the liner trace and the <u>initial</u> pressure distribution -- then all other quantities will be determined. Let us see how this comes about.

If one introduces (9) into equation (3), it is easy to deduce that, because of the reality of p and λ,

$$\begin{cases} \text{(a)} & \lambda_{tt} = 0 \\ \text{(b)} & (p\lambda^2)_t = (p\lambda)_a \end{cases} \tag{10}$$

provided the trivial case in which the initial velocity distribution vanishes is excluded.

Equation (10a) shows that λ must be a linear function of "t" with coefficients dependent on "a". If one puts

$$h_t = p\lambda$$

$$h_a = p\lambda^2$$

then (10b) is satisfied and h must satisfy

$$h_a = \lambda h_t \tag{10c}$$

an equation whose characteristics (along which h is constant) are the same as those of (9). If $g(a,t) = $ const. is the equation of any characteristic, we see that we may take

$$\begin{cases} g(a,t) = R(a) + S(a)t \\ \lambda(a,t) = \dfrac{R'(a) + S'(a)t}{S(a)} = \dfrac{g_a}{g_t} \end{cases} \tag{11}$$

while

where $R(a)$ and $S(a)$ are arbitrary functions of "a" (to be determined perhaps from initial conditions). Then since h is an arbitrary function of g, insofar as equation (10c) is concerned, we see that the pressure p must have the form

$$p(a,t) = \frac{g_t^2}{g_a} h'(g)$$

or:

$$p(a,t) = \frac{S^2(a)}{R'(a) + S'(a)t} h'(R(a) + S(a)t) \tag{12}$$

where h' denotes the derivative of h with respect to its argument "g". It is easy to show that initially we must have

$$\begin{cases} \psi_t(a,0) = S(a)e^{ih(R)} \\ \psi(a,0) = \int_0^a R'(a)e^{ih(R)}da + X(0) + iY(0) \end{cases} \tag{13}$$

68

whereas at any later time the solution ψ is simply written in either of the equivalent forms as

$$\psi(a,t) = \tag{14}$$

$$\begin{cases} \int_0^a (R'(a) + S'(a)t)e^{ih(g)}da + \int_0^t S(0)e^{ih(R(0) + S(0)t)}dt + X(0) + iY(0) \\ \int_0^a R'(a)e^{ih(R)}da + \int_0^t S(a)e^{ih(g)}dt + X(0) + iY(0) \end{cases}$$

It is quite clear now, that an arbitrary choice of the functions R, S, h (and the constant X(0) + iY(0)) completely characterizes one dimensional motion (and the pressure acting!). On the other hand, one might choose a pressure function in the form of (12) which would similarly serve to determine the appropriate initial conditions, and the motion, up to a multiplicative constant and an additive constant. Or we might have given $\psi(a,0)$, in which case R'(a) (and hence R(a) or a(R)) and then h(R(a)) as a function of "a" (and hence h as a function of R) will be determined (except for a constant added to R). Then if either p(a,0) or the initial speed distribution S(a) are given, all other quantities may be found. Examples of "solutions"* of these kinds are given in the next section.

C. Composite Solutions

We are now in a position to write down several solutions which may correspond to some extend to the actual motion of a collapsing shaped charge liner. Their chief interest perhaps is that they may serve to collate certain experimental data. One of these turns out to be the well-known Birkhoff approximation in which the particles of the liner in succession receive impulsive accelerations by a very large pressure pulse (detonation wave) acting for a very short time.

Case 1. Birkhoff motion

Let us assume that in a frame of reference whose origin coincides with the detonation front at the point where it meets the liner, the collapse process appears as a steady one, with the liner material of linear density γ, flowing into the origin at a speed $S = \dfrac{U}{\cos \alpha}$, where U is the detonation front velocity, α is the angle the liner makes (at the origin) with the positive x-axis (half-wedge angle).

The liner particles change direction of motion as they are accelerated by the pressure pulse, which we shall treat as proportional to a Dirac δ-function whose peak is situated at the origin.

If at time t = o, particle a = o was at the origin, then at time

$$t = \frac{a}{\gamma S} \tag{15a}$$

_____

* "Solutions" appears in quotes here since we are considering p as a function of "a" and "t" instead of the more natural arguments x and y.

particle "a" is at the origin and is being given an impulse, -I, per unit length by the linear pressure

$$p = -I\delta(St - \frac{a}{\gamma})$$ (15b)

Guided by the fact that the function h is to be dimensionless, we choose

$$\begin{cases} g = St - \frac{a}{\gamma}, & R(a) = -\frac{a}{\gamma} \\[2mm] h^1(g) = \frac{I}{\gamma S^2}\, \delta(St - \frac{a}{\gamma}) \end{cases}$$ (15c)

in agreement with (11) and the equation preceding (12).

Since

$$\int_0^t p\ dt = \begin{cases} -I, & t \geq \frac{a}{\gamma S} \\[4mm] 0, & t < \frac{a}{\gamma S} \end{cases}$$

we have

$$h(g) = \begin{cases} \dfrac{I}{\gamma S} + C, & g \geq 0 \\[4mm] C, & g < 0 \end{cases}$$ (15d)

The additive constants must be chosen so that initially the liner makes an angle α with the x-axis at the origin, and the particles are moving toward the origin. That is, $C = \alpha + \pi$. Then, according to (13),

$$\psi_t(a,o) = -Se^{i\alpha}$$
$$\psi(a,o) = \frac{a}{\gamma}\, e^{i\alpha}$$ (15e)

At any time $t \geq o$, the description of the motion is given by

$$\psi(a,t) = \begin{cases} (\frac{a}{\gamma} - St)e^{i\alpha}, & t < \frac{a}{\gamma S} \\[4mm] (\frac{a}{\gamma} - St)e^{i(\alpha + \frac{I}{\gamma S})}, & t \geq \frac{a}{\gamma S} \end{cases}$$

Hence we see that the effect of the impulsive pressure is to change the direction of

70

motion of the particles by the angle $\frac{I}{\gamma S}$, while the magnitude of the velocity is unchanged, a result which is to be expected.

Now if we transform to the laboratory frame of reference, by adding the velocity $Se^{i\alpha}$ to all the particles, then

$$\psi = \begin{cases} \dfrac{a}{\gamma} e^{i\alpha} & , \ t < \dfrac{a}{\gamma S} \\[3ex] Ste^{i\alpha} + (\dfrac{a}{\gamma} - St)e^{i\left[\alpha + \frac{I}{\gamma S}\right]} & , \ t \geq \dfrac{a}{\gamma S} \end{cases} \tag{15f}$$

We shall not discuss the Birkhoff theory further, but shall pass on to a generalization, which takes into account the aspect that the pressure exerted by the explosive actually must act for some time on each particle.

Case 2. (Finite Pressure Pulse)

Let the frame of reference as before be the detonation front frame, and assume a steady motion. Define the pressure pulse, applied over an interval of the liner, by

$$p = \begin{cases} 0 , & t < \dfrac{a}{\gamma S} \\[2ex] -P, & \dfrac{a}{\gamma S} \leq t \leq \dfrac{a}{\gamma S} + \tau \\[2ex] 0 , & \dfrac{a}{\gamma S} + \tau < t \end{cases} \tag{16a}$$

where τ is the time of application of the constant pressure P on each particle. Now we may take

$$g = St - \frac{a}{\gamma} \tag{16b}$$

as before while:

$$h'(g) = \begin{cases} 0 , & g < 0 \\[2ex] \dfrac{P}{\gamma S^2} , & 0 \leq g \leq S\tau \\[2ex] 0 , & S\tau < g \end{cases} \tag{16c}$$

An application of (14) again, with the same initial conditions as in the previous case, yields, after again transforming to the laboratory frame of reference:

71

$$\psi(a,t) = \tag{16d}$$

$$\begin{cases} \frac{a}{\gamma} e^{ia} & , \ t < \frac{a}{\gamma S} \\[2mm] Ste^{ia} + \frac{\gamma S^2}{P} e^{i(\frac{\pi}{2} + \alpha)} \left\{ e^{i\frac{P}{\gamma S}(t - \frac{a}{\gamma S})} - 1 \right\}, \ \frac{a}{\gamma S} \le t \le \frac{a}{\gamma S} + \tau \\[2mm] Ste^{ia} + \frac{\gamma S^2}{P} e^{i(\frac{\pi}{2} + \alpha)} \left\{ e^{i\frac{P\tau}{\gamma S}} - 1 \right\} + (\frac{a}{\gamma} - S(t - \tau)) e^{i(a + \frac{P\tau}{\gamma S})}, \ \frac{a}{\gamma S} + \tau < t \end{cases}$$

This is clearly interpretable (in the detonation frame) as indicating that the liner particles are accelerated at constant angular speed, $\frac{P}{\gamma S}$, around a segment of a circle of radius $\frac{\gamma S^2}{P}$, and then move off rectilinearly with the same speed S that they had in approaching the origin, but in a direction making an angle $\frac{P\tau}{\gamma S}$ with the original wedge direction. Such a solution is clearly derivable using the most elementary of physical concepts -- it is produced here as an illustration of the mathematical procedure to be followed in more complicated cases. Incidentally, if $P \longrightarrow \infty$, $\tau \longrightarrow 0$, and $P\tau \longrightarrow I$, this solution reverts to the simpler Birkhoff motion.

Thus by choosing various forms of the function h'(g), the effect of the continuing pressures acting on the liner can be estimated. On the other hand, by varying the functions R and S, it might be hoped that effects due to the variable release of pressure at the outer explosive edge could be estimated. This however turns out to be fruitless, insofar as one-dimensional motion is concerned, since the initial contour and velocity distribution depend critically on the form of R and S. Indeed as we also have intimated previously it is possible for at least two reasons that further investigation of our formulation, in the direction we have pursued in this section, may really lead to illusory conclusions. One is that the dependence of p on ψ itself (and its derivatives) has been entirely neglected. Second, the effects of liner strength properties have also been ignored, a consideration which in part leads to the important phenomena pointed out in the following paragraphs.

IV. STABILITY OF SOLUTIONS

It was soon evident after formulating the Cauchy problem (3) and (4), that its solutions might exhibit a remarkable "unstable" behavior, particularly when the pressure function p is regarded as a function of "a" and "t". This was pointed out by C. Gardner, who mentioned that a similar situation arises in the case of Laplace's equation or the equation of heat conduction, when the problem of finding a solution is posed in a certain way. (4). Although we have by no means fully investigated this behavior, it may be illustrated by the following example.

Consider the special solution of (3), with $p = \frac{m\omega^2}{2\pi} = $ const

$$\psi(a,t) = Re^{i(\omega t + 2\pi \frac{a}{m})} + \frac{A}{n^3} \cosh n\omega t \ e^{-2\pi i \ n^2 \frac{a}{m}} \tag{17a}$$

where n is a very large integer, and A is a constant. Then initially

$$
\begin{cases}
\psi(a,o) = \mathrm{Re}^{2\pi i \frac{a}{m}} + \frac{A}{n^3} e^{-2\pi i n^2 \frac{a}{m}} \\[2mm]
\psi_t(a,o) = i\omega\mathrm{Re}^{2\pi i \frac{a}{m}}
\end{cases}
\tag{17b}
$$

which represents a closed curve approximating as closely as we like, for large enough n-values, the initial circular distribution of the solution (6a). In fact we have merely superimposed on the circular distribution a periodic crinkle -- and since ψ_a also approximates as closely as we like the smoothly turning tangent vector of the circular distribution, while the rotational velocity ψ_t has exactly the same values, the initial data for the cases agree as closely as we like. Nevertheless, for $t > o$, the solutions (6a) and (17a) diverge from one another by as large an amount as we desire, if n is taken large enough. This peculiar situation is characteristic of problems for which, in mathematical terminology, the solutions do not depend continuously on the initial data. According to Hadamard, the Cauchy problem (3) and (4), for p = constant at least, is "not properly set". (i.e., continuous initial data can not be prescribed arbitrarily and be expected to lead to a solution satisfying (3).)

However, it is hard to escape the feeling, based on physical intuition, that the initial assumptions made (of a very thin, weak liner material, acted on by a pressure differential which could conceivably remain constant) are not so radical an approximation to the physical situation that no physically significant information could be gleaned from the theory. When then is the interpretation of the instability exhibited above? According to the writer's view it means two things: (a) in order to obtain a properly set mathematical problem, effects of thickness and liner strength must be included, and (b) the motion of weak liners is an inherently unstable phenomenon, in the sense that unless extreme care is taken in the preparation of shaped charges (machining, detonation) the results obtainable with them will at best exhibit a wide scatter around a mean value. As partial evidence for these conclusions we may point to the tendency toward large statistical fluctuations in the experimental results, if not too great care is taken in the experimental conditions, and to the fact that lead, a weak material, or steel, a brittle material, do not appear to yield as consistent results as copper, a ductile material stronger than lead.

V. CONCLUSIONS

In considering the general motion of a two-dimensional shaped-charge liner, we have omitted many important phases and effects. We have not considered the jet extrusion process or the mechanism of formation of a velocity distribution in the jets, although it is to a certain extent quite simple to treat these questions from the point of view of the present formulation. We have not taken into account the fact that real shaped-charge liners are surfaces in three-dimensions (cones, hemispheres, etc.) and that irregularities in the third dimension certainly must influence the motion markedly. As mentioned before the effects of material strength and liner thickness have not been included. If they are, as indeed they must be some time for a complete theory, terms

which represent the effect of constraints, contributions due to non-uniform thickness
and pressure distributions, and stretching and bending stresses in the liner, must be
added in. Finally the motion of the explosion gases, already investigated to some ex-
tent by Friedrichs, must be taken into account in order to obtain an accurate estimate
of the pressure difference p, as well as to complete the formulation of the problem.

We have, however, concentrated on certain aspects of the problem with certain aims
in mind. Several heuristically usable descriptions of the motions have been obtained,
and their relations to previous investigations pointed out. The important question of
the stability of the motion has been posed, and in some respects, from the present point
of view, considered -- as a result the importance of treating more exhaustively the
problems mentioned in the previous paragraph is accented. Finally the important engi-
neering question, "Given a certain jet shape and velocity distribution, what sort of
shaped-charge configuration will produce it?" can now be considered more fully. For
if we pose part of this question "What shaped-charge and liner configuration will pro-
duce a certain liner collapse motion?" then within the limitations of this formulation,
we may give a partial answer. If the given collapse motion is

$$\psi = \psi(a,t) = x + iy$$

then x and y must satisfy

$$x_a x_{tt} + y_a y_{tt} = 0,$$

and the pressure which will produce this motion is

$$p = \frac{\psi_{tt}}{i\psi_a}.$$

REFERENCES

(1.) Friedrichs, K O.; Keller, J.; Lax, A. "Remarks About the Effect of the Deto-
      nation Wave on the Liner of a Shaped Charge", Preliminary Report, I.M.M.,
      May, 1950.

(2.) Birkhoff, G.; MacDougall, D. P.; Pugh, E. M.; and Taylor, G. I. "Explosives
      with Lined Cavities", Jour. App. Physics, 19, No. 6, June, 1948.

(3.) Touart, C. "Theoretical Interior Ballistics of Lined Wedge-Shaped Charges",
      Unpublished Report, I.M.M., July, 1951

(4.) Hadamard, J. "Lectures on Cauchy's Problem in Linear Partial Differential
      Equations," Yale Univ. Press, 1923.

SOURCES OF DISPERSION IN SHAPED CHARGE PERFORMANCE

R. v. Heine - Geldern

Department of Physics, Carnegie Institute of Technology, Pittsburgh, Pennsylvania

ABSTRACT

Dispersion in the performance of hollow charges can be assigned to three distinct causes:

(a) Lack of homogeneity of the explosive

(b) Geometric liner imperfections

(c) Improper alignment between charge and liner

Of these three causes, only the last two have been evaluated quantitatively. The importance of perfect axial symmetry in zones perpendicular to the axis can hardly be stressed enough. Very little is known about the effect of (a). Further attempts at reducing charge variability should be directed at improving the homogeneity of the explosive.

Anyone familiar with shaped charges, has been confronted with the fact that two apparently identical charges can produce widely different penetrations. A typical experiment is illustrated in **Fig. 1**, where the penetration produced by a single lot of 224 charges are plotted in the form of a histogram. It will be noted that the penetration values range from 5.2 to 9.5 inches, with an average penetration of 8.16 inches. The outstanding feature of this distribution is its marked skewness, which makes data of this type very difficult to treat by established statistical methods. If the long tail of this distribution, which contains about one-third of the individuals, were amputated, then the remaining two-thirds of the individuals would be distributed approximately in accordance with the normal distribution law and the data would thus become amenable to routine statistical treatment. The first objective of any work on charge variability should therefore be the removal of the long tail of low penetrations. Only when this has been done will it be profitable to make an attempt at reducing the spread of the remaining near-normal distribution.

In this paper, an attempt is made to show that those factors which affect the symmetry of cone collapse are the ones which determine the degree of skewness of the frequency distribution. In addition, it will be shown that pronounced asymmetry of collapse gives rise to a bi-modal frequency distribution of which the skewed distribution shown in Fig. 1 is a limiting case with a relatively small number of charges falling within the lower distribution.

For proper formation of a jet from a conical liner, it is essential that all liner elements around a circular zone of the cone meet axially with the same momentum. **Fig. 2** shows a number of charge imperfections which tend to destroy the required
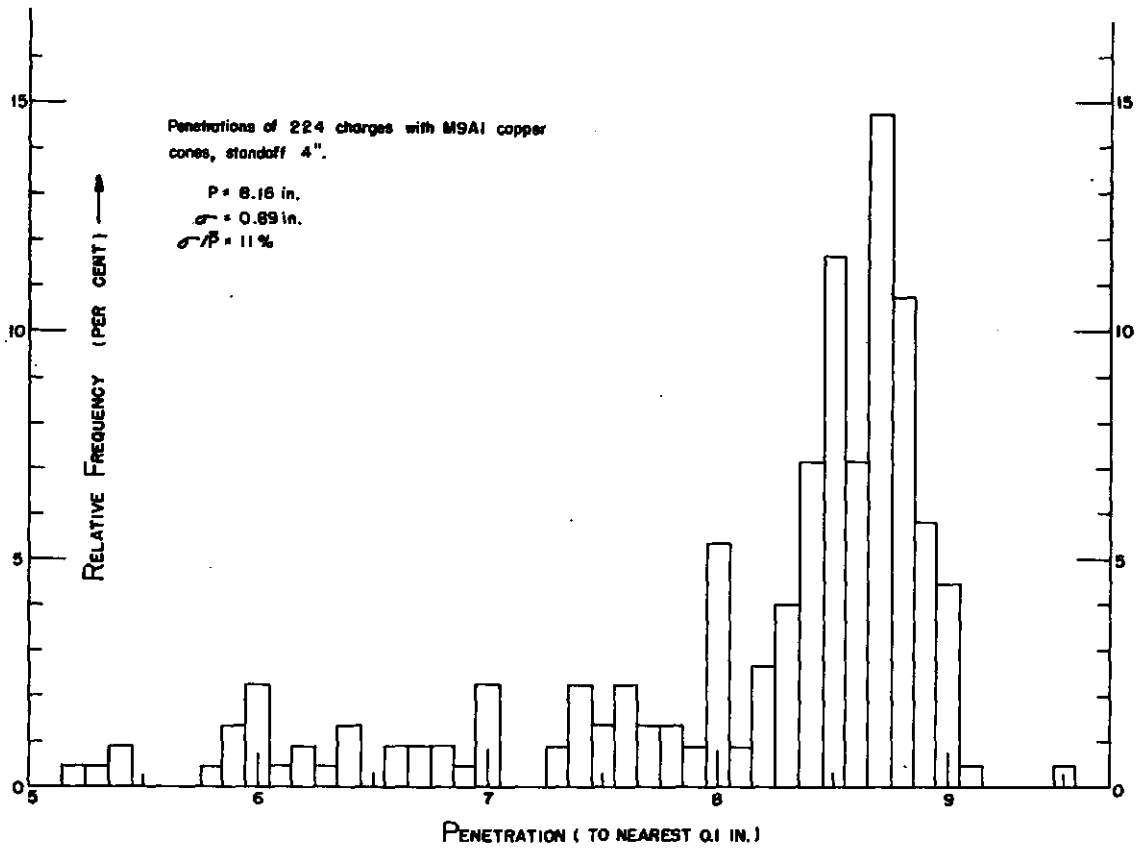
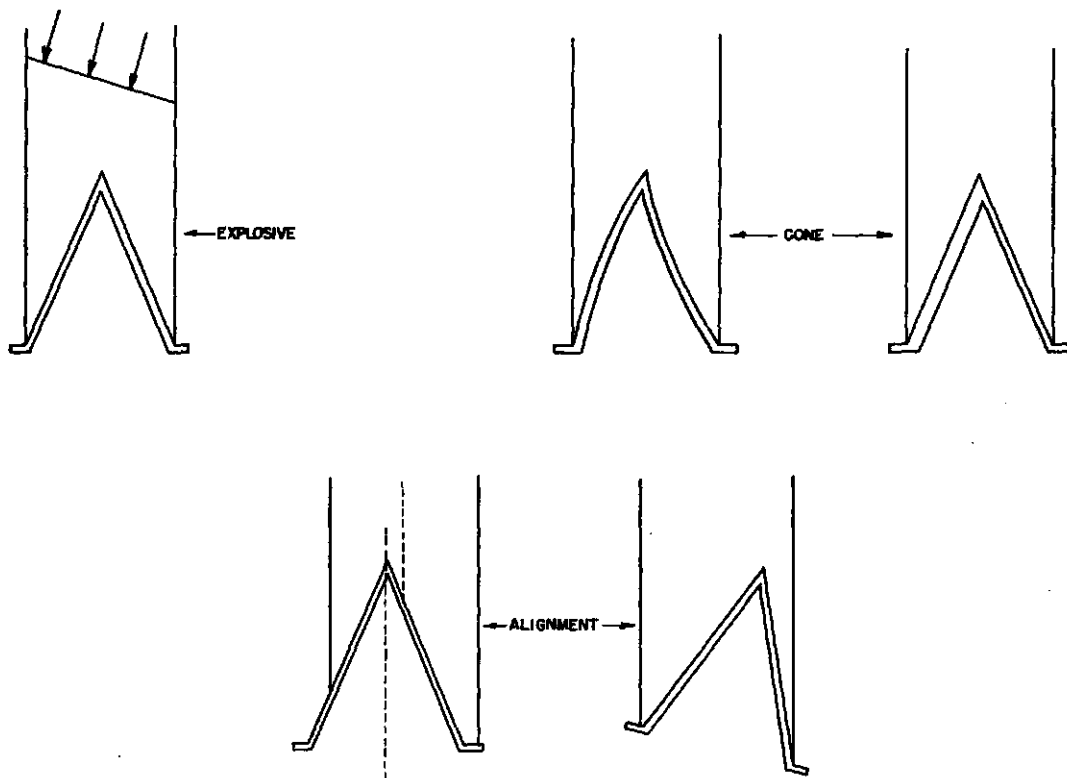Figure 1—Penetration of 224 charges with M9A1 copper cones, standoff 4″.

Figure 2—Schematic of serious charge imperfections.

76

symmetry of collapse. For the purpose of this discussion, these defects are divided into those originating from (a) faulty detonation of the explosive charge, (b) geometric liner imperfections, and (c) faulty alignment between explosive and liner.

The first type of defect, most readily illustrated by off-axial initiation, is not usually encountered in a well-designed charge. Some time ago, this group obtained 50 experimental charges from a commercial source. These consisted of bakelite-confined charges with conical liners; at the top of the charge, a hole in the bakelite allowed the insertion of a piece of primacord with its axis at right angles to the axis of the charge. The primacord was intended to take the place of a conventional blasting cap for initiating the charge. With such an arrangement, a tilt of the detonation wave amounting to several degrees can be expected. The penetration histogram obtained from 50 of these charges is shown in Fig. 3, where the bi-modality of the distribution can be noted. The Kerr cell pictures in Fig. 4 show the effect of off-axial detonation on the jet itself. Both of these jets resulted from charges detonated off-axially, the radial displacement of the detonator amounting to 1/8 in. for the jet on the left and 1/4 in. for the one on the right.

The second type of charge imperfection, namely geometric imperfection of the conical liner, is encountered very frequently. It is very well illustrated by the following example: when this group obtained its first shipment of cones from a new source of supply, it was found that most of the cones displayed a skewness such that the axis near the tip of the cone was inclined at about twenty minutes of arc with respect to the axis near the cone base. The performance of 100 charges made with these skewed cones is illustrated in Fig. 5. The bi-modal character of this distribution is again quite evident. The next shipment of cones from the same manufacturer did not display the skewness shown by the first one, and charges made from them and subsequent shipments displayed the long "tail" of low penetrations discussed earlier, but not the obvious bi-modality of the first group.

The third cause of imperfect charge performance, namely lack of alignment between charge and liner, used to be the most frequently encountered and the most serious of the three imperfections. It has been largely eliminated by casting the charges in a mold, designed by this group, which is shown schematically in Fig. 6. This casting procedure aligns the cone with the charge more accurately than is possible by the old procedure of casting the charge in commercial steel tubing, where alignment is determined by the cone flange. The development of this modified casting procedure constitutes the biggest single step in reducing charge variability. This is demonstrated by Fig. 7, which shows the penetration histogram of 104 charges made by the conventional procedure with that of 50 charges made by means of the C.I.T. mold. It will be noted that the standard deviation of the first group (0.87 in.) is nearly three times the one of the second group (0.31 in.).

Recent evidence indicates that C.I.T. molds must be made to very rigid specifications for optimum charge performance. In comparing two groups of 60 charges each made in two different molds, one of the groups performed significantly better than the other. This difference in performance was eventually traced to the inclinations of the alignment pin in the C.I.T. molds used; in the case of the mold which yielded the better charges, this inclination amounted to 3 minutes of arc, while the other pin was inclined at 9 minutes of arc.

$\bar{P}$ = 2.82 in.
σ = 1.13 in.
$\sigma/\bar{P}$ = 40 %
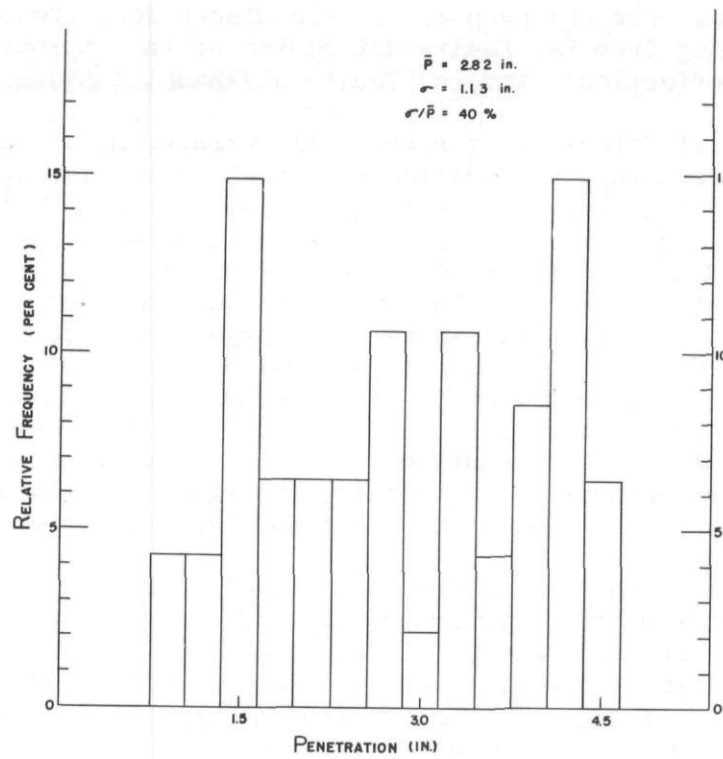
Figure 3—Performance of 50 experimental
charges, standoff 2.5 cone diameters.
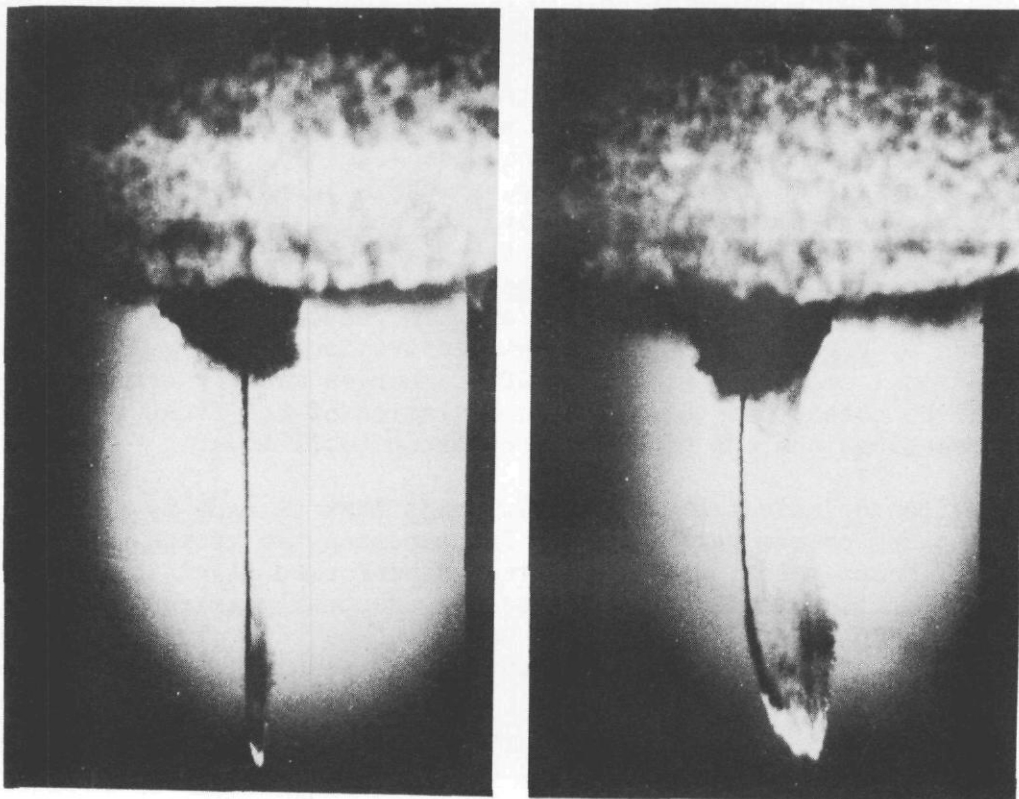
Figure 4—Effect of off-axial detonation on jet.

78
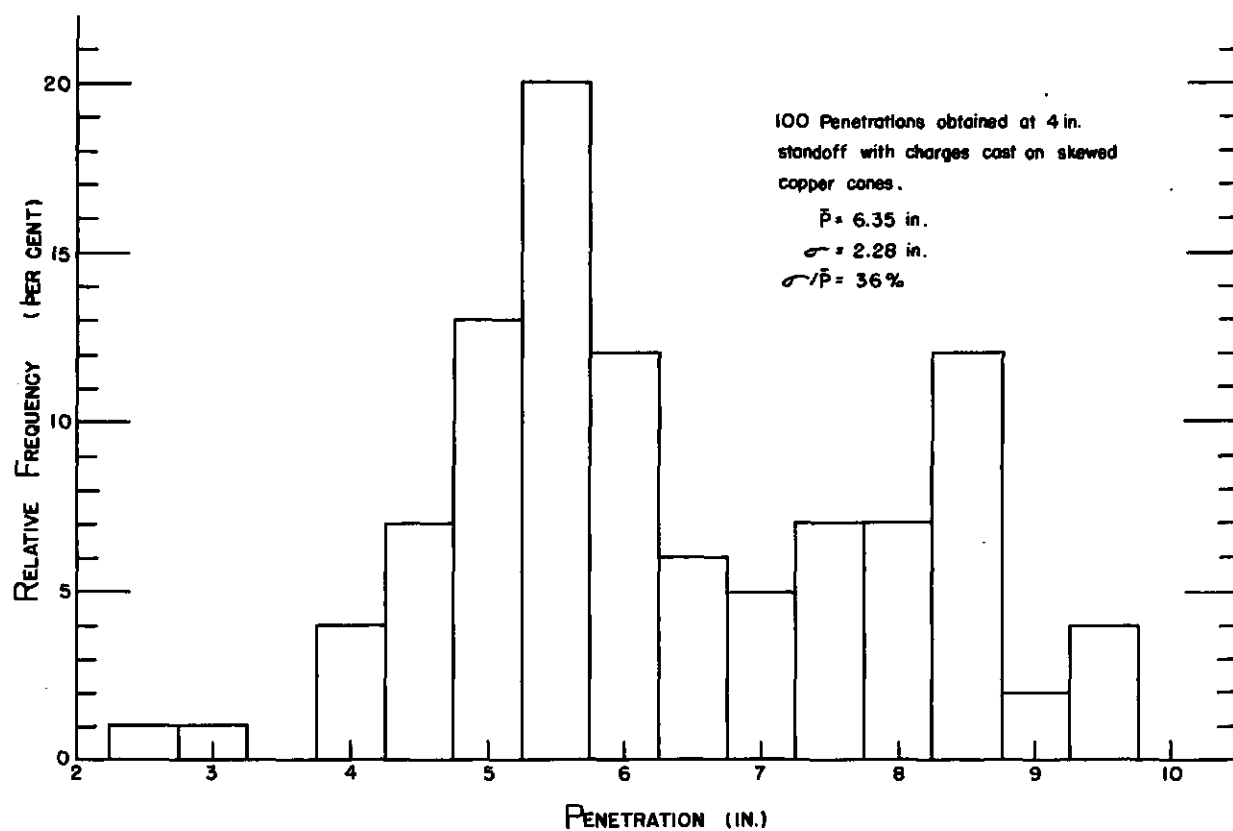
Figure 5—100 penetrations obtained at 4″ standoff with charges cast
on skewed copper cones.
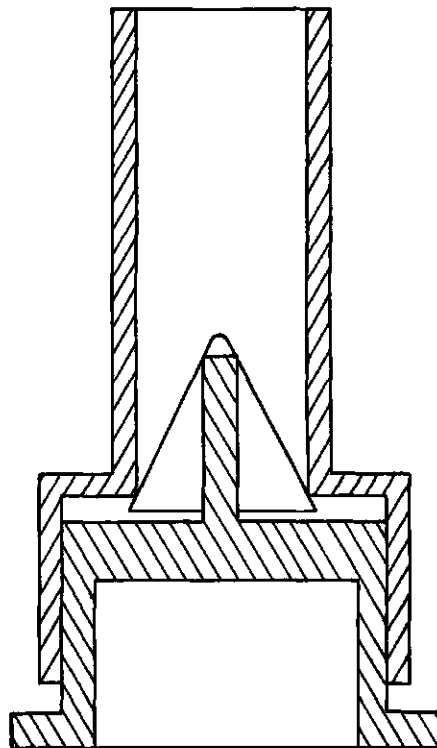
Figure 6—C.I.T. Mold.
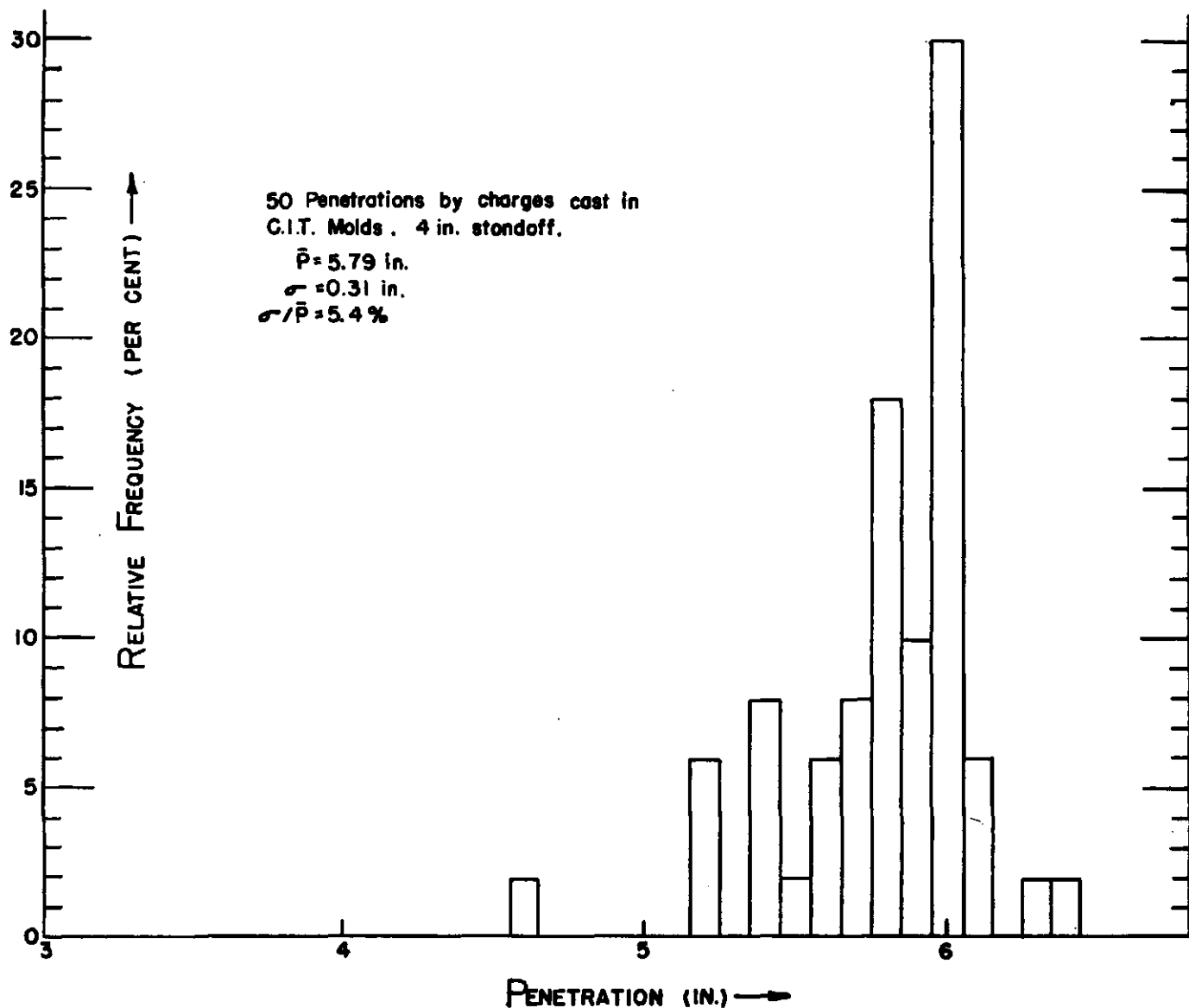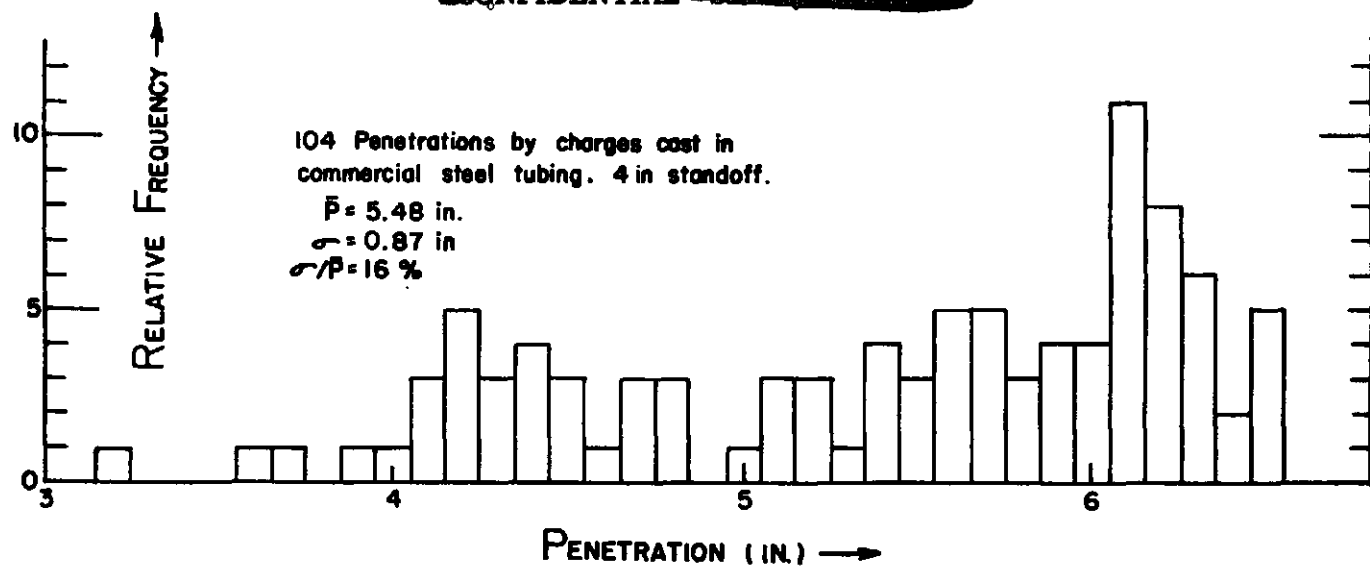
Figure 7—(a) 104 penetrations by charges cast in commercial steel tubing, 4″ standoff.
(b) 50 penetrations by charges cast in C.I.T. Molds, 4″ standoff.

This last example illustrates the extreme accuracy in alignment which is necessary for good charge performance. The requirements for liner symmetry are hardly less exacting, while the inclination of the detonation wave can amount to several degrees before charge performance begins to deteriorate.

To summarize, it can only be repeated that all those factors which affect symmetry of the collapse process should be rigidly controlled, while other factors, not directly concerned with charge symmetry, can be allowed considerable tolerances without impairment of charge performance.

The above considerations have some bearing on all experiments designed to compare the performance of liners made from different materials. It is known, for example, that steel liners give more consistent performance than copper liners. When such liners are subjected to measurements of their contours and wall thicknesses, it is generally found that the steel liners come closer to the requirements set forth in this paper than the copper liners. In the literature, statements are frequently found to the effect that metal A is a better liner material than metal B. In particular, lead has frequently been quoted as being a poor liner material. It is the opinion of this group that such statements express nothing more than the machinability of different materials and that a fair comparison between two metals can be made only if both of them can be machined or worked to the same symmetry tolerances.

PERFORMANCE OF PERIPHERALLY INITIATED SHAPED CHARGES

A. D. Solem

W. T. August

U. S. Naval Ordnance Laboratory, White Oak, Silver Spring, Maryland

ABSTRACT

The performance of experimental cone-lined shaped charges is being investigated under the condition of peripheral initiation of the charges. Peripheral initiation is simultaneous initiation of the entire top periphery of the charge in contrast to point or plane wave initiation. It is obtained by use of a cup-shaped inert-filled initiator placed over the top of the charge such that initiation is transmitted to the periphery of the charge but is delayed in passage through the inert material in contact with the top surface of the charge. The behavior of penetrations from peripherally initiated charges into mild steel targets for variation of charge height, stand-off, cone material, cone wall thickness, and cone apex angle are being studied and compared with the behavior of penetrations from point initiated charges for like conditions. The results are described and reasons for the observed behavior discussed. Experimental evidence showing why peripherally initiated charges produce greater penetrations are presented.

INTRODUCTION

One of the means available for improving shaped charge penetrations and performance is that of shaping the detonation wave in its passage through the explosive. The interaction of detonation wave and liner will thereby be altered, and conditions for increasing shaped charge performance will be enhanced. Various wave shapings are possible; the most obvious one is that of initiating the charge simultaneously around its periphery at the top. The detonation wave then sweeps into the charge like an expanding torus to strike the liner surface more nearly normal than is obtained with ordinary point initiation. This method of wave shaping is not new, variations of it were tested during World War II and were tried in some weapons (reference a[*] gives a list of references to this early work), but as far as is known no systematic study of the system had ever been carried out. In the autumn of 1950 the shaped charge group at the Naval Ordnance Laboratory undertook as one of its programs a general investigation of the behavior of peripherally initiated shaped charges. The purposes of the tests were to establish conditions optimizing shaped charge performance under this system of initiation, to observe limitations of the system, and to determine if peripheral initiation were feasible in practical applications. This present paper reports some of the early results obtained in the tests.

---

[*] Reference (a) - Nav Ord Report 1722 "Peripherally Initiated Shaped Charges" dated 1 November 1950

EXPERIMENTAL CHARGES

The system used to obtain peripheral initiation is given in Figure 1, which shows a sketch of a typical assembled experimental charge. The charge proper consists of a cylindrical charge cast over a conical liner. In the present tests the charge diameter was 1.63 inches, and the liner dimensions were those of the standard M9A1 cone (1.63 inch base diameter, 44 degree apex angle, 0.037 inch wall thickness)[*]. The charge height and the liner material were the factors varied in the tests. The explosive used for these charges, except for one series of tests comparing different explosives, was 50/50 Pentolite.

The peripheral booster consists of a cup-shaped, 50/50 Pentolite charge which fits over the charge proper in contact with the charge proper only at its periphery. The top surface of the charge proper is separated from the booster charge by inert filled cavity of the booster. The inert material is lead oxide, mono (other inert materials have been tried and the results have not been as good as with the lead oxide), and, except for one series of tests where the thickness was varied, the thickness of the lead oxide is 0.5 inches. The assembled charge is initiated on the charge axis by an electric detonator and is boostered by a Tetryl pellet.

Conditions for symmetry are much more critical for these charges than for ordinary point initiated charges. Unless complete simultaneous peripheral initiation of the charge proper is obtained inferior performance results. The initiator must be situated on the axis of the charge so that the detonation wave passing the barrier is essentially plane and normal to the charge axis; the peripheral booster must make good uniform contact with the charge proper so there is no delay of detonation at any point in passage into the charge proper. In test these conditions are not always met even with care in assembly. The spread of results is somewhat greater than obtained with experimental point initiated charges. The spread diminishes as the charge height increases.

EXPERIMENTAL RESULTS

Behavior of Various Liner Materials. Figure 2 compares the penetrations obtained with point, plane wave, and peripheral initiation of M9A1 steel cone lined charges with variation of charge height. Note the increase of penetration as the charge height is increased when point or plane wave initiation is used as is expected. Note also the peaking of penetration with peripheral initiation at the 2.35 inch charge height. This high penetration is some 30 per cent greater than obtained with a standard point initiated charge 4.00 inches in height. This increased penetration furnished incentive to further investigations of the effect.

Figures 3 and 4 show the penetrations obtained with other liner materials as the charge height is varied. Liner materials considered consisted of cast iron, glass, copper, brass, aluminum, and magnesium. Note that while there is reasonably regular variation of the penetration pattern there is considerable scatter of penetrations for

---

[*] The work with glass cones was with 1.90 inch diameter charges; the cones had a 1.90 inch base diameter, and a 60 degree apex angle.
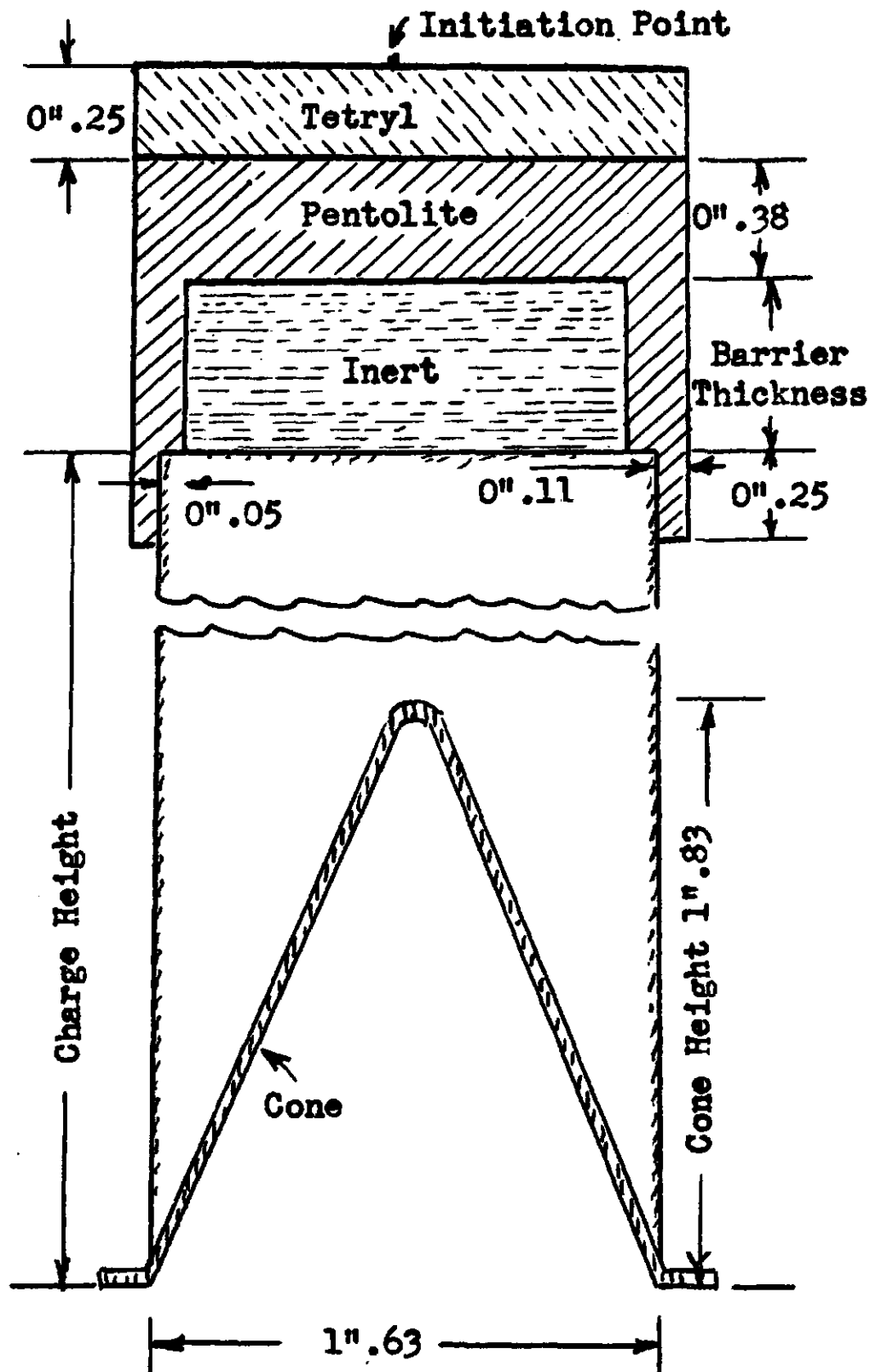
Figure 1—Experimental peripheral initiation charge.
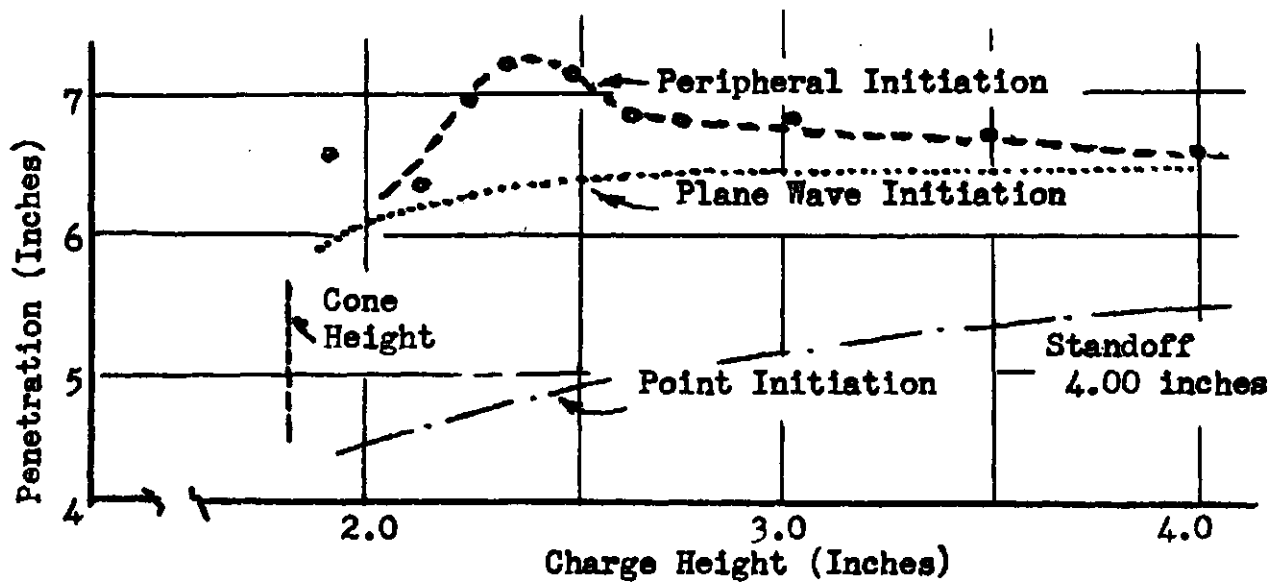
Figure 2—Effect of charge height variation for steel liners.
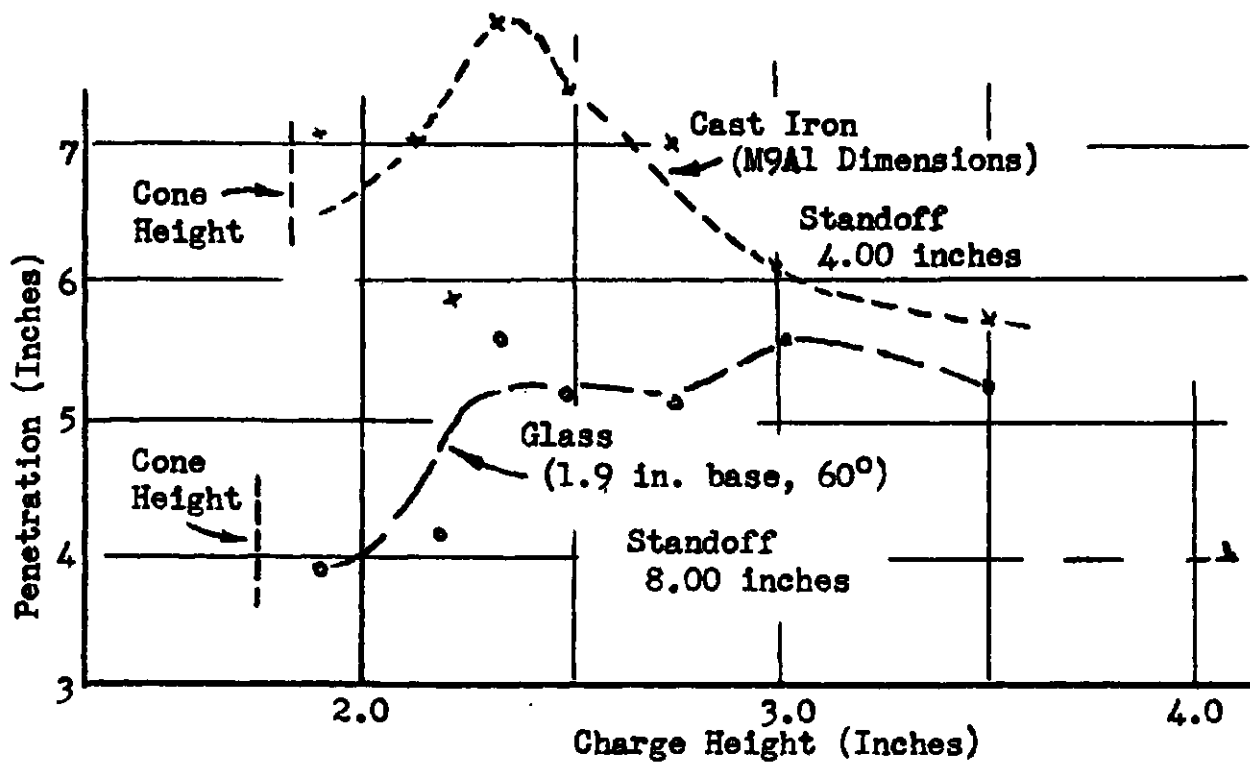
Figure 3—Effect of charge height variation for cast iron and glass
liners under peripheral initiation.
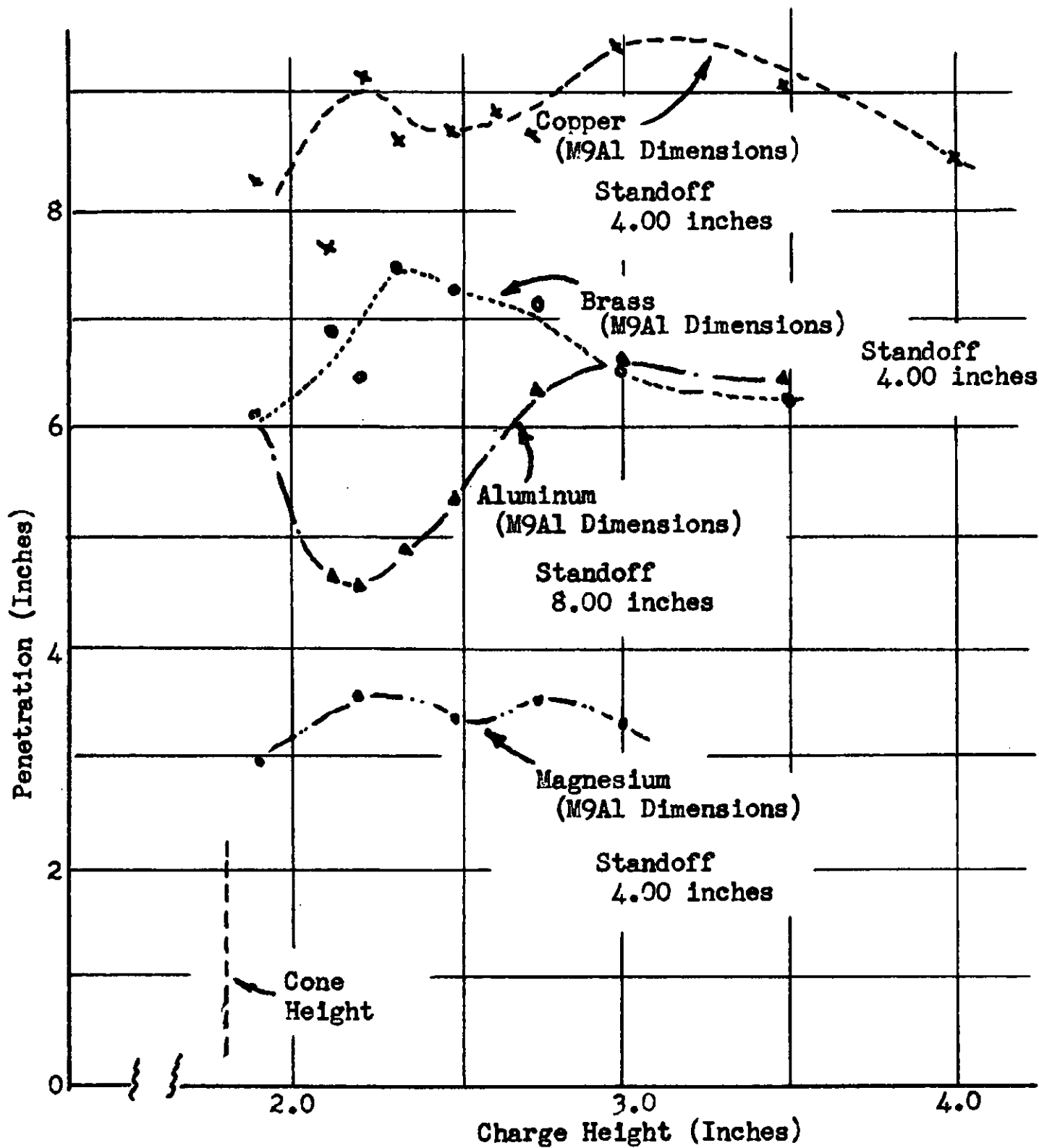
Figure 4—Effect of charge height variation for copper, brass, aluminum,
and magnesium liners under peripheral initiation.

Table 1

PERFORMANCE OF VARIOUS LINERS

44° CONES 1.63" BASE DIAMETER

50/50 PENTOLITE

Liner	Point Initiation		Peripheral		Percentage Increase
	Charge Height	Pentration	Charge Height	Penetration	
Copper	4.00	8.46	3.00	9.51	12
Steel	4.00	5.60	2.35	7.30	30
Cast Iron	4.00	7.49	2.35	7.91	6
Brass	4.00	7.08	2.50	7.28	3
Magnesium	4.00	1.70	2.25	3.58	106
Aluminum	4.00	5.27	3.00	6.50	23
Glass*	4.00	4.27	3.50	5.74	34

* Glass: 60° Cone, 1.9" Base Diameter

Table 2

PERFORMANCE OF VARIOUS EXPLOSIVES
M9A1 STEEL CONES

	Penetration (Inches)		
Explosive	Point Initiation	Peripheral Initiation	Percentage Increase
50/50 Pentolite	5.56	7.41	33
Comp B	6.17	7.20	17
PTX-2	6.57	7.16	9
Comp A-3	6.22	6.82	10
BTNEU/WAX	5.64	6.79	20
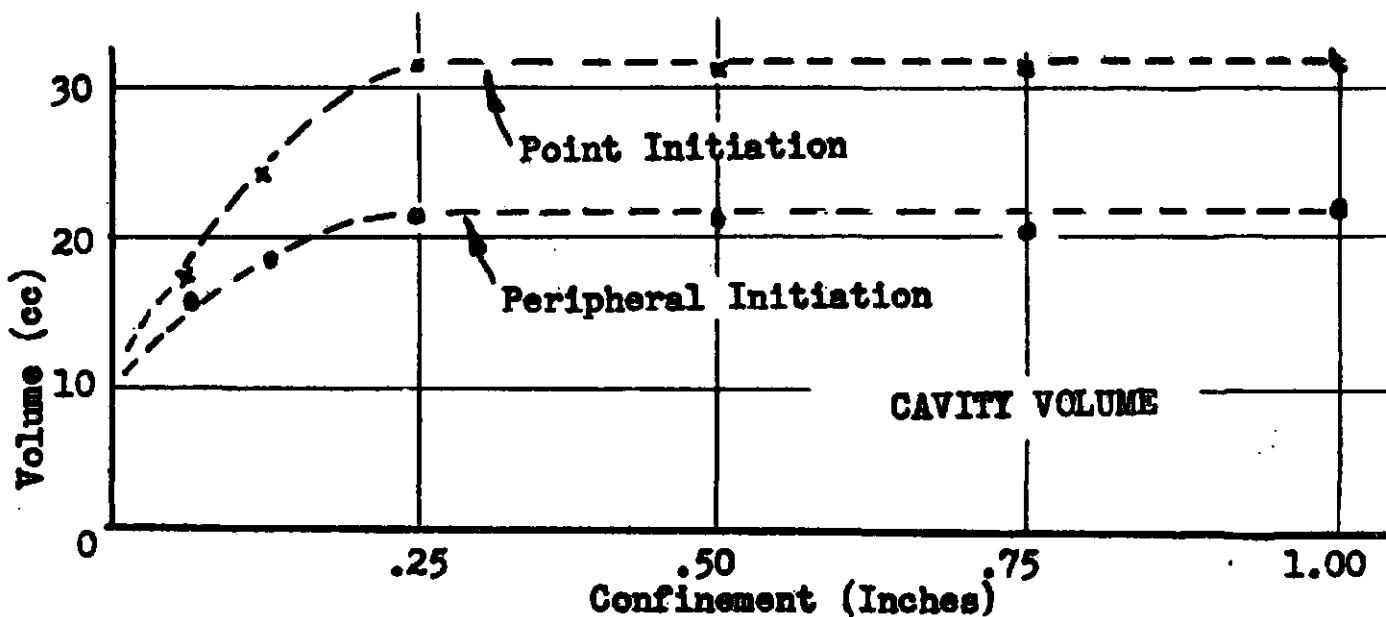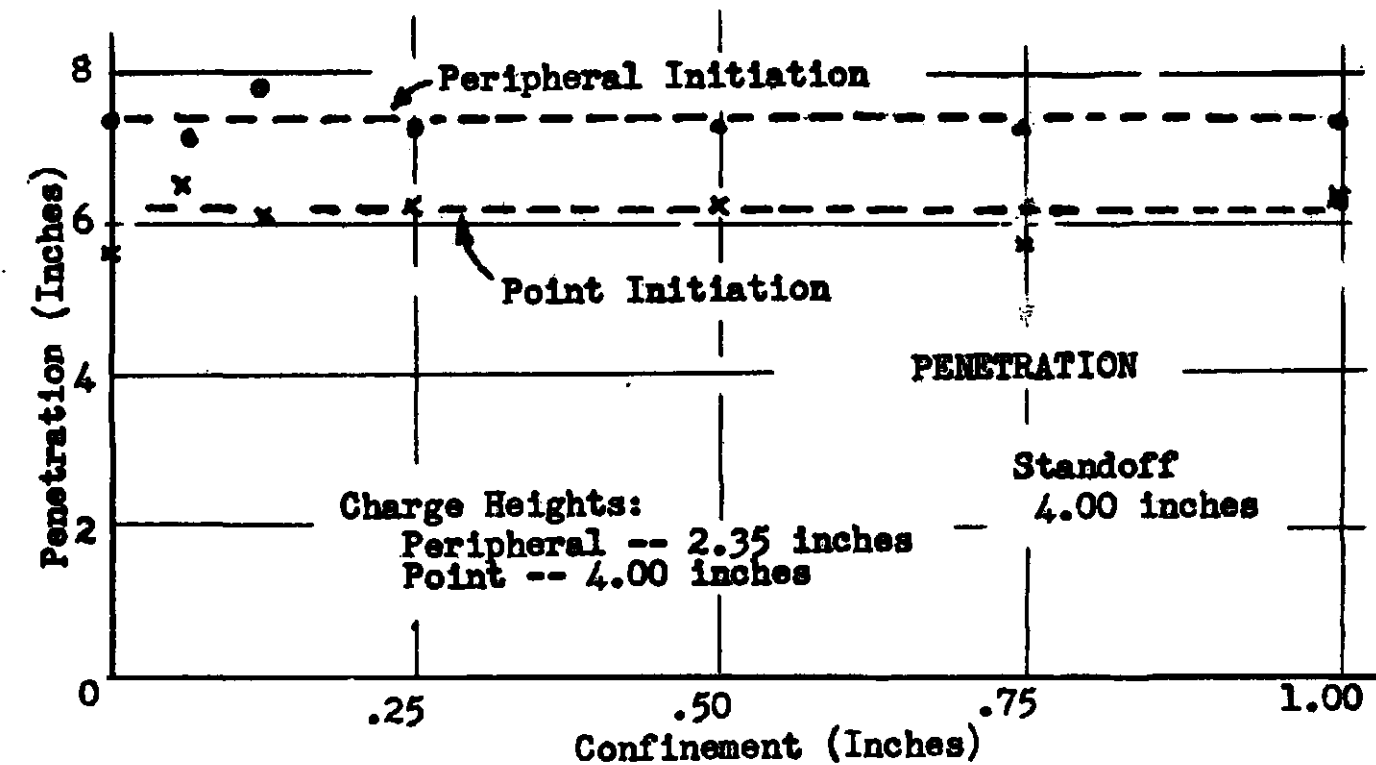
Figure 5—Effect of confinement variation for M9A1 steel cone liners under point and peripheral initiation.

90

the different charge heights for the cast iron, glass, and copper cones. Note also that the penetrations are not typified by a simple behavior pattern, although some order may be made from the chaos. The results are not complete but are given to show the type of behavior observed.

Some comments on the results are pertinent:

    a. The penetration pattern for steel liners is fairly stable. The results have been checked, and the peaking at the 2.35 inch charge height has been verified with many shots.

    b. Only a few shots were fired (on the order of five) to determine each of the points shown for the other materials. Thus the stable position for each point may vary considerably from that shown.

    c. The double-humped behavior of the copper liners is believed to be real. This behavior has been verified qualitatively by work performed at the Carnegie Institute of Technology, although their results do not agree quantitatively with those shown here.

    d. The variation in charge heights tested is somewhat limited and further testing will extend the charge heights in both directions.

Table 1 summarizes the increases in penetration obtained to date in going to peripheral initiation for the various liners tested. Some of these, of course, have no practical applications. The results are encouraging for steel, aluminum, and glass; they are disappointing for copper, brass and cast iron.

Behavior of Various Explosives. Another series of tests that has been considered has been a comparison of the behavior of various explosives on M9A1 steel cones under point and peripheral initiation. The results of these acts are shown in Table 2. All point initiated charges were 4.00 inches high; all peripheral initiated charges were 2.35 inches high. Note that as the penetration under point initiation goes up the percentage increase when peripheral initiation is used goes down. Two comments on these results are offered: 1. The charge height under peripheral initiation was optimum for 50/50 Pentolite; it might not have been optimum for the other explosives. 2. It appears that a saturation effect is being approached, so far as peripheral initiation is concerned, as the explosive power goes up. The choice of 50/50 Pentolite and steel cones for the first peripheral initiation tests was surely a very fortunate one.

Behavior Under Confinement. Figure 5 shows the results of a series of tests to observe the effect of confinement on point and peripherally initiated shaped charges. Standard 50/50 Pentolite charges lined with M9A1 cones were used. The charge height for the point initiated charges was 4.00 inches; the charge height for the peripherally initiated charges was 2.35 inches. Insofar as penetrations are concerned it is concluded that confinement has little or no effect on the results for the case considered. Cavity volume does increase with degree of confinement up to a nominal confinement of 0.25 inch thick steel cylinder. The volume increase is on the order of 300 per cent for both point and peripherally initiated charges. It should also be noted that cavity volumes for peripherally initiated charges are always 20 to 25 per cent less than for point initiated charges. If cavity volume is any measure of total energy in the jet less energy is associated with the peripherally initiated charges, but is so distributed to increase penetrations.
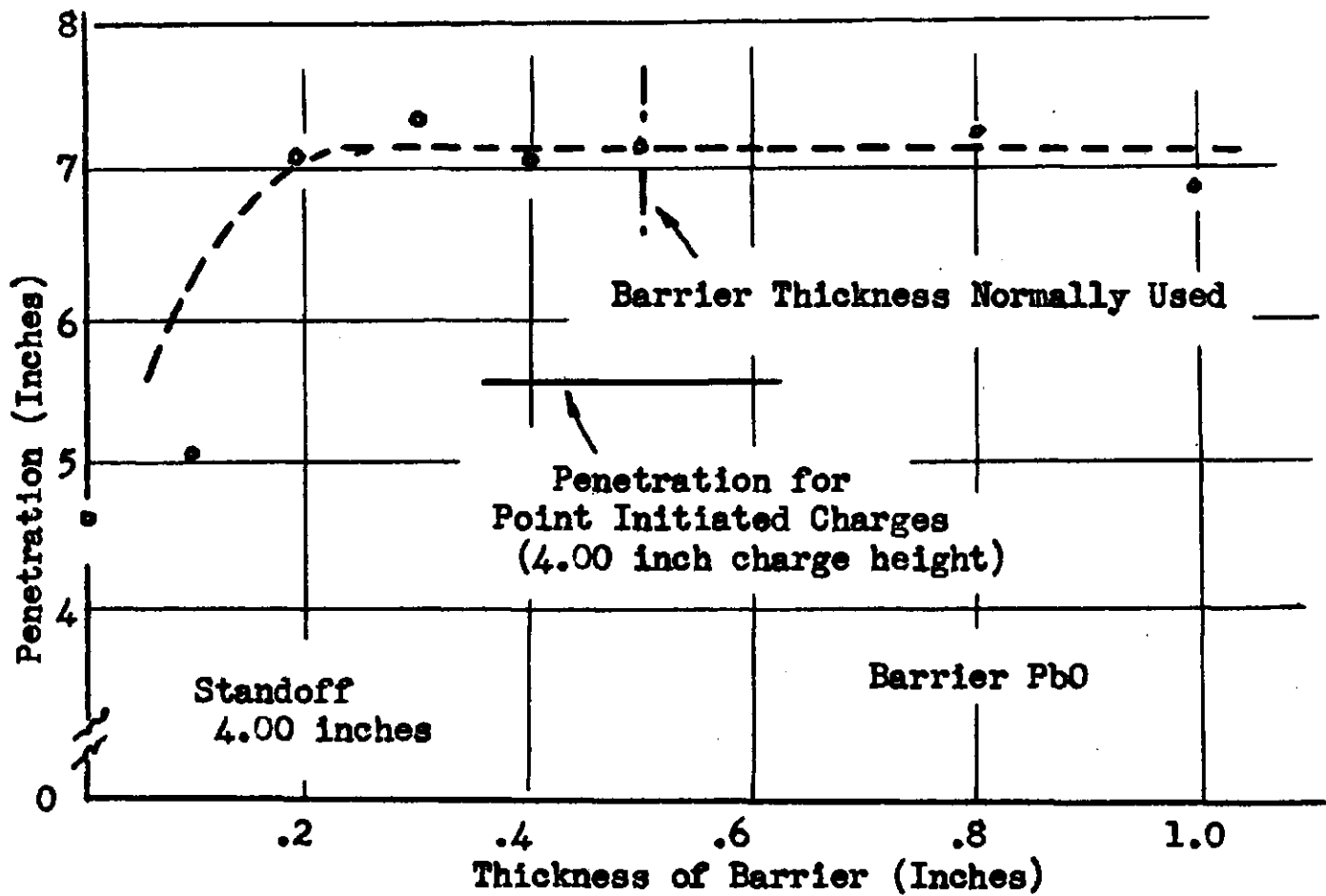
91

Figure 6—Effect of varying barrier thickness for M9A1 steel cone
liners under peripheral initiation.
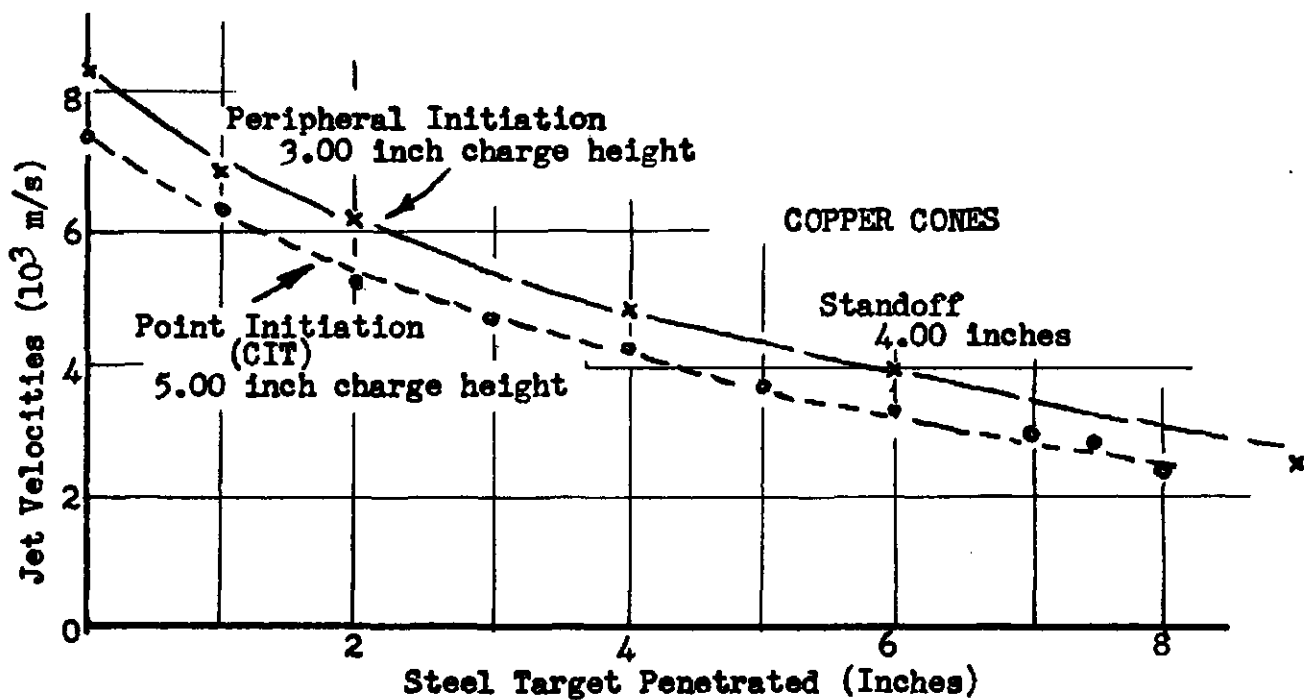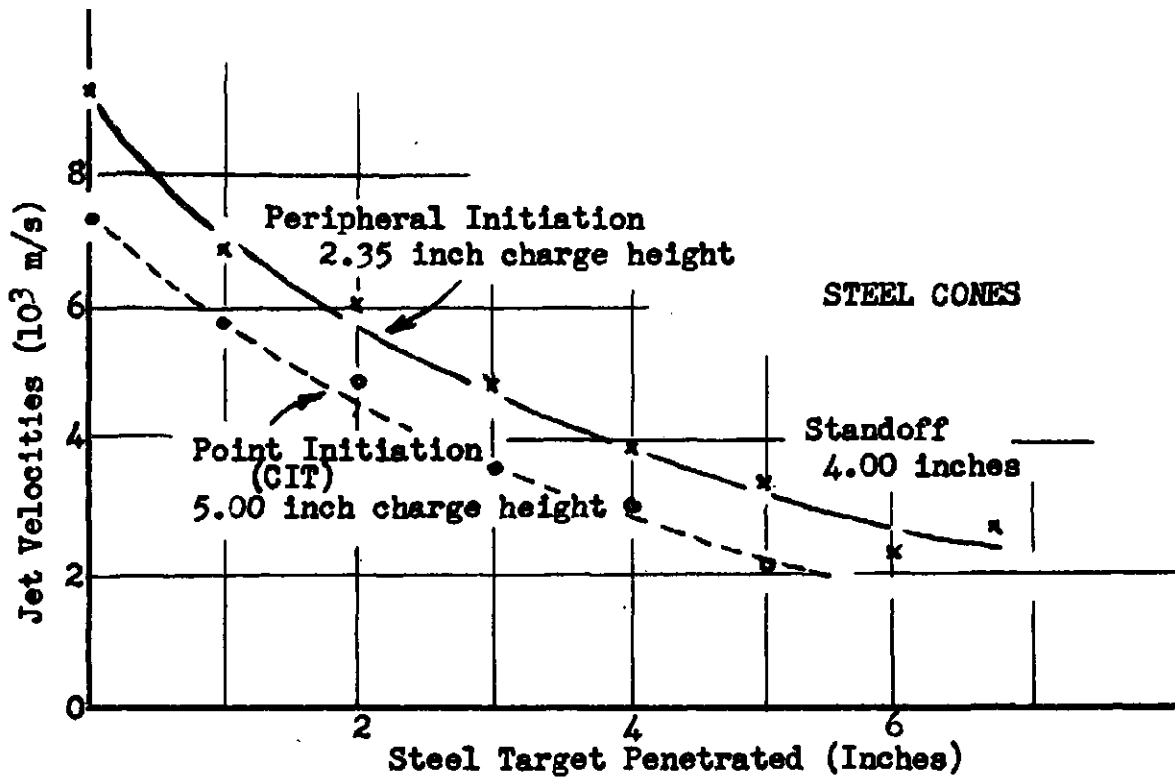
Figure 7—Initial and emergent jet velocities from steel and copper
M9A1 cone liners under point and peripheral initiation.

93

Behavior Under Variation of Barrier Thickness. Figure 6 shows the results of a series of tests to determine the amount of barrier required to produce peripheral initiation. Standard 50/50 Pentolite charges 2.35 inches in height cast over M9A1 steel cones were used in the test. The barrier material was lead oxide, mono. Note the uniformity of penetrations as the barrier thickness is increased beyond 0.2 inches. The standard barrier thickness used in all other tests was 0.5 inch. It is therefore concluded that true peripheral initiation was obtained. The exact nature of initiation for the 0.2 inch barrier thickness is not known, but it is speculated that it approaches true peripheral initiation. For the thinner barriers initiation is surely transmitted through the inert material.

JET VELOCITY STUDIES

A final series of tests to be reported here is some preliminary work on jet velocities which it is hoped will explain the behavior of peripherally initiated shaped charges. Figure 7 shows the initial and emergent jet velocities after penetration of a given target thickness for both point and peripherally initiated charges. Results are shown for both steel and copper cones. The velocities for the point initiated charges were taken from Carnegie Institute of Technology data (reference b)*. Charges 5.00 inches in height were used in each case. The initial and terminal velocities were checked at the Naval Ordnance Laboratory for both the copper and steel cones. Agreement within 2 per cent of the Carnegie data was obtained, and it was concluded that intermediate velocities would also be duplicated. The velocities for the peripherally initiated charges obtained at the Naval Ordnance Laboratory came from charges 2.35 inches high for the steel cones and 3.00 inches high for the copper cones. These charge heights were selected as the ones giving the greatest increase of penetration when using peripheral initiation of the charges.

Note in each case that the emergent jet velocities were always higher for peripherally initiated charges than for the point initiated charges. The increase is much greater for the steel cones (shorter charge height) than for the copper cones (longer charge height). From these results one can say that peripheral initiation does increase jet velocities and hence jet velocity gradients; however, the exact bearing this has on penetration will depend upon the velocity and mass distribution spectra of the jets which have not yet been obtained. Efforts are being directed toward obtaining these distributions but they will not be immediately forthcoming because of complications of the derivations. Initial jet velocities for other charge heights have been obtained to observe how they vary with charge height. The results are tabulated below:

INITIAL JET VELOCITIES
(meters/second)

Charge Height (inches)	Steel cones	Copper cones
3.00		8800
2.35	9330	9410
2.15	11440	
2.00	12660	

* Reference (b) - Sixth Bimonthly Report (CIT-ORD-9) Annual Summary, "Fundamentals of Shaped Charges" dated 30 June 1947 Carnegie Institute of Technology.

94

The initial jet velocities at least increase as the charge height is decreased.

The reasons for shaped charge behavior under peripheral initiation (increased penetrations) cannot be definitely explained by these tests, but one might speculate on the mechanism which increases penetration. For steel liners where the penetrations peak for a single charge height one set of factors (jet velocity, velocity gradient, jet mass, and energy) is optimized at the one charge height. For copper liners on the other hand where penetrations peak for two charge heights two sets of factors must be optimized. For the short charge height such things as jet velocity, mass and energy are optimized; for the longer charge height factors such as jet velocity gradient and jet ductility are optimized. With the short charge the velocity gradient is too strong and the jet is pulled into particles so that full benefit of the optimum jet velocity, mass and energy is not realized. These factors are not optimum for the longer charge height, but this is over balanced by conditions of optimum velocity gradient. These comments are of course only speculations; their possible validity must depend upon further experimental results.

THE PERFORMANCE OF PRECISION-MADE CONICAL LINERS

J. Dewey

H. I. Breidenbach, Jr.

J. Panzarella

J. Longobardi

Terminal Ballistic Laboratory, Ballistic Research Laboratories,
Aberdeen Proving Ground, Maryland

ABSTRACT

Small drawn, cast, and machined cones in bare Pentolite charges have been investigated for a determination of fabrication control necessary for good reproducibility of performance. Explosive casting was carefully controlled. Deliberately introduced flaws in cones produced effects which are usually those predictable from consideration of the time at which each portion of the cone reaches the axis. Flash radiography of the jets supplemented observation of target blocks. Precision cast cones gave about the same reproducibility as drawn cones. Three fabricators made electroformed and machined copper cones of widely differing precision and performance. Warping and metallurgical non-uniformity were sources of large spread in the performance of the products of two fabricators. The third manufacturer produced 3/4" copper cones to 0.1 mil tolerances from which straight jets of uniform penetration were obtained. A 3% cone gave 6.8 cone diameters penetration.

The Terminal Ballistic Laboratory has been investigating the effects of variations in liners on jet performance. In order to radiograph cone collapse, as well as the jet, cones of 3/4" and 1" base diameters have been used. The uniformity of the explosive was investigated by the technique developed in the plastics industry, low voltage radiography of the bare charge. Except very near the edge of a cylinder, where the density gradient is high, this method reveals 2% variations in mass per unit area. In preliminary work, just completed, drawn steel cones and copper electroformed cones of slightly better construction than drawn ones were used. As these have random variations in thickness of the order of 0.001", large deliberate variations and the particular defects characteristic of the method of manufacture were the only ones studied. Figures 1-6 show some results, starting with a jet from a charge having a cavity near the base, for comparison. All the effects shown can be explained by assuming that

thin portions of cones collapse rapidly, not meeting the other portions so as to form a jet. Warped cones, such as are sometimes obtained by drawing and when electroformed cones are removed from a mandrel without annealing, give very poor penetrations.

Very recently cones have been obtained which meet specifications to within a few ten-thousandths of an inch. These are of soft copper, of uniform high density and large grain size. They give straight jets which reach a considerably greater length before breakup than jets from drawn cones, as shown in Figure 7. Figure 8 shows the penetration of jets from these liners, with some Bruceton and Carnegie Institute of Technology results. The 3% cones show considerable spread at optimum stand-off. This stand-off is twice as great as for drawn cones. The results suggest that the rapid decrease in penetration with stand-off usually observed results from wandering, as well as from break-up of the jet. The difference in the shape of the holes in the targets confirms this. Figure 9 shows radiographs of blocks penetrated by jets from various types of cones. The precisely made liners form a slug which always enters the hole symmetrically, filling it. With the 3% liners it was necessary to saw the block to see the hole. When tapered cones of this type were fired, the conical slug formed hung together better, giving a more open hole.

Another difference between liners is seen when stacked or spaced plates are the targets. Penetration is not reduced unless the spacing is large, and no copper is seen around the exit holes. (Figure 10)
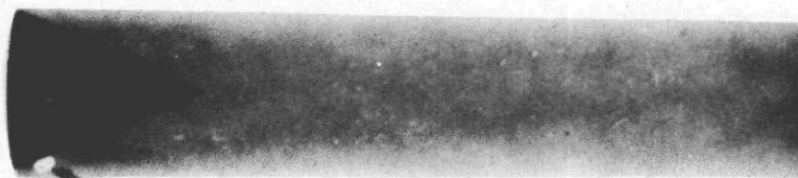
Cavity in Cast H.E.

Dispersed Jet   Slug

Dispersion and Curvature of Same Jet
2 Microseconds Later

NOTE: Radiographs 1 & 2 were made from x-ray
sources 90° apart.

Figure 1—46° copper liner having .015″ radial and .0007″ vertical variation
in wall thickness.   Air bubble in cast H.E. visible.

99

DOUBLE FLASH RADIOGRAPHIC
STUDY OF ELECTROFORMED COPPER CONES
3/4" base dia. , 46°, 0.025" wall
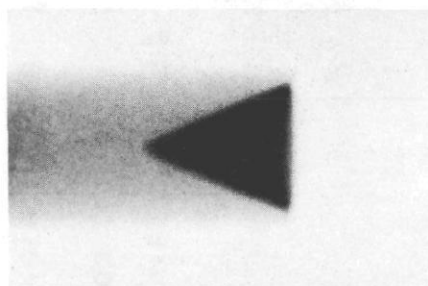
Static

Round
No.

194

VARIATIONS IN CONE WALL
THICKNESS

VERTICAL   (10^{-4} IN.)   RADIAL

12:00 3:00 6:00 9:00   .25 .50 .75
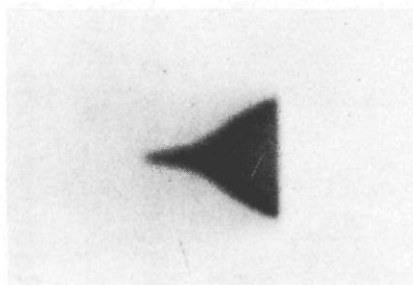
4   2   1   1   3   3   3

Penetration : 3-5/8"
Collapse Angles: Upper 33.5°
Lower 36.25°

Jet Curvature : 7.5°

Figure 2—Double flash radiographic study of electroformed copper cones,
¾" base dia., 46°, 0.025" wall.
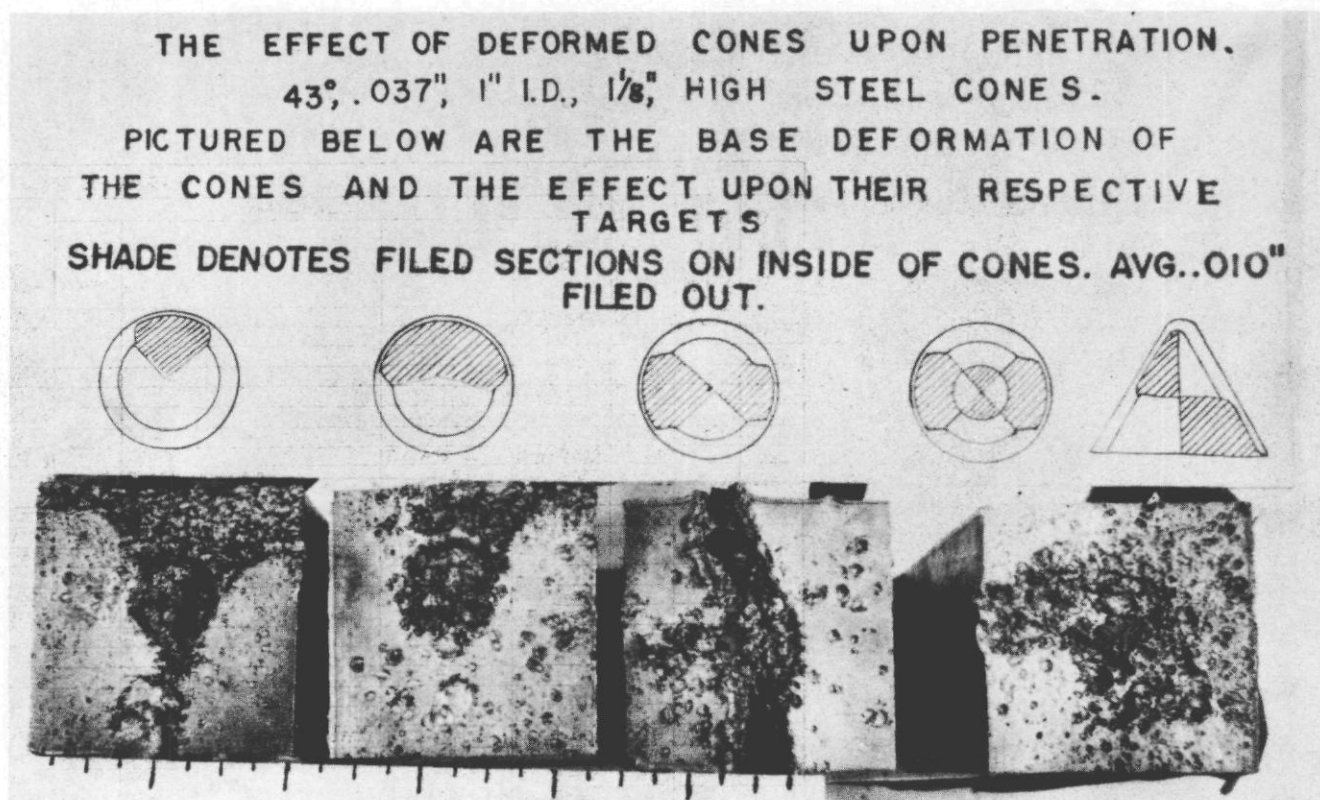
Figure 3—The effect of deformed cones upon penetration.
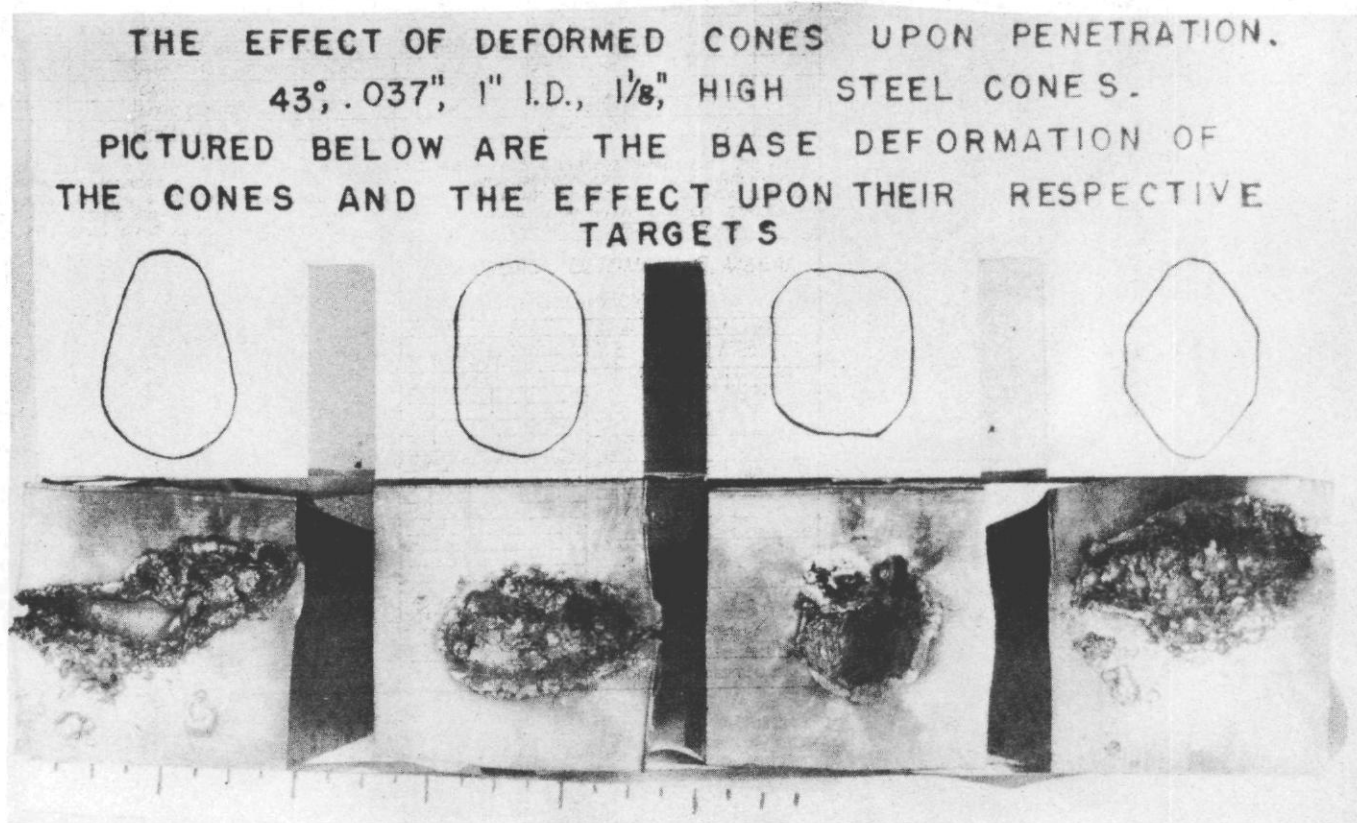
Figure 4—The effect of deformed cones upon penetration.

101

THE EFFECT OF DEFORMED CONES UPON PENETRATION.
43°, .037", 1" I.D., 1⅛", HIGH STEEL CONES.
PICTURED BELOW ARE THE BASE DEFORMATION OF
THE CONES AND THE EFFECT UPON THEIR RESPECTIVE TARGETS
A LINE OF WELD, APPROX. ⅛" THICK, ON EACH CONE FROM APEX TO BASE EDGE.
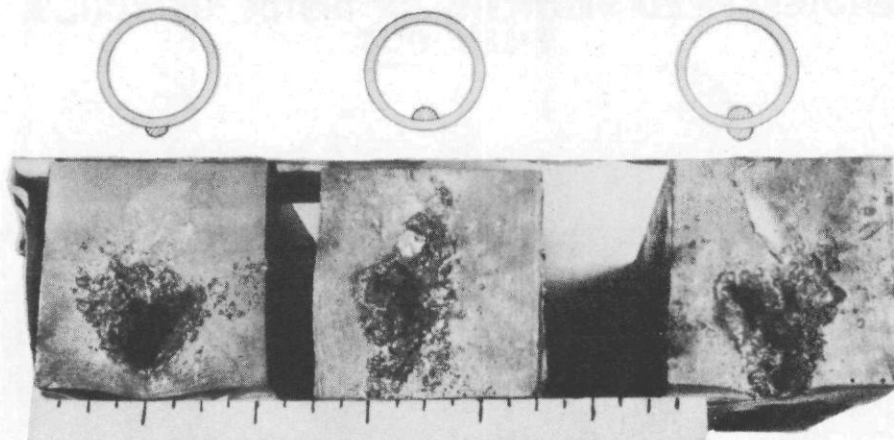
Figure 5—The effect of deformed cones upon penetration.

EFFECT OF THIN WALL SEGMENTS ON STEEL CONES
.037" WALL THICKNESS, 1" I.D.
TARGET, 2" X 2" X 6", 1020 STEEL
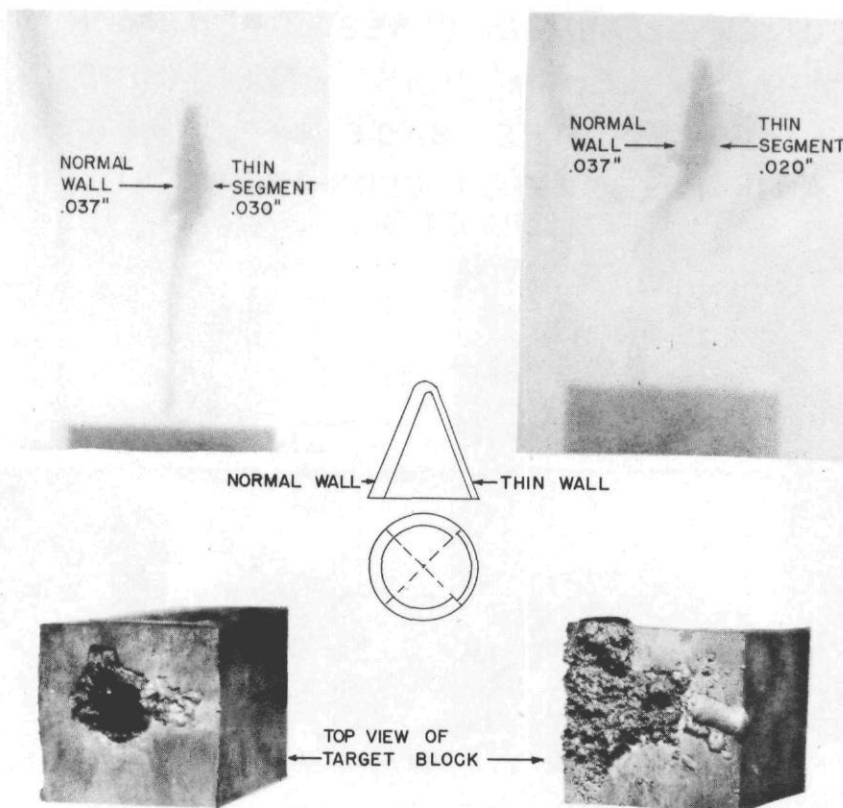
PENETRATION, 1.5 CONE DIAMETERS   PENETRATION, 3/8 CONE DIAMETER

Figure 6—Effect of thin wall segments on steel cones.

102
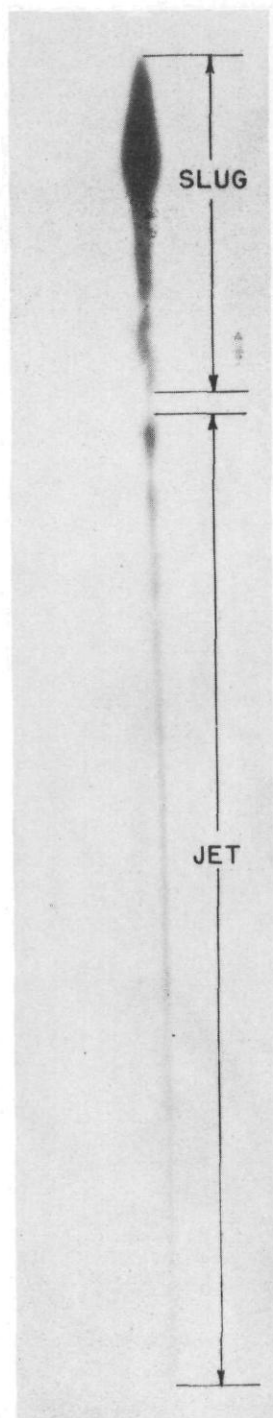
ELECTROFORMED COPPER
.050" Wall, 46°, .75" I.D.
34 us After start of collapse
of cone.

JET LENGTH, 7-3/4"
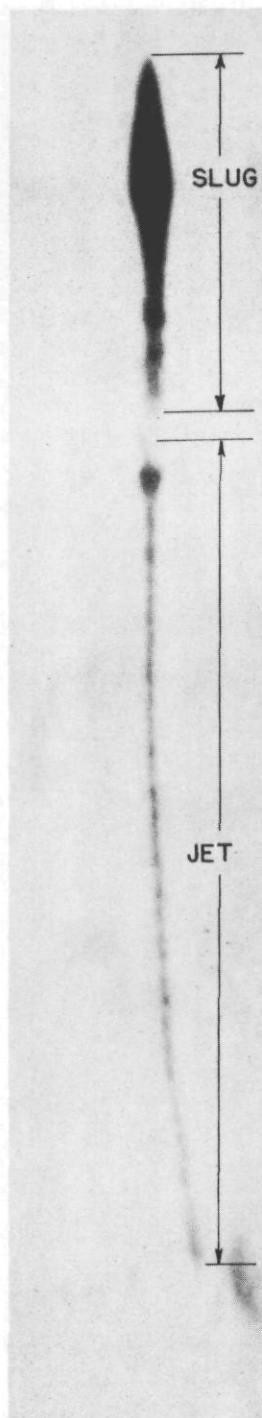
CAST COPPER
.050" Wall, 46°, 1" I.D.
31 us After start of collapse
of cone.

JET LENGTH, 6-1/2"
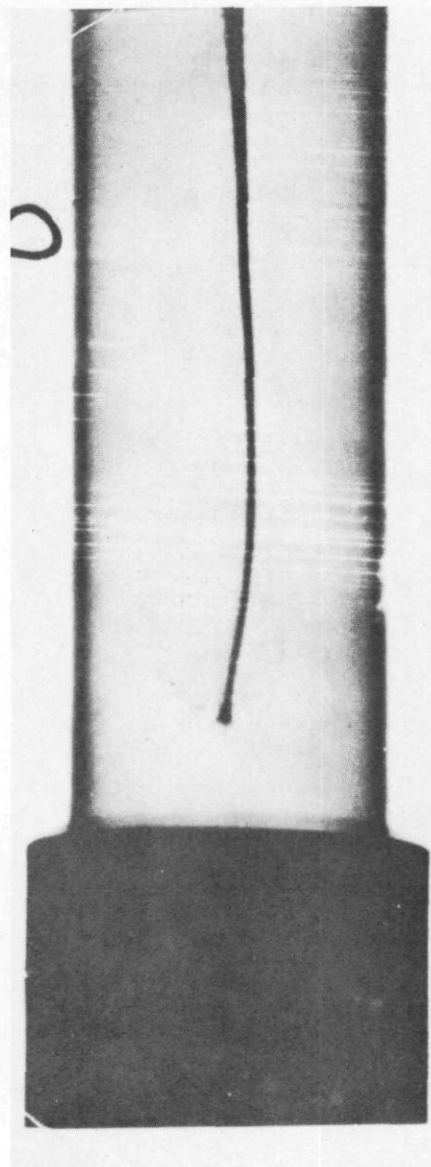
DEEP DRAWN COPPER
.050" Wall, 43°, 1" I.D.
Shot in vacuum, 67 microns, 29 us after
start of collapse of cone.

PENETRATION, 2.75 CONE DIAMETERS

Figure 7—Comparison of jets from different types of cones.

103
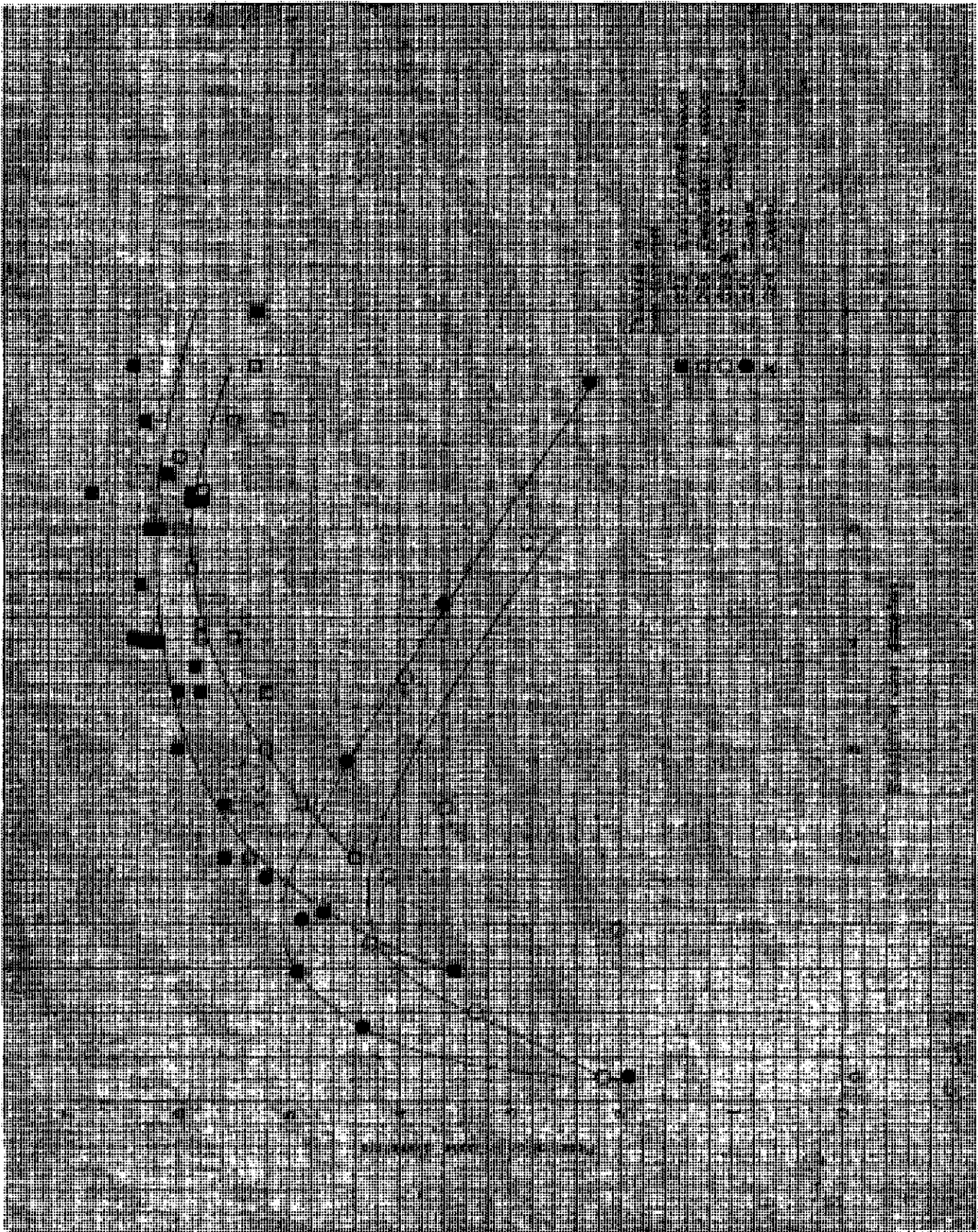
Figure 8—Comparison of penetration by precisely made and drawn copper cones.

COMPARISON OF JET PENETRATION
FROM VARIOUS TYPES OF CONES.
TARGET: 2" X 2" X 6", 1020 STEEL
ALL PENETRATIONS IN CONE DIAMETERS

025" WALL, D-42
PENETRATION, 6.40

.050" WALL, D-12
PENETRATION, 5.35

TAPERED WALL, D-67
.025" APEX TO .050 BASE
PENETRATION, 5.87

.025" WALL, S-73
PENETRATION, 5.50

.025" WALL, C-61
PENETRATION, 5.80

.050" WALL, P-59
PENETRATION, 4.75

.037" WALL
PENETRATION, 3.06

ELECTROFORMED COPPER CONES
.750" BASE I.D.

CAST COPPER CONE
1" O.D.

DEEP DRAWN STEEL CONE
1" I.D.
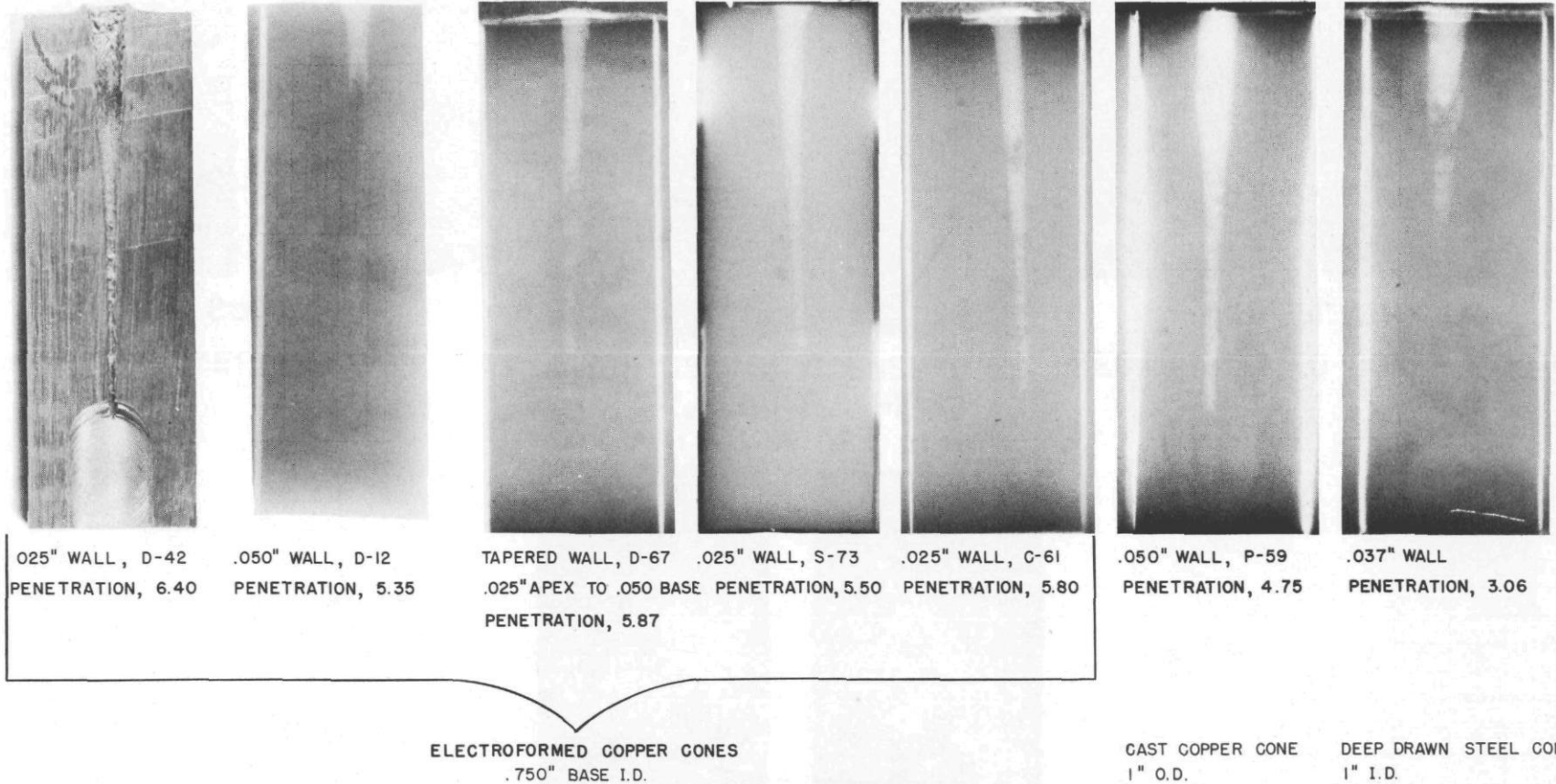
Figure 9—Comparison of jet penetration from various types of cones.

105

SOFT LEAD CONE
JET SPLASH

SPLASH FROM JET FROM
3.5" ROCKET HEAD

STEEL CONE
SPLASH

DEEP DRAWN COPPER CONE

ELECTROFORMED COPPER CONE
NO SPLASH
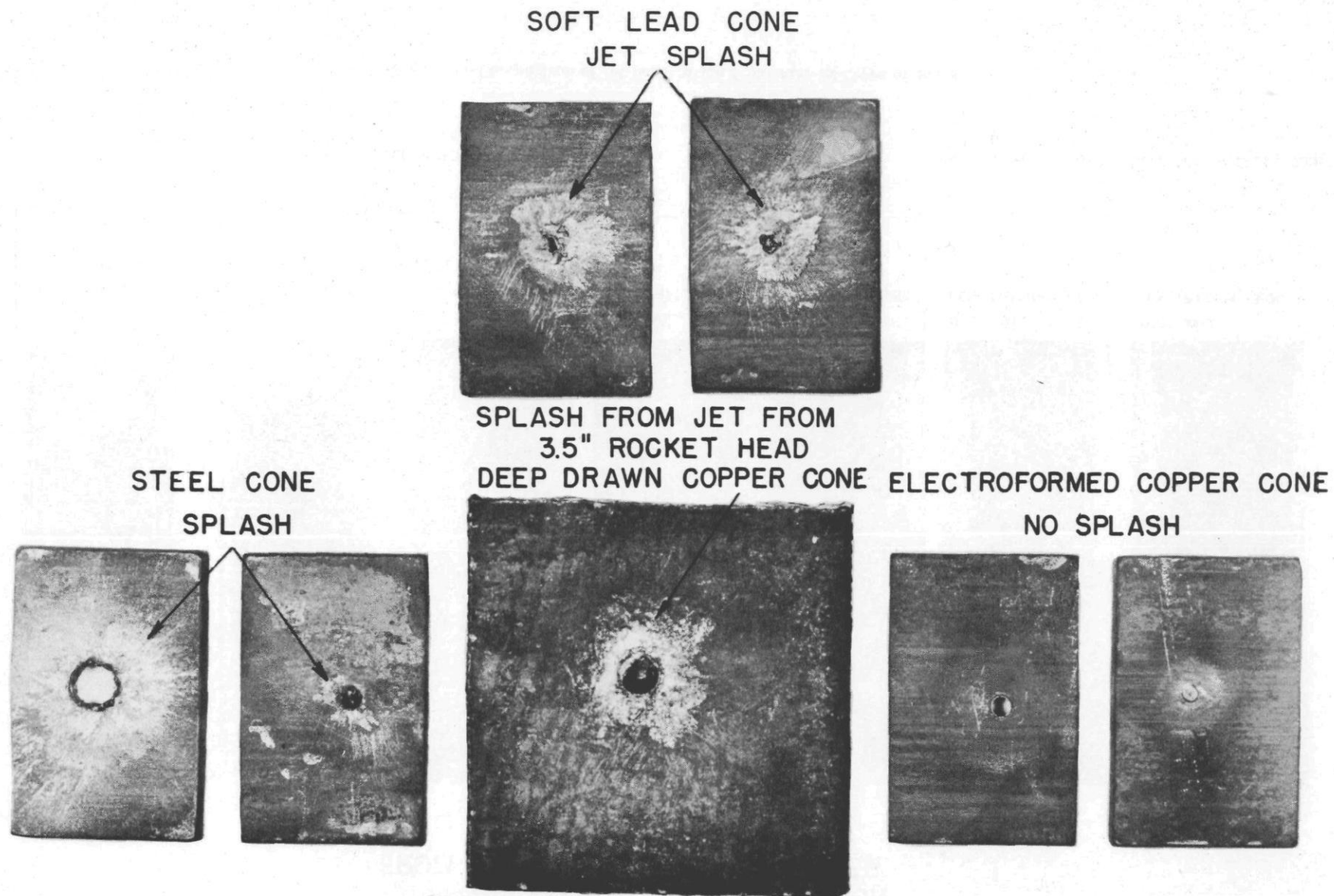
Figure 10—Exit holes of jets from various material cones through steel target plates.

LOW VOLTAGE FLASH RADIOGRAPHY

J. J. Paszek

B. C. Taylor

J. L. Squier

Ordnance Engineering Laboratory, Ballistic Research Laboratories

Flash radiography is generally accepted as being the best means of obtaining direct pictorial presentation of the dynamic performance of shaped charges. Optical methods, although useful in other studies of detonations, are not altogether suitable, due to both the luminescence of the object and the fact that the view is often obscured by material given off by the jet. Flash radiographs give a direct picture of the material in front of the film while optical pictures often require interpretation. Up to now most if not all the radiographic work on shaped charges has been done at voltages of 100 KV, or more. We believe there are advantages in using softer X-rays. A system for taking sub-microsecond duration flash radiographs of shaped charge phenomena using low-voltage (34 KV) X-rays will be described. The system consists of a simplified low-voltage X-ray pulse generator circuit and a method of protecting the X-ray tube and film.

Particular advantages accrue from the use of low voltage. Of prime importance is the ability to get greater detail from objects small in size or of low density. The break-up of a jet, for instance, taken with high voltage X-rays may be lacking in detail due to the transparency of the smaller particles of the jet to the X-rays. Likewise, materials of low atomic number such as aluminum which would be almost transparent to high voltage X-rays show up quite well when the voltage is reduced. When working with low voltages, the useful life of the X-ray tube is not directly determined by arc-over along the inner wall of the tube. The inner wall of a flash X-ray tube becomes coated with a metallic coating as it is flashed and, when this coating becomes heavy enough, arc-over along the wall may occur. In addition, other practical advantages result from the use of low voltages. The equipment is simplified considerably. Components are less expensive and much more readily obtainable. Corona which plagues all high voltage equipment is all but eliminated, making possible the use of the equipment in the field even under high humidity conditions. The equipment becomes compact and light in weight. A photograph of the original equipment is shown in Figure 1. By using smaller components (standard catalog items) the equipment can be made small enough to fit into a 5 cubic foot carrying case permitting full portability. Flash radiography is thus taken out of the category of special laboratory equipment and becomes a general purpose tool.

It may be of interest to relate briefly how the present circuit evolved, at the same time giving acknowledgement to those who were of assistance to the authors. As part of the Ordnance Engineering Laboratory's program for shaped charge investigation flash radiography was required. An order had been placed for a flash X-ray unit of the type developed by H. I. Breidenbach and described in published reports.[1,2] This circuit has been in use since 1947 by the Terminal Ballistics Laboratory.
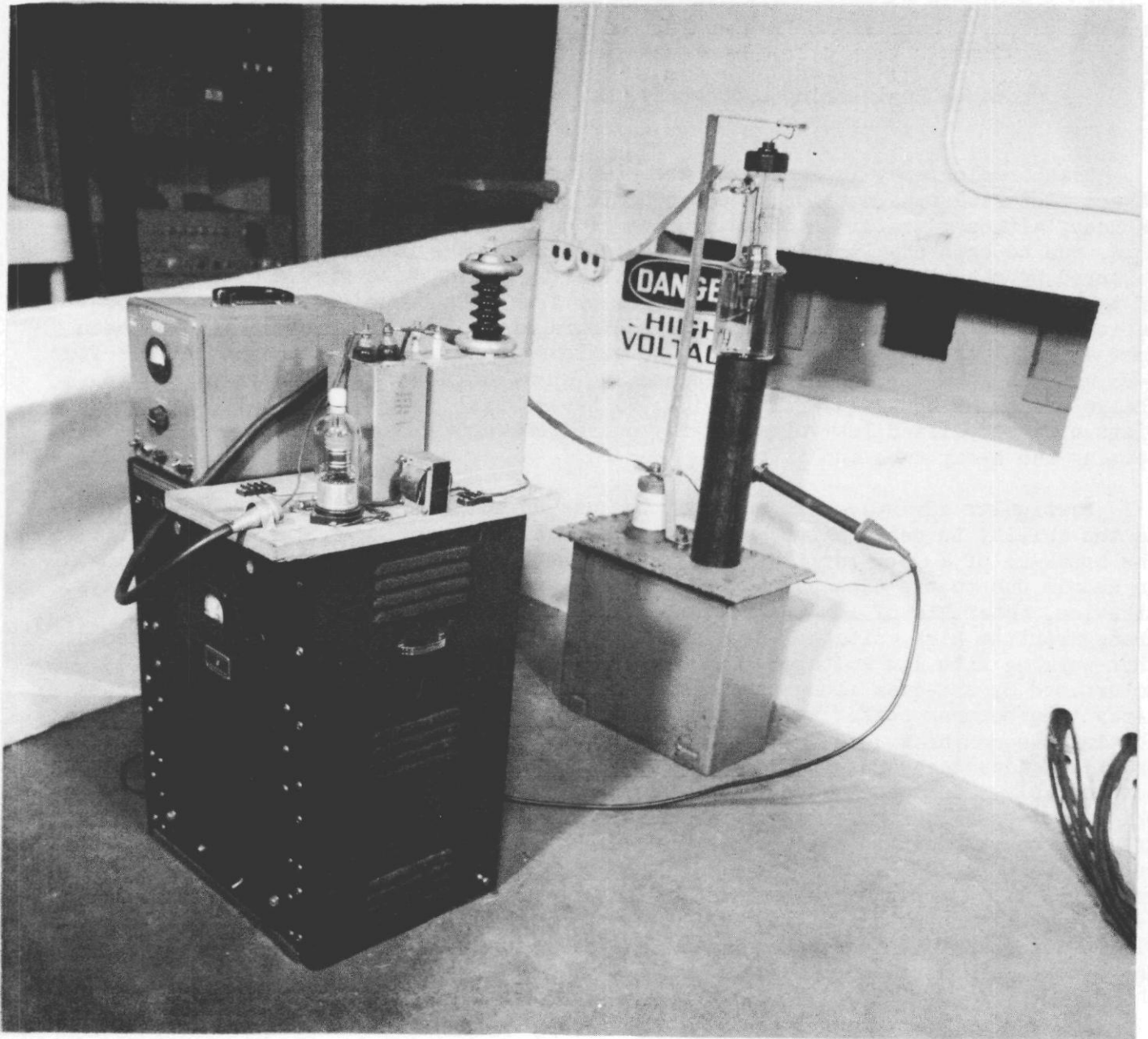
Figure 1

While we were waiting for the delivery of this equipment, R. O. Fleming[*] of Old and Barnes, Inc. visited this laboratory and delivered a paper entitled, "A Simple Flash X-Ray Circuit".[3] In addition, Fleming gave us personal instruction as to how to reproduce his circuit. An attempt to duplicate Fleming's circuit using available components was unsuccessful. It should be emphasized that the use of substitute components prevents us from making a proper appraisal of his circuit. The low voltage X-ray circuit which is the subject of this paper came into being as the result of our being required to work with components at hand.

Brief reference has been made to three X-ray circuits. The Breidenbach circuit is not typically a low voltage circuit and thus will be described only briefly. The basic circuit is shown in Figure 2. It uses a Westinghouse WL-389 three electrode cold cathode field emission X-ray tube operated at approximately 100 KV.[4,5] This tube has a trigger electrode, mounted very close to the cold cathode, which is used to initiate cathode-to-anode breakdown. In the circuit of Figure 2 the trigger electrode voltage is derived from the anode voltage, so that the anode voltage must be at least as high as that required to break down the trigger gap. As we shall see this voltage is relatively high.

The Fleming circuit operates at a cathode to anode voltage of 80 KV. The circuit is unique in the manner in which it makes possible the use of a two electrode tube. Reference to figure 3 will reveal the basic circuit. The tube is the very small 45 X dental X-ray tube made by Amperex. While this tube has a filament, it is used here as a cold cathode tube. A capacitor is connected between anode and ground, while the secondary of a pulse transformer is connected between ground and cathode. Effectively, the capacitor and the pulse transformer are in series. Fleming gives B. Cassen the credit for suggesting this connection of the transformer. The capacitor is charged to 40 KV positive by means of a small r.f. type power supply. A simple pulsing circuit (not shown) supplies a negative 10 KV pulse to the primary of the 4:1 step-up ratio transformer. The 40 KV across the capacitor is alone insufficient to break down the tube. The additional negative 40 KV pulse raises the total cathode to anode voltage to 80 KV causing the tube to flash. Triggering is thus accomplished by direct cathode to anode pulsing without the use of a trigger electrode.

Our reproduction of the Fleming circuit used substitute components. The tube was a Machlett LCP-L, which is a small size dental X-ray tube. The power supply provided 34 KV instead of 40 KV. The pulse transformer had a 10:1 step-up ratio and consequently a higher secondary impedance. Using these components we were unable to produce X-rays.

In addition to the power supply and the pulse transformer mentioned above we had, at the time, several 1 mfd. capacitors rated at 25 KV and one WL-389 X-ray tube. As previously stated, the WL-389 is a three electrode cold cathode field emission X-ray tube having, in addition to the cathode and the anode, a trigger electrode. Availability of the WL-389 suggested a return to a circuit utilizing a three electrode tube. Direct cathode to anode pulsing is not practical inasmuch as the breakdown voltage of the WL-389 may be as high as 100 KV or more. Properly used, the trigger electrode, which is mounted very close to the cathode, can cause the tube to flash at lower

---

[*] Now of Microtime Laboratories, Los Angeles, California.
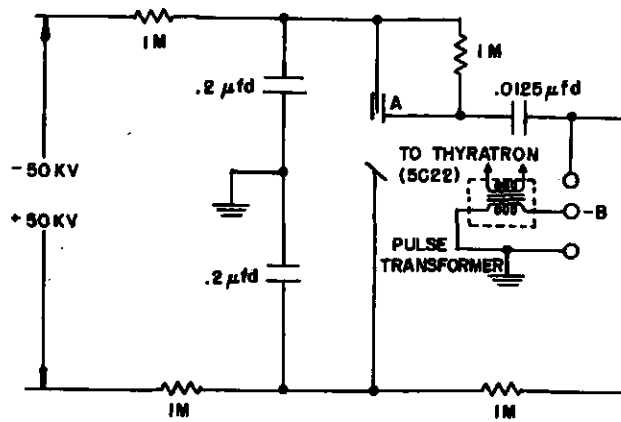
Figure 2
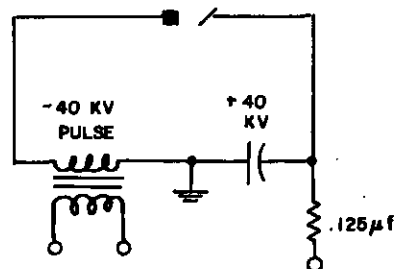
Figure 3

Figure 4

Figure 5

110
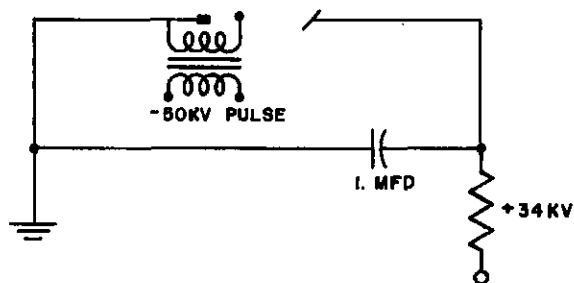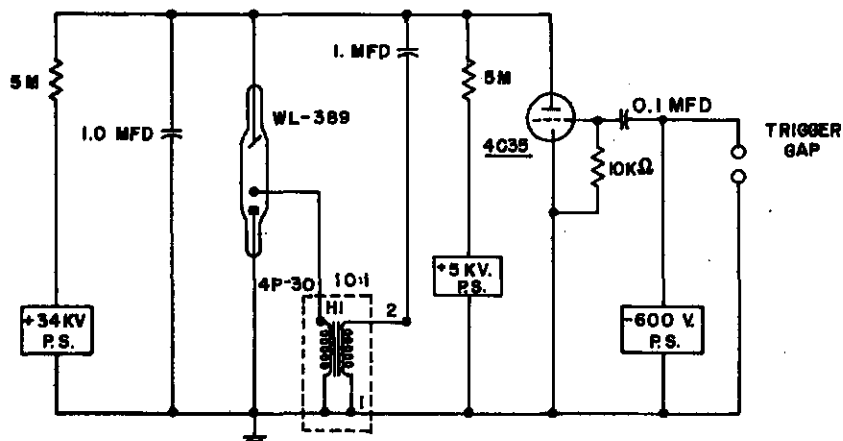
voltages. Circuits that use some fraction of the anode voltage as the trigger voltage require the anode voltage to be at least as high as that needed to break down the trigger gap. Being limited by the 34 KV power supply, our problem was to flash the tube with only this voltage on the anode. This was accomplished by connecting the pulse transformer directly to the trigger electrode so as to apply a negative trigger pulse between the trigger electrode and the cathode. This connection made it possible to trigger the tube independently of the anode voltage, permitting operation of the tube at an anode voltage as low as 17 KV.[*] A 50 KV trigger pulse proved necessary to flash the tube reliably.

The simplified schematic shown in Fig. 4 will help make clear what has just been stated. The circuit consists of a 1 mfd. capacitor with the positive terminal connected to the anode of the X-ray tube, and the negative terminal connected to the cathode. The secondary of the trigger transformer is shown connected between the trigger electrode and the cathode. A small pulsing circuit (not shown) applies a pulse across the primary winding of the transformer. The resultant secondary pulse breaks down the trigger gap, causing the tube to flash.

The operation of the complete circuit is best understood by referring to the schematic diagram shown in Fig. 5. A 1 mfd. capacitor is again shown connected between the cathode and the anode of the WL-389 X-ray tube. The capacitor is charged, through the 5 megohm isolating resistor, by the 34 KV r.f. type power supply. This voltage is insufficient to break down the tube and will, therefore, remain across the tube until some additional energy is supplied to break it down. This is accomplished by applying a negative 5 KV pulse to the primary of the 10:1 step-up ratio transformer. The resultant 50 KV pulse which appears at the trigger electrode causes an initial breakdown between the trigger and the cathode, which in turn causes a breakdown between cathode and anode. This allows the 1 mfd. capacitor to discharge through the tube, producing a burst of X-rays. The WL-389 X-ray tube is thus made to flash with an anode voltage lower than that required to break down the trigger gap.

The negative 5 KV pulse is provided by the trigger circuit which is included in the schematic in Figure 5. A 1 mfd. capacitor is shown connected in series with the primary of the pulse transformer. One side of this capacitor is grounded, under static conditions, through the transformer primary winding while the other side is charged to a positive 5 KV level by the power supply. A 5 megohm resistor serves to isolate the power supply from the rest of the circuit during pulsing. The plate of the 4C35 hydrogen thyratron tube is connected directly to the positively charged side of the 1 mfd. capacitor while its cathode is connected to the grounded terminal of the pulse transformer primary winding. No bias is needed on the grid of the thyratron tube to hold off 5 KV. A 1 mfd. capacitor is connected in the grid circuit of the thyratron tube. One side of the capacitor is grounded, under static conditions, through the 560 ohm grid leak resistor; while the other side is charged to a negative 600 volt level by the 600 volt power supply. The trigger gap serves to initiate the trigger circuit when its terminals are shorted.

Shorting the trigger gap raises the negatively charged side of the 0.1 mfd. capacitor to ground potential, causing the oposite side of the capacitor to rise

---

[*] It has recently come to our attention[6] that the Germans had used a circuit exactly like this at high voltages (100 KV) without apparently realizing the advantages of the lower voltages.

suddenly in a positive direction producing a pulse at the grid of the thyratron tube.
The normally non-conducting thyratron tube now conducts, shorting the positively
charged side of the 1 mfd. capacitor to ground. This produces a negative going
pulse on the opposite side of the capacitor which develops across the transformer
primary winding. This voltage is applied thru the transformer to the trigger elec-
trode which causes the tube to flash.

It might be appropriate to say a few words about the components used in the
circuit described. Except for the X-ray tube, all the components are standard
catalog items and can be purchased for a total cost of less than $1,000.00. The
power supplies are small units of the r.f. type. Less than one milliampere output
is required of these supplies. The capacitors used are filter type capacitors. The
1 mfd. capacitor is rated at 25 KV and was obtained from surplus at a cost of $75.00.
It has been used at voltages up to 50 KV. The pulse transformer is a Westinghouse
4P-30. Although the secondary is rated at 36 KV, no trouble was experienced as long
as the input voltage did not exceed 5 KV. Two transformers failed at higher voltages.

Once the circuit was completed the immediate questions that arose were those
concerning flash duration, resolution, and X-ray output. At present these questions
are best answered by the results obtained from the application of the circuit to jet
radiography.

The first tests were made with small 3/8" diameter copper lined shaped charges
or spitters which proved ideal for testing the low-voltage flash X-ray unit. Three
radiographs of the jets from these spitters are shown in figures 6, 7, 8. DuPont jet
tappers, 1-3/4" diameter shaped charges with conical copper liners, were also used to
test the circuit. The radiographs in figures 9, 10, 11 show the jets from these
charges. The spitter radiographs are the more interesting at this point in that they
provide a good deal of information on the performance of the circuit. Note that the
jet breaks up into small particles some of which are little larger than the head of
a pin. This fact permits direct estimation of particle resolution and flash duration.
The fine resolution and excellence of detail shown in these pictures illustrates and
lends support to our contention that low-voltage X-rays are particularly suited to
jet studies. The tip velocity of the spitter jet is known to be approximately 1/4"
per microsecond. Some of the particles in the leading portion of the jet are less
than 1/16" in length, as measured along the direction of jet travel. Now the length
of the smallest particle in the leading portion of the jet is indicative of the
effective duration which can be inferred from an estimate of the maximum amount of
blurring of the jet particle. The amount of blurring is estimated by assuming that
the length of a given small tip particle represents the distance through which a very
small particle has moved during the duration of the flash.

The spitter pictures indicate a very short effective flash duration, whose
upper limit is conservatively estimated at 1/4 microsecond. This should surprise
the reader as much as it did the authors, if one remembers that the capacitor across
the X-ray tube has a value of 1 mfd. and is not constructed so as to have low in-
ductance. For this reason it seems better to speak of effective flash duration
rather than actual flash duration. It is likely that the operation of the WL-389 at

Figure 6

Figure 8

Figure 7

0   1   2   3   4

INCHES

113
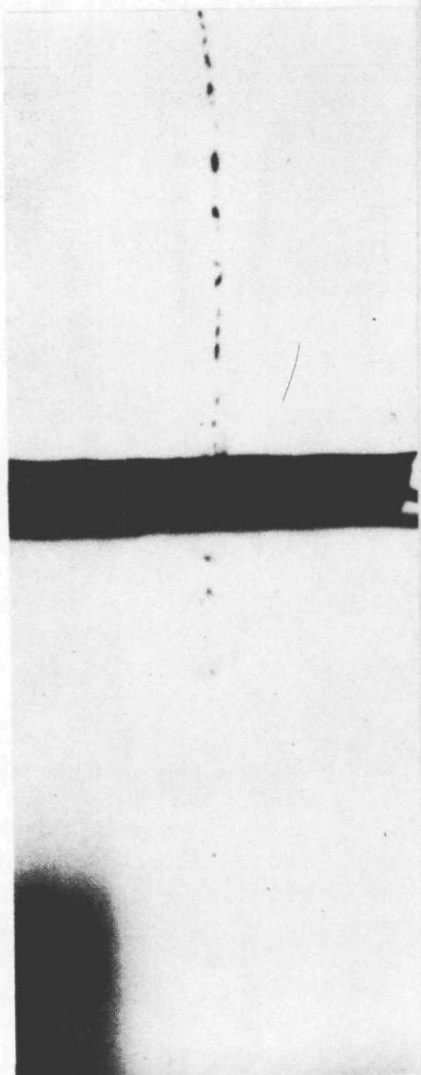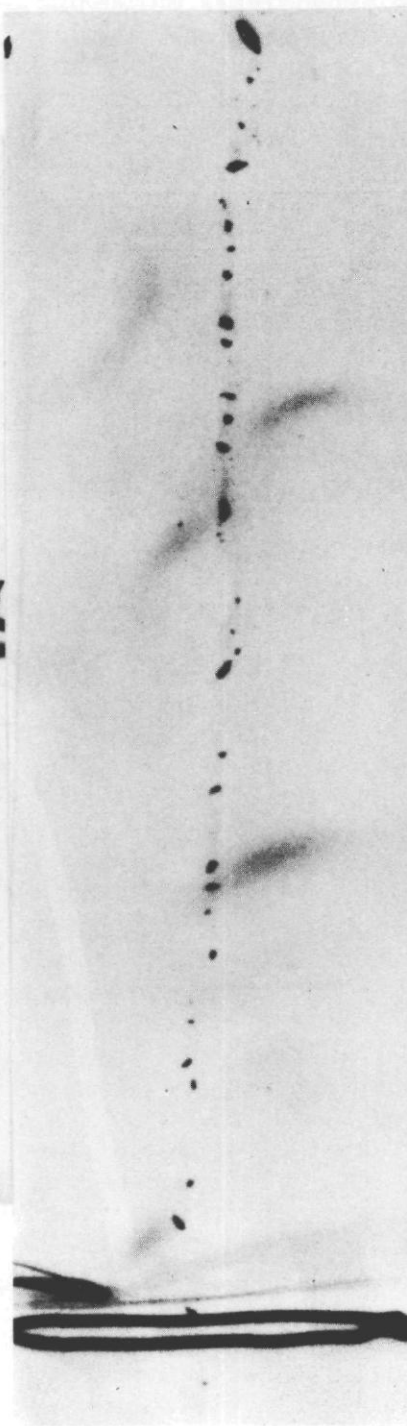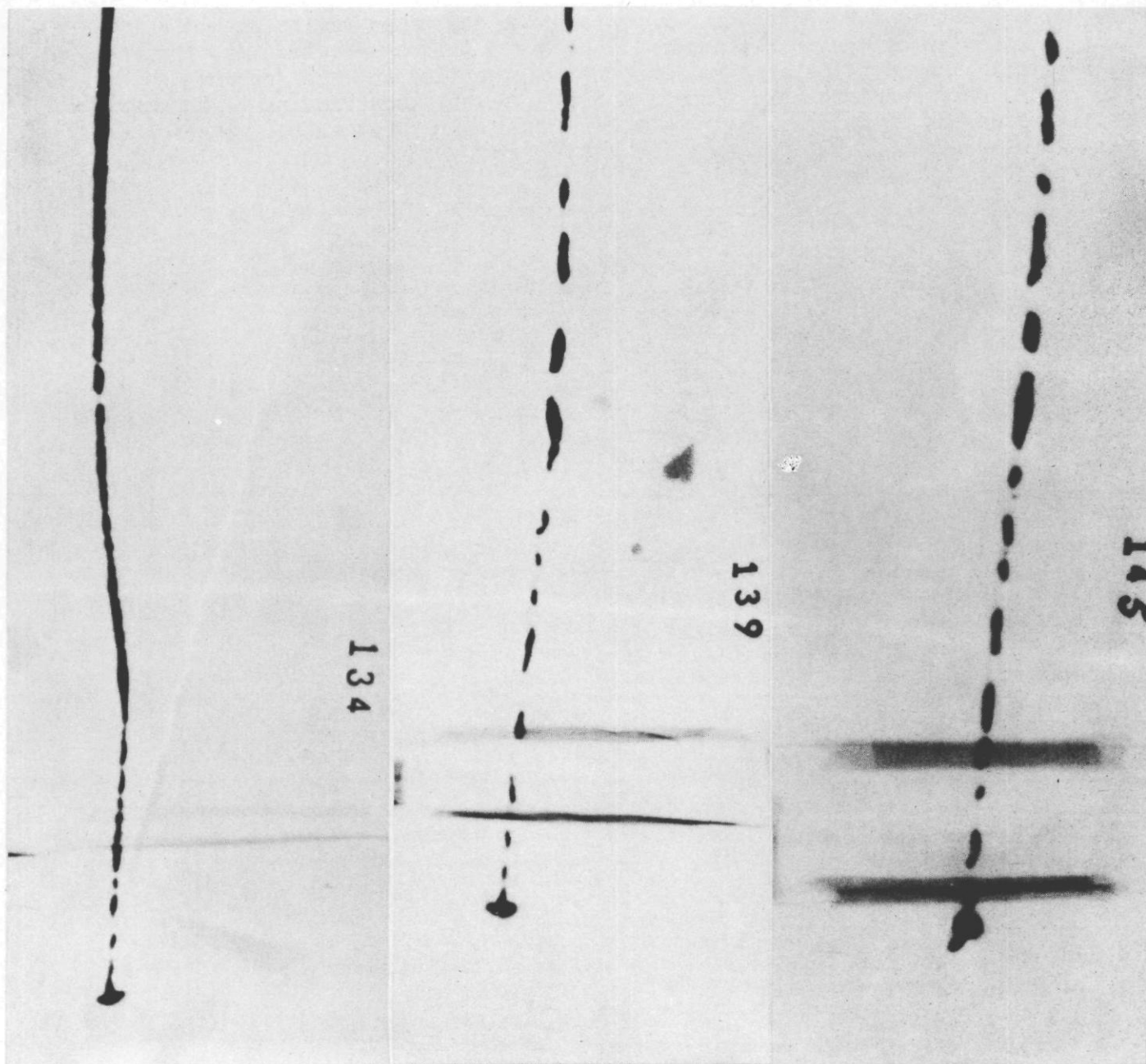
Figure 9

Figure 10

Figure 11

a low voltage causes the effective output to be of shorter duration than the total flash. For instance, the thick glass wall of the tube does not transmit the very soft X-rays. Likewise, the spectral response of the film and the screens may be such as to record or respond to only a portion of the flash, thus serving to shorten the effective exposure duration. The possibility that a low voltage arc within the tube terminates X-ray output soon after it begins has not been overlooked. [4,5] It is the intention of the authors to examine the problem of exposure duration in greater detail. Presently, however, it is interesting to note that even the simple and relatively crude flash X-ray equipment that has been described is capable of producing such a short effective flash duration.

The film used in all our work is Kodak Type F Industrial X-Ray Film. DuPont Fluorazure (zinc sulfide) intensifying screens were chosen because of their sensitivity to soft X-rays.

Additional radiographs revealed further information about circuit performance. It was found that approximately every third flash was a double flash closely spaced in time (Figure 8). It has been reported [2] that reducing the resonant frequency of the trigger circuit has helped to eliminate multiple flashes. We do not yet know whether the double flashing indicates a retention of control by the trigger circuit, or whether the multiple flash is due to some other mechanism. We hope to control the multiple flash. However, we have found that such double exposures furnish a unique and accurate method for determining the velocity gradient along the jet since they provide two superimposed images of the jet slightly displaced in time.

Of more concern is the observed fact that, at 34 KV, every fourth flash is of too low an intensity to be useful. This is most probably due to the fact that the WL-389 X-ray tube was originally designed to be used at approximately 300 KV. Several avenues are being explored in hope of obtaining a more suitable tube. A modification of the WL-389 may prove to be the solution; however, work is being done at this laboratory by G. Hauver and G. Bryan on a small, low cost X-ray tube. This work is reported in the paper following this one in the Transactions of the November 1951 Shaped Charge Symposium, entitled, "Expendable Flash X-Ray Tube." Present efforts promise solution of the problems mentioned. Moreover in practice the advantages of the low voltage system far outweigh its present limitations.

The low voltage flash radiography circuit was originally developed to investigate the jets from 105mm. steel cased rounds. Accomplishment of this, however, hinges upon devising a suitable method for protecting the tube and film from fragments and blast. The 105mm. steel cased round presents a very difficult shielding problem as it is necessary to place the film very close to the jet in order to get good definition. This stems from the fact that the tube is not a point source of X-rays, so that unless the penumbra effect is minimized a sharp image will not be formed. In order to reduce the penumbra the film to jet distance must be made as small as possible. Making the tube to jet distance large will also improve definition, but the X-ray intensity will fall off as the inverse square of the distance. In practice, the film to jet distance is of the order of 6 inches and the tube to jet distance is of the order of 74 inches.

We have said that low voltage X-rays are particularly suited to jet investigation because they are stopped by low density materials. But this means that very

Figure 12

584

584

584
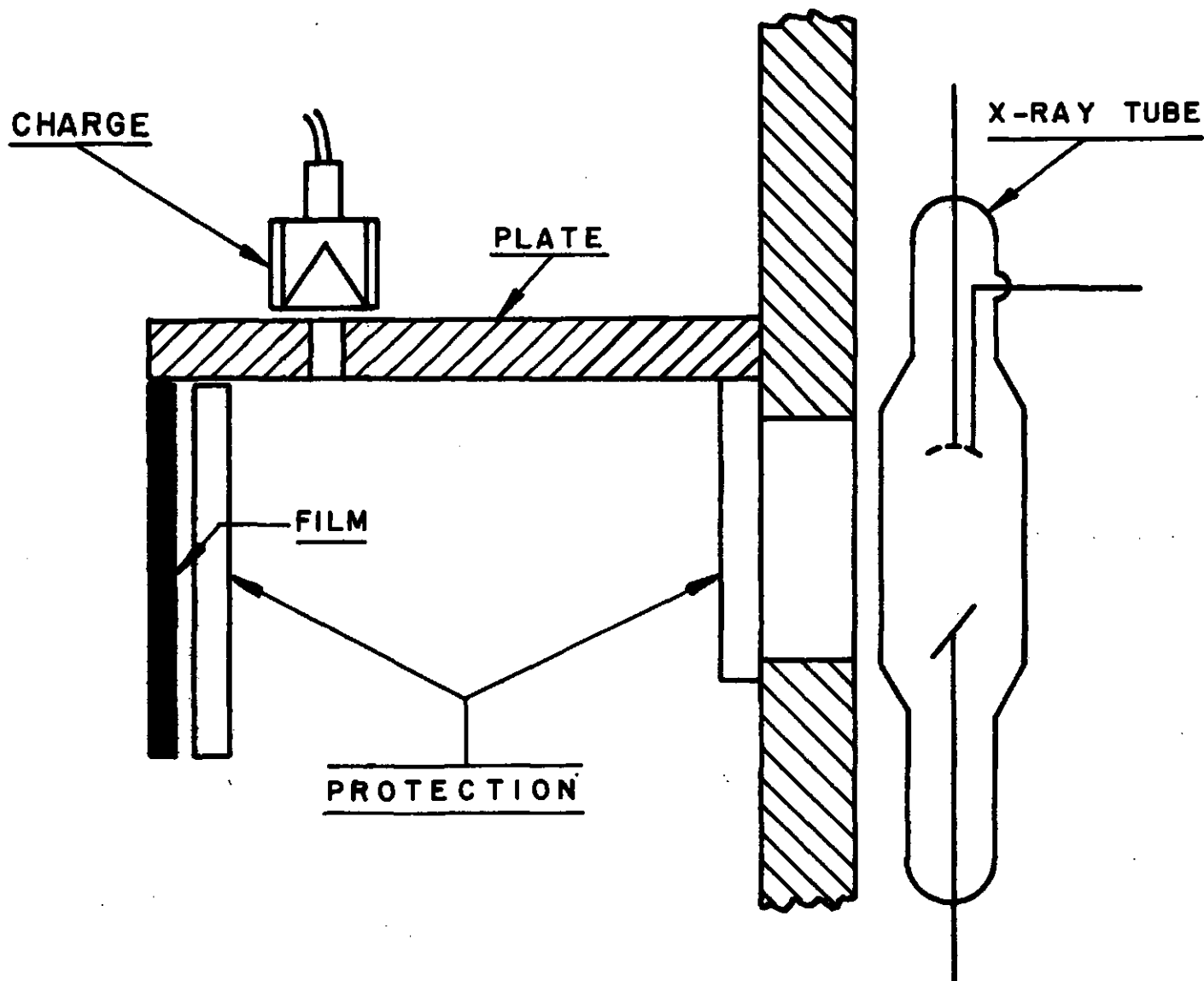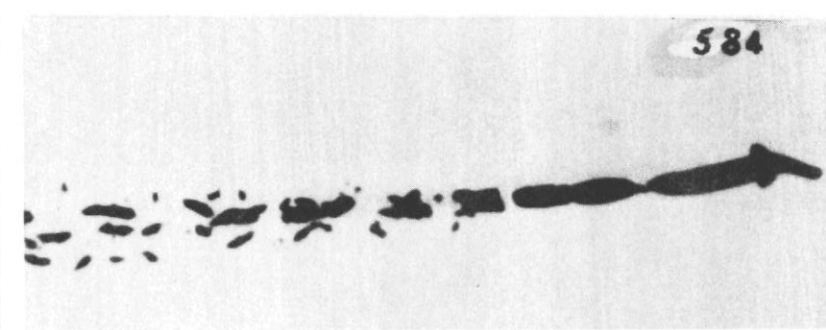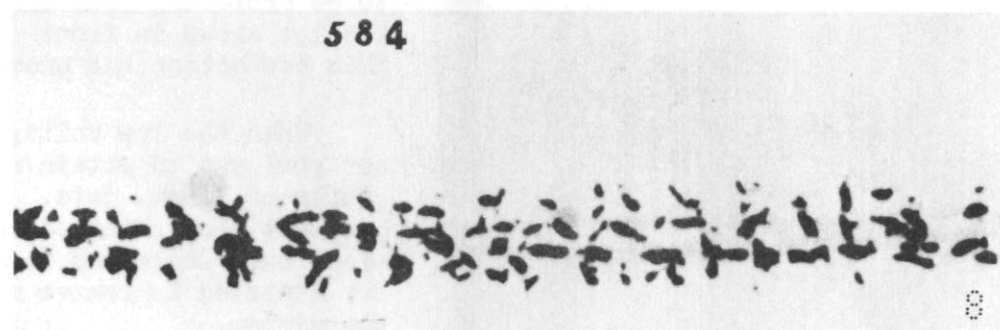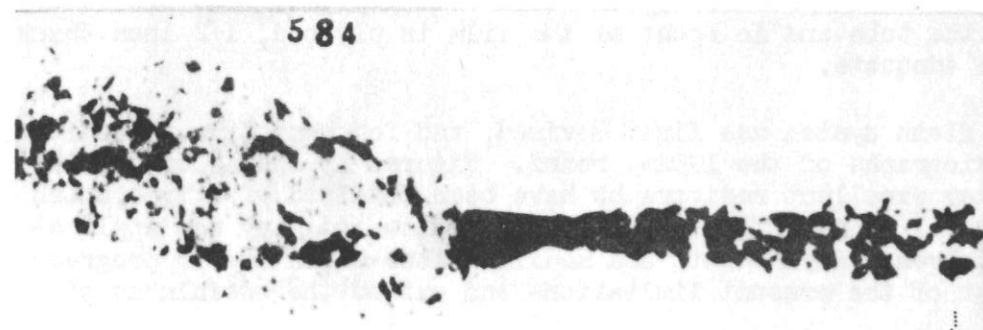
FIGURE 14

FIGURE 13

0 1 2 3 4
INCHES
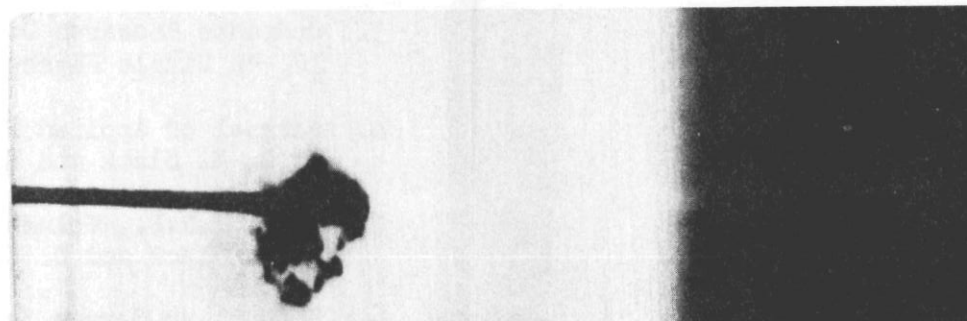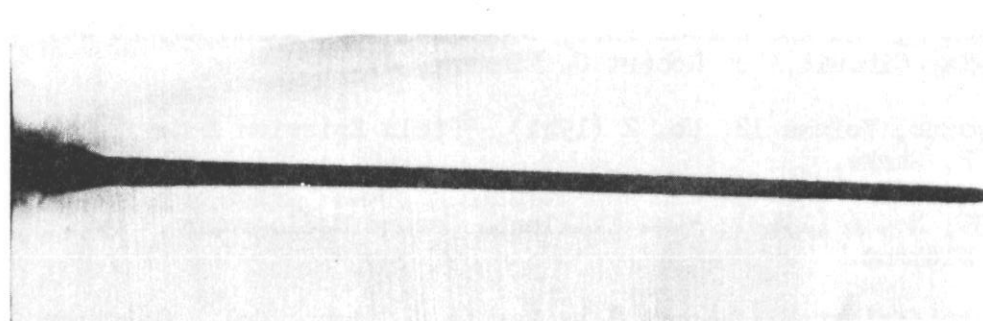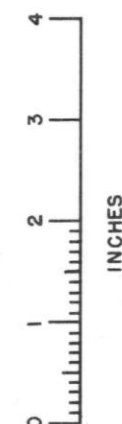
little blast and fragment shielding material may be placed in front of the film and in front of the tube. The problem is solved by obtaining this protection outside of the tube to film path.

Figure 12 shows how this is done. The X-ray tube is mounted behind a steel plate through which a small window has been cut. A second plate is mounted, horizontally, against the first plate and above the window. The round is placed above the horizontal plate and fired downward (through a small hole) past the film, which is mounted below the plate. By this device the tube and the film are shielded from most of the blast and all of the fragments from the round. The tube and the film now need to be protected from only the shock produced by the high velocity jet. The protection shown in front of the tube and in front of the film is plywood, 1/2 inch thick. This protection has proved adequate.

When the low voltage flash system was first devised, and for some time thereafter, our goal was to obtain radiographs of the 105mm. round. Figures 13 and 14 are radiographs of 105mm. jets. Many excellent radiographs have been obtained of a type which have not been obtained before. The system has proven its value and many new applications have suggested themselves. Refinements and modifications which are in progress are expected to remove most of the present limitations and extend the usefulness of the system.

REFERENCES

1. Ballistic Research Laboratories Report No. 678, "Ultra-Fast X-Ray for Multiple Radiography," by H. I. Breidenbach, March 1949.

2. Review of Scientific Instruments, Volume 20, No. 12, December 1949, "A Fractional Microsecond X-Ray Pulse Generator for Studying High Explosive Phenomena," by H. I. Breidenbach.

3. Ordnance Research Division, Old and Barnes Inc., Technical Memorandum Report No. 16, "A Simple Flash X-Ray Circuit," by Robert O. Fleming, Jr.

4. Journal of Applied Physics, Volume 12, No. 2 (1941), "Field Emission X-Ray Tube", by C. M. Slack and L. F. Ehrke.

5. Proc. I.R.E., Volume 35, No. 6 (1947), "One Millionth Second Radiography," by G. M. Slack and D. C. Dickson.

6. "Report on German Scientific Establishments," by Leslie E. Simon, Col., Ordnance Department, September 1945, Office, Chief of Ordnance, Washington, D. C., Page 144.

FLASH RADIOGRAPHIC STUDY OF JETS FROM UNROTATED 105MM SHAPED CHARGES*

L. Zernow

S. Kronman

J. Paszek

B. Taylor

Ordnance Engineering Laboratory, Ballistic Research Laboratories,
Aberdeen Proving Ground, Maryland

ABSTRACT

Jets from conical copper and iron lined shaped charges of
105mm caliber are compared at various jet lengths. The early
breakup of iron into a particle jet is clearly shown. The taffy-
like streching of the copper jet due to the velocity gradient is
also quite evident.

Jets from copper trumpet and hemispherical liners which per-
formed poorly in penetration tests are shown to be badly formed
and associated with an unfavorable velocity distribution along the
jet.

HISTORICAL

Ever since the first pioneering work of J. C. Clark, and independently of the
British and the Germans, flash radiography of shaped charges has been confined to
small charges. The largest charges reported in the literature have been of the order
of 1.5 inches in diameter with most of the work being done in the 1" diameter range.
This is attributable to two things. First, the major interest in the early days was
in the collapse of the liner. Secondly, the blast shielding problem appeared to be-
come rapidly more troublesome with the increased mass of high explosive, and it was
therefore easier to work with small charges.

MOTIVATION FOR PRESENT WORK

Examination of the best flash radiographs available indicated that although the
collapse process seemed to be as clearly delineated as the small cone size would allow,
there was a serious gap in the available radiographic detail of the jet itself. This
was partly due to the fact that the jet from a small charge was difficult to radiograph
clearly, especially in the early days when the flash durations were of the order of one
microsecond. Even with newer techniques claiming shorter flash durations, radiographs
of the jet left much to be desired in the way of detail because most of the radiographs
were taken under conditions necessary for the collapse to be visible, and these were
definitely not the best for showing up jet detail.

---

* Also published as Ballistic Research Laboratories Report No. 802.
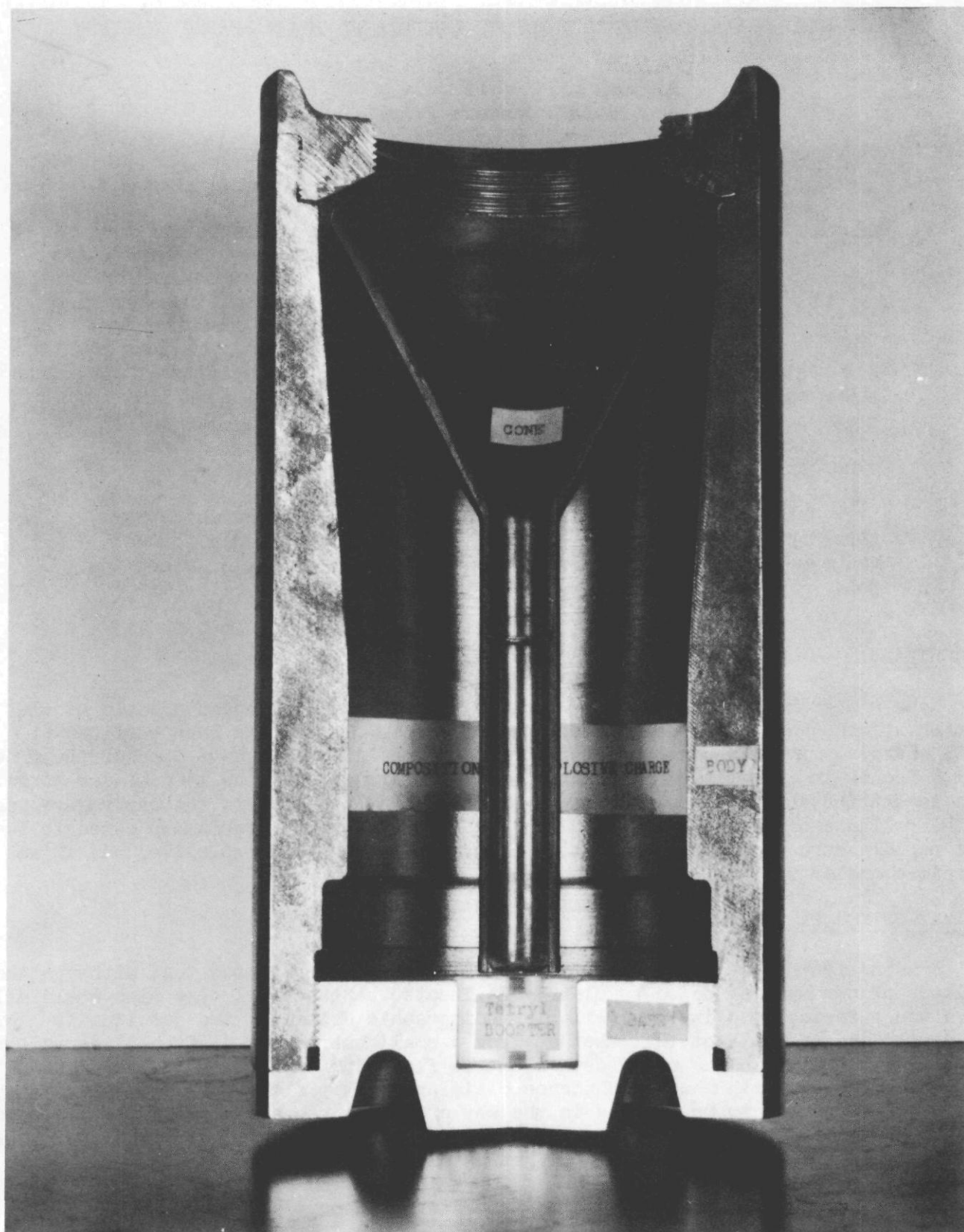
Figure 1—Cut-away view of the 105 mm projectile used in the experiments.

120

CHARGE

ARMOUR PLATE

BARRICADE
WALL

JET

FILM
HOLDER

TUBE
SHIELD

X-RAY
TUBE
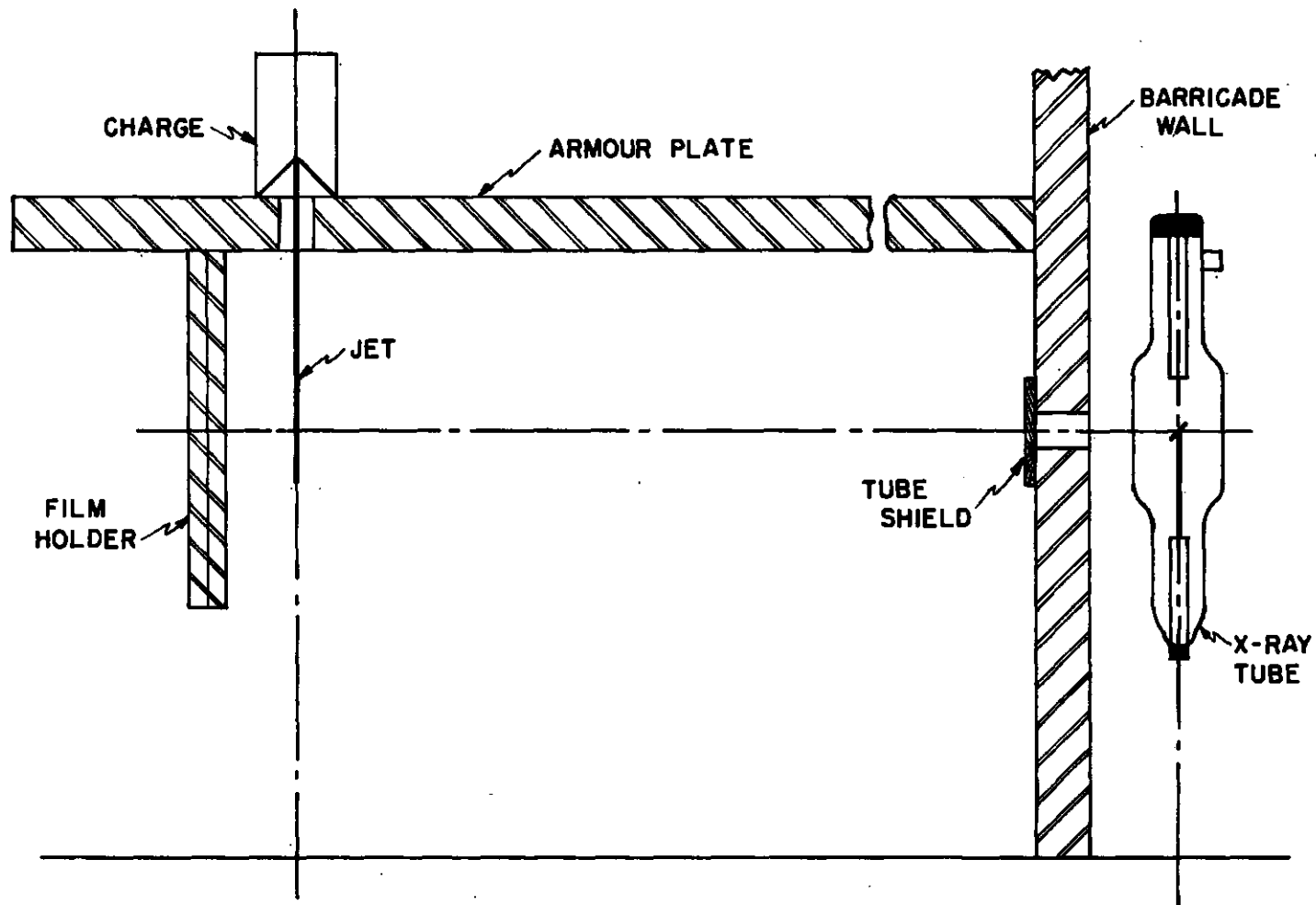
Figure 2—Sketch of field set-up for flash radiography of shaped charge jets.

In the work of this group with large caliber shaped charges (90mm and 105mm caliber), it had been found in the penetration studies that large improvements in both uniformity and performance level could be achieved with larger caliber liners. We therefore expected that if flash radiography could be applied to the study of these large liners, one could achieve from this alone an improvement in the visible details of the jet. Furthermore if these studies were separated from collapse studies, conditions more favorable to jet examination could be achieved.

The low voltage flash radiographic technique developed by Paszek and Taylor[1] was well suited for field adaptation to this problem because of its comparative insensitivity to conditions of high humidity and because of its relatively small bulk and high mobility. We were therefore in a good position to undertake this work with large charges.

METHODS

The shielding of the X-Ray system and the film from the blast and fragments was accomplished by detonating the 105mm cased projectile (shown in Fig. 1) above a 4" armor plate and allowing the jet to travel through a hole in the plate past the film. (Fig. 2 shows the set-up.) The X-Ray tube and film were therefore subjected only to the blast effects accompanying the jet, to the indirect shock transmitted via the supports and to the blast that could get thru the small jet aperture or around the top plate. It is of course essential that fragment ricochets be prevented by proper orientation of the walls of the barricade if the firing is done in an inclosed barricade.

It was found possible to protect both the film and the X-Ray tube aperture by means of approximately 1/2" of plywood. The film holder was designed to allow some flexing of the shielding material without allowing the shielding to touch the film. The holder is shown in Fig's. 3 and 4.

The triggering of the X-Ray tube in these initial experiments was accomplished by means of a simple double aluminum foil switch which was closed by the passage of the jet itself thru the two .005 inch Al foils.[2]

It was also possible to measure penetrations into stacks of plate for the same jets being radiographed. The standoffs of course would be determined by the jet length desired in the radiograph.

EXPERIMENTAL PROGRAM

Machined copper liners of $45°$ angle with and without spitback tubes and approximately 0.10" in thickness were compared with drawn steel liners of the type used in

---

1. Paszek, J., Taylor, B., and Squier, J., "Low Voltage Flash Radiography," Transactions of the Shaped Charge Symposium (November 1951).

2. Improved systems with electronically generated time delays have been developed since these experiments.

122
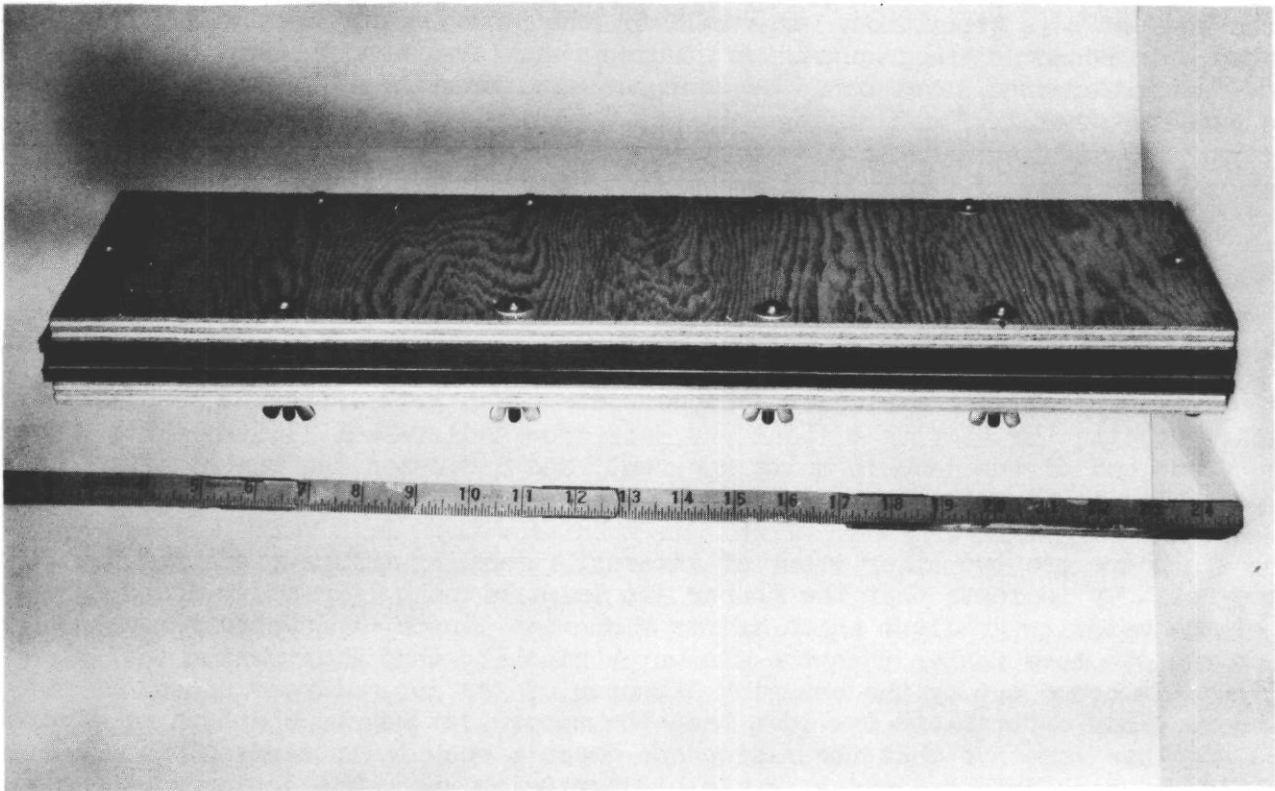
Figure 4.—Assembled view of film holder.
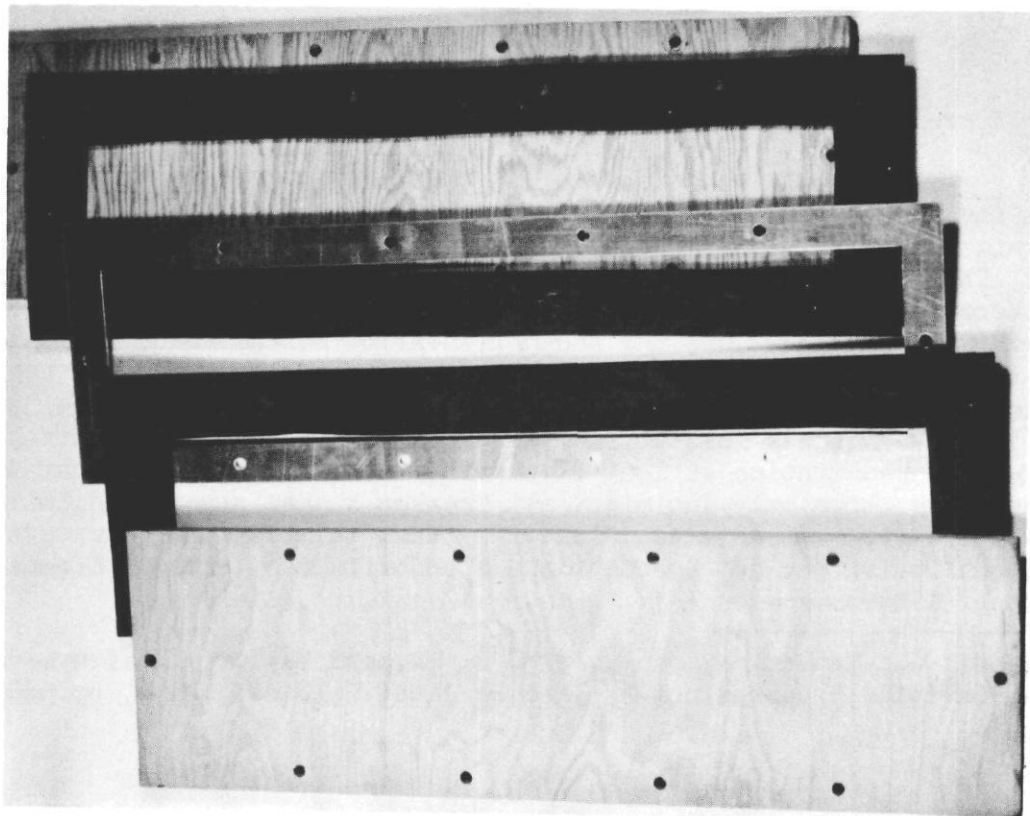
Figure 3.—Exploded view of film holder.

123

standard 105mm H.E.A.T. ammunition. In addition, the jets from trumpet and hemispherically shaped liners were radiographed. All charges were loaded with Comp B (60-40) and were initiated with tetryl Boosters. The charges were cased in steel bodies having a wall thickness of about 3/8".

EXPERIMENTAL RESULTS

All of the radiographs included in this report have been reduced to approximately 40% of full size.

a. Copper Jets from Machined 45° Cones.

Fig. 5 shows a series of 3 copper jets taken at 3 different conditions of jet length. Despite the fact that these are jets from 3 different liners, the similarity of the front end of the jets is quite apparent, and indicates the reproducibility that is possible with large charges.

There are two other items of interest regarding this set of pictures. First, they clearly indicate that the copper jet is stretching like taffy under the influence of the velocity gradient which exists along its length, and which makes each element of the jet move faster than the element behind it, thus lengthening the jet in flight. This is borne out by the changing diameter of the jet, decreasing as the jet grows longer. This contradicts the idea that the copper jet may be composed of discrete particles so close together that the radiograph doesn't show their separation. Such a system would separate into individually visible particles under the action of the existing velocity gradient and would not be expected to show a continuous jet whose diameter decreases with increasing jet length. The latter implies the action of cohesive forces.

Finally the last picture in Fig. 5 shows evidence of the beginning of breakup of even the copper jet at long standoff.

It is well known[3] of course that shaped charges show a standoff effect, in which the penetration increases to a maximum as the charge is spaced farther from the target. Further increase of the standoff is accompanied by a decrease in the penetration. This has been attributed to two things. First, a leveling off of the penetration because of the decrease in average density of the jet resulting from a breakup into particles. In addition, the non-collinearity of the velocity vector of each element of the jet which arises as a result of deviations from perfect symmetry in the liner and the detonation wave, results in a radial dispersion of the jet which begins to make itself seriously felt at the longer standoffs and hence contributes to a reduction of the penetration at long standoffs. It is interesting that the radiograph at this late stage shows only incipient jet breakup and no strong indication of radial dispersion effects. It is also interesting that this picture corresponds rather closely to the condition of the jet near optimum standoff which is about 6 cone diameters for these copper liners.

---

3. Birkhoff, G., MacDougal, D. P. Pugh, E. M., and Taylor, Geoffrey, "Explosives with Lined Cavities," Journal of Applied Physics, Vol. 19, No. 6, pp 563-583, June 1948.
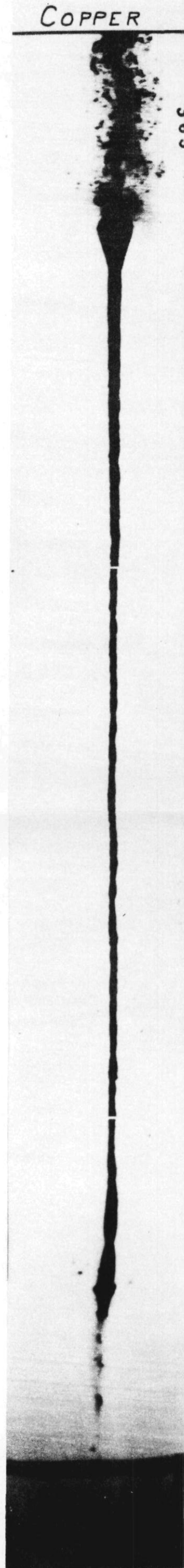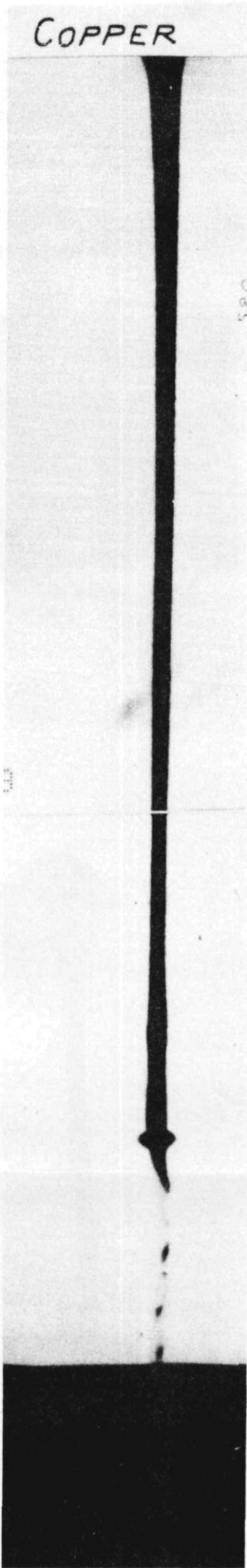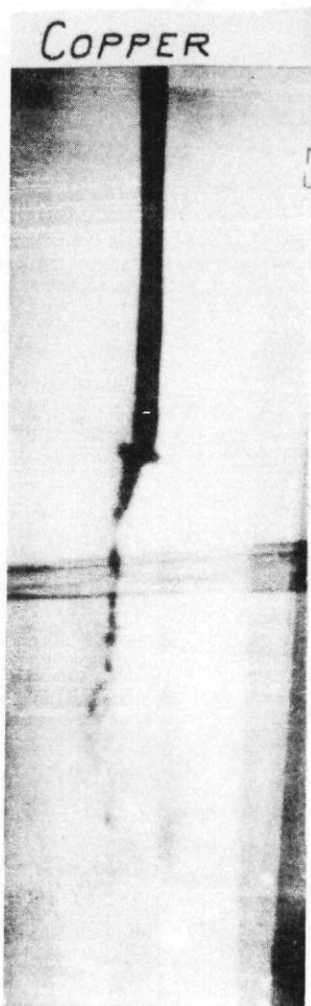
Figure 5—Jets from 105 mm copper liners with spitback tubes.
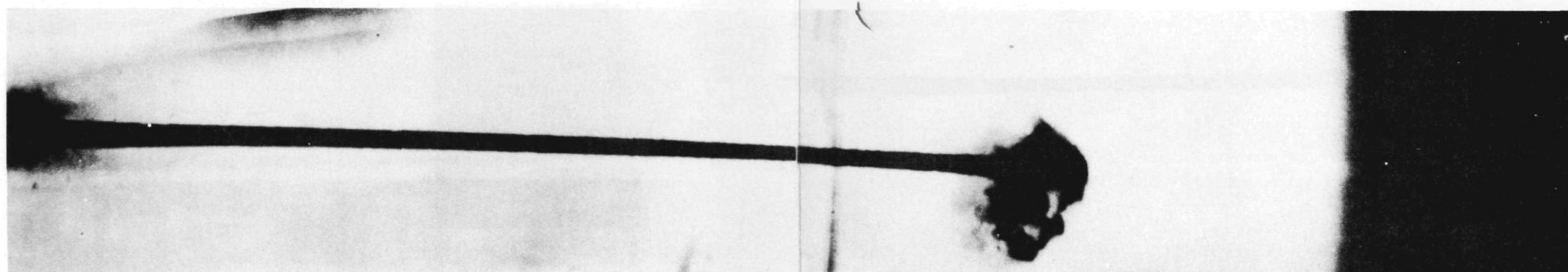
Figure 6.—Jet from simple 105 mm conical liner without spitback tube.

A second item of interest is the "pre-jet" which has been found to precede the main jet from liners which contain a spit-back tube.[4]

The pre-jet is believed to have its origin in the cylindrical spitback tube. This view is supported by the evidence that simple conical liners without spitback tubes do not show this characteristic pre-jet. A typical jet from a simple conical liner is shown in Fig. 6. In Fig. 5 it is the pre-jet which has triggered the flash radiograph in all 3 cases.

The presence of the pre-jet in the jet from spit-back liners suggest that it may be one of the contributing factors[5] to the greater penetration of this type of liner.

b. Steel Jets from Drawn 42° Cones.

The experiments with drawn steel liners resulted in the radiographs shown in Fig. 7. In this case it is quite evident that the steel jet has started to break into fragments very early in its life. The characteristic increasing separation of the individual fragments as the jet lengthens is clearly visible. Also evident is the relatively constant particle diameter independent of the length of the jet. The steel liner was a simple liner without a spitback tube so that, in the absence of the pre-jet the trigger was actuated by the main jet itself. This results in a small part of the main jet passing thru the trigger foil prior to the X-Ray flash, because of the few microseconds delay between the triggering, and the flash. The steel and copper jets are compared in Fig. 8.

There is an interesting speculation possible at this point, which hinges on some work done recently at the Johns Hopkins University by Kramer and Maddin.[6] These investigators have found that there is an observable delay in the initiation of slip in body centered cubic systems of single crystals, (to which Fe belongs) whereas face centered cubic system (to which copper belongs) showed no measurable delay. This means that a stress applied at a rate greater than a certain critical rate, will result in brittle fracture for the B.C.C. System (Fe) while the F.C.C. System (Cu) will yield plastically at this same strain rate. While admittedly the strain rates in these experiments were not comparable to those which result from a detonation yet they strongly suggest what may be the first real clue to the basic physical reasons for the difference between iron and copper.

---

4. The spit-back tube was originally built into liners to permit the initiation of the base booster by means of a so-called "spit-back" fuze. Such a fuze contains a small shaped charge initiated on target impact and firing backward down the "spit-back tube" to initiate the booster. Such fuzes are much faster than inertia type fuzes, but are being superceded by still faster electrical systems. The spit-back tube is being retained in many cases however because it has been shown that its presence improves the penetration of the shaped charge, especially at lower stand-offs.

5. Wave shaping resulting from the effects of the cooling of the explosive (Comp B) by the spitback tube during casting is considered an additional possible contributing factor.

6. Kramer, I. R. and Maddin, R., "Delay Time for the Initiation of Slip in Metal Single Crystals," Trans. AIME (1952) p. 197; Journal of Metals (February 1952).

127
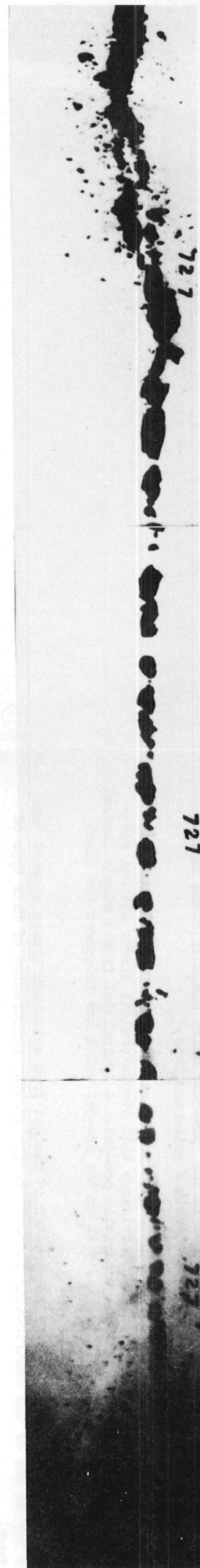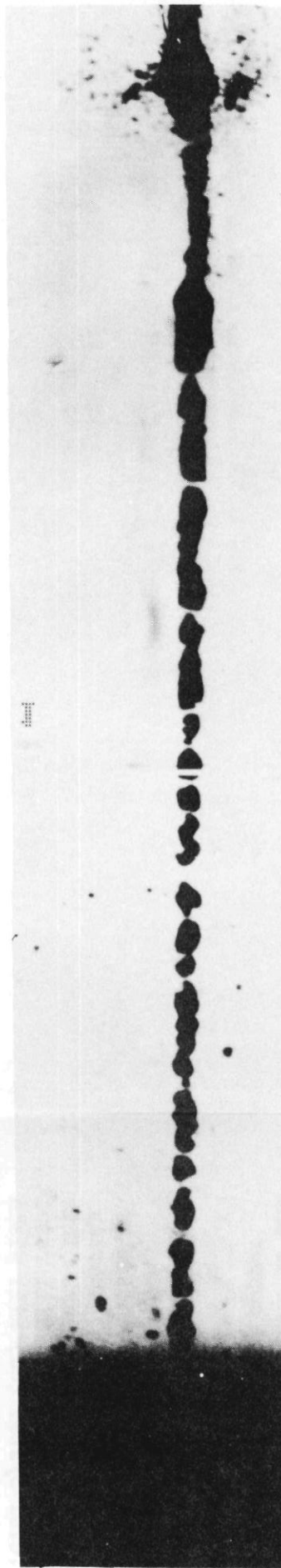
STEEL STEEL STEEL
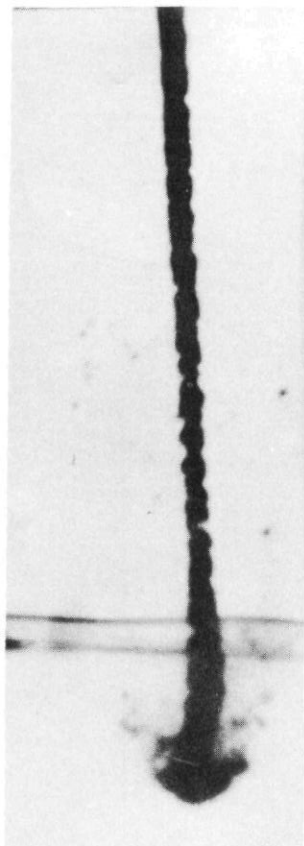
Figure 7—Jets from drawn 105 mm steel liners without spitback tubes.
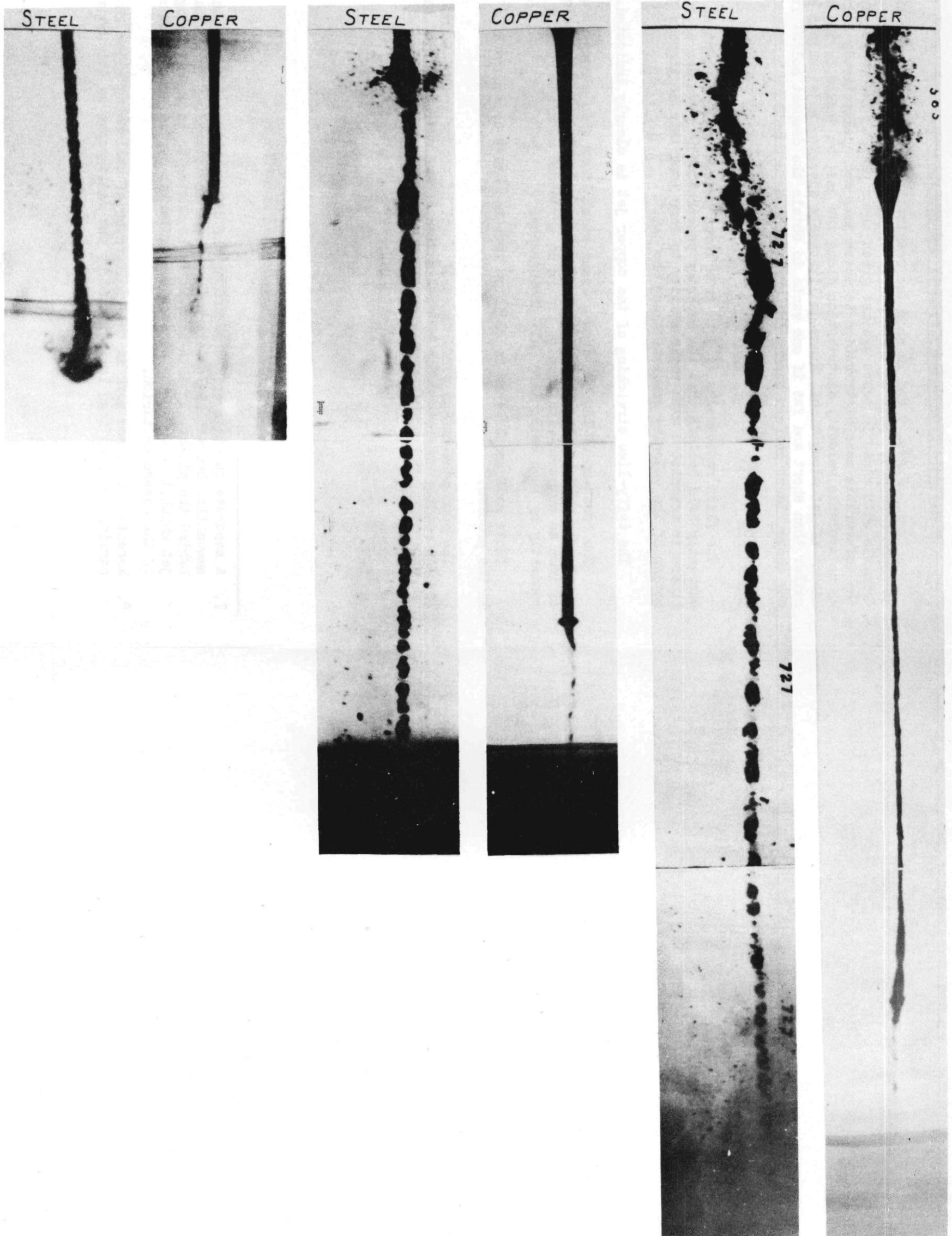
Figure 8—Flash radiographs of the jets from 105 mm shaped charges comparing copper
and steel at several standoffs. The early break-up of the steel jet and
the continuous nature of the copper jet are clearly visible.

c. **Jets from Copper Trumpets and Hemispheres.**

Fig's. 9 and 10 show the results that were obtained with trumpet and hemisphere shapes. Both of these had given approximately 1/2 of the penetration obtainable with cones in tests against green armor plate. The radiographs clearly show the unfavorable mass distribution in these jets and qualitatively indicate in addition an unfavorable velocity distribution along the jet, as judged by the relatively small amount of jet elongation. Since qualitatively speaking a jet should be long and thin rather than short and fat if one wants to obtain the deepest holes[7] it is readily seen why these liners perform poorly in penetration experiments.

CONCLUSION

The flash radiographs of jets from large charges add substantial weight to the currently held beliefs that the superior penetration performance of conical copper liners is associated with their ability to form long thin continuous jets, under the action of the velocity gradient along the jet.

The taffy-like stretching of the copper jet is clearly indicated.

The break-up of the jet from a drawn steel liner also strongly corroborates the previously held beliefs that this was the reason for the poorer penetration performance of iron as compared with copper, and is in agreement with the results obtained independently by Pugh using Kerr Cell photography.

These radiographs show in addition that the break up occurs at a very early stage in the process.[8]

The poor penetration performance of a set of copper trumpets and hemispheres can be made readily understandable by examination of the radiographs of their jets.

---

7. A separate question arises regarding the desirability of a long thin jet if the ammunition overmatches the target, and one is interested in the maximum damage behind the plate. In this case it is beginning to be widely recognized that a jet which is poor on the penetration criterion may be greatly superior on the basis of the damage criterion.

8. Recent unpublished work in the radiography of collapsing 105mm liners shows even earlier break-up than is indicated by the radiographs on this paper.
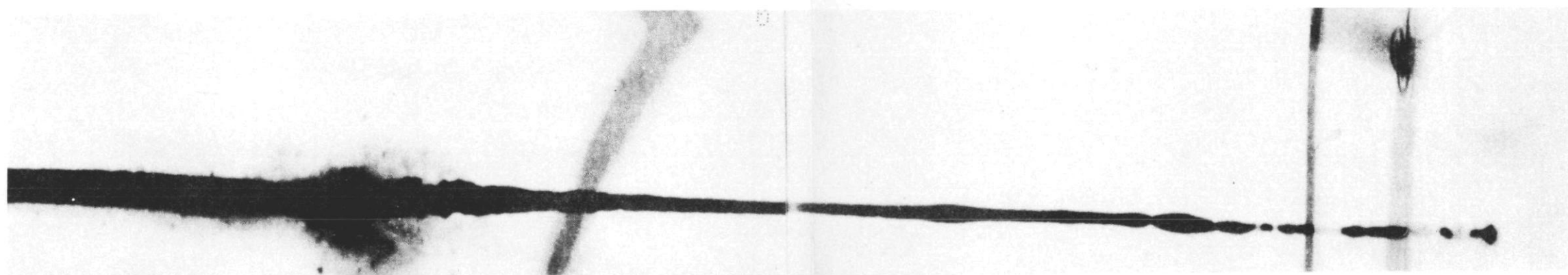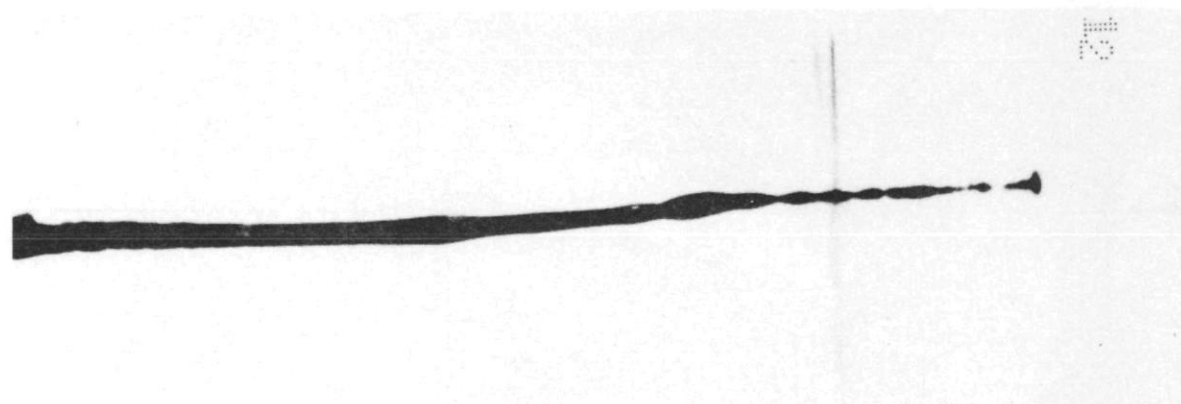
Figure 9—Jets from 105 mm trumpet.
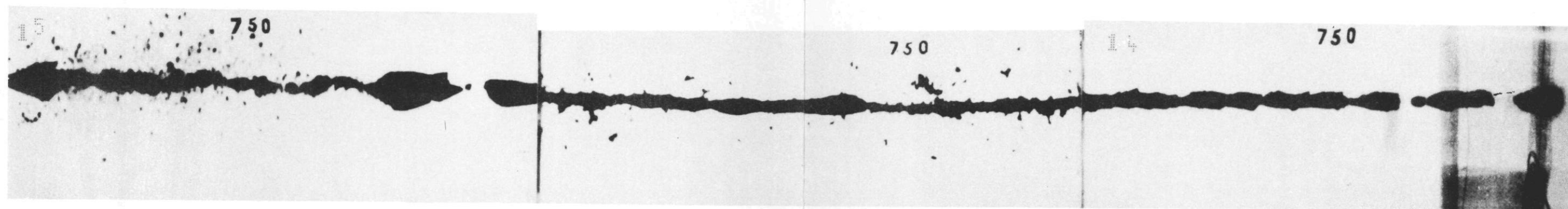
Figure 10—Jet from 105 mm hemisphere.

FLASH RADIOGRAPHIC STUDY OF JETS FROM ROTATED 105MM SHAPED CHARGES

L. Zernow

S. Kronman

F. Rayfield

J. Paszek

B. Taylor

Ordnance Engineering Laboratory, Ballistic Research Laboratories,
Aberdeen Proving Ground, Maryland

ABSTRACT

The development of new techniques for rotation of large projectiles and for low voltage flash radiography has made it possible to obtain successful flash radiography of jets from 105mm cased shaped charge projectiles which are rotating. The first radiographs of this type are discussed.

The effects of rotation are seen in considerable detail. Two distinct effects are observable in terms of which the deleterious effects of rotation may be more readily analyzed. These are (1) axial breakup, and (2) radial dispersion. A tentative hypothesis which distinguishes these two effects from each other is proposed.

The possibility of using the shaped charge as an experimental device for studying otherwise inaccessible properties of liner materials under very high strain rates and unusual stress combinations is pointed out.

The advantages of a cylindrical liner are discussed, and, in particular, attention is called to its expected resistance to spin deterioration. There is also noted the additional advantage that the penetration from such a liner can be made to depend upon the liner length rather than the projectile caliber.

HISTORICAL BACKGROUND

The first published information on possible deleterious effects of rotation on the performance of shaped charges seems to have come simultaneously from the British and the Germans. Tuck[1] in 1943 qualitatively explained the effects of rotation by a

_____

(1) AC 3596 - "A Note on the Theory of Munroe Effect" - James L. Tuck.

widening of the jet which could be predicted from the resultant of the collapse velocity and the tangential velocity due to rotation. His work may have been motivated by the preliminary experimental results[2] which were formally reported some months later. Trinks[3] in April 1943 estimated "considerable reductions" in the penetration due to the expansion of the jet diameter resulting from centrifugal force effects. He also remarked that the final result would probably be a radial spray of "droplets" rather than a simple expansion of jet diameter. At essentially the same time in May 1943 the British formally reported their first experimental evidence of rotation effects in a 3" field gun.[2] They verified that the observed deterioration in performance was attributable to rotation, by spinning the projectiles with an automobile starter motor and observing similar deterioration. This appears to be the first reported instance of a projectile rotating device for shaped charge studies. It is also noteworthy because of the large caliber (3") involved.

Following the British experiments, the study was taken up in this country by the Explosive Research Laboratory of the OSRD.[4][5][6] The British results were confirmed and extended. Most of the work reported by ERL was done with smaller caliber M9A1 cones of 1 5/8" diameter. Considerable work with 57mm and some experiments with 75mm were reported. A single case was reported of a 105mm projectile which was rotated during detonation. Several years after the end of World War II, additional contributions were made by Carnegie Institute of Technology in connection with spin compensation studies. The experimental work by C.I.T. also was mainly carried out with small calibers of the order of 57mm.

All of the work so far described involved studies of penetration into targets.

In a BRL Report published in 1948, Clark & Fleming,[7] described earlier work that had been done in flash radiography of jets from cones and hemispheres of 1 3/8" base diameter. The work described was carried out prior to May 1945 and was probably the first flash radiographic work on rotated shaped charges. The radiographs in the report of Clark and Fleming indicate that the jet was dispersed and broken into particles by the rotation, but their pioneering radiographs were not clear enough to give a quantitative idea of the dispersion process.

No other flash radiographic studies of rotating shaped charges have been found, although the Germans reported[8] multiple Kerr cell studies which indicated the "spreading" of the jet due to rotation.

---

(2) AC 3987 - "Hollow Charge Rotated Projectiles" - (M.D.I.)

(3) Dr. Walter Trinks - "Mathematical Study of Lined Hollow Charges" - Report 43/6 Translated as OTIB No. 1484 - 30 April 1943.

(4) OSRD 1680 - "Target Penetration by the Jet from a Rotating Cone Charge" - August 5 1943.

(5) OSRD 3874 - "Target Penetration by the Jet from a Rotating Cone Charge" - July 10, 1944.

(6) OSRD 5598 - "Target Penetration by the Jet from a Rotating Cone Charge" - November 5, 1945.

(7) J. C. Clark and R. O. Fleming, Jr. - "Effect of Rotation Upon the Explosive Collapse of Thin Metal Surfaces of Revolution" - BRL Report No. 671, July 1948.

(8) Leslie E. Simon, Col., Ord Dept. - "Report on German Scientific Establishments" - Chief of Ordnance, Washington, D. C., Sept. 1945, Page 97.

A theoretical treatment of the effects of rotation, based on conventional hydro-dynamic theory, was given by Birkhoff[9] who predicted a hollow jet under rotational forces. He also suggested that the jet may break into droplets.

The uncertainty regarding the details of the "spreading" process and the need for additional experimental data which could be used as a basis for further development of the theory motivated the undertaking of the present work. It is believed that only by means of an understanding of the detailed mechanism of spin deterioration can the most efficient attack be planned on the problem of spin compensation.

BASIS OF PRESENT WORK

The development of the wire-driven projectile rotator[10] so simplified the prob-lem of rotating large caliber shaped charge projectiles that 105mm projectiles could be easily rotated at frequencies in excess of 350 revolutions per second. The only ex-pended element in this rotation system is the steel drive wire and contactor assembly. Figs. 1, 2 and 3 show the pertinent details of the wire driven rotation system, which is located on Spesutia Island and has been nicknamed "Big Mo" because of its massive construction. The rotating projectile is so stable in this system that during the summer time, flies repeadedly try to alight on the spinning projectile, only to be violently thrown away.

The second essential development was that of the simple low voltage system of flash radiography described by Paszek, Taylor and Squier.[11]

These two recent developments have been combined and have made possible this study of jets from rotated 105mm shaped charges. These liners are more than twice as large as any previously reported in radiographic studies. The advantages of the large caliber are two-fold in these experiments:

1. There is a gain in detail and reproducibility resulting from the larger dimensions of the jet and the dimensional uniformity easily obtained with large cones.

2. The greater sensitivity of large calibers to rotational deterioration makes it possible to cover almost the entire range of interesting phenomena in the frequency range from 0 to 350 rps. Smaller calibers would require correspondingly higher rotational frequencies, so that if, for example, 1 3/4" diameter liners were used, rotational frequencies up to 700 rps would be required to bring out corresponding effects.

(9)   Garrett Birkhoff - "Hollow Charge Anti-Tank Projectiles" - BRL Report No. 623, 10 February 1947.

(10)   S. Kronman, and L. Zernow - "A Wire Driven Projectile Rotating Device for Hollow Charge Investigations" - BRL Report No. 798, March 1952.

(11)   J. J. Paszek, B. C. Taylor and J. L. Squier - "Low Voltage Flash Radiography" - Transactions of Symposium on Shaped Charges, held November 1951 at BRL.
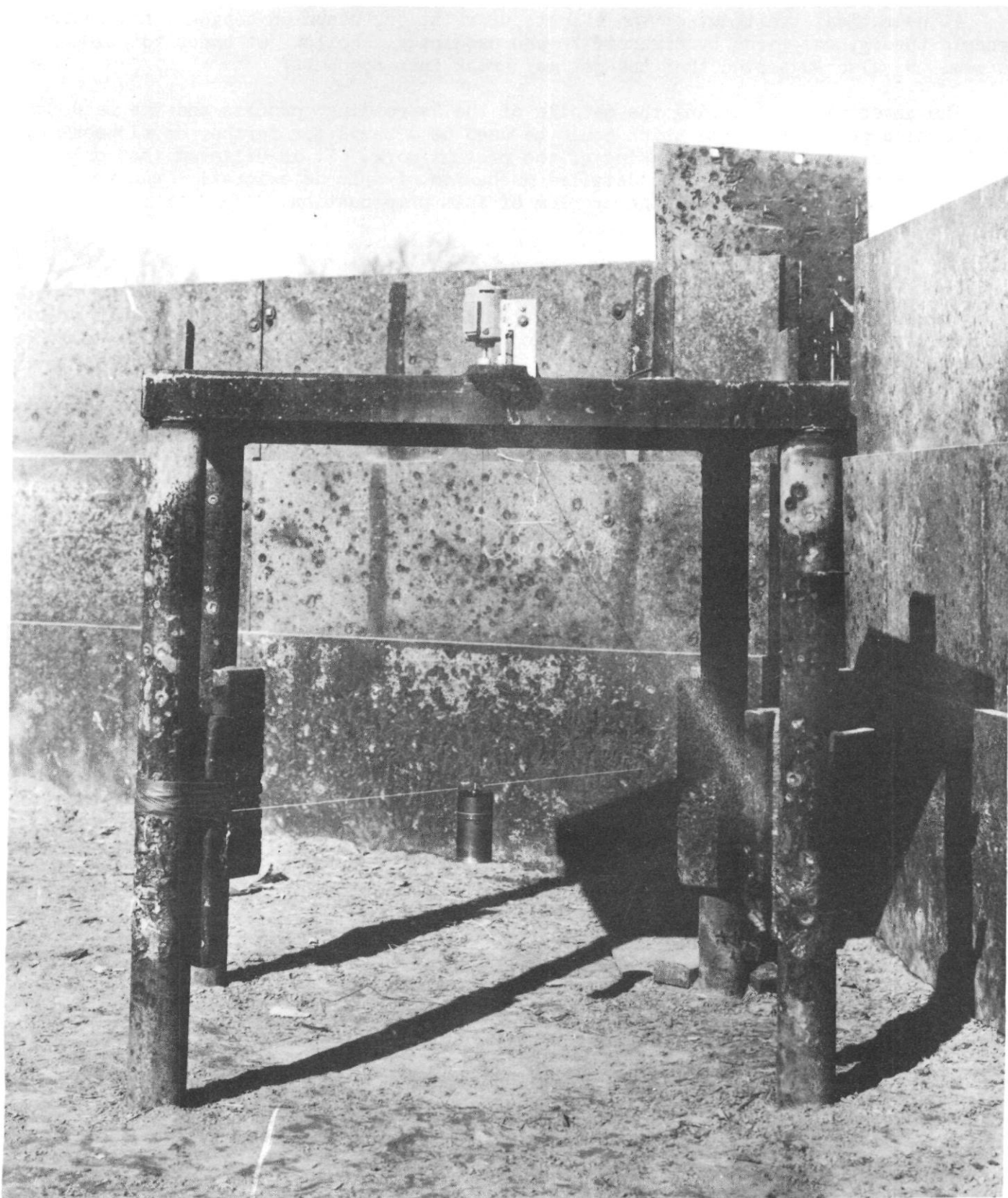
Figure 1—Overall view of wire driven rotator.
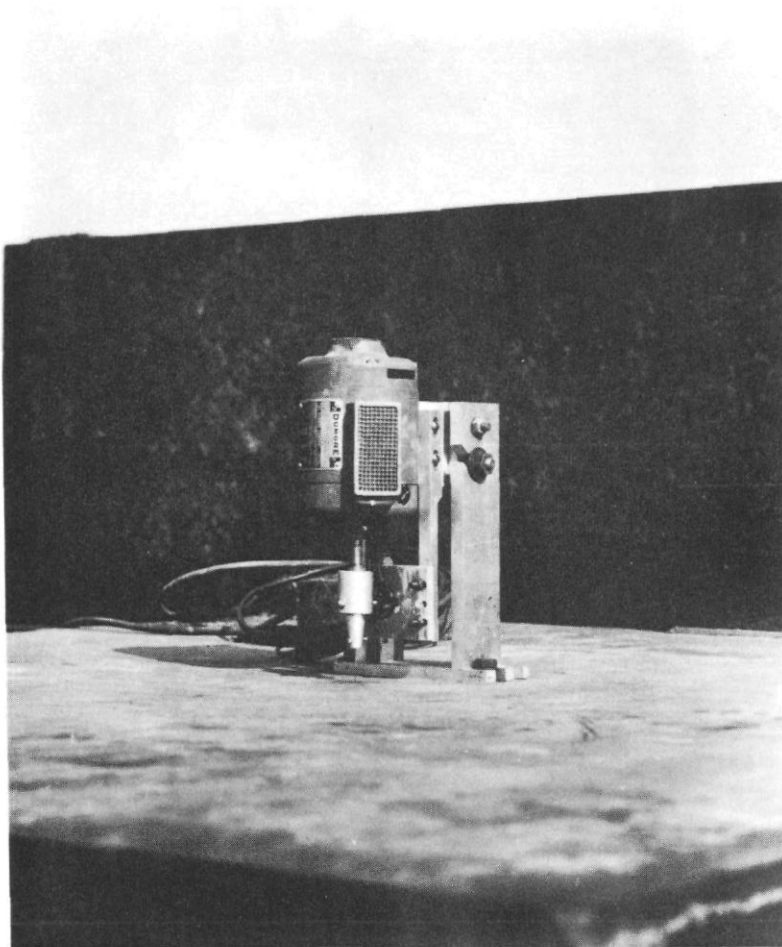
Figure 2—View of motor and monitor of spin frequency.
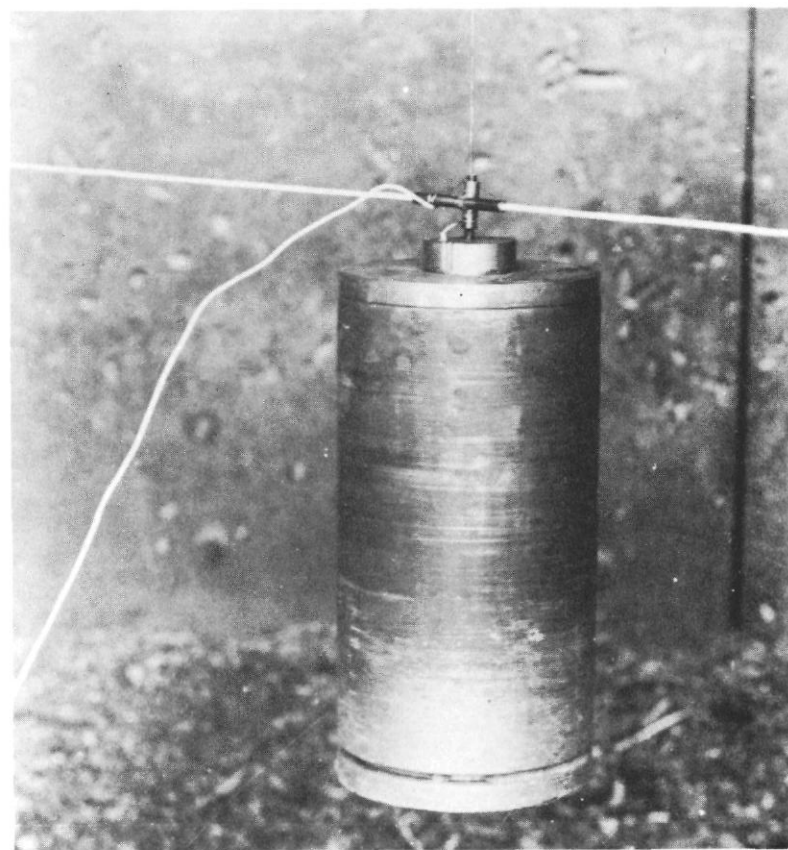
Figure 3—Closeup view of 105 mm projectile on wire, and electrical firing system.
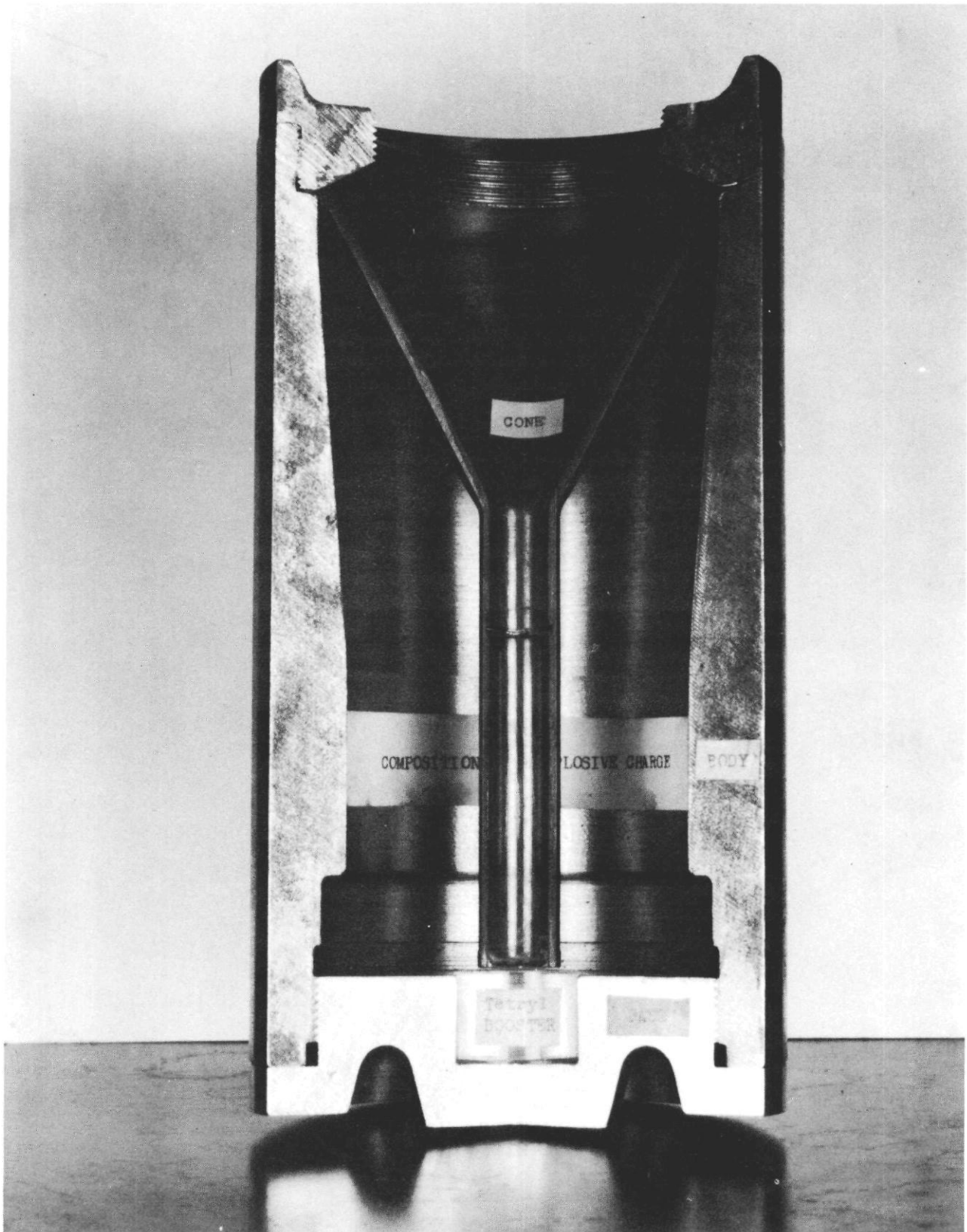
Figure 4—Cut-away view of the 105 mm projectile used in the experiments.

138

EXPERIMENTAL PROGRAM

The work described here was done during the summer and fall of 1951 and represents the initial effort to study the jet from rotated liners at various rotational frequencies. Flash radiographs were taken of 105mm caliber 45° apex angle machined copper liners rotating at 0, 30, 45 and 60 rps. In addition some steel liners were fired for comparison.

Fig. 4 shows the details of the projectile used in these experiments;

The details of the flash radiographic set-up are essentially the same as those reported in the study of unrotated jets.[12] The projectile is hung from the motor driven wire in these experiments, as shown in Fig. 3.

ANALYSIS OF EXPERIMENTAL RESULTS

Fig. 5a compares copper jets from an unrotated projectile and a projectile rotated at 60 rps. For the purpose of reproduction the radiographs have been reduced to about 40% of natural size. The tip of the rotated jet is seen to be essentially unaffected by the rotation. At point A we see the radial break up of the jet into what looks like two separate particle jets (bifurcation). This effect is seen to become more pronounced from point A upward until finally at point B we see what appears to be still further break-up (polyfurcation) of the already bifurcated jet, with the radial spread of the fragments still increasing. At point C the fragment spread has reached a maximum. The significance of the bifurcation process will be discussed in a following paper.

The radial disturbance of the jet seen in the radiograph is at least partially understandable in terms of the simplest notions of jet formation. The tip of the jet has its origin at the apex of the inner liner surface. The portions of the jet which follow the tip come from portions of the liner successively further from the apex, and hence from successively greater radial distances from the axis of rotation, as shown in Fig. 5b. Hence, it is to be expected that the front tip of the jet would be unaffected by rotation, and that the rearward portions of the jet would be progressively more seriously disturbed in a radial direction. This type of disturbance extends to point C (Fig. 5a). The region from C to D will be discussed later.

The early break-up of the rotated jet into particles in the axial direction is a more subtle phenomenon. The apparent trend toward uniformity of the size of these particles suggests that they may have their origin in multiply reflected shocks either in the liner* or the jet. The jet from an unrotated liner of the same type (Fig. 5a) shows incipient jet breakup in the form of a pseudo-periodic necking down of the jet.

The next question that arises concerns the reasons for the marked effects of rotation upon the axial breakup process. We believe that the explanation involves the introduction, as a consequence of rotation, of a rotational velocity gradient in addition to the ordinary axial linear velocity gradient. This rotational velocity

---

(12) L. Zernow, S. Kronman, J. Paszek, and B. Taylor - "Flash Radiographic Study of Jets from Unrotated 105mm Shaped Charges" - Transactions of Symposium on Shaped Charges, held November 1951 at BRL.

Dr. A. W. Hull, among others, has suggested that such vibrations in the liner may be responsible.

140
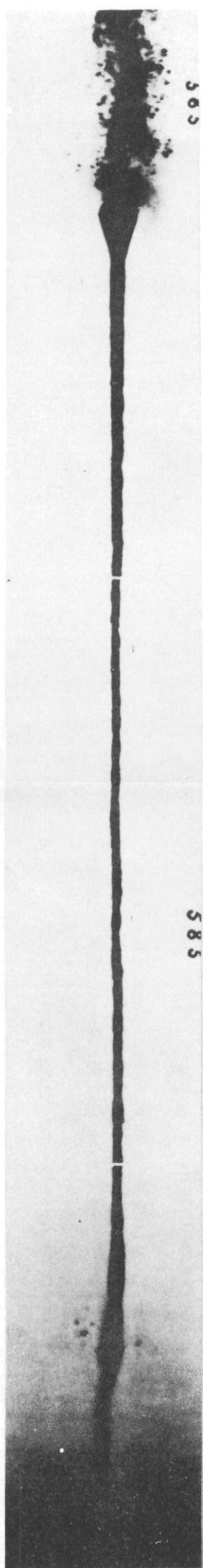
FLASH RADIOGRAPHS
OF JETS FROM 105mm
SHAPED CHARGES

fig. 5A

D

C

B

A

Figure 5a—Flash radiographs of jets from 105 mm shaped charges.
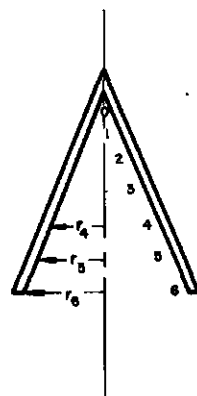
INITIAL POSITION
OF LINER

RELATIVE POSITION OF
JET ELEMENTS OF AN
UNROTATED JET AFTER
DETONATION

DIRECTION
OF JET
FLIGHT

Figure 5b—Sketch showing how successive jet elements come from
greater radial distances.
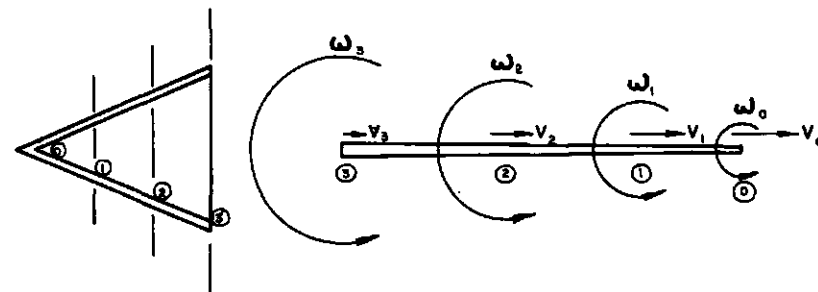
Figure 6a
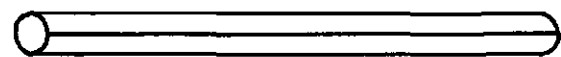
LOCATION ON JET OF AN INTERIOR CONE ELEMENT
(WITHOUT ROTATION)
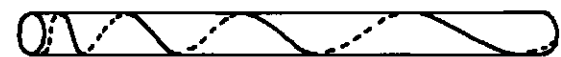
LOCATION ON JET OF AN INTERIOR CONE ELEMENT
(WITH ROTATION & WITHOUT AXIAL VELOCITY GRADIENT)

Figure 6b

LOCATION ON JET OF AN INTERIOR CONE ELEMENT
(WITH ROTATION & AXIAL VELOCITY GRADIENT)

Figure 6c

FOR THESE SKETCHES THE JET IS ASSUMED TO BE A
CONTINUOUS ELASTIC SYSTEM

gradient could arise naturally from the variations in the angular velocity of a jet element at the extrusion point due to the variations in the radial distance of its parent ring in the liner. Thus, in the light of this concept, the jet, if it remained continuous, would not only be stretching due to the ordinary axial liner velocity gradient, but would also be undergoing a torsional deformation. The forward tip would have an angular velocity about the jet axis initially equal to ω_0, the projectile's angular velocity, because it originates at the apex of the liner. Successive rearward portions of the jet could have increasingly larger angular velocities about the jet axis. The jet would thus be stretching and winding itself up simultaneously as illustrated schematically in Figs. 6a and 6b. It is interesting that as shown in Fig. 6c the axial linear velocity gradient would tend to decrease the variation in pitch of spiral representing the angular displacement of an interior cone element making it more nearly a uniform spiral.

The "winding up" process would superimpose an additional torsional stress on a continuous jet. This torsional stress would increase with time if the continuous jet were considered to be an elastic system. Now, if this time dependent stress system is superimposed on the one resulting from the axial linear velocity gradient, in which the stresses also would increase with time, it would be possible to account for the accelerated axial breakup of the rotated jet on the basis of the known reduction in torsional ductility of a wire subjected simultaneously to tension and torsion. A uniform rotational velocity gradient along the jet could explain the uniform logitudinal breakup.

It might also be pertinent to consider the effects on the angular velocity gradient in the vicinity of the extrusion point which would result both from the initial contraction and from the subsequent expansion of the jet following its attainment of minimum diameter at what might be called the "vena contracta" by analogy. This process of contraction and subsequent expansion (which is strongly suggested by both the radiographs and the target data to be reported separately) occurs over a fairly small axial distance and therefore a large gradient of angular velocity will be established in that region. It is interesting to note that the jet appears to be continuous in the vicinity of the "vena contracta" and shows breakup clearly only after the expansion. Also, the expansion is much more marked in the rotated jet than in the unrotated one. Since it is likely that the jet is more nearly a plastic system than an elastic system, these considerations would therefore need to be modified from this point of view.

Let us now return to the region C-D of Fig. 5a. Here the jet appears to be behaving anomalously since the rearmost portions of the jet seem to be less affected, although they should be more dispersed. Various explanations may be given, including the possibility that because of their later extrusion, these parts have not had time to spread to the full extent. However, the results from a single radiograph are not sufficiently conclusive. A multiple flash system now under development should furnish the required additional information.

MEASUREMENT OF VELOCITY DISTRIBUTION ALONG THE JET

Fig. 7 compares the flash radiographs of copper lined charges rotated at 30, 45 and 60 rps. The 30 rps radiograph is an especially useful one of the double flash type, which makes it possible to measure easily the velocity gradient along the jet.
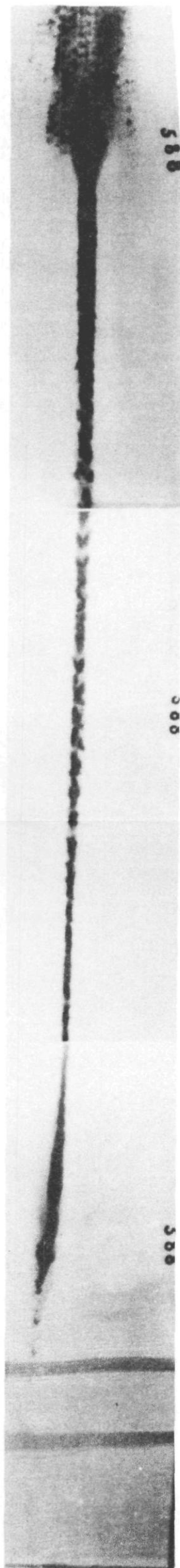
30 RPS   45 RPS   60 RPS

JETS OF 105 mm CHARGES

45° COPPER CONES WITH
SPITBACK TUBES AT VARIOUS
RATES OF ROTATION.

143

Figure 7—Jets of 105 mm charges.　45° copper cones with·spitback
tubes at various rates of rotation.

VELOCITY GRADIENT OF JET

CALIBER 105 MM
LINER 45° CU/W SPITBACK TUBE
ROTATION 30 RPS
ROUNDS NO S86 & 588
MEASURED FROM DOUBLE FLASH
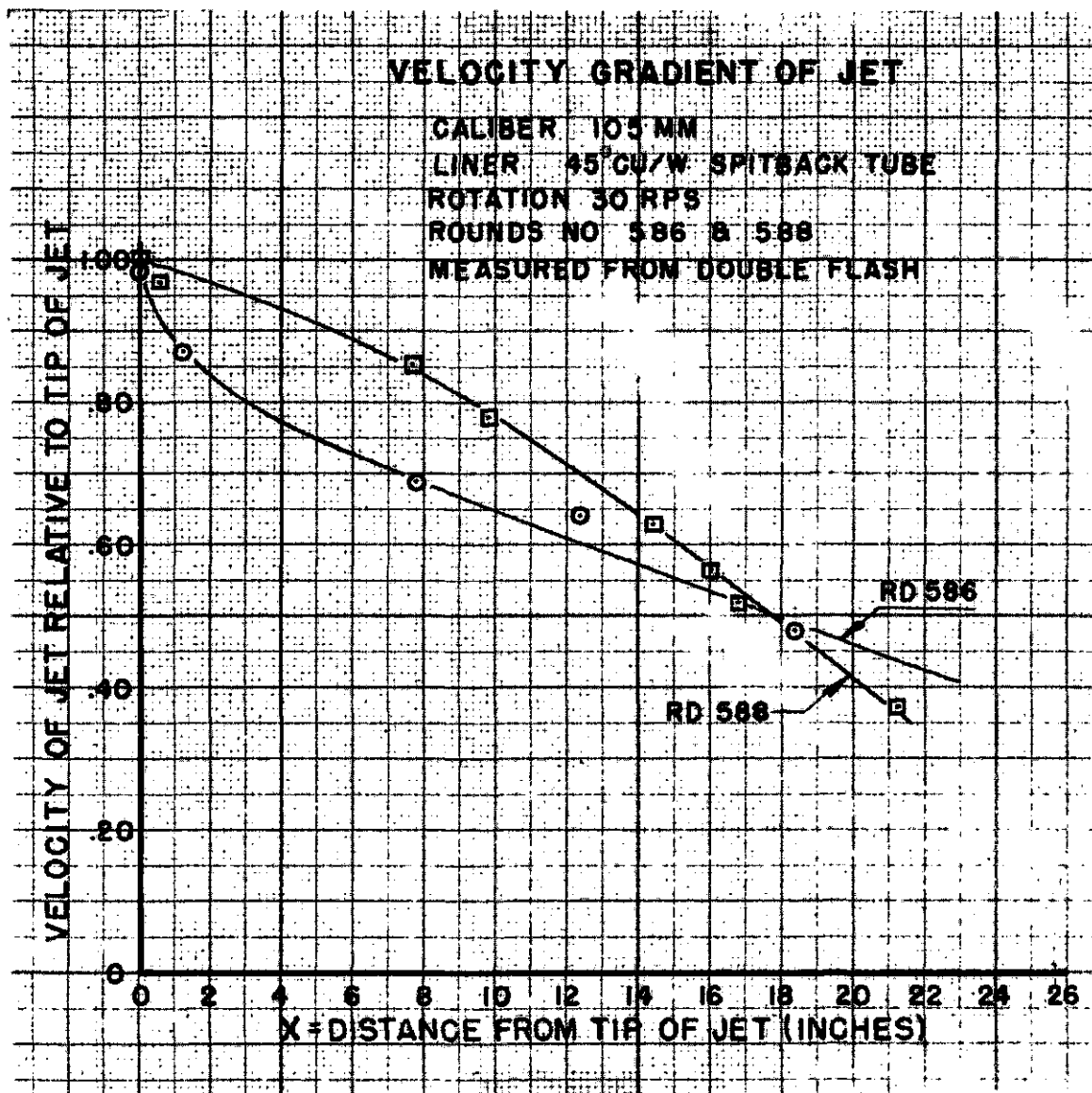
Figure 8

The results of such measurements are plotted in Fig. 8. It is evident that the velocity does not vary linearly along the jet. The deviations from linearity are believed to be real. However, these deviations are fairly small. In addition the average of the two rounds closely approaches linearity. It can therefore be assumed that pending a more detailed analysis and extension of the experimental data this result is not inconsistent with that from measurements made by the Carnegie Tech. group[13] using the rotating mirror technique in conjunction with slug recovery experiments. The simplicity of these measurements from a double flash radiograph constitutes a distinct advantage. However, this is partly offset by the following disadvantages: (1) the double flash method is not as readily applied to a continuous jet and (2) the double flash, at present, is a random occurrence.

EFFECTS OF VARYING ROTATIONAL FREQUENCY

The first effect of rotation appears to be the axial breakup process, which appears to be the predominant process at 30 rps. Evidence for incipient bifurcation can be seen in this radiograph although there is other evidence[14] that it may already be well under way at the rearmost part of the jet.

At 45 rps the bifurcation is clearly apparent. In addition, the axial breakup appears to be much more severe than at 30 rps. However, a single radiograph could conceivably fail to show the bifurcation if it occurred in a plane perpendicular to the film. At 60 rps, the breakup of the jet appears to be not appreciably greater than at 45 rps. In fact in this particular radiograph the dispersion of the particles seems to be smaller. This is also attributable to randomness in the orientation of the plane of bifurcation relative to the film plane. Although radiographs of jets of 30 rps have not shown a discernible bifurcation, all radiographs of jets at 45 or 60 rps show the bifurcation clearly.

If the 30 rps radiograph is considered to be one showing incipient bifurcation, the breakup of the jet under rotation may be interpreted as resembling a catastrophic process, in which up to a critical rotational frequency there is no breakup. Past that critical frequency the onset of axial breakup occurs. Finally at a higher frequency bifurcation of a singificant portion of the jet length occurs. This hypothesis is qualitatively presented in Fig. 9. Two critical frequencies are postulated; ω_o, for longitudinal breakup and ω_1, for significant bifurcation. There is no apparent physical reason that both axial breakup and significant bifurcation should occur at the same critical frequency. However, that a critical frequency ω_o may exist below which no marked effects are apparent can be shown from physical considerations. It is to be expected that such considerations would involve the elastic and plastic properties of the liner. Because of the potential importance of these phenomena, they are being investigated in greater detail.

COMPARISON OF COPPER AND STEEL LINERS

Fig. 10 compares copper and steel liners rotated at 45 rps. The uniformly poor behavior of the steel liner is in agreement with the radiographs of jets from unrotated

(13) C.I.T. - ORD-31 - p. 33.

(14) L. Zernow, J. Regan, J. Simon, and I. Lieberman - "Study of the Effects of Rotation upon the Penetration of Jets from 105mm Shaped Charges" - Transactions of Symposium on Shaped Charges, held November 1951 at BRL.

CURVE DEPICTING
PROPOSED HYPOTHESIS OF CRITICAL
BREAKUP FREQUENCIES

ω_e =CRITICAL FREQUENCY FOR
INCIDENCE OF LONGITUDINAL
BREAKUP

ω_l =CRITICAL FREQUENCY FOR
INCIDENCE OF BIFURCATION
OVER MAJOR PART OF
JET LENGTH

PENETRATION

ω_e ω_l

ROTATIONAL FREQUENCY
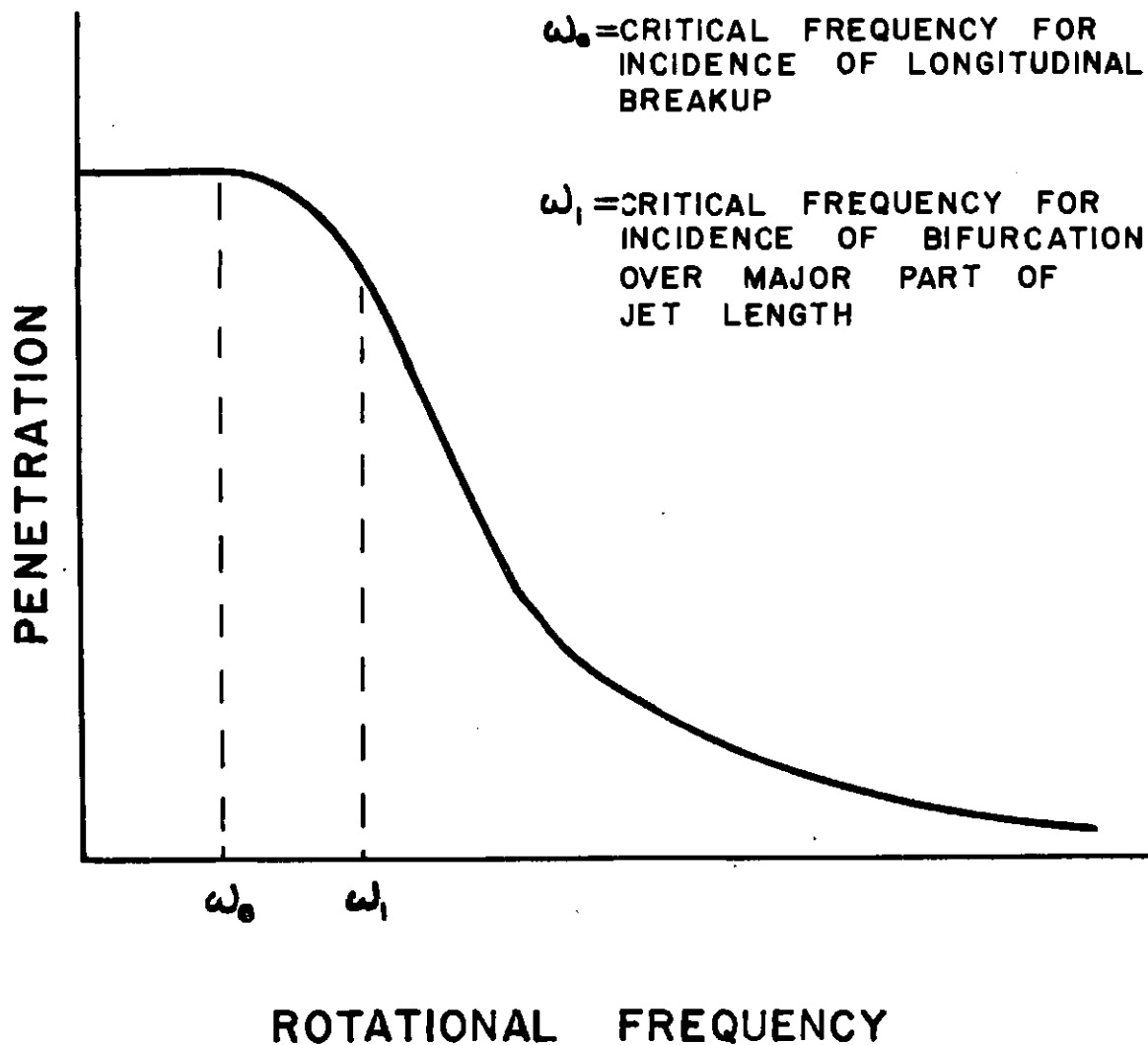
Figure 9—Curve depicting proposed hypothesis of critical break-up frequencies.

charges as reported in a previous paper.[12] The unrotated steel liner breaks up into particles at a very early stage. Rotation seems to have resulted in a further break up of the particles which now are smaller on the average than those in the unrotated steel jet.

The massive jet tip from the steel liner is attributable to the peculiar construction of the particular steel liners, which have a blunt hemispherical apex of about 1/4" radius.

The early breakup of the steel liner apparently results in a rather uniform radial spread of particles, which suggests that the rotated steel jet may already be broken up at the "vena contracta". The material from the blunt apex, however, has obscured the shape of the jet tip sufficiently to make the analysis of radial dispersion somewhat dubious. These experiments will be repeated with better steel liners before further analysis is undertaken.

THE SHAPED CHARGE AS AN EXPERIMENTAL HIGH STRAIN RATE DEVICE

The fact that the shaped charge can be used as an experimental means of applying very high strain rates and unusual stress combinations to a liner seems not to have been generally recognized. A good start has been made in the quantitative study of the interactions of simple slabs of explosive and slabs of metal, for example, as in the work of Rinehart,[15,16] and it has been noted that the processes observed are to some extent characteristic of the high strain rates as well as the high pressure amplitudes. The relatively simple geometry of these experiments is a desirable feature, both from the experimental and the analytical points of view. However, it appears from these initial studies of rotational effects that by the use of the shaped charge additional information may be obtained which may not otherwise be accessible; for example, rotation apparently permits the superposition of a torsional and tensional stress system. The liner need not be a cone, but for simplicity may be a cylinder.

THE CYLINDRICAL LINER

Experiments* have been performed with cylinders which indicate that a jet can be obtained. Also, there is flash radiographic evidence of jets from cylindrical liners; for example, such as reported in a previous paper.[12] The cylinder, in addition to its simplicity has several other potential advantages: (1) The cylindrical liner should be relatively insensitive to rotational effects since all of the material entering the jet can be made to come from near the axis of rotation. This is of very great importance from the viewpoint of application. (2) The penetration from a cylindrical liner could

---

(15) J. S. Rinehart - J. Applied Physics, 22, 555 (1951)

(16) J. S. Rinehart - "Scabbing of Metal Under Explosive Attack - Multiple Scabbing" - NOTS TM No. 348.

* This general problem of cylindrical liners has been discussed with Prof. Richard Courant of N.Y.U. who has independently arrived at essentially the same conclusions, which he discussed briefly at the Symposium in an unrecorded invited paper.

726

726

726

STEEL

COPPER

COMPARISON OF JETS
FROM ROTATED LINERS
OF COPPER & STEEL
105 MM CALIBER, 45 RPS

584

584

584
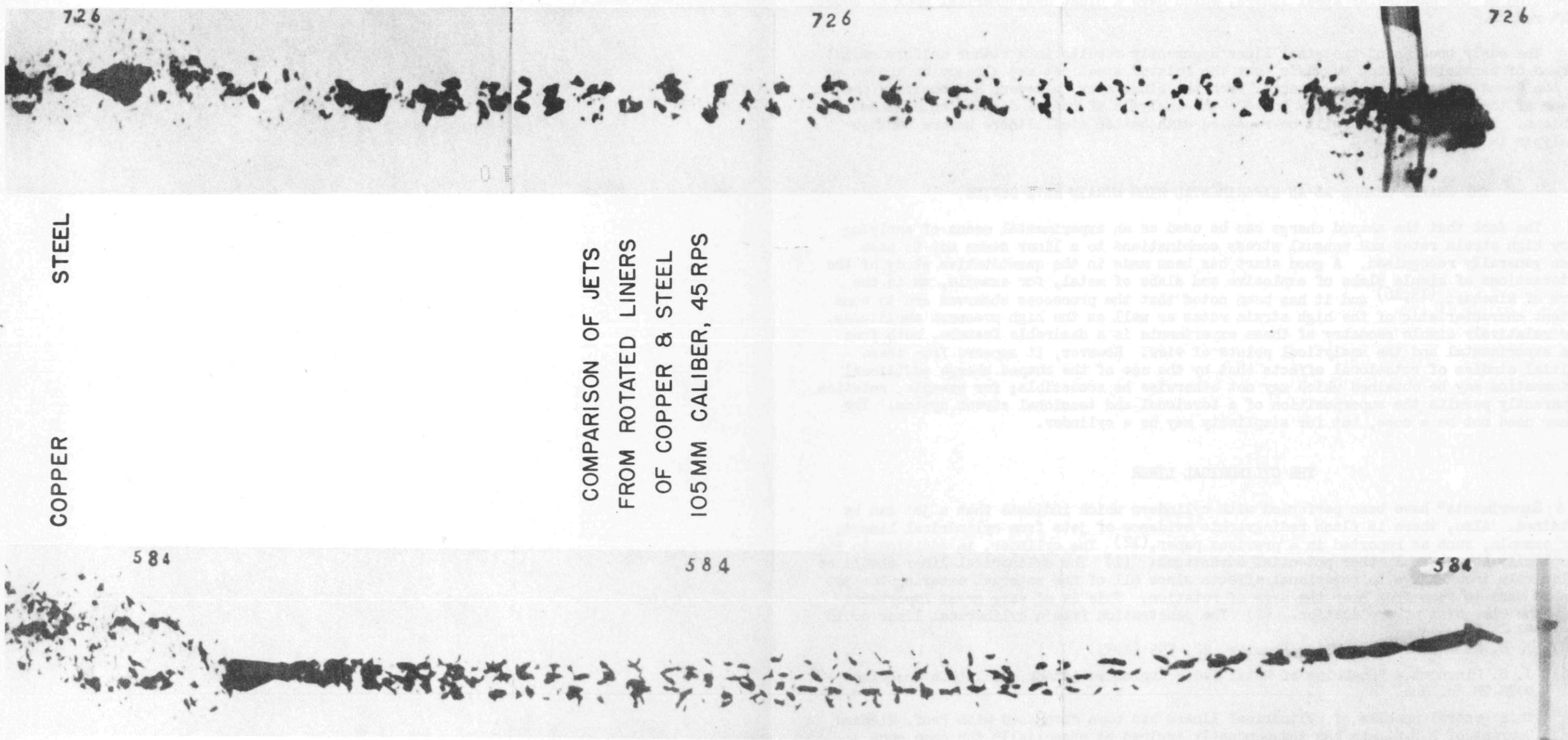
Figure 10—Comparison of jets from rotated liners of copper and steel
105 mm caliber, 45 RPS.

148

be made a function of the liner length rather than of the diameter of the projectile. This characteristic therefore makes it possible in principle to design a long projectile of small diameter which can pierce a target much thicker than that which can be defeated by a cone of that caliber. Moreover, there are other independent reasons why such long thin projectiles are desirable. (3) The collapse of the cylinder could be made to be a true steady state process, and therefore more amenable to analysis. This is distinctly advantageous in correlating experimental results. (4) The modification of the collapse process to incorporate a velocity gradient in the jet appears to be achievable by a variety of means among which is simple wave-shaping.

It is felt therefore that much more attention should be paid to cylindrical liners both because of their simplicity and because of their important potentialities in a weapon. A comprehensive program has been under way for the past year. Although the jet from a cylinder so far has not achieved a penetration as good as that obtainable from the cone that can be put into the same body, the payoff will be big if it can be accomplished.

SUMMARY

The radiographs discussed represent the first ones obtained with the new wire rotator and low voltage flash radiography techniques. They represent only a start on the task of understanding the fine details of the effects of rotation on shaped charge liners.

The attempts to interpret these radiographs must also be considered preliminary. The large amount of visible detail in the radiographs seems to make them quite fruitful in providing a firmer experimental basis for a theoretical approach. However, additional radiographs are needed to remove some of the uncertainties which remain because these first radiographs are single exposures.

CONCLUSIONS

It is concluded that rotation of a conical copper shaped charge liner causes two distinct defects to appear in the jet. The first is the early break-up of the jet axially into particles, which, therefore, even in the absence of any other effects would tend to make copper behave like steel and hence reduce its penetration. The second effect is a radial break-up of the jet which appears to be assignable directly to the action of the centrifugal forces resulting from the rotation of the liner. It takes the form of a bifurcation of the main jet followed by what may be successive bifurcations of each branch (polyfurcation).

The understanding of these phenomena is progressing rapidly. It is believed that this understanding is a prerequisite in the process of bringing new quantitative ideas to bear on the problem of how to overcome the deleterious effects of rotation.

Analysis of the radiographs from rotated liners suggests the possible use of the shaped charge, perhaps in simplest form with a cylindrical liner, as an experimental

device for making accessible otherwise elusive physical properties of liner materials subjected to high strain rates and unusual combinations of stresses such as torsion and tension.

The cylindrical liner is expected to exhibit several very useful properties, among which are the ability to resist rotational deterioration, and the possibility of making its performance depend on length rather than caliber of projectile.

EXPENDABLE FLASH X-RAY TUBE

George Hauver

George Bryan

Ordnance Engineering Laboratory, Ballistic Research Laboratories
Aberdeen Proving Ground, Maryland

ABSTRACT

For the flash radiography of explosive phenomena, an expendable
x-ray tube may be used without protective shielding, facilitating
flexible instrumentation. Experimental expendable tubes of the field
emission type are described, along with preliminary performance data.

INTRODUCTION

Upon preliminary considerations an expendable or inexpensive x-ray tube seems to
offer several advantages over the tubes currently used for the flash radiography of
explosive phenomena. As mentioned by Fleming[1], an expendable tube may be used without
shielding. Ordinarily, massive protective shielding is essential for the radiographic
study of heavy charges and rearrangement of instrumentation then becomes a major con-
struction job. By eliminating the necessity for shielding (or at least reducing the
required shielding by a substantial amount), the great advantage of flexibility of
field instrumentation is attained.

The tubes under investigation have been designed for use with the low voltage
x-ray circuit developed by Paszek, Taylor and Squier[2] for flash radiographic studies
at Aberdeen Proving Ground. A schematic diagram of the circuit and a 3-electrode
field emission type x-ray tube appears in Figure 1. A potential, less than the
critical breakdown potential of the tube, is applied between the cathode and target.
A negative pulse is applied to the trigger electrode, breaking down gap AB, and con-
sequently gap AC. It should be noted that, at present, the x-ray tube is a major item
in the cost of a low voltage unit and that an inexpensive tube would greatly reduce
the total cost.

CONSTRUCTION

Of the tube types first constructed, some were made at the Ballistic Research
Laboratories while others were made to order by a commercial manufacturer. The design
of those constructed in the Laboratories is shown in Figure 2, which represents a tube
with a Pyrex envelope into which is sealed 40 mil tungsten leads. The tungsten target,
5 mils thick and 1/4 inch in diameter, is spot-welded to a 15 mil nickel strip which
in turn is spot welded to the tungsten lead.
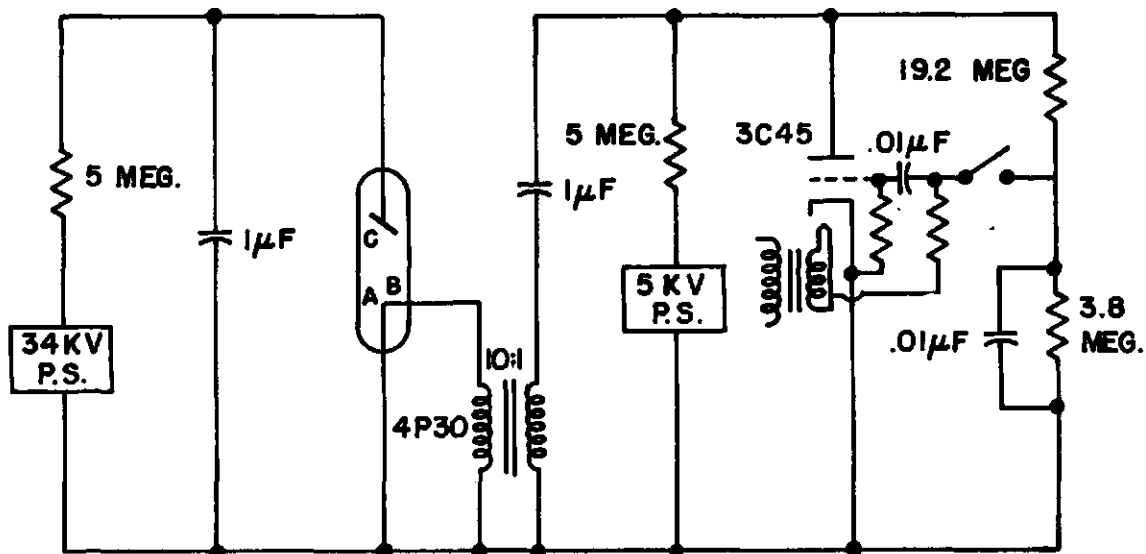
Figure 1—Low voltage flash x-ray circuit.
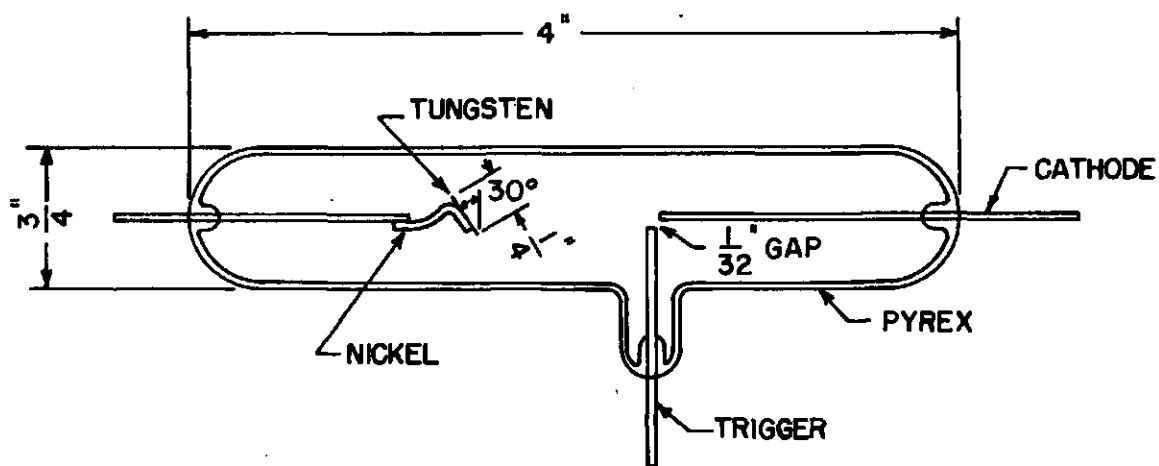
Figure 2—Ordnance Engineering Laboratory Tube.

152

Tubes were evacuated to pressures of from 10^{-2} to 10^{-3} microns and tested while still on the vacuum system. The vacuum system consisted of a three stage oil diffusion pump backed by a Welch Duo-Seal forepump, with a liquid nitrogen cold trap between the tube under evacuation and the diffusion pump. Pressure was measured with National Research Corporation Type 507 ionization gauges. Tubes were not carefully degassed but baked at 350 degrees Centigrade for periods of 12 hours.

The commercial tubes are of the types shown in Figures 3, 4, 5, and 6. These types differ only in their trigger and cathode structures. Tube envelopes are of Kovar sealing glass, into which are sealed leads of 60 mil Kovar. Tungsten targets, 42 mils thick and 1/2 inch in diameter, are spot welded and copper brazed to the Kovar leads. The standard target-cathode spacing is 5/8 inch, although for the tube type of Figure 6 this spacing varies between limits of 3/8 inch and 1 inch. The commercial tubes were evacuated to pressures of about 10^{-3} microns, but were not thoroughly degassed by standard procedure.

TESTING

Tubes were tested with the circuit shown in Figure 1, and x-ray outputs were measured by Victoreen ionization chambers of the 0-10 milliroentgen size. Radiographs of lead test patterns were taken on Kodak Type F x-ray film, using Patterson Fluorazure (zinc sulfide) intensifying screens. Previous tests indicated Fluorazure screens to be the most efficient type for low voltage radiography. Photographs of the visible flash in the tube were taken along with pinhole radiographs of the target.

The highest consistent output from the BRL tubes, measured 20 inches from the tube, was 0.4 milliroentgen. An image of specular density 0.12 was formed on x-ray film placed at the same distance from the tube. After several flashes, the interior of the envelope between the cathode and target was observed to have developed craze or fine surface fractures, presumably caused by heating. Optical pictures indicated a concentration of vapor along tube walls.

Values of some circuit components were changed during tests of the commercial tubes. Tubes tested with the circuit as shown in Figure 1 gave, on the first flash, an output of 1.0 milliroentgen at 36 inches. An image of specular density 0.8 was formed on x-ray film placed at the same distance. Pinhole radiographs indicated greater x-ray emission from that portion of the target nearest the cathode, and optical pictures indicated a greater concentration of vapor near the same portion of the target. With the main capacitance reduced to 0.25 microfarads and the trigger capacitance reduced to 0.01 microfarads, an output of 1.0 milliroentgen was still maintained for the first flash. In all cases, the tubes became gassy after the first flash, and the second flash yielded 0.5 milliroentgen measured 36 inches from the tubes. Further flashing produced no output measurable at this distance.

DISCUSSION

The preliminary investigations lead to the obvious conclusion that some changes in design and construction are necessary to obtain increased and consistent x-ray output.
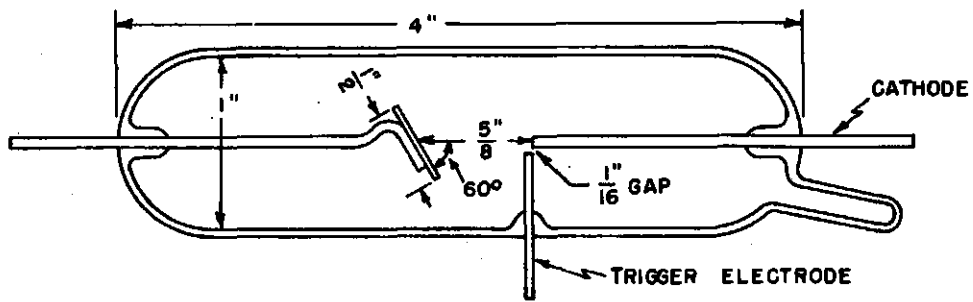
Figure 3—Commercial tube.
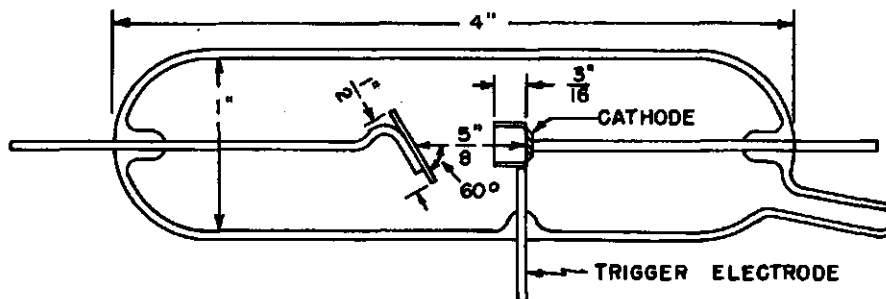
Figure 4—Commercial tube.
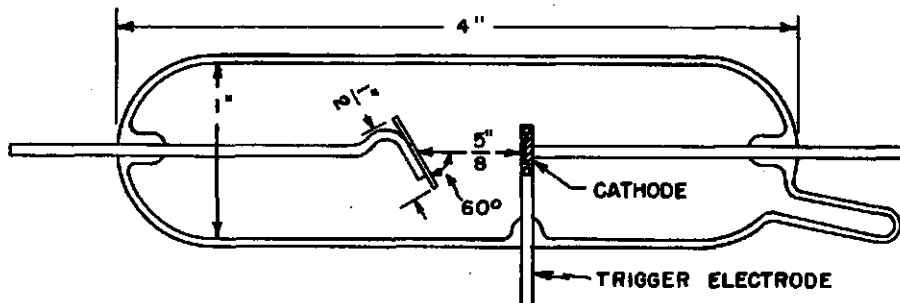
Figure 5—Commercial tube.
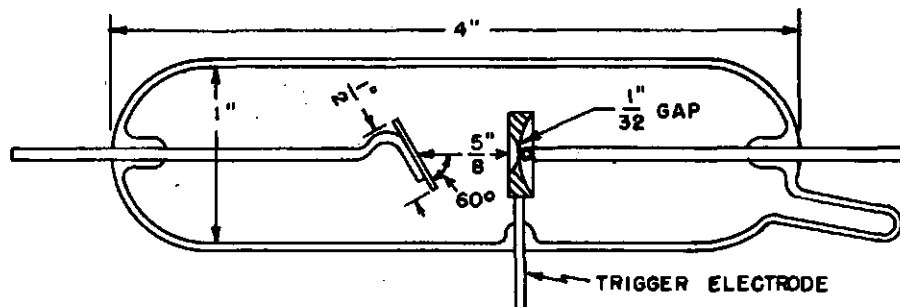
Figure 6—Commercial tube.

Several possibilities for improving the output are suggested by the mechanism presented by Kingdon and Tanis[3]. When the tube is flashed, the electrons initially fall through the entire applied potential. As the voltage falls off from this maximum, the radiation becomes softer and is finally cut off entirely by the formation of a low voltage arc. This arc is caused by the presence of gas or metallic vapor which, when ionized, neutralizes the space charge and allows large currents to flow. With large currents, most of the voltage drop occurs in the leads with little energy going into the production of x-rays. If gas or vapor is evolved too rapidly the x-ray output is cut off prematurely.

Apparently there are three sources of gas or vapor. First, the commercial tubes were not thoroughly degassed and became gassy after the first flash. When the main condenser was slowly charged for the second flash, the gas was cleaned up but was rapidly re-evolved and ionized by the second flash. Second, photographs of the visible flash and surface fractures in the glass indicate that vapor was evolved from the bombarded walls, in which case the envelope should be enlarged. Third, if vapor is boiled from the target, a larger area should increase the maximum output. In fact, preliminary tests indicate a dependence upon target area.

1. R. O. Fleming, "A Simple Flash X-Ray Circuit", Progress Report 16, Technical Memorandum Report 16, Ordnance Research Division, Old and Barnes Inc., Pasadena, California. (1951)

2. Paszek, Taylor, and Squier, "Low Voltage Flash Radiography", Transactions of the Hollow Charge Symposium, Aberdeen Proving Ground. (November 1951)

3. K. H. Kingdon and H. E. Tanis, Physical Review 53, 128-134. (1938)

THE KERR CELL CAMERA AND ITS APPLICATIONS

E. C. Mutschler

Department of Physics, Carnegie Institute of Technology, Pittsburgh, Pennsylvania

ABSTRACT

The Kerr cell method of high speed photography has been used by this group to photograph both luminous and non-luminous transient phenomena at exposure times down to 1/2 microsecond. In the case of non-luminous phenomena, the opening of the Kerr cell is synchronized electronically with the light flash obtained from an electrically exploded wire having a peak intensity of about 5×10^8 candle power. The Kerr cell is of sufficient size to allow the use of a 7 inch, f/2.5 lens at an effective aperture of f/4. To operate such a large Kerr cell requires a voltage pulse of amplitude 25KV.

This method is ideally suited to the photography of detonating explosives, metal jets in shaped charges, shock waves in transparent liquids and solids, and other phenomena having propagation velocities up to 10,000 meters/sec.

INTRODUCTION

A number of unusual difficulties must be overcome if the metal jets from lined cavity charges are to be successfully photographed. The sub-microsecond exposure time required to "stop" the jet rules out the use of mechanical shutters for this purpose. The intense luminosity of the exploding charge rules out "open flash" methods in which the phenomenon is lighted by a flash of light of very short duration from a spark or from a flash tube. Fig. 1, a Kerr cell photograph of the detonation of a cylinder of pentolite, will serve to point up the unusual conditions encountered in the photography of intensely self-luminous phenomena. Note that, in spite of the short exposure time of one microsecond, there is sufficient self-luminosity available for photography. Furthermore, close inspection of the picture reveals a blurring of the image at the detonation front due to movement during the one microsecond the film was exposed. Cavity charge jets are relatively non-luminous when compared with the exploding charge. Consequently, a brilliant light source synchronized with a shutter able to produce one half microsecond exposures is required to photograph these jets by visible light. In the C.I.T. setup, a length of fine wire, exploded electrically, fulfills the light source requirement by giving a peak intensity of approximately 500 million candle power,[1] and a Kerr cell electro-optic shutter determines the duration of the exposure.

I. KERR CELL CAMERA AND LIGHT SOURCE

Fig. 2 shows a schematic diagram of the setup for Kerr Cell Photography. The explosion takes place in a bombproof separated from the observation room by a thick
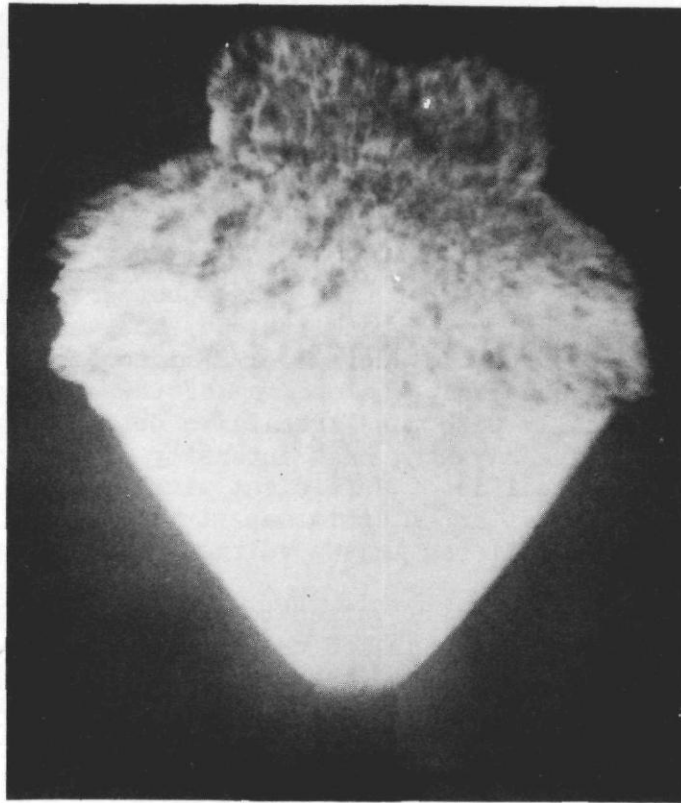
Figure 1—Kerr cell photograph of the detonation of a cylinder of pentolite.
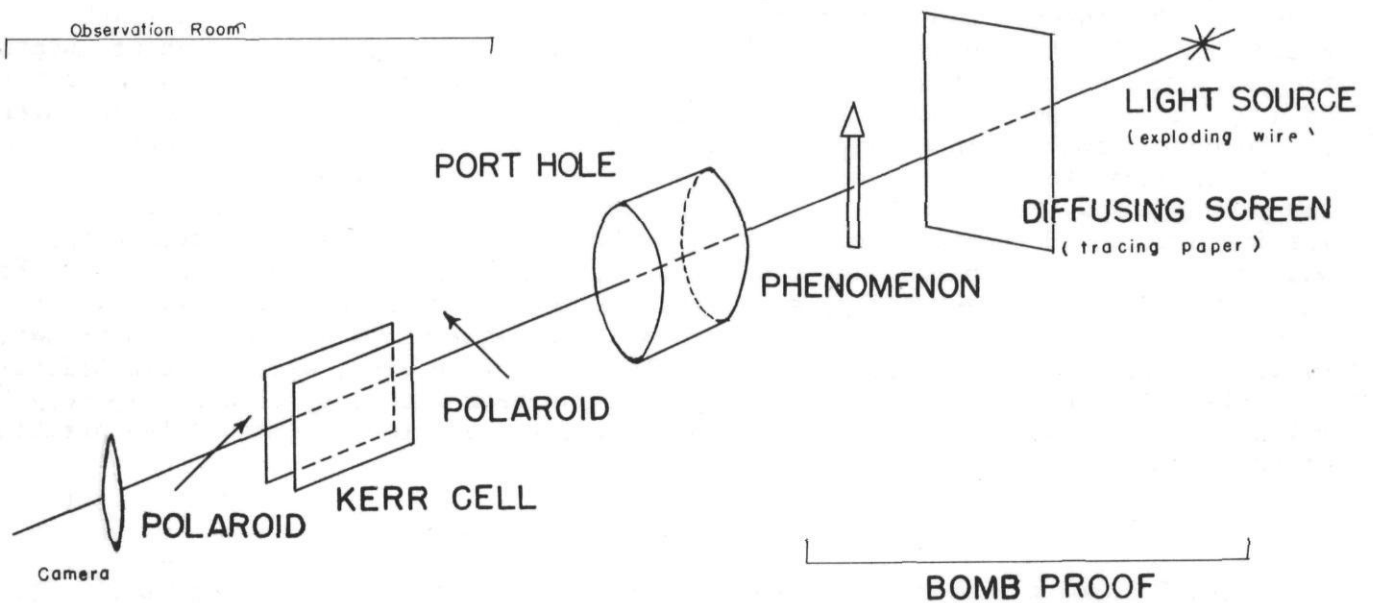
Figure 2—Schematic setup for Kerr cell photography.

158

concrete wall. A window of bullet proof glass permits the camera to take pictures of events occurring in the bombproof. The phenomenon is outlined against a light-diffusing screen of tracing paper illuminated from behind by the exploded wire. The Kerr cell shutter, consisting of a Kerr cell between crossed polaroids, transmits light only during the one half microsecond when a high voltage pulse is applied to the electrodes of the Kerr cell.

For maximum Kerr effect, the front polaroid is oriented so that light entering the cell is plane polarized at an angle of 45 degrees to the vertical. The back polaroid is set at 90 degrees to the front polaroid. The electrodes are immersed in nitrobenzene, a transparent fluid exhibiting the highest Kerr activity known.[2]

When no electric field exists between the electrodes, the polarized light passes through the cell unchanged except for some absorption. However, when a potential is applied to the electrodes, the polarized light is changed progressively to various states of elliptic polarization and, in an ideal case, emerges from the cell plane polarized at 90 degrees to its original direction. Because the Kerr effect depends on wave-length, this "full-open" or maximum transmission condition can be obtained only with monochromatic light. For other wave lengths, only the component of the elliptically polarized light parallel to the plane of polarization of the back polaroid passes through the cell.

For the type of Kerr cell described here, it can be shown[3] that the intensity I of monochromatic light transmitted by the back polaroid is related to the original intensity I_0 from the front polaroid, by the equation given at the top of **Fig. 3**. Here the term e^{-md} is the fraction of the light intensity remaining after absorption, m is the absorption coefficient, d the length of the light path, B the Kerr constant, V the instantaneous potential, and a the spacing of the electrodes. In addition to the absorption of light by the nitrobenzene, there are several other factors that reduce the transmission, namely a non-uniform electric field and the lack of a monochromatic light source.

On the bottom left of this figure is a line drawing of a two electrode cell showing the electrode spacing a and the electrode length d. The aperture of the Kerr cell shutter can be nearly doubled by using three electrodes as is shown at the bottom left. This arrangement is used in the C.I.T. camera.

Fig. 4 shows the disassembled Kerr cell shutter. At the top center is the electrode assembly consisting of three copper screen electrodes and two supporting frames. The center electrode is suspended between two glass rod insulators. The cell body, a rectangular box of glass plates cemented together, is directly below the electrode assembly. At the bottom left is the light proof Kerr cell box with a needle point spark gap mounted on its top. The function of this needle gap will be given later. To the right is one end of the Kerr cell box with a polaroid mounted on it. For use in photography, the glass cell body must have end plates that are distortionless and also free of strain. The latter requirement is necessary because glass that is strained alters the polarized light causing light leakage through the closed shutter. Likewise, internal reflection must be minimized since this also causes light leakage. For this reason, screen mesh electrodes are used to reduce the reflection of light striking their surfaces.

$$I = I_0 \exp(-md) \cdot \sin^2\left(\frac{\pi d B V^2}{a^2}\right)$$

I = Light Transmitted by Back Polaroid
I_0 = Light Transmitted by Front Polaroid
m = Light Absorption Coefficient
d = Length of Electrodes
a = Spacing of Electrodes
B = Kerr Constant
V = Voltage Applied to Cell
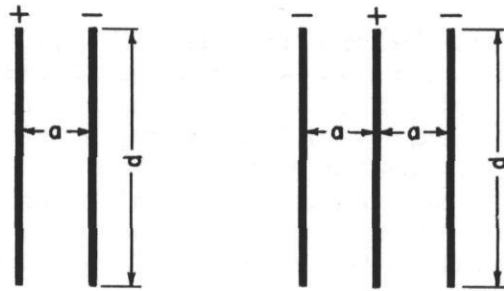
Arrangement for
Doubling Aperture

Figure 3—Transmission of a Kerr cell.
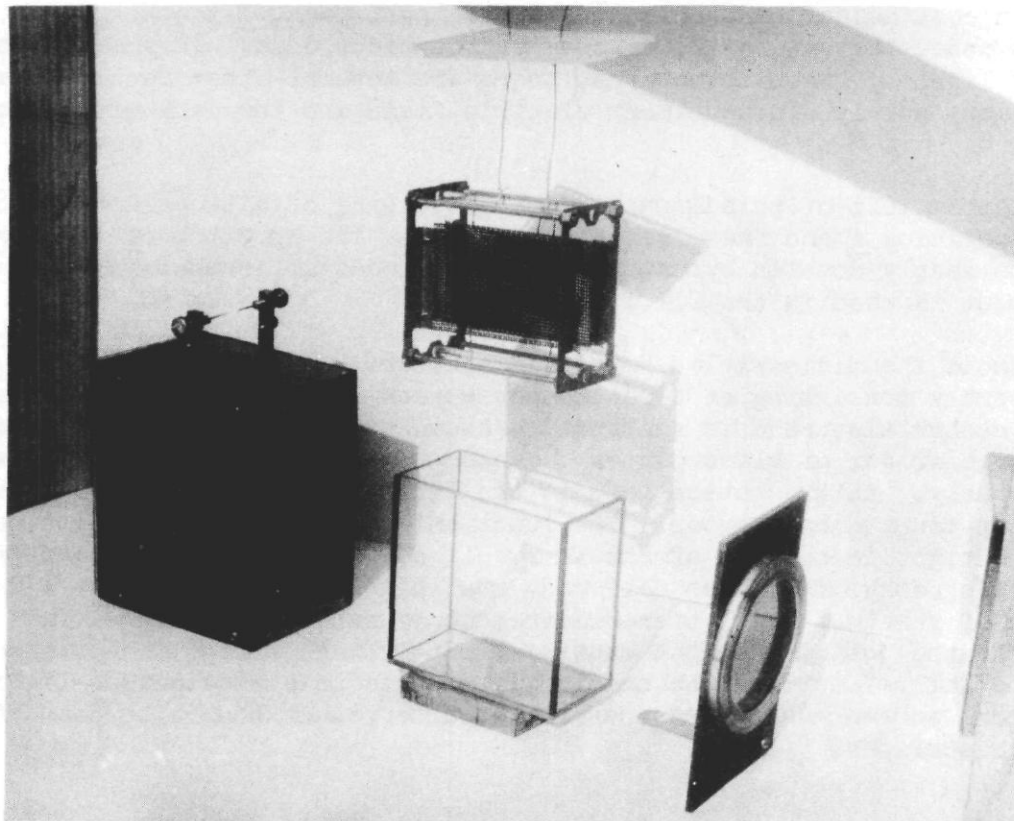
Figure 4—Disassembled Kerr cell shutter.

160

The camera used with the Kerr cell shutter is made up of a 4 x 5 inch Graflex camera back, a cloth bellows and an f/2.5 Aero Ektar lens having a seven inch focal length. Because the aperture of the Kerr cell covers less than half the area of the lens, the effective speed of the combined lens and Kerr is reduced to approximately f/4. At present the camera is being fitted with an f/2 Xenon lens which when combined with the Kerr cell will give an effective speed of f/2.9. A long focal length lens was selected to yield a large image without enlargement. The use of high speed film and harsh development methods increases grain size so much that resolution is limited, even for a 3 inch image obtained without enlargement.

High intensity light for theKerr cell photography of jets is obtained by suddenly discharging a 3 microfarad condenser charged to 24 kilovolts through a fine wire, causing the wire to "explode" with an intense flash of light. This light source reaches a peak intensity of about 500 million candle power in 7 microseconds and has a duration of about 25 to 50 microseconds.

Fig. 5 is a block diagram of the high speed photography system showing the sequence of operations. The phenomenon initiates the synchronization circuit in one of two ways. For non-rotated charges, a pair of enameled trigger leads are twisted together and taped to the explosive. When the force of the explosion shorts these leads, a thyratron is put into conduction forming a triggering pulse. For rotated charges, a photocell is used to pick up the light from the luminous jet front.

A variable delay of 1 to 500 microseconds, is provided for in the delay unit. The delayed pulse is then fed into the high voltage circuit, which is made up of the switching and synchronizing circuit, the exploding wire circuit, and the Kerr cell circuit.

Fig. 6 shows a circuit diagram of the high voltage circuit. Drawn in heavy lines is the exploding wire circuit consisting of condenser C1, three-sphere spark gap SS and the fine wire. The Kerr cell circuit, drawn in medium width lines, is made up of condensers C2 and C3, and spark gap GG. The remaining components, drawn in fine lines, serve as control elements. Both sections of the spark gap SS are adjusted to break down at 15 kilovolts. When a trigger pulse is applied to the 5C22 hydrogen thyratron thus firing it, the center electrode of gap SS momentarily goes to ground potential. The full 24 kilovolt potential then appears across the upper section of gap SS causing it to break down followed immediately by the breakdown of the lower section. With gap SS ionized, a heavy surge of current from condenser C1 passes through the fine wire exploding it. Referring again to the circuit diagram it is seen that spark gaps SS and GG have a common air space. The ionization of this common gap serves to couple together and to synchronize the exploding wire and Kerr cell. The time of breakdown of gap GG can be varied through a range of about 10 microseconds by adjusting the spacing of its electrodes. Condensers C2 and C3 of the Kerr cell circuit discharge through gap GG applying a voltage pulse to the Kerr cell shutter thereby making it transparent. After a very short time, needle gap MG breaks down rapidly discharging the Kerr cell to its opaque state.

Fig. 7 demonstrates the operating characteristics of the Kerr cell shutter. Shown at the upper left is an oscillogram of luminosity vs time for an exploding wire, as seen through an "open" Kerr cell, that is, one with its polaroids parallel. In this instance, transmission was reduced 90 per cent by the application of a voltage

161
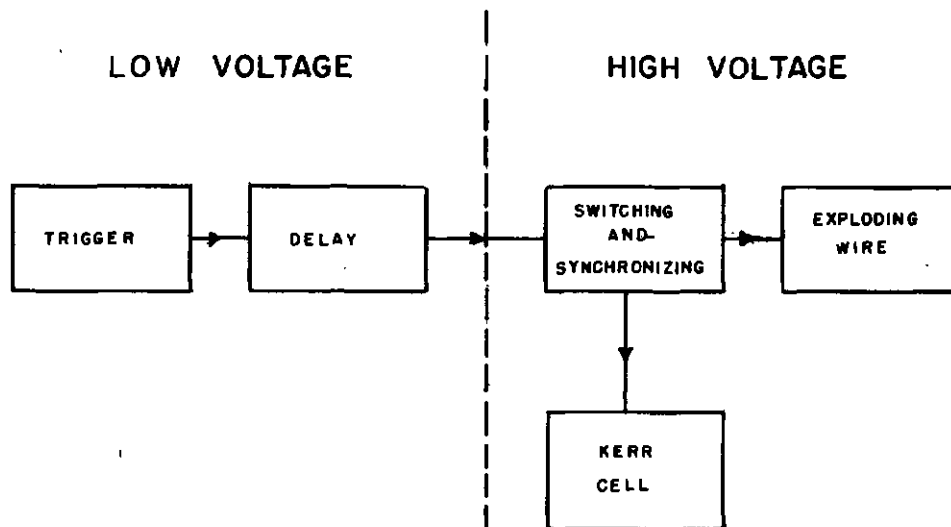
Figure 5—Block diagram of Kerr cell camera system.
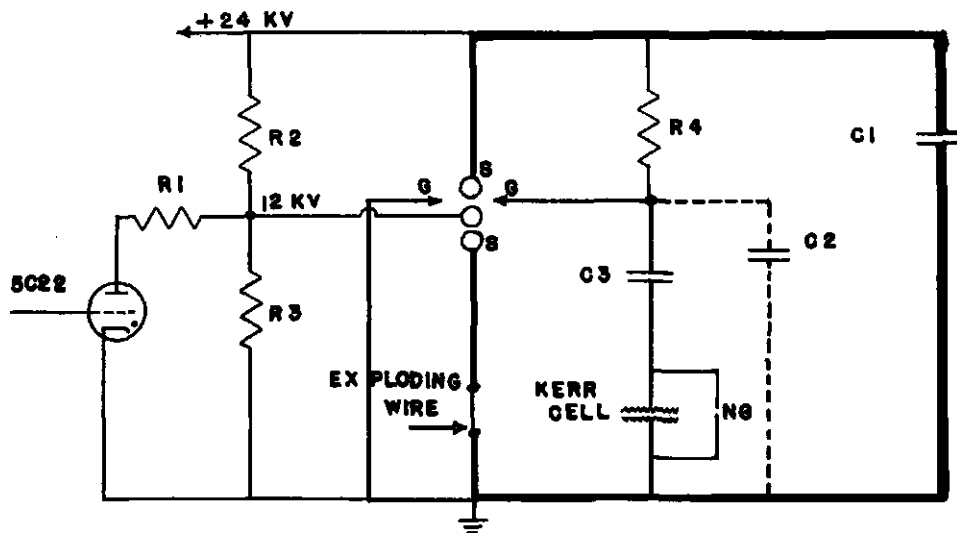
HIGH VOLTAGE CIRCUIT DIAGRAM

R1=10000 OHM	C1= 3 uF	SS = WIRE CIRCUIT SPARK GAP
R2=100 MEGOHM	C2=.1 uF	(THREE SPHERES)
R3=100 MEGOHM	C3=1000 uF	GG= KERR CELL CIRCUIT SPARK GAP
R4= 2 MEGOHM		NG= KERR CELL DISCHARGING SPARK GAP
		(NEEDLE POINTS)

Figure 6—High voltage circuit diagram.
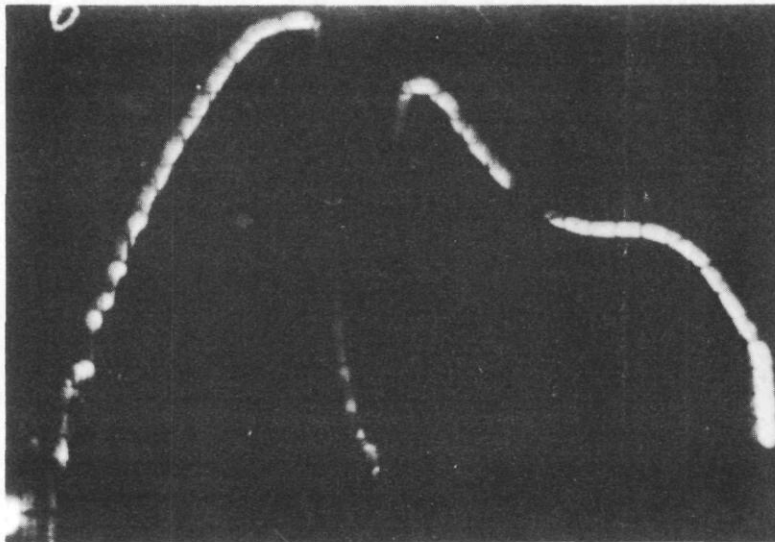
Polaroids Parallel
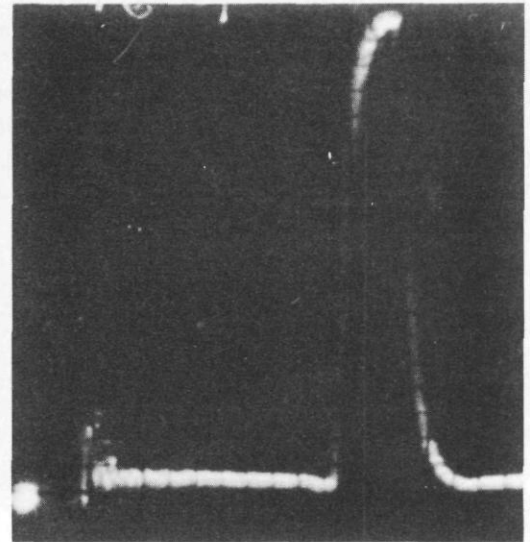
Polaroids Crossed
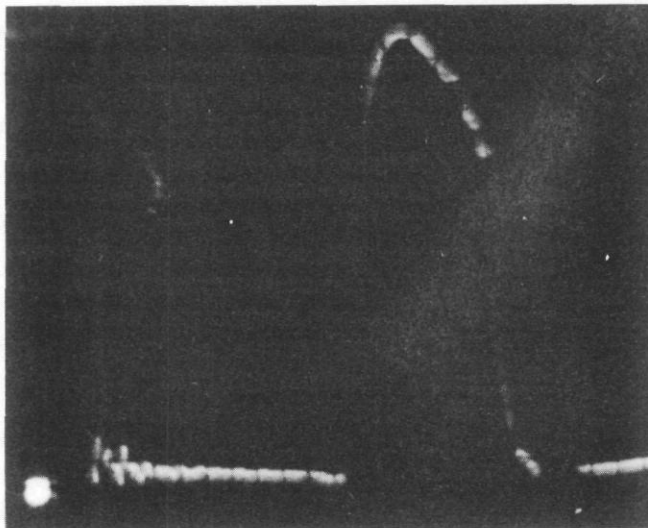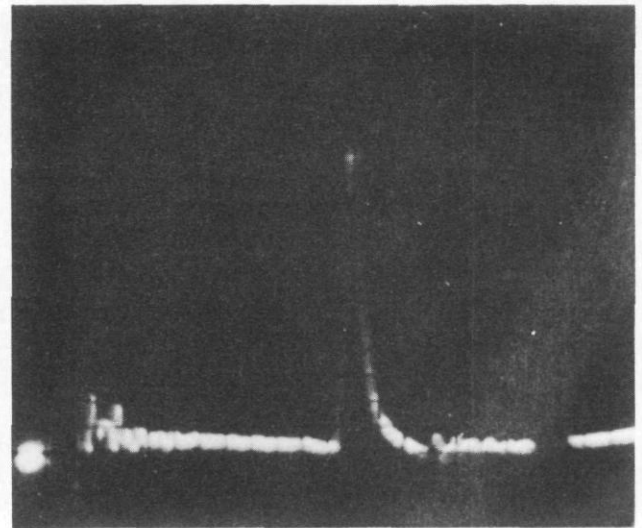
Polaroids Crossed.

Polaroids Crossed.

Figure 7—Oscillograms of typical Kerr cell operation for various needle gap settings.
Each horizontal division corresponds to 0.5 microsecond.

163

pulse to the Kerr cell as is indicated by the dip at the middle of the light trace. This corresponds to a 90 per cent opening efficiency for a similar cell with polaroids crossed. Synchronization, efficiency and exposure time can be checked with this type of oscillogram. The other three pictures in Fig. 7 were obtained with the polaroids crossed as for normal operation. These light intensity versus time oscillograms show the exposures obtained for several needle gap settings. At the upper right is a one microsecond exposure which has nearly a square wave shape. At the lower left is a three microsecond exposure, and at the lower right is a one half microsecond exposure. In this last oscillogram, the decreased amplitude indicates that the transmission efficiency of the cell at this needle gap setting has decreased considerably. Exposure times from one half microsecond to five microseconds are possible through adjustment of the needle gap.

Before proceeding to applications of the Kerr cell photographic technique, some of the advantages of the exploding wire as a light source should be pointed out. First, it gives a peak luminosity that is much higher than that of any comparable light source. Second, because of its negligible cost, it can be used in the bombproof where it will do the most good.

II. APPLICATIONS AND RESULTS

The photography of jets traveling in air was the first application of the Kerr cell technique attempted. Fig. 8 shows a jet picture from a typical charge. While a small portion of the actual jet can be seen near the top of the picture, most of it is obscured by an opaque shroud. In fact the early pictures did not show any jet at all until shadowgraph methods were adopted and the exposure time was made short enough to stop motion.

The opaque shroud appeared to consist of a large number of high-speed particles traveling nearly parallel to the jet and vaporizing continuously. This conclusion was verified by taking a photograph of a jet passing through an evacuated glass tube. Fig. 9 shows such a jet in a tube evacuated to a pressure of 10^{-3} millimeters of mercury. No shroud is seen in this picture, the particles being too small to be visible in the photograph, and no metal vapor is formed at the jet tip in the absence of air.

The shrouded jet shown before in Fig. 8 was from a copper liner with a flat apex as shown in cross-section at the left of Fig. 10. The lack of a pointed apex was found to be responsible for most of the shroud, for when the pointed cones pictured at the right of Fig. 10 were used, shroudless jets like that of Fig. 11 were obtained. Note, however, that a small portion of the jet at the tip is obscured by the metallic vapor produced by its reaction with the air.

In order to determine how two simultaneously detonated cavity charges might interfere, the setup given at the left of Fig. 12 was used. The two shaped charges are detonated simultaneously by equal lengths of primacord running to a single detonator. At the center is the action picture of this setup showing two perfectly formed jets. However, when the detonation of the right hand charge is delayed 8 microseconds, interference results as seen at the right of Fig. 12.
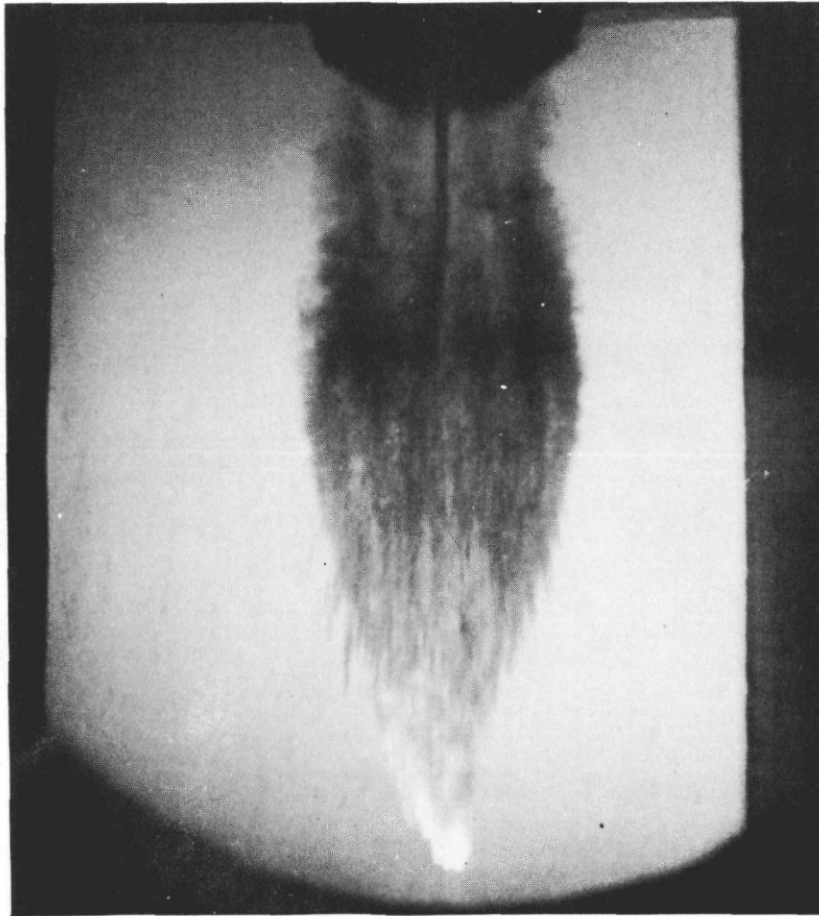
Figure 8—Jet from copper cone
with flat apex.
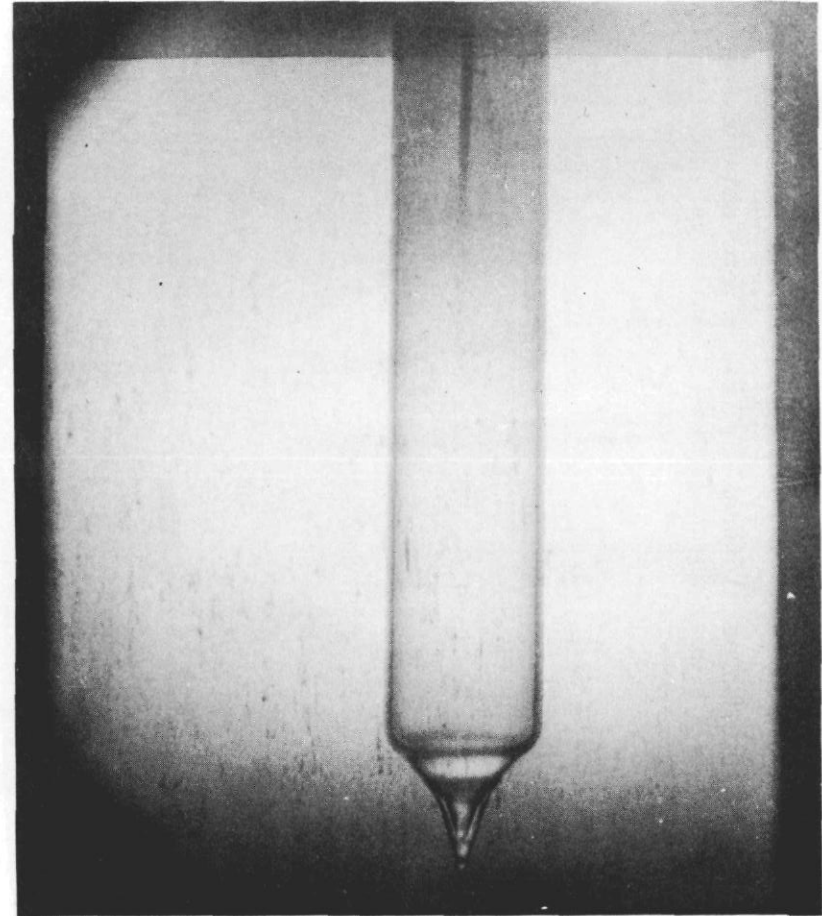
Figure 9—Jet in a tube evacuated to a
pressure of 10^{-3} mm Hg.
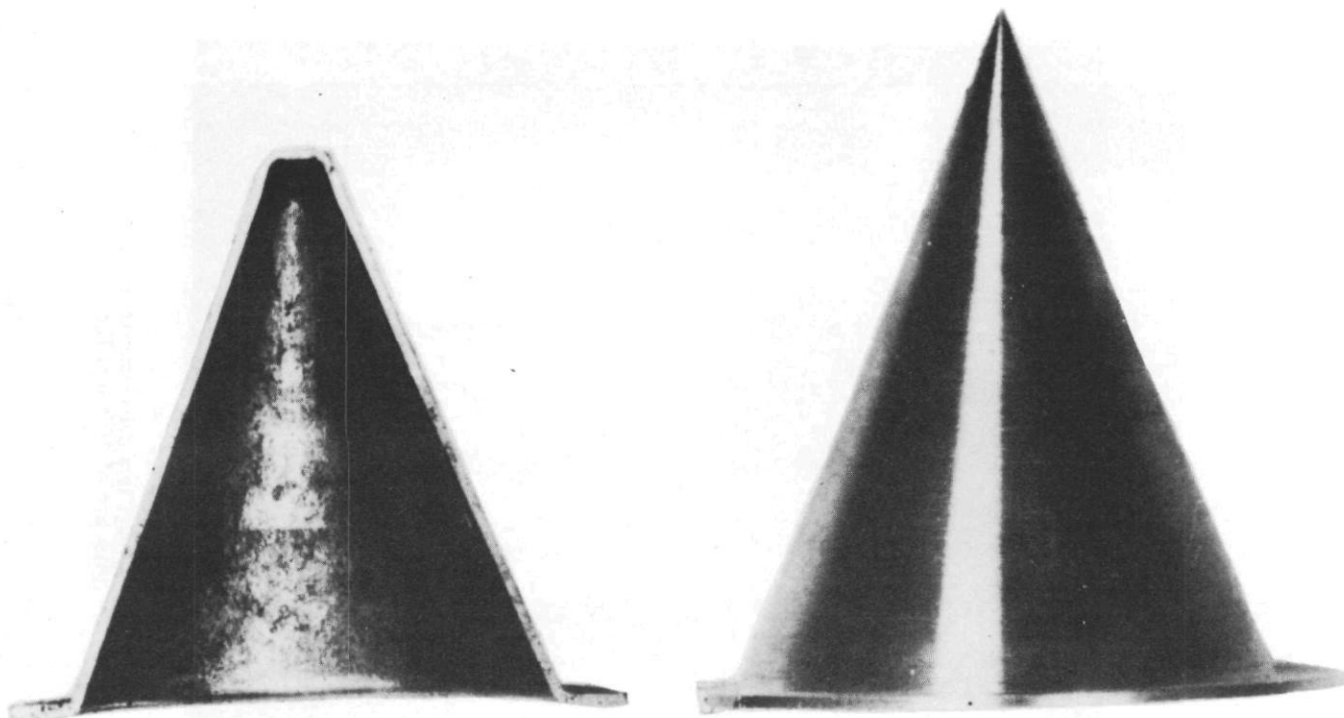
Figure 10—Copper liners with flat and pointed apexes.
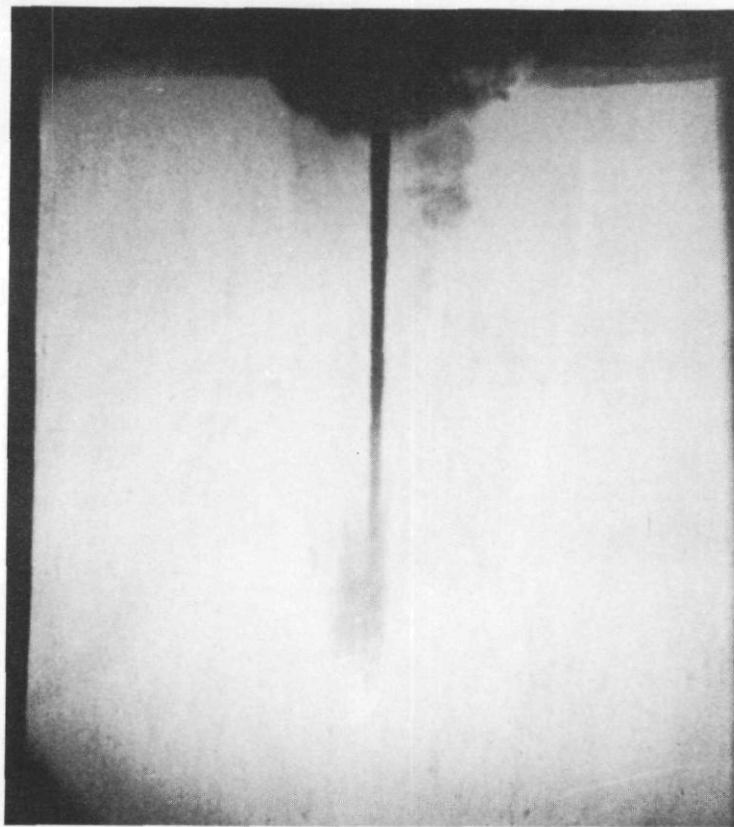
Figure 11—Shroudless jet from pointed cone.

166
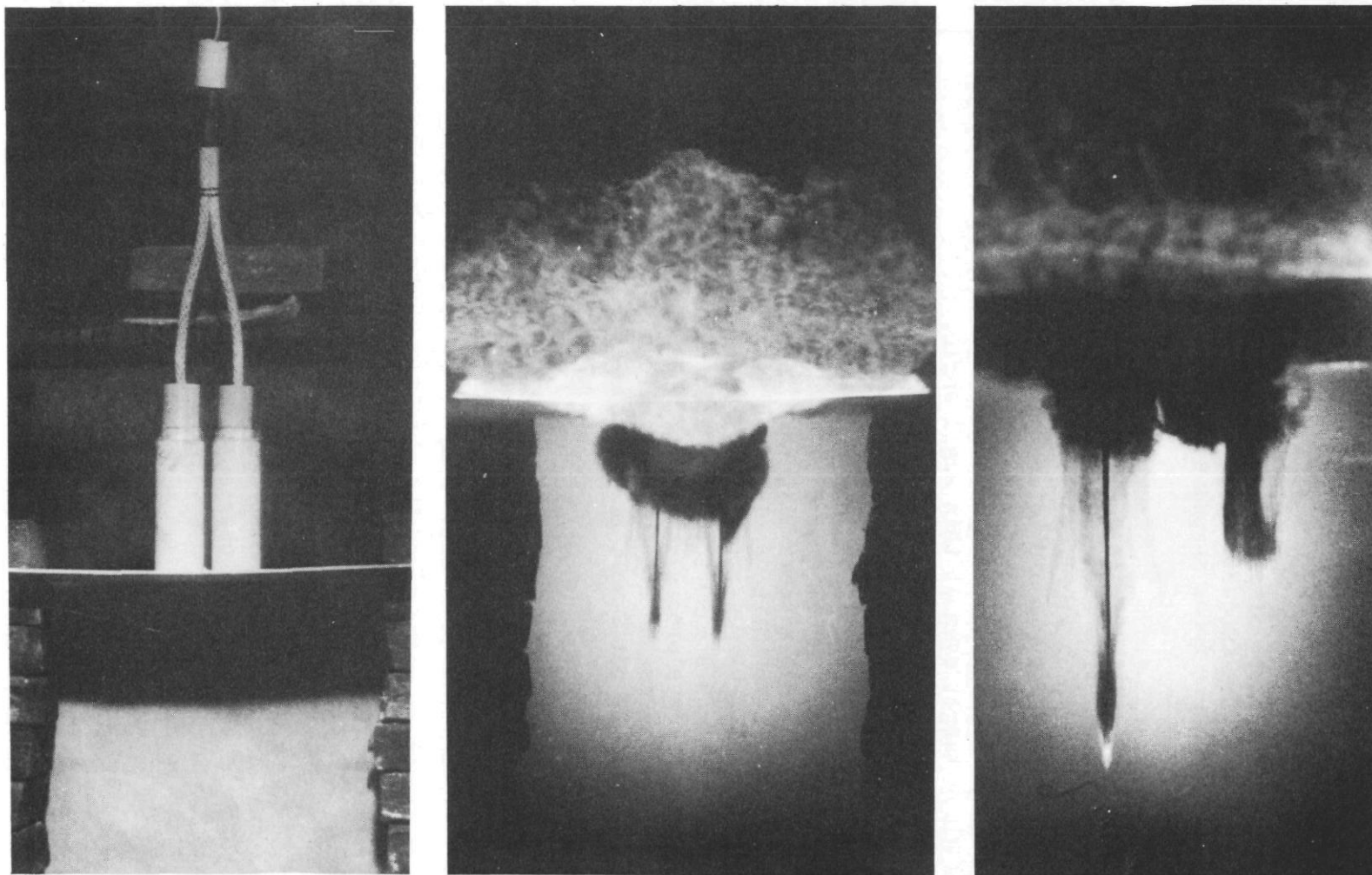
Figure 12—Interference of simultaneously or sequentially detonated cavity charges.

Shown in Fig. 13 are pictures of jets formed from very small cavity charges known as spit-back fuses. This charge is 1 inch long and 3/8 inch in diameter and has a conical aluminum liner with an 80 degree apex angle. The jets shown in these pictures are less than a millimeter in diameter and are probably the smallest jets that have been photographed. Note that one of these jets is quite curved.

A jet penetrating a piece of plexiglas of dimensions 6 x 6 x 1-1/4 inches is seen in Fig. 14. The plexiglas just above the jet tip has been shattered causing this area to become opaque. A bow shaped shock wave is seen extending laterally across the plexiglas block.

Fig. 15 shows a jet entering a glass target at an angle of 20 degrees to the target surface. The jet inside the glass is surrounded by a transparent region which in turn is bounded by a dark line. This dark line cannot be the result of a shock wave since a shock wave would be conical rather than cylindrical. It has been theorized[4] that the transparent region consists of molten glass which has been melted by the high pressure produced by the jet tip. Note that the jet is not deflected by the glass target even at this small angle.

Fig. 16 shows a steel jet in air which has separated into segments. This results from the negative velocity gradient that exists along the jet which causes the jet to lengthen and break up as it travels. This same effect can be shown indirectly by pictures of the jet penetrating water. Fig. 17 shows two pictures of copper jets with 2 and 12 inch standoffs respectively, that is, the distance from the liner base to the surface of the water. Although the jets are not seen in these pictures, their nature can be inferred by the cavitation they produce. At the left the outline of the cavitation for the two inch standoff case is smooth, indicating that the penetration in this case is a continuous process. However, the cavitation becomes progressively more irregular in outline as the standoff is increased, as shown in the other picture in this figure. Hence, the jet itself must become increasingly broken up as standoff is increased.

Fig. 18 gives a similar comparison of jets penetrating water after penetrating 1-1/4 inches of steel, on the left, and 1-1/4 inches of glass, on the right. Here the cavitation outline is much more irregular for the case of the jet that penetrated the glass target.

Fig. 19 demonstrates the use of two Kerr cell cameras to obtain two successive pictures of the same phenomenon. A jet from a brass liner is shown penetrating a 1/2 inch steel plate. The picture at the right was taken 4 microseconds after the one on the left.

Fig. 20 is the setup used to photograph the collapse of a wedge liner. The liner is extended beyond the edges of the charge to prevent explosive products from obscuring the action taking place inside the wedge. Fig. 21 shows the collapsing wedge liner and the resulting "jet" being formed.

III. CONCLUSION

The Kerr cell photographic technique has proven to be applicable to a variety of special problems in the investigation of jet phenomena. This technique can be used to
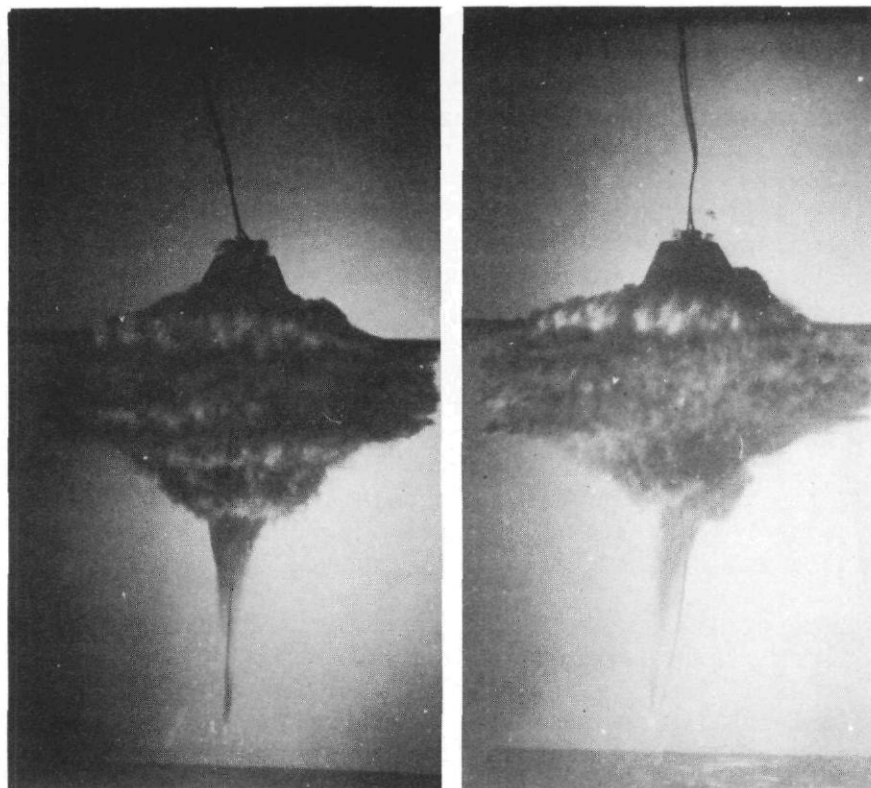
Figure 13—Jets from small cavity charges in spit-back fuses.
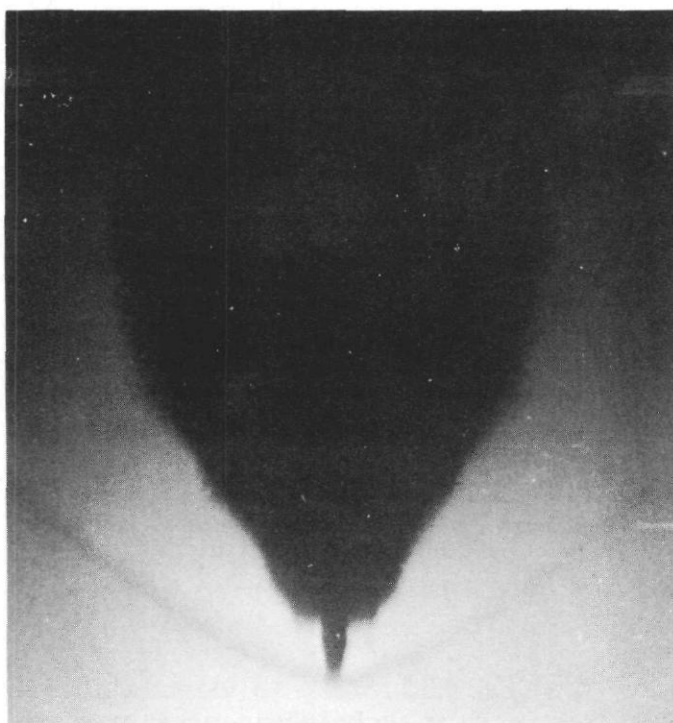
Figure 14—Jet penetrating plexiglass.
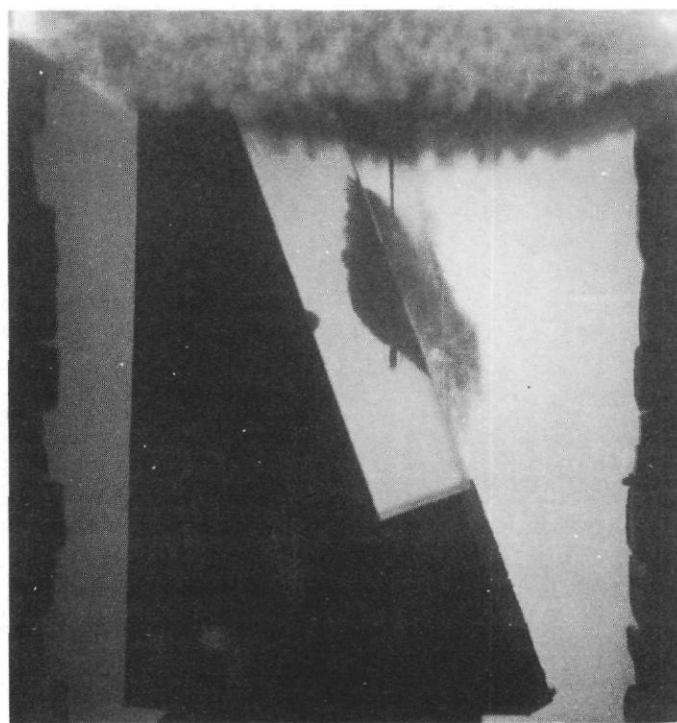
Figure 15—Jet entering a glass target at an angle of 20° to the target surface.

169
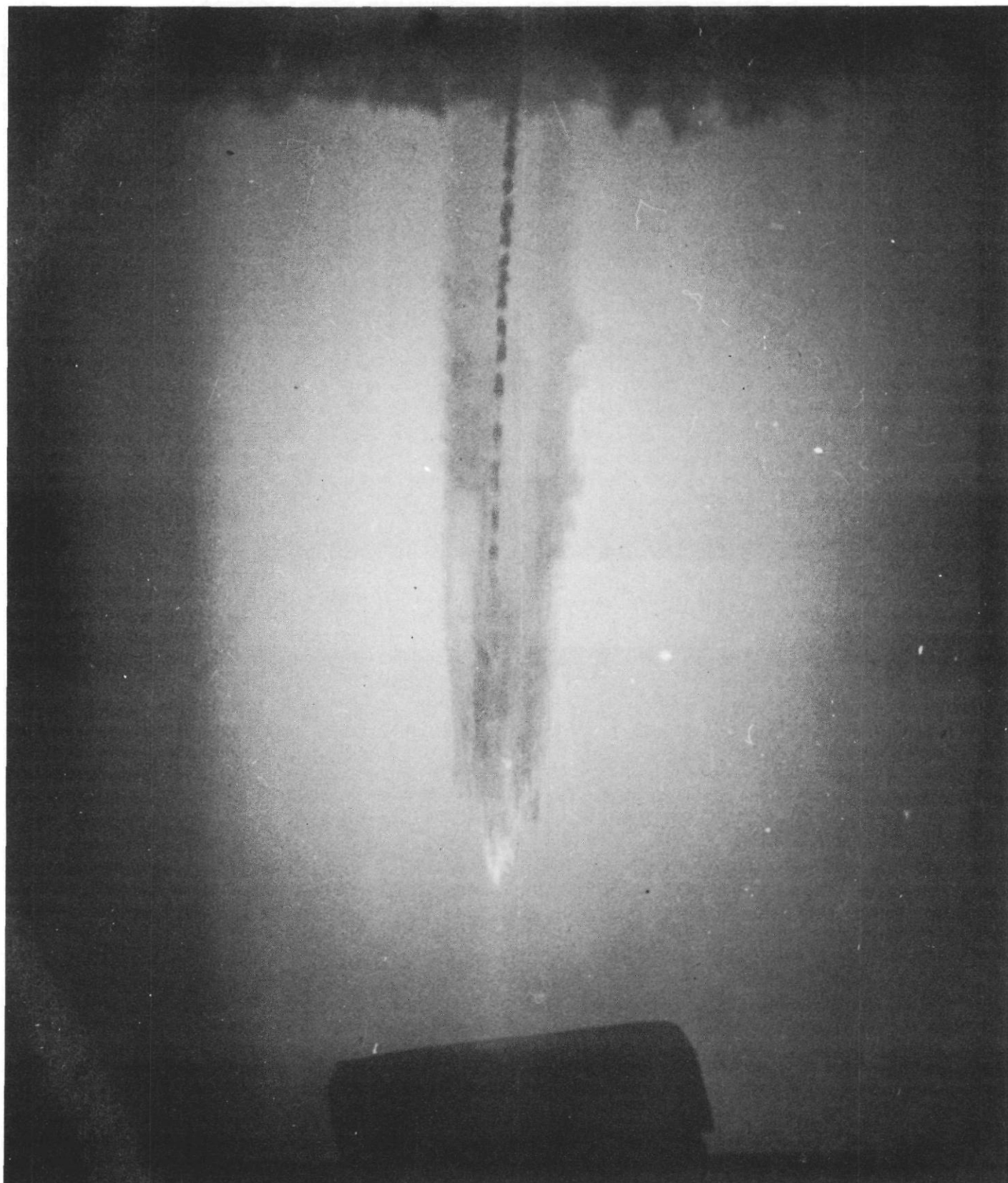
Figure 16—Steel jet in air.
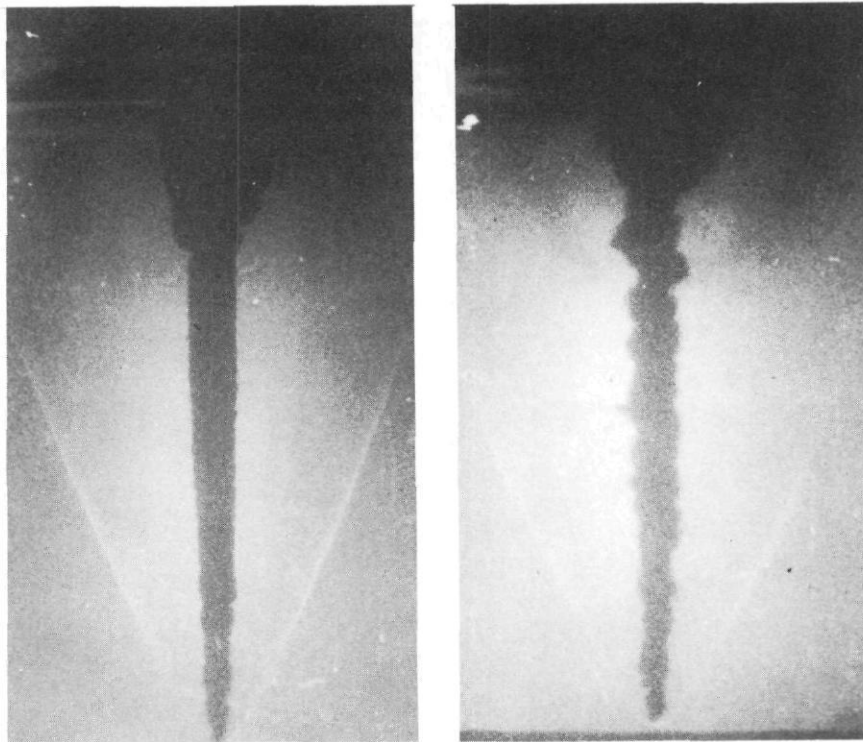
Figure 17—Copper jets with 2 and 12 inch standoffs respectively.
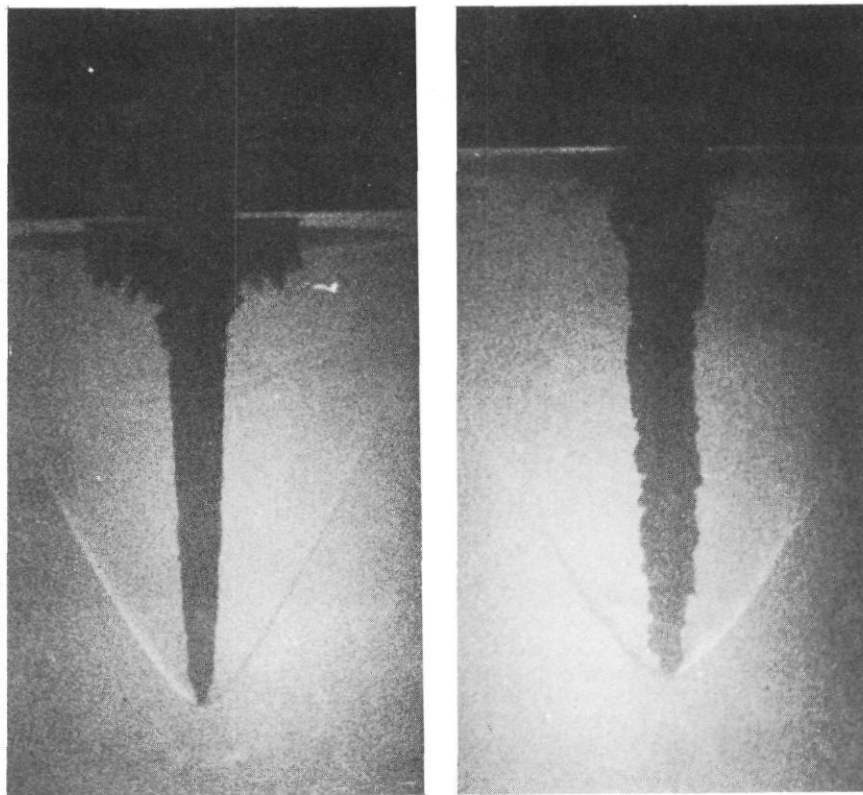
Figure 18—Jets penetrating water after penetrating 1¼ inches
of steel (left) and glass (right).

171

Figure 19—Two successive pictures of a jet penetrating ½ inch steel plate, taken with two Kerr cell cameras.

172
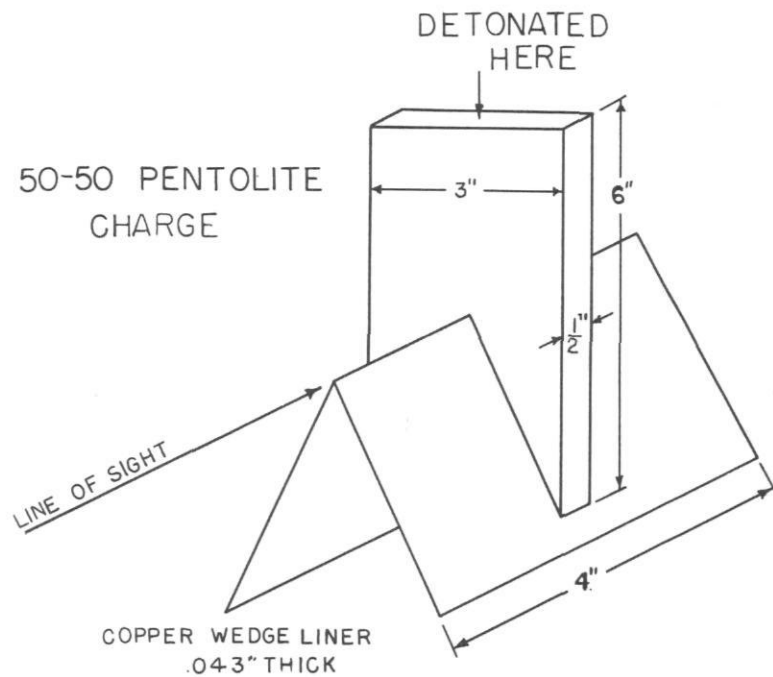
Figure 20—Setup for photographing the collapse of a wedge.
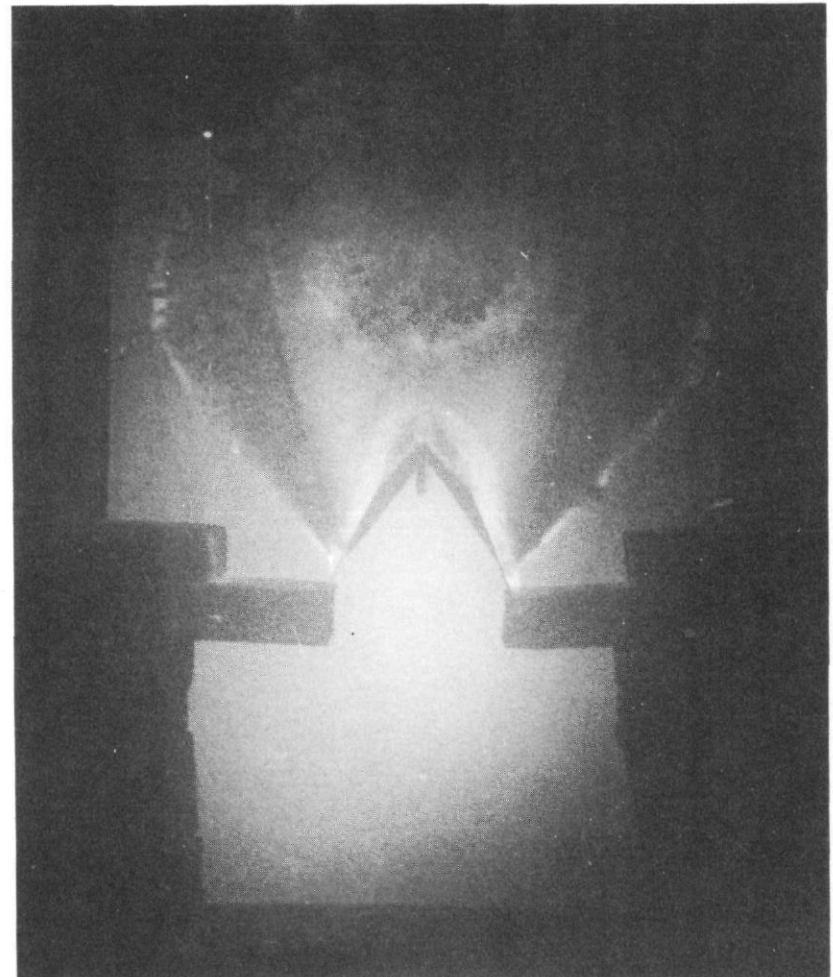
Figure 21—Collapsing wedge liner.

supplement the flash X-ray technique in the study of the fine structure of jets. However, it is not applicable to the liner collapse problem except in the two dimensional case. Multiple Kerr cell cameras can be used to take a number of pictures of the same phenomenon. Available light intensity should be increased so that slow, fine grain film can be used to improve the quality of the pictures. Also an exposure time of 1/10 of a microsecond would give better time resolution and improve the rendering of detail in the pictures.

1 Fundamentals of Shaped Charges, CIT-ORD-21, p. 87, June 30, 1949.

2 Kingsbury, E. F., "The Kerr Electrostatic Effect," Rev. of Scientific Instruments, 1:22

3 Same as reference 2.

4 CIT-ORD-31, Part III, p. 49, February 28, 1951

THE PIN TECHNIQUE FOR VELOCITY MEASUREMENTS

H. Dean Mallory

U. S. Naval Ordnance Laboratory, White Oak, Silver Spring, Maryland

ABSTRACT

This is an electronic method for determining arrival times
of an event at various positions during its motion. The method
takes its name from the electrical switches which are charged,
pointed pins. The moving metal target or ionized shock wave is
electrically grounded so that on contact with a pin, a pip is
generated on an oscilloscope screen. Pips from a sequence of
pins are photographed by a still camera as they appear on the
screen. Time is determined from a crystal controlled sine wave
superimposed over the pips.

We believe that with this method, time can be resolved
better than can reasonably be expected of a photographic method
alone. Also, it is possible with the pin technique to investi-
gate the initial motion of a moving object over the interval
from zero to one millimeter with good reproducibility. It is
over this close-in range that photographic methods are at their
worst and the pin technique is at its best.

The pin technique is an electronic method for determining the arrival time of a
shock wave or moving metal target at various points. It consists of electrically
charged pins connected to one or more oscilloscopes through somewhat complex circuits.
Pips from a sequence of pins are photographed by a still camera as they appear on the
cathode ray tube. Time is determined from a crystal controlled sine wave superimposed
over the pips. Requirements on the rise time of the oscilloscope pips and the duration
of the sweep are sufficiently strict so that very few commercial circuits are adequate.

This paper will be concerned only with the technique as a whole, some experimental
details and results rather than electrical circuitry. Most of the required schematics
can be found in the recent book, "Electronics", by Elmore and Sands.

The pin technique is being used at Naval Ordnance Laboratory in a program to
evaluate various explosives by measuring shock velocity through metals and free surface
velocities of targets propelled by exploding charges. We have for the most part
limited ourselves to the study of aluminum because its shock velocity and density
are such that the data obtained can more easily be related to the particle velocity
and pressure developed in the explosive than can similar data on other easily
available material.

If the detonation pressure is developed according to the von Neuman concept of a
high pressure spike which includes the reaction zone, followed by a square step wave

behind the Chapman-Jouget point, it is apparent that thin targets will have an abnormally high velocity since they are propelled outward before the pressure-peak is eroded. A free surface velocity versus target thickness graph should then show a modified facsimile of the high pressure spike developed in the detonation wave. This has been shown; subject to the uncertainties to be discussed. (Figure 1.) The experiment has been designed to enable 8-time readings to be made within a minimum of about 1 microsecond. The surface velocity readings are obtained from 8 sharp brass pins, electrically charged and connected to an oscilloscope, and which are arranged in a small circle within a few millimeters of the face of an aluminum target. This target is an electrically grounded flat disk, 6 inches in diameter and of any thickness from 1-1/2 inches down to two mils. The target is propelled toward the charged pin contactors by the explosion of a massive charge - the term massive is used in the sense that all measurements are completed before edge effects become operative; actual dimensions of the charge are 6 x 6 x 5 inches. Since the pins have a circular configuration, it is expected that the detonation wave impacting on the target plate be planar and furthermore, that it strike the target exactly normal. The plane waves are generated in the explosive by so-called lense charges or plane wave boosters. As the target strikes a pin contactor, a conical shock wave will be set up in the target metal with its apex at the point of the pin. In order that this disturbance does not influence the planarity of flow before successive pins are discharged by contact with the grounded target, the pins must be spaced a certain distance apart. By consideration of the shock cone around the pins, the target thickness and the distance the target must travel to contact all the pins, one can determine the minimum circle diameter on which the pins can be placed. A minimum diameter is desirable inasmuch as the flatest portion of the plane wave is likely to be near the charge axis. (Figures 2 and 3.)

The rate of propagation of a shock wave through metal is determined in a manner very similar to that used for free surface velocity. In this case however, the charged pin contactors are set in holes drilled to various depths in the target. Passage of a shock causes the pins to short out. Considerations of shock cone and wave flatness also apply to shock measurements.

Experimental difficulties may be classified into two broad groups - those which can effect the magnitudes of measured velocities but not their reproducibility, and those which can effect the reproducibility. They will be discussed briefly in this order.

First of all, it is of prime importance to make measurements on the free surface of the target and not on the air shock which is built up in front of it. The intense air shock contains ionized particles and is electrically conducting. It can therefore effectively short the charged pin contactors and give pips on the oscilloscope which are not a measure of target velocity. The problem here can be appreciated by a description of events occurring at the moment of explosion: The target plate is moving toward the pins at a velocity upward of 1800 m/sec. It is a piston compressing air ahead of it. Thus if the air shock is in some way electrically grounded, the pins will short out on arrival of the air shock front and the records will give only this velocity instead of that of the target behind. Now the pin contactors, in sequence, are charged to opposite polarities in order to facilitate reading the oscilloscope records. Since the air shock has a finite and increasing depth - not the front but
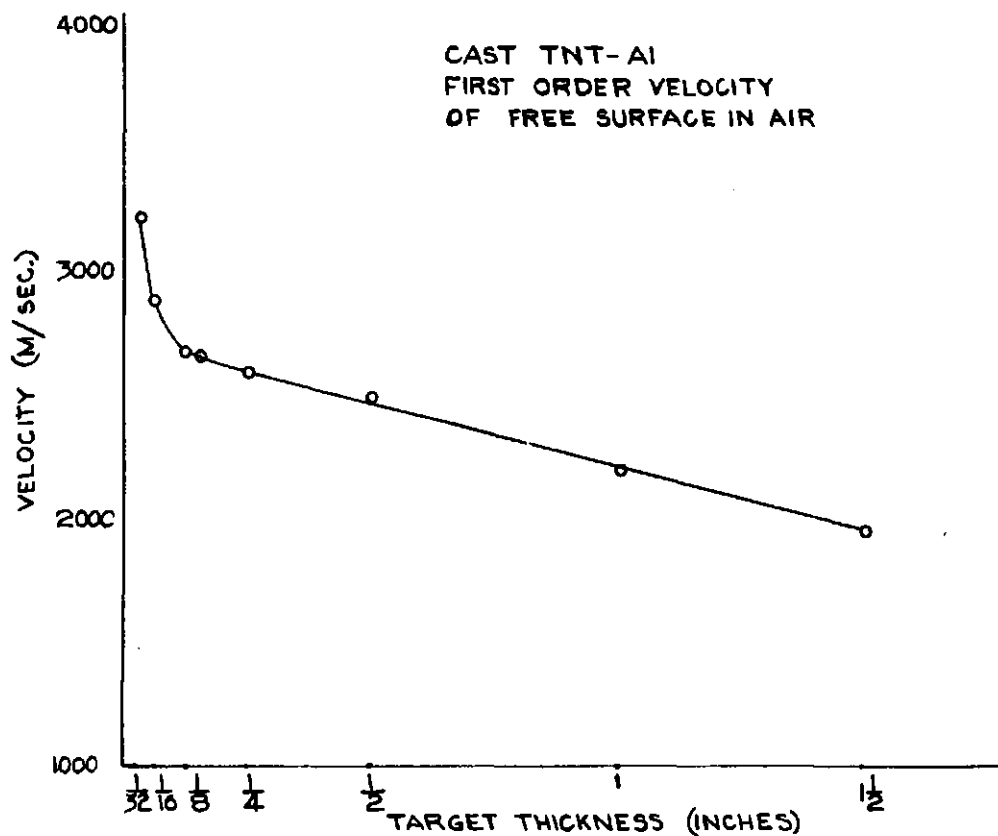
Figure 1—Cast TNT—Al. First order velocity of free surface in air.
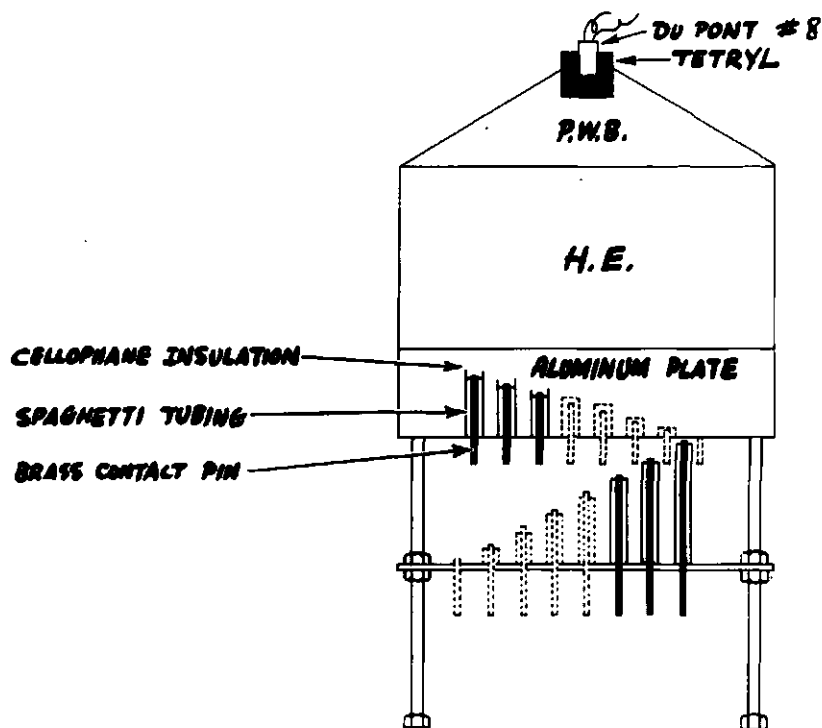
Figure 2—Contact pin setup—Schematic.

177
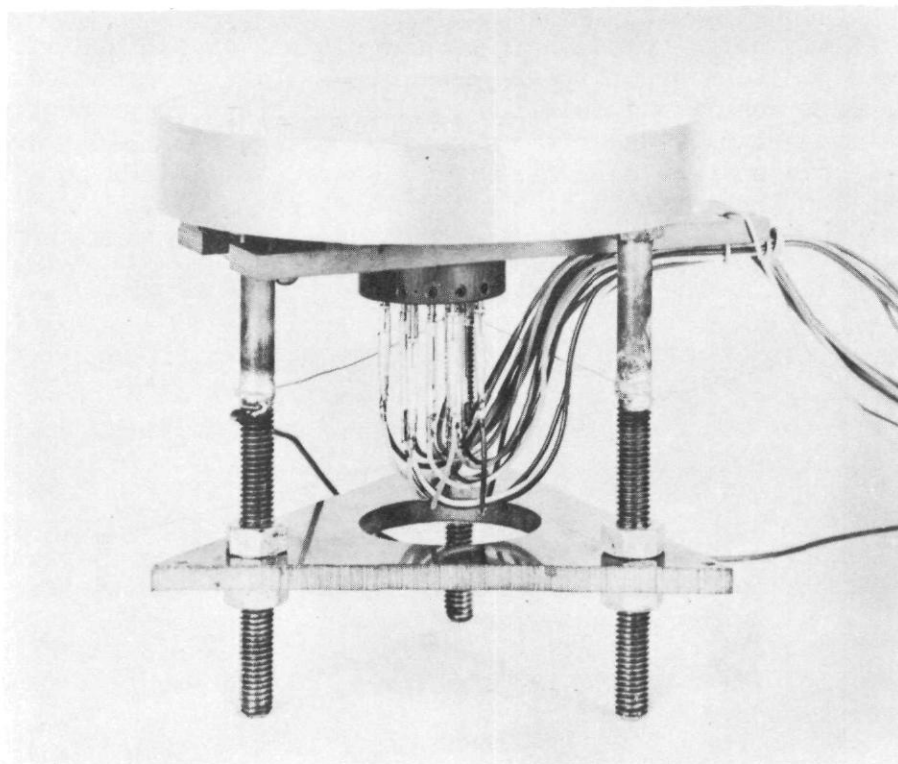
Figure 3—Photograph of plate.
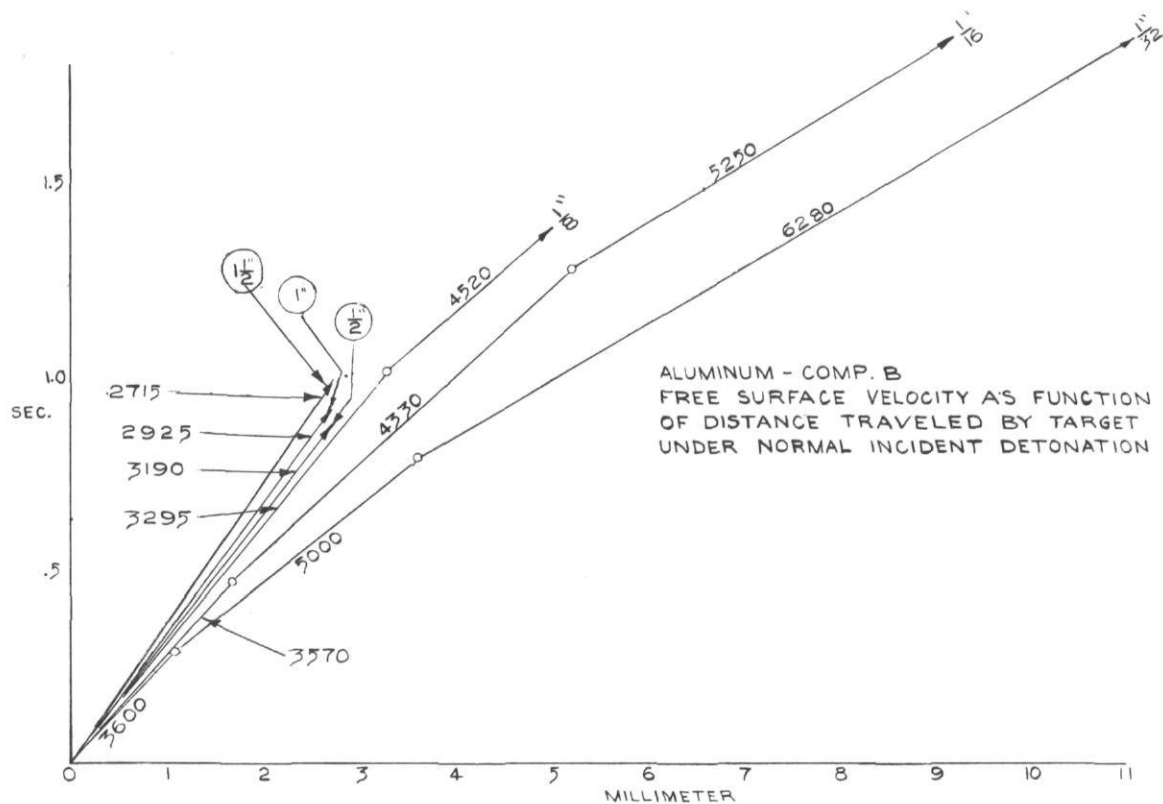
Figure 4—Aluminum—Comp. B.   Free surface velocity as function of distance
traveled by target under normal incident detonation.

178

the mass of shocked air being moved ahead of the piston, it can therefore also short a postively charged pin to a negative one even when it is not grounded. In this case unintelligible records result. Insulation requirements are consequently twofold. The air shock must be electrically separated from the moving, grounded, target and also the pins must be insulated from each other in a manner sufficient to withstand erosion by the hot wind in the shock but lightly enough to break down immediately on metallic contact. We have used films of kerosene or vasoline on all moving parts of the target to keep the air shock from grounding. The pin contactors are painted along their shafts with glyptal over which is slipped plastic spagetti tubing. The pin tips are left bare except for a drop of light oil. It may be noted in passing that if the pins are uninsulated, clean cut pips are observed on the oscilloscope only during approximately the first 0.7 mm of target motion. This has been taken to mean that the shocked air has a depth of about 0.4 mm, which is the approximate distance between consecutive pins, before the target (i.e. piston) has moved 1 mm.

Throughout this work we have neglected the air ahead of the target and considered its free surface velocity as being that which would be observed in vacuum. This approximation appears reasonable in the calculations and some substantive experiments have been performed by firing into an atmosphere of butane. Despite the higher density of butane compared with air, no detectible differences in target velocities were noted. Although the experiment is somewhat less tractable, firing into an atmosphere of hydrocarbon gas has an advantage in that no insulation is required on the surface velocity pins.

Among the experimental difficulties which influence reproducibility of data, one can mention such things as flatness of target plates, planarity of the detonation wave, variation in quality of the explosive used, straightness of pin contactors, accuracy of pin measurement and changes in pin placement due to handling and transportation to the shooting site. Some comments will be given on these items.

The detonation wave striking the target should be plane since the pin contactors are displaced laterally to avoid the effects of one interfering with measurements from all the others. It is believed that the wave is flat to within 0.01 microseconds or better so that this factor is under control. The presence of blow holes in the explosive along with variation in crystal sizes are factors which are difficult to control and we believe have been the most important contributors to fluctuations in the data. We therefore used the procedure of firing numerous shots at each target thickness in order to get a statistical average.

Targets less than 1/8 inch thick introduce their own peculiar problems, in part due to flatness requirements which are especially trying when working with thin foils, but principally the difficulties seem to be due to the very nature of the shock from a detonation. It is in this thin target range that effects due to high pressure in the reaction zone of the detonation show themselves. The reproducibility of free surface velocities here, depends on reproducibility of reaction zone pressures which decay rapidly after the onset of reaction and consequently the slope of the free surface velocity vs. target thickness line is very steep. One might therefore epect the large velocity fluctuations of thin targets which sometimes occur. However, results are on the whole gratifying.

179

Insulation requirements for thin targets are somewhat more stringent than for thick ones due to their higher velocities. As has already been mentioned, the heated shocked air ahead of the moving target erodes the pin insulation. Due to the increasing depth of the shocked air mass, those pins farthest removed from the target are subjected to this erosion for the longest time. The later pins are prone to short out prematurely unless completely covered with a film of oil. This difficulty is of course more pronounced as the distance over which measurements are made is increased. The present studies involve distances up to 11 mm of target travel from its rest position. We believe that 3 orders of velocity have been observed for 1/32" aluminum targets with Comp. B explosive and that it has not yet reached its terminal velocity in this interval. These velocity orders are thought to be due to reverberations of the shock wave in the target. When the free surface of the target begins to move, a backward traveling rarefaction wave goes into the metal. When it reaches the explosive-metal interface, a new shock enters the target which on reaching the free surface causes a sudden jump in velocity. This process is repeated until terminal velocity is reached. It may be seen from the graph (Figure 4) that the 1st order (initial) velocity for 1/32" aluminum extends over only about 1mm and that the target moves through this distance in less than 0.3 microseconds. In the interest of accurate measurements it is desirable to place as many pin contactors as possible within the 1st order range but in order to use 8 pins here, our electronic equipment would have to be faster by a factor of three or four. Thinner targets would require still faster response. At the present time, the more interesting thin target velocities cannot be as accurately measured as we would hope for. However, there are oscilloscopes in existence with which such short intervals can be measured.

We believe that the pin technique is better than photographic methods for some applications. Certainly when the two are used together, more reliable information can be obtained. Application of the technique to shaped charge work would require some changes in procedure but there should be no inherent reason why it cannot be done.

HIGH SPEED PHOTOGRAPHY WITH AN IMAGE CONVERTER TUBE

R. D. Drosd

T. P. Liddiard

B. N. Singleton, Jr.

U. S. Naval Ordnance Laboratory White Oak, Silver Spring, Maryland

ABSTRACT

The results of an investigation in the use of an image con-
verter tube as a high speed camera shutter and an image brightness
intensifier are given. With the 1P25A (sniperscope) image con-
verter tube it was found that exposure times of thirty millimicro-
seconds with a gain in image brightness of two are easily attain-
able. The relative merits of the image converter and the Kerr cell
cameras are discussed. The construction of the 1P25A camera is
shown.

All systems of high speed photography are compromises between exposure time,
light gathering power, optical resolution and field of view. Attempts to improve
these systems generally require a large expenditure of effort and money for rela-
tively small gains. However, there is one system, introduced by J. S. Courtney-
Pratt in 1949, that is basically different and offers, among other advantages, the
unique ability to produce an optical image that is brighter than the image which
is put into it. The device which makes this possible is the image converter tube.

Probably the most common example of an image converter tube in this country is
the 1P25A. This tube was used in the sniperscope and the snooperscope to convert
infra-red images to visible images. It was chosen for this investigation mainly be-
cause of its availability. It consists essentially of a 1.25 inch diameter photo-
cathode, a series of cylindrical electrodes and a 0.63 inch diameter flourescent
screen. (Fig. 1)

The photocathode consists of a semitransparent film of silver and caesim oxide.
It is sensitive principally to light in the 7,000 to 12,000 angstrom range. Its peak
sensitivity is at 9,000 angstroms. When an optical image is focussed on the photocathode
a corresponding electron image is produced on the inner surface.

The electrons of this image are accelerated and focussed on the screen by the
various potentials on the electrodes. The ratios between the potentials must be constant
in order to maintain the proper focus. The overall potential may be varied over a wide
range without appreciably changing the focus or the image size. The maximum potential
that may be applied statically is 4,500 volts but at least 14,000 volts may be applied

NAVORD REPORT 1811
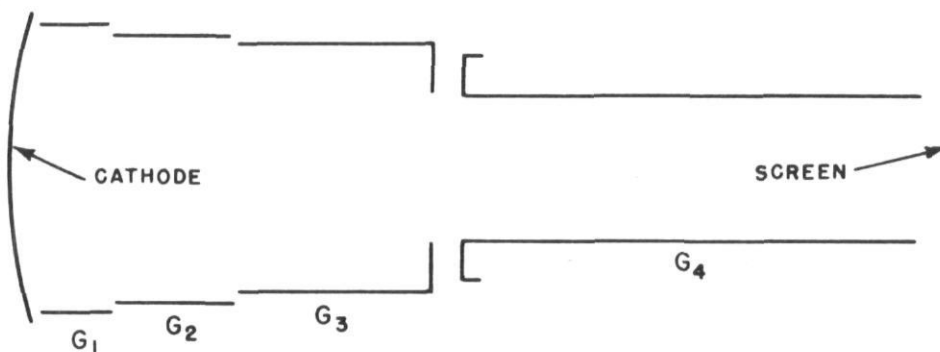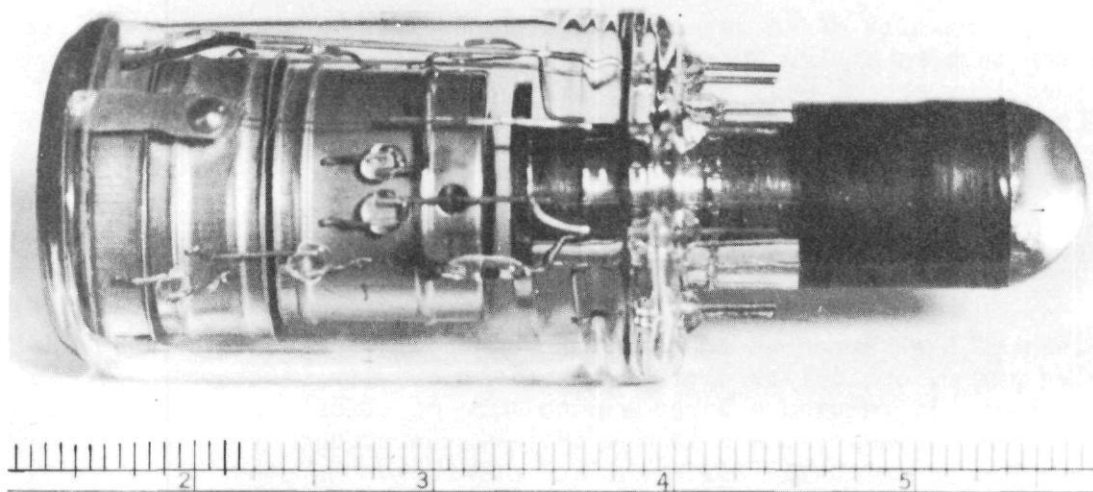
Figure 1—1P25A Image converter tube.
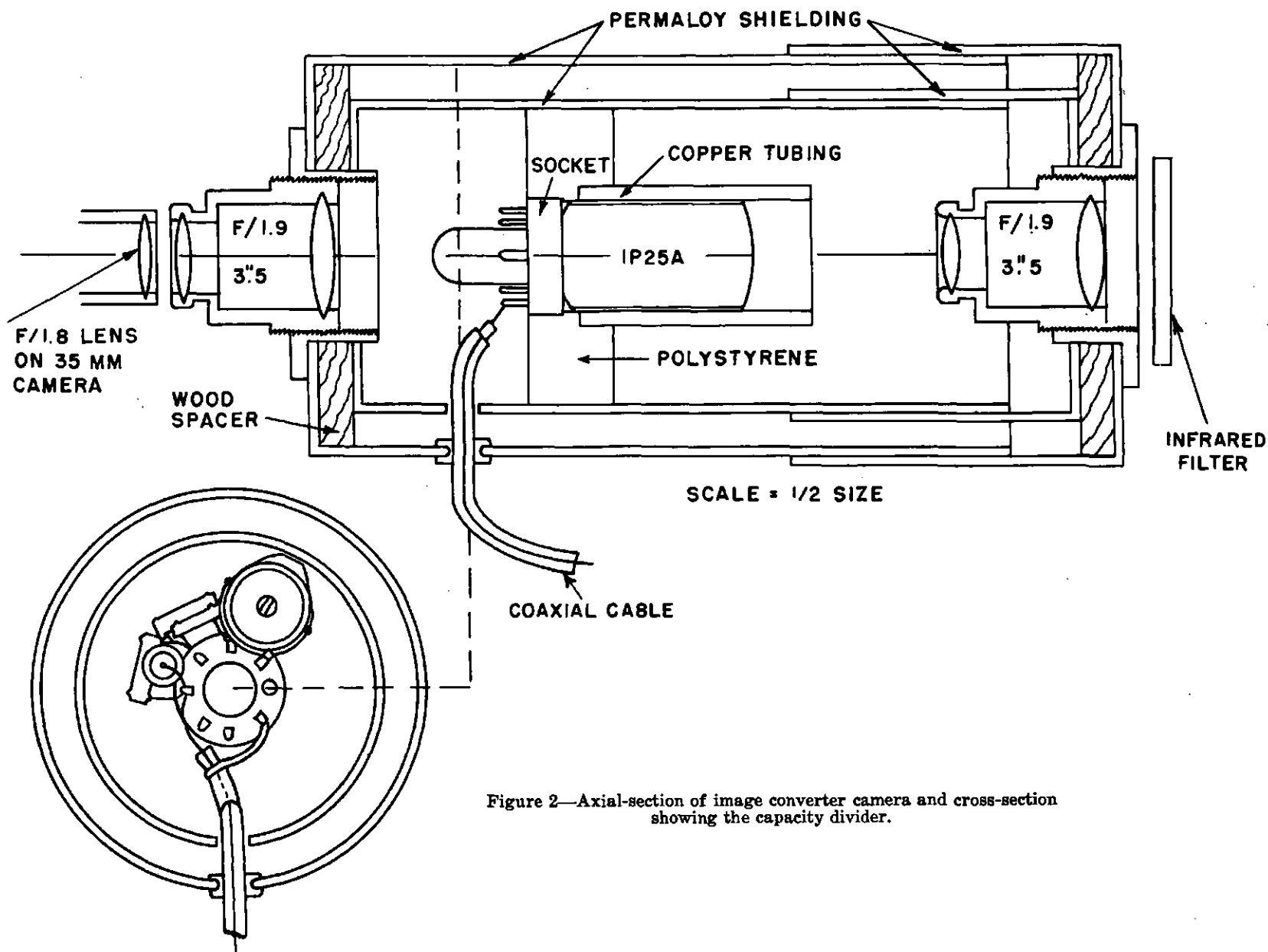
Figure 2—Axial-section of image converter camera and cross-section
showing the capacity divider.
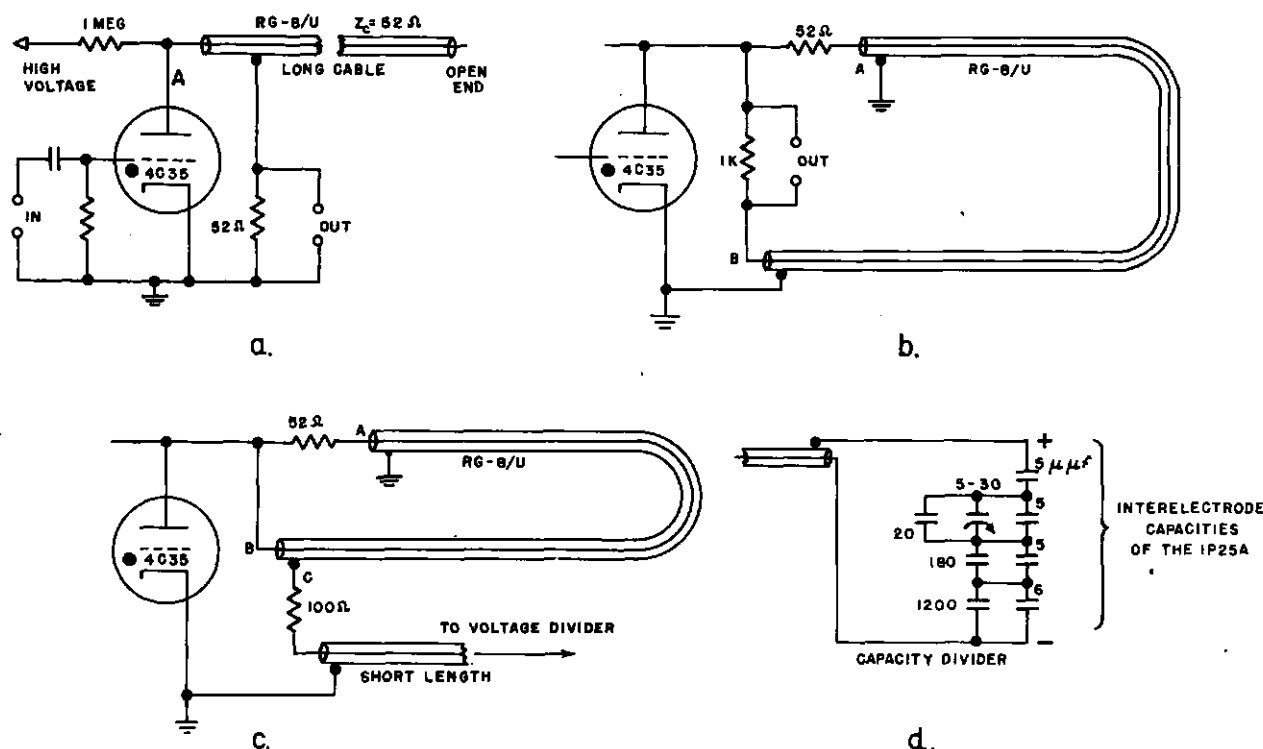
Figure 3—Circuits for three square-pulse generators and a capacity
voltage divider for the 1P25A.

OUTER HOUSING | EXPLOSION CHAMBER
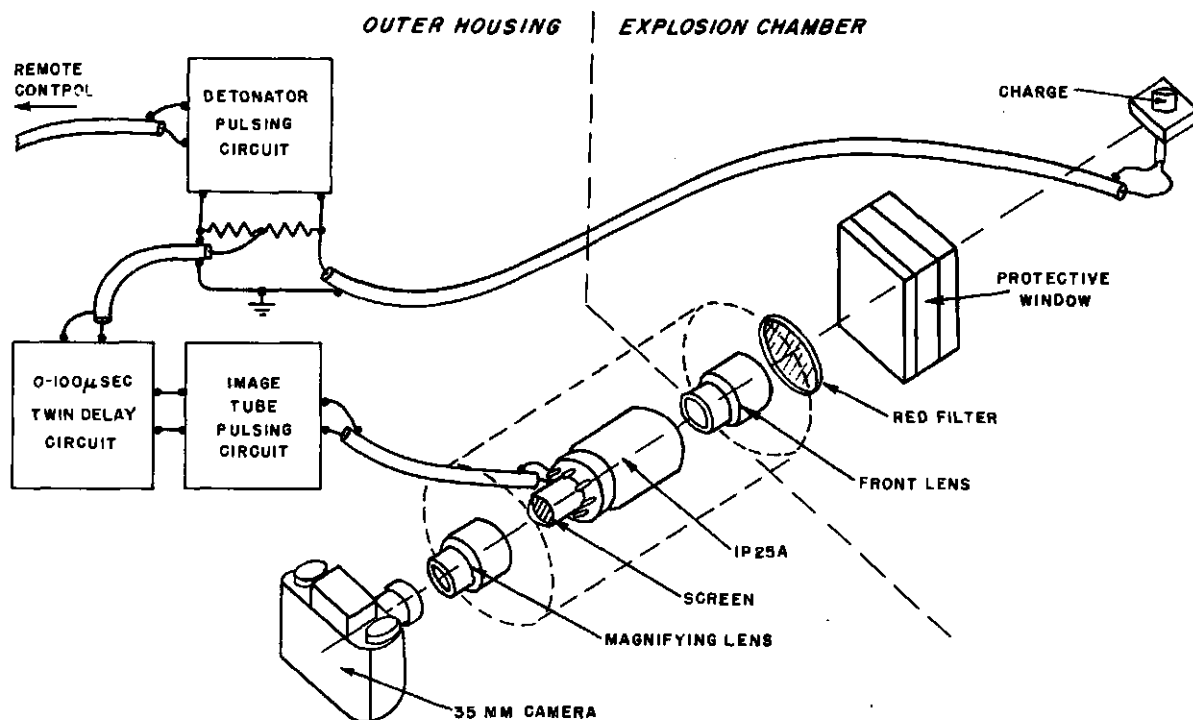
Figure 4—Typical set-up for taking instantaneous photographs of
detonation phenomena with the 1P25A image tube.

in short pulses without danger of breakdown. The duration of the pulse determines the exposure time and is limited only by the transit time of the electrons. At 14,000 volts this is about 3×10^{-4} microsecond.

When the electrons strike the screen the optical image is reproduced in the visible spectrum. This image is one half the size of the original image.

According to the manufacturer's specifications this tube has a gain of light of as much as one when a potential of 4,000 volts is used. This means that the image on the screen is four times as bright as the image on the photocathode since the same amount of luminous energy is concentrated in an area only one fourth as large. With 14,000 volts the calculated brightness relative to the image on the photocathode is about 12. If f1.9 lenses are used at both ends of the tube the overall gain in brightness from object to the photographic film in the camera is approximately 2.4. In an ordinary camera using the same lenses the relative brightness would be about 0.2. (Figs. 2 & 3)

In the experimental investigation it was found that it was necessary to shield the 1P25A from stray magnetic fields. Even the presence of a magnetized screw driver a foot away from the tube caused the image to shift several millimeters and produced blurred images. Double permalloy shields proved satisfactory. A heavy copper tube was placed over the tube to act as a shield against any surge magnetic fields that might have been set-up by the high voltage pulses. (Fig. 4)

The f/1.9 lenses were all of 3.5" focal length. The camera used to record the screen image was a Bolsey 35 mm with an f/1.8 lens.

The various electrode voltages were most easily obtained by means of a voltage divider. A voltage divider made up of carbon resistors proved unsatisfactory for pulses under one microsecond. Attempts to use a capacity compensated divider gave no better results. A purely capacitive divider worked quite well. Apparently, the carbon resistors acted like non-linear elements under the influence of the very short pulses. With comparatively simple circuits it was found possible to obtain pictures with a 0.03 microsecond exposure time. The tube offers an electrical load of only five micromicrofarad to the circuit.

Since both the photocathode and the screen are semi-transparent special precautions are necessary to prevent visible light from leaking through to the photographic film. This is easily done by placing a red filter in front of the image converter and using orthochromatic film. The red filter is very efficient in the near infra red. It was found that orthochromatic film was as efficient as panchromatic film as far as the predominately green light from the screen was concerned.

In detonation experiments only one special provision was required. The three inch thick glass protective windows were found to pass only about 30% of the infra red light. It was found that an equal thickness of lucite passed more than 90% of the light.

In the first detonation experiments a sinusoidal potential of 2,500 volts peak at 100,000 cycles per second was used. This permitted the tube to produce images at ten microsecond intervals with exposure times of less than five microsecond. The explosive was a stack of tetryl pellets encased in a jacket of water to suppress the shock light.
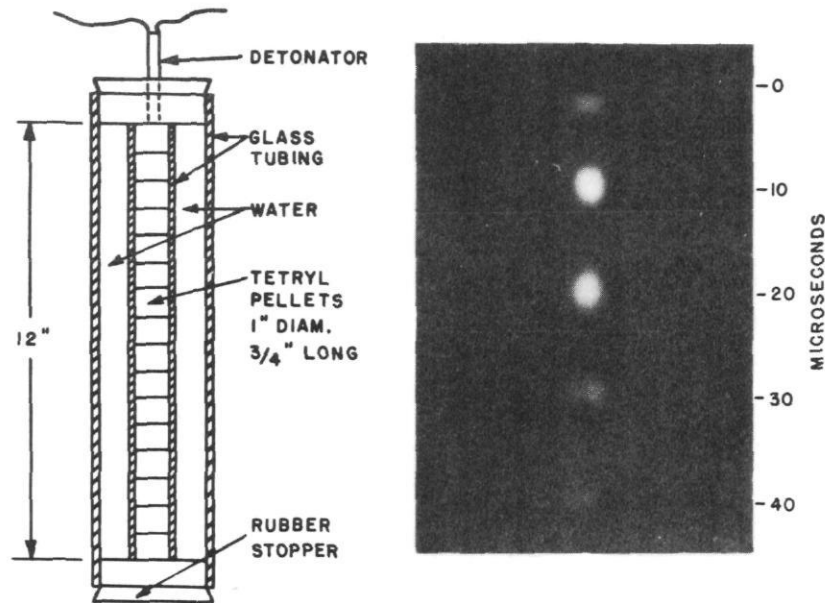
a. *MULTIPLE EXPOSURE OF DETONATION WAVE IN TETRYL AND CORRESPONDING CHANGE SET-UP*

DETONATOR

GLASS TUBING

WATER

TETRYL PELLETS 1" DIAM. 3/4" LONG

12"

RUBBER STOPPER

MICROSECONDS

—0

—10

—20

—30

—40

12-TETRYL PELLETS 5/8" DIAM., 3/4" LONG

(WRAPPED IN CELLULOSE ACETATE FILM)

DETONATOR
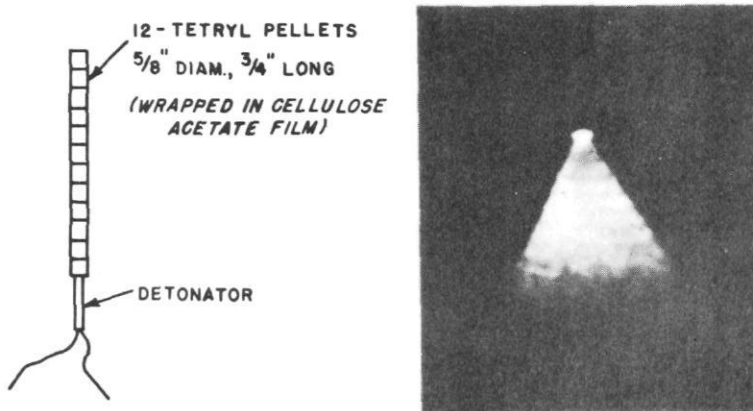
b. *ONE-HALF MICROSECOND EXPOSURE OF TETRYL PELLETS EXPLODING IN AIR*

Figure 5

a
$t = 3\,\mu\,SEC$

CHARGE

b
$t = 4\,\mu\,SEC$

WOOD

c
$t = 5\,\mu\,SEC$

DETONATOR
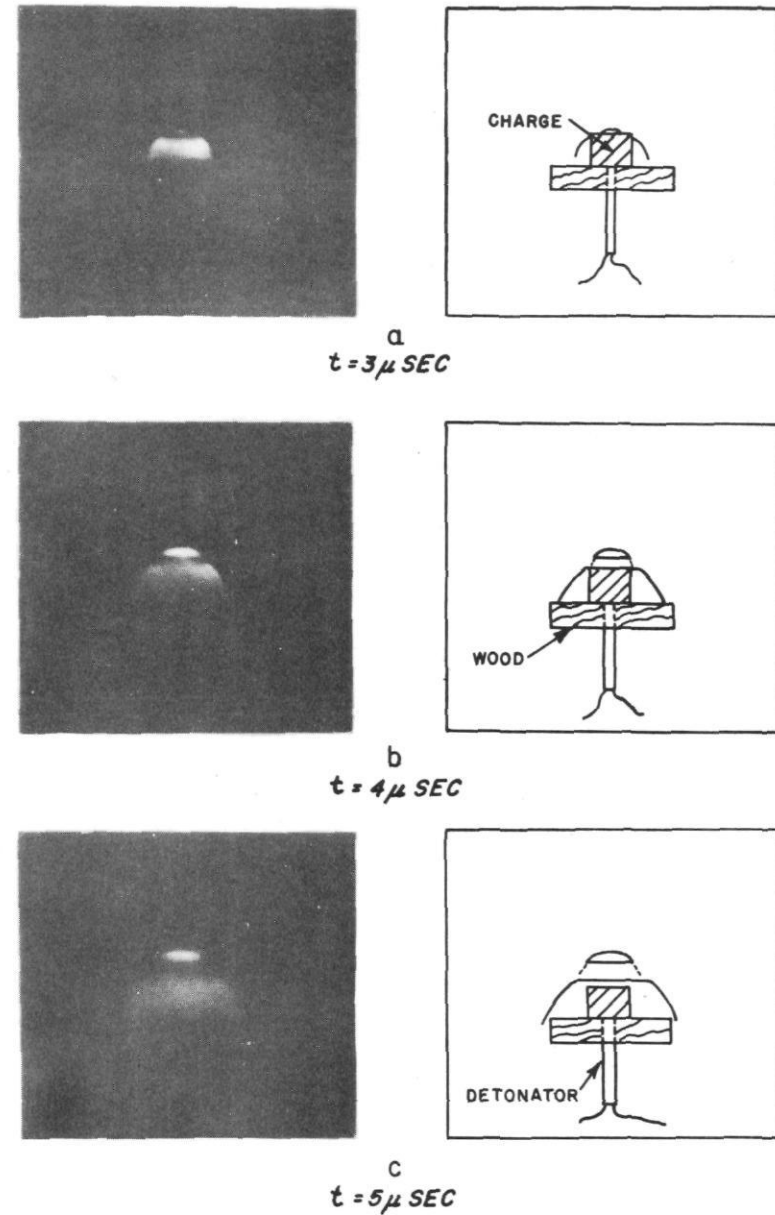
Figure 6—Exploding tetryl pellets photographed at 0.03 μ sec. for various times after initiation.

a
$t = 2\mu SEC$
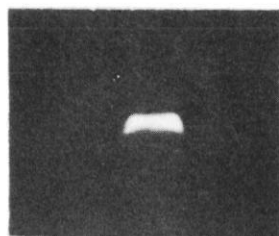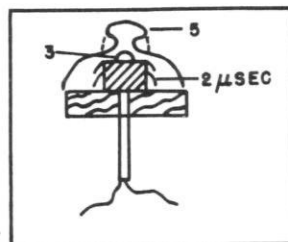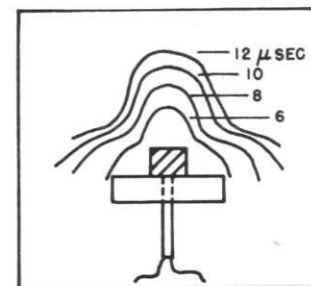
b
$t = 3\mu SEC$

c
$t = 3.5\mu SEC$
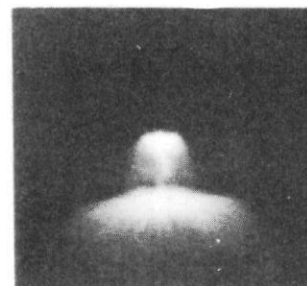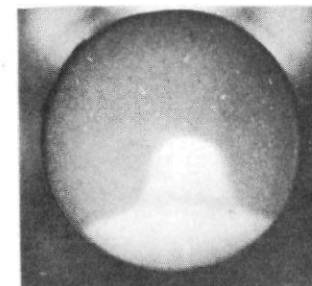
d
$t = 5\mu SEC$

Figure 7—Exploding tetryl at various times
after initiation; one-tenth microsecond
exposures.

a
$t = 6\mu SEC$

b
$t = 8\mu SEC$

c
$t = 10\mu SEC$

d
$t = 12\mu SEC$

Figure 8—Exploding tetryl for various
times after initiation; one-tenth
microsecond exposures.

187

Five exposures were obtained as the detonation proceded down the pellets. From this picture the rate of detonation could be calculated. The quality of this picture is poor due to the poor magnetic shielding which was used at that time. However, it does indicate possible applications. (Fig. 5)

A half microsecond picture of a detonating stack of tetryl pellets was obtained with a 5,000 volt pulse. In this picture the gas front is well defined. The wavy pattern in the gas front is due to the gaps between the pellets and nonuniformity of the density of the pellets. The detonation zone is vastly overexposed and halated.

All the remaining pictures are of the detonations of single tetryl pellets. With 14,000 volts it was possible to obtain exposures down to 0.03 microsecond although most of the pictures are 0.1 microsecond exposures.

The image converter camera has several advantages over a Kerr cell camera using the same lenses. With the Kerr camera one must limit the field of view to maintain approximate parallelism of the light in the Kerr cell. Practical Kerr shutters transmit less than 20% of the light. The relatively high capacitance of the Kerr cell makes pulsing more difficult and high voltage and higher power becomes necessary. One serious disadvantage of the Kerr shutter is that it depends on crossed polaroids to create a "closed" shutter. Limitations of quality of the best polaroids result in a closed shutter having a transmission of at least 0.1% of the transmission of an open shutter. This leads to background exposure and the requirement for auxiliary shutters for its control. The image converter shutter when properly designed has zero transmission when closed.

In only one respect does the Kerr cell camera exceed the 1P25A camera. The resolution of the 1P25A is about 450 lines per inch while the resolution of a Kerr cell camera may be 1000 or more lines per inch. However, new and much better image converter tubes will be soon developed which will have resolutions equal to the best the Kerr cell cameras can offer.

HIGH SPEED HIGH RESOLUTION STREAK PHOTOGRAPHY

C. T. Linder

Carnegie Institute of Technology Pittsburgh, Pennsylvania

ABSTRACT

A simple rotating mirror camera with high space and time resolution, and great versatility in the photographing of various explosive phenomena is described. The camera features a thin single surface plane mirror so that the locus of the image is circular to a high degree of accuracy, and employs film strips which are six inches in width. The selection of the appropriate mirror width, speed of rotation, and radius of film track permit the choice of a variety of fields of view and of writing speeds up to 3 mm/µsec. The design employs a single lens and an expendable external slit placed at the location of the phenomenon to be photographed. An effective lens aperture of f/3.5 can be retained and a 1/1 magnification ratio is possible. Various applications to which the camera is particularly suited are discussed.

INTRODUCTION

There are two types of cameras which are generally used in streak photography. They are the rotating drum camera and the rotating mirror camera. There are many contributors to the development of them. Among these are MacDougall and Messerly,[1] Cairns,[2] Payman, Shepard and Woodhead,[3] Beams,[4] Jacobs,[5] and numerous others. The drum camera is limited to film speeds of less than 300 meters per second because of the mechanical strength of the drum materials. When higher writing speeds are desired a rotating mirror camera is used. In this type of streak camera the image is reflected from a mirror, which is rotated at a known high speed, onto a stationary film strip. In this way both a time and space record is present on a photograph of a rapidly progressing luminous phenomenon. Such a camera was designed by Jacobs[5] while he was at the wartime Explosives Research Laboratory, Bruceton, Pennsylvania. When the C.I.T. group moved to the Bruceton location, they were so fortunate as to obtain the use of this camera. Writing speeds of the order of 1 mm/µsec and an effective aperture of F/5 were obtainable with it.

As our interests at C.I.T. shifted to fundamental details of shaped charges, the limitations of the E.R.L. camera restricted the scope and the accuracy of such investigations. The image size was limited by the 35 mm film width and the placement of the optical components of the camera. Because of the loss of definition in the enlargement of the negative, this permitted only partial compensation for the small image size. We desired better time resolution and larger image size in a camera of simple design so as to be easily adaptable to the photographing of various kinds of explosive phenomena. Our new camera intends to increase the space and time resolution by using film

strips which are 6 inches in width and by increasing the radius of the film track. A range of image sizes and writing speeds are available by employing three different size mirrors and three film tracks of different radii.

DESIGN DETAILS

The camera was not designed for the photographing of a single type of explosive phenomenon. Rather the attempt was made to construct a multi-purpose camera which could be easily modified for any type of investigation which is feasible with a streak camera. Simplicity and dependability were of prime importance. Also we desired to keep the operation and maintenance such that sub-professional personnel could obtain satisfactory results with it.

The dependability and the small amount of maintenance required by the E.R.L. camera made it seem desirable to borrow many of its design features. Jacobs[5] has shown that the best effective aperture obtainable with a two-lens optical system using commercial lens is about F/8. Since a larger effective aperture is desirable for certain types of investigations, he chose a single-lens system and used an expendable external slit placed at the location of the phenomenon to be photographed. In order to make use of the full lens aperture we also have employed the single-lens system. The lens is an Eastman Anastigmat with a focal length of 13 1/2 inches and an aperture of F/3.5.

The mirror is made from stainless steel plate 5 inches high, 3 1/4 inches wide and 1/4 inch thick. Two additional mirrors of widths 1 and 2 inches are in the process of manufacture. When the full aperture of the lens is not desired the smaller mirrors will be used thus permitting a higher rotational speed because of reduced air drag. The mirror surface is obtained by polishing one side of the steel plate until optically flat to within 1/2 wave length and coating it with aluminum. A protective coating of quartz is then put over the aluminum to reduce the abrasive action of dust particles.

Three film tracks have been constructed which accommodate a film strip 6 inches in width. These tracks have radii of 7, 11, and 15 inches, thus giving a wide range of writing speeds and image sizes.

Due to the fact that the mirror is of finite thickness, the locus of the image is not quite circular, hence the angular velocity of the image is not constant. In all measurement work with the camera, a correction for variations in image velocity is taken into account. However, since the mirror thickness is much smaller than that of the square mirror employed in the E.R.L. camera, the correction factor is consequently much smaller.

The driving system consists of two 1/2 H.P. Dumore Electric Company universal motors. It was not possible at the time of construction to obtain universal motors rated higher than 1/2 H.P. with a speed of 8,000 r.p.m. Hence it was necessary to use two motors and to match them by the proper adjustment of the tensions in the driving belts so that the load was equally shared. The speed of these motors is varied by means of a variac.

Figure 1

Figure 2

191
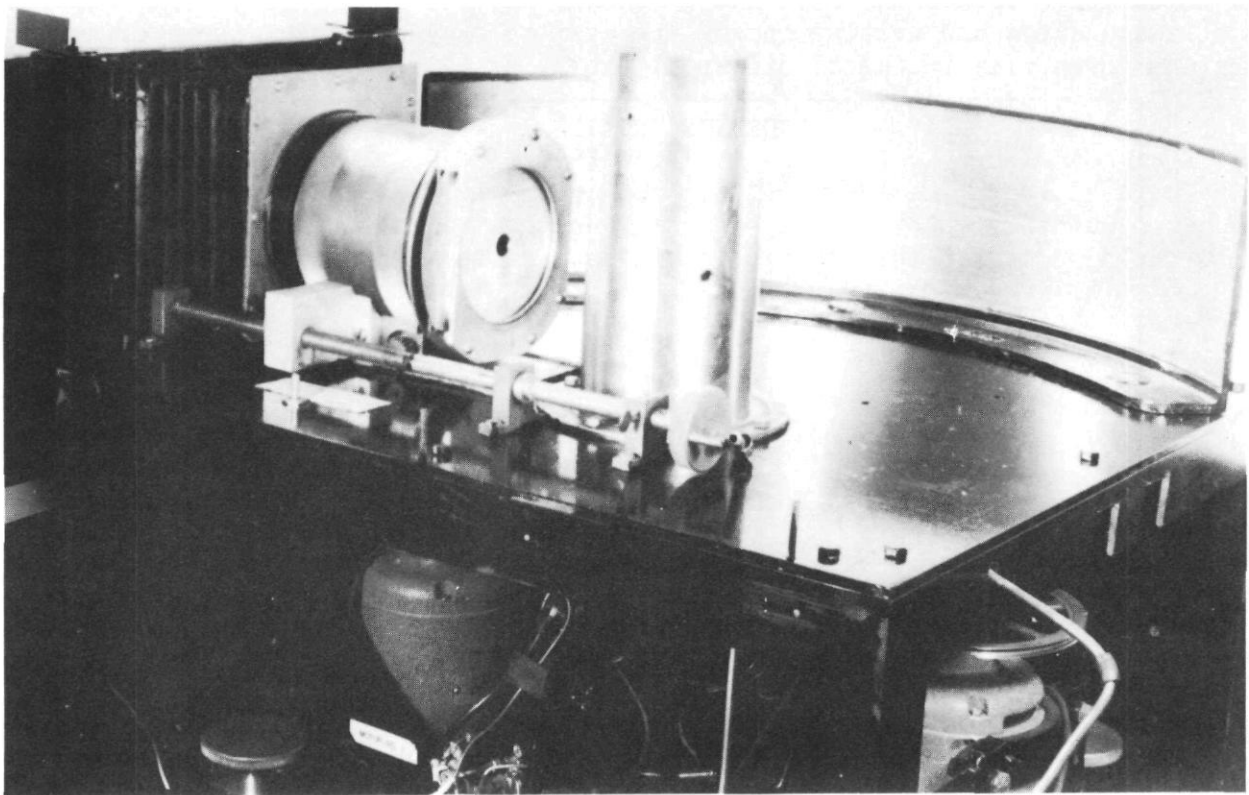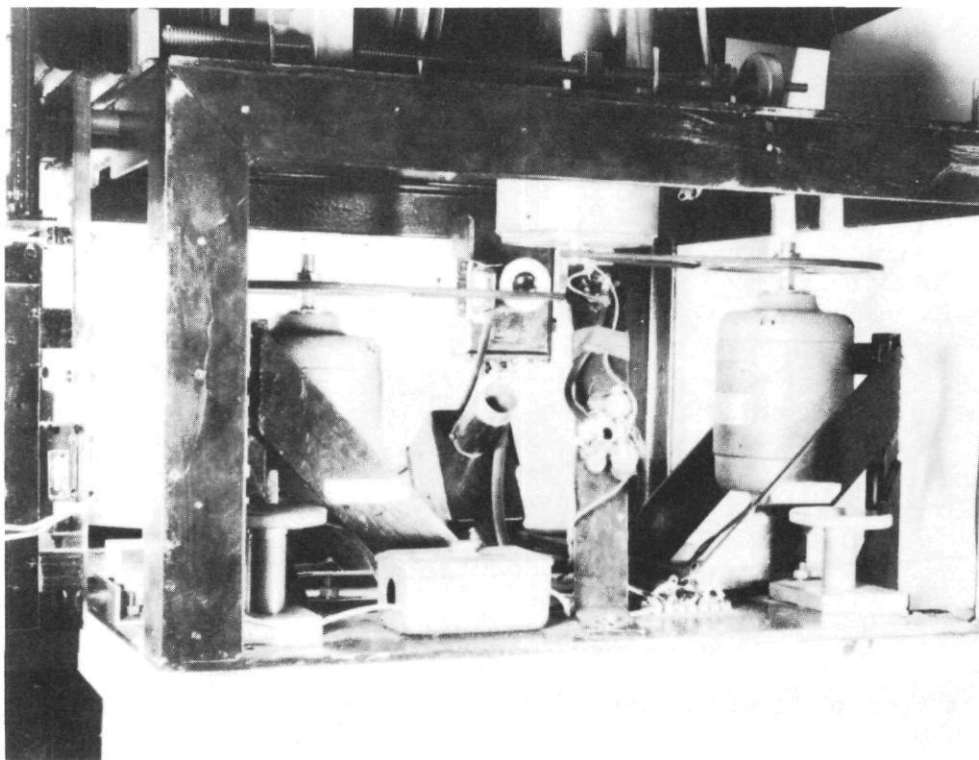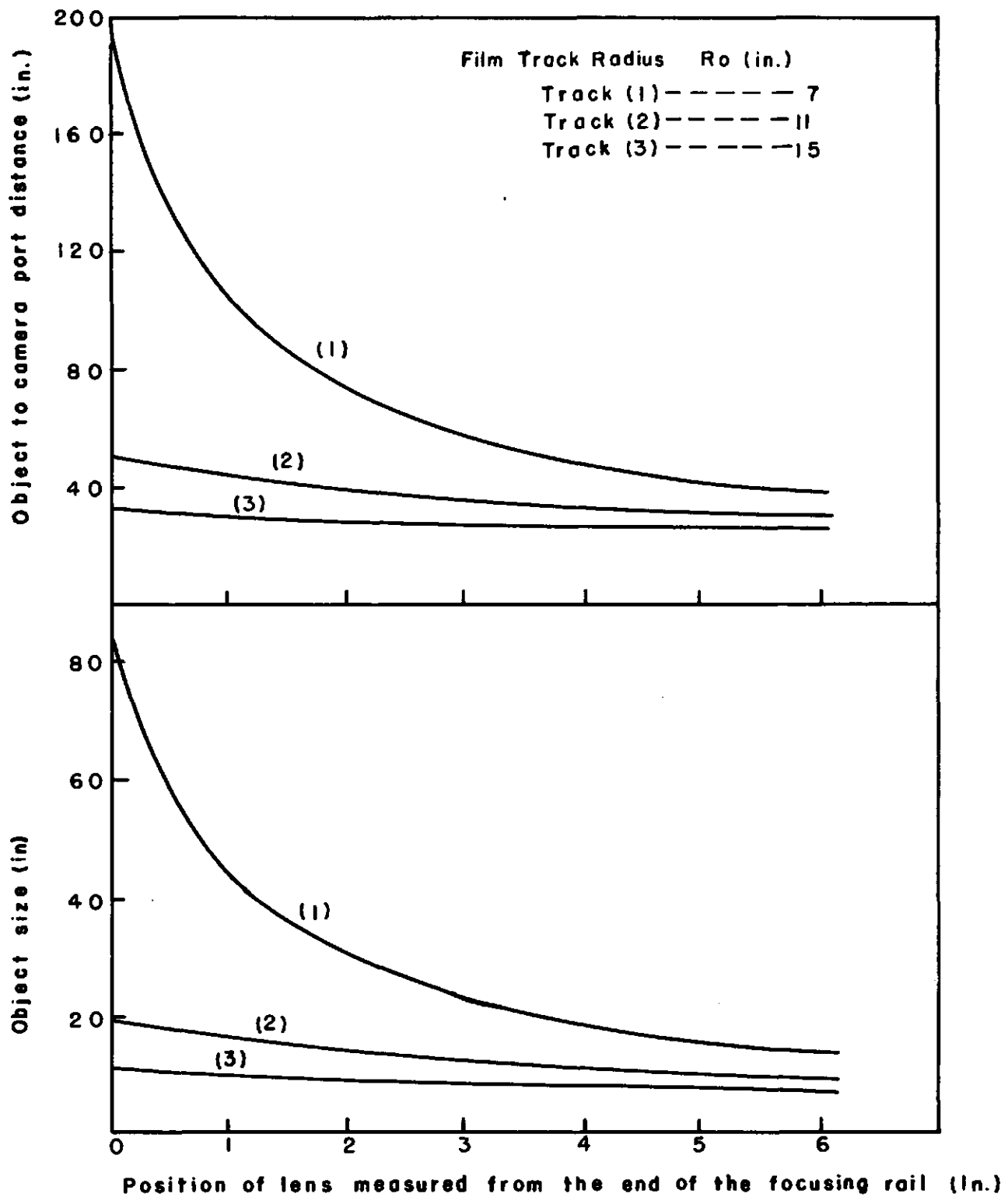
Figure 3—Object size and distance from camera port corresponding to an "in focus" image which exactly covers the 6 in. wide film track.

The speed measuring system is essentially the same as that employed in the E.R.L. camera. The bottom surface of the mirror shaft is half polished and half black. The "chopped" light reflected from a light source to a phototube produces a signal which is amplified and applied to the vertical plates of an oscillograph. The controls of the oscillograph are set to synchronize the horizontal sweep to a full wave rectifier operated from the 60 cycle supply voltage. The horizontal sweep frequency is 120 cycles with the accuracy of the a.c. supply. Stationary patterns of simple form are obtained when the vertical input frequency corresponding to the camera speed is a multiple of 120 cycles.

Since the camera features a thin one-sided mirror and a short film track, it is necessary to predetermine the time of the event to be photographed relative to the time when the mirror reflects light to the desired position of the film. This is accomplished by firing detonators by the discharge of a 1.5 μf condenser charged to approximately 10KV. The condenser discharges through a mercury thyratron which is triggered by means of a light pulse reflected from the shaft of the rotating mirror.

Firing of the detonator is accomplished by the following sequence of events: a light source is turned on, the light from the source is reflected from a polished section of a collar attached to the rotating mirror shaft and is picked up by a phototube, the signal is amplified and triggers a type 884 thyratron, this reduces the grid bias of a type FG-41 thyratron causing it to fire, which permits the discharge of the 1.5 μf condenser, thus firing the detonator.

The position of the image on the film is determined by the orientation of the reflector collar relative to the main mirror. The consistency of picture position, however, depends on the reproducibility of the times required to fire detonators. The firing circuit exclusive of the detonator is reproducible to within approximately three micro-seconds.

A view of the camera proper is shown in Fig. 1. The bellows, lens barrel, aperture stop holder, mirror housing, and a film track are visible. When it is desired a graded filter on a wire frame can be placed in front of the film track. Thus it is possible to make full use of the F/3.5 aperture in photographing the less luminous, slower moving portion of the phenomenon without losing the detail at the more intense beginning. A light tight canopy fits over this section of the camera. The two driving motors and the light sources for speed measurement and synchronization are shown in Fig. 2, which is a view of the lower section of the camera.

OPERATING CHARACTERISTICS

The object size, corresponding to a 6 inch film width exactly covered by an in-focus image, and the object distance measured from the camera port are shown in Fig. 3 for the entire travel of the lens and for the three different film tracks. The magnification ratio can be obtained simply from the object size curve. It is given by 1 : 1/6 the object size.

The maximum image velocity attained with the 3 1/4 inch wide mirror, which permits the use of the full aperture of the lens, has been 2.3 mm/μ sec. This corresponds to a mirror rotational speed of 480 r.p.s. Higher writing speeds will be obtained with the smaller mirrors at the expense of a reduction in the effective aperture.

When smaller apertures are desired the appropriate one can be selected from a group of waterhouse aperture stops ranging from F/10 to F/128. An adapter is located at the rear of the lens barrel to accommodate them.

The film employed at the present time is Kodak linagraph ortho safety film. It can be purchased in convenient 100 foot rolls which are 6 inches wide.

There is little or no trouble with synchronizing the image location with the time of the event to be photographed. Once the reflector collar on the mirror shaft is properly oriented the reproducibility is easily within the detonator variability of 20 μ sec or about 1 1/2 inches on the film strip at the most frequently used operating speeds.

Incorporated in the circuits employed in the camera are the usual safety features. The charging of the condenser, operation of the camera, and firing of the charge are completely controlled from a single firing station. In accordance with the safety requirements at Bruceton, the firing line circuit is completed by a second firing station. The condenser and the firing line are normally shorted to ground except when in actual use.

APPLICATIONS

In operation as a general purpose camera a wide variety of measurements such as detonation rates, shock wave velocities, jet velocities, fragment velocities, and wave shapes can be made. It is possible to make such a variety of measurements with accuracy because of the 6 inch wide film, and the time and space resolution obtained with the three different film tracks. It is useful for studies with small charges because of the large magnification ratio. On the other hand, a wide field of view and large aperture make multiple jet velocity and fragment velocity pictures possible.

As is always the case with such laboratory equipment, improvements are continually in the making. It is now possible to obtain more powerful and faster universal motors. It is hoped that in conjunction with the mirrors of smaller width this will mean greater writing speeds will be available. The use of a lens of 36 inch focal length will permit the construction of a fourth film track and an image velocity in excess of 6 mm/μ sec should be obtainable. These modifications will greatly facilitate wave shape studies.

The range of usefulness of the camera can be further extended by taking shadowgraphs of relatively slow moving fragments of large size.

1 MacDougall, D. P. and Messerly, G. H., OSRD No. 682, July 8, 1942.
2 Cairns, R. W., Ind. Eng. Chem., 36, 79-85, 1944.
3 Payman, Shepherd and Woodhead, Safety in Mines Research Board Paper No. 99, H. M. Stationery Office, London 1937.
4 Beams, J. W., Rev. Sci. Instr. 1, 667, 1930; 6, 299, 1935.
5 Jacobs, S. J., OSRD No. 5614, January 2, 1946.

EXPERIMENTS ON DETONATION PHENOMENA

G. R. Walker

Canadian Armament Research and Development Establishment, Valcartier, Quebec

In an attempt to investigate some of the fundamental aspects of HE detonation, a project was carried out at the University of Saskatchewan from 1944 to 1949 in which photographs of detonating explosives were taken by a camera of the rotating-mirror type. The results obtained will not be dealt with at any length here because detailed reports have been available for some time, and because none of the results have any apparent practical value in the field of shaped charges. Instead, I shall briefly describe our experimental set-up, and shall indicate what new facilities are being planned for similar investigations at CARDE.

Fig. 1 is a plan view of our camera. The mirror is any one face of a 1" cube, and is mounted on a Beams-type rotor turning at speeds up to 800 rev/sec for a maximum writing speed of 5000 m/sec. The effective aperture is about f/20. At CARDE, consideration is being given to the design of a similar camera with a comparable high writing speed but with a much greater aperture. A detonation chamber designed for photographing charges up to thirty pounds TNT is in the final stages of planning. It is in the shape of a cylinder of length 40 feet and inside diameter 16 feet with light doors at both ends which are opened before firing. The observation window is in the middle of one side, and in the opposite side is a similar window for Schlieren photography. It is planned to collect structural data by means of strain gauges built into the reinforced concrete.

Fig. 2 is a photograph to illustrate the operation of the camera. The charge consisted of a large number of 5-gram HE pressed pellets in tandem, contained in a glass tube 32 mm I.D., and initiated at one end by an electric detonator. The vertical charge was imaged on the (vertical) slit by a field lens, and so vertical distance on the photograph indicates distance on the charge. Horizontal distance indicates time, and so the slope of the trace indicates velocity of detonation. Fig. 2 shows two and one half RDX pellets and three tetryl pellets, and shows a sudden decrease in velocity at the junction.

For fig. 2 the residual space within the glass tube was filled with water. Fig. 3 shows a similar charge with this space filled with propane. With the latter, there is strong luminosity as the shock wave hits the glass wall of the tube. In both, the thin sloping trace is luminosity from the "hot" detonation zone. These photographs illustrate the well-known effect of water or propane in quenching the luminosity of the shock wave.
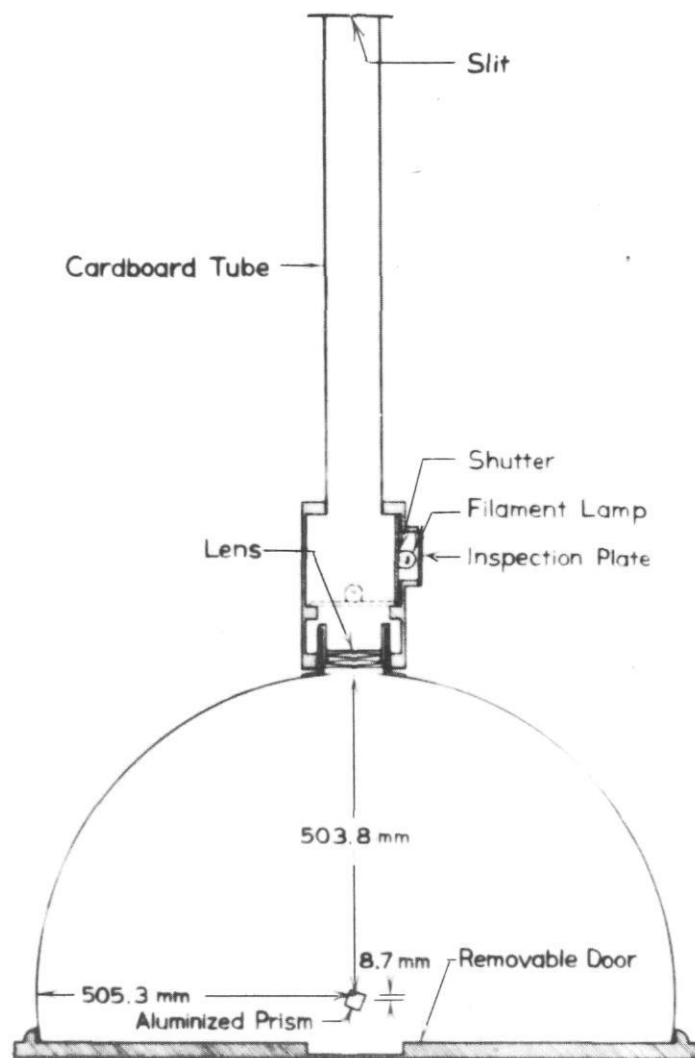
Figure 1—Rotating Mirror Camera,
Horizontal Section
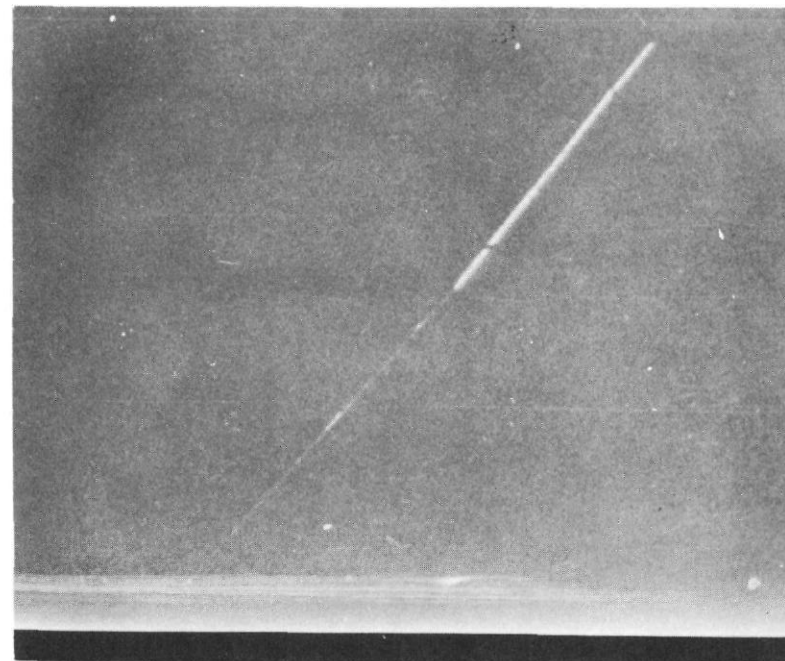
Figure 2
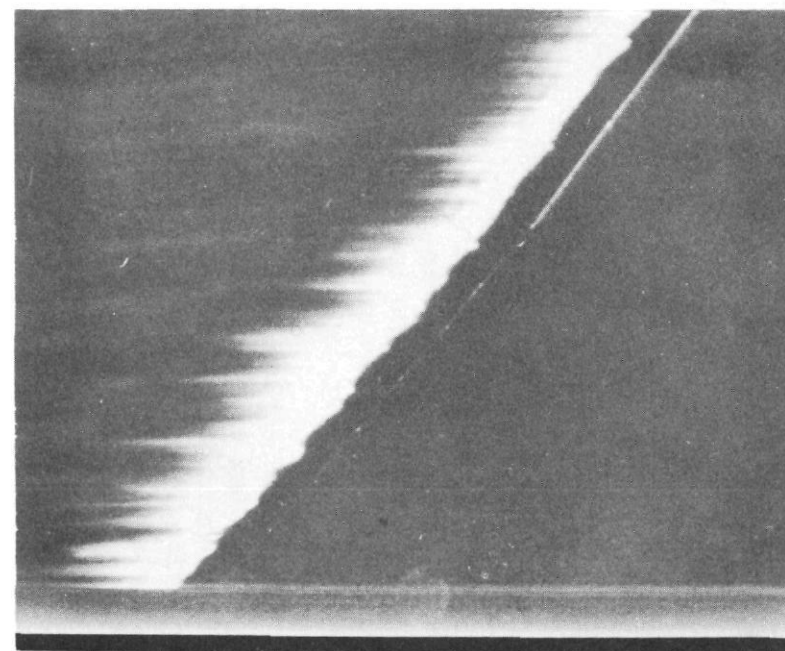
Figure 3

COMPARATIVE EFFECTIVENESS OF ARMOR-DEFEATING AMMUNITION

A. Hurlich

Watertown Arsenal Laboratory

Watertown Arsenal, Watertown, Massachusetts

ABSTRACT

Presentation of the comparative armor penetration performance of the various types of kinetic-energy armor-piercing ammunition (AP, APC, HVAP, and discarding sabot shot) against single armor targets as influenced by the type, thickness, mechanical properties, and obliquity of armor. Performance of kinetic-energy armor-piercing projectiles against spaced armor structures. Performance of HEP ammunition against solid and spaced armor targets. Projectile design criteria and their relation to target characteristics. Influence of tank design and construction upon selection and development of armor defeating ammunition.

There are, at present, two major types of armor-defeating ammunition; projectiles which depend upon their own kinetic energy to pierce or punch a hole through armor, and explosive-loaded shell which, upon impact and detonation against armor, generate the energy required for the defeat of the target.

The Kinetic energy projectiles consist of more or less massive, cylindrical, ogival-nosed inert shot made of hardened steel or tungsten carbide compacts designed to have sufficient strength to remain substantially intact during the penetration cycle. The armor penetration characteristics of such projectiles depend largely upon their mass and velocity, consequently best armor penetration performance results when they are fired from high velocity guns. Kinetic energy projectiles may be further subdivided into a number of types; monobloc (AP) and capped (APC) steel shot, also composite-rigid (HVAP) and discarding sabot (HVAPDS) tungsten carbide cored shot. Monobloc steel shot are the most simple in design and least expensive of all types, consisting of a solid steel body to whose nose a windshield, made of a thin steel stamping, may be attached to improve its exterior ballistic performance. The steel bodies of AP and APC shot are made of alloy steel differentially heat treated so that the nose sections have maximum strength and hardness, with the hardness gradually decreasing towards the bases to provide tough fracture-resistant body sections. The APC shot differ from the AP shot only in the possession of a steel cap placed over the nose of the shot for the purpose of cushioning the forces on the nose of the shot resulting upon impact against armor. The cap thus assists in keeping the point of the projectile intact.

HVAP shot contain sub-caliber sized tungsten carbide cores fixed within light-weight metallic carriers of gun bore diameter. The carrier accompanies the core to

the target, at which point the core breaks out of the carrier to effect the penetration.
By virtue of its high density and high strength, tungsten carbide is a more effective
penetrator than steel. In addition, because of the combination of a light-weight
carrier and a sub-caliber core, the HVAP shot weighs less than a full caliber steel
shot and thus achieves a higher muzzle velocity when fired from the same gun. Since
the energy required to effect penetration is approximately proportional to the volume
of the hole produced in the armor, the greater armor penetration performance of the
HVAP projectile is, under ideal conditions, obvious.

Because of the lighter weight and consequent lower sectional density of the HVAP
shot, this type of projectile has poorer range-velocity characteristics than steel shot.
Although it may have a muzzle velocity initially 500 to 700 ft/sec higher than an AP
shot, the HVAP shot will have dissipated most of this advantage within 2000 yards'
range. In order to overcome this deficiency, the HVAPDS shot was developed. The
tungsten carbide core is carried within a thin steel sheath and supported, during firing,
in a metallic or plastic carrier which is discarded shortly after the projectile emerges
from the muzzle of the gun. The sub-projectile of high sectional density proceeds to
the target unencumbered by any useless mass.

The explosive loaded or chemical energy armor-defeating ammunition consist of the
high explosive plastic (HEP) shell and the hollow charge (HEAT) shell. The HEP round
has a thin, hemispherical, deformable ogive and a base detonating fuze. Upon impact,
the forward portion of the shell collapses against the target and, upon detonation, a
compressive shock wave parallel to the plate surfaces travels through the armor, is
reflected as tensile waves, and produces a fracture parallel to the plate surfaces. A
disc, having a thickness of approximately 25-30% of the plate thickness, is detached
from the back of the armor at velocities of 500-1000 ft/sec and, within the narrow con-
fines of the interior of a tank, may produce considerable damage. The HEP shell rarely
perforates armor in the true sense of the word, unless the armor is quite brittle, but
inflicts damage by a combination of disc formation and shock. The force of the deto-
nation of HEP shell may produce considerable damage of a secondary nature through
disruption of tank treads, detachment of fittings, etc.

The hollow charge round produces a high velocity jet of discrete particles which
perforate armor by accelerating the plate material away from the path of the jet. The
metal around the hole produced by the jet is compressed. This type of ammunition is
too well known by this audience to justify any further discussion of its functioning.

I will first describe the armor penetration performance of kinetic energy and
chemical energy projectiles against simple targets and then discuss their performance
against more complex targets.

PERFORMANCE OF KINETIC ENERGY PROJECTILES AGAINST SIMPLE ARMOR TARGETS

I shall not attempt to present any equations to describe the armor penetration
performance of kinetic energy projectiles; firstly because all equations which have
been proposed in the past are found to apply, with a good degree of accuracy, to only
a limited range of target conditions, and secondly, because a large number of geo-
metrical, metallurgical, and mechanical property variables existing both in present

service projectiles and armor exert a profound influence upon the mechanisms of armor penetration and projectile reaction.* Variables such as plate hardness may be introduced into penetration formulae, but factors such as variations in projectile nose shape, microstructure, toughness, and soundness of the projectile and armor steels cannot be readily reduced to mathematical terms.

An important consideration in the penetration of armor by kinetic energy projectiles is the ratio of armor thickness to projectile diameter (the e/d ratio) since the mechanisms of armor penetration and projectile behavior vary with the e/d ratio. When the e/d ratio is greater than 1 (armor overmatches the projectile), the penetration tends to be effected by a ductile pushing-aside mechanism. Relatively sharp nosed shot are most effective, and the resistance of the armor generally increases as its hardness increases. When the e/d ratio is less than 1 (armor undermatches the projectile), the penetration tends to be effected by the punching or shearing out of a plug of armor in front of the shot. Relatively blunt nosed shot are most effective under this condition of attack, and the resistance of the armor generally increases as its hardness decreases.

Data on the comparative armor penetration performance of kinetic energy projectiles of the AP, APC, and HVAP types are included in Table I. This table compares the penetration performance of the 90MM AP T33, the 90MM APC T50, and the 90MM HVAP M304 shot when fired at cast and rolled homogeneous and face-hardened armor from 3" to 7.6" in thickness at obliquities of 30° to 70°. The comparative performance of these kinetic energy projectiles against solid armor targets may be summarized as follows:

a. Monobloc steel shot are more effective than capped steel shot for the defeat of undermatching armor at all obliquities of attack and are more effective than both APC and HVAP shot for the defeat of moderately overmatching armor (up to at least 1-1/4 calibers thick) at all obliquities of attack above approximately 45°.

b. Capped steel shot are superior to monobloc steel shot for the defeat of greatly overmatching armor, (over 1-1/4 calibers in thickness) at obliquities in the range of 20° - 45°, but both capped and monobloc shot are greatly inferior to HVAP shot in the low obliquity range against heavy armor targets.

c. HVAP and HVAPDS shot are most effective against heavy armor targets at low and moderate obliquities of attack (the 90MM tungsten carbide cored shot can penetrate 10 to 12 inches at 0° obliquity and at short ranges) but their effectiveness is markedly degraded at obliquities above approximately 45° - 50°.

The preceding statements regarding the comparative performance of AP and APC shot are well illustrated by Figures 1 and 2. Figure 1 represents data obtained from terminal ballistic tests conducted at the Watertown Arsenal Laboratory in which caliber .40" scale models of the 90MM AP T33 and 90MM APC T50 shot were fired at plates from 1/2 to

---

* This is not to imply that the factors which influence penetration are unknown, that the performance of kinetic energy projectiles is very variable, or that penetration data are either scanty or unreliable. As a matter of fact, it is because penetration data are so reliable and so extensive that we are not satisfied with equations that yield only approximately correct estimates.

APC SHOT SUPERIOR

AP SHOT SUPERIOR

COMPARATIVE PERFORMANCE OF AP VS APC PROJECTILES
FOR THE DEFEAT OF HOMOGENEOUS ARMOR OF VARYING
THICKNESSES AND OBLIQUITIES
BASED UPON DATA INVOLVING SCALE MODEL PROJECTILES
AND ARMOR

OBLIQUITY — DEGREES

$OBLIQUITY = \frac{1}{\cos \theta}$

WATERTOWN ARSENAL LABORATORY
WTN.639-8646

Figure 1—Comparative performance of AP vs. APC projectiles for the defeat of
homogeneous armor of varying thicknesses and obliquities, based upon data
involving scale model projectiles and armor.

Figure 2—Comparative performance of 90 MM AP T33 vs. 90 MM APC T50 projectiles
for the defeat of homogeneous armor of varying thicknesses and obliquities.
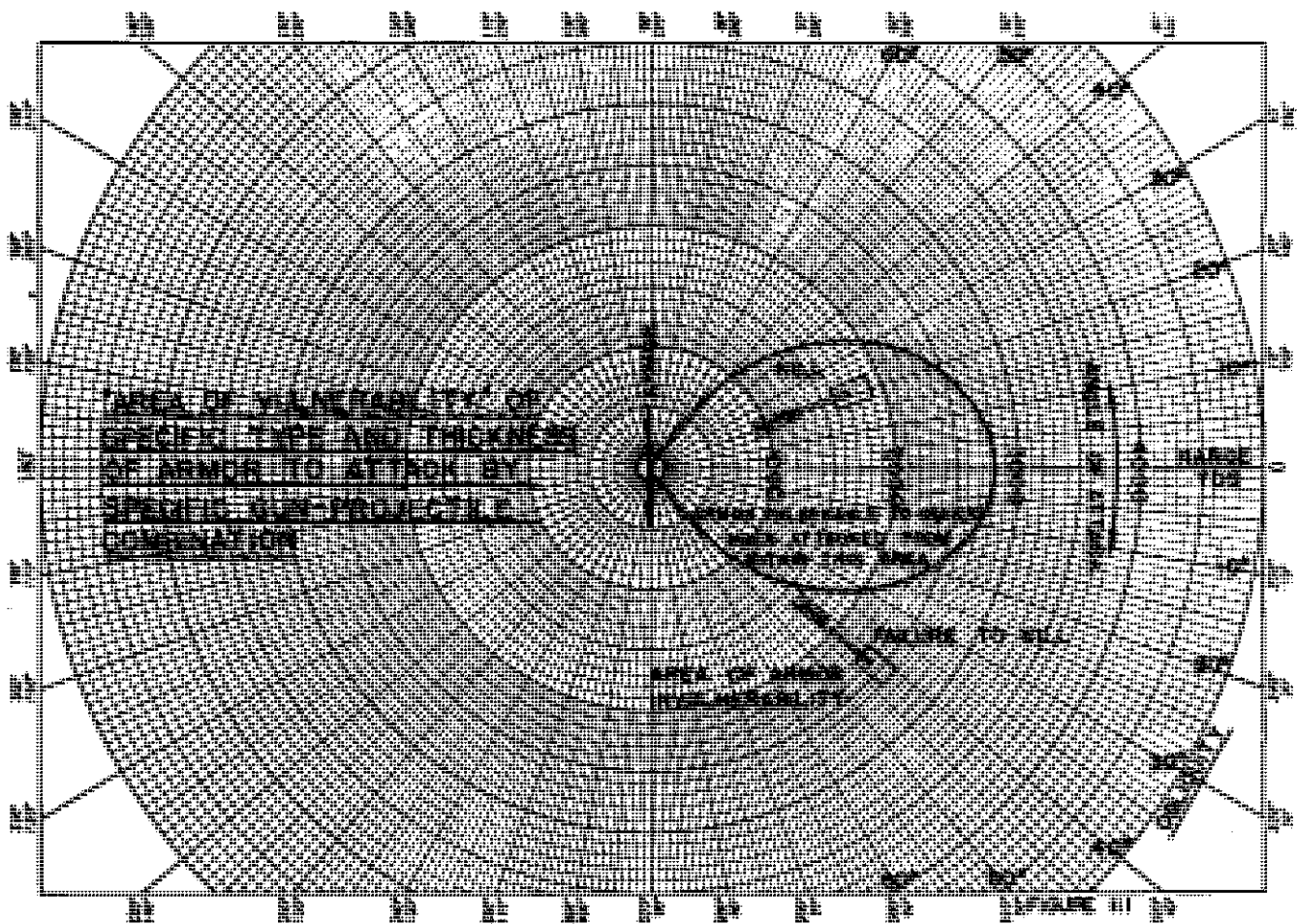
Figure 3—Schematic area of vulnerability curve.
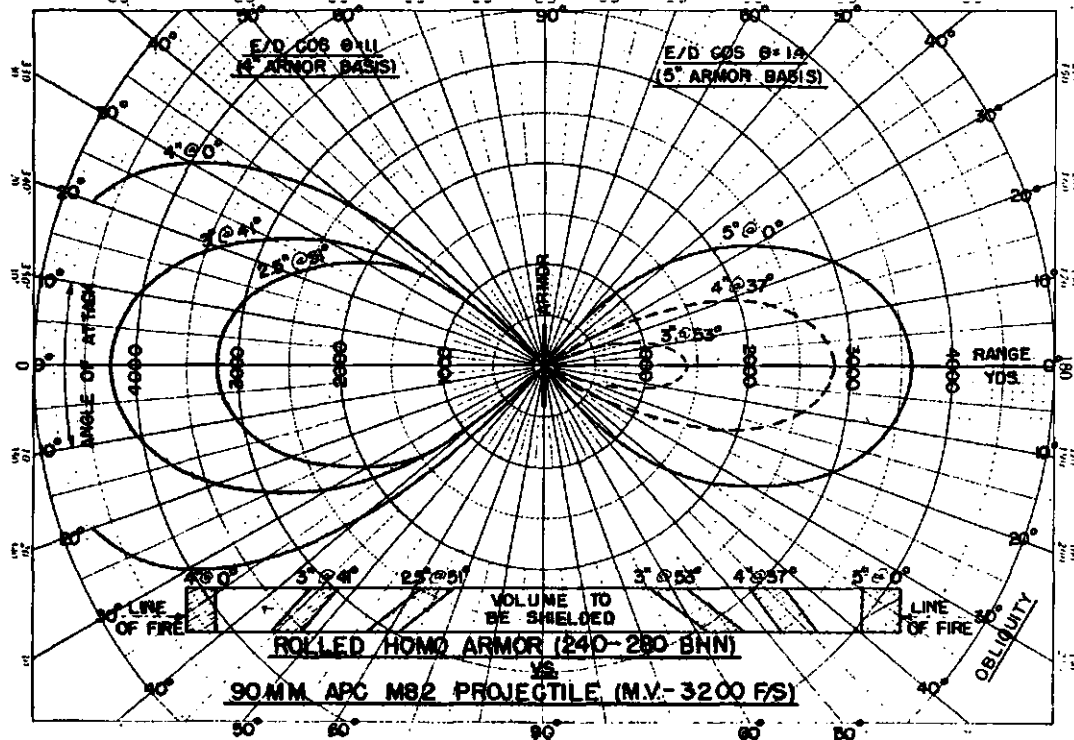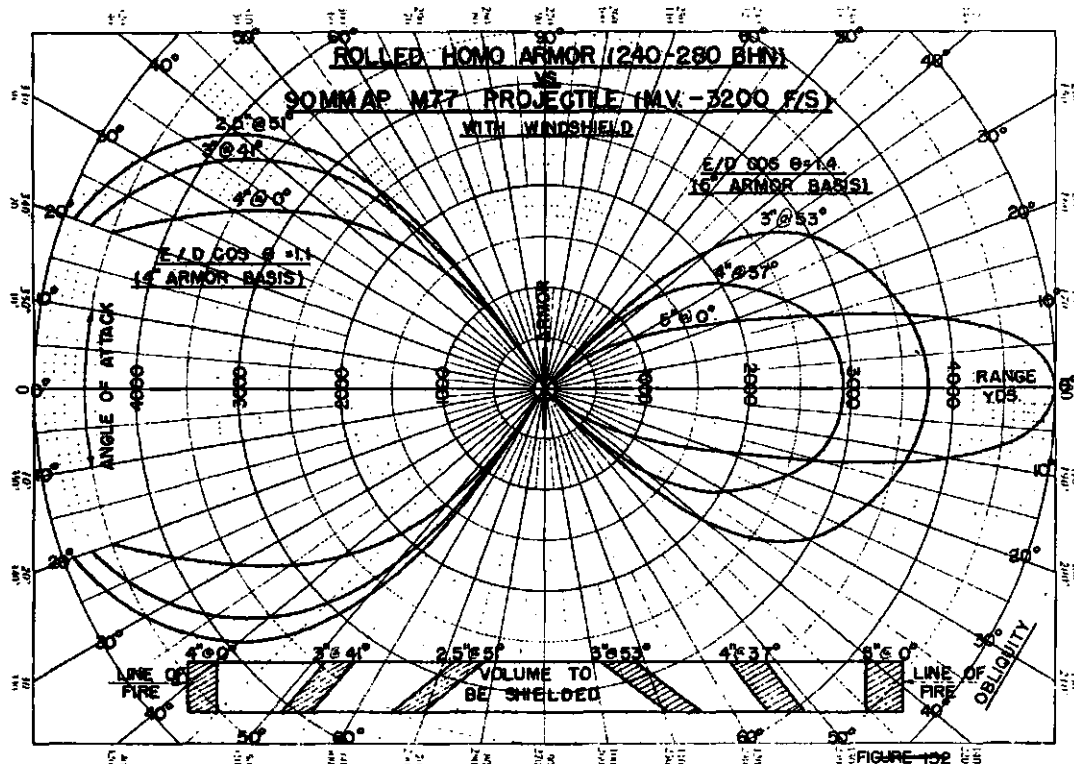
Figures 4 & 5—Comparison of areas of vulnerability for various combinations of armor
thickness and obliquity having equal weight per unit of shielded volume
when attacked by 90 MM steel projectiles.

203

2 calibers in thickness and at obliquities from 0° to 70° inclusive. The curves on Figure 1 represent equal resistance curves; i.e. all plate thicknesses and obliquities whose coordinates fall on the line designated 3000 have ballistic limits of 3000 f/s. The lines furthermore represent the minimum ballistic limit for the target conditions, whether the minimum ballistic limit was obtained with AP or APC projectiles. The dashed line represents the boundary between target conditions where the AP shot was superior and where the APC shot was superior. It will be noted that the areas of superiority of the AP over the APC shot and vice versa are in accord with the previous conclusions.

The data plotted in Figure 1 represent very precisely determined ballistic limits obtained over a wide range of target conditions. Similar data in full scale would involve the expenditure of several million dollars, hundreds of tons of steel armor and thousands of rounds of 90MM armor-piercing projectiles.

Figure 2 represents a similar treatment of data obtained in full scale tests conducted at Aberdeen Proving Ground. These data are necessarily more limited in scope than those used to obtain the curves shown in Figure 1 and hence the boundary conditions of Figure 2 are considerable less reliable than those shown in Figure 1. The same general type of curve results, however.

A useful way of presenting penetration data on kinetic energy projectiles is by means of vulnerability diagrams of the type shown in Figure 3. A roughly elliptical area exists for each gun-projectile-armor combination within which penetration of the armor can be effected and beyond which the armor is invulnerable to the particular attack. The gun must enter into this consideration since it influences the velocity and hence the kinetic energy of the shot at all ranges.

Figures 4 and 5 show the use of vulnerability diagrams to illustrate the comparative performance of AP and APC projectiles against various thicknesses of armor sloped at different obliquities. It will be noted that, for a fixed weight of armor per unit vertical height, thinner plates sloped at higher obliquities (at least up to 53°) provide progressively more protection against APC shot. Against AP shot, however, a given weight of armor sloped at 37° obliquity provided considerably more protection than the same weight of armor in the form of a thinner plate sloped at 53° obliquity. A comparison between the righthand curves of Figures 4 and 5 illustrates the improved effectiveness of AP shot in attacking highly sloped armor targets.

Figure 6 illustrates the weights of steel armor required to protect against kinetic energy projectiles at ranges of 1000, 2000, and 3000 yards as functions of the obliquity of disposition of the armor and the caliber and type of armor-piercing projectile. Note the steep downward slope indicating the marked degradation in performance of HVAP projectiles with increasing obliquity of attack. It is also apparent that protection against APC shot increases constantly as the obliquity increases, whereas armor is most effective against AP shot at about 30° obliquity, then becomes progressively more vulnerable with increasing obliquity above 30°.
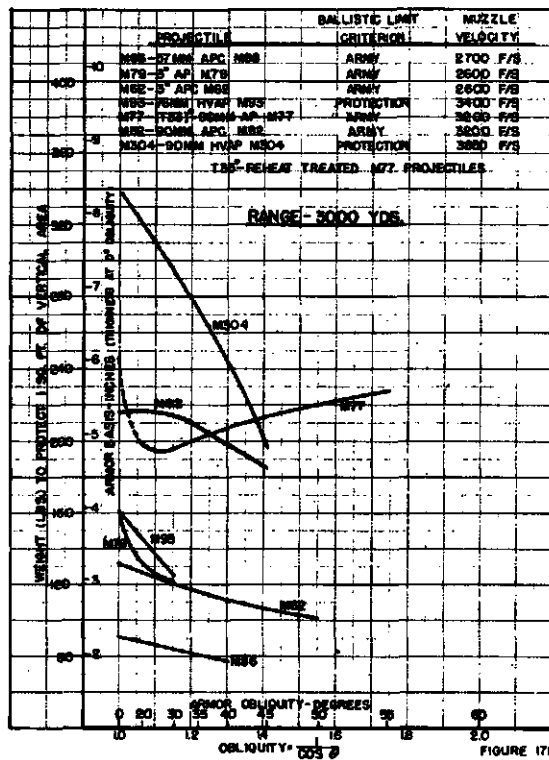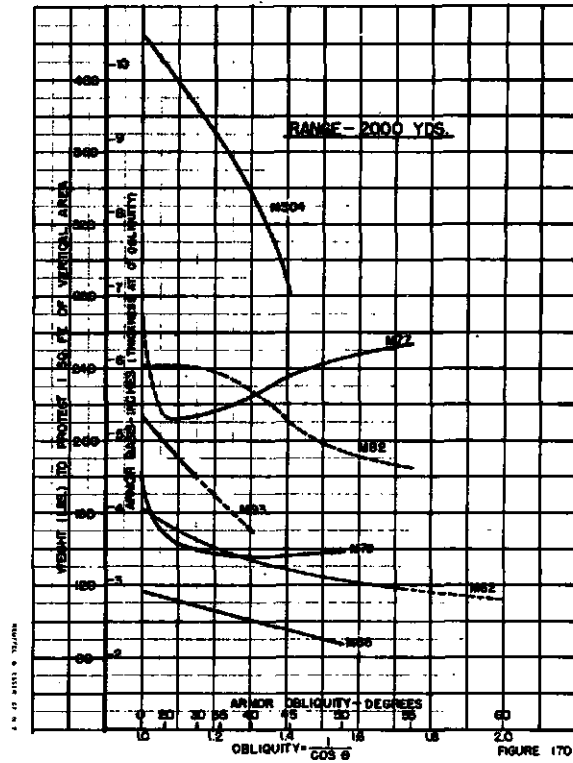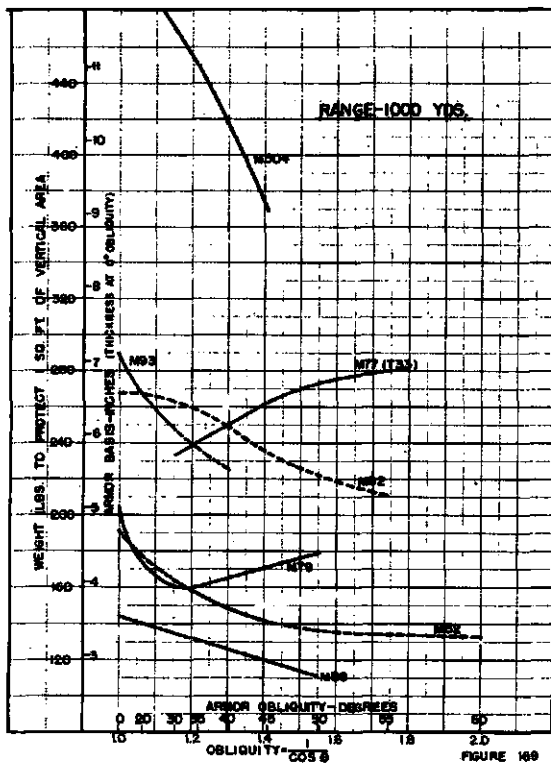
Figure 6—Weights of rolled homogeneous armor at various obliquities required to protect one unit of vertical area against various projectiles at selected ranges.

205

Early in World War II, kinetic energy projectiles were fired from guns with muzzle velocities of 2000-2700 ft/sec. By the end of World War II, steel shot were being fired at velocities up to 3200 f/s and present guns are being built to fire solid steel shot at velocities up to 3500 f/s and HVAP and HVAPDS shot at velocities of 4000-4500 f/s. Coupled with these high velocities are good stability, high accuracy, and high rate of fire. These factors combine to yield a high probability of registering a damaging hit with kinetic energy shot. It is firmly believed that kinetic energy shot will, at least in the foreseeable future, play an important role in tank and anti-tank warfare.

PERFORMANCE OF CHEMICAL ENERGY PROJECTILES AGAINST SIMPLE ARMOR TARGETS

The available data on the armor-defeating performance of high explosive plastic (HEP) shell indicates that this round can cause the scabbing or spalling of armor up to 1.3 calibers in thickness over a wide range of obliquities. Unlike kinetic energy armor-piercing projectiles, the performance of HEP shell is not greatly influenced by obliquity of attack at least within the range of 30° to 60°; the same thickness of armor can be defeated over this whole range of obliquities. As a matter of fact, the performance of HEP shell is worse in the range of 0° to 30° obliquity than at higher obliquities due primarily to the fact that the explosive charge is not spread over the face of the armor as effectively at very low obliquities as it is at higher obliquities. The HEP shell is also degraded at obliquities of attack above approximately 60°.

HEP shell perform satisfactorily at striking velocities up to approximately 2500 f/s, but at higher impact velocities this shell is relatively ineffective because of shock detonation of the explosive which initiates at the nose of the shell at these high velocities. To perform satisfactorily, detonation must be initiated at the base of the shell to permit the generation and travel of a shock wave from the explosive to the target.

It has been determined that brittle steel armor and unsound steel containing laminations or segregations of inclusions are more readily defeated by HEP shell than are tough, sound steels. There is reason to believe that HEP shell become increasingly effective in cold climates since the toughness of steel armor decreases with decreasing temperature, particularly if the steel is insufficiently alloyed or poorly heat treated.

In view of the lower velocity of HEP shell as compared to kinetic energy projectiles, errors in range estimation assume more serious proportions than in the case of kinetic energy shot. The probability of hitting the target, particularly at longer ranges, is thus lower with HEP shell than with kinetic energy shot.

Chemical energy armor-defeating ammunition do, however, have one very great advantage over kinetic energy projectiles. Since they generate their destructive energy upon impact against the target, chemical energy shell inflict as much damage when hitting from long ranges as from short ranges, whereas kinetic energy projectiles become less and less effective as the range from which they are fired increases.

The jet generated by the hollow charge (HEAT) shell continues in a relatively straight line along the line of flight of the shell, consequently the armor penetration performance of this type of ammunition closely follows the cosine law. The penetration performance of kinetic energy projectiles follows the cosine law fairly well up to approximately 30° obliquity, but at higher obliquities the deviation is very considerable and is markedly influenced by the geometrical and metallurgical design of the shot. Since the HEAT shell does follow the cosine law, a round which can penetrate 12" thick plate at normal obliquity can defeat 6" thick plate inclined at 60° obliquity. For comparison, the 90MM HVAP M304 shot can defeat 12" thick plate at 0° obliquity at ranges up to approximately 1300 yards, but cannot defeat even 4" thick plate at 60° obliquity when fired at point blank range.

The presently available data on the armor penetration performance of HEAT shell indicate that the thickness of armor which can be penetrated 90% of the time is approximately 4 times the inside diameter of the cone. This behavior holds over a wide range of obliquities up to possibly 70°. Thus a 90MM HEAT shell having a cone diameter of approximately 3" should be able to penetrate about 12" of armor. The data contained in Table II shows that the 90MM HEAT T108E15 shell can defeat 5" armor at 60° obliquity and 4" armor at 68° obliquity.

In the case of defeat of armor by kinetic energy and chemical energy HEP shell, more or less massive pieces of metal flying at considerable velocities become available to inflict damage behind the armor. In the case of HEAT shell, however, only a thin beam of tiny, incandescent particles emerges behind the armor. Personnel or equipment directly in the path of the jet will become casualties, but the damage may not necessarily be serious. In order, therefore, to insure that the emerging jet will possess a significant degree of lethality, it has recently been agreed that the jet must have a residual penetrating ability of 2" of armor after defeat of the main armor to be considered effectively lethal.

It was found early in World War II that spin stabilized HEAT shell fired from rifled guns suffered a 30 to 50% loss in penetration performance as compared to non-rotating shell. The centrifugal force of spin was sufficient to cause the jet to cone out and dissipate much of its energy. This factor led to the intensive development of fin-stabilized non-rotated HEAT shell. The depth of penetration of 4 times the cone diameter applies only to non-rotated shell.

The depth of penetration by HEAT shell is inversely proportional to the square root of the density of the material under attack, therefore the thickness of material required to defeat the attack is also proportional to the square root of its density. Since the weight of material varies directly as its density, the weight of material required to defeat HEAT shell varies directly as the square root of its density. Low density materials are thus more resistant, on a weight basis, than are high density materials. Thus aluminum and magnesium will offer better resistance to HEAT attack than will the same weight of steel armor. In their present stage of development, however, aluminum and magnesium alloys in section thicknesses comparable to 2" and more of steel are significantly inferior to steel armor in resistance to attack by kinetic energy projectiles.

In their present stage of development, fin-stabilized HEAT shell do not match the accuracy of kinetic energy projectiles, and this, coupled with their lower velocities, results in lower hit probabilities than are possible with kinetic energy projectiles. The higher velocity and greater accuracy of kinetic energy projectiles make them considerably more accurate than all present types of chemical energy armor-defeating ammunition.

PERFORMANCE OF KINETIC ENERGY PROJECTILES AGAINST COMPLEX ARMOR TARGETS

Kinetic energy projectiles have been tested against spaced armor targets consisting of relatively thin (approximately 1/2") plates placed some distance in front of the more massive main armor. The function of the skirting plate is not to extract a significant amount of energy from the attacking projectile, but to so affect it by yawing, decapping, or fracturing the shot that its performance against the main armor is degraded.

Results of firing various types of 57MM and 90MM kinetic energy projectiles against spaced armor targets are shown in Table III. These tests were conducted at Aberdeen Proving Ground under the technical supervision of the Watertown Arsenal. Photographs of the projectiles were also taken as they emerged behind the skirting plate in order to observe the effect of the skirting plate on the projectiles.

It was found that 57MM AP and APC shot were not fractured by passage through 1/2" thick skirting plate but were considerably yawed. In addition, the cap was always removed from the APC shot. Surprisingly, the 90MM AP shot were found to be readily fractured by passage through 1/2" thick skirting plate. Since the 57MM shot were not fractured, parallel plate arrangements were found to be worse than the basic armor since the shot were yawed in the direction of lower obliquity against the main armor. Oppositely sloped spaced armor arrangements are indicated for cases where the shot cannot be fractured by the skirting plate.

Since the 90MM AP shot was broken by the skirting plate, both parallel and non-parallel placement of the skirting plate were equally effective in degrading this shot. The 90MM APC shot was not readily fractured by skirting armor, but its performance was degraded against the target conditions shown in Table III because, once its cap was removed, it behaved essentially the same as monobloc shot, and the target conditions chosen, namely 30° and 40° obliquity, are those where monobloc shot are less effective than capped shot.

Tungsten carbide cored projectiles may be seriously degraded by spaced armor arrangements since the very brittle core may be rather easily fractured by skirting plates. Once the core is fractured prior to impact against the main armor, the HVAP type of shot is rendered comparatively ineffective.

It is essential that spaced armor arrangements to defeat kinetic energy projectiles be very carefully chosen, because it is entirely possible that some arrangements cause the projectile to penetrate far more efficiently than it would against the main armor alone.

Spaced armor arrangements can readily be designed to fracture capped shot. This can be done by using two skirting plates separated from each other. The first skirting plate removes the cap and the second fractures the shot. The test described in Table III, where the 90MM APC T50 was fired against two 1/2" thick plates parallel to and separated from each other and the main plate (3" at 55°) by 8" of space shows what can be done with this type of plate arrangement. This arrangement could not be defeated even at point blank range, whereas 4" armor at 55° obliquity can be defeated by the same projectile at ranges up to 600 yards and 3" armor at 55° at ranges up to 1600 yards.

PERFORMANCE OF CHEMICAL ENERGY PROJECTILES

AGAINST COMPLEX ARMOR TARGETS

Since the HEP shell defeats armor by the application of a severe shock which induces stress waves of high magnitude, it is obvious that the best way to cope with the attack of this type of ammunition is to prevent the shock wave from getting started in the armor. It does not help much to increase the thickness of the plate since large increases in thickness are required to defeat HEP shell. The British have done an extensive amount of firing of HEP shell against spaced armor structures and have found that they could be readily defeated by spaced armor combination, by rubber pads placed between armor sandwiches, etc. The skirting plate of spaced armor arrangements designed to defeat HEP shell must be supported well enough to prevent contact with the main armor during detonation of the shell, since then the shock wave will be transmitted to the main armor.

Table IV contains some data recently obtained at Aberdeen Proving Ground on the performance of the 105MM HEP T81E17 shell against 3" armor at 55° and then against a spaced armor combination consisting of a 1/2" plate 8" in front of the 3" armor at 55°. This shell can normally defeat 5" plate at this obliquity. Its inability to defeat a spaced armor combination consisting of a total of 3-1/2" thickness of steel indicates how greatly this type of shell can be degraded by spaced armor.

There has been extensive work on the development of defense against HEAT shell. This type of ammunition can penetrate such a great thickness of solid steel that other means must be found to defend against it. Since it was apparent that low density materials offered better protection against HEAT shell for a given weight of material, a considerable amount of effort was expended during World War II in developing low density materials for this purpose. The best low density material developed was HCR-2 which consists of a mixture of quartz gravel in a mastic base of 75% asphalt and 25% wood flour. This material when placed behind a thin steel plate and attached to the main armor of vehicles was found to give much better protection against HEAT shell than a similar weight of steel or other materials with the exception of solid or laminated glass.

Another type of defense against the HEAT round was provided by fixing 7" to 8" long closely spaced steel spikes to the surface of the main armor; the function of the spikes being to break up the cone before initiation of the jet. Spiked armor structures have been found to be effective against several models of HEAT rounds.
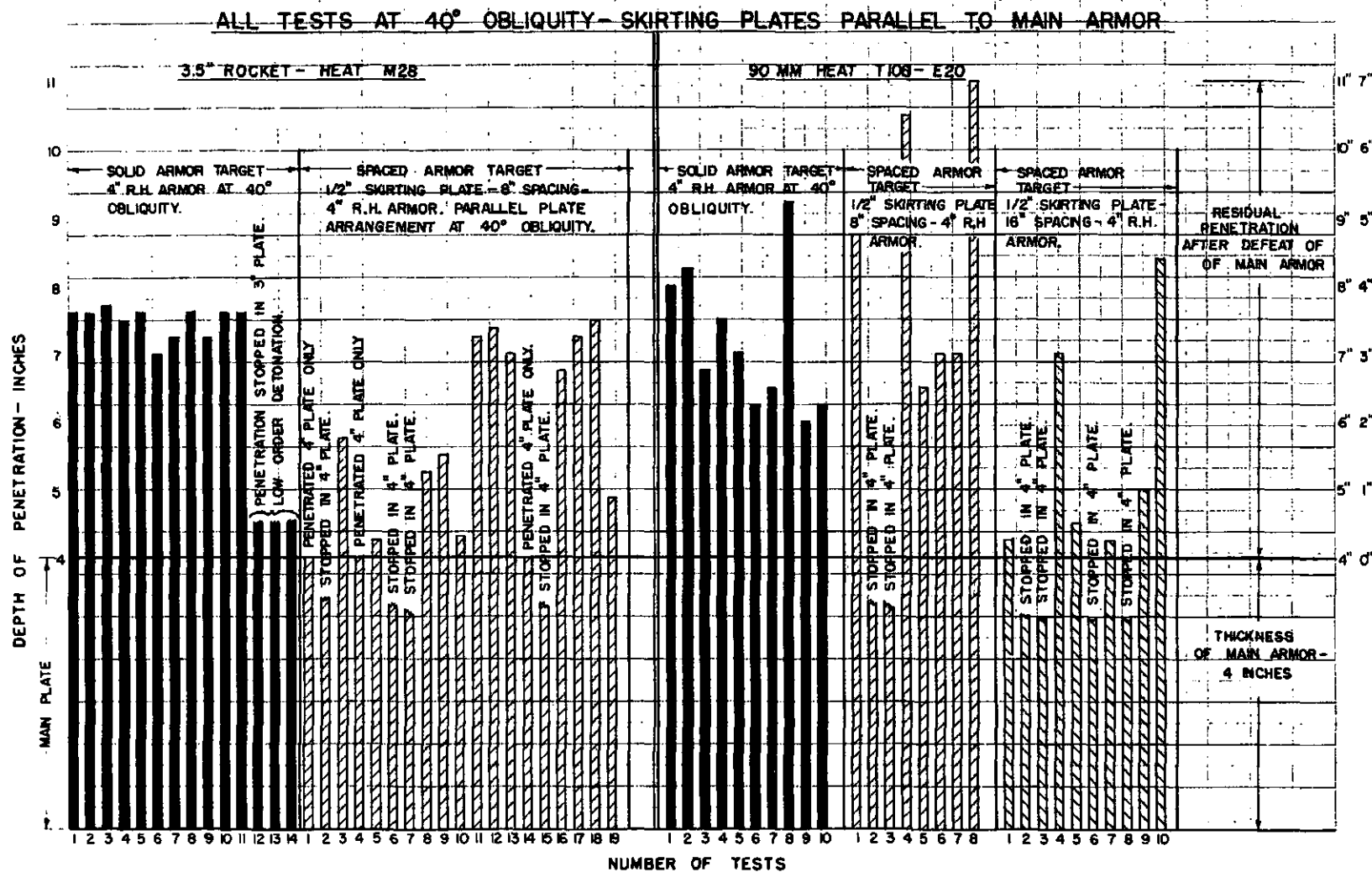
Figure 7

More recent developments sponsored by the Detroit Arsenal show that an arrangement of parallel angle irons, made of armor steel, placed on the surface of the main armor offer considerably increased protection, particularly at high angles of attack, against both HEAT and HEP shell. Although these angle irons did not defeat all the HEAT shell fired at them, they were effective in significantly reducing the probability of a perforation when hit by a HEAT shell.

It was found during World War II that spin stabilized HEAT shell could be fairly readily defeated by spaced armor due to the degrading effect of the spin, particularly when the standoff was increased by the spaced armor. More recent tests have shown that spins even as low as 10 rev./sec. result in a 20% decrease in penetration performance of 105MM HEAT shell against a spaced armor target consisting of a 3/4" plate 12" in front of the main armor. This 20% decrease represented degradation in performance of the same round compared to its performance against the same target when the shell was not rotated.

Very recently, tests of the 3.5" HEAT M28 rocket and the 90MM HEAT T108E20 shell have been conducted against spaced armor targets. The basic armor consisted of 4" plate at 40° obliquity; firings were first conducted at this target, then at spaced armor targets consisting of a 1/2" thick plate parallel to and 8" in front of the main armor. In one case a 3" plate was placed behind the 4" armor, with 1/4" thick plates stacked behind the 3" plate in order to measure the residual penetrations, but in all other cases, a series of 1/4" thick plates were stacked behind the main armor for this purpose.

Figure 7 tabulates the data resulting from the tests described above. Starting at the lefthand end of the chart, 14 rounds of the 3.5" rocket were fired against 4" armor at 40° obliquity. Eleven rounds completely perforated the 4" plate and achieved residual penetrations of 3" to 3-5/8" into the 3" and 1/4" thick plates behind the 4" plate. Three rounds appeared to produce low order detonations; the 4" target, however, was perforated, but relatively little residual penetration into the 3" back-up plate was achieved.

Nineteen rounds of the 3.5" rocket were then fired at spaced armor consisting of the 1/2" skirting plate parallel to and 8" in front of the 4" plate. Of these nineteen rounds, four failed to perforate the 4" main armor, three perforated the 4" main armor but had no residual penetration ability, three more perforated, but had residual penetration abilities of less than 1", three achieved residual penetrations of 1 to 1-1/2" in depth, and the remaining six rounds achieved the same residual penetrations as were obtained against the solid armor target.

The performance of the 90MM HEAT T108E20 was found to be very variable against a simple armor target consisting of 4" plate at 40° obliquity. Of ten rounds fired, all perforated the target, but the residual penetrations varied from 2" to 5-3/8". When tested against spaced armor with 8" spacing, two rounds of eight 90MM T108E20 shell fired failed to defeat the target. Four rounds perforated the target and achieved residual penetrations of the same order of magnitude as were obtained against the solid

armor target, while two rounds achieved even higher residual penetrations; 6-1/2" to 7" in depth. This increase in residual penetration probably resulted from a more efficient standoff caused by the 8" spacing.

A 16" spacing between the skirting armor and the main plate greatly improved the effectiveness of spaced armor against the 90MM HEAT T108E20 shell. Of ten rounds fired, four were totally defeated, 4 perforated but achieved residual penetrations of but 1/4" to 1" in depth, while only two rounds performed as well as they did against the main armor alone.

While the above tests are only elementary in nature, there appears good hope that spaced armor combinations may be devised which will be even more successful against HEAT shell. Spaced armor may be particularly effective at higher obliquities of attack.

Combinations of the main steel armor, low density materials, and spaced armor may yet provide real defense against chemical energy armor-defeating ammunition

In conclusion, the thought should be expressed that both types of armor-defeating ammunition should be brought to the field of battle. Any decision to adopt one type of the kinetic and chemical energy ammunition to the exclusion of the other type would greatly simplify the enemy's armored vehicle design and construction problems. It is possible to devise a reasonably simple defense against either type of ammunition alone, but the problem of defense against both types together is an extremely complicated one.

TABLE I

PENETRATION PERFORMANCE OF 90MM AP T33, 90 MM APC T50, AND 90MM HVAP M304 vs ROLLED AND CAST HOMOGENEOUS AND FACE-HARDENED ARMOR

| | Armor | | | Ballistic Performance of | | | | | |
| | | | | 90MM AP T33 | | 90MM APC T50 | | 90MM HVAP M304 | |
Thick-ness, in.	Type	BHN*	Obl. of Attack	Bal. Lim. f/s	Max. Range yds	Bal. Lim. f/s	Max. Range yds	Bal. Lim. f/s	Max. Range yds
3	RH	280	45°	1983	5000	2216	3975	----	----
3	RH	280	60°	2629	2200	2853	1300	3145	1575
3	RH	280	65°	3026	625	3101	350	3543	675
3	RH	320	60°	2645	2150	2795	1550	3246	1350
3	RH	320	65°	2870	1225	3109	350	3611	525
3	CH	260	45°	1979	5000	----	----	2437	3225
3	CH	260	53°	2315	3550	----	----	2725	2550
3	CH	280	55°	2313	3550	----	----	2754	2475
3	CH	280	60°	2586	2400	2683	2000	----	----
3	CH	280	65°	----	----	3112	325	----	----
3	CH	280	70°	3073	375	----	----	----	----
3	FH	---	55°	2059	4725	2248	3825	----	----
3	FH	---	60°	2505	2725	2635	2175	2903	2125
3	FH	---	65°	2648	2125	2902	1100	3300	1225
4	RH	280	30°	2054	4750	2149	4275	----	----
4	RH	280	45°	2469	2875	2831	1400	----	----
4	RH	280	55°	2742	1750	3010	700	3571	625
4	RH	280	60°	3079	450	3162	125	3638	475
4	RH	320	55°	2719	1850	3138	225	3503	775
4	RH	320	60°	3075	450	----	----	3748	225
4	RH	360	60°	2943	975	3097	375	3680	375
4	CH	240	55°	2785	1575	----	----	----	----
4	CH	240	60°	2933	1000	3208	Above MV	3800	100
4	CH	280	55°	2620	2250	2744	1750	----	----
4	CH	280	60°	3007	700	3135	250	----	----
4	CH	280	65°	3129	250	----	----	----	----
4	CH	320	60°	2947	950	3175	75	3669	400
4	FH	---	45°	----	----	2391	3200	2868	2225
4	FH	---	50°	----	----	----	----	3160	1550
4	FH	---	55°	----	----	2765	1650	3397	1000
4	FH	---	60°	2763	1675	3069	475	----	----
5	RH	240	30°	2804	1500	2343	3400	----	----
5	RH	240	45°	3146	200	2976	825	----	----
5	RH	320	30°	2967	875	2461	2925	----	----
5	RH	320	45°	3167	100	3177	75	----	----

TABLE I (Cont'd)

Thick-ness, in.	Armor Type	BHN*	Obl. of Attack	Ballistic Performance of					
				90MM AP T33		90MM APC T50		90MM HVAP M304	
				Bal. Lim. f/s	Max. Range yds	Bal. Lim. f/s	Max. Range yds	Bal. Lim. f/s	Max. Range yds
5	CH	240	30°	2543	2575	2234	3900	----	----
5	CH	240	45°	2740	1750	2905	1100	----	----
5	FH	---	30°	2475	2850	2394	3175	2819	2325
5	FH	---	45°	2866	1250	2879	1200	3208	1425
6	RH	260	30°	3214	Above MV	2750	1725	2562	2925
6	CH	240	30°	2907	1100	2632	2200	2487	3100
6	FH	---	30°	----	----	2863	1275	3333	1150
7.6	RH	260	30°	----	----	3182	50	2892	2150

* BHN - Brinell Hardness   RH - Rolled homogeneous armor
  Greater than   CH - Cast homogeneous armor
  Less than   FH - Face-hardened armor
  mv - AP, APC - 3200 f/s
  mv - HVAP - 3850 f/s

TABLE II

PENETRATION PERFORMANCE OF HEAT SHELL AGAINST ARMOR

Projectile	Thickness of Armor	Obliquity of Attack	No. of Rounds Fired	Results
90MM HEAT* T108E15	Approx. 5"	60°	5	3 complete penetrations 2 partial penetrations
"	4.1"	68°	1	Complete penetration
"	3.4"	73°, 75°	2	Ricochet, no penetrations
"	4.5"	72°	1	Ricochet, no penetration

* fired from range of 50 yards, 2400 f/s muzzle velocity

TABLE III

PERFORMANCE OF KINETIC ENERGY PROJECTILES AGAINST SPACED ARMOR COMBINATIONS

Projectile	Main Armor* Thick-ness	Main Armor* Obli-quity	Thickness Skirting Plate	Arrange-ment**	Spacing	Ballistic Performance Ballistic Limit f/s (Protection)	Ballistic Performance Maximum Range for Penetration - yards
57MM AP M70	2"	40°	None	-	-	1997	1850
"	2"	40°	1/2"	A	16"	1772	2500
"	2"	40°	1/2"	B	16"	2620,2638	175
57MM APC M86	2"	40°	None	-	-	2149	1500
"	2"	40°	1/2"	A	16"	1943,1940	2000
"	2"	40°	1/2"	B	16"	2755	Above m.v.
90MM AP T33	3"	55°	None	-	-	2505	2725
"	3"	55°	1/2"	A	8"	2952	950
"	4"	30°	None	-	-	2025	4875
"	4"	30°	1/2"	A	16"	2383	3250
"	4"	30°	1/2"	A	8"	2368	3300
90MM APC T50	3"	40°	None	-	-	2040	4800
"	3"	40°	1/2"	A	16"	2452	2950
"	3"	40°	1/2"	A	8"	2501	2750
"	4"	30°	None	-	-	2171	4200
"	4"	30°	1/2"	A	16"	2681	2000
"	4"	30°	1/2"	B	16"	2657	2100
"	4"	30°	1/2"	A	8"	2669	2050
"	3"	55°	None	-	-	2777	1600
"	3"	55°	3/4"	B	20"	2657	2100
"	3"	55°	two 1/2" plates 8" apart	A	8"	partial at 3249	Above m.v.
90MM HVAP M304	3"	55°	None	-	-	3018	1850
"	3"	55°	1/2"	A	8"	3832	50
"	4"	30°	None	-	-	2226	3750
"	4"	30°	1/2"	A	8"	2690	2625
"	4"	30°	1/2"	A	16"	2780	2425
"	4"	30°	1/2"	B	16"	2702	2600
"	6"	30°	None	-	-	2590	2900
"	6"	30°	1/2"	A	12"	3689	350

* Main armor is rolled homogeneous plate of 260-280 BHN.
** Arrangement:
      A - Skirting plate parallel to main armor
      B - Skirting plate and main armor sloped towards each other, each inclined at same angle but in opposite directions from normal.

TABLE IV

PERFORMANCE OF HEP SHELL AGAINST SPACED ARMOR COMBINATIONS

Projectile	Main Armor		Thickness Skirting Plate	Arrangement	Spacing	Result on Target
	Thickness	Obliquity				
105MM HEP T81E17	3"	55°	None	-	-	Average spall size 10" x 7"
"	3"	55°	1/2"	parallel	8"	No spalling, target not defeated

The 105MM HEP T81E17 shell is normally capable
of spalling 5" thick rolled homogeneous armor.

REVIEW OF THE PRESENT POSITION OF HOLLOW CHARGE AND SQUASH
HEAD RESEARCH AND DEVELOPMENT IN UNITED KINGDOM

W. E. Soper

Armament Research Establishment, Fort Halstead, Kent

Introduction

During the years following 1945, the attention devoted to armament research was naturally severely curtailed, and, in this process, research on the hollow charge and squash head virtually ceased, apart from a few sporadic attempts at ad hoc work. This state of affairs is now ceasing, but the process of re-establishing a good research team equipped with modern apparatus is a comparatively slow process. For this reason, this paper will be devoted largely to a survey of the field as it appears in Great Britain, and the directions in which the now growing research effort will be expected to turn. It cannot be a record of considerable achievement, although an account will be given of such ad hoc work as has been carried out.

1. Hollow Charge

Cone Production

It was obvious from the American results during the war years that, were deep penetration is required, copper must replace steel as the material for the conical liner.

A limited amount of work of a rather ad hoc nature was undertaken to try to formulate the requirements to specify for given cases. The first results, obtained with cones with $30°$ and $45°$ apex angles, 2.45 inches in diameter, pressed from 1/16 inch sheet metal were rather disappointing, although in the main somewhat better than with steel cones. These first copper cones were, however, rather poor and had obvious ribs, although the variation in wall thickness was not large.

It was therefore decided to attempt to set a standard by making cones which were not pressed. These cones were all to have apex angles of $45°$. Two methods were tried. The first was electrodeposition on to a graphited steel former. This produced a cone, the thickness of which diminished in a regular manner from apex to base, the mean thickness being about 0.06 inch. Under certain conditions, the surface was fairly good and free from pits, and these cones were made up into charges without any machining, apart from cutting off the skirt to leave the cone 2 inches in diameter at the base. In other cases the outside was machined. The difficulty was to obtain reproducible specimens.

The charges made from these cones perforated 200mm of homogeneous armour and this was a considerable improvement in performance over the pressed cones. The second course was to machine cones from 2 inch drawn bar. This method is, of course, much more flexible and probably the best method to use for cones for research purposes.

With this method cones of different wall thickness were studied including some with wall thickness tapering either from base to apex or from apex to base.

The results of these tests are rather interesting.

Cone			Result
Electrodeposited	thickness	0.041	Perforated 200mm homogeneous armour
	"	0.065	200mm
Turned	thickness	0.035	Failed at 200mm " "
		0.045	Perforated 230mm homogeneous armour
		0.066	230mm " "

Turned tapered thickness Apex 0.08 Base 0.05 Perforated 200mm
                  Apex 0.05 Base 0.08   "   "

                 Apex 0.066 Base 0.032 Failed to perf. 200mm

Experiments were then abandoned on the tapered wall. This does not necessarily imply that the tapered wall thickness is abandoned for all time; it merely means that continuation on an ad hoc basis was not thought to be profitable, in view of the promising results obtained from cones of uniform wall thickness.

From this basis, a contract was given to a firm, Messrs. Plessey, to develop a pressing technique, and, in fact they produced, after some months of experiment, some very satisfactory cones of 2.6 inches diameter and nominally 0.060 inch thick. These cones turned out surprisingly uniform. The apex was thin being of the order 0.050 to 0.055, but below this the thickness measured at four places at four different heights did not differ by more than 0.003 inch. This cone perforated 300mm of armour. The cones were produced by seven successive pressing operations, each step being followed by annealing. Encouraged by this the Armament Design Establishment put an order on to the Royal Ordnance Factories to produce a large 5-inch diameter cone 0.1 inch thick. These did not turn out so well, but after machining on the outside a more or less uniform thickness of 0.096 inch was obtained. These cones have not so far been fired statically, but dynamically, in the 5 inch rocket, a perforation of 10 inches at 60° from normal (equivalent 500mm) was obtained by one shot in the A.D.E. trial.

Lethality

This discussion leads directly to a question on which a great deal of interest now centres. When assessing the performance of a given hollow charge, it has been the custom to base it upon the thickness of armour which is perforated irrespective of what damage is done behind the armour plate. This, however, does not appear to be completely logical because the primary aim is to cause lethal damage behind the structure which the hollow charge has to penetrate.

It has almost always been the custom in Ordnance Board trials against armour to place behind the rear face of the armour, two mild steel plates 1/16 inch thick, separated by a distance of 6 inches from one another, and situated so that there is a

distance of 3 feet between the rear face of the armour plate and the first surface of the target plate structure. The evidence of damage which would occur within a structure protected by the armour is thus obtained. It has been a common experience to find that at the extended limit of its performance a hollow charge will do little or no damage to the target plate structure.

This then leads to the question of what criterion should be adopted by the designer when called upon to defeat a specified target. Should he design on the basis of perforation or should he allow some overmatching coefficient in order to do lethal damage behind this specified target? This question is now being hotly debated in Great Britain. It is obvious that, if an overmatching coefficient is introduced, it will mean an increase of calibre, and, thus, of weight of the round designed; and it is important then to know a precise value to put to this coefficient.

Experiments to this end are now in progress and, at this moment, it is impossible to give any very clear or emphatic decision. This work has been primarily sponsored by the Ordnance Board, and a programme has been arranged to fire, statically, in order to eliminate some of the firing variables, a number of Service munitions against plate at and around the critical penetrating thickness with targets of wood, A.P. shot complete with filled cartridge cases and tanks containing Diesel Oil. The hollow charges to be used are the Energa Grenade, the 3-1/2 inch rocket head both of which have copper liners, the 95mm shell with steel liner to be followed later by the 5 inch and 4-1/2 inch rocket heads with copper liners.

Some of this programme has been fired and in giving the present trends, it is with the understanding that as the trial proceeds these trends may be profoundly altered. What appears to be emerging at the moment is that, at the critical thickness of plate, round to round variations are considerable both in penetration and damage; but if a point is taken for the performance where a series of 9/10 successes against the plate is achieved, then at this level of performance considerable lethal damage may be inflicted inside the armour protected structure.

This conclusion is, naturally, of little help to the designer who wants to know whether to add a constant thickness to his specified target, or whether it is better calculated on the basis of a percentage of armour thickness.

Later experiments with the larger 4-1/2 inch and 5 inch heads, none of which have yet been fired, may help to resolve this scaling question.

Meanwhile a short series of firings of the standard 2 inch experimental charge using various thicknesses of liner are to be fired to ascertain how nearly the maximum penetration and maximum damage criteria can be reconciled.

Regularity

It is obvious from what has been stated in the previous passage that one of the greatest improvements that could be made to the conventional hollow charge would be to increase its regularity. In the United States a very great volume of painstaking

work has been done on this theme. The regularity and symmetry of the liner has been studied from the point of view of thickness and axial symmetry; the uniformity and homogeneity of the high explosive charge has also been studied together with the effect of off-axial initiation. It has been shown that careful attention to these details has made a considerable improvement to the range of spread but has not eliminated it. Particular attention is now being directed in Britain to the question of symmetrical initiation. There is some evidence to show that with the ordinary method of initiation with a detonator and booster pellet it cannot be assumed that a symmetrical detonation wave will result from the most careful geometrical set-up, and an investigation was started by Evans and his group on improved methods of initiation. This work has now been taken over by the new hollow charge group. It is as yet too early to give any results but the purpose of the present preliminary investigation is to see if there is any improvement in regularity with a true point initiation and a symmetrical detonation wave.

Lines of Future Investigation

There is still a chance that some advantage may be obtained from the liner with a tapered wall thickness if it can be adjusted to the optimum collapse velocity possibly with the help of a shaped detonation wave. There is a very considerable field for enquiry here and it may be necessary to depart from the conical shaped liner. The primary object will naturally be to increase the mass of the jet without decreasing the velocity gradient. There is a large source of untapped energy in the explosive if only we can devise the means to obtain it.

Not much attention has been given at the present time to the shock waves which are involved in the various steps of cone collapse, jet formation and target penetration.

Consider the collapsing conical liner, the detonation wave coming through the explosive starts a shock wave through the thickness of the liner. At the other side a shock wave is transmitted into the air and a shock wave or rarefaction wave returns through the liner. Work on this problem is now being started and the simple case of transmission through a flat plate is first being studied. This work acts as a link between the hollow charge and the squash head which is the responsibility of the same group at the Armament Research Establishment.

Work is also being started on the study of the penetration phenomenon by the hollow charge jet with special reference to the shock wave which must precede the head of the jet.

It is unfortunate that this work is not yet in a stage where some concrete results could be exhibited.

These problems are being tackled by a combination of methods including oscillography, Kerr-Cell cameras and rotating mirror cameras. We are also very interested in the promising technique being developed by Stanton at the N.O.T.S. using tracers to record the paths of collapsing elements of the cone.

The Filling of Hollow Charges

The standard British filling for hollow charges is RDX/TNT 60/40. There is, however, a certain amount of difficulty attendant upon this as British manufactured RDX/TNT 60/40 tends to be a rather thick unmanageable mass. It is thus very difficult to avoid the formation of cavities in the filling and to get the filling down to the flange of the cone without bridging. Consequently the filling factory organisation has often extracted a reluctant concession to reduce the proportions to 50/50. This is a bad and retrograde step for two reasons, the more obvious being the loss of power inherent in the charge between the proportions 60/40 to 50/50. The second reason is that the filling is now very much more fluid and the RDX tends to segregate, and zonal examination of the segregated filling shows that the settling is not symmetrical and the case may arise where there may be for example a zone of 65/35 RDX/TNT on one side of the charge with perhaps 55/45 RDX/TNT on the other side at the same level. The manufacture of RDX/TNT must be pursued in the zone of physical chemistry.

Rotation

The problem of compensating for the effects of rotation on the performance of the hollow charge jet has proved to be very troublesome. One of the first difficulties is to ascertain what exactly is the mechanism by which the jet is perturbed. Quite simply, it may be due to tangential velocity effects during cone collapse or it may be due entirely or in part to centrifugal effects acting against the forces causing collapse as visualised by Schumann. The former effect seems to be unlikely if the collapsing liner is conceived to be coherent. But in either of these cases the effect of rotation is to prevent the complete formation of the jet by reducing the forces causing collapse.

The other mechanism by which the jet may be perturbed after formation is by centrifugal spreading due to the conserved angular momentum. Shell trials against homogeneous armour, and armour protected by a thin (1/4 inch) skirting plate at 5 inches distance suggest from the obvious instability of the jet that this effect at least is operating.

With regard to compensation it is considered that with the wealth of experience which has been gathered in the last few years on the fluted cone it would be unprofitable for us in Great Britain to enter this field on the research side. But we are not satisfied that the last word has been said on behalf of the cylindrical liner. This type of liner has obvious advantages if it can be made to work efficiently, the chief of which is that it will have a smaller angular momentum, and it might be possible to use it in practice without compensation.

There is obviously quite a big field of work on the unrotated cylindrical liner before any rotation work is begun. There are many obvious theoretical difficulties, but it is intended as soon as possible to survey the ground with a view to increasing the collapse forces while delaying the collapse process by suitable shaping of the detonation wave and adjustment of the thickness of the cylindrical liner.

Weapon Design

The endeavour of our designers is mainly concentrated on obtaining a high level of performance at large angles of incidence. The electric nose switch developed by the

Design Establishment has established that functioning can be obtained up to angles of 60° from normal with the rocket head at striking velocities of the order of 700 ft/sec. It is hoped that with introduction of the new A.R.E. detonator which will function with very small delay when actuated by a very low current, a performance comparable with that obtained statically will be possible at high angle of incidence and high rate of striking.

Trials with an electric switch in shell have shown that some re-design may be necessary in order to get good results.

2. Squash Head

The squash head shell has developed on very different lines from the hollow charge. It has been very largely a matter of empirical development without any pure research. As a consequency a great many trials have been carried out and it is often quite diffi-cult if not impossible to correlate them.

The principle is firmly established that a thin walled shell filled with a plastic or semi-plastic H.E. filling and fitted with a fuze with a small delay will under certain conditions release a 'scab' from the back of the plate on detonation.

It has been assumed that during the short time of delay between the impact of the shell on the plate and the functioning of the fuze that the thin nose of the shell is squashed out on to the plate giving a fairly close contact between a comparatively large section of the plate and the H.E. filling.

Kine camera records have been taken of the impact of shell on plates but the actual mechanism of collapse and spreading is to a large extent obscured by flash, smoke and debris.

This type of shell works reasonably well at low velocities of impact up to about 1500 ft/sec and at angles from normal up to about 60° from normal.

At higher velocities a general deterioration in performance takes place especially at angles near normal.

At higher velocities still, a poor performance is marked at angles from normal up to 30° and again at larger angles of the order 50° to 60°. This poor performance appears to be associated with premature detonation or explosion of the H.E. filling by impact shock.

This study of this phenomenon is the major investigation on squash head shell at the present time.

It has already been remarked that our knowledge of the exact mechanism of squashing is extremely sparse and our knowledge of the behaviour of explosives under high rates of strain is very poor.

Apart from obvious weakness in design of many squash head shell, there are several possibilities for the cause of this premature detonation. They will be listed: -

1) Aeration of the filling leading to detonation by adiabatic compression on impact.

2) Heat of deformation of case leading to ignition of the filling.

3) Heat generated by the shock wave running back into the filling.

The subject of (1) is under investigation and the scope of the investigation is to extract the air from the plastic explosive in a vacuum incorporator and then to fill by extrusion into an evacuated shell. It is thought that this is a practical proposition and a pilot plant is being constructed.

Under (2) it is proposed to line the shell, more especially the nose, with an inert material which will absorb or delay the transmission of heat to the high explosive. Trials of this nature have not yet been carried out.

The heat generated by the shock (3) is thought to be the most likely cause of premature ignition or detonation.

From the theoretical side some calculations have been carried out by Thornhill in the A.R.E. on the possible shock temperatures in the filling at different striking velocities. This calculation can only be very approximate because the equation of state of plastic explosive is entirely unknown and it was necessary to assume data by analogy with certain organic compound for which data is available.

It is clear from these results, without ascribing any accuracy to the actual temperatures involved, that at higher striking velocities the shock temperature rises very sharply and from this point of view it is obvious that there is a maximum striking velocity beyond which it is impossible to go.

Again using the actual temperatures which Thornhill obtained and combining them with the heat of formation of R.D.X. the time of survival of the explosive and different striking velocities was obtained. It happens that between 2000 ft/sec and 2500 ft/sec striking velocity the time of survival works out at 1 millisecond and 1 microsecond respectively. It is not claimed that this agreement with practice is anything more than fortuitous but it does demonstrate that there is a limiting velocity at striking.

Attempts to damp out this shock wave have been made and suggested. The simplest is to fill a quantity of inert plastic in the nose of the shell. This has been tried out in the new 120mm and gave some successful shots at 2400 ft/sec. This result needs confirmation with a large number of shots. A suggestion by Thornhill was to encourage streamline flow of the plastic H.E. by putting in the nose of the shell along the axis a streamlined plug.

Another problem which has not yet been resolved is the filling of squash head shell. There are two possible fillings, Plastic Explosive and pourable RDX/Paraffin Wax. Owing to the design of the British squash head shell it is difficult to fill with Plastic Explosive except by hand stemming. The competitive pourable RDX/Paraffin Wax is not always pourable without trouble and there are varying reports that it is not so efficient in bringing off a 'scab' as P.E.

Research on the mechanism of squashing is now being studied photographically on the small scale and it is hoped that the results of these studies will assist in designing a more efficient shell, the problem being to get the largest spread of H.E. in the shortest possible time at all angles of attack.

HELLER WARHEAD DEVELOPMENT*

R. W. Foster

Canadian Armament Research and Development Establishment, Valcartier, Quebec

1. INTRODUCTION

The Heller is a platoon anti-tank weapon of 3.2 inch or 81-mm calibre undergoing final engineering trials. Canadian User trials are expected to take place in December 1951. The rocket burns all propellant within the launching tube so that it is non-propulsive during flight. This method was chosen as it provides more regular external ballistics than the orthodox rocket which may burn and provide thrust after launching.

The rocket is fin-stabilized with a chamfer on the leading edge of the fins which imparts a slow spin in the launcher to compensate mis-alignment or dissymetry obtained in manufacture. (Fig. 1).

The shaped charge warhead is initiated by a spit-back fuze. However, it is intended to replace this at a later date by an electric fuze under development.

2. WARHEAD DESIGN

2.1 The Copper Cone Liner

When the design of the warhead was first considered, it was decided to use a copper cone liner with a solid angle of 42°. The warhead was filled with RDX/TNT 60/40. These decisions were made on the basis of work on shaped charges in other countries. An independent investigation into these variables would have involved more work than C.A.R.D.E. could complete within a reasonable length of time.

Tools were designed and manufactured for producing the copper cone liner, and 300 warheads were manufactured for full-scale static penetration trials. These penetration trials were fired to find the optimum stand-off and cone liner thickness for the shaped charge. For stand-off, suitable wood stands were used to give a range of stand-offs from 1.5 cone diameters to 2.25 cone diameters. The range of cone thicknesses was obtained by pressing cones of .09 inches wall thickness and machining the outside surface of the cone. In this way, wall thicknesses from .05 to .09 inches were obtained. (Fig. 2)

Briefly, the results from these first trials showed that the optimum stand-off was 1.75 cone diameters and the wall thickness should be greater than .09 inch.

A new set of tools was then made to produce cones up to .125 inches wall thickness and it was possible to fire trials with cone thickness of .100, .115 and .125 inches, again machining the outside surface as required - (Fig. 3). Penetration decreased with these greater thicknesses and it was decided from the curve of penetration versus cone wall thickness that .095 should be the thickness for the cone.

---

* Project S/N-17-1; Reference N-17-1; Tech. Letter N-17-1-5.

Figure 1—Heller Round.

226
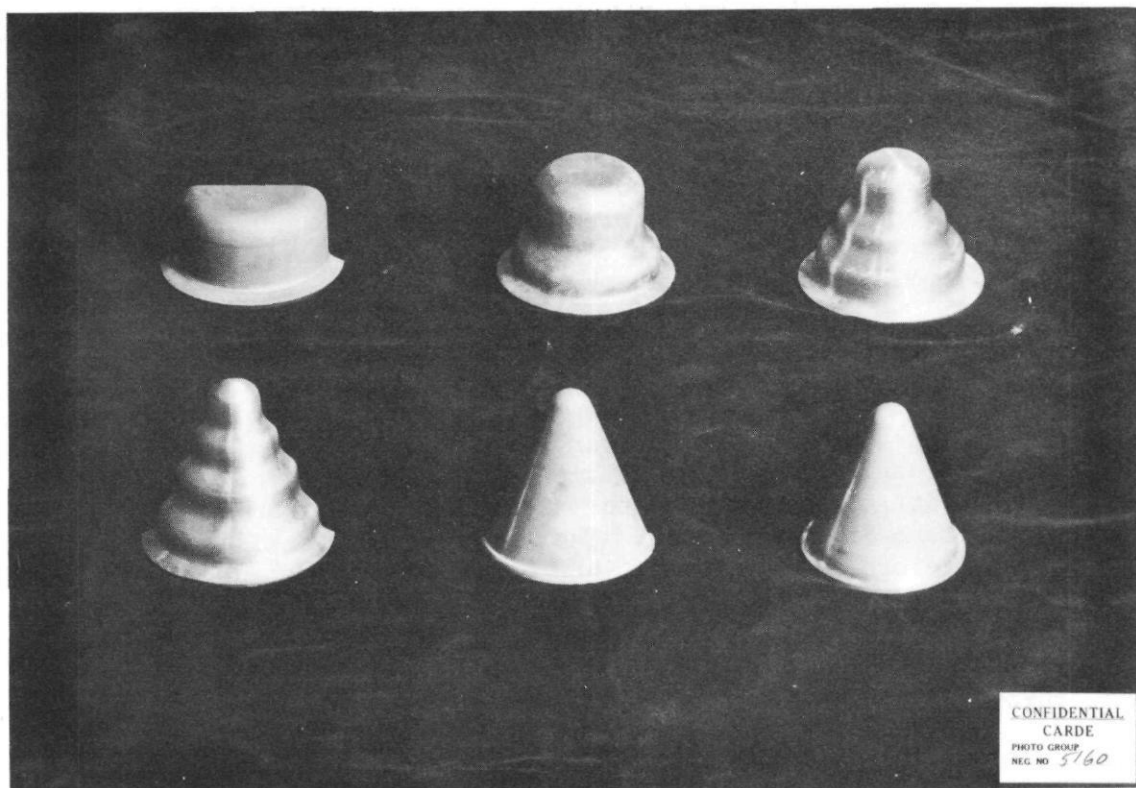
Figure 2—Cone Liner.
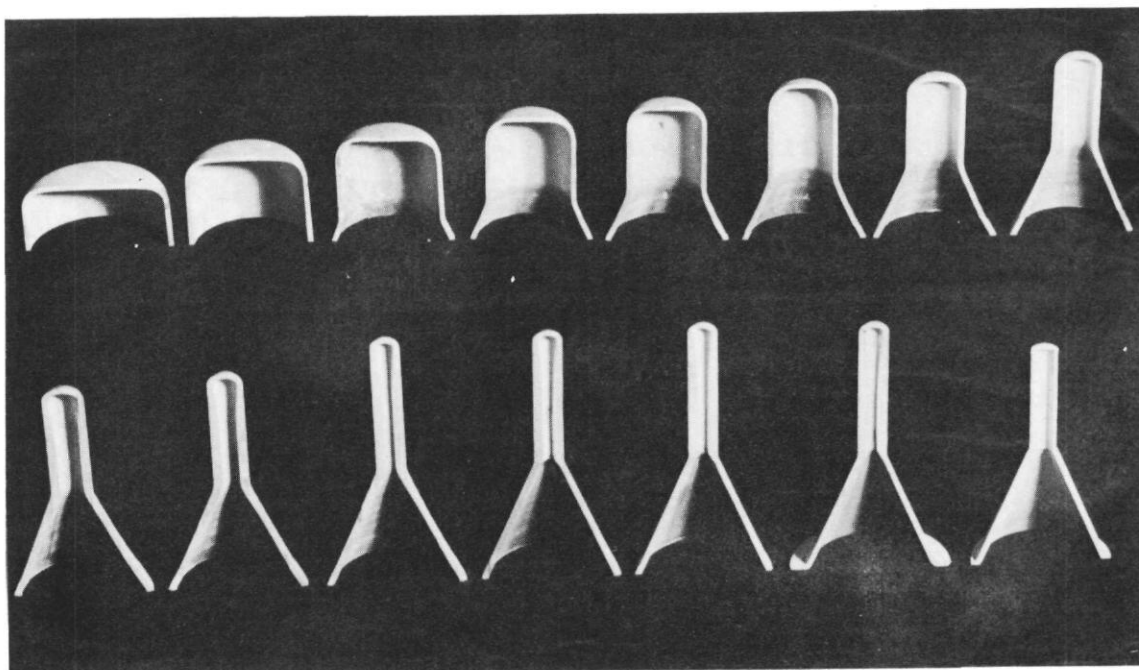
Figure 3—Cone Liner.

However, considerable difficulties have been encountered with the cones manufactured from the second set of tools. The tools are simple in design and use unguided punches. The cones are drawn in 11 operations and two ironing operations instead of four operations and two ironing operations used with out first set of tools. The new tools produced cones with better control over metal flow but it was difficult to keep the inside surface of the cone concentric with the outside. The variation in wall thickness around any circumference of some cones was as much as .005 of an inch. It was found that this type of variation caused an unacceptable degradation in penetrative performance and a considerable number of double jets were formed.

Tools are at present being designed at C.A.R.D.E. to produce cones to tolerances which are considered to be necessary from trial results. The wall thickness will be .095 ± .005 but within this range, the wall thickness must not vary more than .0015 around any circumference. They must not vary more than .005 along the slant surface. Hardness of the inside surface must be between 70 and 75 on the Rockwell 15T scale. Runout of the cone flange with respect to the longitudinal axis must not exceed .002 as this locates the cone in the warhead. The temperature and time of the final annealing treatment before ironing operations have not yet been decided; it is believed that a temperature between 500°F. to 600°F. for one hour will be suitable. This should give a uniform grain size from cone to cone.

2.2 WARHEAD CASING

The warhead casing material is SAE 4130 steel heat treated to give 30-32 on the Rockwell C Scale. It varies in wall thickness from .115 to .160.

Two types of warhead have been used for static trials. The first type (Fig. 4A) is 7 inches in length and has a parallel section of .16 inches at the front end. However, in flight trials the warhead (Fig. 4B) was found to have a better ballistic shape and was much easier to load into the launcher. The warhead with the parallel front section had a tendency to jam during loading in the launcher unless the rocket was very carefully aligned by the loader.

Static penetration trials were carried out with the warhead design as shown in Fig. 4B, and it was found that penetration had improved about 15% although the H.E. content had been reduced from 1 pound 6 ounces to 1 pound 1 ounce. It is believed that this increase in penetration is due to the length between apex of the cone and the exploder pellet approaching the optimum length for this warhead design. This variable is being investigated by firing trials but they will not be completed in time to affect the present design.

3. FILLING

The use of a low viscosity RDX/TNT 60/40 has eliminated much of the trouble from entrapped air and shrinkage originally encountered when the standard filling was used.

The following steps are used for the present method of filling: -

(a) The warhead is filled to just below the required height of filling with low viscosity RDX/TNT 60/40 which is poured at a temperature of 85°C.
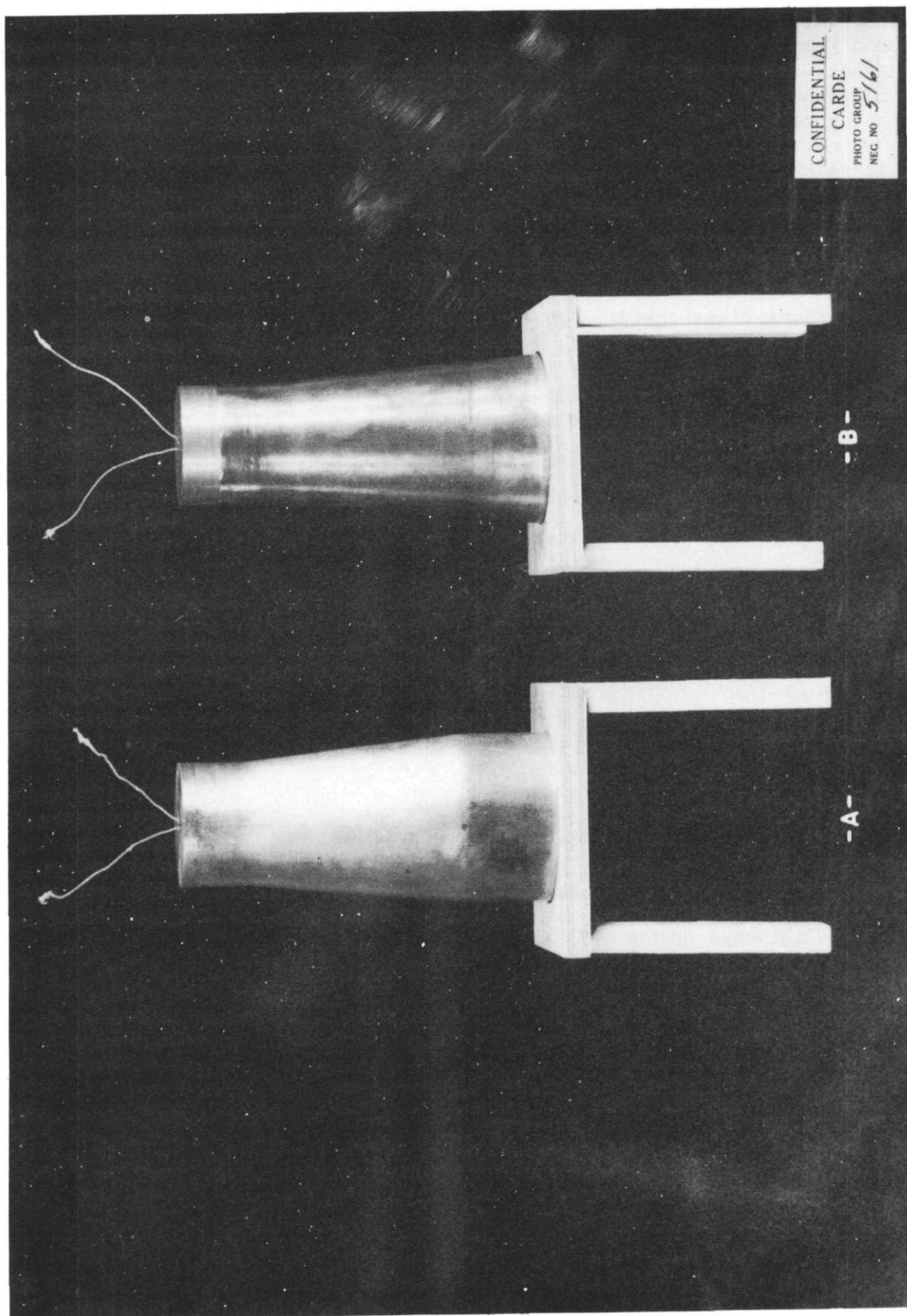
Figure 4—Warheads.

(b) A special riser is preheated to 95°C and is set onto the neck of the war-head. This riser is filled with H.E.

(c) A heat insulating cardboard cover is then placed over the riser and the whole assembly is set aside to cool for 3/4 of an hour.

(d) As the filling cools, shrinkage cavities are prevented from forming by the molten H.E. in the riser. When the filling has solidified the riser is removed by inserting a bar through holes in the upper riser wall and giving a sharp twise. This breaks the filling and allows the riser to be removed.

The special riser consists of a hollow aluminum cylinder having a thin per-forated base. The height of the filling is controlled by the depth to which the riser is allowed to set into the warhead. By this method, the height of filling is controlled by riser design and no scraping of the filling surface is required. The method has given perfect fillings in 95% of the warheads filled.

High and low viscosity RDX/TNT 60/40 have been compared in penetration trials but there was no difference in performance.

Trials have also been fired to compare 50/50 and 70/30 with the 60/40 RDX/TNT. These trials have shown 60/40 to be the most suitable for the present design of warhead.

4. STAND-OFF

The static penetration trials have shown that the optimum stand-off for the warhead is approximately 1.75 cone diameters. The ballistic cap and fuze provide a stand-off of 2 cone diameters; with a fuze functioning time of between 50 to 60 micro-seconds, the effective stand-off after fuze functioning is very close to 1.75.

5. FUZING

A modified American M52 fuze for the rocket is used.

The modifications consist of: -

(a) An all ways mechanism, which will work up to 70° from normal, to replace the original striker.

(b) A spit back charge liner and housing to replace the booster magazine.

This fuze has functioned extremely well in all firings to date.

An electric fuze is also under development and it is hoped to hold the first firing trials with this fuze within the next two or three weeks. A few warheads have been fired statically with a mock-up of the electric fuze to check the functioning of the detonation train and this has been satisfactory.
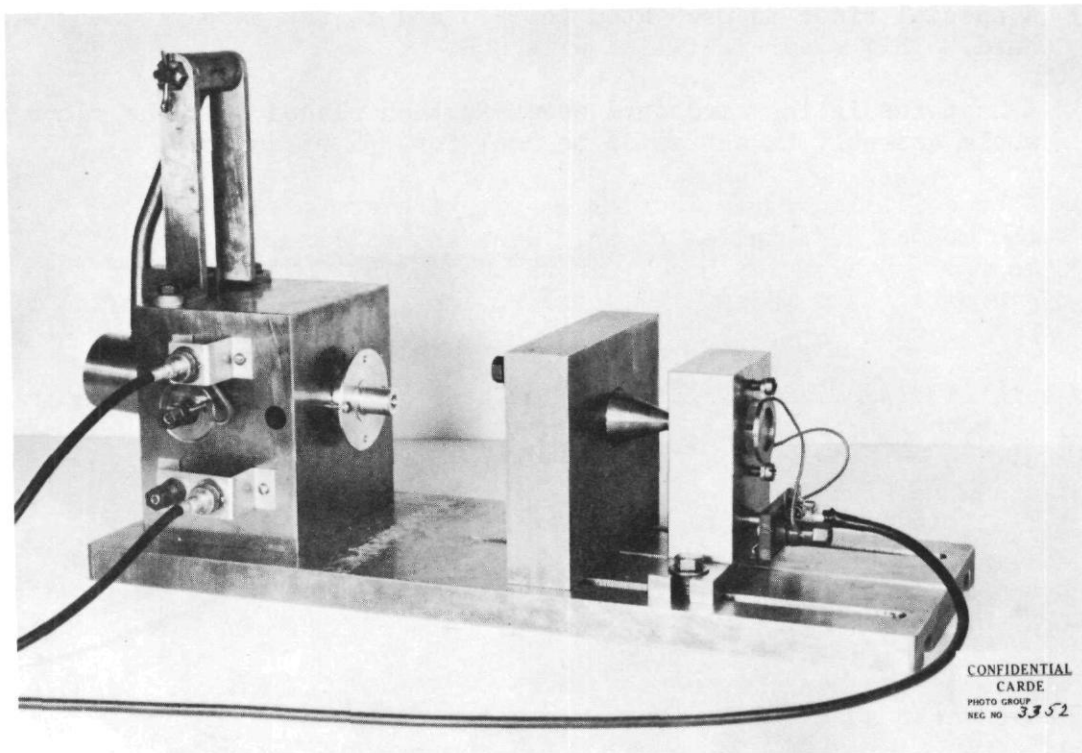
Figure 5—Test Fixture.
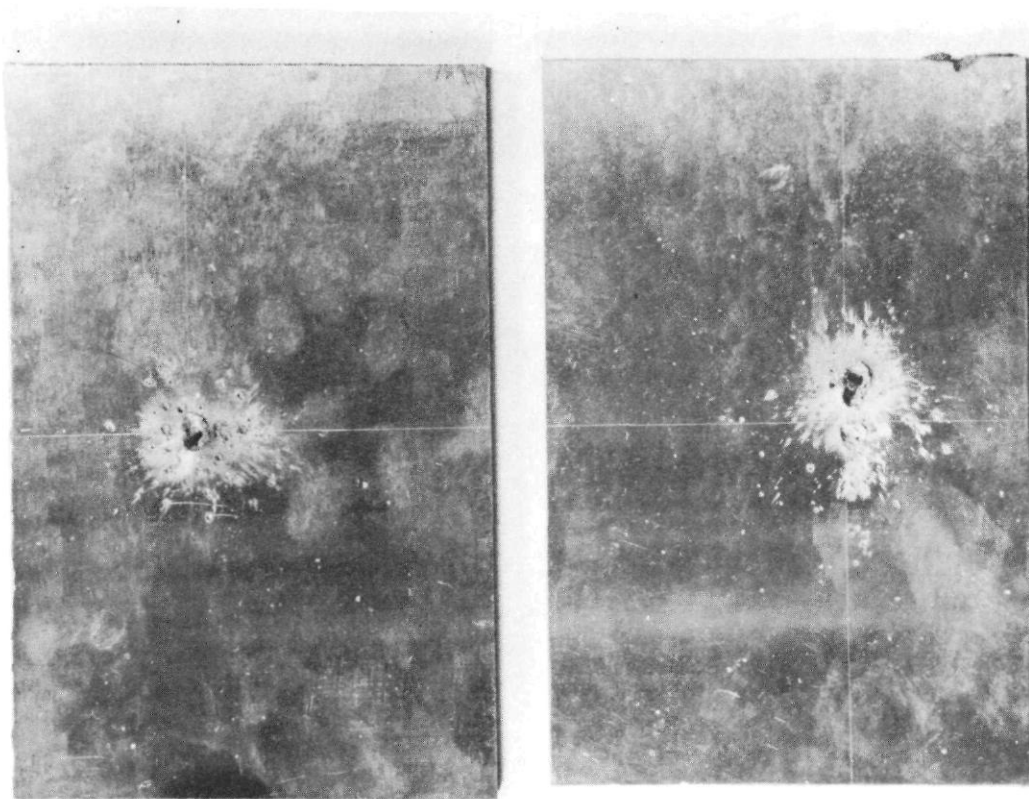
Figure 6—Target plate for Spit-back Fuze.

231
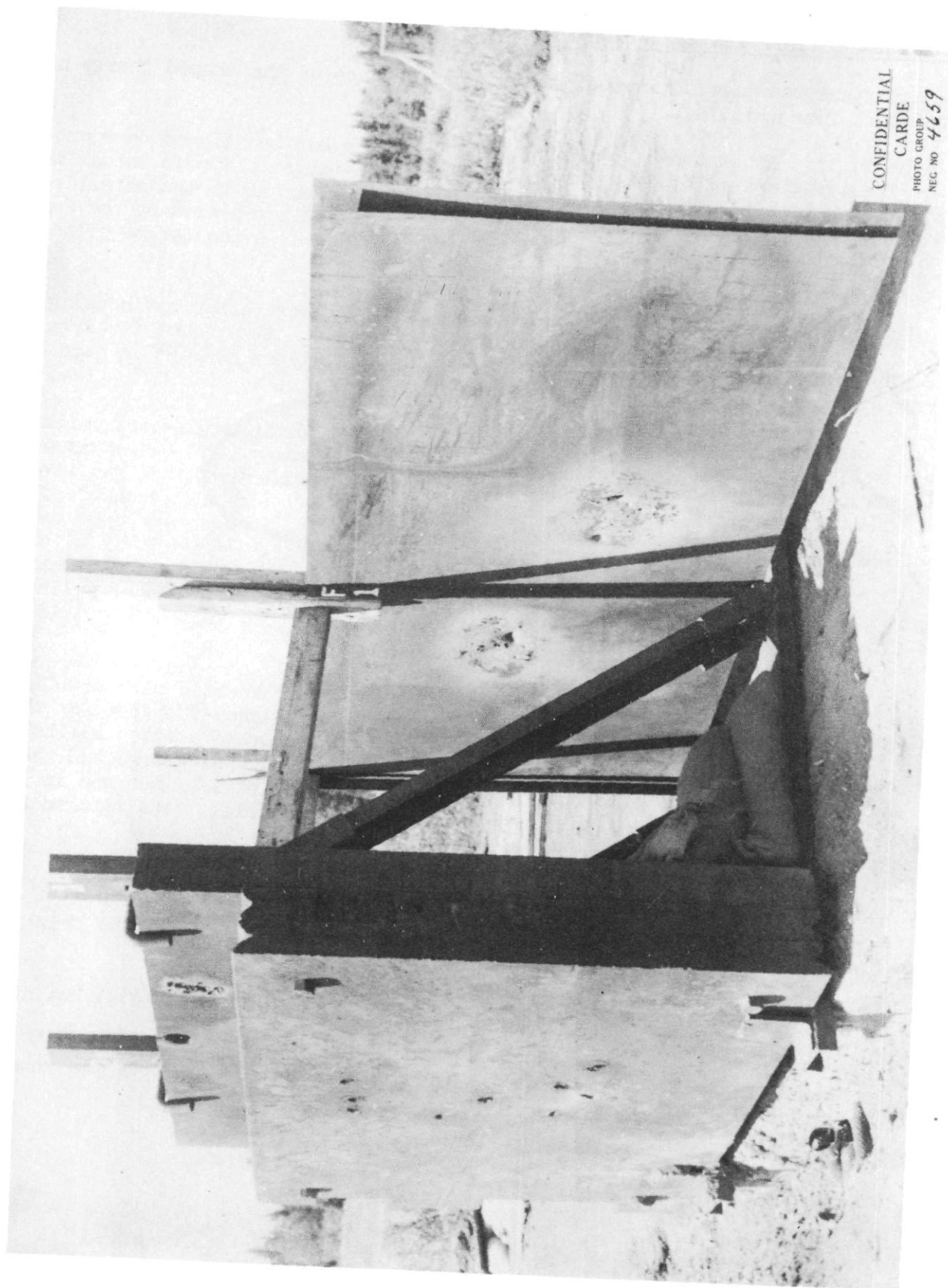
Figure 7—280 mm Target.

6. SHAPED CHARGE LINER FOR SPIT-BACK FUZE

A fixture was made to investigate the performance of the shaped charge used in the spitback fuze (Fig. 5).

The fixture is arranged so that the charge liner can be aligned on a cross scribed on the target plate of 1/4 inch mild steel. The target plate is set at the same distance from the spit-back pellet as the exploder pellet is in the actual round. (Approximately 7-1/2 inches.) The efficiency of the charge is assessed by the damage caused to the target plate and by the distance from the cross on the target plate to the jet centre. (Fig. 6.)

From these trials, materials and shapes for the charge liner and housing, and methods of filling the charge liner can be investigated. At present a charge liner of aluminum with hemispherical shape fitted in an aluminum housing is used but this may be changed if other types prove more suitable.

It was noticed during these trials that the jet from the spit-back pellet did not always strike the cross on the target plate. Under actual conditions, this would result in off centre initiation of the shaped charge. The effect of this was investigated in penetration trials by placing the detonator 1/4 inch off-centre and results showed that penetration was decreased 30%.

To reduce this possibility of off-centre initiation it is proposed to use a cone liner stem with tapered bore, the diameter of the bore at the exploder pellet to be .25 to .3 inches. With this design, any mal-alignment of the spit-back jet is corrected and the C.E. exploder pellet initiated on centre.

The guiding properties of the tapered bore have been checked with the fixture used for trials with the small shaped charge liners. A small shaped charge for the spit-back fuze was mounted in the fixture and aligned on the cross scribed on the target plate. A copper cone liner was then mounted between the shaped charge and the target plate with the stem of this cone liner aligned on a point 1/4 inch and in later trials 1/2 inch from the cross on the target plate. In both trials, the tapered stem iid deflect the jet from the spit-back pellet.

SUMMARY OF TRIALS

The Heller warhead is 3.2 inches calibre and in static penetration trials has given 13 inches penetration in homo armour plate.

In flight trials against 280mm of armour at normal angle of attack 80% of the rounds fired have defeated the armour.

In flight trials against 120mm of armour at 60° to normal 80% of the round fired have been successful.

233

CURRENT PROGRAM ON HEAT AND HEP ARTILLERY PROJECTILES

Lt. Col. R. E. Rayle

Office, Chief of Ordnance, Washington, D. C.

ABSTRACT

The current program for fin-stabilized HEAT artillery projectiles is discussed. Status of development is given in each of the various calibers. Principal development has been in 90mm and 105mm sizes, and developments in these calibers are being extended to other sizes. Highlights of these developments are discussed, including the electric fuze, the effect of standoff and slow spin, and the effect of cone variables on penetration. A definition of K factor as employed in a recent tripartite conference is given. A K factor of 4 appears descriptive of current HEAT rounds. Accuracy of fin-stabilized HEAT rounds is discussed. The accuracy appears to be about .35 mil horizontal or vertical probable error, compared to about .15 for spin-stabilized projectiles.

The current program for HEP shell is discussed. A number of designs have been released for production in 75mm, 76mm, 90mm and 105mm sizes. Principal development has been in 75mm and 105mm sizes. Most significant recent improvements are use of one-piece type shell construction, and use of a new plastic filler. An electric fuze is under development, which should further improve performance. Present HEP shell are shown to be capable of defeating about 1.3 calibers of plate, regardless of obliquity, at velocities up to 2600 fps.

1. HEAT Projectiles

    a. Introduction

        The current program on HEAT fin-stabilized artillery projectiles will provide rounds for recoilless rifles in 57mm, 75mm, 90mm and 105mm sizes, for tank guns in 76mm, 90mm, and 120mm sizes, for howitzers in 75mm and 105mm sizes. Programs for the immediate future will cover such rounds for 105mm and 155mm tank guns and for 110mm howitzers.

        The principal development efforts during the past two years have been on the 90mm T108 round for tank guns, the 105mm recoilless rifle rounds under the BAT program, and the 105mm T131 round for the standard howitzers. From these programs, a number of features which either improve accuracy or penetration, or which permit simpler fabrication have been determined, and are being applied across the board to other rounds wherever possible.
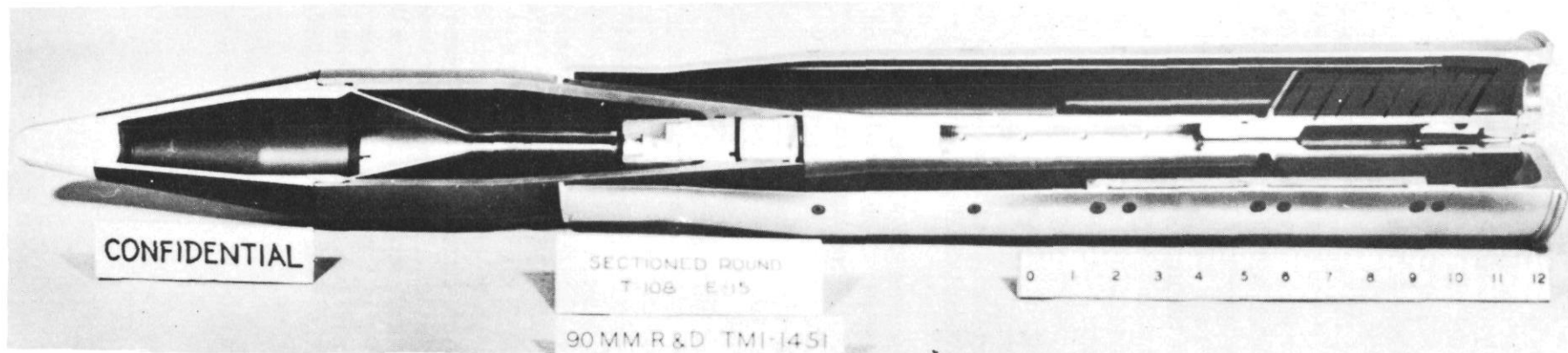
Figure 1—Sectioned round, T-108, E-15, 90 MM R&D TM1-1451.
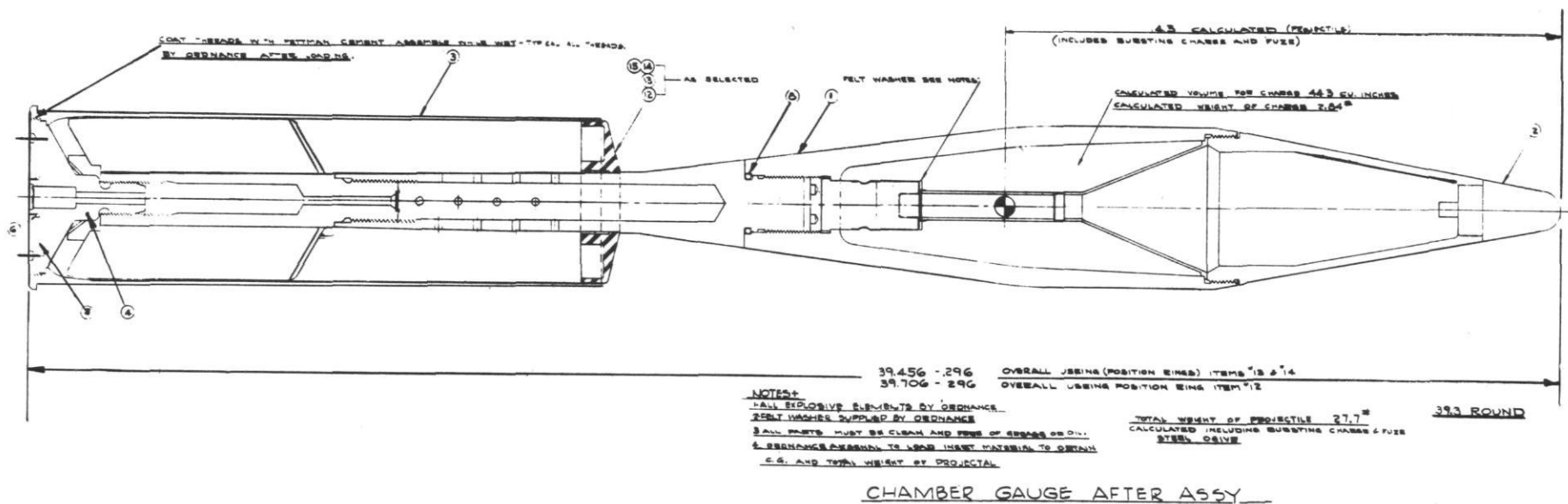
Figure 2—Flight test round, 105 MM HEAT TM1-1526.

The Figures illustrate a few typical new HEAT rounds.

First, Figure 1 shows the fin-stabilized, 90mm, T108 HEAT round for tank guns. Note the long boom extending back into the case, the guide rails in the case, the shot-pull device. Several thousand of these spit-back fuzed 90mm T108 rounds are now in field service stocks. Production is currently being switched over to electric fused rounds. Next, in Figure 2 is the 105mm T131 FS HEAT round for howitzers. Note the boom extending beyond the case. Production of the 105mm T131 round for howitzers will begin in December at the rate of 5000 per month. No BAT rounds have yet been released for procurement, but substantial R&D quantities are on order, including 5000 105mm T184 rounds and 3000 T118 rounds which are similar in general to the 90mm T108 round, and 1000 105mm T138 potato-masher shaped rounds for the Firestone BAT weapon. The latter is the only HEAT round of current development being procured in substantial R&D quantities, which is not fin-stabilized. Figure 3 is a drawing of this shell. The T138 spins slowly at about 25 rps, and is stabilized through its unusual nose shape.

b. Penetration of HEAT rounds

(1) Fuzing

Under the 90mm T108 program, an electric fuze has been developed which, due to its fast and more reliable action, is replacing the spit-back nose fuze. The time of functioning, from first nose contact to jet reaching the plate is of the order of 60 microseconds compared to about 120 microseconds for the spit-back fuze. The electric fuze has the added advantage of simplicity (the fuze being essentially a crystal in the nose which generates its own current on impact), the ability to function properly up to 71 degrees, and by use of inner and outer ogives, a more difficult fuze to defeat by such devices as spikes and angle irons.

(2) Stand-off

Tests in 90mm and 105mm sizes have indicated optimum stand-off occurs at 4 to 5 cone-diameters. Built in stand-off for most of the current rounds is 2 to 3 cone diameters, and in this region, about 3/4" in penetration is gained for every inch increase in stand-off for 90mm and 105mm rounds. Figure 4 is a curve showing penetration vs. stand-off for 105mm BAT rounds. The lower curve here illustrates the fact that cones with a simple conical apex have less penetration than with a spit-back tube. This result has been obtained in both 90mm and 105mm sizes. The first electric-fuzed 90mm T108 round employed a cone located deeper in the shell body at about 2.8 cone diameters stand-off, instead of 2.4 as used in the spit-back type. The penetration increased from about 9" to about 12" for this 3" cone when electric fuzed. Of this 3" improvement, about 2" can be attributed to increased stand-off due to faster action of the electric fuze and about 1" to the increased built-in stand-off. Recent static 3.5" rocket tests have shown that the explosive behind the cone can be considerably reduced without significantly degrading penetration where constant stand-off was used, indicating cones should be as far back in the shell as practical.
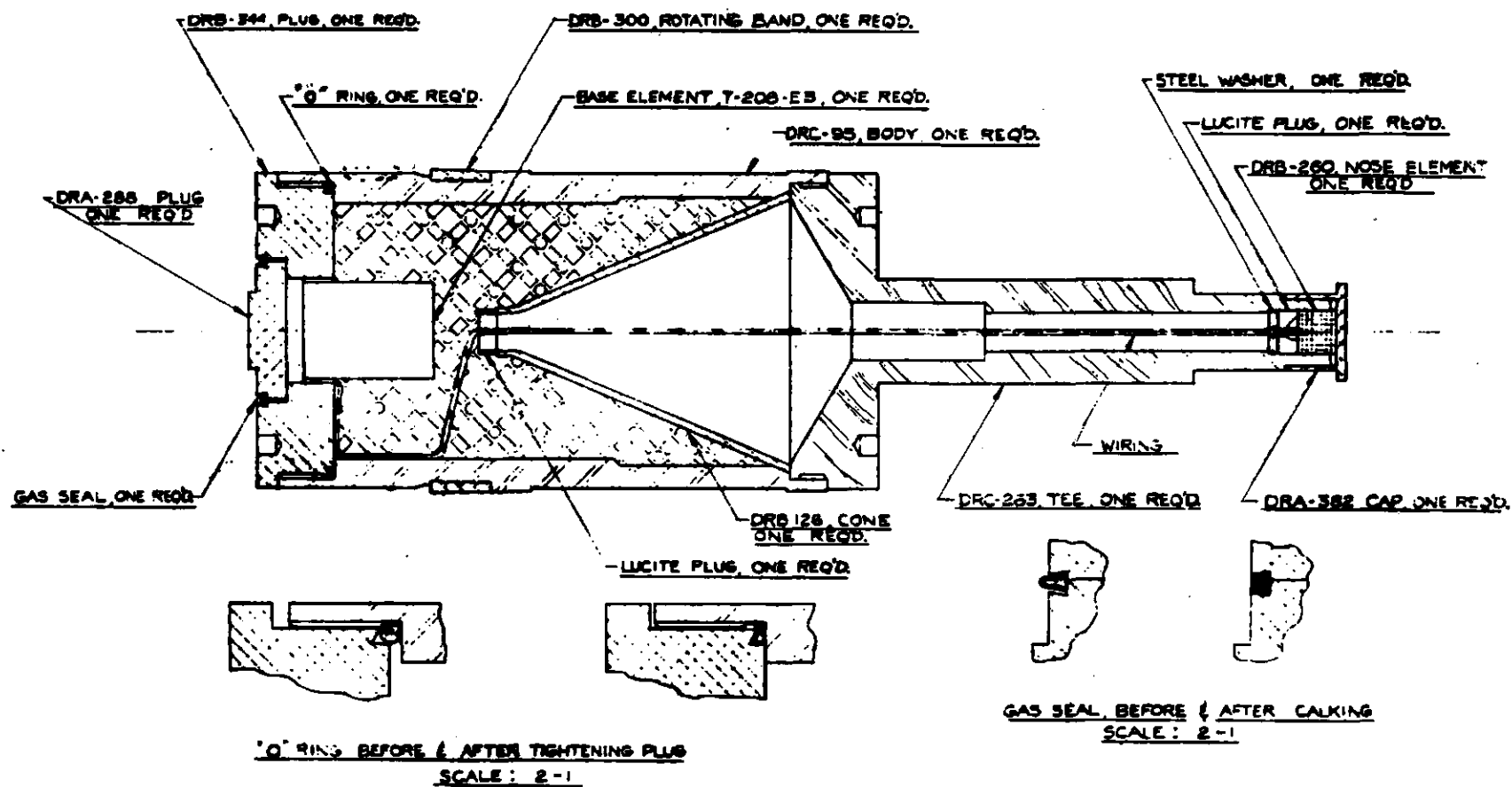
Figure 3—Assembly T-138 Projectile for initial trial firing.

STANDOFF VS PENETRATION
105MM T 138 CONE-.100 INCH WALL
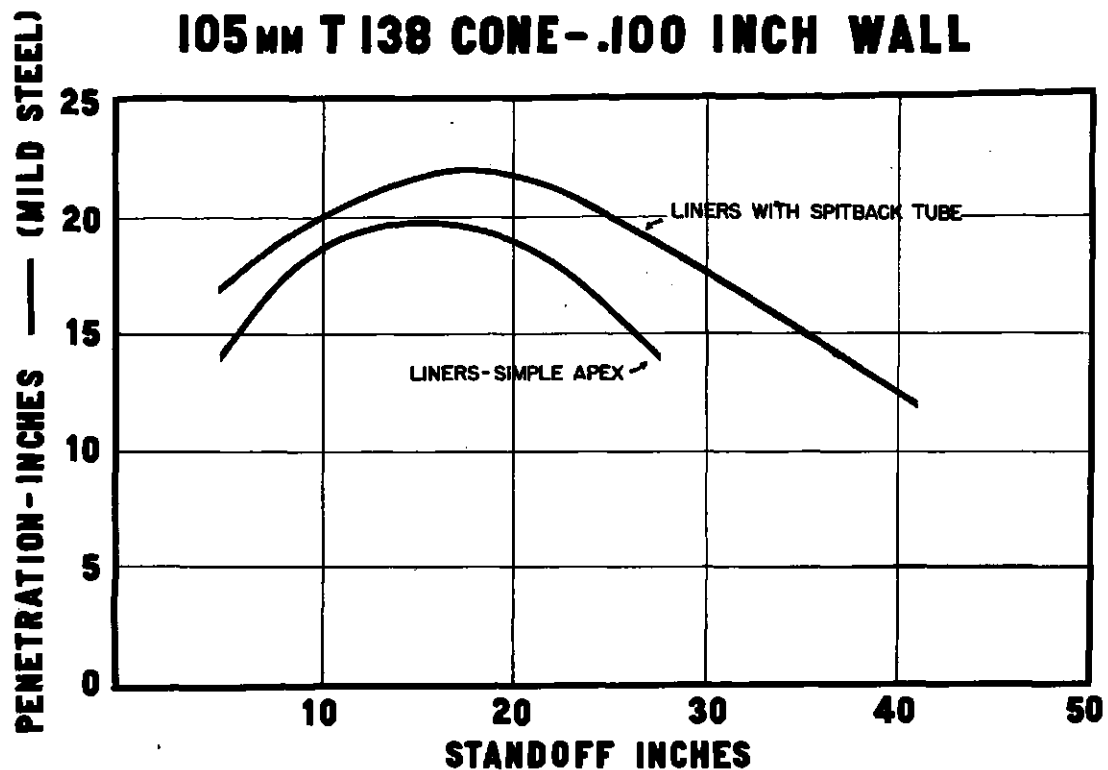
Figure 4—Standoff vs. Penetration, 105 MM T-138 Cone—.100 inch wall.

SPIN RATE VS PENETRATION
105MM T138 CONE -.100 INCH WALL
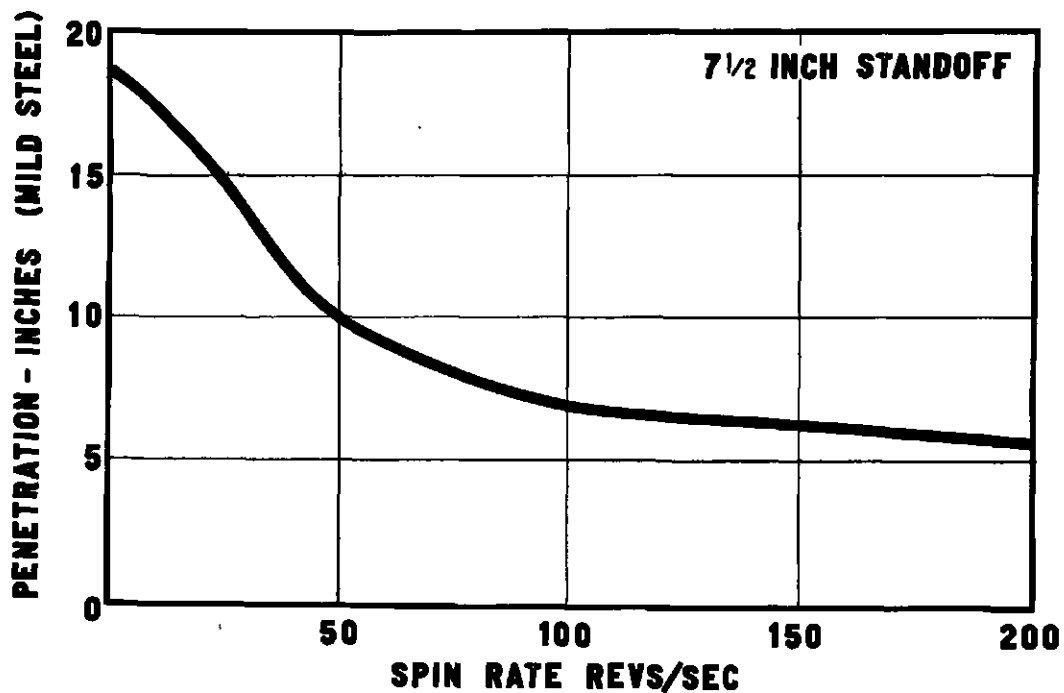
Figure 5—Spin rate vs. Penetration, 105 MM T-138 Cone—.100 inch wall.

ACCURACY FIRINGS OF SHELL HEAT-FS 90MM T108

(2800 FPS - 1000 YDS)

SUPERIMPOSED ON T34 TANK

EFFECT OF CONE VARIABLES OF 90mm HEAT

RS-5 CONE .010 TRANSVERSE BODY EII STD VARIATION

RS-6 CONE .010 WALL WAVINESS BODY EII STD

REFERENCE ACCURATE CONES (88 ROUNDS)

NOTE: ARMOR PLATE -2 CONE DIAMETERS STAND OFF

RS-6

RS-5

PERCENT OF ROUNDS FIRED

PENETRATION INCHES

10 FT

Figure 6—Effect of cone variables
of 90 MM HEAT.

Figure 7—Accuracy firings of shell
HEAT-FS 90 MM T-108.

(3) Rotation

Current fin-stabilized HEAT rounds rotate about 10 rps, this spin having been found necessary for best accuracy. The potato-masher shaped, 105mm T138 round previously shown, rotates about 25 rps. Figure 5 is a curve showing the effect of spin on penetration as determined for 105mm projectiles. It is noted that about 1" penetration is lost for 10 rps, 3" for 25 rps, and for 200 rps (as encountered in the M67 105mm standard rotated HEAT rounds), penetration drops from 18" to 6". The scaling law may be applied to these results by plotting penetration in cone diameters vs. V/N (instead of RPS = V/ND), but this scaling law is not accurate for moderate changes in scale. V is muzzle velocity, N is twist of rifling in calibers per turn.

(4) Cone Variables

A number of cone variables have been examined in 90mm and 105mm sizes, such as eccentricity, waviness, wall thickness, cone angle and other factors. Figure 6 is a curve showing the results of studies of cone variables of the 90mm T108 round. The data is plotted in terms of percent of rounds fired versus penetration in inches. For the 88 reference, accurately made cones, it is seen that 50% defeat 13-1/2", 90% defeat just under 12", at 2 cone-diameters stand-off, against armor plate. The lower curves show that 2" to 3" penetration is lost if wall thickness in a transverse plane varies .005, or if the exterior cone elements are sinusoidal waves of .010 amplitude. Similar curves, not shown here, indicated that other factors investigated did not appreciably degrade penetration, such as having thicker walls at top than bottom of cone, or having the shell cavity as forged, which resulted in a certain amount of ovality. Other tests in 105mm size have indicated that provision of a wide flat at the base of the cone is harmful, that the cone angle should be about 45°, and that the cone wall thickness should be about 3% of cone diameter. In the 105mm T131, various cone thicknesses have been tried, and penetration was 3" better with .100 inch walls than with .065 inch walls.

(5) K Factor

In a recent tripartite tank gun conference it was agreed that the K factor should be defined as that depth into homogeneous armor measured in cone diameters to which 90% of the rounds will penetrate, and that a K factor of 4 on this basis closely describes actual performance of current HEAT (FS) rounds. This does not allow for overmatch required to give full lethality, which appears to be about 2 inches, based on both U.S. and U.K. tests. Incidentally cone diameter is taken as the inside diameter at the base of the cone.

c. Accuracy

Spin-stabilized shell average about .15 mil horizontal and vertical probable error. A primary factor in development of fin-stabilized HEAT rounds has been the problem of achieving acceptable accuracy. It has been necessary to use high-alloy aluminum fins and booms, close tolerances, unshrouded tails and a slow spin (of the order of 10 rps) to achieve the current accuracy of about .35 mil horizontal and vertical probable error. Figure 7 shows a chart of the hits of a typical group of 90mm T108 rounds fired at 2800 fps against a vertical target at 1000 yds. The silhouette of

a Russian T34 tank is shown to provide a sense of the relative scale. A typical spin-stabilized projectile would show a little under half the spread obtained here but it is observed that all of the shots fall within the silhouette of the tank. A total of 239 T108 rounds fired have averaged .35 mil. Other tests involving shrouded fins, uncemented joints, and relaxed tolerances have shown poorer accuracy, and therefore such designs have been discarded. The first production lots averaged .42 mil. The latest production lot from a new manufacturer gave .20 mil for a 9 round group. Recoilless rifle HEAT rounds, including the potato-masher type T138, have average about 1/3 mil probable error. Smooth-bore firings of non-spinning rounds gave poor accuracy. If fins were canted enough to achieve accuracy, spin built up to over 50 rps at 1000 yds, reducing penetration. Hence, best results are achieved by obtaining about 10 rps at the muzzle by simply making use of friction between the projectile body and rifling within the bore. Use of full twist and depth of rifling appears satisfactory, and has the advantage of permitting the firing of cheaper, more accurate spin-stabilized HE and WP rounds. Loss of gases through the rifling around the projectile has little effect on tube life or muzzle velocity.

2. HEP Projectiles

    a. Introduction

        The HEP round is another armor defeating type which does not depend on kinetic energy to defeat the plate. The plate defeating ability of such a round depends on the use of a soft thin-walled nose containing a plastic explosive which is deformed on striking plate, to the general shape of the plate. In Figure 8 we have a diagram, somewhat exaggerated, showing its principle of operation in spalling the back side of the plate by means of a shock wave. A number of individuals have written papers covering the nature of the wave, and the distribution of pressure within the wave. Essentially, a compression wave is reflected as a tension wave strong enough to cause tensile failure.

        Over 100,000 105mm HEP shell have been produced. The basic shell was developed for howitzers; by splining the rotating band, it has been adapted to the standard 105mm recoilless rifle. HEP shell designs have also been released for procurement in 75mm size for rifle, howitzer and tank gun, in 76mm size for tank guns. Other development type HEP shell range in caliber from 57mm to 165mm.

        If the nose of a HEP shell strikes the plate at too high a velocity, shock detonation occurs, and the resulting explosion occurs before sufficient explosive is in contact with the plate, and the explosive wave moves away from the plate. Failure to spall is the net result. The HEP shell designer attempts to get a high-capacity shell by using walls as thin as set-back forces and stability calculations will permit. He chooses a powerful, plastic explosive, with as little impact sensitivity to shock as possible. He tries to select a base fuze which will set off the explosive wave after just the right amount of deformation, or squash. The delay time required is a function of striking velocity, plate obliquity and caliber. A new electric fuze utilizing a probe extending up toward the shell nose is now in the planning stage, which, if successful, should permit more nearly ideal fuze action. The length of probe will be adjusted to give optimum crush-up.

243

ACTION OF SQUASHHEAD PROJECTILE

DEFORMED SHELL

PLATE

FACIAL IMPRESSION

DIRECT SHOCK WAVE

REFLECTED SHOCK WAVE

BACKSPALLS
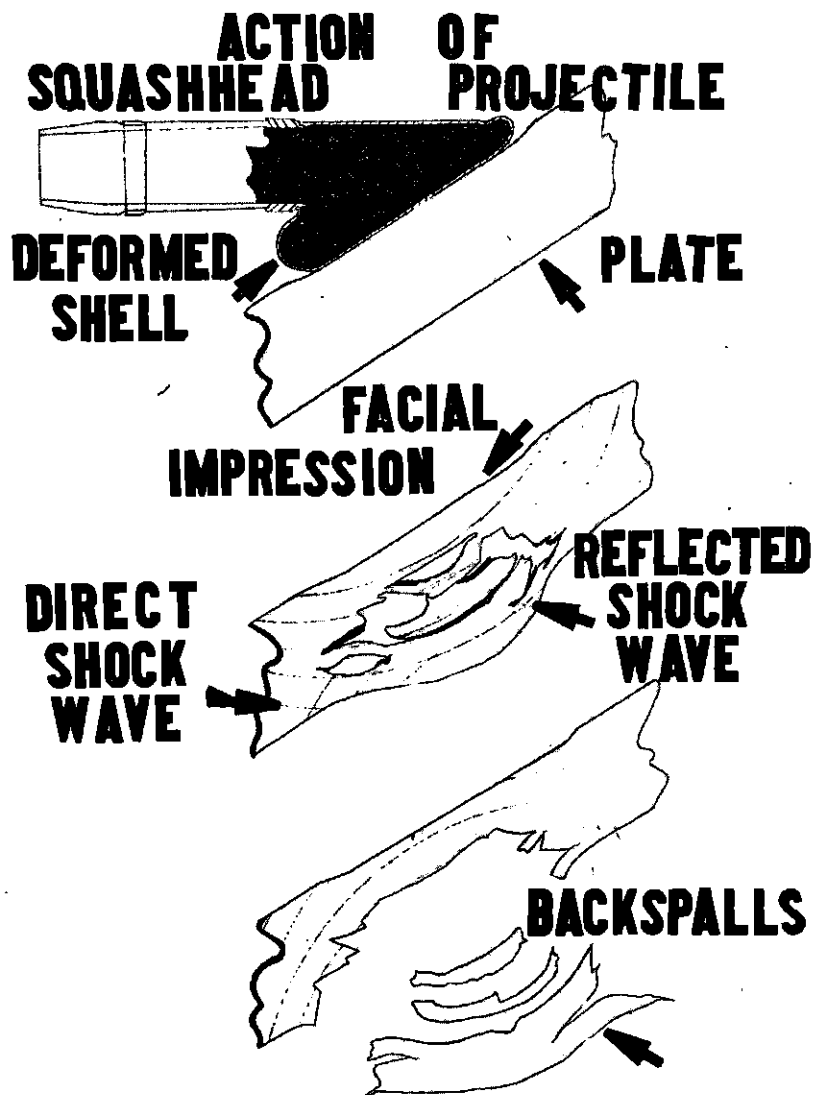
Figure 8—Action of squashhead projectile.

ARMOR PLATE DEFEATED BY HEP SHELL
(High Charpy, High Obliquity Plate)

SLOPE = t/d = 1.3

161 MM

180 MM

UPPER LIMIT

90% ASSURED SUCCESS

ARMOR DEFEATED (INS.) (t)

75mm 90mm 105mm 120mm

CALIBER (INS.) (d)
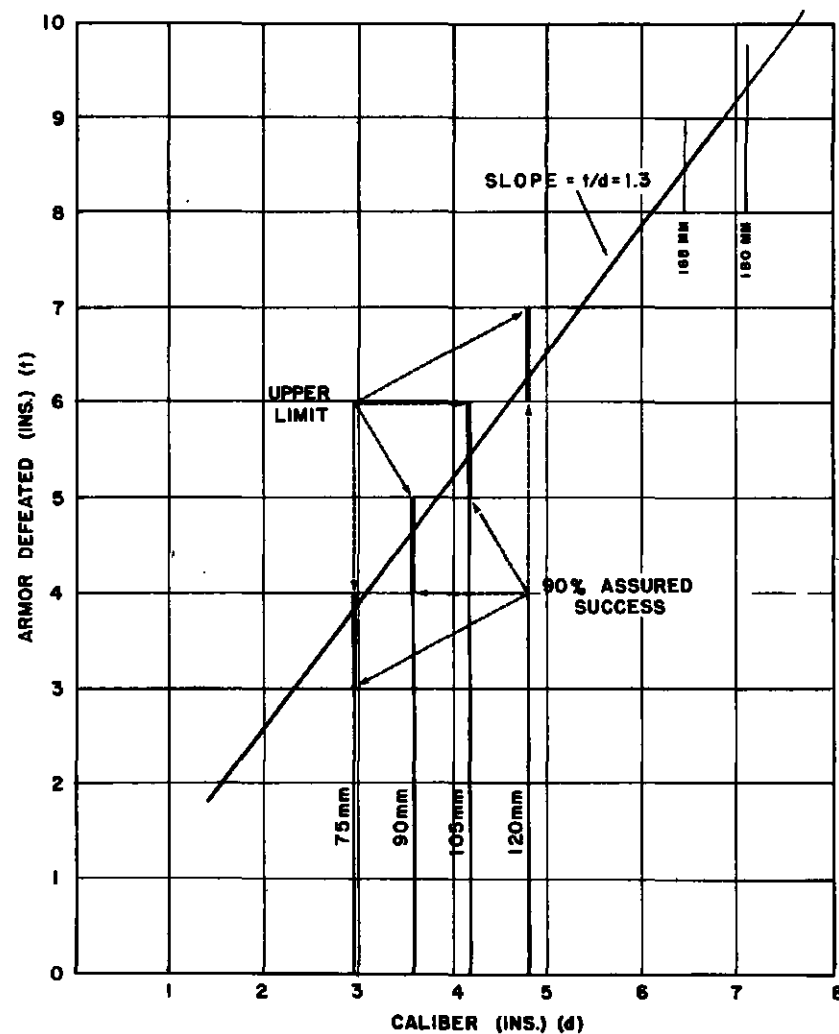
Figure 9—Armor plate defeated by HEP shell.
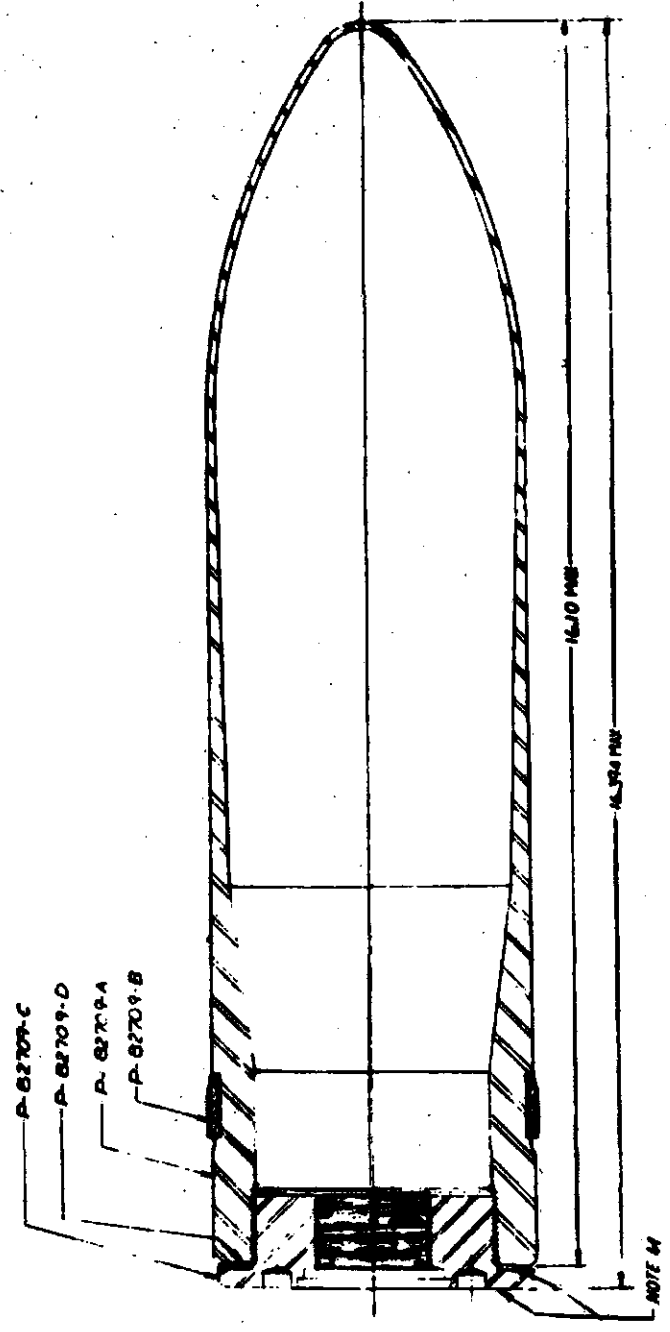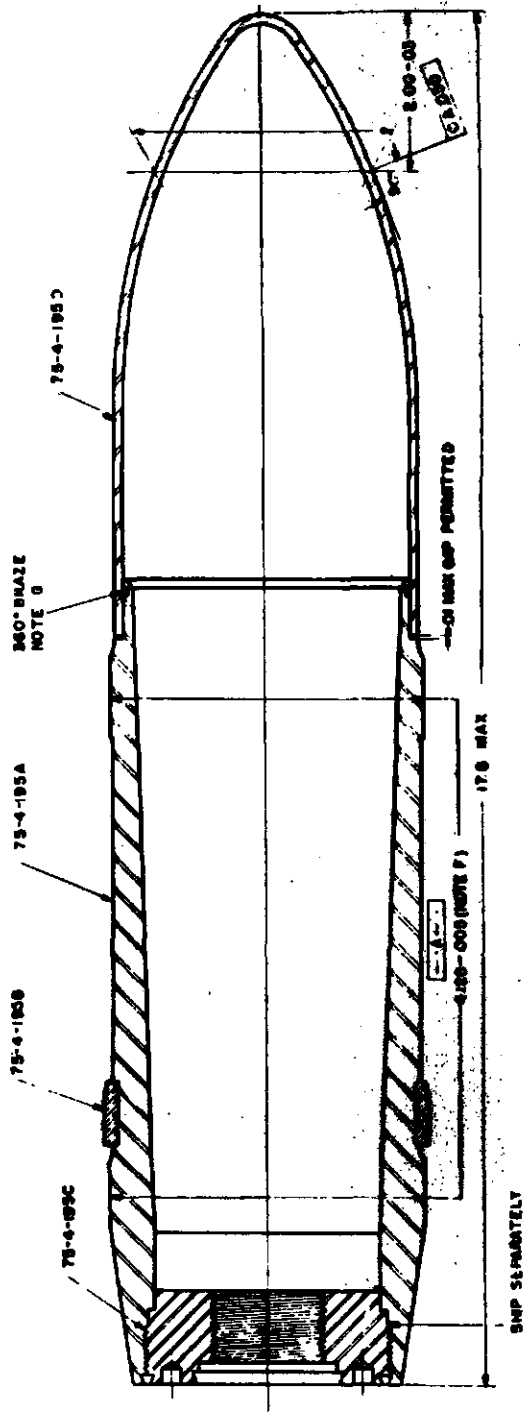
Figure 10

b. Plate Defeating Ability

Considerable experience has been obtained in four sizes, 75mm, 90mm, 105mm and 120mm. The performance of these rounds are plotted in Figure 9 against ability to defeat plate at high obliquity. The points are plotted as one-inch bands, based, for example, on the ability of the 105mm HEP to defeat 5" plate but not 6" plate. Thus, the performance is bracketed, and the line represents expected average performance. However, the lower point for each caliber has been used in the chart since this is a known or demonstrated capability. It is noted that in 75mm size, the line runs close to the 4-inch point. A few 75mm rounds have actually defeated 4-inch plate, but at only one velocity, 1700 fps. Also, in 105mm size early firings against very low charpy 6" plate were successful. When it was learned that plate toughness, or charpy value, strongly influenced results, all firings subsequently have been against tough, high charpy plate. The charpy test measures toughness by the ft. lbs. of energy required to break a notched bar. Low charpy is considered 5 to 15 ft. lbs., high charpy above 35 ft. lbs. This plot indicates the HEP round to be capable of defeating about 1.3 calibers of tough, high-obliquity plate, regardless of caliber. It is not known if the slope of the curve is actually a constant, but from the firings to date it is not far from constant for the range 75mm to 120mm. For very large calibers, one would expect the curve to droop, or for HEP to become less effective. However, the line is fairly close to the plate thickness of 8-inches defeated when Aberdeen Proving Ground fired UK 6.5" rounds.

There have been three principal methods of fabricating a soft-nosed HEP shell. (1) The UK HEP shell used butt welding. (2) The US was wary of production difficulties of welding, and first used an overlap, brazed joint to produce the two-piece HEP shell. (3) More recently, production methods have been developed to produce a one-piece HEP shell with inner walls gradually tapering outward toward the front, then closing in to the nose with no joint. In Figure 10 are cross-section drawings of the 105mm one and two-piece designs. The technique of making the one-piece type involves a series of drawing operations followed by a final nosing and spinning operation to close in the nose. The method is cheap, and many private facilities have the type presses and other machines required. The advantage of the one-piece type shell has been that the walls can be gradually thickened toward the rear, being only thick enough to withstand set-back forces, which permit maximum nose capacity and insures a better squashing action of the shell on striking plate. The principal effect of the one-piece design on plate performance has been to raise the effective velocity range, permitting better hit probability. Any HEP shell has an upper and lower striking velocity limit of effectiveness, the upper limit set by wall strength, and deflagration on short range impact, the lower limit is set by the walls being so strong that proper crush-up, or squash, does not occur. For example, the latest 105mm HEP shell for howitzers has an effective striking velocity range from 2100 down to 1400 fps, compared to 1700 down to 900 fps for the original two-piece HEP shell. HEP shell for tank guns now appears to have the upper effective limit near 2600 fps. Up to recently the HEP shell filler has been the new plastic explosive, Comp C-4. Tests now indicate certain superior features of Comp A-3, an explosive which is press-loaded (in granular form) to produce a firm, solid filler, but which flows plastically on impact. Use of A3 has permitted the velocities to go up as high as 2600 fps without shock detonation, and has permitted defeat of plate at normal impact of thickness equal to that defeated at high angles of obliquity. For example, with 105mm shell loaded with C4, the shell defeats 5" oblique plate and 3" normal plate, but with A3, 5" plate is defeated at any angle of attack.

Nose shape has been varied, between hemispherical and ogival with no significant difference noted. The ogival nose was chosen because of reduced drag. It is considered that future improvement of HEP shell performance is more likely to come from use of the electric fuze previously mentioned, than from further changes in shell geometry.

c. Accuracy

In general the average rotated shell, whether HE or HEP, has an accuracy of about .15 mils HPE or VPE. The HEP shell differs from the HE shell in that the walls are thinner, resulting in lower stability factors but results to date indicate accuracy at 1000 yds. of HEP shell is about the same as for HE shell. In the fabrication of HEP shell, special attention has been paid to keeping wall eccentricities to a minimum. At long ranges, there is some evidence that HEP shell accuracy is less than that of other spin-stabilized shell. The actual accuracy figures for tank guns range from .12 to .16 mil HPE and VPE, based on firing results in 75mm, 76mm and 90mm tank guns. Accuracy of HEP shell fired from howitzers has averaged about .2 mil HPE or VPE, and from recoiless rifles about .25 mil HPE or VPE.

DEVELOPMENT OF SHOULDER FIRED SHAPED CHARGE ROCKET HEADS

H. S. Weintraub

S. Fleischnick

I. B. Gluckman

Picatinny Arsenal, New Jersey

ABSTRACT

In order to evaluate the design features to be incorporated into a lightweight T205 Head, this arsenal conducted a shaped charge investigation by varying different parameters in the standard 3.5" M28A2 Head. Results obtained through this investigation and pertinent to designing the prototype T205 Head were as follows:

     a. The optimum cone thickness for the 3.5" M28A2 Rocket is .075" ≤ .003".

     b. The HE charge can be reduced to 1.3 lbs. without affecting penetration.

     c. The optimum standoff distance for the 3.5" M28A2 Rocket is 9".

     d. The booster pellet may be placed as close to or atop the apex of the copper cone without any significant difference in penetration being noted.

Preliminary tests with a modified 3.5" M28 type rocket head which eliminated the flat at the base of the cone (the M28A2 Head has a flat of approximately .1" at the cone base) indicated that an increase in penetration of approximately 2 inches might be expected.

Studies to improve the performance of the 2.36" T59E3 Rocket Head (1) by the use of explosives having higher rate of detonation than Composition B, such as 70/30 Cyclotol and 75/25 Cyclotol, (2) by shaping the detonation wave front traveling through the charge and (3) by use of a tandem cone arrangement, have resulted in no marked improvement in penetration to date.

Investigations are being conducted with the T2016 and T2017 Rocket Heads to determine whether increased standoff and correspondingly decreased explosive charge (overall length of head being constant) would result in increased penetration.

INTRODUCTION

This paper is divided into four parts. The first and major part covers the development of a 3.5" T205 lightweight Rocket Head. The second part deals briefly with the development of a 2.36" T59E3 Rocket Head. The third part gives a very brief description of the development of the 2.75" T2016 and T2017 Rocket Heads. Although the T2016 and T2017 Rocket Heads are not shoulder fired, they have been included in this report because the design problems are closely allied to those encountered in the development of the 3.5" T205 Rocket Head. The fourth part gives a very brief description of an independent investigation conducted for the 105mm T43 (M324) HEAT Shell. The results of this investigation are now being reviewed to determine the feasibility of incorporating the data into a 3.5" Rocket Head design.

DEVELOPMENT OF A 3.5" T205 LIGHTWEIGHT HEAT ROCKET HEAD

BY: H. S. WEINTRAUB

1. A conference, which was attended by representatives of ORDTU, Redstone Arsenal Division of the Rohm and Haas Company, Ordnance Rocket Center, Redstone Arsenal, Aberdeen Proving Ground and Picatinny Arsenal, was held at this Arsenal in April 1951. The object of this conference was to establish a high priority program for the development of a 3.5" Rocket having greater accuracy, range, penetration and velocity than the now Standard 3.5" M28A2 Rocket (Figs. Ia, Ib). The new rocket is designated as the 3.5" T205 Rocket.

2. The responsibilities for the development of the 3.5" T205 Rocket were fixed as follows:

    a. Picatinny Arsenal -

        (1) Coordination and technical supervision.

        (2) Design and development of a lightweight HEAT Head for the T205 Rocket.

        (3) Design and development of an alternate T205 Motor design, employing trap-type construction.

    b. Rohm and Haas -

    Design and development of the T205 Motor, employing head-end suspension.

    c. National Bureau of Standards -

    Design and development of the Piezo Electric Type Fuze for the T205 Rocket.

3. The characteristics to be achieved by the T205 Rocket, as put forth by ORDTU, especially those pertinent to the head design are listed as follows:
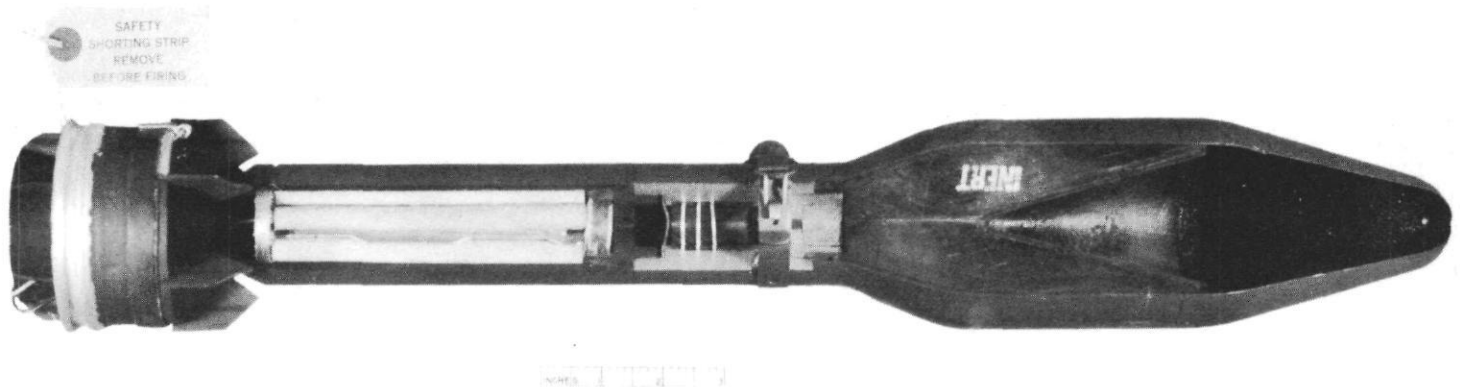
Figure Ia—Rocket, HEAT, 3.5″, M28A2.
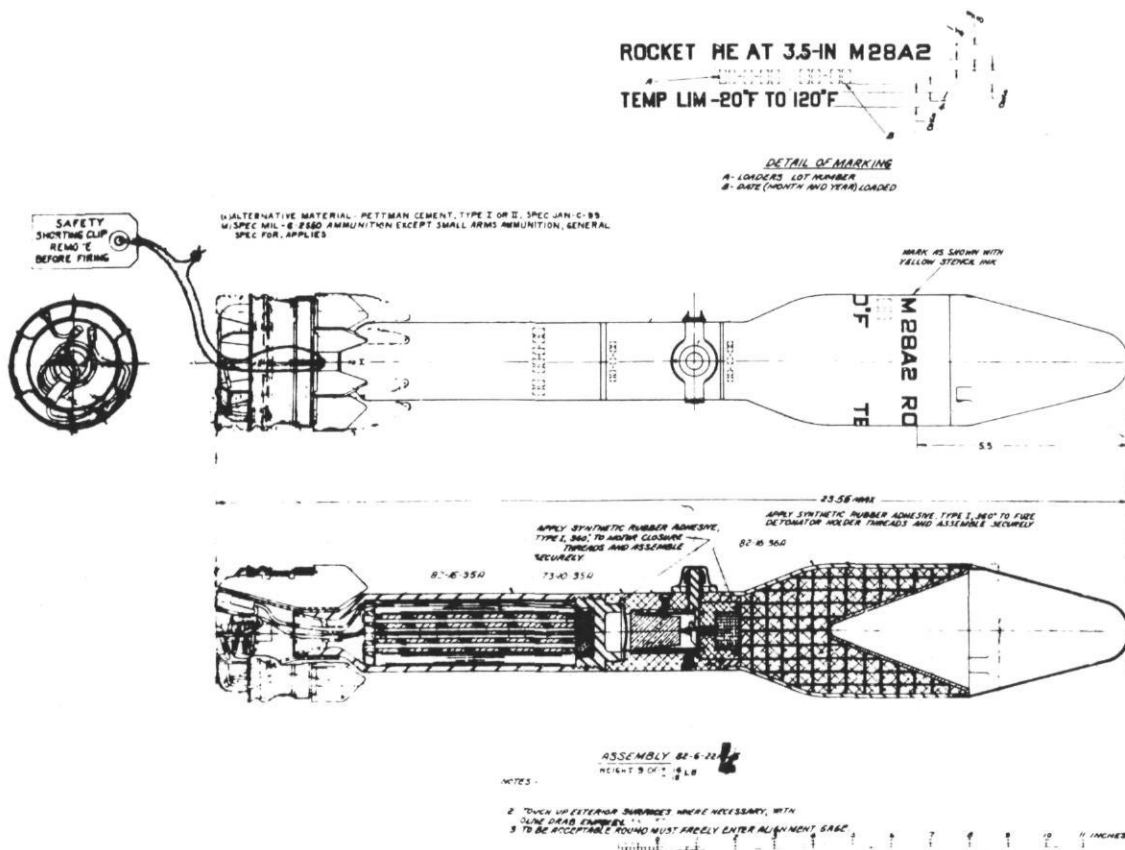
Figure Ib—Rocket, HEAT, 3.5″, M28A2, Assembly.

a. Penetration to be achieved by 90% of the rockets:

   (1) 6" penetration of armor plate at 60° obliquity is required.

   (2) 5" penetration of armor plate at 70° obliquity is desired.

b. Lethal Fragmentation:

   Fragmentation equal to that obtained with the M28A2 Heads is desired.

c. Accuracy:

   (1) 80% probability of the first round hitting a target 7.5' x 7.5' at 500 yards is desired, with the rocket having a probable error of 1 mil.

   (2) The rocket has to exhibit equal or better aerodynamic stability when compared to the M28A2 Rocket.

d. Initial Velocity:

   500 ft. per second is required.

e. Weight:

   (1) A weight of 7.5 pounds for the complete T205 Rocket is required.

   (2) A weight of 7 pounds is desired if possible of attainment.

f. Length:

   A maximum overall length of 23.55" (same as M28A2) is required. In addition, this round must be able to be fired from the automatic launcher as well as the M20 shoulder-fired launcher.

g. Fuze:

   The PI, BD, T2030 Electric Fuze is required.

4. The Rohm and Haas Company selected for their motor development a design (Fig. II) that had the same metal parts weight (3.3 lbs.) as the M28A2 Rocket Motor. This motor, however, contains approximately 30% more propellant than the M28A2 Motor. The National Bureau of Standards has under design a fuze that weighs .86 lb. less than the M40A1 Fuze of the M28A2 Rocket. The increase in weight of propellant and the decrease in weight of the fuze did not meet the velocity requirement of 500 fps and the maximum weight requirement of 7.5 lbs. for the T205 Rocket. Thus, it became necessary to provide a much lighter head than that of the M28A2 Rocket. To meet these requirements, a head weight of approximately 3.5 lbs. or 25% less than that of the M28A2 Rocket was required (Fig. III). Thus, the main problem for this Arsenal was to design a much lighter 3.5" HEAT Head that would have better performance characteristics with respect to penetration than those of the 3.5" M28A2 HEAT Head.

Figure II

Figure III—Rocket, HEAT, 3.5″, M28A2, and practice, M29A2,
Head metal parts, Assembly and details.
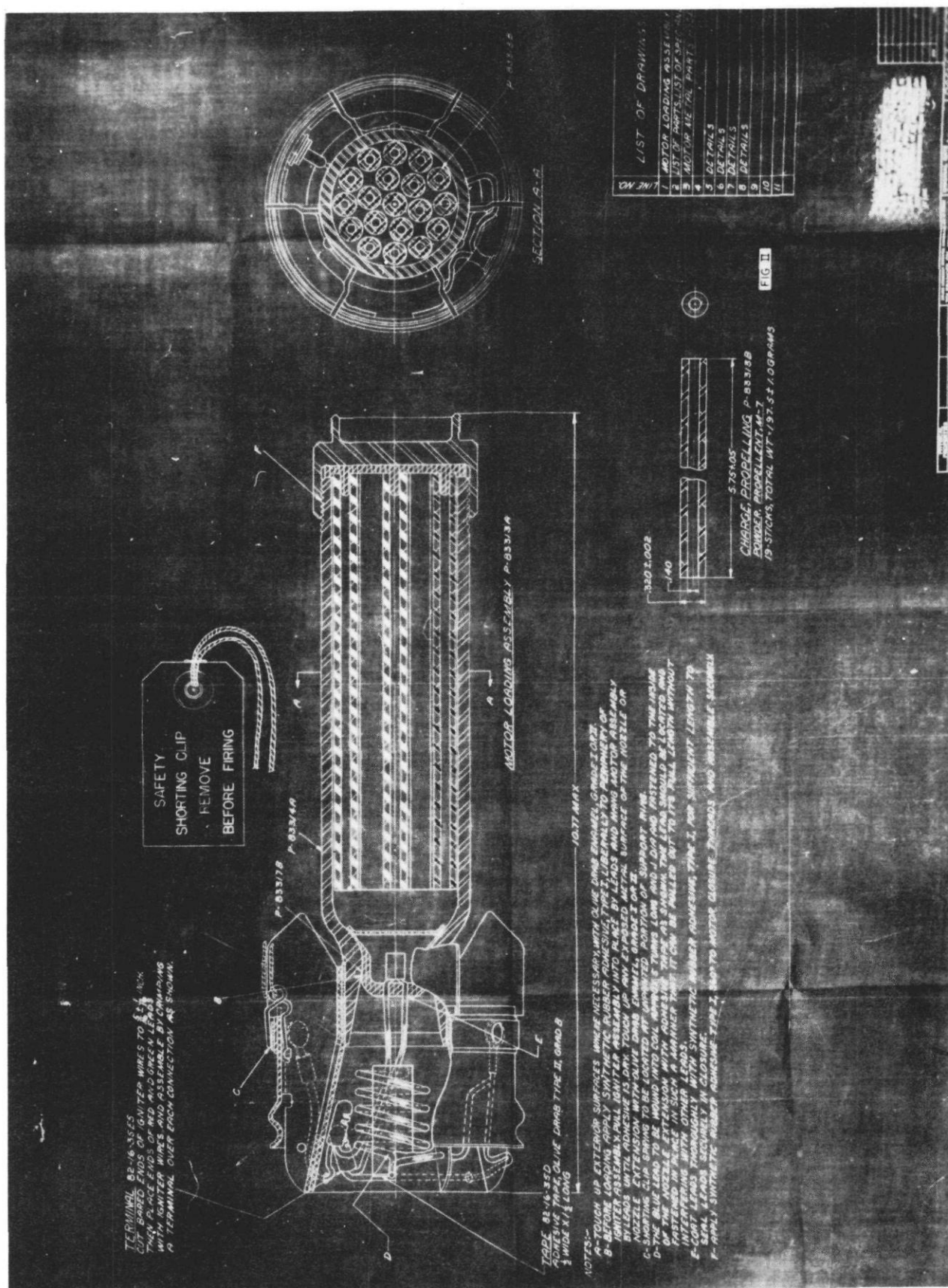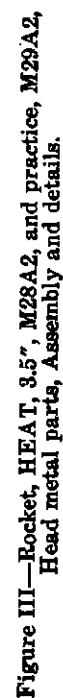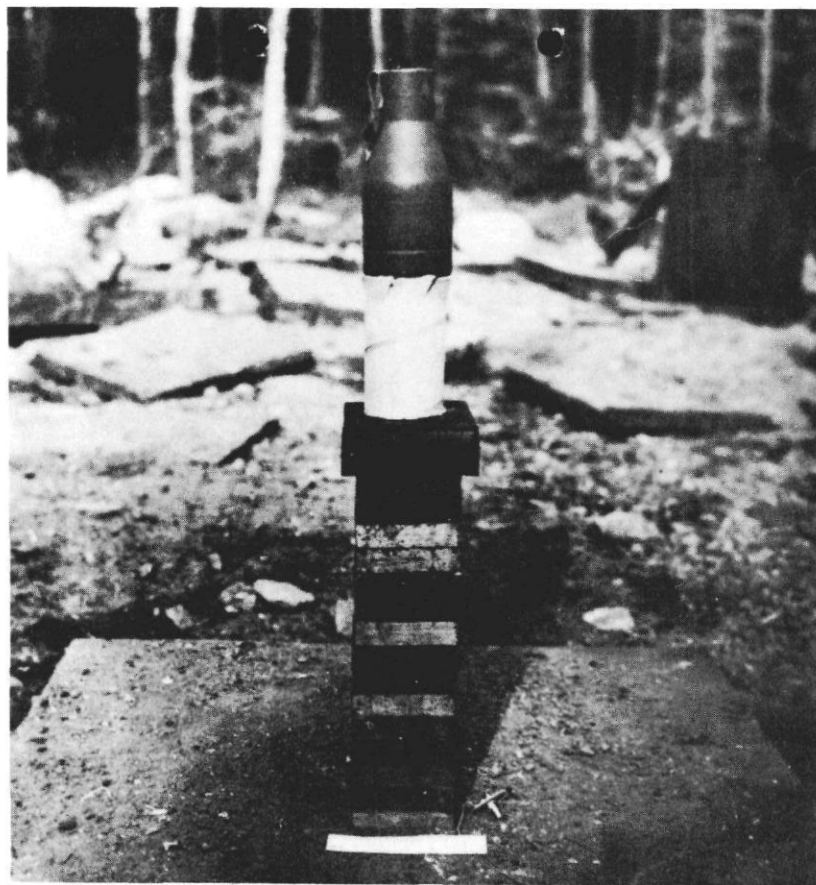
Figure IV—Head, Rocket, HEAT, 3.5″,
T205 Pc Mk P-83152A Assembled with
tetryl pellet (See photograph M-39684)
Prior to assembly with blasting cap.
Plates are hot-rolled (RHN B-70)
FS 1015 Spec QQ-S-633.

Figure V—Rocket, HEAT, 3.5″, T205,
design No. 6 as shown on Dwg. PX-8-720
assembly with booster detonator assembly
& Du Pont No. 6 Blasting Cap.
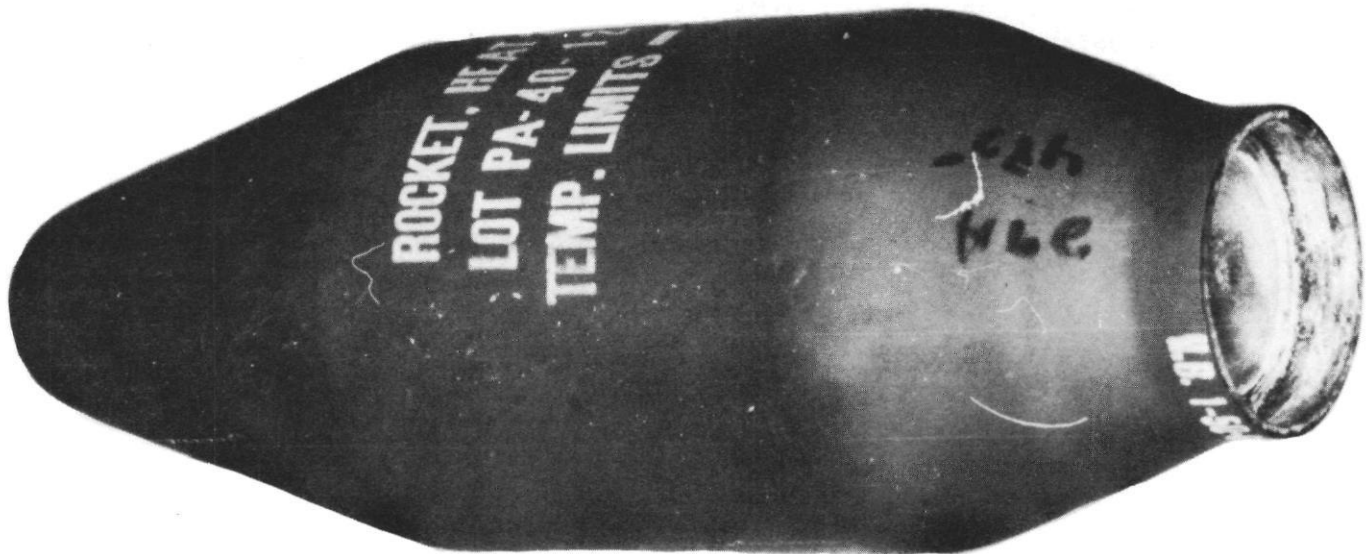
Figure VI—3.5″ M28A1 Rocket head of ammunition Lot PA-40-12.
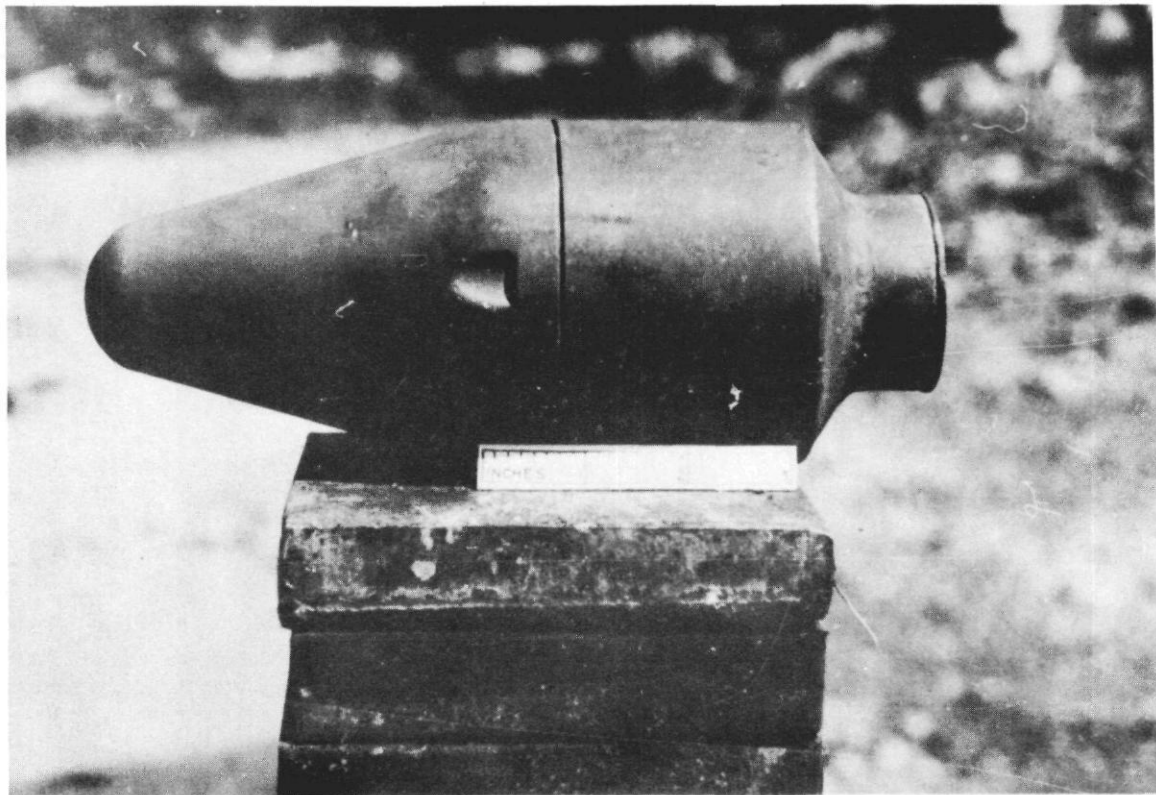
Figure VII—Head, Rocket, 3.5″ modified T205 head to contain
1.01 pound H.E. as shown on piece marked P-82795F.

5. Development of the lightweight head was investigated by conducting static penetration tests for a variety of modified heads. The following is a list of the more important variables that were investigated:

    a. Reductions in the weight of the HE charge.

    b. Changes in the body contour to determine the best distribution for the reduced HE charge.

    c. Reductions in cone thickness to save weight.

    d. Decreases in the distance between the apex of the cone and the booster pellet to save weight without sacrificing penetration performance.

    e. Changes in standoff distance to increase penetration.

    f. Reductions in thickness of head wall to save weight.

    g. Changes in ogive shape to obtain more stable flight characteristics.

6. In order to expedite the test program, most of the initial static firings were made with modified M28A2 Heads. The firings were conducted by placing the modified heads perpendicularly on top of a stack of 1-inch mild steel plates 16 to 20 inches high. As shown in Fig. IV, the stack was usually arranged with three 5" x 5" x 1" steel plates at the top and 4" x 4" x 1" plates for the remaining height. These plates were of FS 1015 hot rolled steel, in accordance with Specification QQ-S-633, and had an average Brinell hardness of 140 (Rockwell B-70). Detonation was accomplished so as to simulate, wherever possible, the conditions that take place when the head is assembled to the rocket. To accomplish this, the M28A2 Heads were assembled with booster detonator assemblies, and the detonation of the heads initiated by a duPont No. 6 blasting cap. Although this method of obtaining the static penetration data does not exactly duplicate firing against homogeneous armor plate, it does afford a good evaluation of the performance of a design relative to other designs tested in the same manner. In addition, it has been shown that the penetration of armor plate is approximately 80% of the value obtained with mild steel plates.

7. The following tentative conclusions may be drawn from the tests:

    a. The reduction in the weight of the HE charge from 1.9 lbs. (Fig. VI) to 1.4 lbs. and 1.01 lbs. (Fig. VII) does not indicate any significant difference in penetration. These heads were fired at a standoff of 4.2", which is the standoff obtained by static firing of a 3.5" M28A2 Head.

    b. The body contour (Fig. VIII) may be modified within limits without adverse effect, provided that the portion of the head body extending from the base to the apex of the cone is approximately cylindrical and maintains a diameter approximately equal to the base of the cone. The portion of the head body for the M28A2 and T205 Heads, which
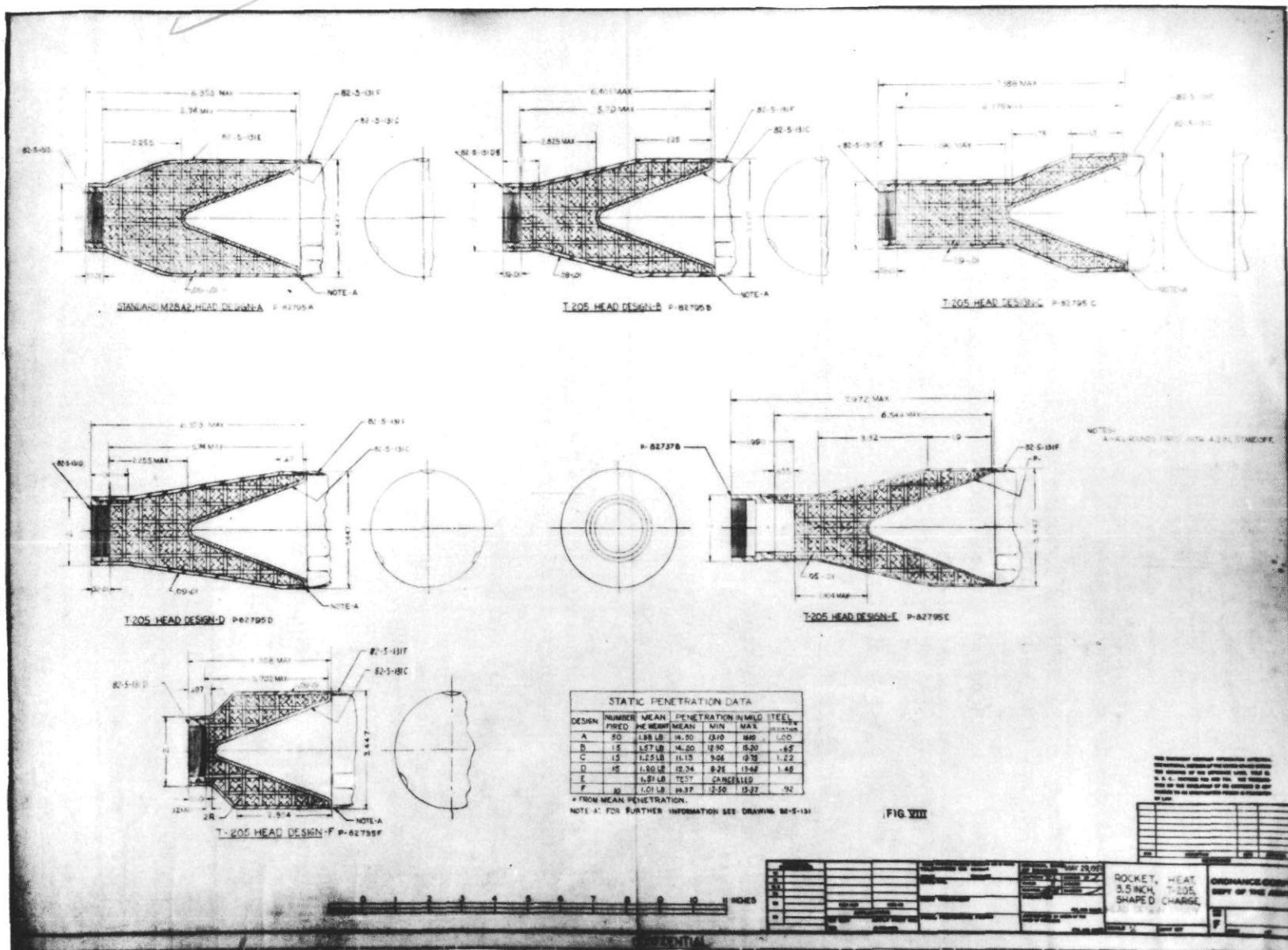
Figure VIII—Rocket, HEAT, 3.5″, T-205, Shaped Charge, head design study.

CONFIDENTIAL

PENETRATION vs CONE WALL THICKNESS FOR THE
3.5" M28A2 HEAD

Point	σ (ins)
1	.582
2	.57
3	.481
4	.393
5	.295
6	.6053

σ = Std Dev

The cone wall thickness tolerance is
± .006" except for the group of .075"
thick cones with ± .003 tolerance.
Standard cone thickness is .093" ± 006.

Std M28A2

PENETRATION (INCHES)

CONE WALL THICKNESS (INCHES)

FIG. IX

Fired statically at Picatinny Arsenal with
head placed in vertical position, perpendicular
to and touching the top plate of 17 - 1"
thick mild steel plates. Each point represents
average value obtained with 20 firings.

Rev 7-13-51
Rev 7-10-51
7 July 1951

Figure IX—Penetration vs. cone thickness for the 3.5" M28A2 head.

CONFIDENTIAL

PENETRATION VS STANDOFF
FOR THE STANDARD 3.5"
M29A2 ROCKET

Fired at Picatinny Arsenal with Head
placed in vertical position, perpendicular
to and touching the top plate of 18 - 1"
thick mild steel plates. Distance "x"
equal to 4.2" standoff for Standard M28A2
Head.

σ = STD. DEV

STD. M28A2

PENETRATION (INCHES)

Point	No. Pound Fired	σ (ins)
1	5	1.40
2	15	.30
3	15	.39
4	15	.71
5	15	.55
6	15	.60
7	15	.49
8	15	.75
9	15	.60
10	11	.98
11	15	1.2
12	13	1.3
13	15	1.4

FIG. X

Rev. 2 October 1951
Rev. 10 July 1951
7 July 1951

STANDOFF (INCHES)

Figure X—Penetration vs. standoff for the standard 3.5" M28A2 rocket.

82-5-131 B OR
82-5-131 H

P-82911 B DESIGN 3A

P-82911 B DESIGN 3

COMPARISON OF HEAD CONTOURS
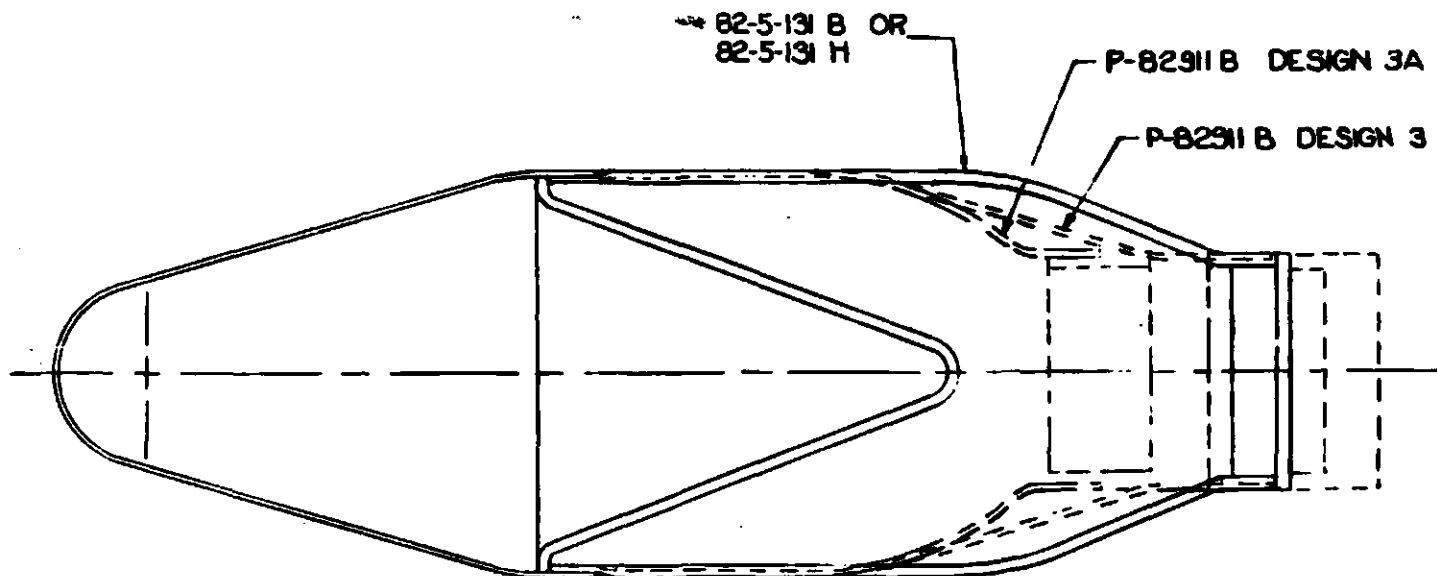
HEAD TYPE PIECE MARK	APPROXIMATE WHGT. OF H.E.	DISTANCE FROM CONE APEX TO BASE OF BOOSTER CAVITY
82-5-131	1.93	2.24
P-82911 NO3	1.55	1.71
P-82911 NO3A	1.35	.24

Figure XIIa—Comparison of head contours.

Point	No. Rounds Fired	Γ(ins)
1	23	.8
2	10	.4
3	22	.9
4	15	.7
5	9	.6
6	10	.6
7	10	.8
8	50	1.0

PENETRATION vs DISTANCE OF BOOSTER PELLET FROM CONE APEX FOR STANDARD 3.5" M28A2 ROCKET

Γ = STD DEV

CONFIDENTIAL

STD M28 A2

Fired at Picatinny Arsenal with Head placed in vertical position, perpendicular to and touching the top plate of 17 - 1" thick mild steel plates. Standard pellet distance "X" equal to 2.2 inches.

FIG. XIIb

PENETRATION (INCHES)

DISTANCE OF BOOSTER PELLET FROM CONE APEX (INCHES)

Figure XIIb—Penetration vs. distance of booster pellet from cone apex for standard 3.5" M28A2 rocket.
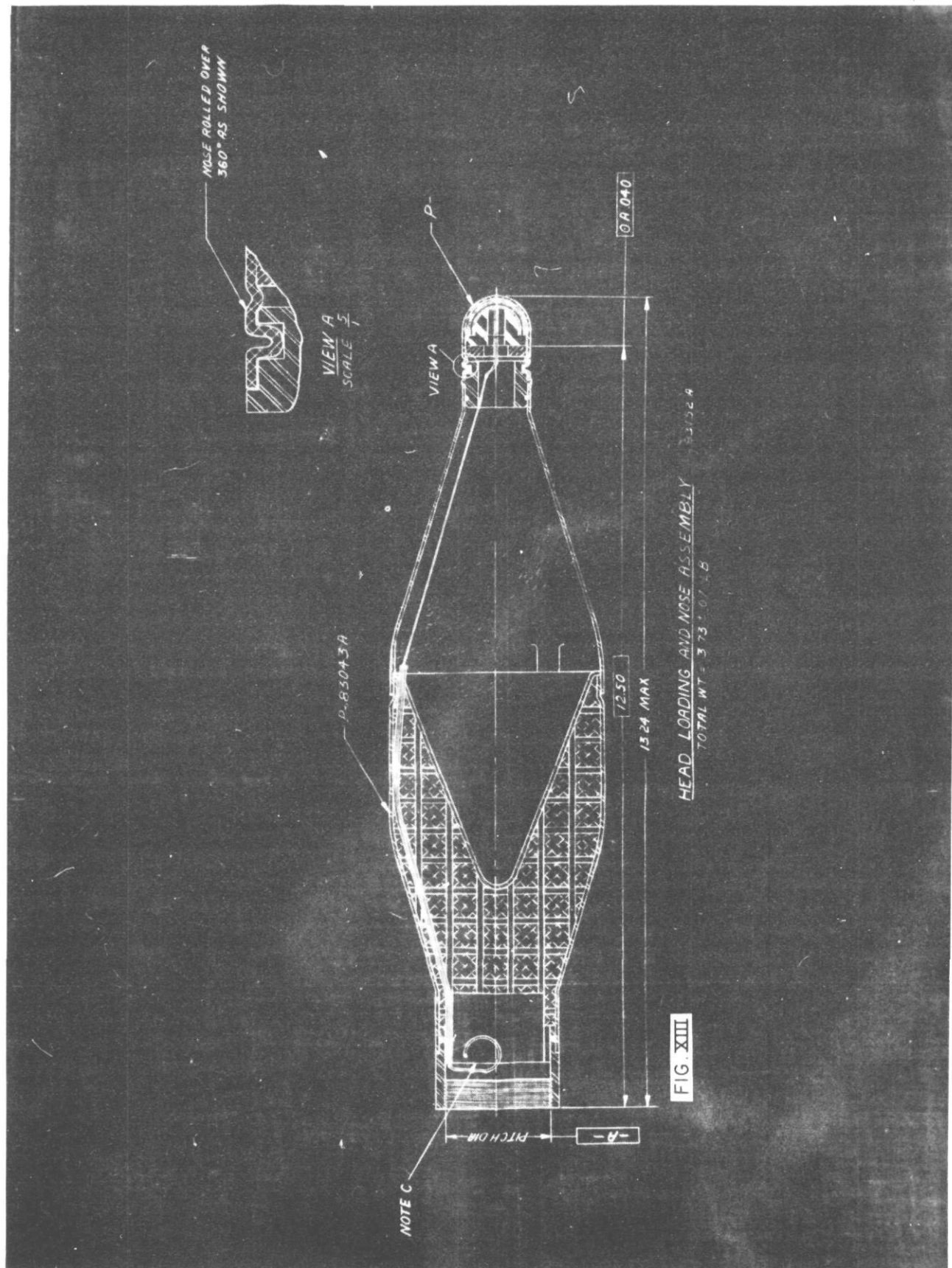
Figure XIII—Head loading and nose assembly.
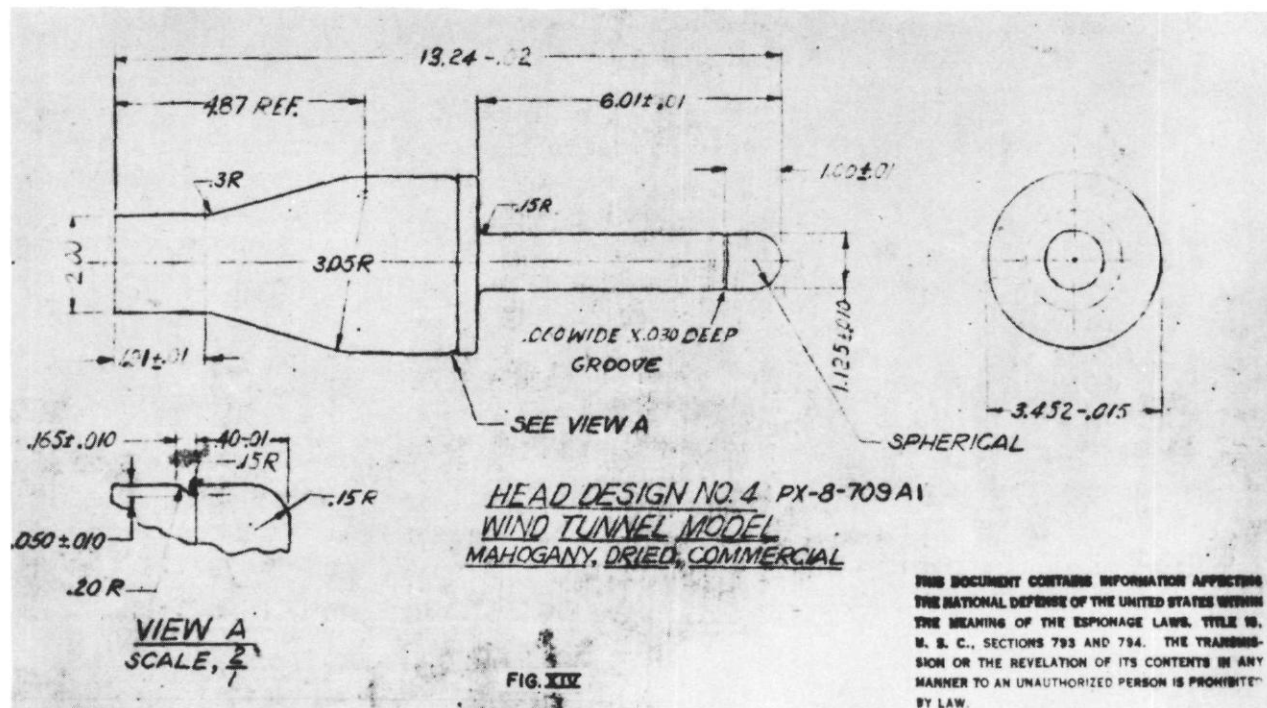
Figure XIV—Rocket, HEAT, 3.5", T205, Head design #4.
Wind tunnel model, dimensioning.
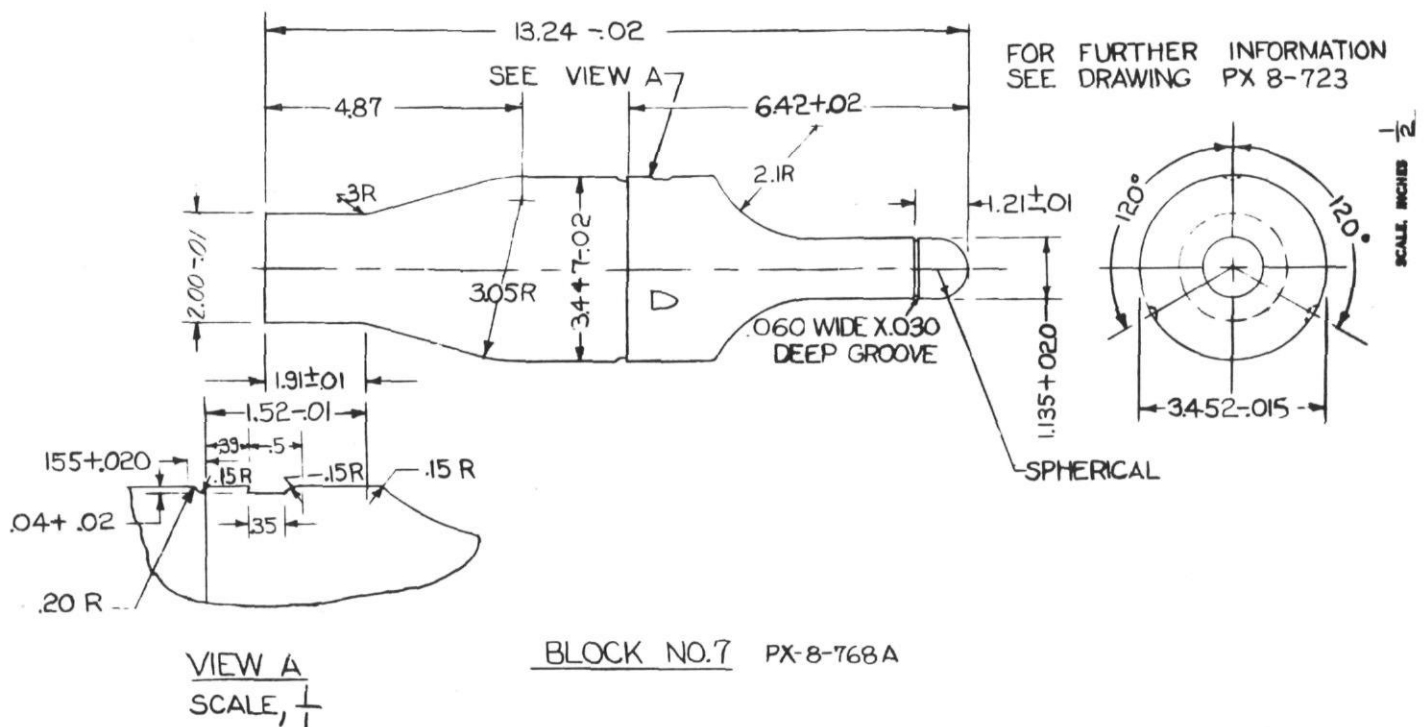
Figure XV—Block No. 7.

runs for the height of the cone, should have a diameter of approximately 3.5 inches. The copper cones of the heads have an apex angle of 42° and a diameter of approximately 3.5 inches.

      c. In the M28A2 Rocket, a maximum static penetration occurs with a cone thickness of .075 inch as compared to a thickness of .093 inch for the M28A2 Cone (Fig. IX). This result was obtained by firings conducted with groups of M28A2 Heads. Each group of heads was assembled with different cones having the following thicknesses:

$$.050" \neq .003"$$

$$.060" \neq .003"$$

$$.070" \neq .003"$$

$$.080" \neq .003"$$

$$.093" \neq .003"$$

      d. The static penetration of the mild steel plates by the 3.5" T205 Rocket increases almost linearally with standoff (Fig. X), until a maximum penetration of about 18 inches occurs at about a 9" standoff. The static penetration of the M28A2 Rockets at full ogive standoff (4.2") is about 14.5 inches.

      e. A head wall thickness of .050" may be used instead of the .090" thickness of the M28A2 Head, but with no significant difference in static penetration. Since the use of a thinner wall head and a smaller HE Charge will undoubtedly affect the fragmentation qualities of the head, this problem is now under investigation.

      f. Reduction of the distance between the booster pellet and cone apex in the M28A2 Rocket does not seem to reduce the static penetration of the head (Figs. XIIa and XIIb). The tests leading to this conclusion were conducted with groups of M28A2 Heads, each group of which had the booster pellet placed at a different distance from the apex of the cone. The distance ranged from 0 inch to 2.2 inches (M28A2) in increments of 1/4 inch. This was accomplished by increasing the depth of the bore of the HE cavity into which the booster pellet was inserted.

    8. The above work indicates that acceptable penetration characteristics can probably be achieved with a head of much less weight than the M28A2 Head. The weight reduction, together with the necessary head contour changes, moved the center of gravity of the T205 Rocket to the rear (closer to the center of pressure). This change in center of gravity was sufficient to decrease the flight stability of the rocket when an ogive of standard contour is used. It was, therefore, found necessary to conduct an aerodynamic investigation of ogives having different contours, so as to develop an ogive shape that would improve the flight stability without adversely affecting penetration. Wind tunnel tests showed that the head designs Nos. 3, 4, 7 and 8 (Figs. XIII, XIV, XV and XVI) had satisfactory flight stability characteristics. However, head design No. 4 gave unsatisfactory penetration because of interference of the ogive with the jet. As a result, an ogive design having longitudinal clearance at the base of the cone to avoid interference with cone collapse and jet penetration was then designed. This design gave satisfactory results when tested for penetration (Fig. XVII). Aerodynamic tests for different type head contours are still being conducted at NACA.

FOR FURTHER INFORMATION
SEE DRAWING PX 8-724

BLOCK NO. 8 PX-8-767A

VIEW A
SCALE, +

Figure XVI—Block No. 8.

JET INTERFERENCE

DESIGN NO.4

DESIGN NO.8

JET CLEARANCE

Figure XVII—Jet interference in T-205 head expressed on basis of
two dimensional cone collapse.
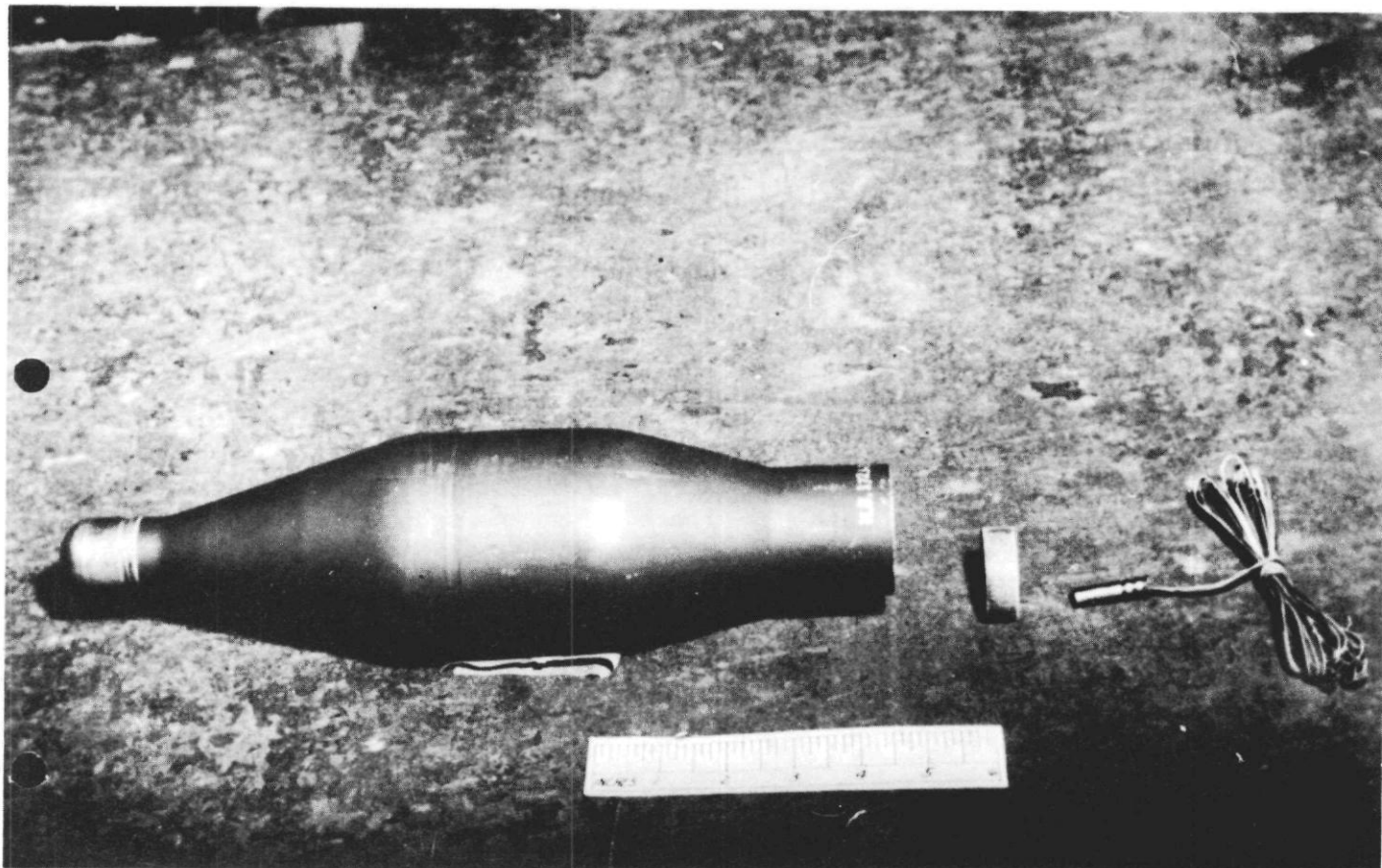
Figure XVIII—Head, rocket, HEAT, 3.5" T205 Pc Mk P-83152A with 1.45"x½" tetryl
pellet and #6 Du Pont blasting cap prior to assembly for static penetration test firing.
See photograph #M-39685.
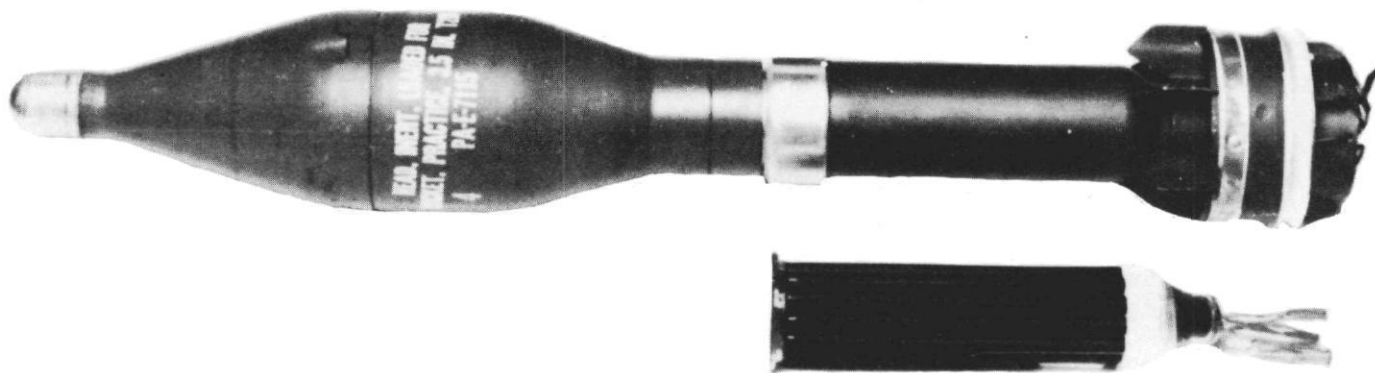
Figure XIX—Rocket, HEAT, 3.5", T205, Design No. 3 with propellant charge & igniter.

263

9. Using the data obtained in the various tests, the lightweight prototype T205 Head design No. 3 (Figs. XVIII and XIII) has been established. This head design differs from the M28A2 in the following manner:

      a. The HE content is reduced to 1.4 lbs.

      b. The cone thickness is reduced to .060".

      c. The distance between the booster pellet and the cone apex is reduced to 1.7".

      d. The outside contour including the ogive is changed to accomodate the reduced charge and to provide satisfactory flight stability.

      e. The total weight has been reduced to 3.5 lbs. The T205 Heads have been manufactured and are about to undergo static firing tests. Flight tests of the T205 Rocket (Fig. XIX) employing the Picatinny Arsenal head are scheduled to be conducted in the near future. It is expected that the characteristics of the rocket will be as follows:

      (1) Length - 23.55" max.

      (2) Weight - 7.2 lbs.

      (3) Velocity - 500 ft. per second.

      (4) Maximum range - 1400 yards.

      (5) Expected penetration - 14-inch homogeneous armor plate.

DEVELOPMENT OF A 2.36" T59E3 HEAT ROCKET HEAD

BY: S. FLEISCHNICK AND I. B. GLUCKMAN

1. The 2.36" T59E3 Rocket (Fig. 1) is a completely redesigned rocket intended to replace the 2.36" M6A6 Rocket. The T59E3 Rocket weighs 6.5 lbs., has a velocity of 420 ft. per second at 70°F, and has a penetration of approximately 8 inches of homogeneous armor plate.

2. Due to the occurrence of some erratic penetration performance of the T59E3 Head, work was initiated and is still being conducted at this Arsenal to improve both the depth and the uniformity of armor penetration. The investigations conducted and those still under investigation include the following:

      a. Tests conducted with explosives having higher rates of detonation than Composition B, such as 70/30 Cyclotol and 75/25 Cyclotol, have not indicated that any improvement in the penetration performance of the T59E3 Rocket Head can be expected.
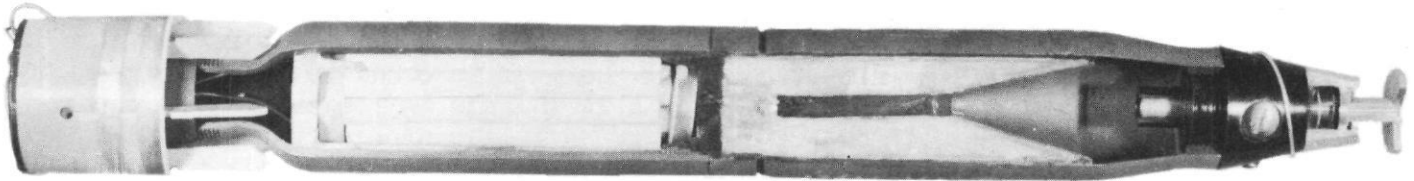
Figure 1—Rocket, HEAT, 2.36", T59E3 with fuze, rocket, T2000 E1 (Mod A).

CHARGE, BURSTING PX-8-634B
.84 LB COMP B, GRADE I (a)
SPEC JAN-C 401

PX-8-633B

(c) SOLDER 360° WITH COMP Sn 50, SPEC QQ-S-571,
WITH SOLDERING FLUX, SPEC 4-103.
(d) LOAD SECTIONS A & B SEPARATELY, SECTIONS
TO BE ASSEMBLED PRIOR TO STATIC FIRING.
TR-176A (MODIFIED TO PROVIDE SECTION A AND B)

NOTE d

.93+.02 DIA

.63 MIN

NOTE C

P-81436 H

SECTION A
2.86-.01

PX-8-633 A

NOTE C

SECTION B
4.64 MIN TO FORWARD END OF HEAD
(a) EXCEPT EFFLUX VISCOSITY SHALL BE 3.5 TO 5.5 SECS
(b) LGTH OF ASSEMBLY 7.58 IN. MAX

LOADING ASSEMBLY PX-8-634 A

FOR EXPERIMENTAL USE ONLY

SCALE, INCHES

Fig 2

Figure 2—Rocket, HEAT, 2.36", T59E3, Loading Assembly.

265

b. Tests, in which it was attempted to shape the detonation wave front travelling through the charge, were conducted with the T59E3 Heads. However, no improvement in penetration was noted.

c. The use of a tandem cone arrangement (Fig. 2) indicated some marked improvement in the penetration of the T59E3 Head. However, several basic difficulties encountered with this type of head design must first be overcome. The first problem is to design a supplementary charge (located behing the smaller cone) to give a very fast jet with little or no slug, which would produce a large hole in the armor through which the main jet could then pass. The second and more difficult problem has been to delay the formation of the main jet so as not to destroy the jet from the supplementary charge. Means of overcoming these problems are still under investigation.

d. An investigation to determine the optimum standoff for the T59E3 Head has indicated, in static tests, that an increase in the existing standoff by approximately one inch (to offset for the nose crush of the fuze on ballistic firing) may result in an additional inch of penetration. It is felt that this change can be made without affecting overall rocket length, since it may only require relocating the cone closer to the rear of the head. A corresponding reduction in the length of the explosive charge, without change in standoff, did not indicate any reduction in penetration.

e. Tests are now being conducted with T59E3 Heads having different cone thicknesses to determine if the .059" thickness of cone now used in the T59E3 Rocket is optimum.

f. An investigation is being conducted of the effects of non-uniformity and eccentricity of the head metal parts. While this investigation is not as yet complete, preliminary results indicate that the amount and uniformity of penetration can be significantly improved by closer control of eccentricities of the head metal parts.

DEVELOPMENT OF A 2.75" T2016 AND T2017 HEAT HEAD

BY: I. B. GLUCKMAN

A development program is now in progress at this Arsenal to design a 2.75" T2016 Heat Rocket Head using a mechanical fuze and a 2.75" T2017 HEAT Head using an electrical fuze. The T2016 (Fig. 3) will have an approximate nose crush of 2 inches while the T2017 will have approximately 1 inch of nose crush. Tests to determine optimum parameters of these heads are in progress. The present tendency is to increase the standoff of these heads by moving the cone to the rear; however, this would result in a smaller amount of explosive and the limiting amount in this regard has not yet been determined. The optimum cone thickness for these heads was found to be .076" in static tests.

RESULTS OF AN INVESTIGATION OF THE 105MM T43 (M324) HEAT SHELL PERTINENT TO 3.5" ROCKET HEAD DESIGN

BY: S. FLEISCHNICK

As a result of a recent investigation conducted by this Arsenal, to determine an optimum design of cone for the 105mm T43 (M324) HEAT Shell, it was found that improved
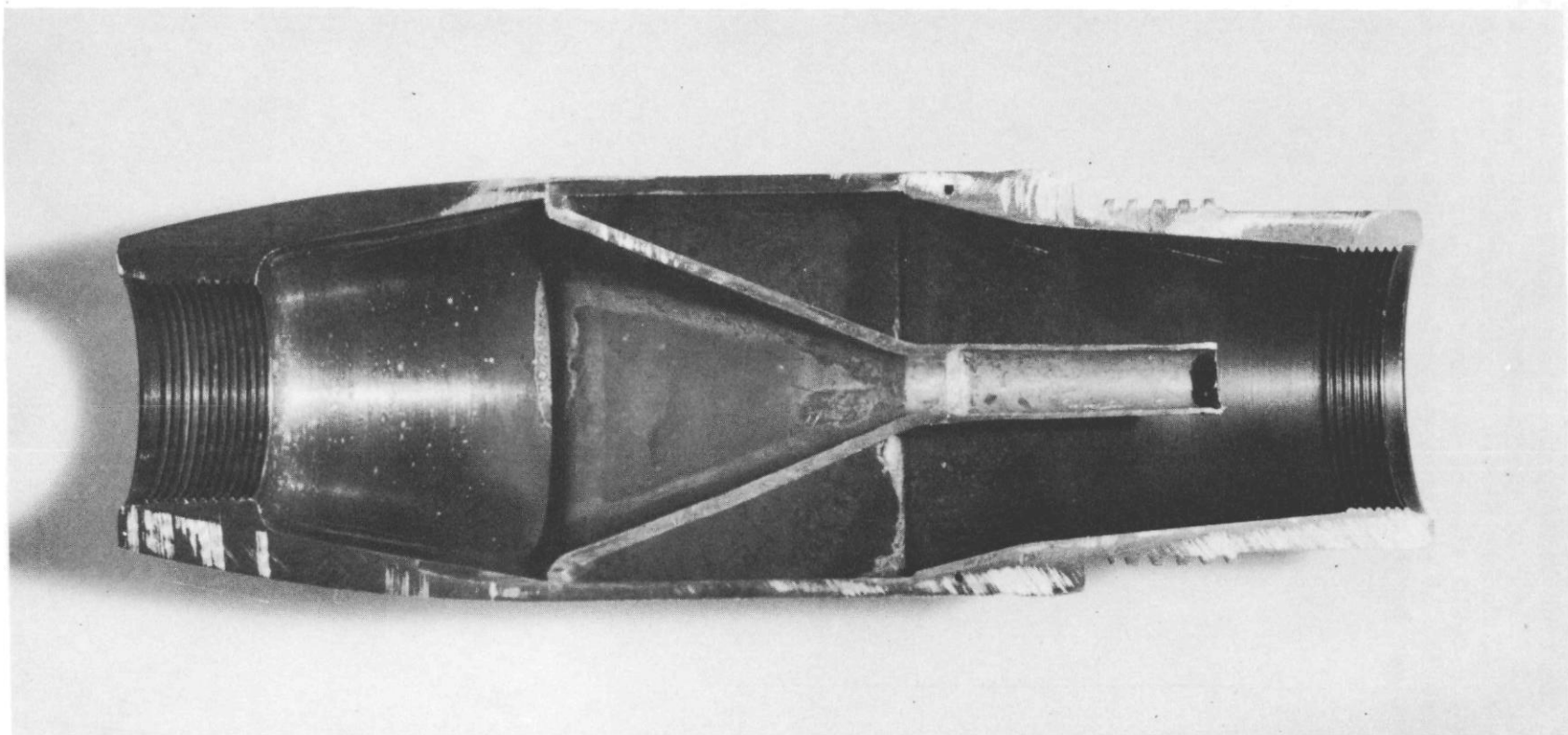
Figure 3—Head, Rocket, HEAT, 2.75″, T2016 metal parts.

penetration was obtained, in static tests, by removal of the "flat" (and/or radius) of explosive at the base of the cone between the slant surface of the cone and the interior wall of the shell. A "flat" of approximately 0.1 inch exists at the base of the cone as assembled in the M28A2 Rocket Head. It was considered desirable to determine whether improved performance could also be obtained in this head by use of a cone which permitted no flat. The results of exploratory tests indicate that as much as two (2) inches more of penetration can be obtained by eliminating the flat.

THE PRESENT PERFORMANCE AND PROBLEMS OF THE 105MM BAT RIFLE

H. P. Manning

C. W. Musser

H. W. Euker

Frankford Arsenal, Philadelphia, Pennsylvania

ABSTRACT

As candidates for "The BAT Rifle" there are three 105mm re-coilless rifles, four mounts, four spotting rifles, one set of fire control, four types of HEAT rounds and five types of spotting ammunition including tracer. These will be assembled into four "weapon systems".

The T136 Rifle, T118 Ammunition and T149 Mount have given accuracy at 1,000 yards represented by HPE of 0.29 mils, and VPE of 0.44 mils. Static penetration tests have given 16.9 inches penetration against homogeneous armor. These data represent ammunition already superseded by improved designs. Caliber .50 tracer and spotting ammunition have shown reasonably good function-ing and matching performance.

The major problems currently being encountered with the T136 Rifle, T118 Ammunition, T149 Mount, T43 spotting rifle combination are: recoil balance seems to be unduly sensitive to loading density; the method of spinning the long boom, fixed fin T118 type projec-tile; the amount of spin to meet accuracy and penetration require-ments; variations in measured jump under different conditions have been encountered; questions of overall evaluation of the spotting device and techniques for its use are yet unanswered.

One of the candidates for the BAT Rifle is the T136 105mm Rifle on the T149 Mount and incorporating the caliber .50 Spotting Rifle, direct and indirect sights. In Fig. 1 you will note the spotting rifle is the T43 and the sight is the interim type. On the T149 Mount the elevating hand wheel is in the vertical plane and the traversing hand wheel in the horizontal plane. The firing button (pull out to fire spotting rifle - push in to fire major caliber) is located at the center of the elevating hand. wheel. The handle for operating the breech mechanism for 105 rifle can be inserted from either the top or the bottom.

The ammunition for the T136 Rifle is shown in Fig. 2, the projectile being the long boom, one caliber fixed fin, T118 type and the cartridge case being the T30 fabricated case. The case is cylindrical and there is no requirement for guide rails.
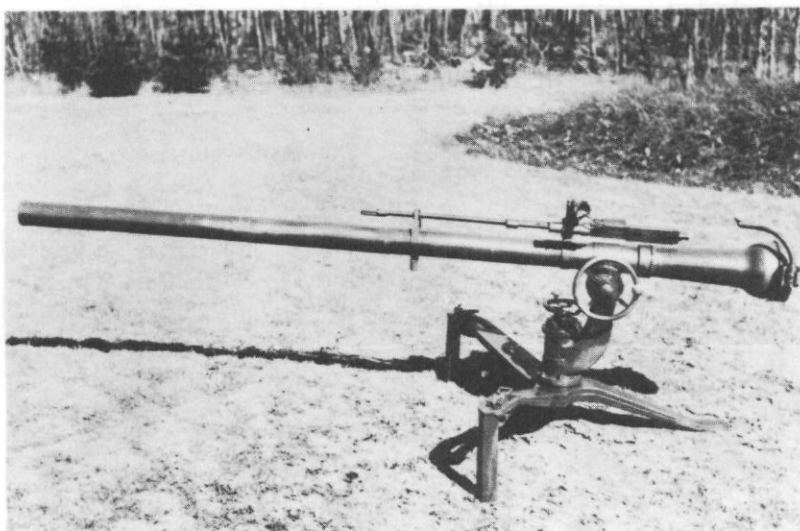
Figure 1—105 mm rifle T136, 105 mm mount
T149, caliber .50 rifle T43 and
the interim sight.
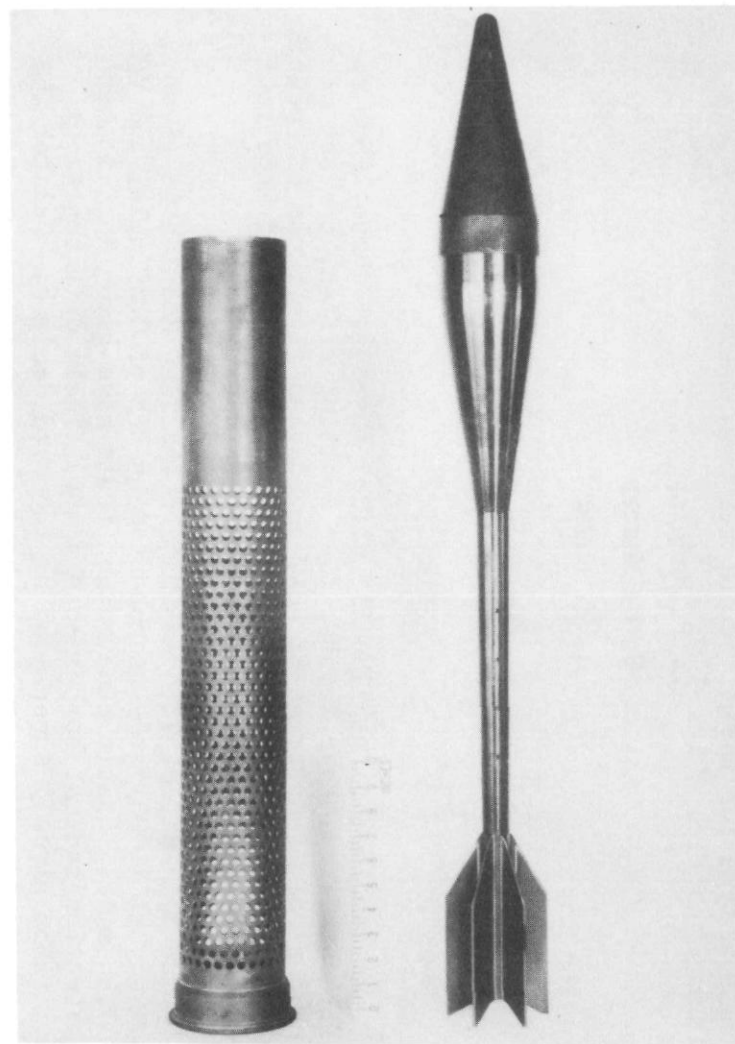
Figure 2—Cartridge case (Dwg. FD15561,
rev. 1) and projectile, 105 mm, T118E2.

Associated with the development program on the T136 Rifle and T118 ammunition and technically inseparable from that development are the development of fin stabilized ammunition T184 type for the M27 Rifle and the development of a T170 Rifle for the "ONTOS" infantry vehicle. Fig. 3 shows the characteristics of these three rifles. The main points to note - that the M27 Rifle has an 800 cu. in. chamber volume and the other two rifles have 500 cu. in. chamber volume. This results in the loading density of .3 for the M27 and .5 for the other two rifles. The barrels on the M27 and the T170 are identical on the inside, the T170 having a thinner wall than the M27. Note also that the M27 was designed for a 70,000 psi working stress, the T136 for 100,000 psi working stress and the T170 for 85,000 psi working stress. The barrels of the M27 and the T170 are rifled one turn in 20 caliber for the stabilization of the thirty pound spin stabilized projectile. The T136 rifle, being designed specifically for fin stabilized projectiles, is rifled one turn in 480 calibers to give it 2.18° per foot roll to the projectile, in order to average out asymmetries which otherwise would cause large deviations from the average trajectory.

One of the major features of the T136 Rifle is the incorporation of the "strain compensation" principle in the barrel design. In order to achieve minimum weight for the rifle, it has been designed so that the working stress of the steel is 100,000 psi at rated maximum pressure. On conventional design, the bore diameter would have been 4.134" + .002 and bourrelet diameter of the projectile would have been 4.128" - .005. With the very thin barrel of the T136 Rifle, elastic strain in the steel would give rise to an increase in diameter of .013". The diametral clearance between the projectile and the bore during firing would be at least .019" and with normal manufacturing tolerances could be as high as .026". This condition is illustrated in the upper sketch in Fig. 4. Several bits of experimental evidence support the contention that all this clearance appears on one side of the projectile. On the "strain compensated" principle of barrel design, the bourrelet diameter is made sufficient to give a small clearance in the bore during projectile firing, while the bore is elastically expanded by the gas pressure, as illustrated in the lower sketch in Fig. 4. In the T136 Rifle the bore diameter is 4.134" and bourrelet diameter is 4.145". During firing, clearance between the projectile and the bore lies between .002" and .007" at the extremes of manufacturing tolerances. The T136 is the second recoilless rifle designed on this principle. It has been shown that, with spin stabilized projectiles, accuracy is greatly improved in this manner. However, sufficient experience has not been gained to be certain difficulties will not be encountered in rifles designed with these high stress levels.

Figure 5 shows long boom fixed fin 105mm HEAT projectile. For the present purposes this can be either the T184 or the T118 projectile since the features which distinguish between them are not shown. These projectiles weigh 16.8 pounds, both will be fired at a muzzle velocity of 1700 f/s. These projectiles contain a 3.6" diameter cone incorporating a spit back tube. The fuze is of the T208 series, actuated by the barium titanate piezo electric crystal. Neither the crystal nor the base element are shown in the sectional view. Stand off is 8-1/2" and fuze time is expected to reduce this by not more than 1/8". The explosive charge is two pounds of composition B with a head of charge of 7.3". The boom is perforated and contains the primer charge for the cartridge. The projectile is fastened into the case by a retainer which acts as a shot start device rupturing in tension at 4,000 pounds pull. Spin rates at the muzzle are of the order of ten to fifteen rps. Penetration tests have been conducted with T184 type projectiles

271

105 mm RIFLE CHARACTERISTICS

Rifle nomenclature	T136	M27	T170
Projectile weight (lb)	16.8	16.8	16.8
Muzzle velocity (f/s)	1700	1700	1700
Rated max pressure (psi)	10,000	9,500	10,000
Chamber vol (cu in)	500	800	500
Charge weight (lb)	8.8	8.6	8.8
Loading density	0.5	0.3	0.5
Projectile travel (in)	98.7	98.7	98.7
(original design) (in)	88	-	-
Min yield strength of steel (psi)	150,000	125,000	125,000
Working stress (psi)	100,000	70,000	85,000
Ratio bore to throat areas	1.35	1.45	1.37
Bore diameter (in)	4.134	4.134	4.134
Bourrelet diameter (in)	4.145	4.134	4.134
Rifling depth (in)	0.005	0.037	0.037
Twist of rifling } (turns/cal)	$\frac{1}{180}$	$\frac{1}{20}$	$\frac{1}{20}$
(deg/ft.)	2.18	-	-
Bare rifle weight (lb)	185	340	220
Wt of complete mounted system (lb)	383	702	-

Figure 3—105 mm rifle characteristics.
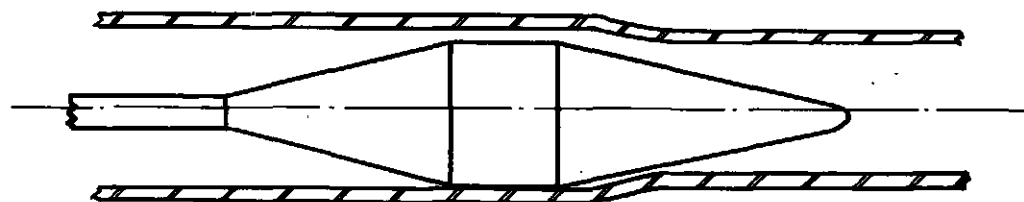
NON—COMPENSATED SYSTEM
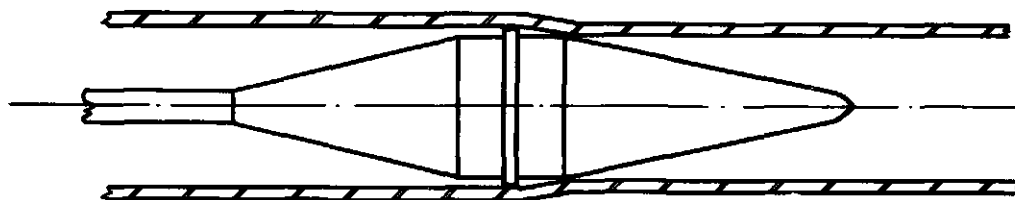
COMPENSATED SYSTEM

Figure 4—Principle of strain compensation.

272

273
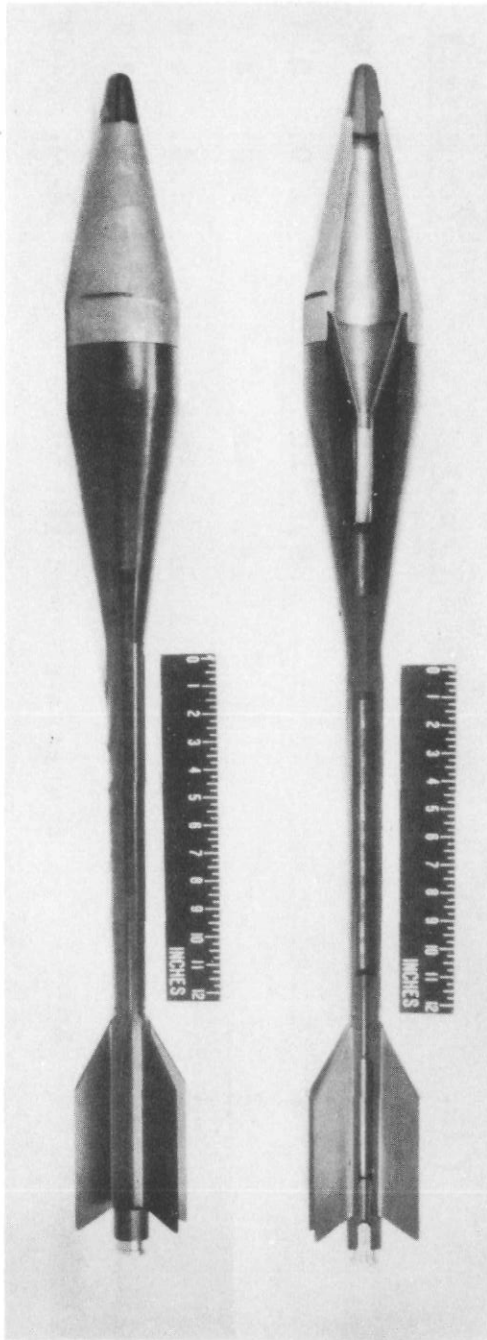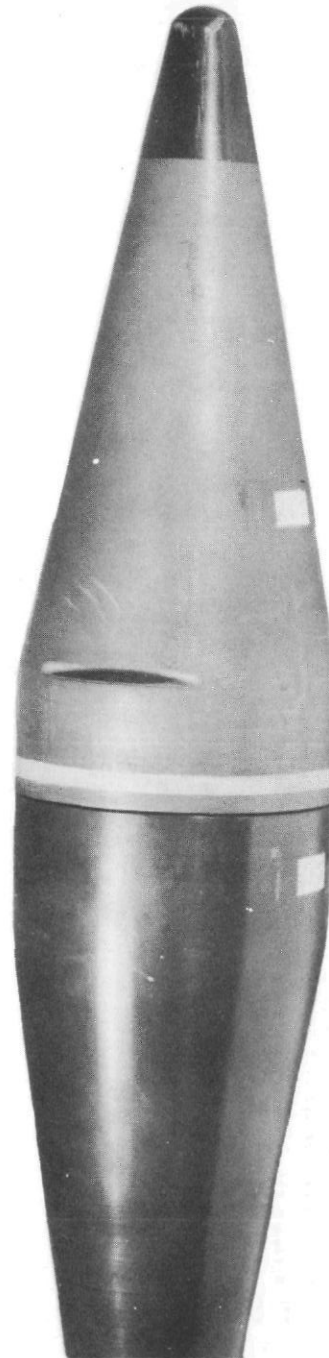
Figure 5

Figure 6—105 mm T118E18 projectile body showing plastic rotating band on bourrelet.
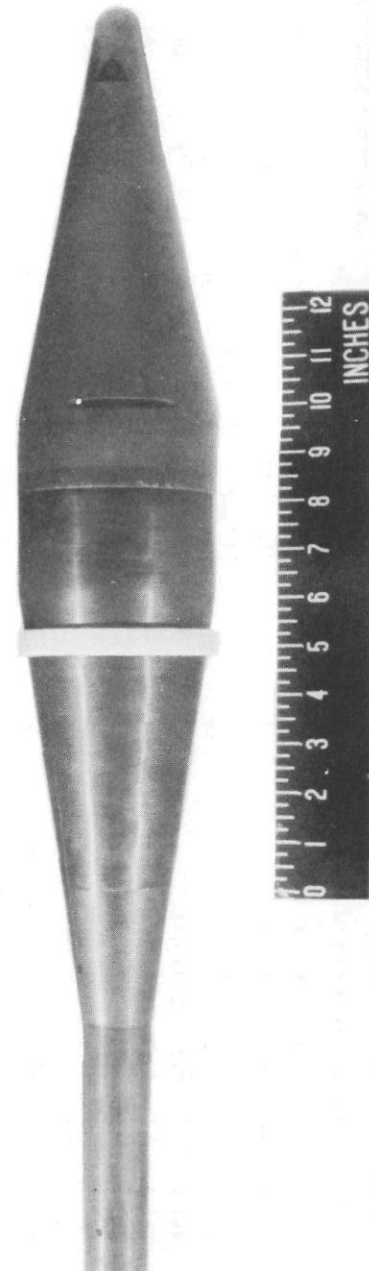
Figure 7

ACCURACY - T118 AND T184 ROUNDS

Model	Gun	Mount	Spin at muzzle		Spin at 900 yds		HPE	VPE	#Rds	Range
			deg/ft.	rps	deg/ft.	rps	mils	mils		yd
T118E2	Test	Rigid		<2		<1	.63 (.63)*	1.9 (.26)*	10 (9)*	900
T118E10	Test	Rigid		<2		<1	.61 (.24)*	.94 (.44)*	10 (8)*	900
T118E13	Test	Rigid		<2		>45	.29	.33	8	900
T118E13	T136	Rigid		<2		>45	.43	.30	12	900
T118E13	T136	T149-Gnd.		<2		>45	.28	.37	8	900
T118E13	T136	T149-Jeep		<2		>45	.37	.25	7	900
T118E13	T136	T149-Jeep		<2		>45	.44	.29 (.24)**	10	1000
T118E13	T136	T149-Jeep		<2		>45	.49	.69 (.35)**	10	2000
T118E13***	Test	Rigid		<2		>45	.35	.36	8	900
T118E11	Test****	Rigid	2.1	10	1.5	5	.26	.35	7	900
T184E2	M27	M75-Jeep		C4		>45	.63	.42		900
T184E2	M27	M75-Jeep		C4		>45	.37	.35		1000
T184E4*****	M27	Rigid	2.5	12	2.3	8.5	.18	.23	7	900

* Wild shots not considered.

** Corrected for velocity variations.

*** Pin diameter reduced by 0.040 in.

**** Rifled 0.005 in deep at twist of one turn in 480 calibers.

*****
** With ¼ in plastic band in machined seat.

Figure 8—Accuracy—T118 and T184 rounds.

SPIN RATES

TI84E3 Projectile - Plastic Rings

Ring widths (inch)	Spin rate near muzzle	
	(rps)	(deg/ft.)
none	3 to 4.5	.64 to .95
⅛	9, 10	1.9, 2.1
¼	18, 19	3.8, 4.0
½	30, 30	6.4, 6.4
½ (improperly positioned)	143, 159	30.3, 33.7
¼ (in machined seat)	11 to 13	2.3, 2.8

Figure 9—Spin rates, T184E3 projectile—plastic rings.

having straight fins and fired from the M27 Rifle so that the muzzle spin is approximately 4 rps. Five rounds fired against 15" of stacked armor at 400 feet gave complete perforations at normal impact. Five rounds fired at 9" of stacked plate at 60° obliquity at 400 ft. range gave an average penetration of 14.6", penetration ranging from 14-1/4" to 15-1/4".

The special features of the T118E18 projectile, shown in Fig. 6, are the step bourrelet and molded plastic rotating band. The step bourrelet is approximately 1/4" wide and appears at the rear edge of the ogive. Immediately ahead of the step bourrelet has been machined a shallow band seat and a plastic rotating band molded into place. This rotating band is not pre-engraved.

The T184E3 projectile, to be fired either in the B27 or T170 rifles, is characterized by a plastic ring located around the tapered portion of the body to the rear of the bourrelet. This may be seen in Fig. 7. During firing the band apparently moves forward, is engraved by the rifling, and imparts spin to the projectile by friction and slippage between the band and the projectile.

Fig. 8 shows the accuracy which has been obtained in the development of the T118 and T184 type projectiles during the program. The top two lines show the fairly poor accuracy obtained with straight fin projectiles fired from a smooth bore rifle. The accuracy targets showed what appeared to be a normally distributed group with occasional projectiles well outside of this group. The figures in parenthesis show the target sizes when only those rounds exhibiting normal distribution were considered. The T118E13 type of projectile had a 4° cant to the flipper at the rear of the fin. The average of horizontal and vertical probable errors for all of these rounds, fired over 900 of 1,000 yards range, is .335 mils. T118E11 design is similar to the T118E18 except that the body metal is aluminum; thus the last line of T118's represent firing from a barrel rifled one turn in 480 calibers. The T184E2 rounds had fins with the rear flippers canted 4°. The T184E4's in the last line of the table were fired with 1/4" plastic bands in a machined seat, as shown in a previous figure, in an M27 with a barrel rifled one in 20 calibers. Spins imparted to the projectile were approximately 12 rps at the muzzle and 8-1/2 rps at the target.

Fig. 9 shows spin rates observed near the muzzle for various widths of plastic rings. Note the 1/2" rings although cemented to the body were knocked loose in chambering the round into the gun and were fired in this condition. Note the very high rates of spin obtained. Note that 1/4" bands placed on the projectiles without a band seat and those which were held in place in a machined seat give entirely different rates of spin. The 1/8", 1/4", and 1/2" bands were properly positioned although not held there by a machined seat. Results such as these increased the mistrust of plastic rings sufficiently so that other methods of inducing spin were designed and investigated.

Fig. 10 shows a design made in accordance with principles laid out in a BRL Report by Mr. Vinte. This has been variously described as the reaction engine or broached bourrelet. The slots operate as nozzles and the passage of the chamber gas through these slots gives rise to thrust, the tangential component of which applies a torque
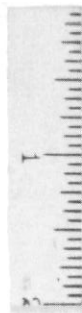
Figure 10—105 mm T184 test slug body
showing eight "reaction engines"
machined in bourrelet.

Figure 11

SPOTTING RIFLE AMMUNITION

Projectile type:	Tracer	Tracer	Spotting
Nomenclature:	T139	T139E3	T140E17
Ballistic Coeff. (C_5):	.765	.666	.423
Muzzle velocity (f/s):	1739	1825	1975
Elevation Bias (mil):	0	-1	-1
Missmatch at 200 yd (mil):	.13	-.55	-.22
" " 400 yd (mil):	.20	-.25	.38
" " 600 yd (mil):	.19	-.02	.59
" " 800 yd (mil):	.09	.06	.40
" " 1000 yd (mil):	-.12	-.02	-.38

Ballistic coeff. of T118 or T184, C_1 = 1.47 $(C_5 \tilde{=} .98)$

Figure 12.—Spotting rifle ammunition.

277

to the projectile. The one shown in the figure incorporates eight such engines around
the bourrelet. No appreciable degrading of performance has been observed in the
firing of these projectiles. Brief tests in the M27 Rifle showed that the desired
spin can be imparted by this method.

A second method for imparting spin in the M27 is shown in Fig. 11. This is
described as the knurled bourrelet or the turbine type. This type operates because
the gases flowing past the bourrelet inside the grooves of the barrel expand into the
knurl and impact angular momentum to the projectile as they strike the surfaces of the
knurl. Analytical studies of this method have resulted in several additional designs
intended to give a range of spin rates. The design shown here has given a one point
check of the analysis.

Experiments with both of these methods of inducing spin within the gun are in the
early stages and will be continued until a definite conclusion can be reached. The
minimum rate of spin which must be imparted to the projectile within the gun in order
to give good accuracy has not been definitely determined, although present indications
are that the spin of $2.18°$ per foot (10 rps) will give good accuracy up to 1,000 yards.
Whether the spin will decay sufficiently to give poor accuracy at 2,000 yards has not
been determined.

A portion of the BAT development program is the spotting device, consisting of a
caliber .50 semi-automatic rifle, tracer cartridge, spotting cartridge, and combined
spotting-tracer cartridge. A tracer cartridge and several spotting cartridges have
been developed. Fig. 12 shows the matching characteristics of several bullets. The
first column represents a tracer with insufficient length of trace. The second column
is a satisfactory tracer bullet. The third column is one of the spotting bullets.
The low ballistic coefficient is undoubtedly due to large yaw of the bullet in flight.
It is believed that the design can be made to eliminate yaw and maintain the good
functioning characteristics upon impact. A combination tracer-spotting bullet is
under development and will probably supplant the separate bullets. The effect of such
large mismatch as shown for the T140E17 bullet is not now completely determined, but
may be sufficiently large that this bullet will be useless at this stage of the
development.

DESIGN VARIABLES AFFECTING THE PERFORMANCE OF THE BAT HEAT ROUND[*]

Earl W. Ford

Defense Research Division, The Firestone Tire and Rubber Company, Akron, Ohio

ABSTRACT

This paper discusses some of the factors investigated in the development of a HEAT round for the BAT project.

Some of the factors investigated are: cone angle, stand-off flange effect, target material, effect of interference, cone shape, wires through cone, base element location, temperature effect, spit back tube length, cone wall thickness, cone material, constant head versus constant volume, and confinement. The more pertinent factors will be discussed.

Firestone has adopted a 42° cone, pressed from sheet copper, having no flange and a short spit back tube, with a wall thickness of .100 inch for use in the T-138 HEAT rounds. This round is to be fired at 25 r.p.s. The design of this round is explained in detail.

Time has not permitted carrying each investigation to the ultimate and hence the data are in many cases only indicative of the trends. Work is continuing on certain features in order to be more specific as to the optimum conditions.

As part of the development of a BAT weapon it has been necessary to study many variables which would effect the performance of a HEAT round. The effect of spin rate on the several variables was unknown and hence had to be studied. It is felt that the results of the various tests can best be summarized in tables and graphs. In practically all cases the data given represents the average of at least five tests.

The variables will be discussed in an order which is not necessarily that of importance. Certain data are common to all rounds to be reported: The liners were turned from copper bar stock purchased to government specification QQ-C-501a. All rounds were fired from cylindrical bodies. In part of the program the cylinders were T-138 bodies and later a slightly less complicated body was developed for use as a test body. Data will be presented to show that the results obtained with the two body types were comparable.

---

[*] Data Obtained at BRL and ERIE
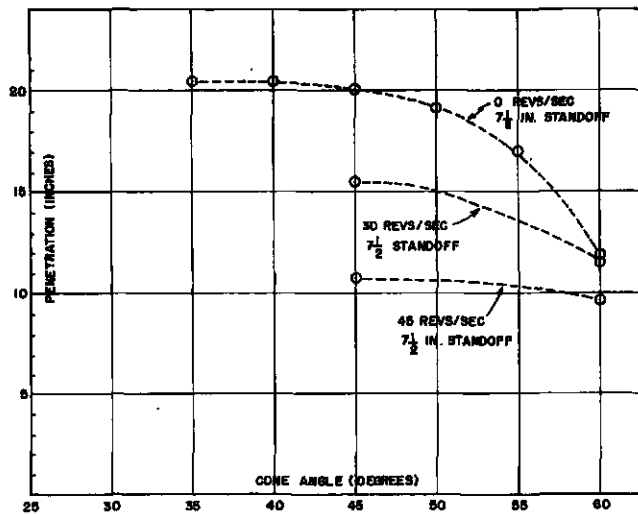
Figure 1—Penetration as function of
cone angle.
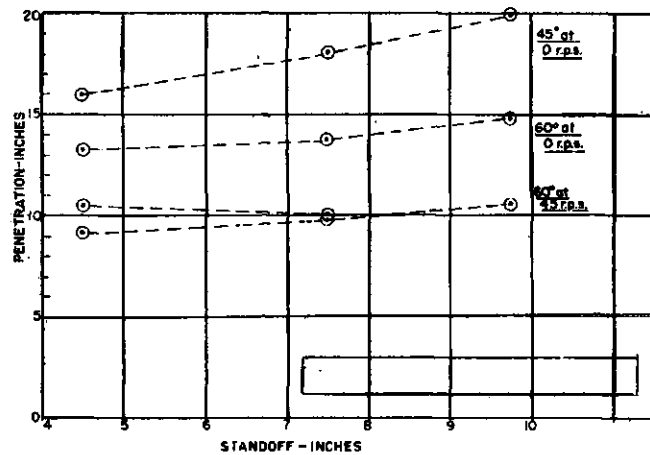
Figure 2—Penetration as function
of standoff.
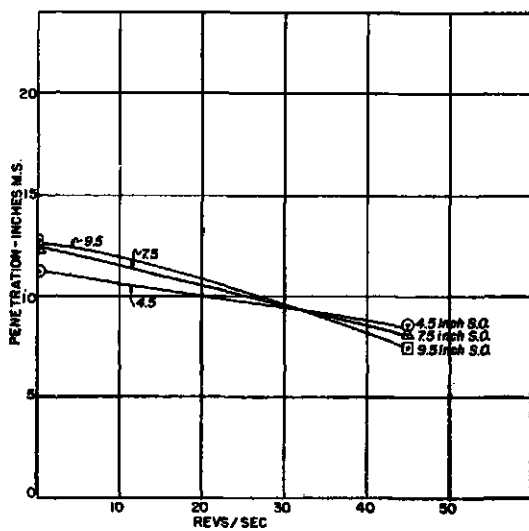
Figure 3
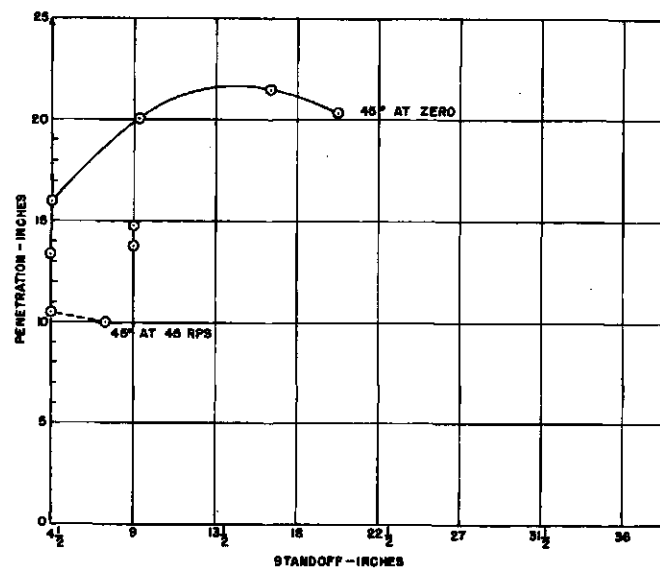
Figure 4—Penetration as a function
of standoff.

280

TARGET MATERIALS		
MATERIAL	SPIN RATE	PENETRATION
BOILER PLATE	0	18.0
ABERDEEN TARGET PLATE ALTERNATED WITH BOILER PLATE	0	17.9
ABERDEEN TARGET PLATE	0	17.5
ABERDEEN TARGET PLATE ALTER-NATED WITH BOILER PLATE	0	17.0
BOILER PLATE	25	14.9
HOMOGENEOUS ARMOR PLATE	25	14.1
ABERDEEN TARGET PLATE	0	18.7
HIGH QUALITY ARMOR PLATE	0	16.0
ABERDEEN TARGET PLATE	45	10.7
HIGH QUALITY ARMOR	45	9.4

Figure 5—Target Materials.

DRC 224
(A)

DRC 230
(B)

DRC 314
(C)
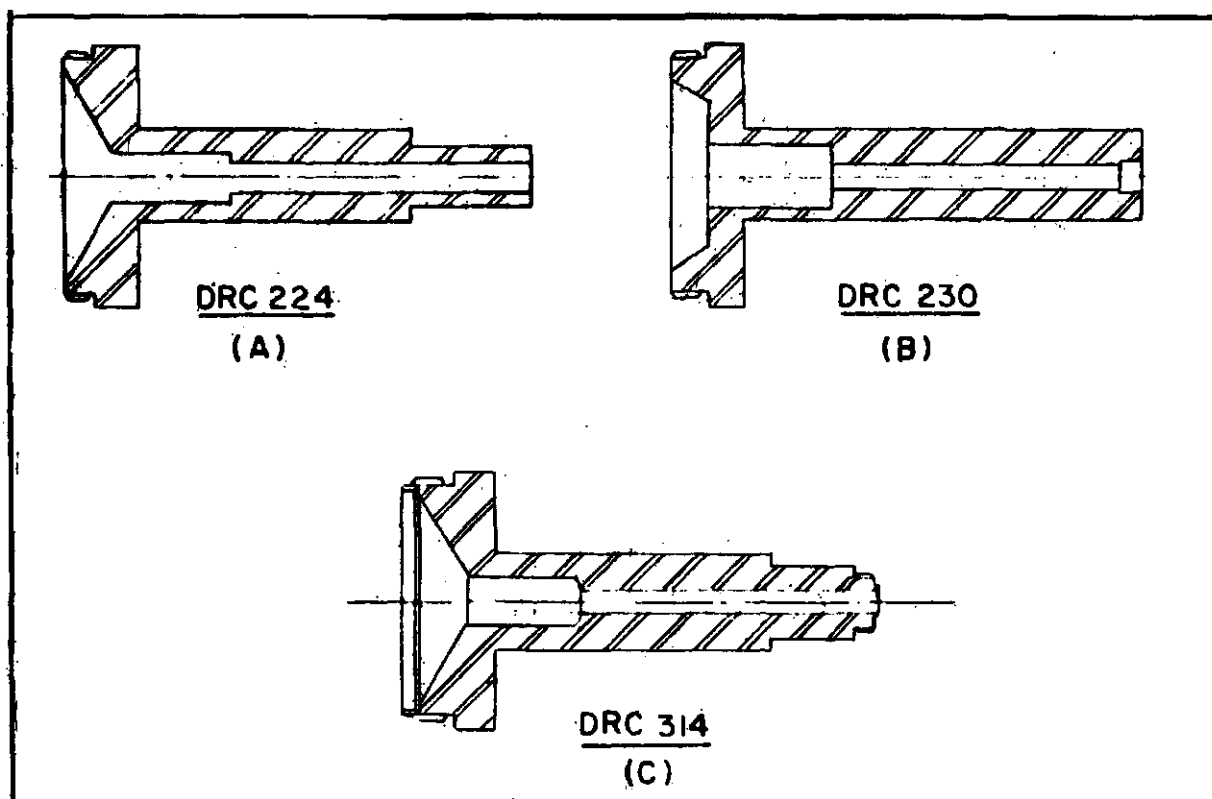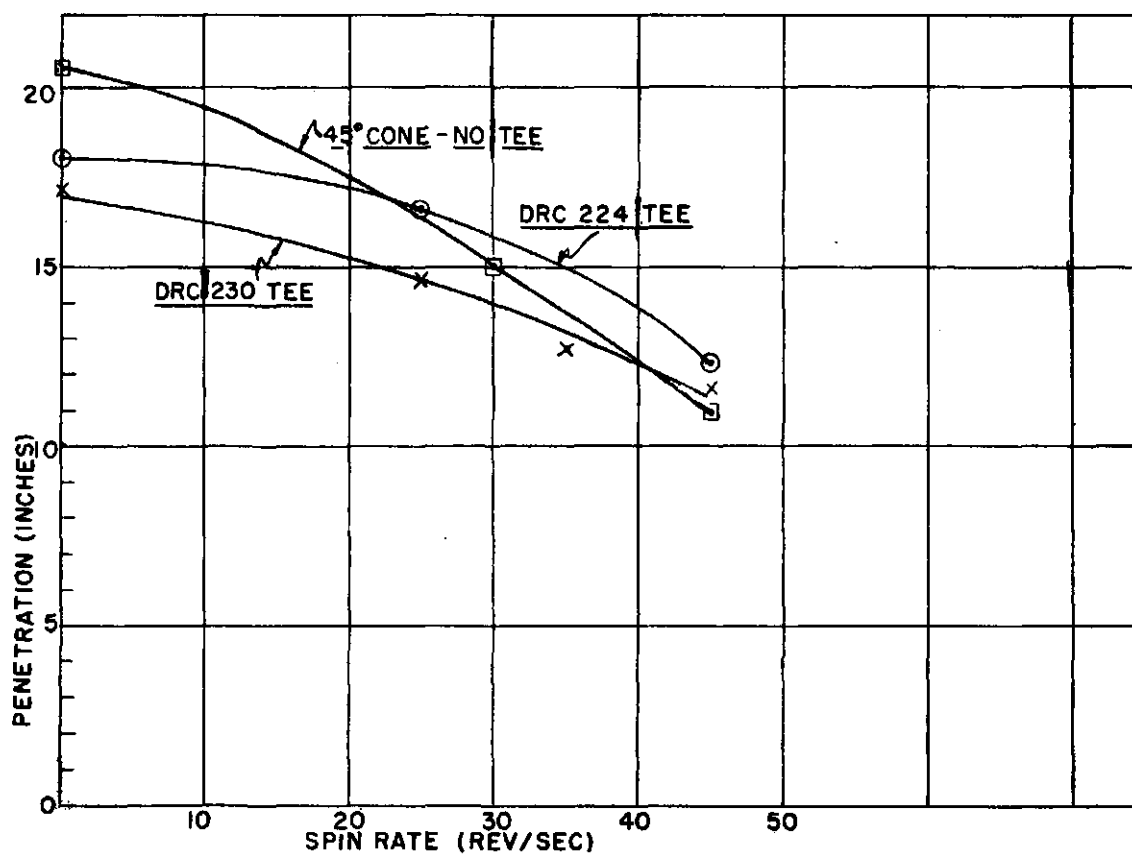
Figure 6

Figure 7

It is obvious that cone angle would affect the penetration obtained. Consequently a program to study the effect of cone angle on penetration at various spin rates was carried out. Figure 1 shows a summary of the data. It should be remarked here that 30° and 25° cones have been made but have not been fired. From the data available it is apparent that a cone angle of approximately 42° is optimum for the 105mm shell of the T-138 type. A consideration not readily apparent is the overall length of the cone and hence the shell body. It is fortunate that the optimum cone angle was 42° since the T-138 projectile body as finally developed would not have accomodated a much longer cone. The effect of cone angle apparently is much less pronounced at higher spin rates.

Another important consideration in the development was the effect of stand-off distance on penetration. Figure 2 shows the effect of practical point detonated fuze standoff distance on penetration for two cone angles at two spin rates, when using copper cones. Figure 3 shows the results for 45° steel cones. Figure 4 shows the penetration obtainable at higher standoff distances. These standoff distances would require something other than a point detonated fuze. The data shows that the standoff distance has an effect on penetration which becomes quite pronounced for 45° cone angle at the lower spin rates. It is also evident that extremes of standoff distance do not result in greatly increased penetration.

A comparison of penetration through mild steel plate and homogeneous armor plate was made. Figure 5 shows the results obtained. It appears that for slowly spinning projectiles the difference in penetration is in the neighborhood of 5% whereas for zero spin rate the difference is about 15%.

Since the T-138 projectile has a large mass of steel in front of the shaped charge it was necessary to find whether the tee would adversely affect the penetration. Some preliminary work at the Ballistics Laboratories using aluminum tees having 1/4" and 1/2" diameter holes had shown that the hole had to be at least 1/2" in diameter. The question of the relief immediately in front of the cone became of importance in terms of the location of the center of gravity of the rounds. After preliminary firings had shown the necessity of considerable relief the interior tee configurations shown in Figure 6a, b, were tested. As a result of the data from these tests the interior tee configuration chosen is that shown in Fig. 6c. The data for the two tees tested and for rounds having no tee are shown in Fig. 7. It is seen that with DRC-224 tee configuration the penetration is essentially as good as with no tee. The design being adopted Fig. 6c is certain to be no worse than DRC-224.

Certain projectiles used by foreign countries were known to have liner shapes other than the conical shape that is standard in this country. Certain special liner shapes as shown in Figure 8 were tested. Figure 9 shows in tabular form the results of these various rounds as compared to the 45° cone. The data are incomplete as to spin rate and standoff distance but clearly indicate that the conical shape is superior to any others tested.

The effect of the booster being buried beneath the rear surface of the Comp B was investigated. In the original test rounds the tetryl booster was placed in the metal plug just tangent to the rear surface of the Comp. B. In the actual round, it is
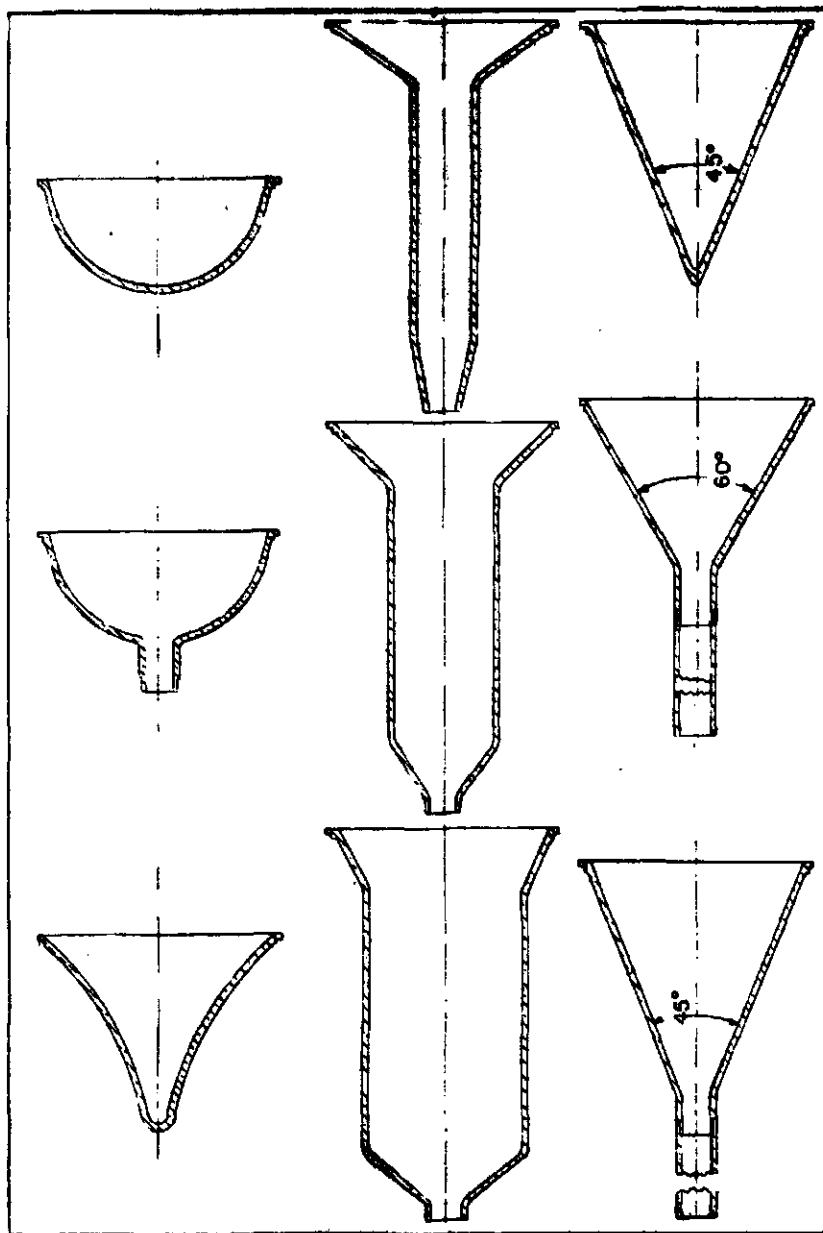
Figure 8

LINER SHAPE DATA			
LINER TYPE	SPIN RATE (R.P.S.)	STANDOFF (IN.)	PENETRATION (IN.)
SEMI-CYLINDRICAL 2.5 IN. O.D.	0	$7\frac{1}{2}$	7.25
SEMI-CYLINDRICAL 1.75 IN. O.D.	0	$7\frac{1}{2}$	11.86
SEMI-CYLINDRICAL 1.00 IN. O.D.	0	$7\frac{1}{2}$	9.55
HEMISPHERE NO SPITBACK	0	7½	8.51
	30	7½	7.68
	0	11½	9.60
TRUMPET	0	7½	9.72
	30	7½	8.73
	0	11½	8.64
45° CONE	0	7½	19.4
	30	7½	13.4
	45	7½	9.4

Figure 9—Liner shape data.

EFFECT OF BOOSTER LOCATION

BOOSTER LOCATION	STANDOFF (inches)	PENETRATION (inches)	CONDITIONS
In base plug	7½	17.33	
In Comp. B	7½	17.16	Maple plug in base plug
In Comp. B	7½	17.44	Steel in base plug
Booster Embedded $\frac{5}{8}$"	7½	17.55	Simple Cone
Booster in base plug	7½	16.67	Simple Cone

Figure 10—Effect of booster location.
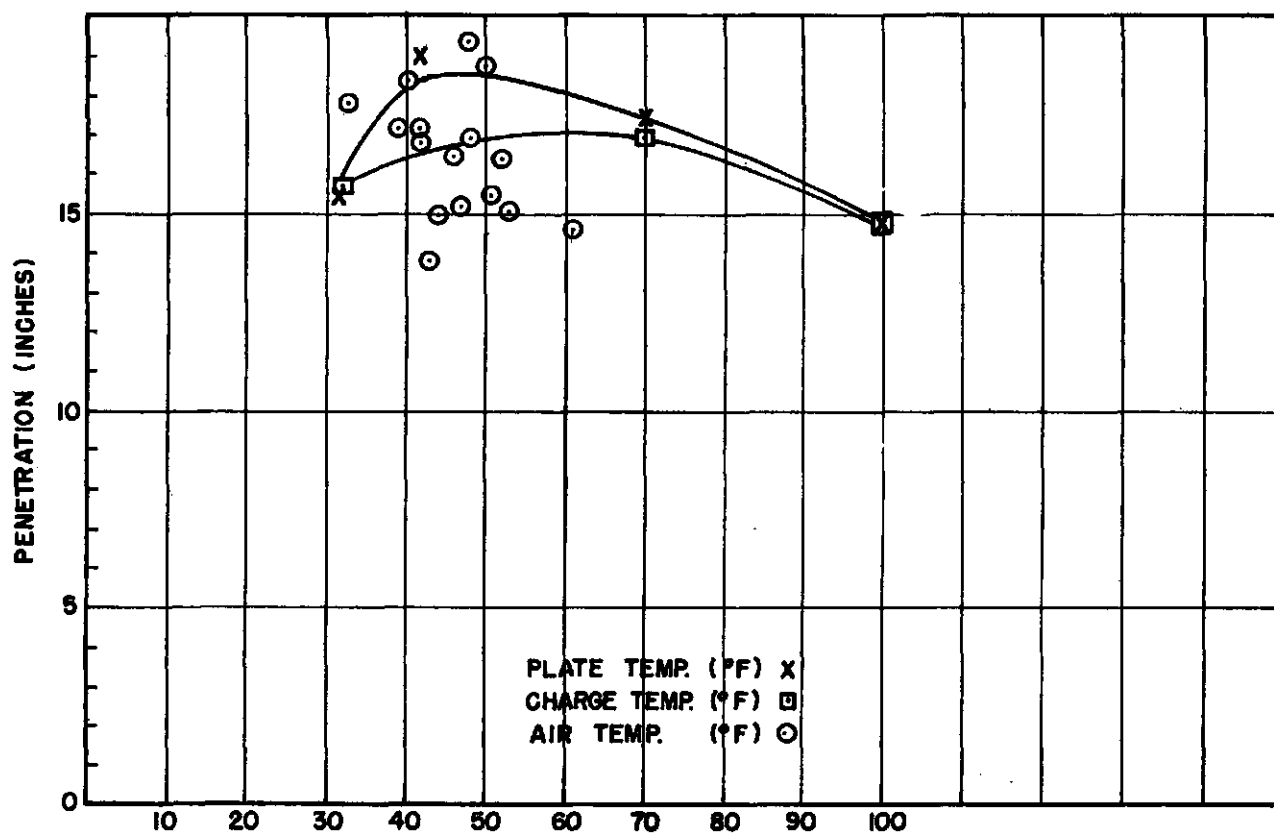
Figure 11

SPITBACK TUBE LENGTH	
CYLINDRICAL TEST BODIES DRC 15-6 NON-ROTATED, $7\frac{1}{2}$ IN. STANDOFF	
SPITBACK TUBE LENGTH (IN.)	PENETRATION (IN.)
0	17.33
1.25	17.50
2.40	17.80

Figure 12—Spitback tube length.
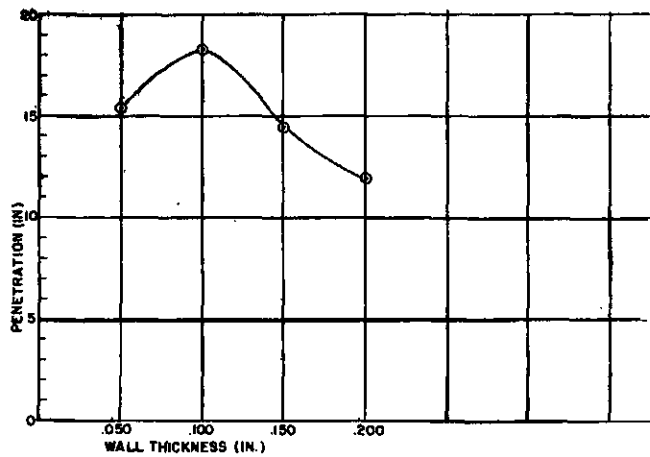
Figure 13
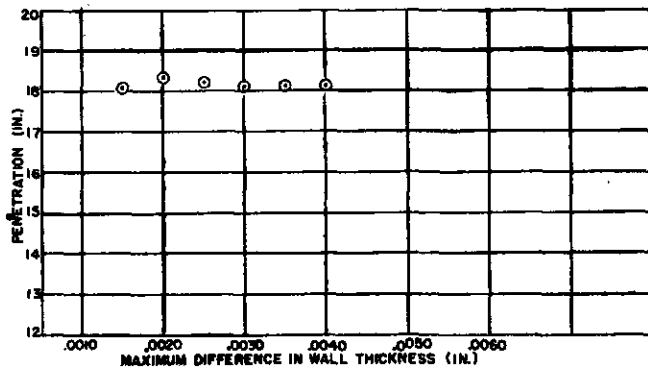
Figure 14

Figure 15

286
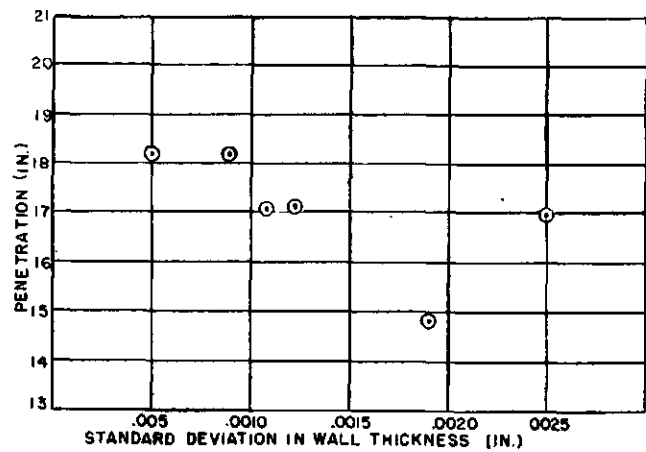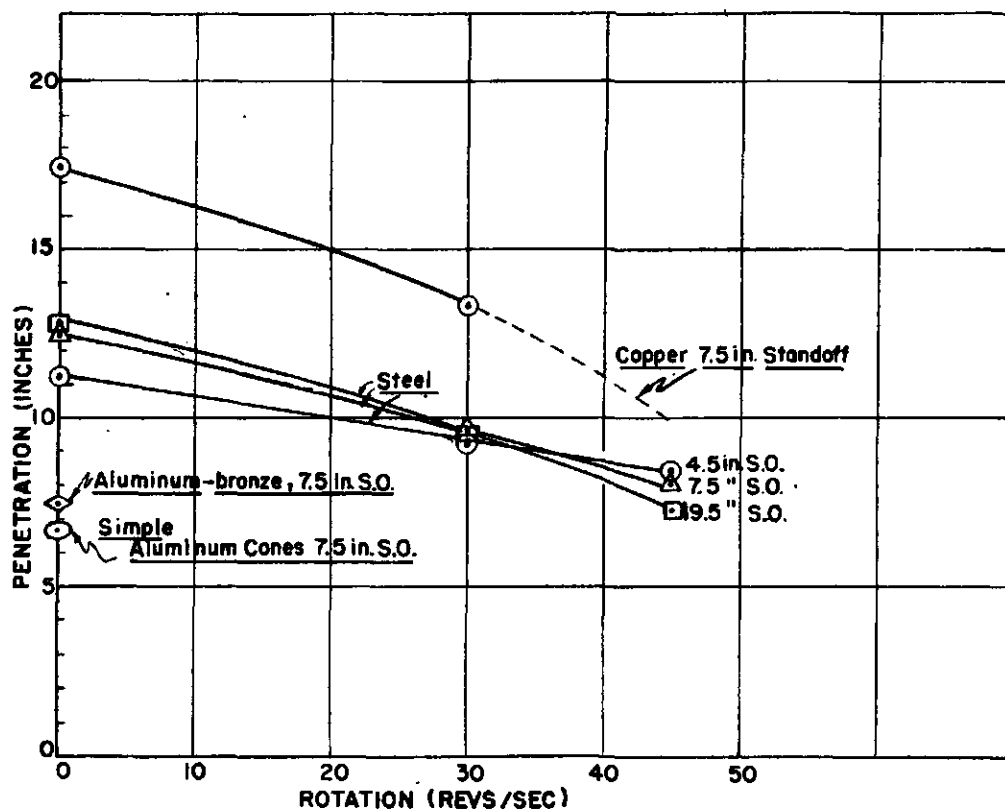
Figure 16

CONFINEMENT-TEST BODIES				
BODY TYPE	SPIN RATE (r.p.s)	STANDOFF (in)	CONE ANGLE	PENETRATION (in.)
T-138	0	7½	45°	17.4
T-138	0	7½	45	18.7
T-138	45	7½	45	10.7
Test Cylinder	0	7½	45	17.3
" "	45	7½	45	10.0
T-138	0	7½	60	14.4
T-138	45	7½	60	9.6
Test Cylinder	0	7½	60	13.8
" "	45	7½	60	9.8

Figure 17—Confinement—Test Bodies.

RING "A"

with pilot ring

with pilot ring removed

shows ring
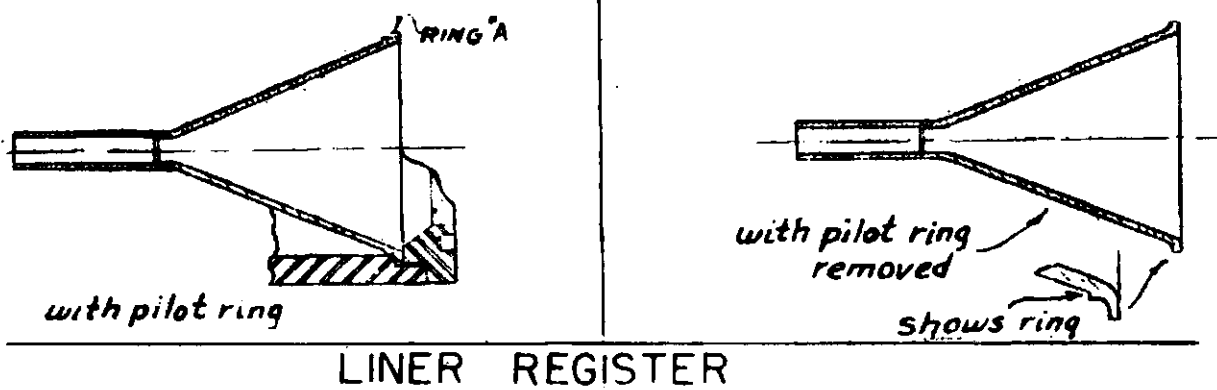
LINER   REGISTER

LINER	SPIN RATE r.p.s.	STANDOFF (in.)	PENETRATION (in.)
STD. 45° Cu.	0	7½	19.26
45° MODIFIED	0	7½	19.98

Figure 18—Liner Register.

necessary to have the tetryl booster buried in the Comp B due to the size of the fuze base element. Several experiments were run under slightly different conditions which indicate that the booster can be ahead of the rear surface of the Comp. B by as much as 1.0 inch without serious impairment of the penetration. Figure 10 shows the results in tabular form.

The effect of the temperature of the high explosive, the target material and the ambient temperature was investigated at considerable length. Figure 11 shows the results. The general conclusions are, that over the temperature range investigated, the penetration is not a function of the temperature of the Comp. B of the target plate or of the ambient temperature.

At the outset of the program a spitback type fuze was anticipated in order to get superquick action to take advantage of as much standoff distance as possible. Consequently, the cones were built with a spitback tube extending back from the apex of the cone to the location of the tetryl booster. When other types of fuzes became available the suggestion was made that the spitback tube be eliminated. Certain data had indicated that some type of inert material back of the apex of a simple cone produced an improvement in penetration. Hence, a series of tests using different lengths of spitback tube were carried out. Figure 12 shows the data from this test. Within the experimental error there is only slight reason for using a spitback tube.

The effect of cone wall thickness has been investigated in two ways. First from rather drastic changes in nominal wall thickness, using .050", .100", and .200". Rounds of each thickness were fired at each of three standoff distances for zero spin and, at one standoff distance, at 45 rps. The data are shown in Figure 13 and show only that there is a maximum between .050" and .200". Using data from other tests on cones of .150" wall thickness it is apparent that the optimum penetration is obtained with a wall thickness of .100 inch. The Second study on cone wall thickness involved the effects of variations in the wall thickness of a given cone. Figure 14 shows a plot of the penetration as a function of the maximum difference in wall thickness and Figure 15 shows penetration as a function of standard deviation in wall thickness. It is evident from these data that within the limits of variation involved the penetration is independent of either variable.

Investigations were made to study the effect of various liner materials. Figure 16 shows the data available. It is quite evident that copper cones are definitely superior to any other materials used.

Another factor which has been investigated is the effect of the wall thickness of the test body or projectile on penetration. The available data are shown in Figure 17. As far as the comparison of T-138 test projectile bodies as compared to the regular penetration test body - the performance is essentially equal. Further work is in progress.

The effect of non-concentricity of the cone axis and projectile body has been the subject of repeated discussions. A series of rounds were modified in that the register on the cone was removed. This resulted in the axes of the cone and test body being non-coincident by as much as .003 inches. For this amount of eccentricity the data shows little or no effect. Figure 18.

SUMMARY

1. A cone angle of approximately 42° has been found to be optimum.

2. A standoff distance of 7 1/2 inches is found to be practical both from the penetration and from the projectile design viewpoints.

3. At spin rates in the vicinity of 25 rps the difference between penetration in armor plate and mild steel is about 5%. At zero spin the difference is about 15%.

4. A tee design for the T-138 projectile has been found which satisfies the flight characteristics and the penetration requirements.

5. A conical shaped liner has been found to be the best for use in the project.

6. The fact that the booster charge is buried beneath the surface of the Comp. B has not been found to be deleterious.

7. The temperature of the Comp. B, target or the air does not affect the penetration over the range investigated.

8. The use of a spitback tube on the cone appears entirely optional.

9. A cone wall thickness of .100 inch appears to be optimum.

10. Copper has been proved to be the optimum liner material. ✓

11. The cone must be fairly concentric with the body, but variations of .003 inches does not materially affect the penetration.

APPLICATION OF THEORY TO DESIGN

Norman Rostoker

Carnegie Institute of Technology, Pittsburgh, Pennsylvania

ABSTRACT

The scope of the discussion will be limited to the design of hollow charges with metal cone liners. Design parameters that will be considered are material, geometry, and confinement of the explosive, and material and geometry of the liner. Performance will be assessed on the basis of penetration depth, hole volume, and hole shape.

Several specific charge designs and their observed performance will be described. On the basis of these examples an attempt will be made to evaluate the guidance afforded by theory, in its present status to the design of shaped charges. The extent to which further developments in theory may assist in predicting performance from design parameters will be considered for the purpose of clarifying research objectives.

At the outset, it is appropriate to consider to what extent physical theory based on representations may be of assistance in the design of shaped charges. There are limitations to the accuracy with which liners and charges can be manufactured to design specifications. Such limitations are hardly unique to the shaped charge problem, but perhaps unique in relative importance. A good illustration of the effects of these limitations is provided by the comparison of penetration-standoff curves[1] in Fig. 1. The two curves were obtained for two lots of cones of identical nominal design specifications cast into supposedly identical charges of 50/50 pentolite. The reasonable agreement of penetrations for low standoffs lead one to believe that such penetrations could be predicted from the nominal charge design. However for large standoffs it is unlikely that any theory will be of much assistance in predicting even the average penetration. In many aspects shaped charge performance, charges that are supposed to be stereotyped turn out to be individuals. The approach to the problem of shaped charge design is consequently twofold.

(1) By means of physical theory based on representations which embrace nominal charge design parameters we should attempt to predict those aspects of performance which experiments indicate to be determined by nominal design.

(2) Many aspects of shaped charge performance are observable, but not predictable from charge design. It is necessary to track down the causes of charge individuality in order to minimize them and increase the class of predictable variables in performance.
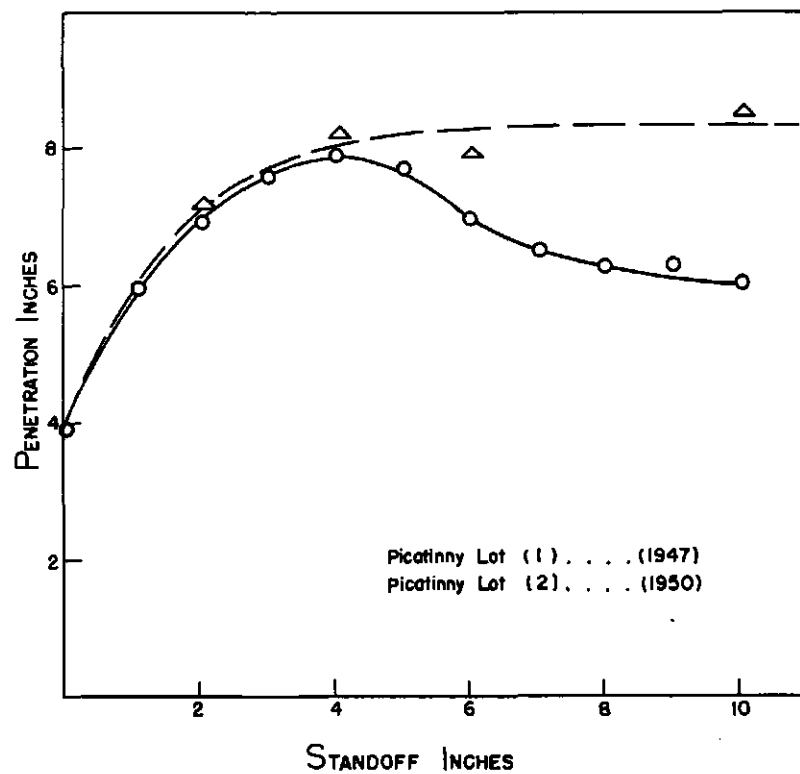
Figure 1—Comparison of two lots of cones
of identical nominal design.

CHARGES : Cast 50/50 pentolite with tetryl boosters.

LINERS : M9AI copper ; thickness .037" ; apex angle 44°
base diameter 1.63".
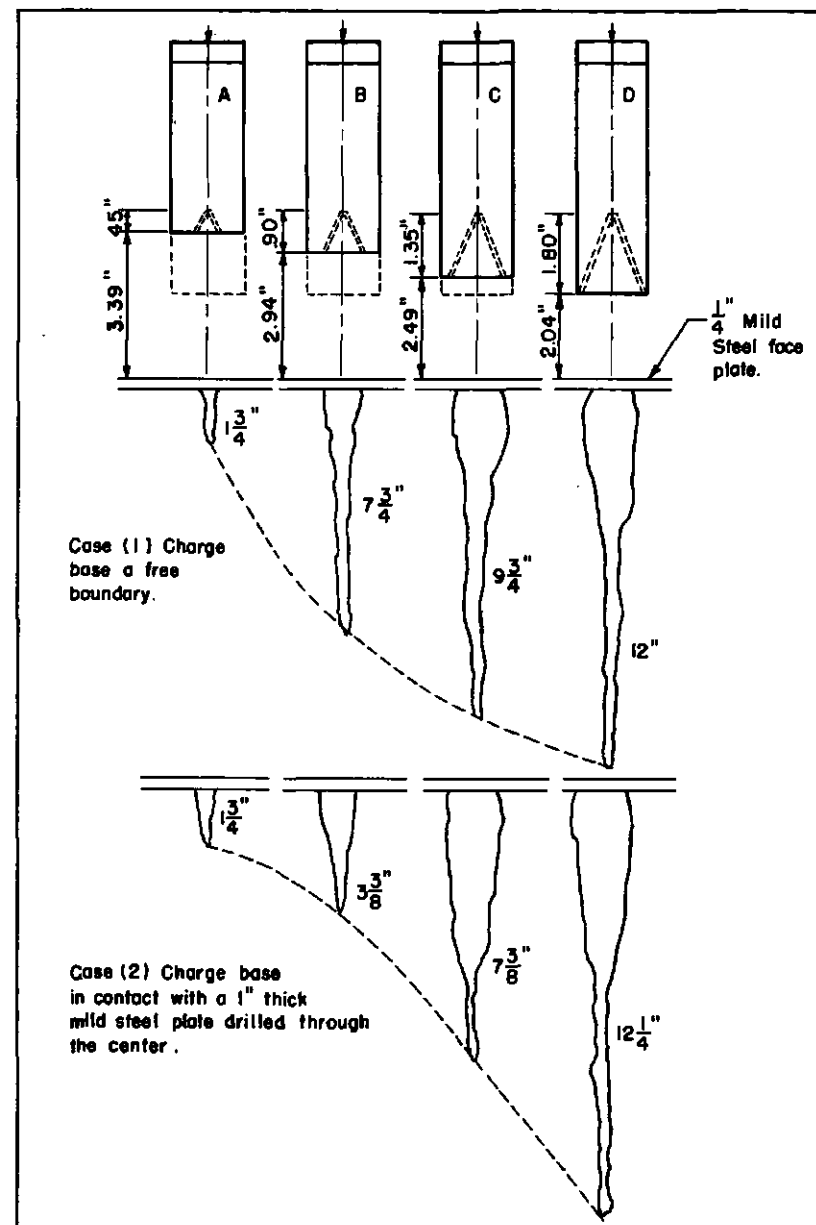
Figure 2—Penetration produced by M9A1
cone-section charges in 2-S aluminum.

In this discussion we shall be concerned principally with the present status of the first approach. As yet the theory of shaped charges contributes little quantitative assistance to design. The main reason for this is that we do not yet have an adequate quantitative understanding of the dependence of the velocities and directions of liner elements upon the geometry of the explosive. However, we do have an apparently sound qualitative understanding that has developed from extensive experimental studies and theoretical investigations of over-simplified representations such as have been carried out by the group at N. Y. U. This claim best be supported by considering several specific charge designs.

1. Cone Section Charges[2/]

When the charge base is a free boundary as in Case (1) of Fig. 2, the penetrations produced by charges B and C are considerably larger than we should expect similar sections to produce when they are part of the full cone. The velocity gradient in a jet is principally due to the rarefactions from the charge boundaries which reduce the pressure acting on the liner and consequently the ultimate collapse velocity attained by liner elements. The ultimate collapse velocity attained by any liner element depends on the mass per unit area of the element and its location with respect to the boundaries of the charge. Elements near the cone base for a standard charge design such as charge D, are closer to a charge boundary and attain an ultimate collapse velocity that is less than the ultimate collapse velocity of elements near the cone apex. The relative magnitudes of velocities of the corresponding jet elements are similarly disposed. In terms of these ideas the behaviour of cone section charges may be understood.

We shall compare the cone section in charge B with an identical section of the liner in charge D. In charge B the rarefaction from the charge base reduces the pressure acting on the liner. The pressure decay is more rapid for basal elements. From the point of view of the same cone section in charge D, the rarefaction from the base has been postponed by the presence of the rest of the charge so that the pressure on the basal liner elements of the cone section should decay less rapidly. Therefore we expect the cone section in charge B to have a greater velocity gradient and produce greater penetration than its counterpart in charge D. Similar remarks apply to the cone section in charge C.

The essential correctness of this explanation may be tested by placing a mild steel plate in contact with the free boundary at the base of charge B. Then a weak compression shock will reflect back into the detonation products, followed by a rarefaction which begins when the steel plate starts to move. In general the pressure near the base will decay much more slowly than it would if the boundary were free, because the steel plate moves slowly compared to the escape velocity of the detonation products. The result is that the jet from charge B has a smaller velocity gradient and produces less penetration as may be seen in case (2) of Fig. 2.
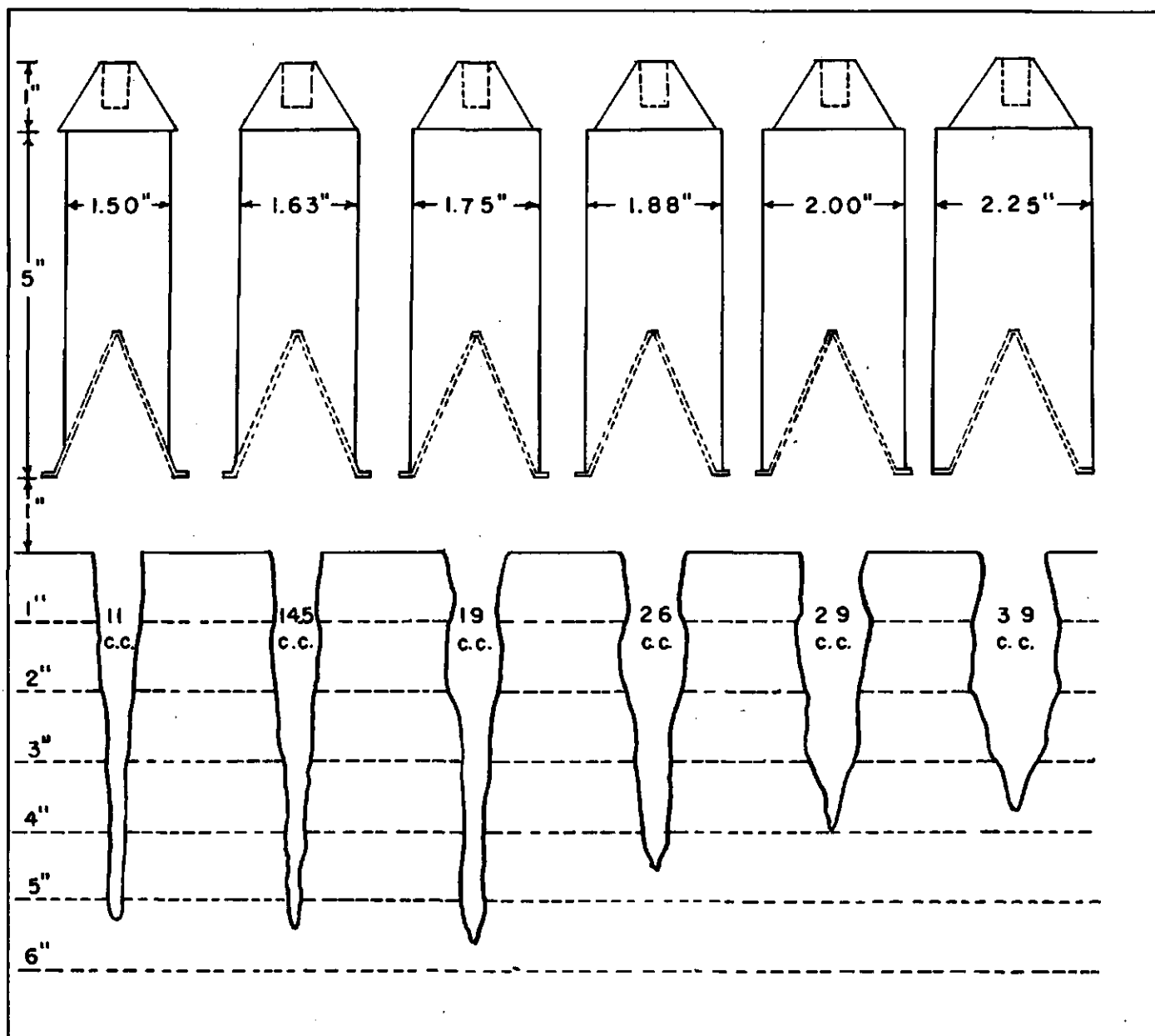
Figure 3—Profile diagram of charges of various diameters and penetrations
produced in mild steel targets.

CHARGES: CAST 50-50 PENTOLITE WITH CYCLOTOL BOOSTER

LINERS: M 9A1 STEEL; THICKNESS .036"; APEX ANGLE 44°;

                           BASE DIAMETER 1.63"
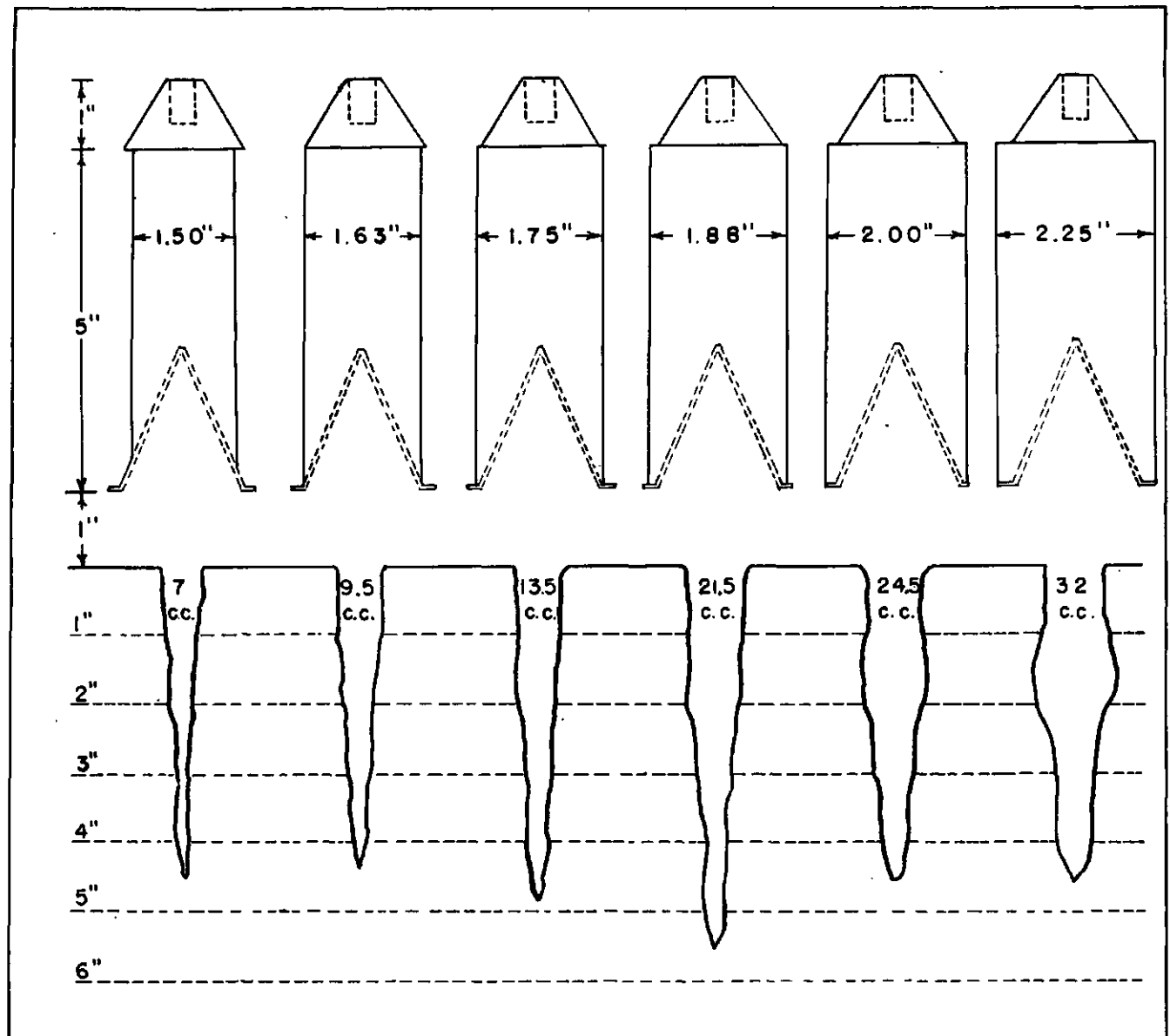
Figure 4—Profile diagram of charges of various diameters and penetrations
produced in mild steel targets.

CHARGES: Cast 50-50 pentolite with cyclotol boosters

LINERS: M-6 steel; thickness .062"; apex angle 42°,

base   diameter 1.63".

295

2. Control of Penetration and Hole Volume by Explosive Diameter

Consider first the case of a $44°$ steel cone with an .037 in. wall thickness for which experimental results obtained by duPont investigators[3] are shown in Fig. 3. The penetration as a function of charge diameter has a maximum for a diameter of 1.75 in. which is slightly greater than the 1.63 in. base diameter of the liner. For charge diameters less than 1.75 in. the basal elements of the cone receive insufficient impulse from the explosive to form a useful jet. By increasing charge diameter the basal elements of the jet are not wasted and the penetration increases up to an optimum charge diameter when the cone is efficiently employed and the velocity gradient of the jet is a maximum. Further increase in charge diameter reduces the penetration because the resultant increase in impulse delivered to the basal elements decreases the velocity gradient in the jet. The hole volume produced is a monotone increasing function of charge diameter.

Additional results of duPont investigators for $42°$ steel cones of wall thickness of .062 in. are shown in Fig. 4. The interpretation is essentially the same. In this case the optimum charge diameter is 1.88 in. instead of 1.75 in. in which case the maximum penetration is the same as for .037 in. cones. The reason for this is that the .062 in. liner has a greater mass per unit area and requires a greater impulse to achieve the same velocity. The hole volume is once again a monotone increasing function of charge diameter.

The performance of the above charge designs can easily be understood from our qualitative notions about the rarefactions from the charge boundaries. Rarefactions proceed in from the free boundaries of the charge and reduce the pressure acting on the liner. If the belt of explosive around a section of the liner is narrow the pressure decays rapidly and the impulse imparted to the liner is correspondingly low. Optimum penetration is achieved when the cone is employed efficiently in that the basal elements are not wasted, and when the jet has the maximum velocity gradient. The hole volume is a monotone function of the total kinetic energy of the jet so that it increases monotonely with the impulse imparted to the liner.

3. Confined Charges

If the free boundaries of the liner are covered with any confinement material that provides inertia, the confinement material moves slower than the escape velocity of the gas. The expansion and consequent decay of pressure at the liner by rarefaction waves is retarded. For design purposes, the addition of confinement tubing is essentially equivalent to increasing the explosive diameter. An increase or a decrease of penetration may be produced depending on whether the original charge diameter is less or greater than the optimum diameter. The hole volume of course increases with confinement.

The effects of confinement are illustrated in Fig. 5 which is a reproduction of duPont[4] data. The charge diameter is 1.63 in. which is slightly less than optimum for .037 in. cones. The .75 in. confinement tube is equivalent to an increase in charge diameter of more than .25 in. so that a decrease in penetration results from
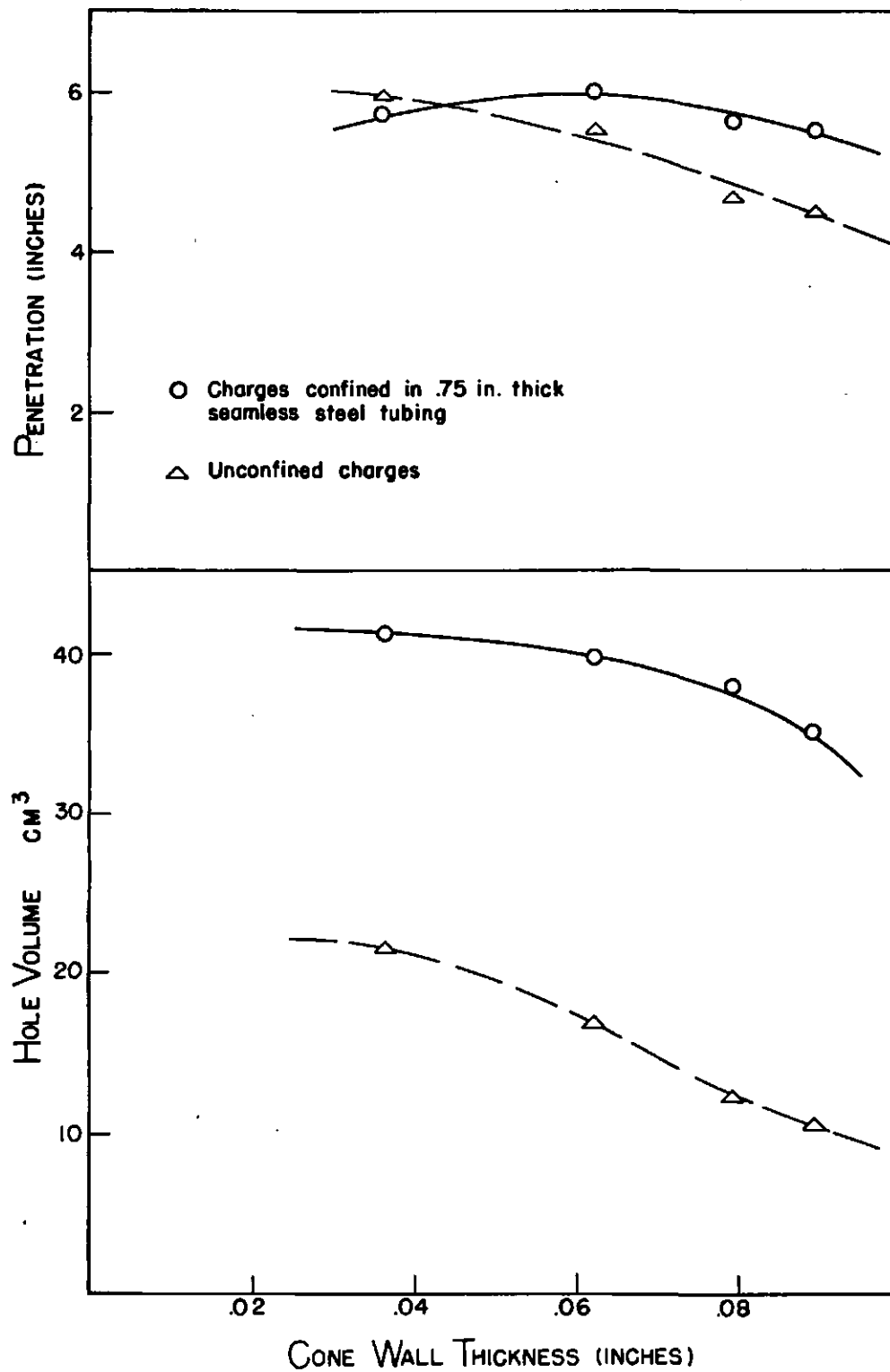
Figure 5—Effects of confinement on penetration and hole volume produced by 44° cones and 50/50 pentolite charges in mild steel.

confinement. Charges for the thicker cones are also 1.63 in. in diameter which is considerably less than optimum. The confinement tube is equivalent to an increase in charge diameter which increases the penetration.

Although the present status of the theory is such that it can only provide qualitative assistance in the design of shaped charges, it is clear from the above examples that even this much assistance permits us to exercise a considerable degree of control over penetration and hole volume by suitable charge designs.

The hole volume can be increased to any desired magnitude by increasing the amount of explosive, adding confinement, choosing an explosive of higher detonation pressure, or a combination of all three. The penetration at a given standoff and for a given liner material is limited by an optimum that is achieved when the basal elements of the cone are efficiently employed, and the jet has a maximum velocity gradient. The optimum penetration may be achieved by adjusting the charge diameter, adding confinement, varying liner thickness, or by a combination.

It is anticipated that current work on the dependence of velocities and directions of liner elements upon explosive design will eventually make possible quantitative application of theory to design. Quantitative success in the application of theory to design will be always limited by the accuracy with which design specifications can be met. However, there is much to be gained in the appreciation of the possibilities and limitations of shaped charge applications by attaining the quantitative understanding of the collapse process that mathematical analysis of realistic representations can provide.

BIBLIOGRAPHY

1/ CIT-ORD-32   April 30, 1951

2/ CIT-ORD-23   October 31, 1949

3/ Theory and Application of the Cavity Effect; May, 1943, Contract W-670-ORD-4331; E. I. duPont de Nemours and Co., Inc.

4/ Theory and Application of the Cavity Effect; March 1943, Contract W-670-ORD-4331; E. I. duPont de Nemours and Co., Inc.

FOREIGN DEVELOPMENTS IN SHAPED CHARGES

Harry Bechtol

Development and Proof Services, Aberdeen Proving Ground, Maryland

ABSTRACT

This presentation deals with recent shaped charge developments from the following sources:

     1. European - France and Belgium

     2. Russia and China

The French 73mm Rocket and the Belgian Energa Rifle Grenade have been selected as being representative of recent European advancements in shaped charge technology. Both of these devices have many excellent features among them being lightness of overall weight, improved mechanical types of fuzes and shaped charges using RDX type filler and copper liners.

The Energa Grenade employs a 2.7" diameter, 45° copper cone similar to late models of U. S. shaped charge ammunition. Penetrations of 10" or 3.7 calibers have been observed. Full standoff is 1.3 calibers.

The French 73mm Rocket is unique in that it employs a trumpet shaped or double angle cone of 2.73" diameter. The cone starts at an angle of approximately 22° at the apex and finishes at an angle of approximately 58° at the base. Cone thickness increases from apex to base (approximately .055" to .084"). Penetrations of 12.0" or 4.4 cone calibers have been observed. Full standoff is 1.5 calibers.

Russian and Chinese designs of shaped charges observed thus far are generally considered to be primitive by current standards.

Russian 76mm and 122mm shaped charge artillery projectiles have been examined and tested. Except for spitback fuzes, they resemble very early U. S. designs, which used steel cones. Penetration is roughly one caliber for either round.

The Chinese 87mm Rocket of very recent manufacture is now under examination. The Rocket Launcher is a close copy of the U. S. 3.5" Rocket Launcher. The 87mm Rocket, strangely enough, is a spinner. The shaped charge for this round has TNT filler and a fabricated (wrapped and seamed) cone. Performance details are not available at the time of preparation of this abstract.

INTRODUCTION

This presentation deals with recent shaped charge developments from the following sources:

    1. European - (France and Belgium)

    2. Russia and China

The description of the French and Belgian developments is not an attempt to enumerate all of the various calibers and types of shaped charges now under consideration. Instead, we have selected two developments which we consider outstanding and about which we have a reasonable amount of knowledge.

The information to be given on Soviet and Chinese hollow charge ammunition is probably the limit of our knowledge of their present application of shaped charge technology.

If our information is accurate, it might be considered comforting, for it shows the Soviets and Chinese to be considerably behind us and our allies in development of shaped charges.

EUROPEAN DEVELOPMENTS

The French 73mm Rocket and the Belgian Energa Rifle Grenade have been selected as being representative of recent European advancements in shaped charge munitions.

The Energa Rifle Grenade is a development of a Belgian firm known as Mecar*. The characteristics of this grenade are as follows:

Caliber	2.87"
Weight	1.32 lb
Velocity	165 fps
Fuze Type	Spitback
Design Standoff	1.3 Cone Diameters
Explosive	Pressed RDX - TNT (81.9% - 18.1%)
Liner Material	Copper - Tin Coated
Liner Diameter	2.715"
Liner Angle	45°
Liner Thickness	.048"
Liner Manufacture	Probably Cold Formed and Annealed

---

* = Societe Anonyme Belge de Mecanique et d'Armement

Armor Performance* - Defeats 10" at 0° consistently. Also defeats 5" at
65° (11.8") consistently. Has defeated 10" at 30°
(11.5") but not consistently. These data may seem to
be contradictory at first glance. However, when we
consider that these are the results of firings at actual
ranges, the explanation is obvious. A low velocity
missile such as a grenade has an appreciable trajectory
at any range. Hence, it has a noticeable angle of fall
at the target. When striking a high obliquity plate, a
small angle of fall makes a considerable difference in
the amount of armour to be defeated. When striking a
low obliquity target (30°) a small angle of fall makes
little difference in the amount of armor to be defeated.

In view of the above, we consider 10" at 30° to be
the upper limit of the Energa Grenade.

Advice received from London indicates that the
Energa Grenade has recently been improved. The cone is
supposedly the same, but the weight of explosive and the
standoff have been increased. This new round is supposed
to defeat 325mm of armor (12.8") at 0° obliquity.

The French 73mm Rocket is a development of STRIM**. The Rocket is designed for a
shoulder fired launcher much like the 3.5" Bazooka.

A quantity of these 73mm Rockets have been tested at Aberdeen Proving Ground with
excellent results. The following summarizes the important characteristics observed:

Caliber	73mm
Weight	3.0 lb
Velocity	525 fps
Explosive	Cast 50/50 Cyclotol
Fuze Type	Base Inertia
Design Standoff	1.5 Cone Diameters
Liner Material	Copper
Liner Diameter	2.73"
Liner Angle	Double 22° and 58°
Liner Thickness	Varies .055" Apex to .084" Base

---

* = As reported by Board No. 3, Fort Benning, Georgia.

** = Societe Technique de Recherches Industrielles et Mechaniques.

Liner Manufacture   Cast*

Armor Performance – Local tests indicate that the round defeats 12" at 0°
consistently. Other targets defeated were 6" at 60°
(12") and 4" at 70° (11.7"). The upper limit of per-
formance was not determined, but it is no doubt slightly
greater than 12". In summary, it can be said that the
French and Belgian designers of shaped charges have made
excellent use of the latest techniques and have come forth
with service rounds which give performance comparable to
the best U.S. rounds to be developed to date.

The French liner is especially interesting since it
embraces a design which has been given very little con-
sideration in this country. In fact, U.S. experiments
along this line with 105mm trumpets showed the trumpet to
be no better than a cone.

RUSSIAN SHAPED CHARGES

Two shaped charge rounds of Russian designs and manufacture have been examined and
tested in this country. The following are the characteristics of these rounds:

Caliber	122mm	76mm
Weight	29.2 lbs	11.93
M.V. (Approx)	1093 fps	850 fps
Fuze Type	Spitback	Spitback
Explosive •	Cyclotol	Cyclotol
Liner Material	Steel	Steel
Liner Angle	42°	28° 40'
Liner Thickness	.080" to .089"	.077" to .090"

Armor Performance – The 122mm Projectile has been subjected to static test
and gave a maximum penetration of 4". No dynamic test
results are available, but Soviet Ammunition Manuals indi-
cate that the round is good for about 4".

The 76mm Projectile has been tested at Aberdeen
Proving Ground recently. Statically, it defeated 2.75"
to 3.0". In dynamic firing tests, the performance was
about the same, the best being 2" at 47° (2.9").

* = The liner examined locally appears to have been cast, machined inside and annealed.
However, advice received from London indicates that similar cones for the STRIM
Grenade are formed from 3mm plate and finish machined.

CHINESE SHAPED CHARGES

Only one example of a Chinese shaped charge has been captured and examined to date. This is an 87mm shaped charge rocket projectile that is fired from a weapon which is evidently a copy of the U.S. 3.5" Rocket Launcher. While the Chinese Launcher bears close resemblance to the U.S. Launcher, the rocket itself is entirely different from the U.S. 3.5" rounds. It appears that the Chinese made no attempt to copy the U.S. Rocket nor any of its good features. In fact, it appears that the Chinese round might have been designed independently of the U.S. model.

The Chinese 87mm Rocket is spin stabilized, resembling somewhat, the U.S. 4.5" M16 design. A small quantity of the Chinese Rockets have been captured and are now at Aberdeen Proving Ground for examination. None have been fired to date, however. The following characteristics have been observed:

Caliber	87mm
Weight	11.75 lbs
Velocity	Unknown
Fuze Type	Spitback
Explosive	TNT
Liner Material	Steel
Liner Angle	55°
Armor Performance –	Unknown, however, it is doubtful that the penetration will be much greater than 1 caliber, based on U.S. experience with rounds of similar design (75mm M66).

ROTATED-NON-ROTATED

REPORT ON 120MM SPIN STABILIZED PROJECTILE WITH NON-ROTATING SHAPED CHARGE

Stanley Dubroff

Artillery Ammunition Department, Frankford Arsenal, Philadelphia, Pennsylvania

ABSTRACT

In order to secure an armor penetrating round in the 120mm caliber which will have greater penetration than the AP shot, this "Shaped Charge" carrying round is being developed. Considerations leading to this design are: compactness of round, due to its spin stabilization; improvement of armor penetration of the "Shaped Charge" by reduction of spin to approximately zero.

The proposed round has an exterior member which is rotated at the full spin rate for this weapon. Because of the large moment of inertia provided by the cylindrical section, stability is secured.

The inner member carrying the "Shaped Charge" cone is carried on ball bearings. Load pressure distribution on the inner and outer member reduces the load on the ball bearings to a very small value during "set back".

The above is an abstract of the paper given at the Symposium. The material discussed in this paper is covered essentially by the Frankford Arsenal RNR Report from which the following is taken.

THE DEVELOPMENT

The development of the subject shell divides itself into four main parts:

1. Investigation of all possible methods of mounting the inner member of the shell in the outer member.

2. The design of first engineering samples.

3. The manufacture of engineering samples.

4. Testing the completed round.

REQUIREMENTS

The following is a tabulation of requirements for the 120mm HEAT T230 spin-stabilized projectile with nonrotating charge:

     1. The projectile should be launched with the least possible rotation imparted to the shape charge.

     2. The projectile should be launched without any damage to the bearings and the bearing races.

     3. After launching, a method must be devised to prevent rotation of the inner member of the projectile caused by bearing drag.

     4. Design a projectile with the largest possible diameter copper cone in order to improve on the performance of the best available 120mm AP shot.

DISCUSSION

HISTORICAL

The following characteristics will exist in all designs of the shell:

     a. The projectile will be stabilized by rotating the outside member, which should have heavy walls, for high axial moment, and should be as short as practicable, resulting in relatively high stability.

     b. The inner portion of the shell containing the shape charge should be restrained from rotating and should be as light as practicable in order to minimize the overturning moment.

Since rotation decreases penetration, the idea of a rotating shell with a nonrotating shape charge is a natural outgrowth. It was discussed in Artillery Division long before it was given any serious consideration. Finally, in December of 1950, the above idea was discussed in a conference at Office, Chief of Ordnance, ORDTA. During this conference many ideas for effecting the design were discussed. Frankford Arsenal received from the Ordnance Office $10,000 and was informed that this Arsenal should proceed with design studies on the 120mm rotating-non-rotating shell (RNR). The initial approach considered the use of a thrust bearing for the rear bearing of the projectile and a needle bearing for the forward. After the initial design studies were completed, an investigation was made to determine the stability of this type of projectile. Preliminary calculations indicated that this type of projectile was very stable and, if launched without damage to the bearings, had a very good chance of performing in the proper manner.

The following approaches were reviewed as possible solutions of this design problem:

      1. The use of a fluid lubricant to be used with mating parts to form an annular orifice between the outer and inner members.

      2. The use of special rifling to engage the inner member while the outer member is being rotated by the normal rifling of the gun.

      3. The use of orifices in the base and ogive to produce a turbine-like effect which will prevent the rotation of the inner member.

      4. Setting the inner member in bearings which will prevent the inner member from picking up full spin on firing of the gun, while the outer member does pick up full spin and provides the stabilizing influence for the projectile.

Of the above mentioned possibilities, the fourth was chosen. The first was rejected because of sealing problems, and heat dissipation through the fluid at high rotational speeds. The second was discarded because of the need of a special gun to fire the round; and the third dropped because of the implied difficulty and expense of manufacture. Therefore, the fourth possibility, which seemed to be the most logical, was chosen for development, since it does away with fluid seals, special type rotating bands or grooves and turbine blading to go with an orifice system.

Assumming that the projectile would be fired at 40,000 psi the design was initiated. The first design incorporated the use of a thrust bearing at the rear of the projectile to take the setback forces. (See Illust. No. 11). Considering the weight of the projectile to be approximately forty (40) pounds, the maximum acceleration of this projectile being fired at a pressure of 40,000 psi would be in the vicinity of 20,000 g's. Were the inner member to weigh eight (8) pounds, the setback forces on a bearing placed at the rear of the projectile would be 160,000 pounds. A thrust bearing to take this load would have to be far larger than that which could be contained in a 120mm shell.

At this time it may be mentioned that a Government contractor had an Ordnance contract to develop a projectile of this type, and upon testing the first designs found that failure occurred at the bearing. A thrust bearing was utilized in the above design, and failure was caused by "brinelling". Personnel at this installation did not have the advantage of any further information than that which told of bearing failure. However, it was quickly perceived that the crux of the entire problem was the rear bearing. That is, the setback forces caused the balls to imbed in the races and cause depressions which prevented the balls from rolling freely.

There was no apparent way to solve this problem of so great a setback force until the personnel working on this project came up with a possible solution: - to limit the setback force by allowing the gases propelling the projectile to act on the inner member, causing little or no relative motion between inner and outer members.

With this solution in mind the first design came off the drafting board with an opening in the back of the projectile. The bearing at the rear of the projectile was a thrust bearing, and a needle bearing was put just to the rear of the cone near the front of the projectile. (See Illust. No. 11).

It was then a problem to see if bearings were available to fit in the spaces set up for them in this design. Representatives were consulted from New Departure Division of General Motors, SKF Industries, Inc., The Torrington Company, Nice Ball Bearing Co., and Fafnir Bearing Co. to get their separate recommendations on the problem. Nice and Fafnir Bearing Companies could not supply the bearings and The Torrington Company presented a needle bearing which would fit, but advised that a needle bearing of the type presented would not take the high rotational speeds of this projectile. The New Departure Division of General Motors and SKF Industries, Inc., recommended a plain single row, deep groove radial type ball bearing, as they were asked to furnish a bearing to take the high rotation of 20,000 rpm, and a thrust of 10,000 pounds (with a life of less than a minute).

The New Departure Division of General Motors and SKF Industries, Inc., advised of the availability of certain sizes of bearings and from this point on the projectile was designed around the bearings.

Since the projectile would eventually be used with the new NBS "Lucky" fuze, it was decided upon to utilize this arrangement. This immediately presented the opportunity to place the front bearing farther forward than in the first design, thus eliminating most of the front overhang in the projectile and affording support for the inner member close to both extremeties.

Due to space limitations, the largest cone which can be utilized at present is 105mm in size. Therefore, the same cone designed for the 105mm fin-stabilized projectile will be used for the first group of engineering samples of this projectile.

Upon the completion of this design, the local representatives from the New Departure Division and one of the factory engineers were consulted on the design and possible problems of lubrication. At the present, storage problems are not considered, therefore, it was concluded that a thin film of oil on the bearing would be enough lubrication for this first test. There were also some alternatives in bearings offered in the event that the deep groove, radial type ball bearing offered too much resistance, and this drag caused undue rotation of the inner member. (The friction exerted on the balls by the high velocity of the outer race revolving may cause additional drag on the inner race causing the inner member to rotate.)

The bearing and bearing seat tolerances chosen were A. B. E. C class three (3). At the present time it is not known whether this tolerance is needed, but the problem at hand is to establish a principle, while the production difficulties encountered may be overcome at a later date. (It must however, be mentioned, that many of these difficulties have been noted and possible production solutions are already available.)

Ten 120mm T147E1 target practice rounds have been modified for use as proof slugs for determining a propellant system for the projectile.

The first five (5) projectiles have been inert loaded and will be fired on the transonic range at Aberdeen Proving Ground, Maryland. The remaining five (5) projectiles will be utilized in another test, possibly against armor plate for penetration, upon the successful conclusion of the first test.

Stability computations were performed on the first design and appeared satisfactory. Information pertinent to flight characteristics will be obtained from the first test of the present design.

In order to be able to tell whether there is any relative motion between the outer member and the inner member, the aluminum nose of the projectile (attached to the inner member) will be anodized and then sand blasted with a spiral in order that it may be photographed in flight. An alternate method for determining the rotation of the inner member is to insert a magnet into the nose of the projectile perpendicular to the axis of the projectile. There would then be set up wires running longitudinally in the range. The projectile when fired would then set up impulses in this field by any rotation of the magnet. These impulses would be recorded, and the rotational speed would be readily available.

To have an absolute check on rotation, two pins are attached to the inner (non-rotated) member and protrude past the base of the rotated member. One pin is cylindrical in shape and the other is conical. The projectile is photographed in vertical and horizontal planes along its trajectory and from these photographs the rotation may be computed.

TECHNICAL

In order that a basis for design would exist, and since no special requirements were announced for this RNR (Rotated-Non-Rotated) projectile, the pressure of 40,000 psi was chosen as a design pressure (based on the pressure at which the 120mm AP Shot is fired).

From the elementary equation

(1) $P \times A = m \, a$ where P = pressure, psi

A = exposed area (sq.in.)

M = weight (lbs.)

A = acceleration (g's)

it is easily seen that for any set conditions where the area and weight are given, the pressure is directly proportional to the acceleration or

(1a) $\dfrac{a}{P} = \dfrac{A}{M}$ = constant

To prevent too great a shock load from acting upon the bearings (see Illust. No. 2), or more exactly, upon the rear bearing, the design problem existed whereby the exposed rear area of the outer member divided by its weight be equal to the exposed rear area of inner member divided by its weight. When this condition exists, there will be no tendency for relative motion between inner member and outer member upon firing.

Under design conditions, the pressure being 40,000 psi, the acceleration of the projectile computed to be 18,951 g's. The setback forces (ma) for the inner member,

weighing seven (7) lbs., came to 132,657 lbs. This force had to be balanced by the pressure of the gun multiplied by the exposed area of the inner member. From equation (1) the exposed area was computed and the diameter determined.

For the given pressure and acceleration:

$$\frac{A1}{M1} = \frac{A2}{M2}$$

where A is the rear area and M is the weight; the subscripts stand for the inner and outer members. This is the condition which must exist in order that there would be no tendency for relative motion between inner and outer members upon launching.

The consultant from New Departure Division recommended an angular contact bearing in the event that there was too much rotation of the inner member due to drag on the inner race. In this event, it is not desirable to leave the forces equal, for if any forces are set up in flight that might cause the thrust to be forward on the inner member, the angular contact bearing would not be suitable. However, if the area of the inner member was so controlled as to permit a set-back force of say 1000 lbs. the bearing would function as designed. From this point of view, and to be sure that the direction of the force be known, the exposed area of inner member was designed to allow for a net force back, of the magnitude of 1000 lbs. This will be useful regardless of whether the single row deep groove radial type or the angular contact ball bearing is used.

One design idea for limiting the rotation of the inner member is to mill a spiral groove in the nose, with the spiral opposite to the rotation of the projectile's outer (stabilizing) member. If the rotation is excessive, this method for limiting rotation may be tried. Another alternative, straight grooves in the nose, may be sufficient to stop rotation.

Another problem existed in the design - concerning aerodynamic forces on the projectile. The first design had the inner member utilizing a nose which took up the entire ogival area. With this arrangement, a large portion of the drag of the shell was taken by the inner member. It is not known whether or not this would set up any undue forces on the bearings. However, to do away with this possibility, the present design utilized frontal exposed areas approximately proportioned to the masses of the outer and inner members. The drag on the inner member is proportional to the area exposed. The drag on the outer member is proportional to its exposed area. The above would minimize the tendency for relative motion between inner and outer member.

CONTRIBUTING PERSONNEL

ARTILLERY AMMUNITION DEPARTMENT

PHASE	DIVISION	NAME
Engineering & Design	Projectile & Case	Mr. W. S. Scheingold
	" "	Mr. H. S. Lipinski
	" "	Mr. S. Dubroff
	" "	Mr. G. Callum
	" "	Mr. J. Brady
	Design	Mr. W. F. Kauffman
	"	Mr. J. J. Luczak
	"	Mr. S. S. Bloom
	"	Miss M. Bostwick
Manufacturing	Experimental Shop	Mr. J. King
	" "	Mr. R. Ganser
	" "	Mr. F. Goepel
	" "	Mr. F. Majke

311

Figure 1—120 MM, T230 projectile metal parts assembly.
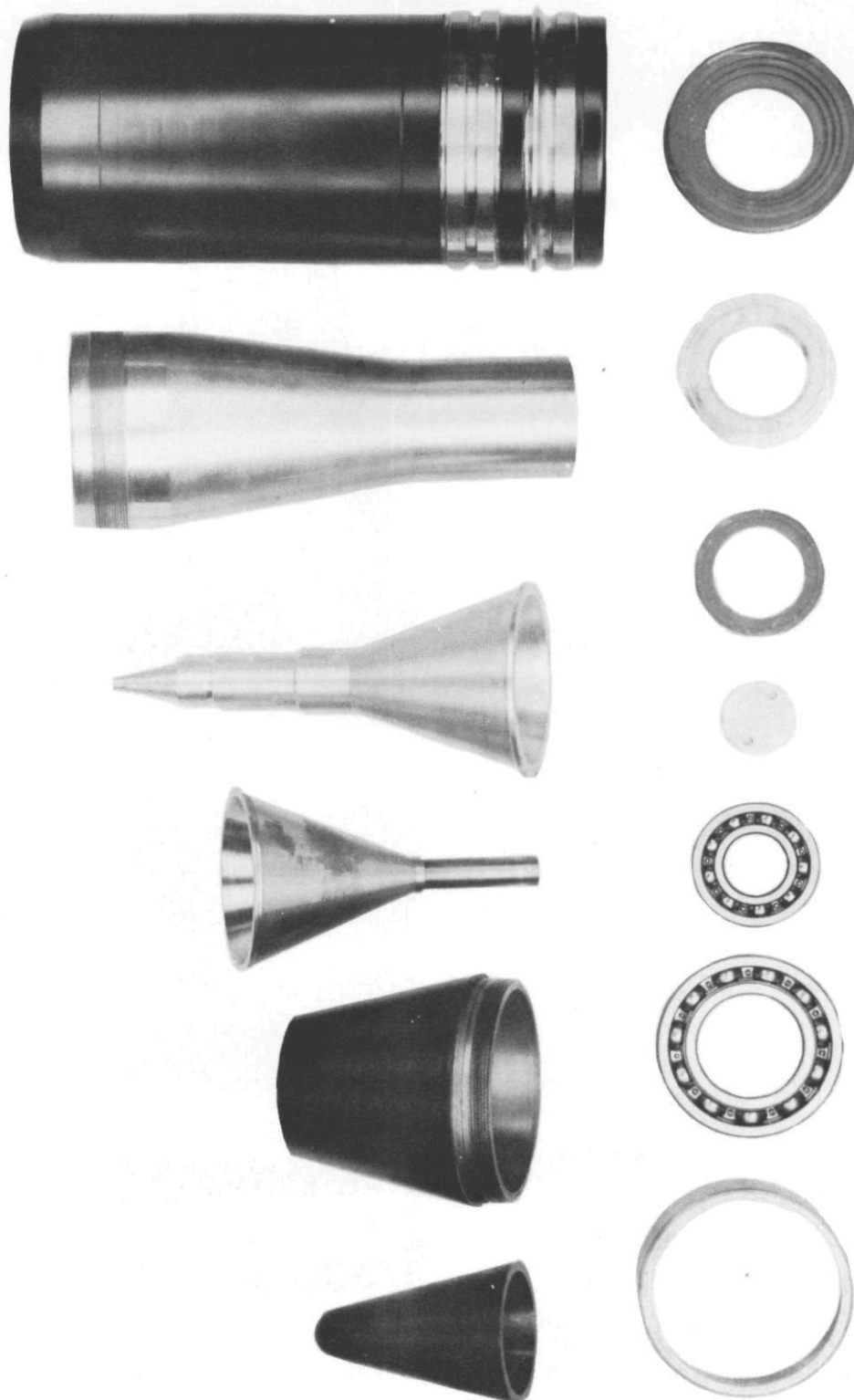
Figure 2—Component parts.

313
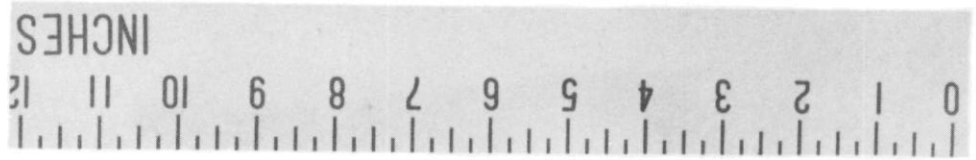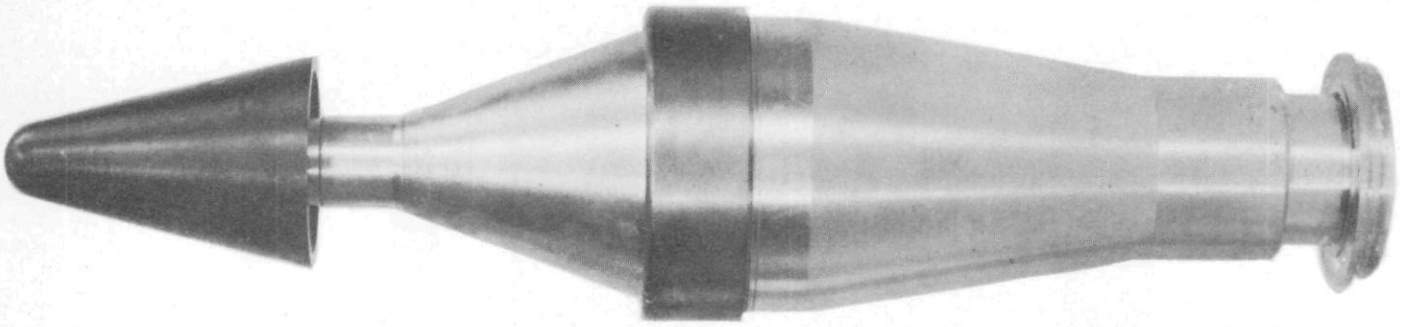
Figure 5—Inner body assembly, nose in place.
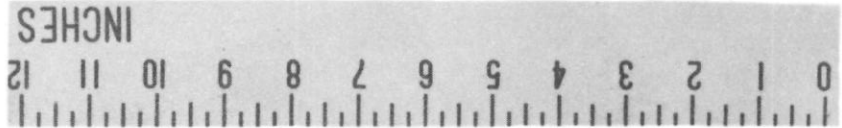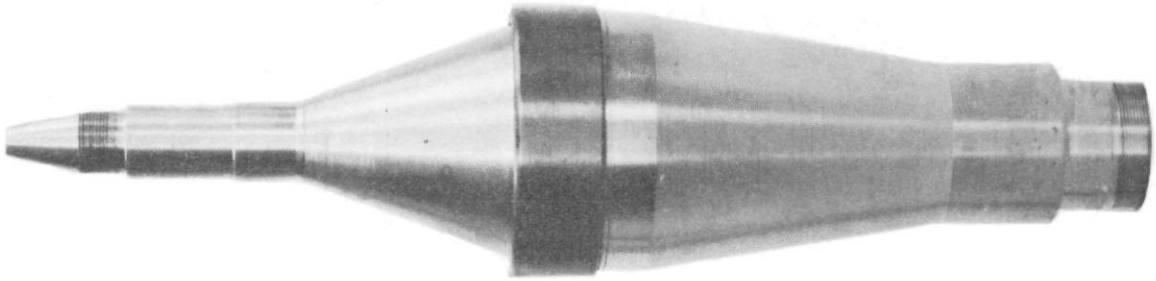
Figure 4—Inner body assembly (after machining).
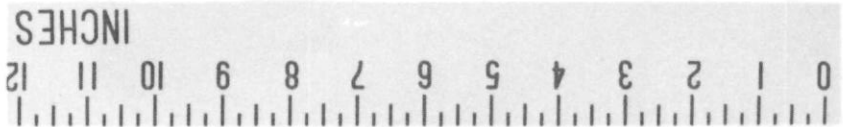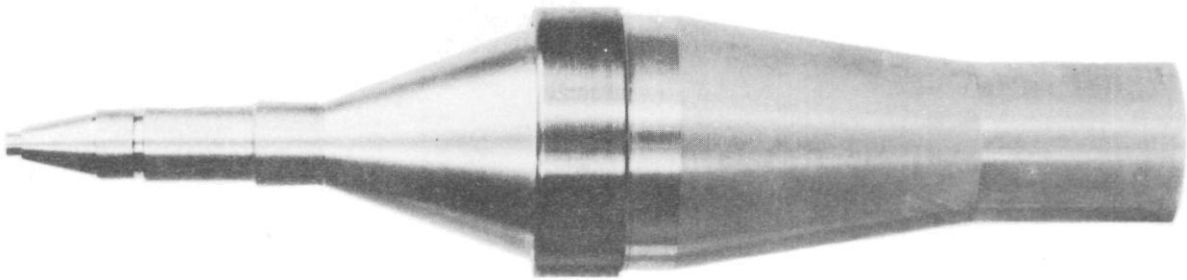
Figure 3—Inner body assembly (before machining).

Figure 6—Inner body assembly, bearings, outer body and ogive assembly.
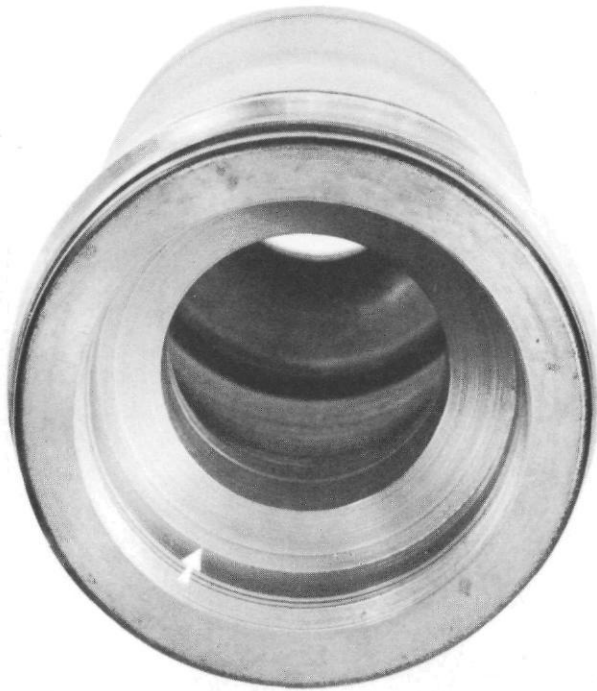
Figure 7—Rear bearing seat.

Figure 8—Forward bearing seat.
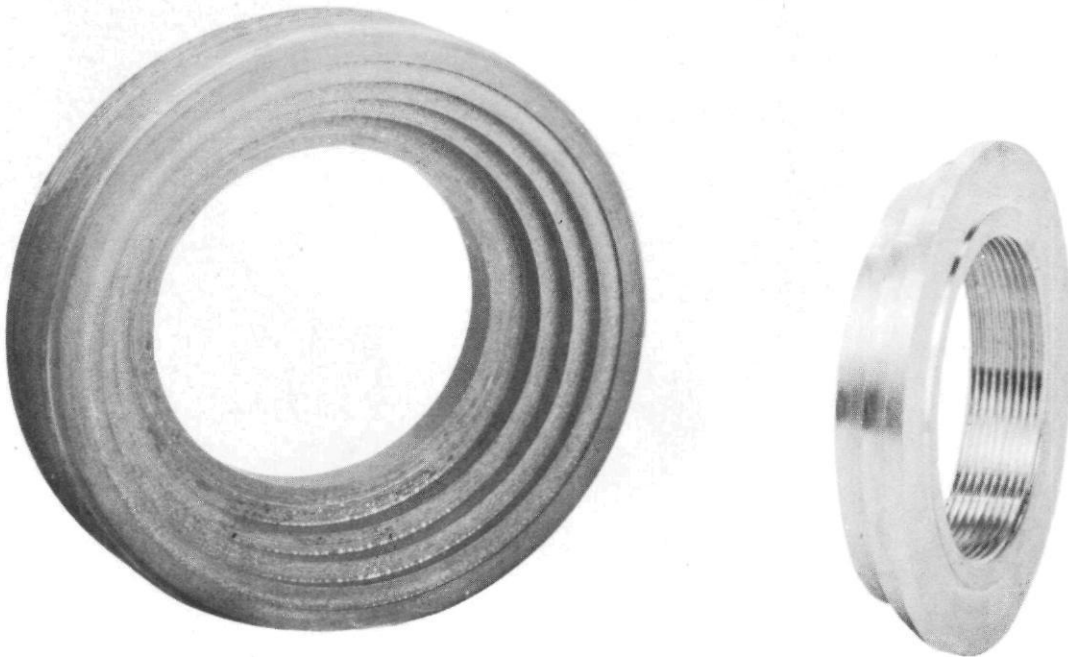
Figure 9—Labyrinth seal (base plug & rear lock nut).
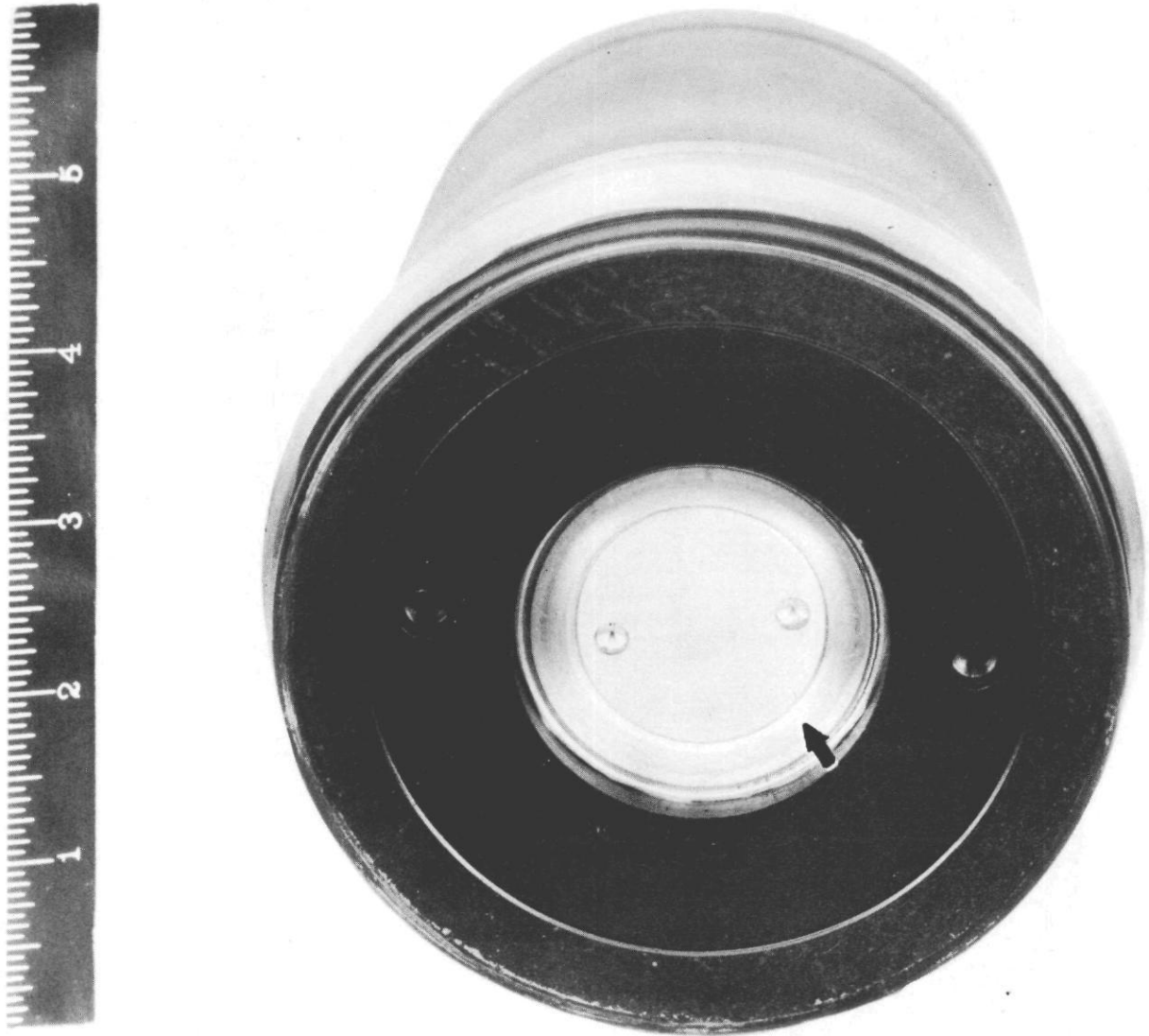
Figure 10—Projectile base (arrow indicates exposed inner member).
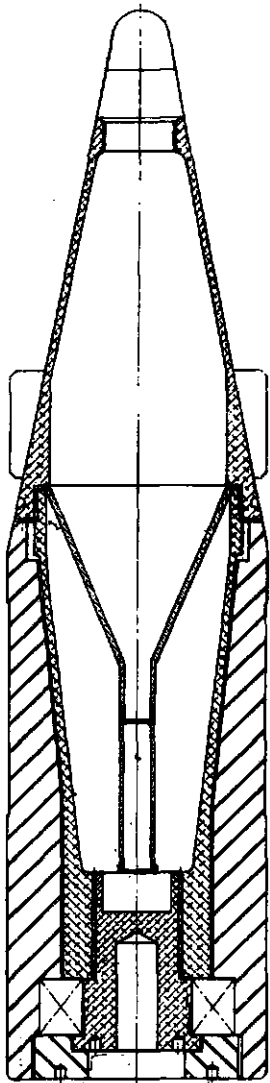
Figure 11—Initial design A.
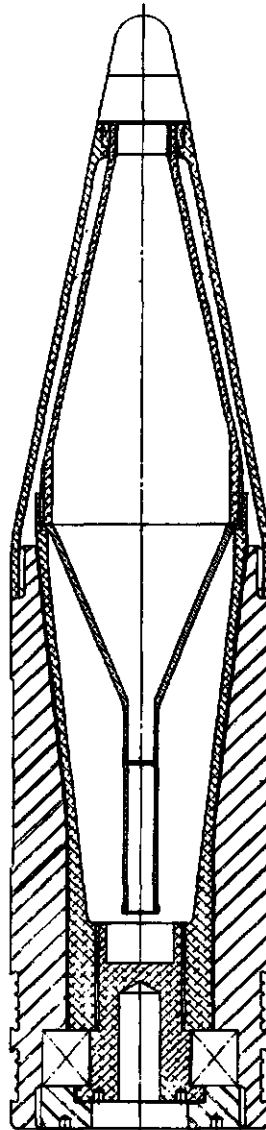
Figure 12—Initial design B.
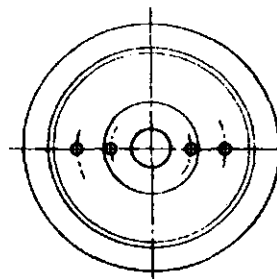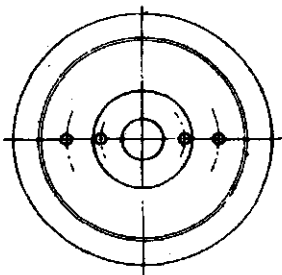
STUDY OF THE EFFECTS OF ROTATION UPON THE PENETRATION
OF JETS FROM 105MM SHAPED CHARGES

L. Zernow

J. Regan

J. Simon

I. Lieberman

Ordnance Engineering Laboratory, Ballistic Research Laboratories
Aberdeen Proving Ground, Maryland

ABSTRACT

An analysis of the targets into which rotated shaped charges
were fired was carried out prior to flash radiographic studies
previously reported.

Clear evidence was found for the bifurcation and subsequent
apparent polyfurcation of the jet at increasingly higher rota-
tional frequencies. Photographs of sample targets illustrating
this effect are shown.

A rotational standoff effect is established, which shows
that the depth of penetration of a rapidly rotated shaped charge
decreases sharply with increasing standoff.

Additional evidence for the importance of shocks and com-
pressibility in the penetration process is found in peculiar holes
of essentially square cross section associated with the jets from
the rotated projectiles. It is noted that these effects may be
important in lethality studies.

A hydrodynamic model of a rotating hollow liquid cylinder
which is unstable under rotation is proposed as a basis for
understanding the bifurcation process.

INTRODUCTION

The need for a systematic study of the effects of rotation on large caliber shaped
charges stimulated the development in 1950 of the wire driven projectile rotator[1]
which greatly simplified the experimental problems. This system was immediately put to

----

(1) S. Kronman, L. Zernow - "A Wire Driven Projectile Rotator for Hollow Charge
Studies" - BRL Report No. 798, March 1952.
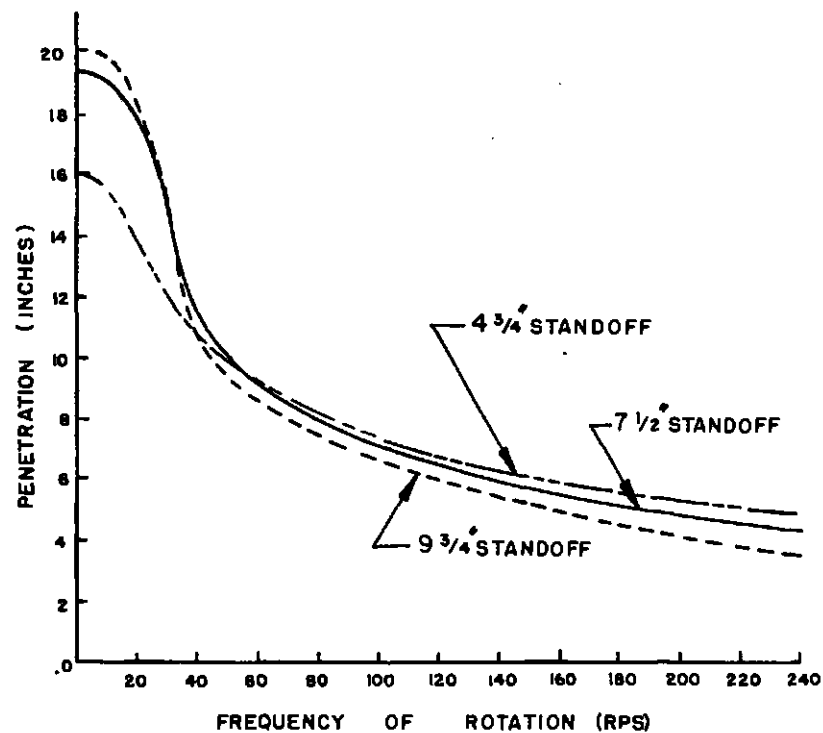
Figure 1—Effect of Rotation on Penetration at various standoffs. 45° cu. cone with spitback tube, 105 mm.
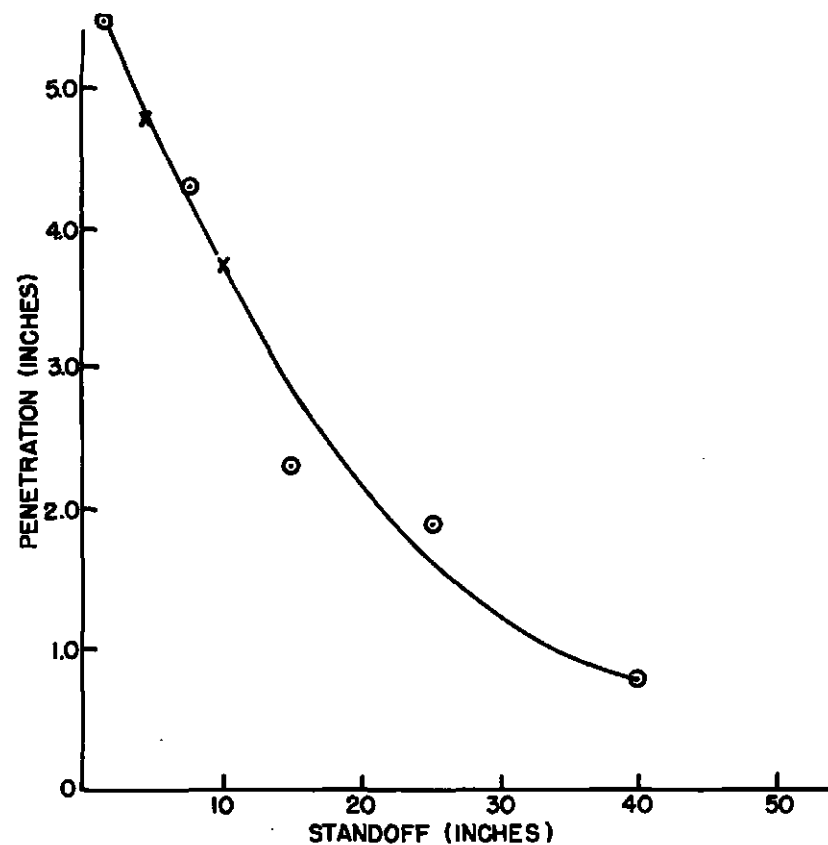
Figure 2—Effect of standoff at 240 RPS. 45° cu. cone with spitback tube, 105 mm.

use in studying the effects of rotation upon 105mm projectiles. This information was urgently needed in connection with the development of a 105mm weapon by the Firestone Tire and Rubber Company as well as by several government agencies. As it turned out, predictions based on the scaled performance of 57mm projectiles were badly in error. The actual experimentally observed deterioration was about twice that predicted on the basis of the 57mm scaling calculations. These calculations have not yet been critically examined so that this deviation from the scaling law may, at least in part be attributed to causes such as non-similarity of the liners.

During the course of these experiments careful attention was paid to the targets which showed several very interesting and reproducible characteristics that could be correlated with the rotational frequency and the standoff. A study of these targets proved illuminating, and it was possible to predict some of the details regarding jet breakup which were later observed in the flash radiographs of the jets from rotating liners.[2]

THE EXPERIMENTAL PROGRAM

The initial experiments which were carried out covered the range of rotational frequencies from 0 to 60 rps. The standoff used in these experiments was fixed at about 2 cone diameters, since this was approximately the standoff at which the service weapon would be expected to function. The data collected in these initial experiments[3] were augmented to include the effects of higher rotational frequencies and of variation of the standoff.

EXPERIMENTAL RESULTS

Figs. 1 and 2 contain a summary of the experimental results. Penetration is plotted against rotational frequency in Fig. 1 and against standoff in Fig. 2.

The points of interest on these plots are:

(1) The crossover of the curves for 9 3/4", 7 1/2" and 4 3/4" standoff,

(2) The clearly evident rotational standoff effect at 240 rps.

The crossover frequency was not established very accurately because it is not of significant importance at present. However, the reality of the crossover is established beyond doubt, and it is understandable simply as the result of the competition between increasing penetration due to standoff and decreasing penetration due to rotation.

Simply stated, the experimental range of standoffs for a copper liner is such that at zero spin, the penetration is still increasing with standoff while at high-spin

---

(2) L. Zernow, S. Kronman, F. Rayfield, J. Paszek and B. Taylor - "Flash Radiographic Study of Jets from Rotating 105mm Shaped Charges" - Shaped Charge Symposium Transactions - November 1951.

(3) Most of the data obtained in the early firings appears in the 1950 and 1951 reports of the development of the B.A.T. weapon by the Firestone Tire & Rubber Company.
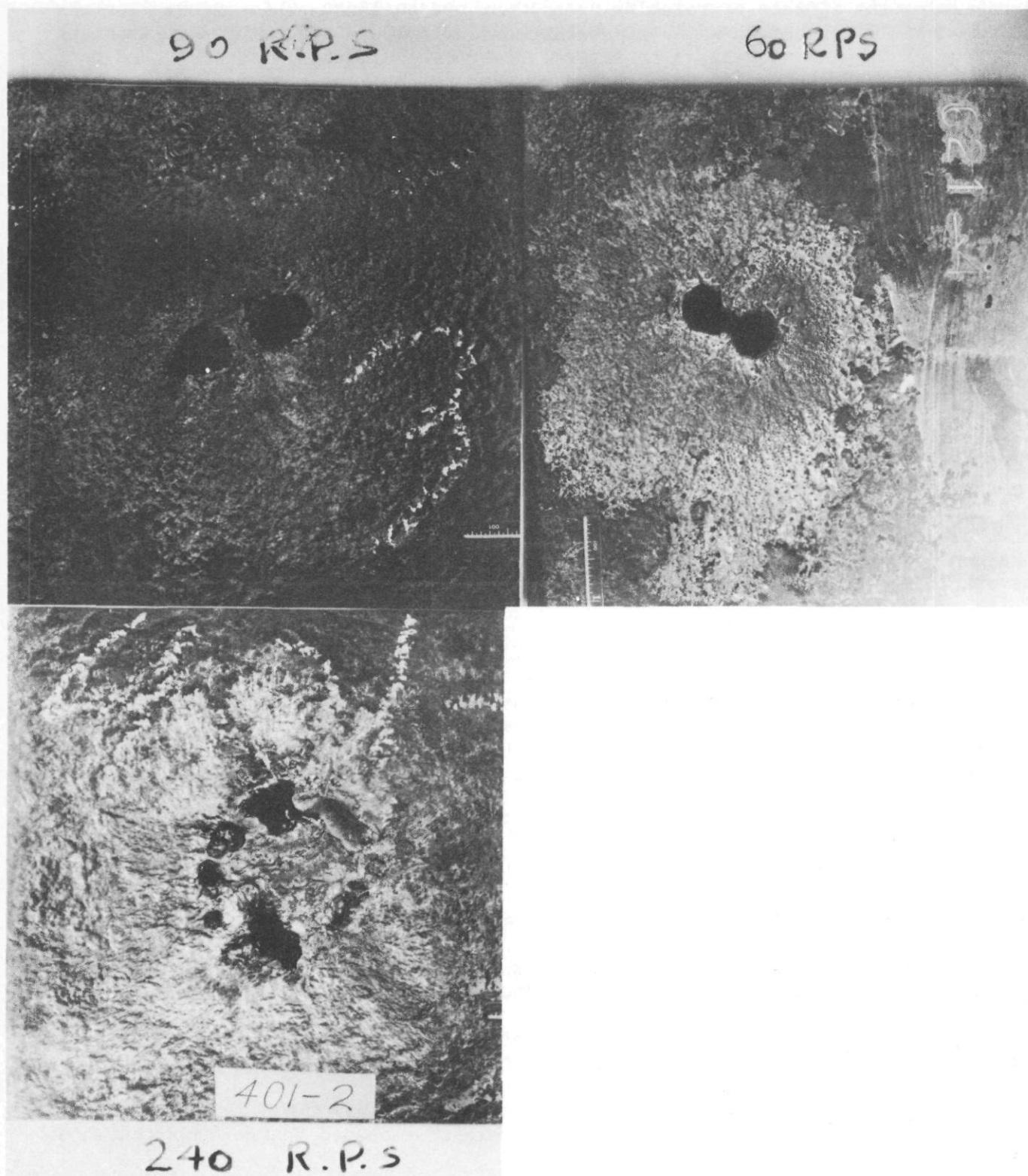
Figure 3—Bifurcation and Polyfurcation in the bottom target plates
resulting from rotation at various frequencies.

(240 rps) the rotational dispersion effect is such as to decrease the penetration with increasing standoff. These two end conditions necessitate a crossover such as is observed.

Some evidence for this rotational standoff effect was observed by the British[4] in 1943 in their original experiments on 3" charges. However, the trend since that time to carry out the experimental work with small charges has resulted in the crossover point being shifted to higher frequencies and hence, the experimental data reported with small charges does not go out far enough in rotational frequencies to firmly establish the rotational standoff effect at high spins. This can be made clear by the following reasoning:-

If, as postulated by Birkhoff, the rotational effects scale with the parameter ωD, where ω is the rotation frequency and D is the caliber, then a cone of 1/2 the 105mm diameter would require a rotational frequency of 480 rps to show effects that we can observe at 240 rps. Very few experiments have been carried out at this high rotational frequency, which is much greater than that attained by H.E.A.T. projectiles in any weapons. As an example, the 57mm H.E.A.T. projectile is fired at 215 rps. It is likely that we could still have observed evidence of the rotational standoff effect at frequency of rotation lower than 240 rps.

A semi-empirical correlation of rotational scale effects proposed by Winn[5] of the Firestone Tire and Rubber Company does not take this rotational standoff effect into account. Therefore, its reliability must be considered limited to the region of rotational frequencies below the crossover frequency.

TARGET STUDIES - EFFECT OF INCREASING ROTATIONAL FREQUENCY AT CONSTANT STANDOFF

As the rotational frequency was increased during these experiments a series of striking changes could be observed on the target plates. The reduction in penetration was found to be accompanied at first by definite enlargement of the hole bottom and finally by a bifurcation in the last plate. The spacing between the two holes increased as the rotational frequency increased at a given standoff. Finally at the very high frequencies, the bifurcation gave way to a series of many holes spread around a circle.

Figure 3 shows pictures of the last plates at 3 different rotational frequencies. These photographs clearly show the increasing spread of the bifurcation and the ultimate polyfurcation.

The data obtained are summarized in Fig. 4 which is a plot of the distance between the centers of the two holes (or the mean diameter of the circle for the polyfurcations) against the rotational frequency.

(4) AC-3987 - Hollow Charge Rotated Projectiles.

(5) Firestone Tire and Rubber Company - Progress Report - June 11, 1951.

DISTANCE BETWEEN CENTERS OF HOLES
vs. FREQUENCY OF ROTATION
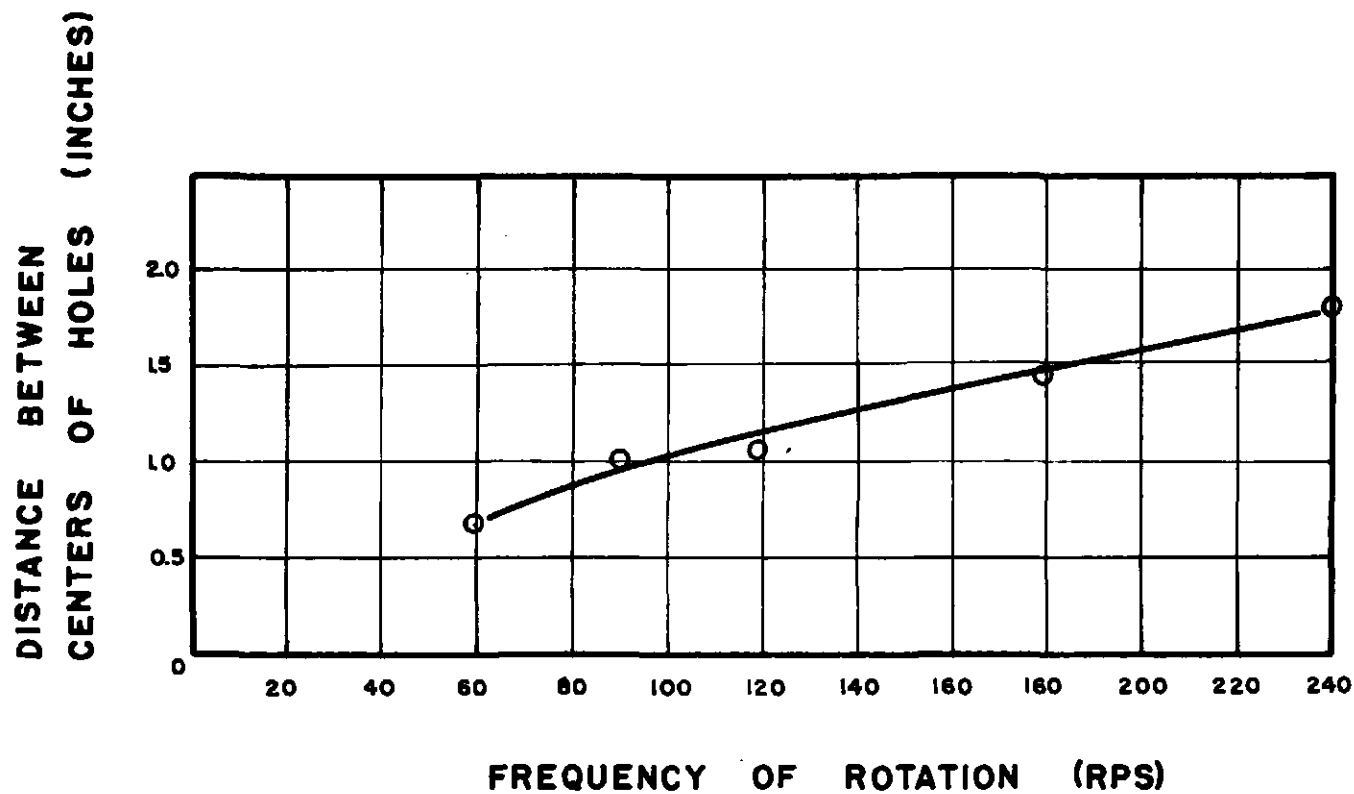
Figure 4—Distance between centers of holes vs. frequency of rotation.

Figure 5—Square hole from a rotated charge.
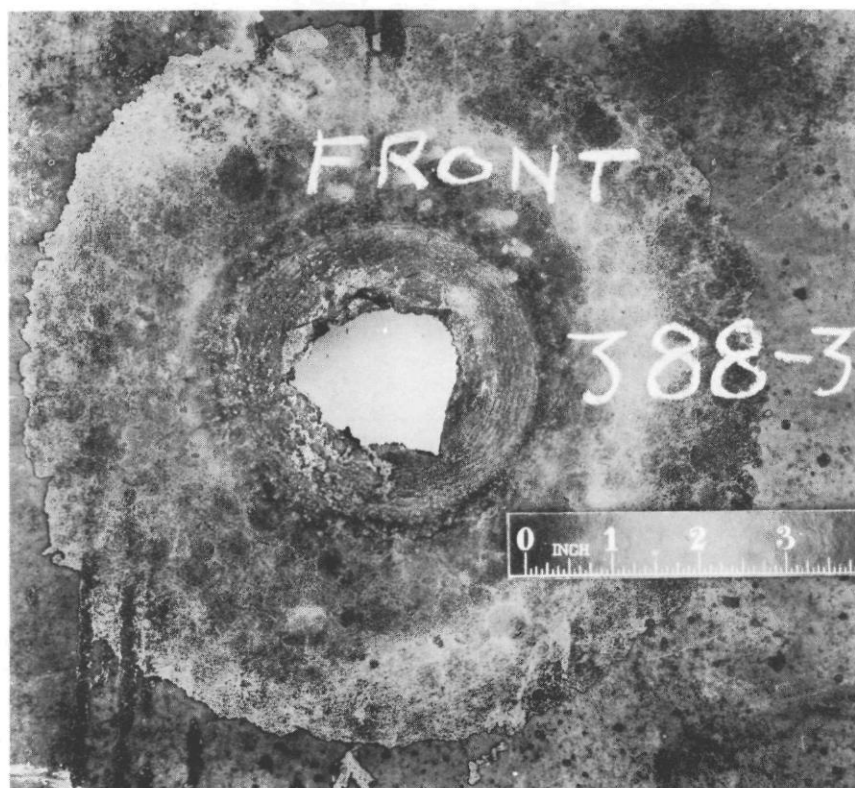
Figure 6—Square hole from a rotated charge.

325
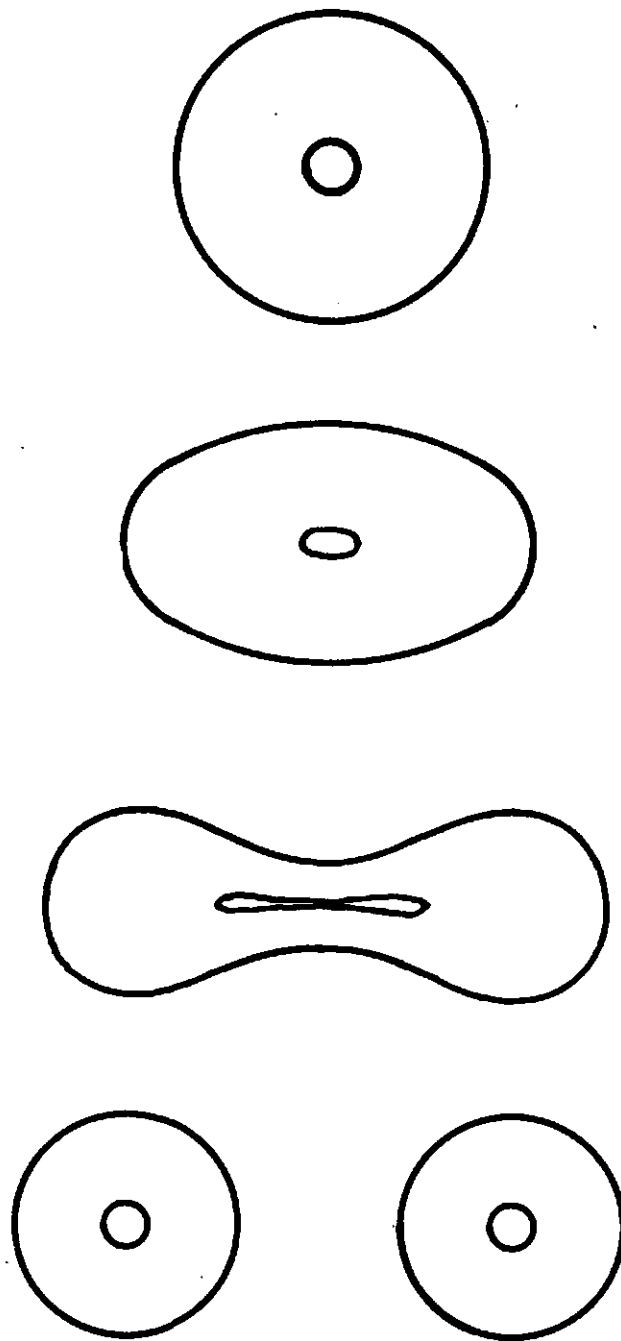
Figure 7—Hypothetical steps in the process of bifurcation
of a rotating hollow liquid cylinder.

Among the other interesting observations are those shown in Figures 5 and 6. Here apparently a hole with approximately square cross section has resulted from the rotation* of the charge!

It is quite evident that processes other than the simple incompressible hydrodynamic ones are needed to explain these results. The need for considering in detail the target compressibility during penetration and the study of shock propagation in the target (and perhaps in the jet as well) is clear. Birkhoff[6] has already considered the effects of compressibility on penetration and concluded that target-compressibility decreases the penetration. Further effort in extending this is believed justified because such studies may make important contributions to the better understanding of lethality of the H.E.A.T. round.

HYDRODYNAMIC MODEL OF THE BIFURCATION PROCESS

In the course of the observations of bifurcation in the target plate it was natural that one should attempt to find a hydrodynamic model which could explain the process. Following Birkhoff's work[6] and extending the reasoning to non-steady state hydrodynamic models, the investigation led to an examination of the stability of a rotating hollow liquid cylinder. This appears to be an extremely difficult problem to solve analytically, although one could make very plausible a posteriori "intuitive" guesses regarding the process of bifurcation of a rotating hollow liquid cylinder, examples of which are sketched in Figure 7.

During the investigation of this problem** it was learned that Sir James Jeans had carried out a theoretical investigation "On the Equilibrium of Rotating Liquid Cylinders".[7] He was interested in the three dimensional problem connected with the behavior of nebulae and the formation of planetary systems, but in this work he treated the simpler two dimensional problem of a cylindrical mass of fluid held together by a gravitational potential, using a very specialized approach. The essential conclusions he reached were:

(1) There was a critical rotational frequency below which the system would be stable,

(2) Above the critical frequency the fluid cylinder would break into two parts.

It must be noted first that Jeans treated the full cylinder, whereas we are really interested in the stability of a rotating hollow cylinder. Unfortunately it appears that his specialized treatment will not work for a hollow cylinder. In any case, it is not presently known whether the stability of a hollow liquid cylinder is markedly different from that of a solid cylinder. Intuitively one might guess that there would be considerable similarity. Jeans predicts a necking down and finally a

---

* Dr. Soper indicated that similar observations had been made by the British.

(6) Garrett Birkhoff - "Hollow Charge Anti-Tank Projectiles" - BRL Report No. 623, February 1947.

(7) Phil. Trans A cc 67 (1902).

** Pointed out to one of the authors (LZ) by Prof. T. H. Berlin of the Physics Dept., Johns Hopkins University.
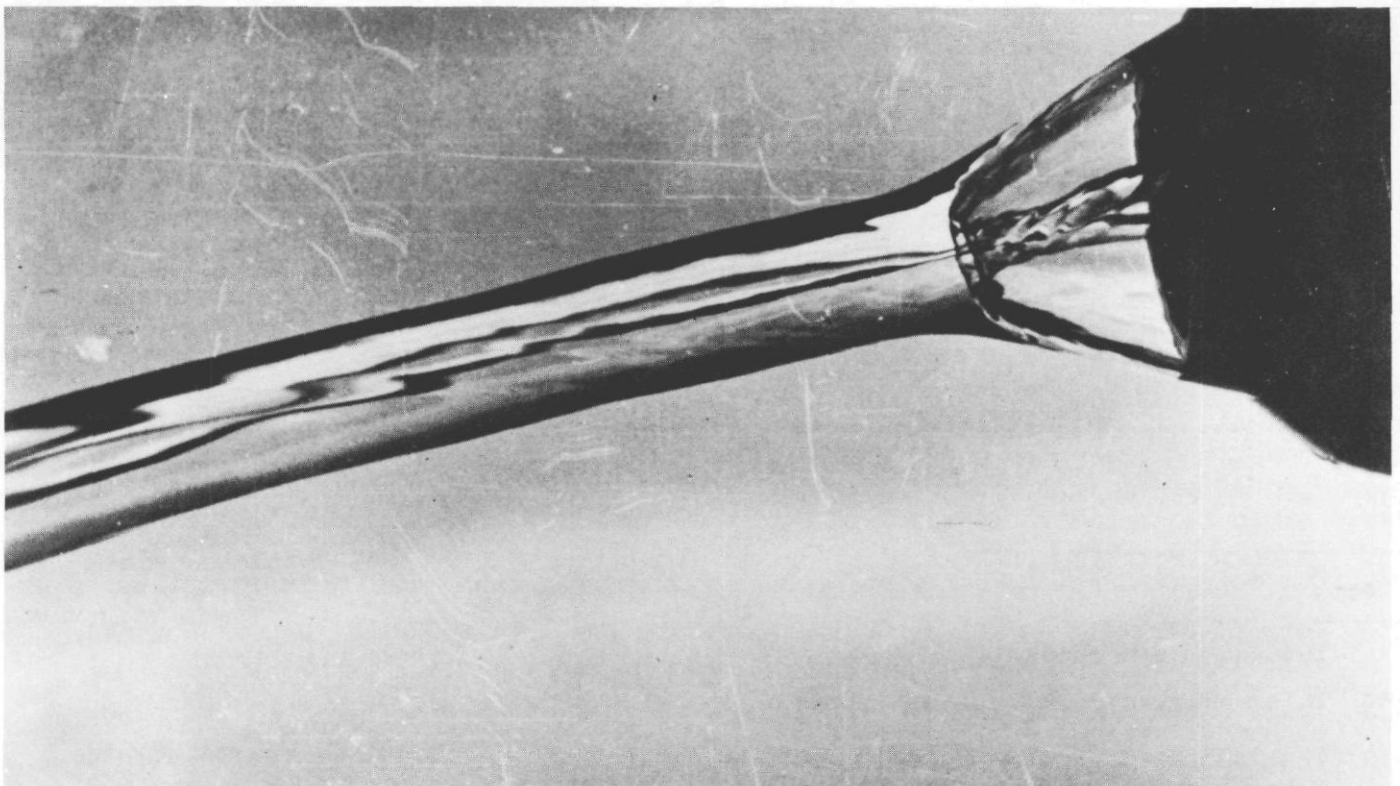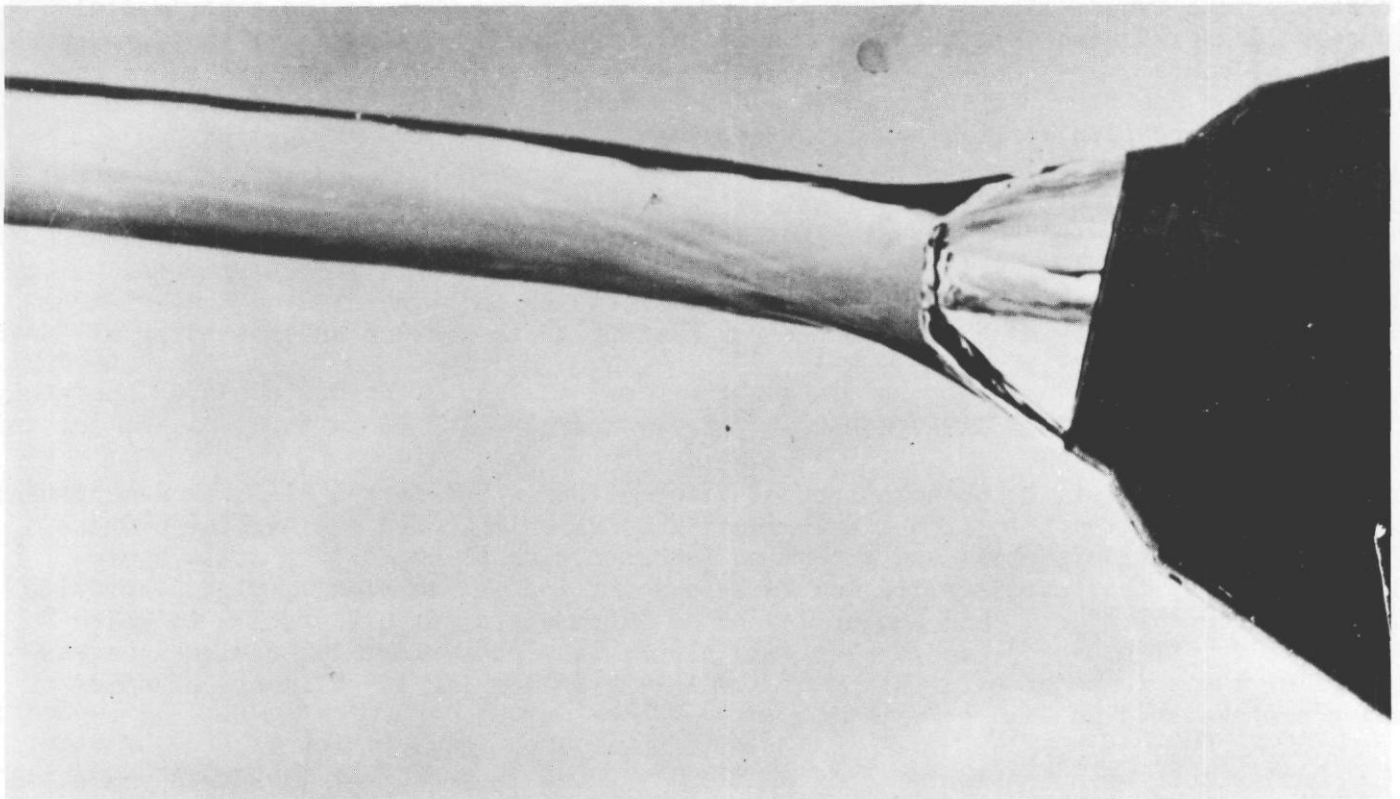
Figure 8 {Water analog of a shaped charge} 8—Unrotated.
Figure 9 {   Jet & Slug} 9—Rotated.

328

break-up into two smaller cylinders of unequal diameters, whereas the experimental observations indicate that the break-up is into two approximately equal portions. One could, of course, postulate successive bifurcation of each of the two cylinders resulting from the first bifurcation in order to account for the experimentally observed polyfurcation at high rotation frequencies.

WORKING HYDRODYNAMIC ANALOG OF JET FORMATION AND THE EFFECTS OF ROTATION

Early in 1950, two pictures were obtained from the laboratory of Dr. Schardin in France.[*] These pictures which are reproduced in Figures 8 and 9 represent a converging conical surface of water forming a jet and a slug as predicted by hydrodynamic theory. In Fig. 8, no rotation was imparted to the water. In Fig. 9, rotation was deliberately imparted to the water. The formation of a hollow region in the interior of the jet and slug can plainly be seen. If one examines the jet in the rotated case, one can imagine that there is incipient bifurcation, although a comparison with the unrotated case leaves one somewhat in doubt, since there appear to be extraneous striations in the unrotated jet as well.

This was an extremely striking demonstration and it was an easy matter to duplicate[**] the unrotated jet with locally fabricated equipment. It has been more difficult to duplicate the rotated jet, although the attempts to do so are still in progress. In addition, a rotating hollow liquid cylinder analog has been constructed. It appears at present that extraneous physical properties of the water, such as surface tension, may mask the effects one is seeking. Steps are being taken to eliminate these and thus make the analog more realistically duplicate the system it is meant to simulate.

One can occasionally obtain definite bifurcation in the water analog of the rotating hollow cylinder, but it is not at present a satisfactorily reproducible simulator. This work is being pursued further and the plans include treatment of the fluid and possibly choice of fluid to eliminate the factors that are believed to be masking the results.

This short discussion of the hydraulic analog has been included because it is indicative of the diversity of the possible methods of attack upon the problem of understanding the rotational deterioration of the jet.

SUMMARY AND CONCLUSIONS

The process of deterioration of a jet by rotation is shown to involve a bifurcation of the jet, at the lower rotational frequencies. Higher rotational frequencies appear to result in polyfurcation.

A clear rotational standoff effect is found at 240 rps which shows the penetration falling off monotonically with increased standoff.

---

[*]   Through the courtesy of Professor Garrett Birkhoff of Harvard University.

[**]   This work was done by Mr. S. Kronman and Mr. F. Rayfield.

Evidence is found for processes other than the simple incompressible hydrodynamical ones normally considered in target penetration. The need for extension of the analytical treatment has been recognized by others before. These observations accentuate the need for an extension.

The postulated instability of a rotating hollow liquid cylinder is proposed as a hydrodynamic model on which to base the understanding of the bifurcation process.

SPIN COMPENSATION

E. L. Litchfield

Carnegie Institute of Technology, Pittsburgh, Pennsylvania

ABSTRACT

Techniques and methods for the manufacture of fluted cones as developed in cooperation with the National Bureau of Standards are discussed. Techniques used in producing C.I.T. laboratory size samples are essentially those required for large scale production of liners for weapons use. It is shown that the problem of obtaining good fluted liners is of the same magnitude as that obtaining good smooth liners.

The results obtained from tests with various fluted liner designs are presented. Several fluted liner designs have produced 100% compensation (i.e. static smooth liner performance) at spin rates as high as 150 to 180 r.p.s.; other liner designs have produced as much as 75% compensation at spin rates as high as 300 to 330 r.p.s. Additional fluted liner groups which may be of importance in future weapons design are also discussed.

The need of compensation for the effects of spin degradation upon the performance of shaped charge ammunition is well known. A typical demonstration of such degradation is given in Fig. 1, which represents the penetration depth vs. rotational frequency data for the copper cone used in the 57mm HEAT shell. The penetration at 210 r.p.s., the spin frequency of the shell fired from the 57mm recoilless rifle, is only 2.8 in. although the liner will give 9.3 in. penetration at 0 r.p.s.

The concept of compensation for the effects of spin through the use of fluted liners first appears in E.R.L. reports[1]. Apparently, the idea was advanced initially by Pauling; and it was tested by E.R.L. with small numbers of relatively crude liners. The first laboratory size group of identical fluted liners was obtained by E.R.L. just before the termination of NDRC at the war's end.

Thus, at the time this investigation was undertaken by C.I.T., neither fluted liners nor methods for the manufacture of such liners were available to permit further testing of the idea. The problem was standardized with the 57mm copper cone (1.69 in. base diameter, 42° apex angle and 0.045 in. wall) because of the higher potential penetration of copper liners; and was to include the development of methods of manufacture applicable to mass production of fluted liners.

---

[1] National Defense Research Committee of the Office of Scientific Research and Development, "Target Penetration by the Jet from a Rotating Cone Charge", Report OSRD No. 3874, July 10, 1944.

National Defense Research Committee of the Office of Scientific Research and Development, "Target Penetration by Rotating Cavity Charges", Report OSRD No. 5598, November 5, 1945.
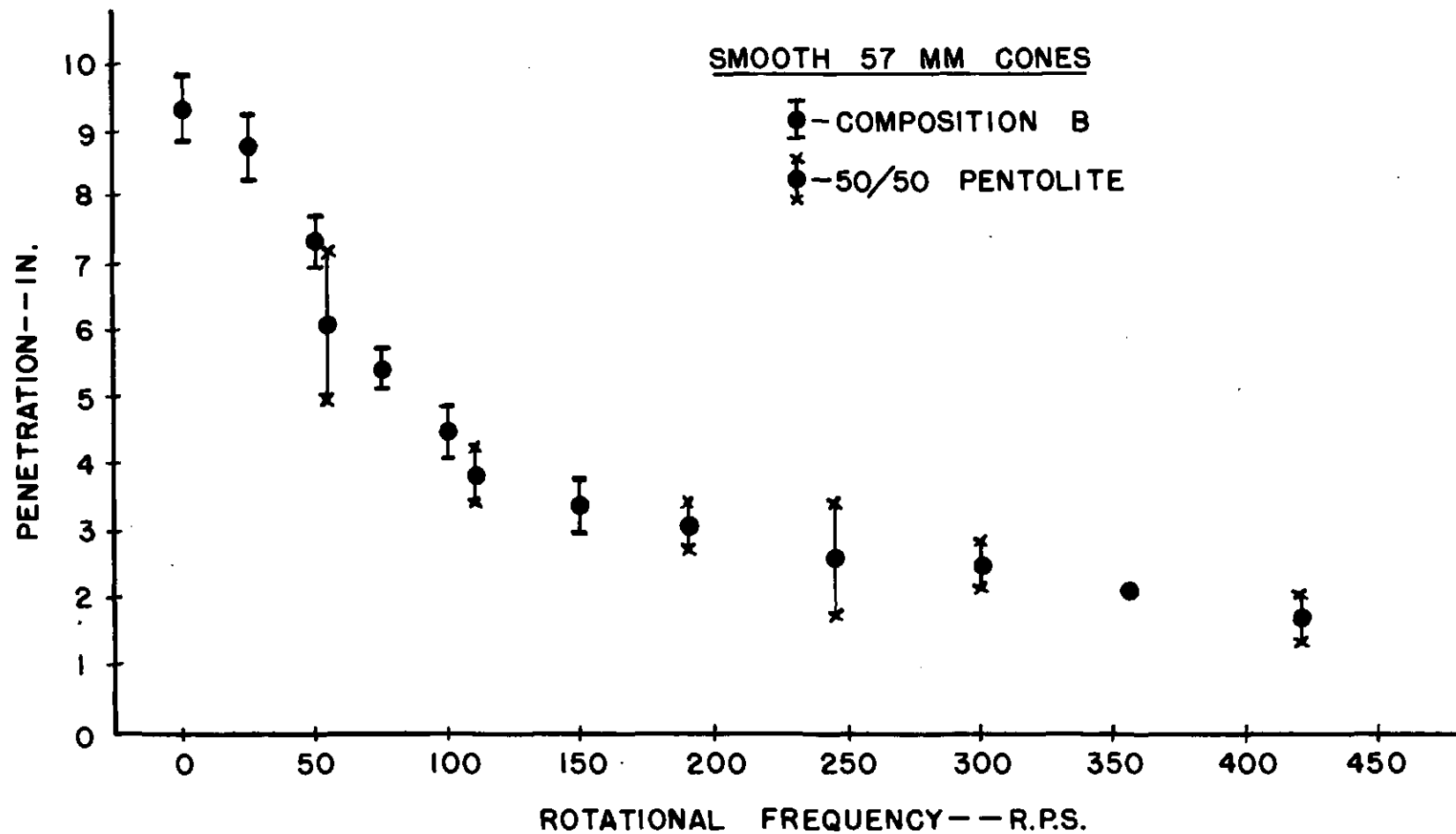
Figure 1—Smooth 57 MM cones.

Responsibility for the development of applicable methods of manufacture was assumed by the National Bureau of Standards; and a number of linear flute designs have been manufactured. A representation of a typical product is given in Fig. 2. This figure shows several cross sections of a fluted cone. The canted surfaces, which are usually segments of circles canted with respect to the pitch circle of the smooth cone, and the flute or offset surface joining the extremities of two canted segments may be observed.

The first cones manufactured by N.B.S. were formed with a fluted punch and a rubber pressure pad. The fluted punch is formed by machining the fluted cone design into a steel replica of the cone to be fluted. This punch and a rubber padded smooth die are then used to form flute contours into the copper cone. The rubber acts as a hydraulic medium, forcing the cone against the punch and causing flute contours to appear in the exterior surface of the cone as well as the interior. Typical flutes formed in this manner are shown in Fig. 3. The contours formed on the interior of the cone are reasonable but not perfect reproductions of the punch; but the contours formed on the exterior of the cone bear little resemblance to the contours actually present on the punch.

Fig. 4 shows profiles which were produced when N.B.S. developed a method of producing fluted dies. The dies are cobalt-phosphorous alloy replicas of the fluted punch. Such a replica, prepared by electro-deposition and seated in a tool steel block, may be used as a fluted die. The contours in Fig. 4 were produced by such a die used in conjunction with a rubber padded smooth punch.

It would seem that the next step in development of fluted liners would be the use of matched metal dies and punches. Fig. 5 shows typical contours for such liners. Little experimental information is available for designs of this type and they will not be discussed further here.

Examples of typical results from fluted liners which are of interest in the 57mm HEAT problem are given in Figs. 6, 7, and 8. Fig. 6 shows data which gives evidence of 100% compensation at 150 r.p.s. and a curve shape which is a reasonable facsimile of that of the smooth liners, except for the shift in the frequency at which best penetration performance was obtained. (The solid curve represents performance data for the smooth 57mm copper liners.) These cones had sixteen linear flutes with a nominal maximum depth (at the cone base) of 0.025 in. formed by the method illustrated in Fig. 3. It should be noted that, with few exceptions, the reproducibility of results is as good as with smooth liners. Penetrations as high as 7.4 in. at 210 r.p.s. should be compared with the 2.8 in. to be expected from smooth liners at the same frequency.

Fig. 7 shows penetration depth vs. rotational frequency data for a group of liners having 16 linear flutes of 0.035 in. nominal maximum depth, also formed by the method illustrated in Fig. 3. These liners show compensation at a much higher frequency than those of Fig. 6; but they do not show as high a degree of compensation. The best performance is about 7 in. penetration, or 75% compensation, at 330 to 360 r.p.s. This penetration is nearly 3 times the penetration of the smooth liners at the same frequency. Even at 210 r.p.s., where only 60% compensation is shown, the penetration of the fluted liners is twice that of the smooth liners.

333
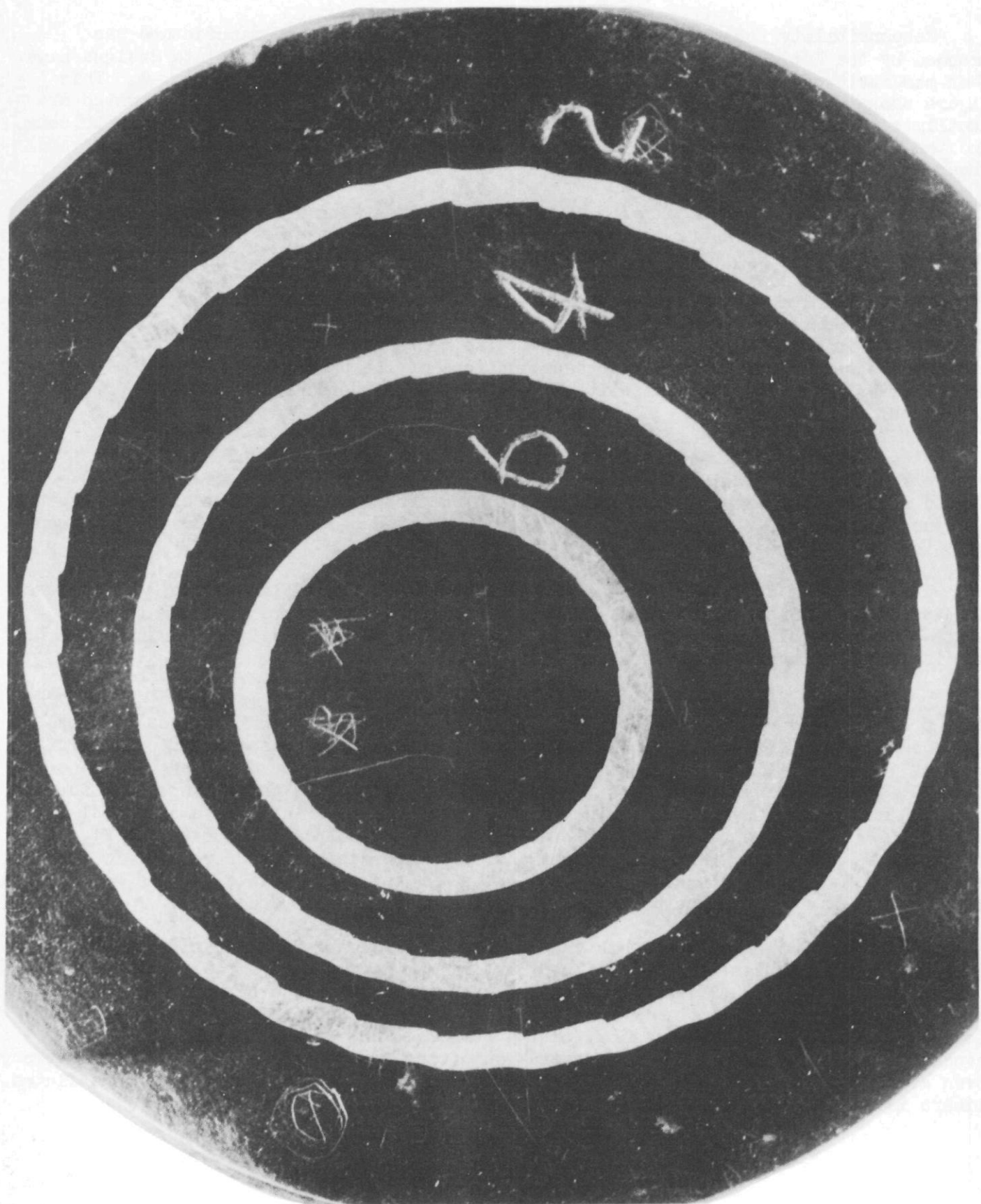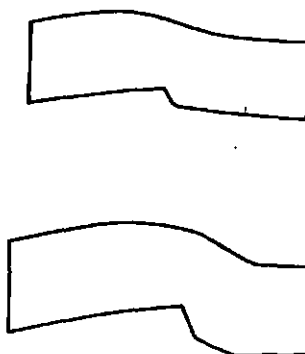
Figure 2

Figure 3—Typical RS flute contours formed with fluted punch and rubber padded die.
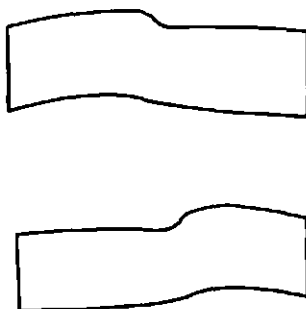
Figure 4—Typical SR flute contours formed with fluted die and rubber padded punch.
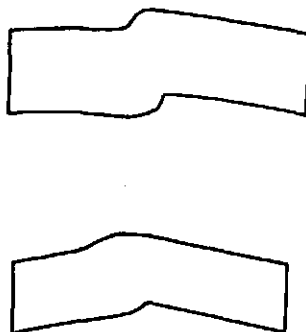
Figure 5—Typical SS flute contours formed with matching steel dies.

335
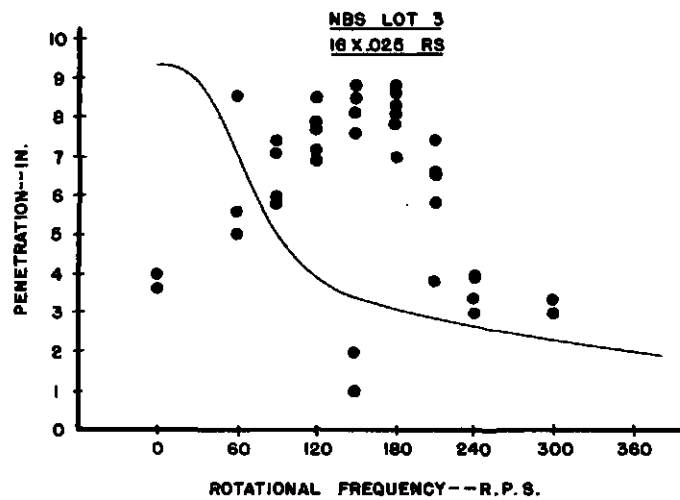
Figure 6—NBS Lot 3, 16 x .025 RS.
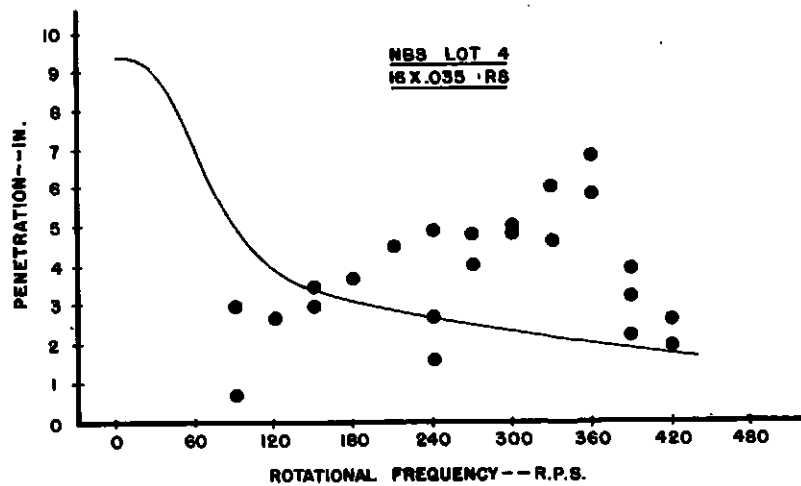
Figure 7—NBS Lot 4, 16 x .035 RS.
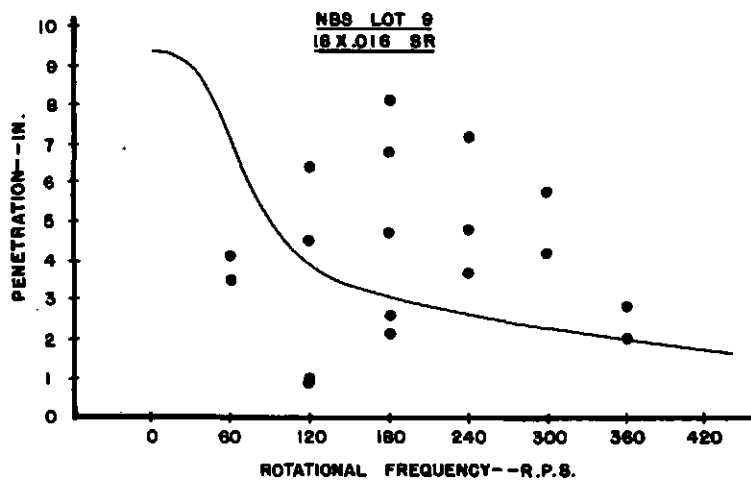
Figure 8—NBS Lot 9, 16 x .016 SR.

Fig. 8 show penetration-frequency data for another group of liners having about the same dynamic characteristics as those shown in Fig. 6. However, the data represented in this figure show quite clearly the variability that some groups of fluted liners have exhibited. The best performance to be expected from these liners at 210 r.p.s. would be about 7.5 in. or about 3 times the penetration of the smooth liners at that frequency. These liners had 16 linear flutes of 0.016 in. maximum depth formed by the method illustrated in Fig. 4. The optimum frequency of the liners of Fig. 8 is more than twice that of the liners having the same nominal specifications formed by the method illustrated in Fig. 3.

The accumulation of data from several lots of fluted liners has indicated certain correlations between design parameters of fluted cones and their performance. For cones having sixteen flutes, the optimum frequency is essentially a linear function of the flute depth. This linear correlation holds for flutes formed as illustrated by either Fig. 3 or Fig. 4, but, for the same nominal flute depth, the liner having flutes formed sharp on the exterior has an optimum frequency which may be as much as 3 times as large as that of the liner fluted with a punch and rubber padded smooth die.

Difficulty has been encountered in obtaining complete compensation at optimum frequencies above 150 r.p.s. If flute depth is increased beyond that required to give an optimum frequency of 150 r.p.s., the performance at the optimum frequency begins to degrade. This is apparently due to mechanical failure of the liners along the corners of the flutes, which in turn is likely due to the fact that the simple linear flutes used thus far are not the ideal. Empirical design of non-linear flutes from data obtained in tests with the linear flutes is contemplated. The interpretation of degradation with increasing flute depth is strengthened by results obtained with heavier blanks. Much deeper flutes can be tolerated when heavier blanks are used but, as would be expected, the optimum frequency for a given flute design decreases with increasing wall thickness.

For constant flute depth, as the number of flutes is increased from 16 to 36, the direction in which the liner must be rotated in order to achieve compensation is reversed if the flute orientation is kept constant. This means that if a 16 flute liner has a positive compensation frequency, the corresponding 36 flute liner will show a small negative compensation frequency. This reversal in direction of compensation was entirely unexpected at the time of the initial observation but has since been established unquestionably by experimental observations. As the flute number is increased from 36 to 60, the magnitude of the negative compensation frequency increases slightly. With flute numbers in excess of 60, no further increase in compensation frequency with flute number has been observed. These experimental observations provide the basis for rejection or modification of early theories of compensation and will provide a critical test of future proposals for such a theory.

There is no apparent reason that a fluted liner design which will compensate at 210 r.p.s. and have good reproducibility cannot be developed. The proper compensation frequency has been closely approximated and offers no real problem. The more troublesome problem of variability is now being investigated through gaugings of each fluted cone before firing. These data require tedious and laborious statistical treatment; but significant results are being obtained.

337

There are two general fields for theoretical work in connection with spin degradation and spin compensation. The first of these, dealing with spin degradation, implies a theory to explain the effects of rotation upon the collapse and penetration of smooth liners. The second general field, spin compensation, means here a theory for the mechanism of compensation by fluted liners.

The effects of spin upon smooth shaped charge liners have been treated briefly by Birkhoff.[2] These equations were derived for steady state collapse geometry but may be adapted readily to non-steady state collapse geometries. No definitive experiment has yet been carried out; but the equations appear applicable to such data as are available.

Theoretical treatment of the mechanism of compensation by fluted cones has been attempted by several groups. The initial version of the E.R.L. theory assumed that only the influence of the canted surface collapsing toward its center was important. It was determined, however, that the observed direction of compensation was opposite to that predicted by the theory. A later theory developed by E.R.L. predicted compensation in the proper direction (for small numbers of flutes) but does not give predictions in quantitative agreement with observation.

Since that time, theoretical work, primarily by C.I.T., has progressed until now it is believed that three effects may influence the behavior of fluted liners. The first of these is the variation in impulse received by a liner from a detonation wave with the thickness of the liner. The second is the variation in impulse received by a liner with the inclination of the liner to the detonation wave. The third effect (the only one of the three considered by E.R.L.) is the tangential component of velocity which (possibly) can be obtained from the collapse of the fluted liner. Of these three effects, it is believed that the first is by far the most important. Each of the first two effects may be experimentally separated and studied by means of plate liners. Experimental and theoretical investigations with these simple models has been accomplished; but application of the results to a theory of fluted liners is difficult.

A theoretical paper to be given later by L. H. Thomas (Watson Scientific Computing Laboratory) treats by shock wave techniques the first effect mentioned for liner designs that actually can be manufactured but which are different from those that have been tested.

In conclusion, although no quantitative theory is yet available, compensation by fluted liners seems to be the simplest and most promising way to counteract spin degradation in shaped charge ammunition. There is no apparent reason that liners manufactured to reasonable industrial tolerances and designed to compensate at service frequencies cannot be developed.

2/ Ballistic Research Laboratory, Report No. 623, "Hollow Charge Anti-Tank Projectiles", Aberdeen Proving Ground, Maryland, February 10, 1947.

MINIMIZING THE EFFECT OF ROTATION UPON THE PERFORMANCE OF LINED CAVITY CHARGES

Hugh Winn

Defense Research Division, The Firestone Tire and Rubber Company, Akron, Ohio

ABSTRACT

The effect of rotation on the penetration of shaped charges is described. An empirical correlation, useful for design purposes, is presented, which permits one to estimate the spin rate penetration curve for shaped charges with reasonable reliability.

In an effort to overcome the deleterious effect of rotation both fluted liners and double body projectiles have been studied. It is shown that a degree of spin compensation has been obtained by each method and that the prospect for an ultimate solution to the problem is bright.

It is well known that the penetration of lined cavity charges is greatly reduced by the rotation required for spin stabilized shell. The extent to which penetration is reduced by rotation is shown in Figure 1. These curves have certain very interesting features. The penetrations at 0 and 240 rps are proportional to the base diameter of the liners. This means that the penetration efficiency-spin rate curves for these two liners coincide at 0 and 240 rps, but at intermediate spin rates, the efficiency of the 105mm liner degrades with increasing spin much more rapidly than does the 57mm liner. As a first approximation it appears that the rate of loss of penetration at stated spin rates is proportional to the non rotated penetration, that is,

$$L = FSP_o \qquad (1)$$

$$\text{and } P_s = P_o(1-FSP_o) \qquad (2)$$

$$\text{where } L = 1 - \frac{P_s}{P_o}$$

$S =$ spin rate, rps

$P_s =$ penetration at S rps

$P_o =$ penetration at 0 rps

Values of the FS vs S function are shown in Figure 2. The curves drawn represent the composite data for several hundred rounds. It is very significant that the curves for the 57mm and 105mm liners coincide up to 45 rps. Thus, over this range equations (1) and (2) hold for both 57 and 105mm liners, and also presumably for a wide variety of

Figure 1

$$L_s = FSP_o$$
$$P_s = P_o(1 - FSP_o)$$

Figure 2

340

Figure 3—Effect of rotation upon penetration.
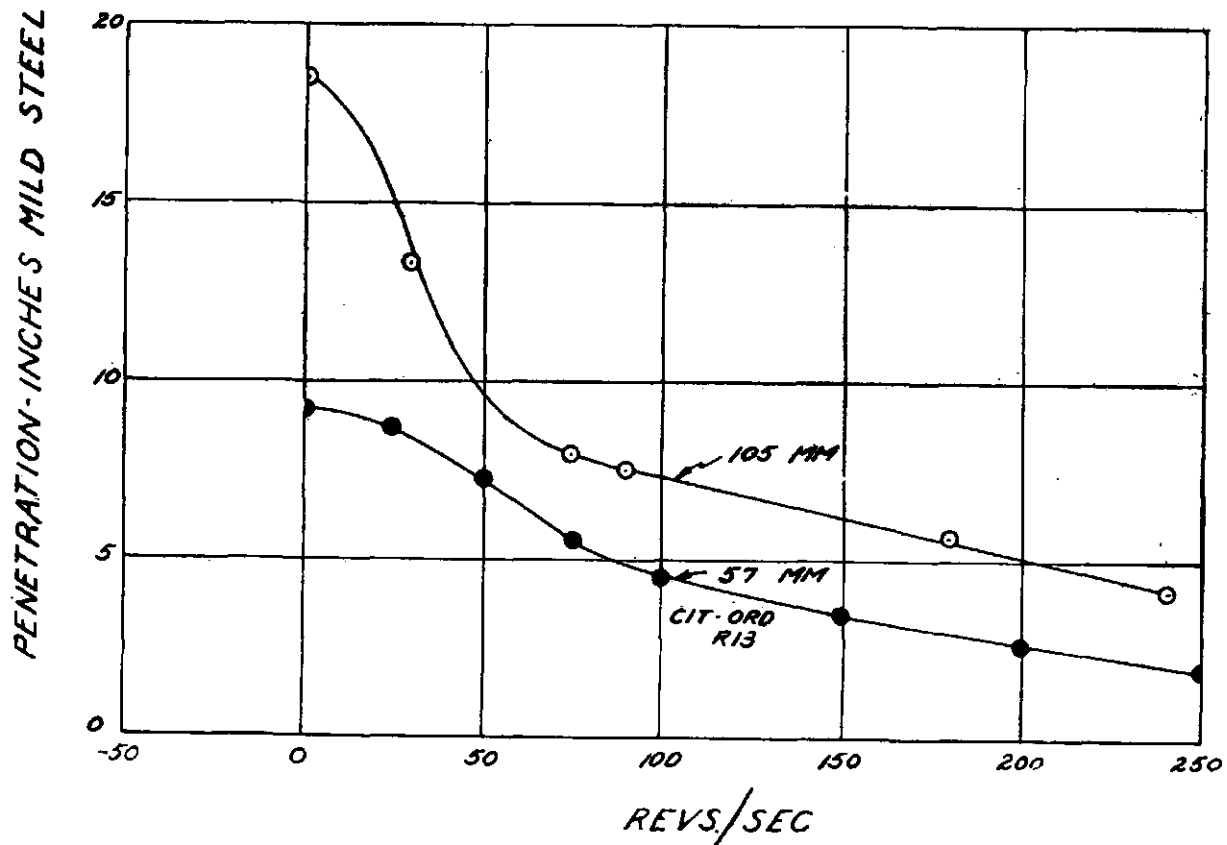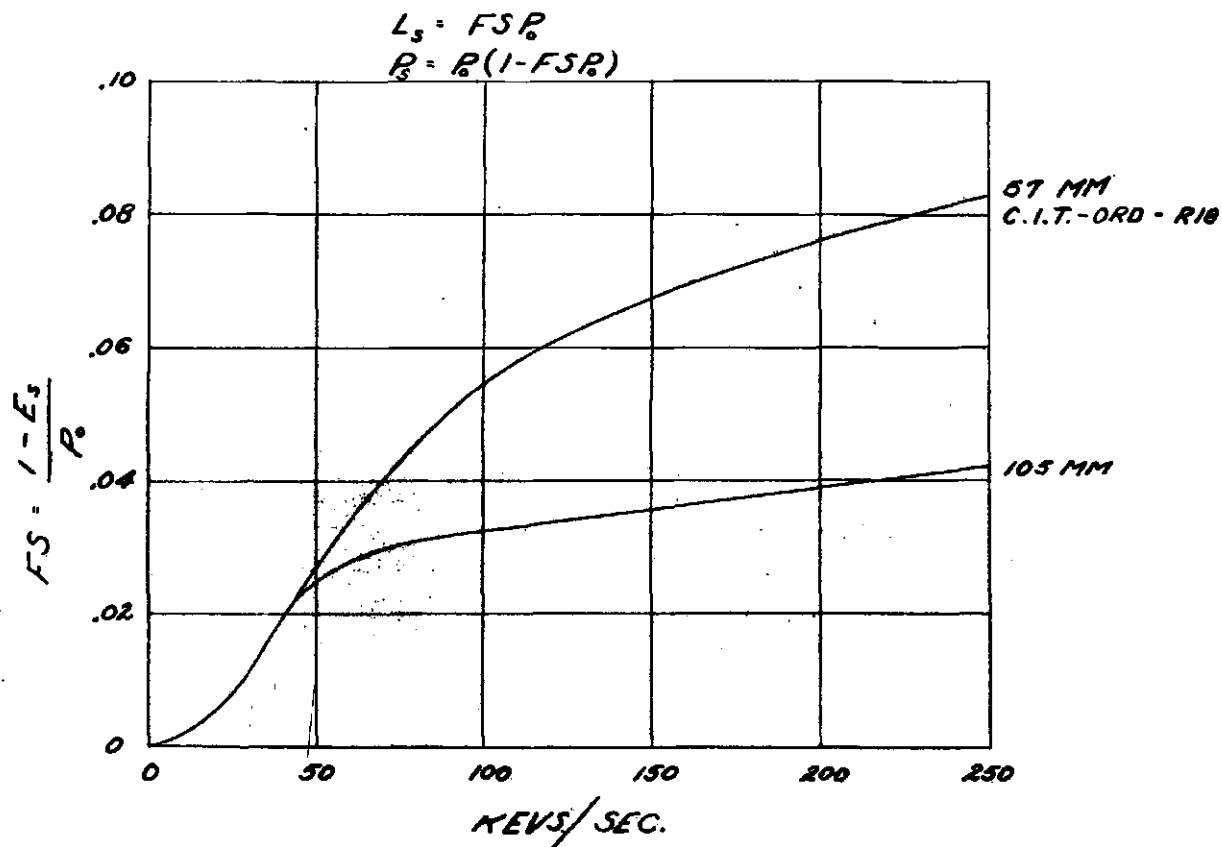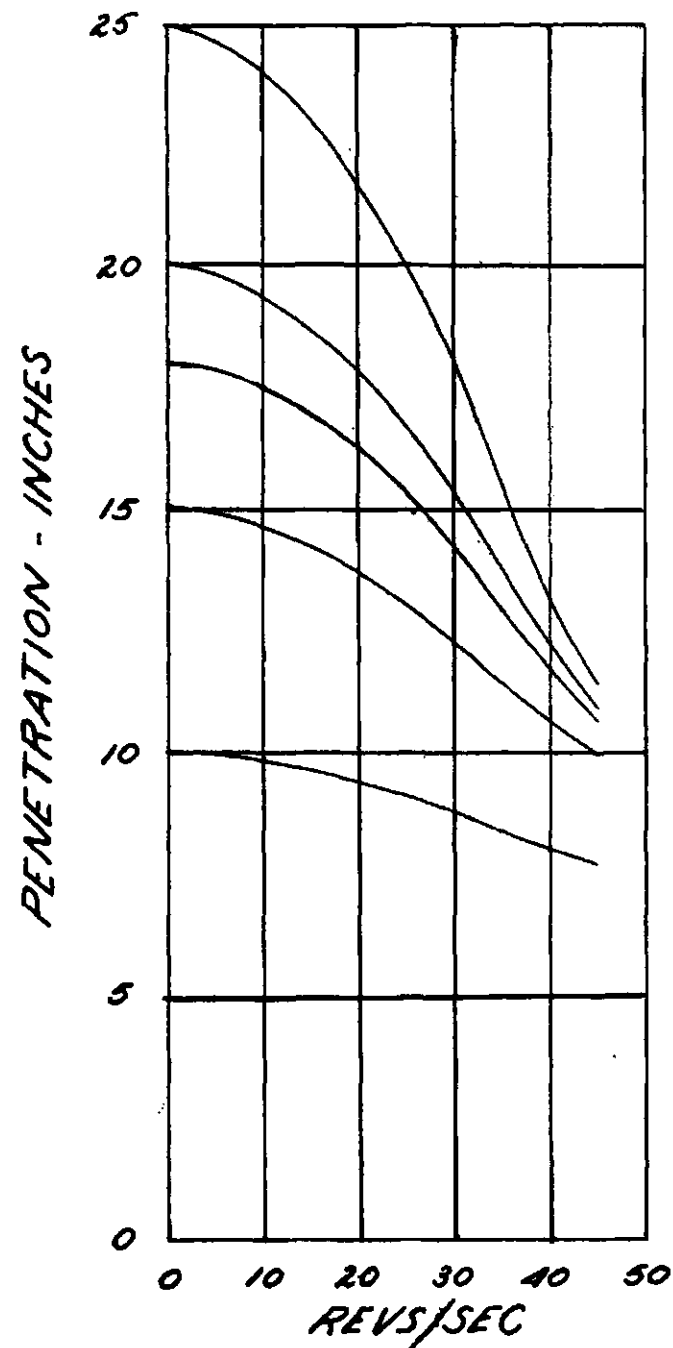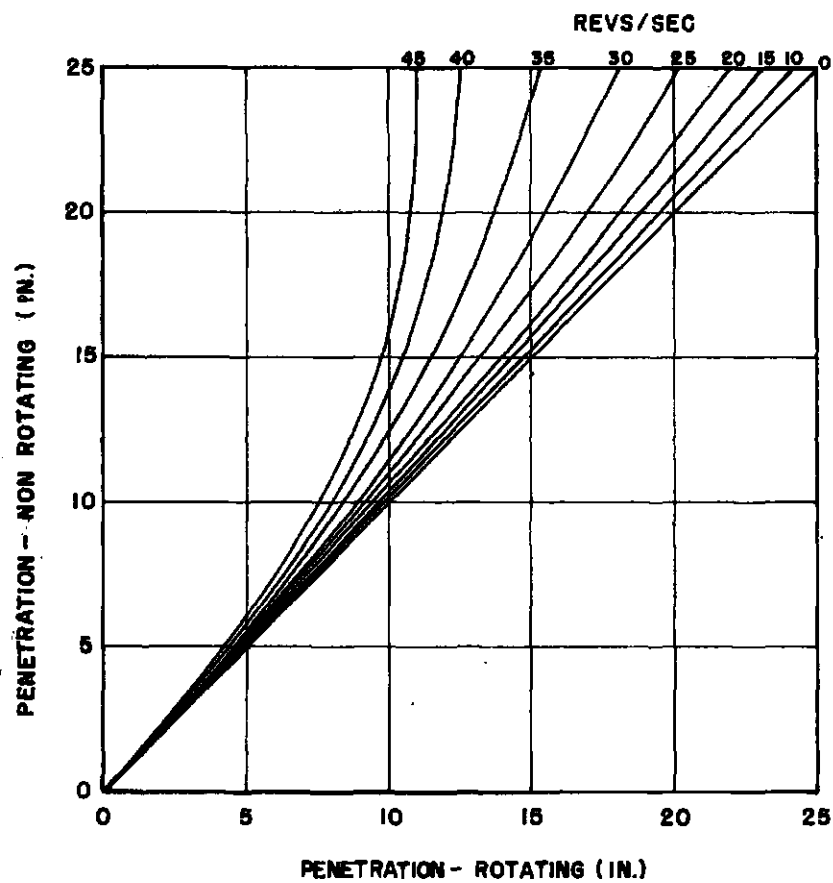
Figure 4

other shapes and types. Equations (1) and (2) and the correlation of Figure 2 have
been used to evaluate the penetration-spin rate behavior for series of liners of vary-
ing non-rotating penetration. These data are shown in Figure 3. Predictions based on
these curves are remarkably sound. In some seventeen comparisons, totaling some 200
rounds and including such variations as 45° to 60° conical liners both with and without
spit back tubes, trumpets, hemispheres, mild steel and armor plate targets, 45 and 105mm
diameters, standoff, and charge shape, the estimated values were within the standard
deviation of the experimental measurements. Based on Figure 3, Figure 4 shows the
estimated penetration curves for liners whose non-rotated penetrations are 10, 15, 18,
20 and 25 inches. It is significant that very little advantage results by using
larger liners, or more perfectly made liners, if they must be spun faster than about
40 rps.

Since rotation tends to cancel out the improvements gained by using larger or more
perfectly made liners, in order to achieve penetrations in the range of 15 or 20 inches
one must either design a round in which the rotation is kept below 30 or 40 rps, or
one must modify the liner and/or charge so as to shift the axis of optimum performance.
Fin stabilized rounds, "slow spin" rounds of the T-138 type, and double body projec-
tiles, which will be described presently, are examples of methods by which the rota-
tional rate may be held at an acceptably low level. The use of fluted or serrated
liners is an example of an attempt to shift the axis of optimum performance from zero
to the higher spin rate where spin stabilized projectiles are feasible.

During the past year, Firestone, working with the groups at Carnegie Institute of
Technology and BRL, has manufactured and tested ten series of fluted liners of varying
design. At the present time a certain degree of success has been achieved, and
certain design factors have been at least qualitatively established.

The penetration-spin rate curves for the ten series of liners are shown in
Figures 5 - 14, inclusive. The flute profile for each design is also shown in these
figures. All liners were conventional 105mm copper liners machined from hard drawn
electrolytic copper bar meeting Federal Specification QQ-C-501a. All rounds were
assembled in cylindrical mild steel test bodies, loaded with Comp. B at Picatinny
Arsenal, and fired at a 7 1/2-inch standoff against a mild steel target. The design
relationships noted will be described after the various curves have been examined.
Figures 5 - 9 show the behavior of 16 flute liners. The performance of the DRD 17-1
and 2 liners shown in Figure 5 is very disappointing. The best performance was only
12 inches penetration at 0 rps. Figure 6 shows the behavior of the DRD 17-6 liners.
This series, with a heavier wall, but being otherwise similar to the DRD 17-1 and 2
liners, has a penetration of 16 inches at 15 rps. Figure 7 shows the performance of
the DRD 32-3 liners. These liners, differing from those of the DRD 17-1 and 2 series
by having a curved rather than a flat flute profile, penetrated 8.5 inches at 35 rps.
Figure 8 is for the DRD 34-3 series. This series, having a deeper flute than the
DRD-17-6 series, but being similar otherwise, has a penetration of 9.6 inches at 55
rps. The DRD 78-2 liners shown in Figure 9 were the only liners with matching internal
and external flutes. The best penetration was 17.0 inches at 5 rps.

Figures 10 - 12 show the behavior of three series of 36 flute liners. It should
be noted that compensation in the positive direction is obtained with 36 or more flutes
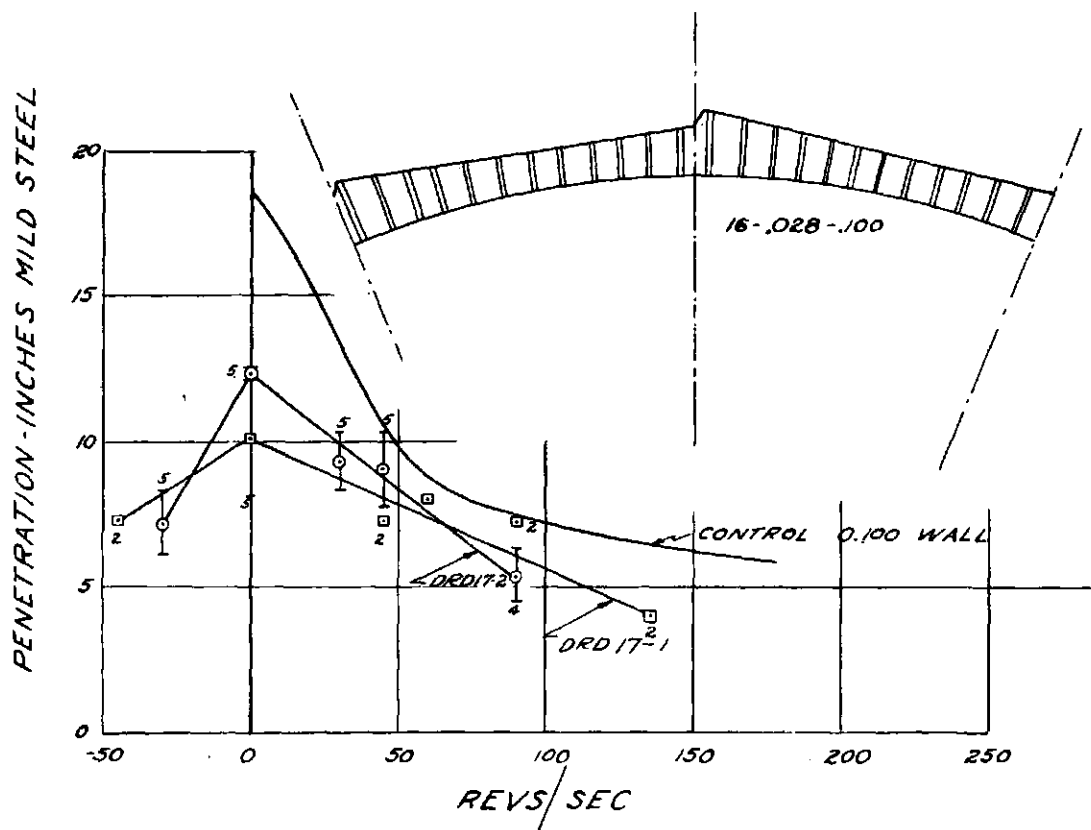
Figure 5
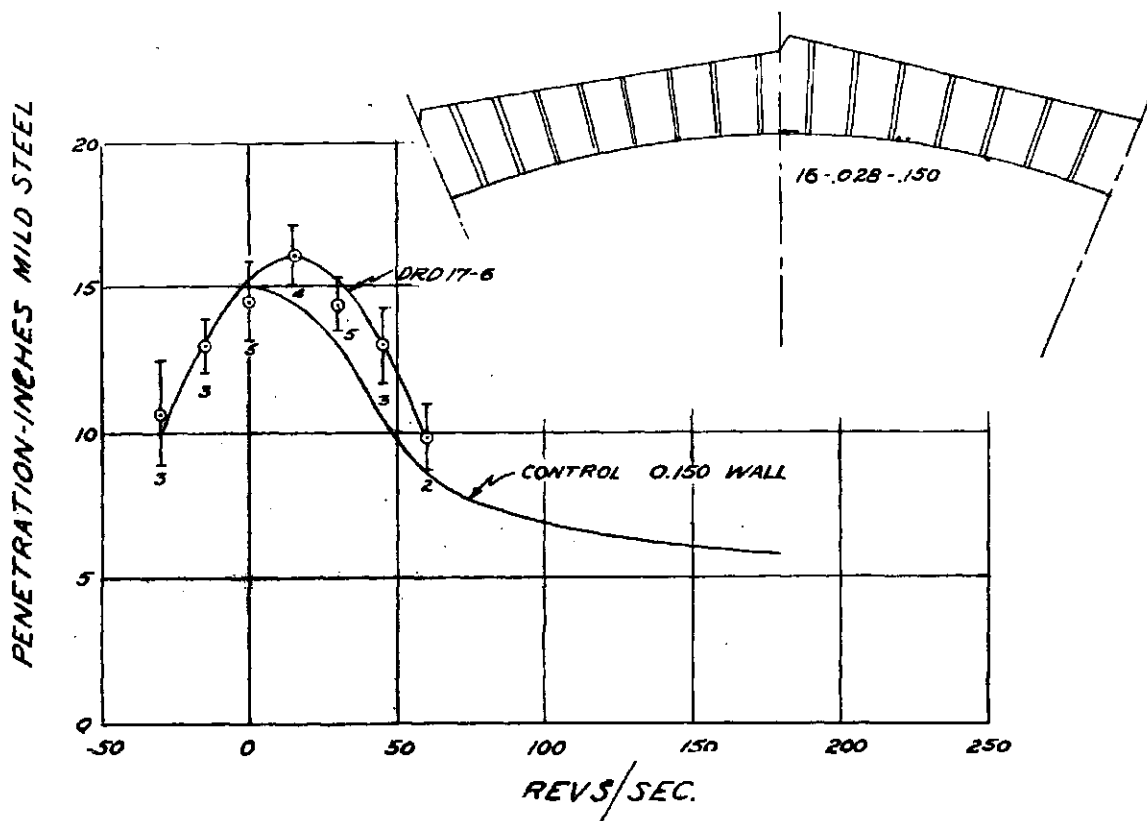
Figure 6
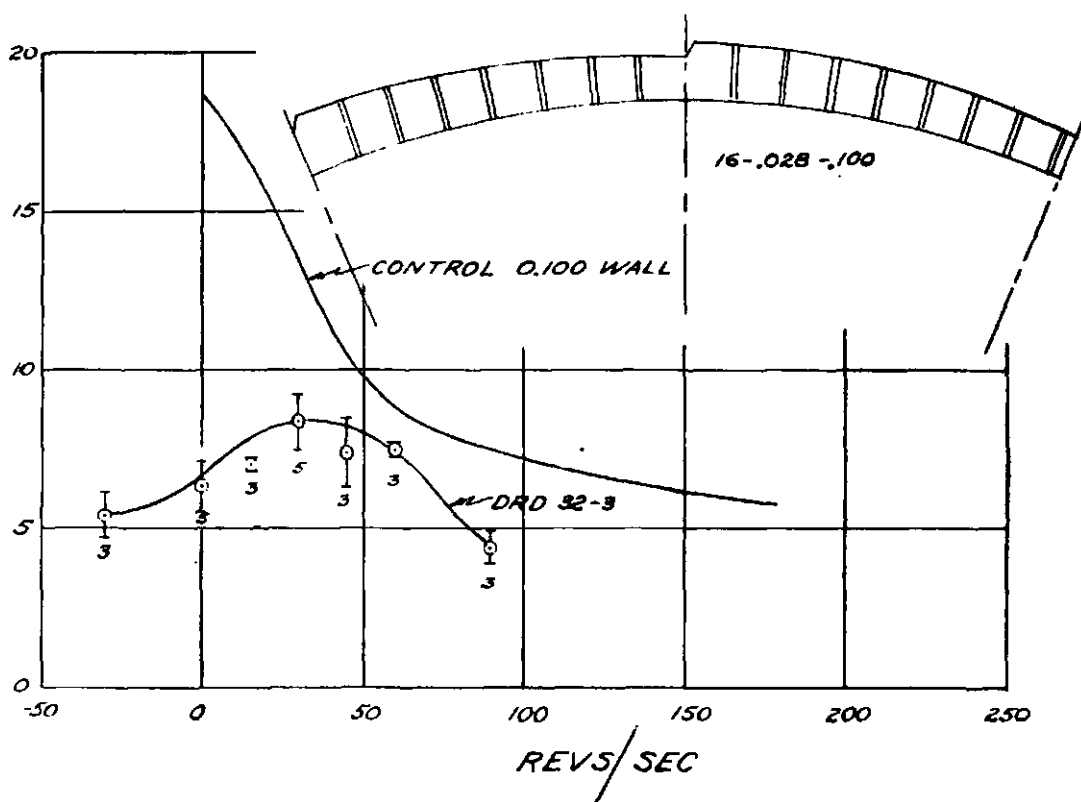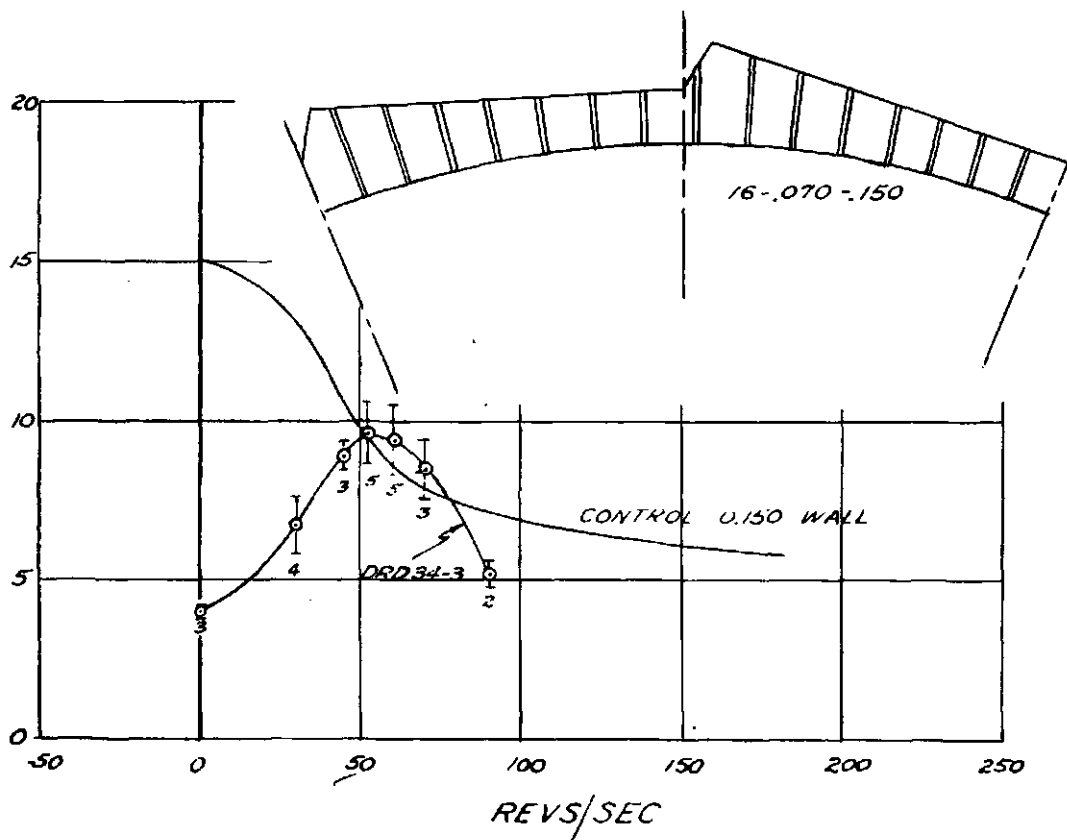
343

Figure 7

Figure 8

344

Figure 9

Figure 10

345

Figure 11

Figure 12

346

Figure 13

Figure 14

347
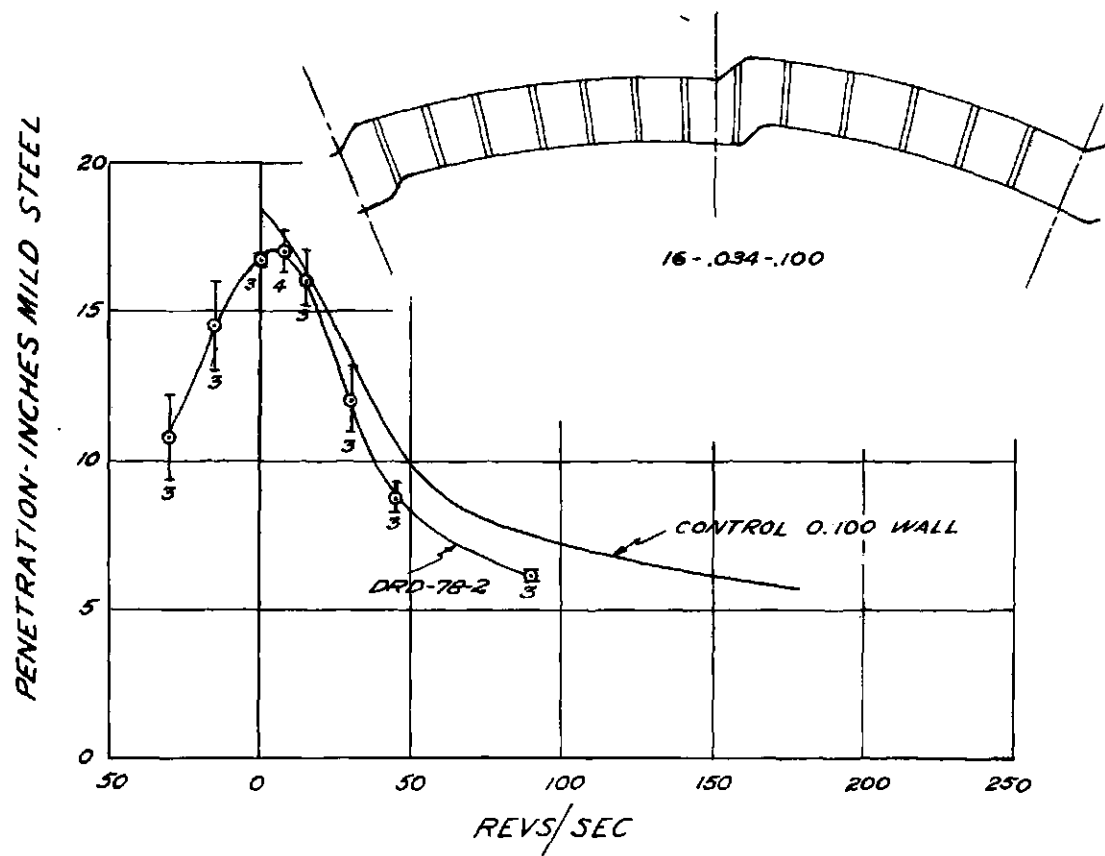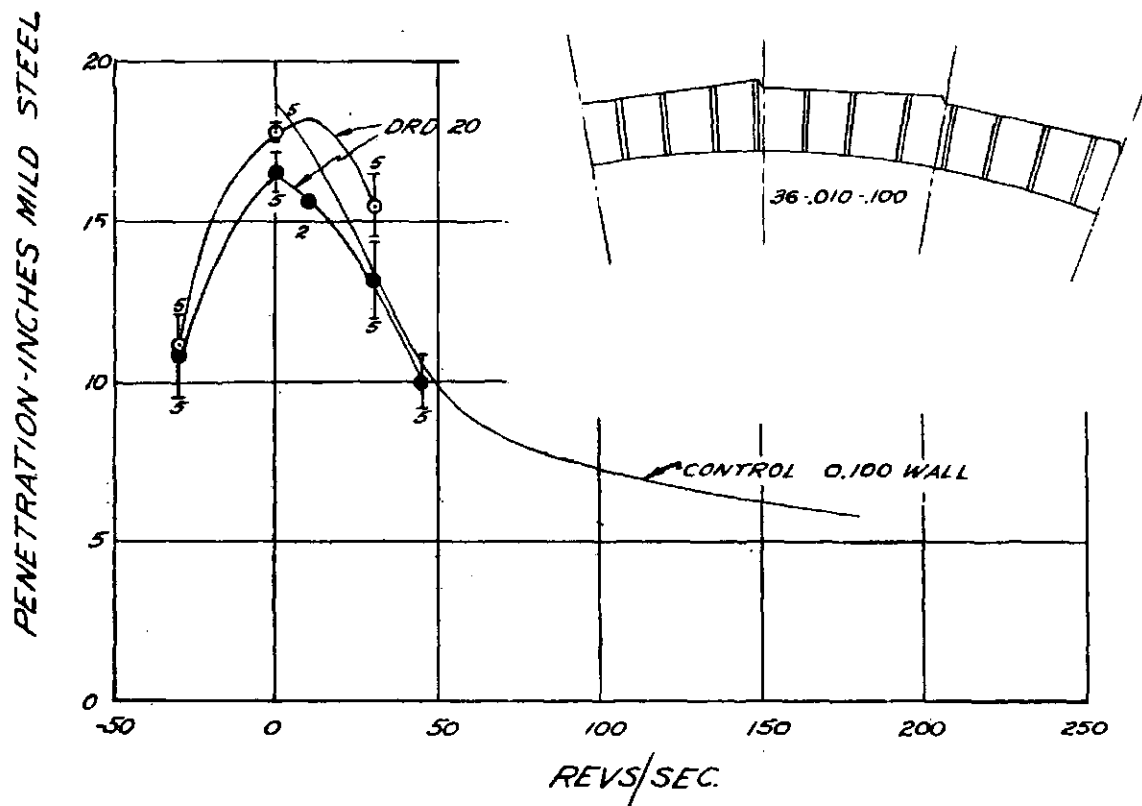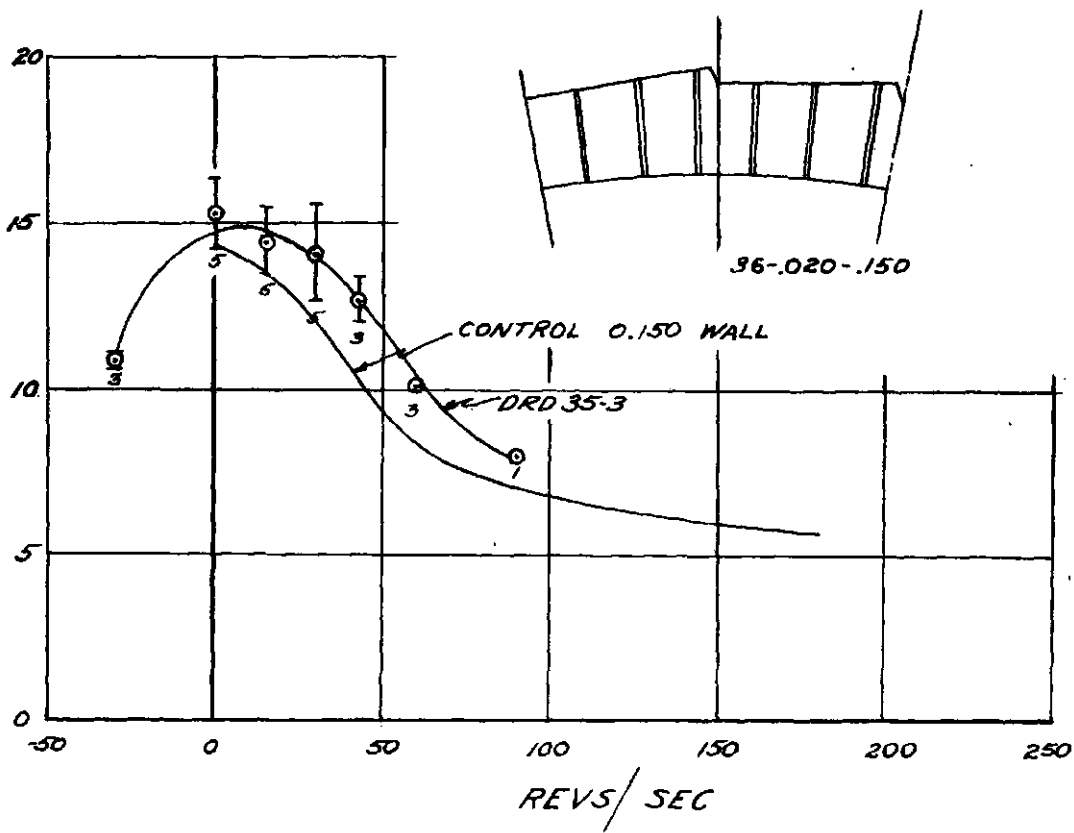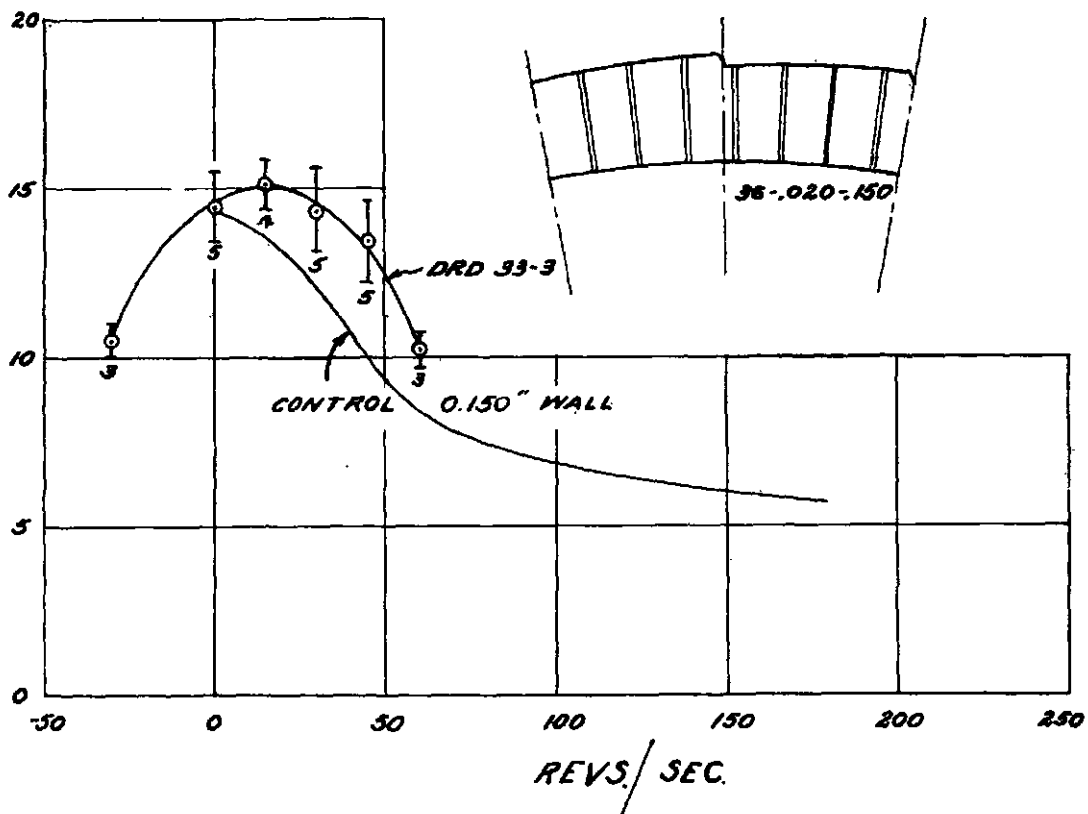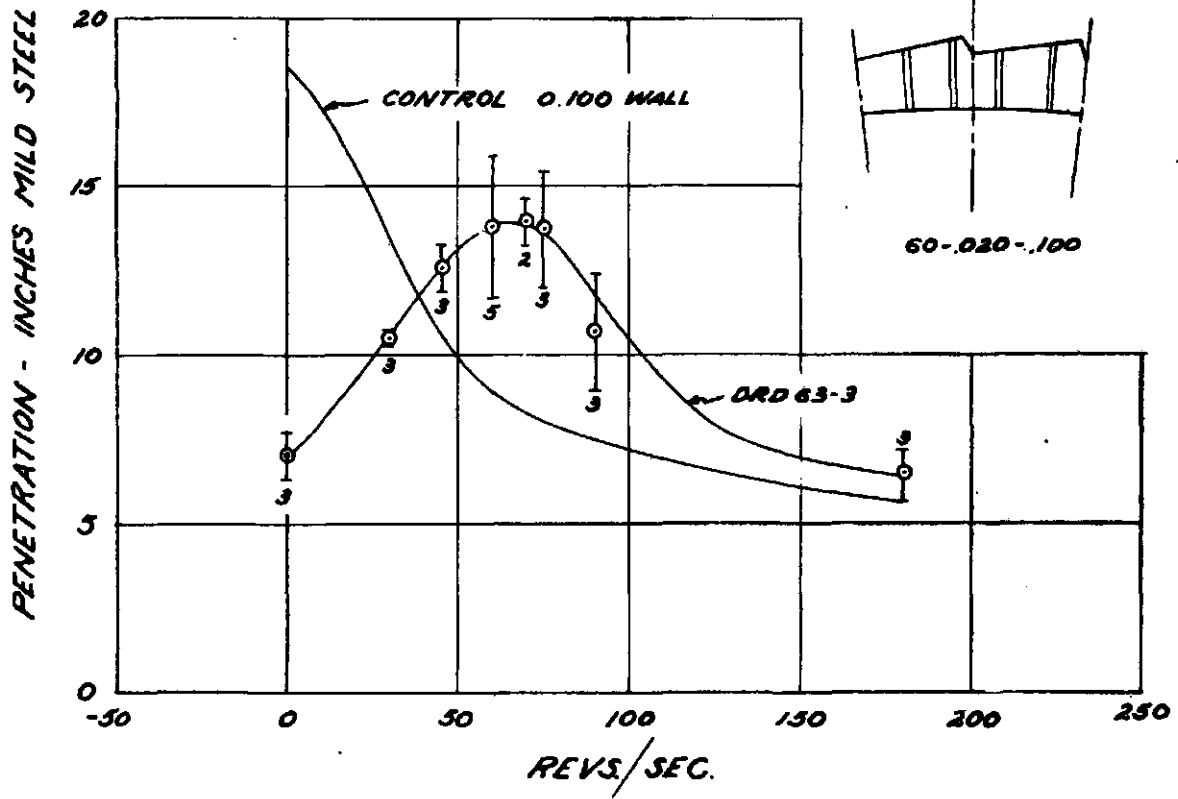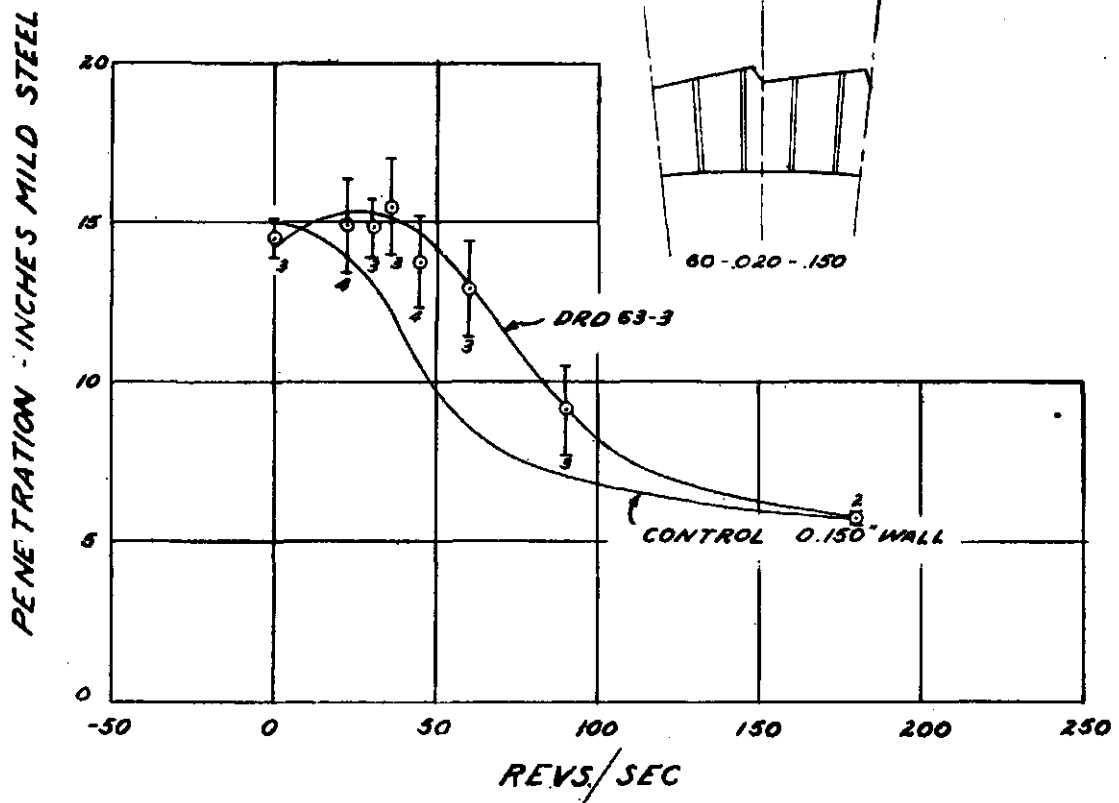
only when the flute orientation is the reverse of that used in the 16 flute series. There are two series of DRD-20 liners, representing different manufacturing tolerances, shown in Figure 10. The close tolerance liners penetrated 18.2 inches at 10 rps, while the second series did not show any compensation. The DRD-20 liners, historically the second series tested in Firestone's program, showed the importance of careful manufacture and all subsequent series met the close tolerance specification. Figure 11, for the DRD 35-3 series, shows a maximum penetration of 15.0 inches at 10 rps. Both flute depth and wall thickness are greater than for the first 36 flute series (Figure 10). Figure 12 shows the DRD 33-3 series having curved flutes instead of flat flutes. A penetration of 15.2 inches was measured at 15 rps.

Figures 13 and 14 show the behavior of two DRD 63-3 60 flute series of liners which differ only in wall thickness. The thinner wall series liners penetrated 14.0 inches at 65 rps and the thicker wall series penetrated 15.3 inches at 25 rps.

The performance of these ten series are summarized in Table I. Let us now consider the effect of design variables upon optimum spin rate and, independently, upon penetration. A comparison of item 10 with 11 shows that for a given flute contour, the optimum spin rate is certainly a function of wall thickness, the thinner wall thickness, the thinner wall compensating at the higher spin rate. A comparison of items 3 and 5 shows that, other things being equal, the optimum spin rate increases with increasing depth of flute. A comparison of item 8 with 11 shows that the optimum spin rate depends upon the number of flutes. As indicated by the negative sign in brackets after the 16-flute series, a given flute orientation causes a 16 flute liner to compensate in a direction opposite to that of a 36 or 60 flute liner. It appears that the inversion point is near 25 flutes.

A comparison of items 8 and 9 shows that with 36 flutes the curved and flat flute designs cause similar performance, but as shown in items 2 and 4, with only 16 flutes a curved flute is better than a flat flute.

Let us now consider the penetration obtained at the optimum spin rate. In each case where the minimum wall thickness of the fluted liner is not less than .090 inch the penetration is as good as the non rotating penetration of a smooth liner having a uniform wall thickness equal to the maximum wall thickness of the fluted liner. When the minimum wall thickness is less than about .090 inch the penetration is proportionately reduced. Therefore, a minimum wall thickness of about .090-.100 inch must be maintained if full penetrating efficiency is to be obtained. Now, in general the optimum wall thickness of smooth 105mm liners is about .100 inch. Thicker walls result in reduced penetration. If it is desired to design a liner for operation at high spin rates relatively deep flutes will be required, and if a minimum wall of .090 inch is to be maintained the nominal wall thickness will be fairly large. Under these con-. ditions the fluted.liner may be expected to show a total penetration at the high spin rate equal to a non rotated smooth liner of equivalent maximum wall thickness (100% compensation), but the penetration will be somewhat less than the non rotated penetration of a smooth liner of optimum wall thickness.

The DRD 78-2 liners showed a rather anomalous behavior. This series did not show an appreciable compensation. All series which do show appreciable compensation have a flute profile with a uniformly increasing wall thickness. Because of the particular

348

geometry of the DRD 78-2 liners, the wall thickness is approximately constant over the major portion of the flute profile. As a result no appreciable compensation is observed even though a portion of the mass of the liner should have been compensated. From this we conclude that compensation arises mainly as a result of a symmetrical variation in wall thickness, and that flute contour is of importance only in so far as it causes a variation in wall thickness. This statement agrees qualitatively with the "thick-thin effect" described by Dr. E. Pugh and his co-workers at Carnegie Institute of Technology and tends to substantiate the recent predictions of Dr. L. H. Thomas of Watson Scientific Computing Laboratory as set forth in BRL Report No. 765. If further studies confirm that a symmetrical variation in wall thickness is a primary and controlling pre-requisite for compensation, then a liner fluted on the inside only should be as effective as one fluted on the outside only, except that the direction of compensation should be reversed. Experiments now in progress should help to clarify this question.

Another different approach to the question of spin compensation which has received some attention in this laboratory is one employing a double body projectile. An exterior portion has a conventional rotating band and spins at the usual stabilizing rate while the charge carrying portion mounted on ball bearings is constrained by its own inertia to rotate at a relatively lower rate. Figure 15 shows one type of such a double body projectile. There are two major problems involved in the development of this type of round. In the first place, either the bearings must be capable of accepting the thrust load caused by setback without developing too large a frictional torque, or both parts of the projectile must be subjected to the same acceleration so that only a relatively low unbalanced thrust load need be sustained by the bearings. It is possible to balance the acceleration by the relatively simple expedient of adjusting the base areas of the two parts so that the area of each exposed to the propellant gases is proportional to its respective mass. This required that the non-rotating body fit inside the stabilizing section and, for a given bore diameter limits the size of the shaped charge. On the other hand, if the total thrust load can be carried by the bearing system it is possible to use a larger size liner. Since the thrust loads developed in the BAT weapon are not unreasonable and because penetration is of supreme importance, the studies in this laboratory have thus far been directed toward the development of a bearing system capable of accepting the full thrust load. A simple annular pivot bearing of the type shown in Figure 15 has demonstrated considerable promise. Lubricated with "molykote", a test slug with such a bearing developed only 40 rps in the non-rotated section, even though the stabilizing section was spinning at about 240 rps. A ball bearing thrust system is under development.

The second basic problem with double body projectiles concerns their flight stability and accuracy. If the round functions properly, and the charge carrying part is indeed rotating at a relatively low rate, how large must the rotating portion be to stabilize the round? Unfortunately we do not now have an answer to this question.

SUMMARY

The effect of rotation upon penetration be shaped charges has been described and a chart has been presented which permits the designer to estimate the spin rate penetration curve of a specific liner with reasonable accuracy.

DRC-215 TEE, ONE REQ'D.

DRA-274 THRUST BEARING, ONE REQ'D

#N-20206 NEW DEPARTURE
BALL BEARING, TWO REQ'D

DRB-229 ROTATING BAND, (ONE IN 20 TURNS), ONE REQ'D.

1"-8 L.H. NC-2 JAM NUT,
ONE REQ'D — — STAKE
IN 3 PLACES AFTER FINAL ASSY

DRC-214 FRONT BODY, ONE REQ'D.

DRC-209 CONE ASSY #1, ONE REQ'D.

DRC-232 REAR BODY, ONE REQ'D

DRB-269 NOSE, ONE REQ'D.

DRA-307-PLUG, ONE REQ'D.
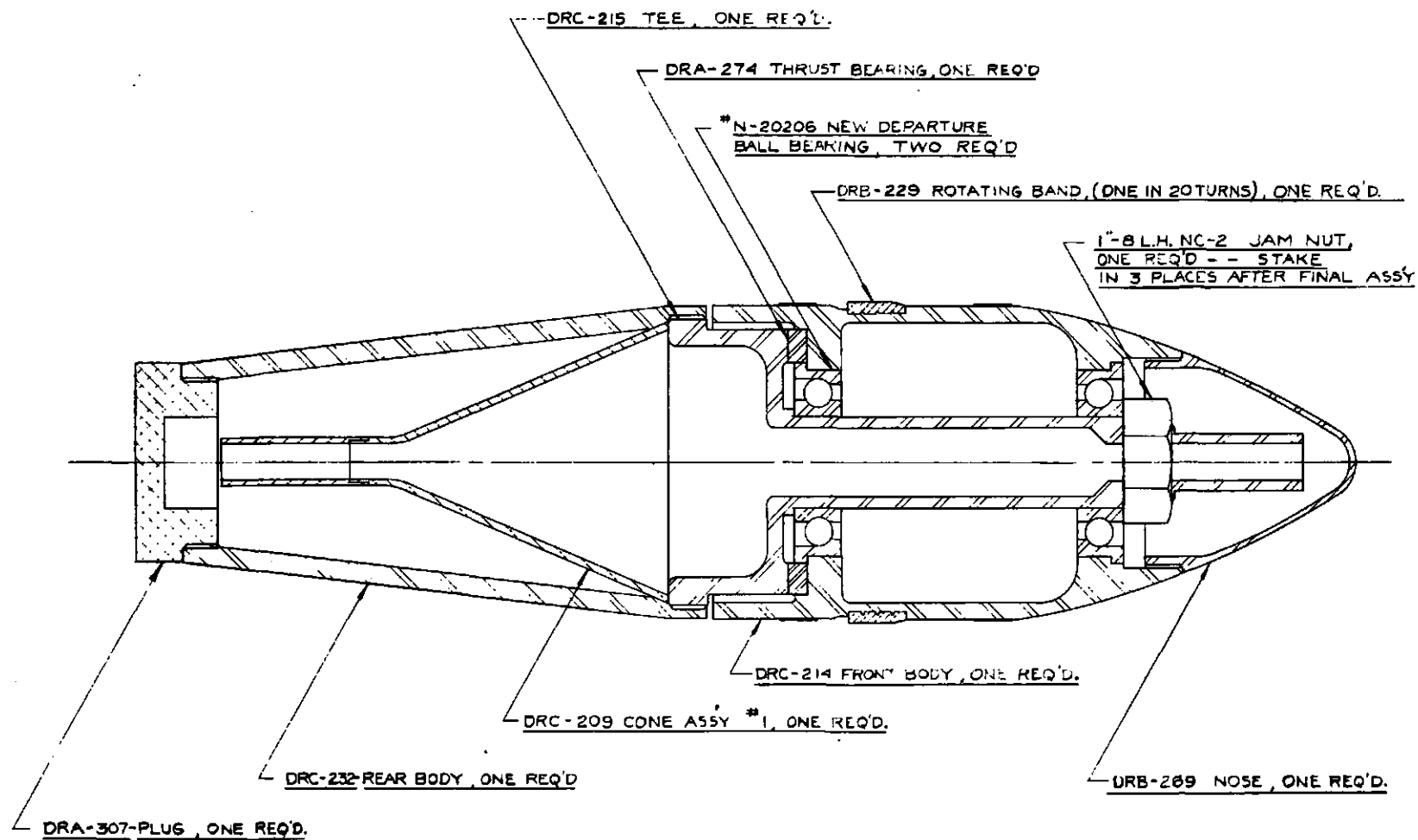
Figure 15—Double body projectile assembly.

Certain of the design variables governing the performance of fluted liners have been presented. It appears that 105mm liners of the type described here show compensation only when there is a significant variation in wall thickness across a flute profile, that a minimum wall thickness of about .090 inch must be maintained in order to secure full penetrating efficiency, and that the spin rate at which the best average penetration occurs is increased by: (1) deepening the flutes, (2) reducing the minimum wall thickness, and (3) by increasing the number of flutes when 36 or more flutes are used, or by reducing the number of flutes when 16 or fewer flutes are used.

TABLE I

Summary: Behavior of Serrated Liners

Item	Drawing No.	Fig. No.	Geometry	V_o	P_{vo}	P_o
1.	DRD17-1	5	16-.028-.100	0	12	18
2.	DRD17-2	5	"	0	10	18
3.	DRD17-6	6	16-.028-.150 (-)	15	16.0	15.0
4.	DRD32-3	7	16C-.028-.100(-)	35	8.5	18.0
5.	DRD34-3	8	16-.070-.150 (-)	55	9.6	15.0
6.	DRD78-2	9	16CP-.034-.100 (-)	5	17.0	18.0
7.	DRD20	10	36-.010-.100	10	18.2	18.0
8.	DRD35-3	11	36-.020-0.150	10	15.0	14.3
9.	DRD33-3	12	36C-.020-.150	15	15.2	14.3
10.	DRD63-3	13	60-.020-.100	65	14.0	18.0
11.	DRD63-3	14	60-.020-.150	25	15.3	15.0

351

A ZERO ORDER THEORY OF THE INITIAL MOTION OF FLUTED HOLLOW CHARGE LINERS*

L. H. Thomas

Watson Scientific Computing Laboratory, New York, New York

ABSTRACT

When a cased charge detonates we may divide the early motion of the casing into three parts: the initial state of rest or steady motion, a confused regime of shock waves and reflected rarefactions, and a more or less steady motion under the continuing pressure of the explosion gases.

For a light casing a plausible zero order theory treats the whole intermediate stage as the motion of a single shock wave forming a refracted extension of the detonation wave into the casing, which sets the casing impulsively into motion. The momentum impulsively given in this approximation to a certain area of the casing is proportional to its thickness, the physical reason for this being the longer time that the material is confined by that adjoining it when it is thicker.

This picture makes it possible to estimate the angular momentum of a zone of a hollow charge liner immediately after the passage of the detonation wave, and the angular momentum is not likely to change much later as equal pressure on the outer surface of the liner would produce no change. The assumption that nearly zero angular momentum is a necessary condition for the formation of a good jet now leads to a prediction of the effect of any given fluting in counteracting initial rotation which is in qualitative, and perhaps rough quantitative agreement with observation.

If this zero order theory is borne out by further comparison with observation, it may assist the design of efficient liners for rotating projectiles.

1. The impulse wave in a light casing. (Compare BRL Report 475 (1944) § 7.)

Consider first a shock front travelling with velocity U into metal of density ρ_0 at rest, and propelled by pressure p. If the metal density at pressure p is ρ_1, and if the subsequent velocity of the metal relative to the shock front, in the opposite direction to U, is U_1, conservation of mass and momentum gives

$$\rho_1 \xleftarrow{} U_1 \quad \Big| \xleftarrow{} U, \ \rho_0 \qquad \text{(velocity relative to the front)}$$
$$p \quad \Big| \quad 0$$

---

* Also published as Ballistic Research Laboratories Report No. 765.
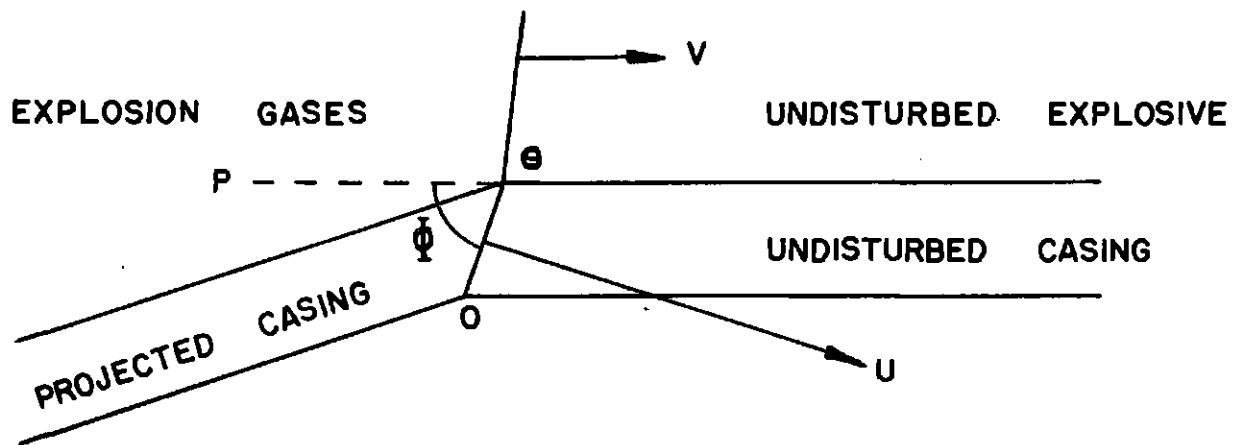
Figure 1

Figure 2

Figure 3

354
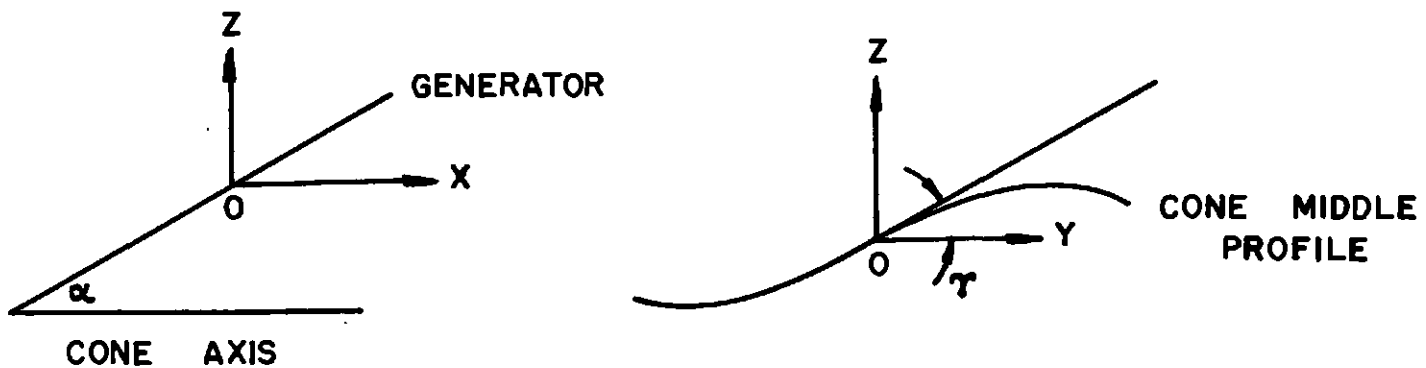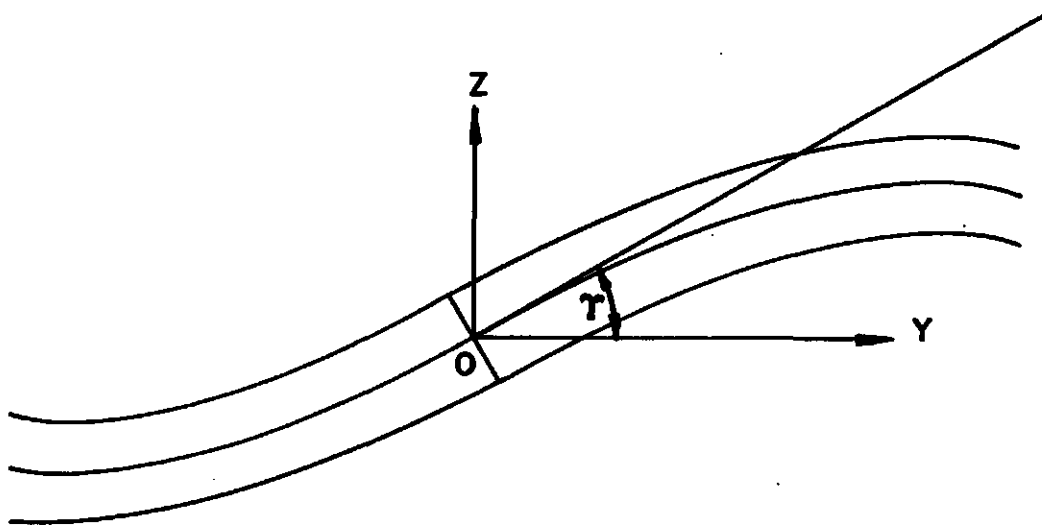
$$\rho_0 \, U = \rho_1 \, U_1$$

$$\rho_0 \, U^2 = \rho_1 \, U_1{}^2 + p$$

The impulse per unit volume, $\rho_0(U - U_1) = p/U$, in the direction of motion of the shock front of velocity $U = \sqrt{(p/\rho_0 \{1 - \rho_0/\rho_1\})}$ into the undisturbed casing.

We picture the detonation wave travelling through the explosive at a definite speed V with a definite pressure jump P extended through the casing by a 'virtual shock wave' in the casing, with a pressure jump varying from P inside to 0 outside, and a mean of $p = \frac{1}{2} P$. We may suppose that this 'virtual shock wave' has a configuration determined by its mean speed U, a property of the casing material, and that this material is set in motion impulsively with impulse p/U per unit volume perpendicular to the virtual shock. (Figure 1.)

If the angle of incidence of the detonation wave on the undisturbed casing is θ and the angle of refraction of the virtual shock is ϕ, as usual

$$\frac{V}{\sin \theta} = \frac{U}{\sin \phi} \, .$$

2. <u>Geometry for a fluted conical casing.</u>

We suppose the detonation wave in the explosive perpendicular to the cone axis. We refer the cone to its middle profile, halfway between the inner and outer surfaces, drawn in a plane perpendicular to its axis. At any point O in the profile take rectangular axes with Ox parallel to the cone axis, Oz produced negatively passing through the axis. (Figure 2.)

If the half angle of the cone is α, the cone generator through O has direction cosines

$$\cos \alpha \, , \, 0, \, \sin \alpha$$

and if the tangent to the profile through O makes angle γ with the y-axis, this tangent has direction cosines

$$0, \, \cos \gamma, \, \sin \gamma.$$

The profile surface normal then has direction ratios

$$-\cos \gamma \sin \alpha \, , \, -\sin \gamma \cos \alpha \, , \, \cos \alpha \, \cos \gamma$$

and the direction of progress of the waves along the surface has direction ratios

$$\cos \alpha \, , \, -\sin \alpha \, \sin \gamma \cos \gamma, \, \sin \alpha \, \cos^2 \gamma$$

Thus the angle of incidence of the detonation wave, θ, is given by

$$\cos\theta = \frac{\cos\gamma\,\sin\alpha}{\sqrt{\cos^2\alpha + \cos^2\gamma\,\sin^2\alpha}} \quad,\quad \sin\theta = \frac{\cos\alpha}{\sqrt{\cos^2\alpha + \cos^2\gamma\,\sin^2\alpha}} \quad,$$

and the angle $\emptyset$ that the virtual shock makes with the cone surface is given by

$$\sin\emptyset = \frac{U}{V}\cos\alpha \Big/ \sqrt{\cos^2\alpha + \cos^2\gamma\,\sin^2\alpha}\;.$$

Impulse p/U, per unit volume, perpendicular to the virtual shock has components $(p/U)\sin\emptyset$ in the direction of progress of the waves along the surface and $-(p/U)\cos\emptyset$ perpendicular to the surface, so that its component in the y-direction is

$$-\frac{p}{U}\sin\emptyset\,\frac{\sin\alpha\,\sin\gamma\,\cos\gamma}{\sqrt{\cos^2\alpha + \cos^2\gamma\,\sin^2\alpha}} + \frac{p}{U}\cos\emptyset\,\frac{\sin\gamma\,\cos\alpha}{\sqrt{\cos^2\alpha + \cos^2\gamma\,\sin^2\alpha}}$$

$$= -\frac{p}{U}\frac{\frac{U}{V}\cos\alpha\,\sin\alpha\,\cos\gamma\,\sin\gamma}{\cos^2\alpha + \cos^2\gamma\,\sin^2\alpha} + \frac{p}{U}\frac{\sin\gamma\,\cos\alpha}{\cos^2\alpha + \cos^2\gamma\,\sin^2\alpha}\sqrt{\cos^2\alpha + \cos^2\gamma\,\sin^2\alpha - \frac{U^2}{V^2}\cos^2\alpha}$$

per unit volume.

If t is the thickness of the cone in the y-z plane perpendicular to the middle profile, the volume per unit area of the x-y plane is $t/\cos\gamma$, so that the impulse in the y-direction per unit area of the x-y plane is, if we abbreviate (Figure 3.)

$$\frac{\sin\alpha\,\cos\gamma}{\cos\alpha}\ \text{to}\ \zeta$$

$$t\,\frac{\sin\gamma}{\cos\gamma}\frac{p}{U}\frac{\left\{\sqrt{1 - \frac{U^2}{V^2} + \zeta^2} - \frac{U}{V}\zeta\right\}}{1 + \zeta^2} = t\,\frac{\sin\gamma}{\cos\gamma}\frac{p}{U}\frac{1 - \frac{U^2}{V^2}}{\sqrt{1 - \frac{U^2}{V^2} + \zeta^2} + \frac{U}{V}\zeta}$$

To get the angular momentum given a zone of the cone, per unit distance along the cone axis, we must multiply the above expression by the distance from the cone axis, r say, variations in which around the cone we may reasonably neglect, and integrate with respect to y completely around the developed profile.

3. Results.

The integrand found in § 2 has the same sign as γ. If we integrate with respect to z separately for parts of the profile with positive γ and parts with negative γ,
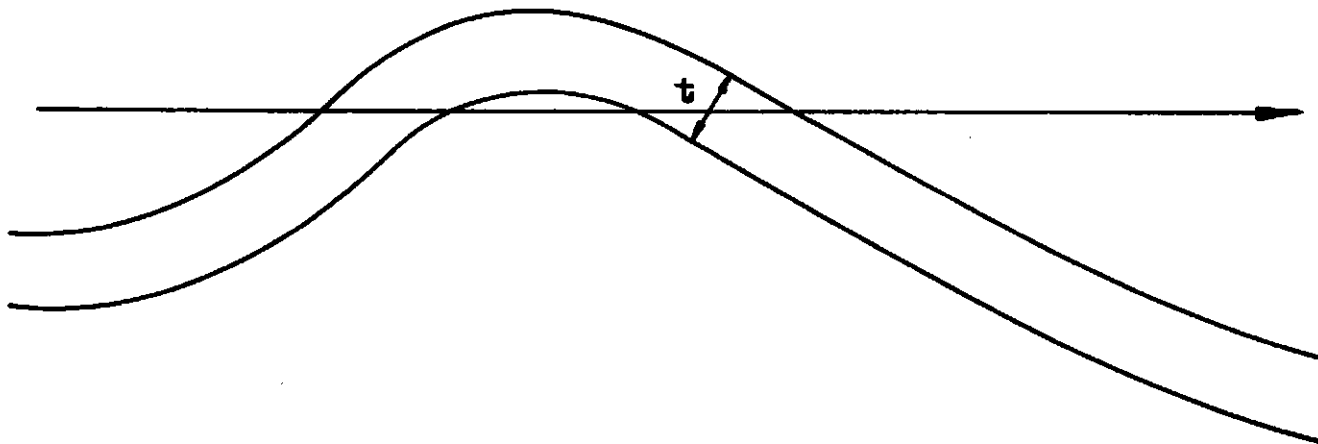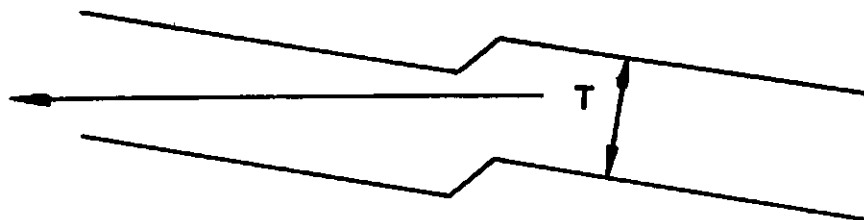
Figure 4

Figure 5

since dz = $\frac{\sin \gamma}{\cos \gamma}$ dy, we have integrand

$$r \ t \ \frac{p}{U} \ \frac{1 - \frac{U^2}{V^2}}{\sqrt{1 - \frac{U^2}{V^2} + \zeta^2 + \frac{U}{V}\zeta}}$$

Suppose now that t is constant; then the integrand continually increases as γ increases and so ζ diminishes. Hence in a profile with t constant and γ on the average larger when positive than when negative, the total angular momentum imparted by the virtual shock is in the y-direction. (Figure 4.)

Suppose on the other hand that the thickness in the z-direction is constant rather than the thickness perpendicular to the middle profile. Then t = T cos γ, where T is constant, and we have integrand

$$r \ T \ \frac{p}{U} \ \frac{\cos \alpha}{\sin \alpha} \ \frac{\zeta (1 - \frac{U^2}{V^2})}{\sqrt{1 - \frac{U^2}{V^2} + \zeta^2 + \frac{U}{V}\zeta}}$$

This expression continually decreases as γ increases and so ζ decreases. Hence in a profile with T constant and γ on the average larger when positive than when negative, the total angular momentum imparted by the virtual shock is in the negative y-direction. This seems to explain qualitatively the difference in direction observed for different profiles. (Figure 5.)

Taking p = 7 x 10^{10} dyne/cm^2, U = 5 x 10^5 cm/sec, and a density ρ = 9 gm/cm^3, $\frac{p}{\rho U}$ = 1.5 x 10^4 cm/sec. This is about 25 times the observed peripheral velocity, and 1/25 is not unreasonable for the mean of tan γ $(1 - \frac{U^2}{V^2})/\sqrt{1 - \frac{U^2}{V^2} + \zeta^2 + \frac{U}{V}\zeta}$.

A more accurate theory obtained by setting up an artificial shock front of constant velocity in actual casing as a refraction of the detonation wave might be worth while.

SHAPED CHARGE DAMAGE BEYOND ARMOR

D. R. Kennedy

U.S. Naval Ordnance Test Station, Inyokern, China Lake, California

ABSTRACT

The development of shaped charge weapons has been concentrated primarily on achieving maximum penetration capabilities of the charge, and little attention has been given to the effects of the jets beyond the defeated armor, or, more specifically, within the enemy tank.

Realizing the need for such information, a program was initiated at the Naval Ordnance Test Station early this year to determine the comparative effects of various shaped charge liner materials and cone angles in producing damage beyond defeated armor.

The charges investigated were identical to the 6.5 in ATAR in size and load. Copper, aluminum, and steel were utilized as cone materials, with cone angles of $42\frac{1}{2}$, 60, 90, and 120 deg.

Three series of tests were conducted to determine (1) the mass, size, number, and spatial distribution of fragments ejected beyond armor, (2) the distribution of jet fragments impinging on angle plates beyond the primary armor, and (3) the pressures and temperatures generated within confined steel targets by the various shaped charge jets.

Aluminum liners were discovered to have unique damaging properties when fired at extremely close stand-off distances against defeatable armor. Indications are that copper liners, although superior in depth of penetration capability, are decidedly inferior to steel and aluminum liners as damaging agents.

Shortly after the onset of the Korean War, the Naval Ordnance Test Station at Inyokern, California was asked to develop a shaped charge warhead adaptable for use on the 5.0 in. High Velocity Aircraft Rocket (HVAR) motor. The design specifications for the warhead required a 100% defeat of 13 1/2 in. of armor since it was thought that this penetration would be required to stop the North Korean armor.

Accordingly, a warhead was developed which incorporated electric fuzing, a 6.125 in. 60o low carbon steel liner, and a 20-lb. Composition B explosive load. The weapon

as issued to the service was designated the 6"5 ATAR (Anti-tank Aircraft Rocket) Mk 1 Mod 0. During the course of the Station's evaluation of the ATAR a test was conducted in which several ATAR's were fired through 12 in. of Class B armor into a confined steel target box encompassing a volume of 240 cubic feet, or about the volume of a typical tank. It was concluded from these tests that lethal fragments ejected beyond the defeated armor were confined to a narrow cone and that the fragment ricochet was negligible.

As a result of the observations made on these tests an exploratory program was initiated to seek some means of increasing the beyond armor damage by shaped charges of the ATAR caliber. The effects of varying the liner material, thickness, and apex angle were studied in a test program composed of three parts, (1) the determination of armor damage, spatial distribution of material beyond armor, and size and mass of the material ejected beyond the armor; (2) the distribution and velocities of fragments impinging on angle plates beyond the primary armor; and (3) the pressures and temperatures generated within confined steel targets (i.e., tanks) by the defeating shaped charge jet.

All of the charges investigated were similar in size and explosive load to the production 6"5 ATAR. Cone materials investigated included copper, steel, and aluminum. Apex angles included 42 1/2°, 60°, 90° and 120°. All liners of a given apex angle were identical in geometry and had a liner thickness of 6%, this thickness being used in preference to the normal 3% (for copper and steel liners) since one of the objectives of this program was to increase the production of material beyond the defeated armor.

The first part of the test program utilized a large ice target structure designed to receive and retain all of the material ejected beyond a massive plate of 6 in. Class B homogeneous armor. A 1/6 in. X 50 in. X 60 in. sheet of aluminum was placed 2 ft. behind the armor plate to record the spatial distribution of the jet and spall fragments. A 7000 lb. ice mass arranged roughly in the form of a cube was placed behind the spatial distribution plate to stop and retain the ejected material.

In addition to the various configurations of 6 in charges discussed above, a few service issue shaped charge heads were also fired for determination of the their comparative effect beyond the 6 in. armor. The service charges included the 3.5 in. Rocket HEAT M28A2 (Superbazooka), the 5"0 Rocket Head Mk 25 Mod 1 (a Navy head for the HVAR), and the 6"5 ATAR.

Some of the conclusions reached as a result of this series of tests were: (1) no strict relationship between the hole dimension in the target plate and the amount of material produced beyond armor were noted, although as a rule the larger the hole in the armor, the greater was the mass of ejected material; (2) doubling the liner thickness for a given size of liner generally more than doubled the mass and number of fragments produced beyond armor; (3) steel cones produced greater numbers of lethal fragments beyond armor than did any of the other materials tested; (4) the smaller cone angles (i.e. 42 1/2° and 60°) produce greater numbers of fragments (as well as being capable of greater penetrations); and (5) increasing the cone diameter increased the output of lethal material greatly in excess of the ratio of diameter increase. The spatial distribution of fragments beyond armor revealed that the small angle steel liners had a maximum spread of approximately 110° with the area of heaviest fragment concentration falling in a spread of 60°.

360

The second part of the program, that of determining the distribution and velocities of fragments impinging on a 45° angle plate placed behind the primary armor plate (6 in. homogeneous armor) was only partially successful. Attempts to record fragment velocities were unsuccessful with the instrumentation than available. Photographic records indicated, however, that steel liners were superior to identical geometry copper liners in the production of large masses of ricocheting fragments off the angle plate.

The third part of the program, the determination of pressure and temperatures generated within confined structures by various shaped charge jets consisted of statically firing each charge through 6 in. armor plate into a welded steel target box 5 1/2 ft. deep, 5 1/2 ft. high and 8 ft. wide (a volume of 240 cubic feet). The interior of the target box was painted white before each shot to record the incendiary flash and fragment impact pattern. The target interior was instrumented to record transient pressure and temperature rises caused by the entrance of the shaped charge jets.

Some of the observations noted from this test were that (1) steel cone charges produced average temperature rises for all charges fired of 1028°F over a recorded 1 second duration as compared to an average rise of only 318° F for copper cone charges including the 3.5 HEAT M28A2, the 5%0 Mk 25, and the various 6 in. charges; (2) the transient pressure rises averaged 18.8 PSI above ambient for the steel cone charges as against 5.3 PSI for copper cone charges; (3) the temperature and pressure rises were independent of the charge size in the range tested; and (4) the scorched surface on the wall of the target box opposite the jet entrance hole was about three times as large in area for the steel cone charges as for the copper cone charges.

Based on the results of the first three parts of this program for the determination of jet effect beyond defeated armor, we submit that as far as possible, the weapons designer should consider the use of soft steel or cast iron for a liner material instead of the commonly used but highly critical (as regards supply) copper. The loss in maximum penetration ability (a criterion which we feel is greatly over-rated) is more than offset by the increased beyond armor effectiveness.

THE DAMAGE EFFECTIVENESS OF SHAPED CHARGES AGAINST TANKS

F. I. Hill

Terminal Ballistics Laboratory, Ballistic Research Laboratories,
Aberdeen Proving Ground, Maryland

ABSTRACT

A summary of the damage from firing over one hundred 3.5 in. rockets and limited numbers of 90mm T108 projectiles vs. the T26E4 tank is made. From these data, it is tentatively concluded that interior damage after a perforation by both these projectiles is comparable. However, the conditions to achieve a perforation with the better fuzed projectile are not so rigorous. A comparison of terminal ballistic data for the 90mm HEAT and kinetic energy projectiles is made indicating that general damage from perforating kinetic energy projectiles is considerably greater than that from HEAT rounds. A further analysis is made in which the vulnerable areas of these rounds are compared. This analysis indicates that the vulnerable areas to mobility, firepower and total destruction are not considerably greater for the kinetic energy projectiles. An explanation of this apparent anomaly lies in the fact that the principal targets inside a tank are ammunition, fuel and the engine, and that the personnel are not the most important targets. A brief estimate is made of the relative overall effectiveness of 90mm HVAP and HEAT rounds to show their expected relative probabilities of a hit being a kill for these projectiles against the M26 tank.

At its present stage of development the shaped charge round from a terminal ballistic point of view is a comparatively effective one against tanks. This statement in no way implies, however, that a perforation by this round will necessarily destroy a tank. It has sometimes been desirable from a terminal ballistic standpoint to approach the 100% level of effectiveness in a weapon for destroying its target once it has hit. Perhaps this would be desirable in antitank weapons provided the attendant sacrifices in rate of fire, weight and possibly hit probability were not too severe. With present weapons such sacrifices are probably too severe. The effort to achieve even a perforation on some surfaces of tank armor has been great enough that the objective of just perforating the armor has been one that was a sufficiently high goal. We may well ask: "What lies behind such an objective?" The answer is that a perforation of the armor usually allows the projectile or jet to enter the tank and initiate the forces of destruction that a tank carries within itself. These forces are primarily resultant from ignition of the ammunition and fuel although they are not the only ones. A shot into the engine compartment may also destroy the tank's effectiveness in a like manner. A shot into the radiator or water jacket will cause the engine to burn itself up or a shot into an oil line or cooler will eventually cause the engine and transmission to destroy themselves. At the present time, we have no antitank weapon that is capable of inflicting comparable damage on a tank independent of

these forces. Some projectiles do more than others, but, still, those projectiles capable of initiating a tank's potential of self destruction compare closely in overall effectiveness caliber for caliber.

At the request of BRL, the Development and Proof Services here at Aberdeen have been conducting extensive firings against some T26E4 tanks (essentially the Pershing) with hollow charge projectiles to determine their terminal ballistic effectiveness. Most of these firings have been performed with the 3.5 in. Rocket. Some have been performed with some early 90mm T108 projectiles and some static firings have been made with the 6.5 in. ATAR. The tanks for the most part have been stowed with radio and fire control equipment, wooden dummy personnel, inert ammunition and in some cases fuel. As long as possible the engine has been operating. Of course, after considerable firing the tank is more damaged and many of these things can no longer be simply repaired to put the tank back in operation.

Assessment of damage is made on the basis of whether the tank is destroyed completely ("K" damage) or whether firepower ("F") or mobility ("M") damage have been done. Since the tanks are usually fired on without ammunition or fuel stowed auxiliary experiments have been performed to determine their susceptibility to attack by HC ammunition. Table I lists the results obtained from firing on gasoline and diesel fuel. To obtain these data firings were made through armor at fuel in small cans (5 gal.), 55 gal. drums and actual fuel tanks. The jets were aimed both above and below the fuel level.

TABLE I

Results of Firing vs. Gasoline and Diesel Fuel

Diesel Fuel				Gasoline			
Armor Penetration ins	Container Size gal	No. of Shots	% Fires	Armor Penetration ins	Container Size gal	No. of Shots	% Fires
7.25	5	8	0	7.25	5	3	100
2.75	5	5	0	3.67	5	5	100
7.25	55	28	36	7.25	55	1	0
2.75	55	24	33	4.25	6	6	100
2.75	55	10	40	3.00	M26 Fuel Tank	13	85
Gross Ave.		75	29			28	90%

Examination of the above table shows the very high susceptibility of gasoline to fuel fires as compared to Diesel fuel. It is notable that small containers of Diesel fuel were not ignited. Of further interest is that the ignition of the fuel in the gasoline tanks appeared to be independent of whether the fuel tanks were full or empty. Data on the effect of fragments against ammunition are very extensive and will not be gone into here. HEAT rounds will explode ammunition if the jet passes through the case. The small high velocity fragments cannot be expected to ignite a case if the fragment does not strike the primer or the black powder booster. Our data on firing at ammunition are limited. However it is adequate for the illustrations to be shown today.

Table II is a summary of the damage obtained in firing on the T26E4 tank with various types of HEAT ammunition. As a gross summary it is of some value in comparing just how much damage can be expected for these rounds. The data from these tests are, of course, used in a different manner to assess overall tank vulnerability because the shots are distributed over the tank. Most of the damage obtained in the tests was determined by the location of the shot and the shot was located at the places where the greatest doubt of the result would be. For instance repeated shots into the ammunition stowage from the side are of little interest.

TABLE II

Summary of Damage from Hollow Charge Rounds

Round	Direction of Attack	No. of Shots	No. of Perforations		Per Perforation Crew Compt		Per Perforation		
			Crew Compt	Eng. Compt	Killed	Wounded	M	F	K
3.5 Rocket	Ground Attack (45° from Front & Side)	70	32	7	.30	.69	.32	.25	.18
3.5 Rocket	45° Air Attack	16	8	6	.25	.75	.64	.53	.43
90mm T108	Ground	10	8	0	.37	.63	.45	.54	.12
6.5 Rocket	45° Air Attack	6	5	0	2.40	.60	.96	.85	.60
90mm HVAP	100 yds 1500 yds	19 26	9 15	0 2	1.80 1.00	.55 2.00	.87 .85	.82 .73	.58 .47
90mm AP	100 yds	23	17	0	1.12	.88	.90	.81	.58

Examination of the detailed data as well as Table II shows that if there is a significant difference in the damage from the 90mm T108 round and the 3.5 inch Rocket is has not been shown with the first 10 rounds fired. However, the 6.5 in rocket does very much more damage. The nature of the damage for all the rounds is such that some wounding of personnel is possible a small distance from the direct path of the jet but little other damage outside the jet path is obtained. This is borne out by the small number of persons killed and wounded by the jet. At the bottom of Table II for the sake of comparison there is shown the damage for the 90mm HVAP and AP rounds. Note that damage after perforation is greater for these rounds.

Because the above shots were selected and nonperforating shots were not even tried the data of Table II are not a fair comparison between the projectiles. A comparison of the average vulnerable area of the 3.5 in. Rocket and the 90mm M304 HVAP projectile has been made in which the vulnerable area of the M26 tank to the two projectiles has been computed. Vulnerable area is the product of the presented area and the kill probability of a hit on that area. Table III lists these data:

TABLE III

Average Vulnerable Area of M26 Tank

Round	Vulnerable Area		
	M	F	K
3.5" Rocket	23.0	12.3	7.2
90 HVAP M304 (500-1000 yds)	26.1	15.7	8.6

The reason for the similarity of the vulnerable areas is attributable to two things: The first is that the chief targets in a tank are the engine, ammunition and fuel rather than the people, and the second is that the 3.5 Rocket can perforate a few surfaces that the 90mm round cannot.

If it is assumed that the damage after a perforation is essentially the same for both the 3.5 Rocket and the 90mm T108 round, an overall comparison can be drawn considering the expected ranges and angles of attack. This has been done using a range and angular distribution function, $f(R,\theta)$, obtained from data on battles fought in NW Europe. The kill probability, $P_K(\theta,R)$, considered as a function of range and angle can be computed from the chance that a hit will be obtained on a vulnerable area at angle of attack θ and range R. The comparison can then be based on the expectation of a kill, P_E, averaged over all ranges and angles of attack. This can be expressed as

$$P_E = \int_0^{2000} \int_0^{2\pi} P_K(\theta,R)\ f(\theta,R)\ d\theta\ dR.$$

The integration for range is taken to 2000 yds. because only a small % of shots occur at ranges greater than 2000 yds. The values of P_E computed for a single shot fired at an M26 Tank by a 90mm M3 gun without a range finder are as follows:

TABLE IV

Type Kill	P_E	
	90mm HVAP M304	90mm HEAT T108
M	.83	.60
F	.79	.54
K	.73	.45

The numbers of this table are satisfactory for a comparison but their value tends to be high because the vulnerable area is assumed to be concentrated in a given area. This overall comparison shows the importance of having a high velocity and good accuracy as well as considerable terminal ballistic damage effectiveness in a round. While some sacrifice in penetration performance of the T108 might be desirable to gain ballistic damage on an M26 tank it probably will not be so for the same caliber round were it to be used against a more heavily armored vehicle such as the Stalin III and it is doubtful if any of its velocity or accuracy characteristics should be sacrificed to such an end.

SHAPED CHARGE DAMAGE TO AIRCRAFT STRUCTURES

G. C. Throner

U. S. Naval Ordnance Test Station, Inyokern, China Lake, California

ABSTRACT

The search for an ideal warhead for ground-to-air guided missiles has been centered upon four different types of heads, the most promising of which, according to some investigators, is one using the shaped charge principle.

Since 1950, the Naval Ordnance Test Station has been engaged in studies of the effects of shaped charges fired at aircraft structures from long standoff distances. Tests have shown that the hypervelocity shaped charge jet fragments can be directed against aircraft targets 100 to 150 feet from the point of detonation and produce K-kill damage. The type of damage incurred is referred to as "vaporific" damage, and is characterized by a brilliant flash which envelopes the target and produces severe structural and skin damage to the aircraft.

Present investigations lead to the hypothesis that "vaporific" damage is the result of target material combining explosively with its surrounding atmosphere because of the high energy imparted to the material by impacting jet fragments. Single hypervelocity (8,000 to 15,000 fps) pellets have been fired from "Pugh charges" against enclosed, multiple-plate aluminum targets containing both inert and reactive atmospheres such as helium, nitrogen, oxygen and engine exhaust gas. It was shown that "vaporific" flashing and the accompanying damage can occur only in an atmosphere which will react with the target material when the latter is produced in finely divided form by high velocity impact. The possibility of protection by purging the interior of aircraft wings with engine exhaust gas is cited.

Since ground-to-air guided missiles at the present stage of development are unable to approach an aircraft target sufficiently close for effectiveness of a blast-fragmentation warhead, it is intended that a shaped charge warhead be gimbaled within the missile and guided so that it will track the target and detonate at the point of closest approach. If the jet misses, this warhead would be no less effective than a blast-fragmentation warhead because a heavy, controlled-fragmentation case for the shaped charge will be incorporated.

K-kill damage is a necessary requirement for this warhead because in operation against flights of more than one aircraft, each individual target must fall immediately when hit so that succeeding missiles will not be wasted on the same target.

A variety of shaped charges ranging from 4.6 in. to 8.5 in. in diameter and with aluminum, steel and copper cones have been fired against small fighter aircraft at long standoff distances of 100 ft. and greater in a cursory and random exploration of their destructive capabilities in this application; most of these charges having been originally designed for use against armor targets at close standoff distances.

In the near future, a preliminary model of the above described guided missile warhead will be tested against B-29 bomber airframe sections. This preliminary test model has an aluminum cone 15 in. in diameter with a 120 lb. high explosive load, much larger than any of the charges tested against aircraft so far.

The specifications of some of the more successful charges fired against aircraft are given in the following table:

Chg. Ident.	Type Expl.	Wt. of Expl.	Length of Chg	Cone Dia.	Cone Wt.	Cone Angle	Cone Wall Thickness	Cone Met'l
A	B	23.6 lb	15 in	6.125 in	609 gm	120°	6%	Aluminum
*B	B	20.0	15	6.125	1375	60°	3%	Steel
C	C-3	69.0	22	8.5	3493	80°	3%	Copper

*The Type B charge is a production model 6"5 ATAR head stripped of ogive and fuze. This charge has a cast, unmachined steel cone.

The target airplanes were stripped of guns, ammunition, fuel, instruments, radio and in some cases the engine, but were structurally sound. They were placed in appropriate positions on the ground, usually with nose down and tail elevated to expose the greatest wing area. Charges were supported statically at the indicated standoff distances.

Type A Charges: Four 6 in. aluminum cone charges were fired against F6F fighter aircraft at 100-ft. standoff distance.
No. 1 The wing was sheared off at a point approximately 6 ft. inboard from wingtip. The remaining part of the wing sustained removal of large areas of skin and severe damage to internal structure. Assessed as K-kill.
No. 2 Aimed at wing-to-fuselage juncture just aft of engine compartment skin at root of wing blown wide open, fire set to empty fuel tank, main spar cut; electrical lines, hydraulic lines and oil cooler destroyed, engine accessories damaged. K-kill.
No. 3 All of wing structure removed in impact area except for main spar and leading edge. Main spar was cracked. K-kill.
No. 4 Aimed just below horizontal stabilizer shooting perpendicular to axis of fuselage. Severe damage to tail of fuselage, all controls destroyed. Skin of horizontal stabilizer bulged outward by internal pressure. Assessed as K-kill.

Type B Charges: Four of the 6"5 ATAR heads using cast, unmachined steel cones were fired against F6F fighter aircraft at 100 ft. standoff distance.
No. 1 was aimed at a wing. The gun and ammunition compartments of that wing were burned out and the main spar was cracked. Assessed as A-Possible Kill. Failure dependent upon presence of ammunition in wing.
No. 2 also aimed at a wing. Approximately 16 ft^2 of skin was removed from both top and bottom surfaces of wing. Three ribs and some stringers were destroyed, however the wing retained most of its strength since the main spar was undamaged. A-Possible Kill.
No. 3 was aimed at side of fuselage 3 ft. aft of canopy. A peppered area about 1 ft. high and 2 ft. wide was produced on the entrance side. On the exit side a hole 3 ft. in diameter was completely blown out. Fuselage structure was weakened to point of failure in flight. K-kill.
No. 4 aimed at side of fuselage 1 ft. aft and 2 ft. below canopy. All cockpit canopy glass was blown out except for heavy, bulletproof windshield. Fires were set in cockpit and along fabric-covered ailerons. Inside of fuselage was buckled and bulged and heavy damage was sustained on the side away from impact. K-kill.

Type C Charge: One 8.5 in. copper cone charge loaded with 69 lb. of composition C-3 plastic explosive was fired against an F6F fighter at 100 ft. standoff distance. This charge was aimed at the folding wing juncture and removed all the wing structure in a path 2 ft. wide except for the spar. Debris from the wing was found 150 ft. from the plane. This round was assessed as K-kill.

CONCLUSIONS

It has been demonstrated that shaped charges fired at long standoff distances are capable of producing K-kill damage to aircraft.

Experimentation to date indicates that the following conditions are necessary for inflicting K-kill damage to aircraft of the F6F type construction:

     a. The charge must be aimed so that the jet will strike the aircraft.

     b. The charge diameter must be 6 in. or greater. This fixes the explosive load at a minimum of 20 lb.

     c. The standoff distance must be 125 ft. or less.

     d. The shaped charge cone material should be aluminum, steel, or copper in order of decreasing effectiveness.

     e. Extensive "vaporific" damage can occur only in an atmosphere which will react with the target material when it is produced in finely divided form by high velocity impact.

371

DEFENSES AGAINST HOLLOW CHARGES

R. J. Eichelberger

Carnegie Institute of Technology, Pittsburgh, Pennsylvania

ABSTRACT

A resume of the principles set forth in recent reports on this subject are given, together with some more recent results on the use of glass as a protective device. (See bibliography)

Glass blocks or plates fastened on the outside of homoplate and protected on the outside surface by a relatively thin homoplate are believed to provide the most practical protection. Aluminum armor fastened to the outside of basic homoplate provides several advantages over glass but would add more weight for the same protection.

Under certain circumstances patterns of spikes or layers of explosives between steel plates may provide very low weight protection.

In principle any low density material can be used for protection, since the weight that must be added for a given protection is proportional to the square root of the density of the protecting material. The protective qualities of aluminum are due to this relation but the protective qualities of glass are much greater than this relation predicts. Glass is the one known exception.

This discussion of means of defense against shaped charges will involve only the phase of preventing perforation of a vehicle that is struck by such a weapon. Such aspects of the problem as reduction of the probability of a hit by increasing maneuverability or decreasing damage by charges that do defeat the vehicle by appropriate disposition of components, personnel, and contents will be completely neglected.

The problem of protecting a vehicle against shaped charges is complicated by the fact that such charges are not exclusively artillery weapons; they are at least equally important as infantry weapons. Consequently, a tank must have its entire surface protected, insofar as this is possible, instead of having only selected vulnerable areas heavily protected while the remainder is only lightly armored. The weight of protection required is much greater on this account. In fact, especially for the lighter vehicles, the weight of armor that must be added is prohibitive unless some active means of defense is used. Heavier vehicles with thicker basic armor could possibly be protected adequately by passive means.

$$\Delta P_\rho = \Delta P_s \sqrt{\rho/7.8}$$

$$P_s' = P_s \cdot \frac{P_r}{P_r + \Delta P_\rho}$$

Figure 1

As indicated above, the means of protecting an armored vehicle naturally divide into two categories: passive armors that simply absorb the energy of a shaped charge jet, and active protective devices that induce malfunctioning of the charge or destroy the jet after its formation. We shall consider the passive types first.

The protection to be expected from ordinary materials added to a reasonable thickness of steel basic armor can be predicted to a fair degree of accuracy by means of the residual penetration theory devised by Fireman and Pugh. Very briefly, the reduction in the residual penetration into the steel backing is computed as illustrated in Plate I. The data that must be available are the penetration-standoff curve for the weapon under consideration, fired into material similar to the basic armor to be protected, and the density of the proposed protective material. The reductions in penetration are in the same ratio as the square roots of the densities of the protective materials.

If an air space is left behind a layer of protective material, the residual penetration is computed from the ratio of the residual penetration immediately behind the protective layer to the penetration at the same distance from the charge with no intervening protection, and the corresponding point on the penetration-standoff curve. That is, as shown on Plate I,

$$P_S' = P_S \cdot \frac{P_R}{P_R + \Delta P_\rho}$$

With this addition, the theory can be applied to layers of various materials and to spaced armor (including skirting plates) as well as to homogeneous layers of protection.

The relative ability of some typical materials to protect mild steel backing is shown by Plate II. The thickness of aluminum, steel, or lead required to protect any given thickness of backing against the standard laboratory charge can be taken directly from the plot.

Very roughly, the theory yields the result that the thickness of material needed to provide a given degree of protection varies inversely as the square root of the density of the material, and the weight varies directly as the square root of the density.

The manner in which skirting plates and spaced armor provide protection is illustrated by means of the residual penetration theory in Plate III. Against the laboratory charge fired at 2 in. standoff, a 1/4 in. steel skirting plate placed 9 in. from the basic armor will reduce the penetration from 5 1/4 in. to less than 3 inches. Similarly, a series of 12 - 1/4 in. plates spaced 1/2 in. apart will reduce the penetration from 5 1/4 in. to 1 1/4 inches. These figures sound rather good, but it must be observed that a considerable part of the effectiveness of the skirting plate and of spaced armor lies in the rather rapid fall in the penetration-standoff curve at large standoffs. Against really well constructed charges, the skirting plate would be practically useless and the spaced armor would have little or no advantage on a weight basis over solid armor.
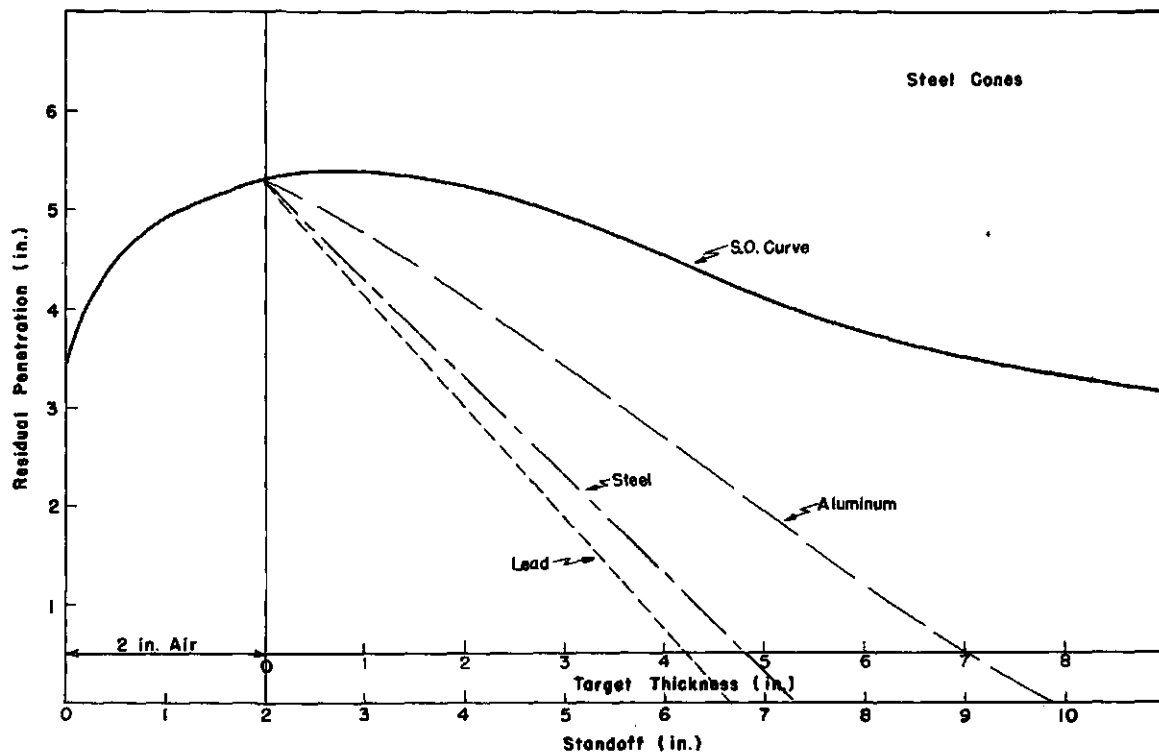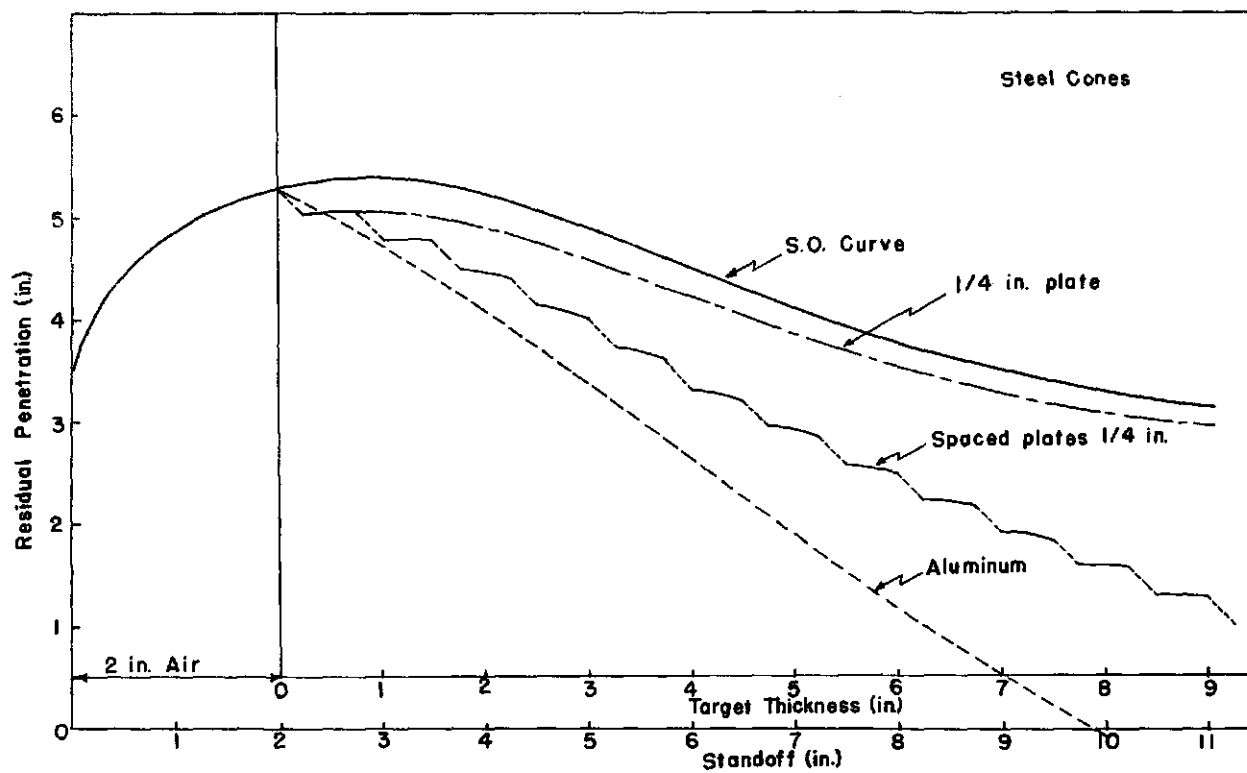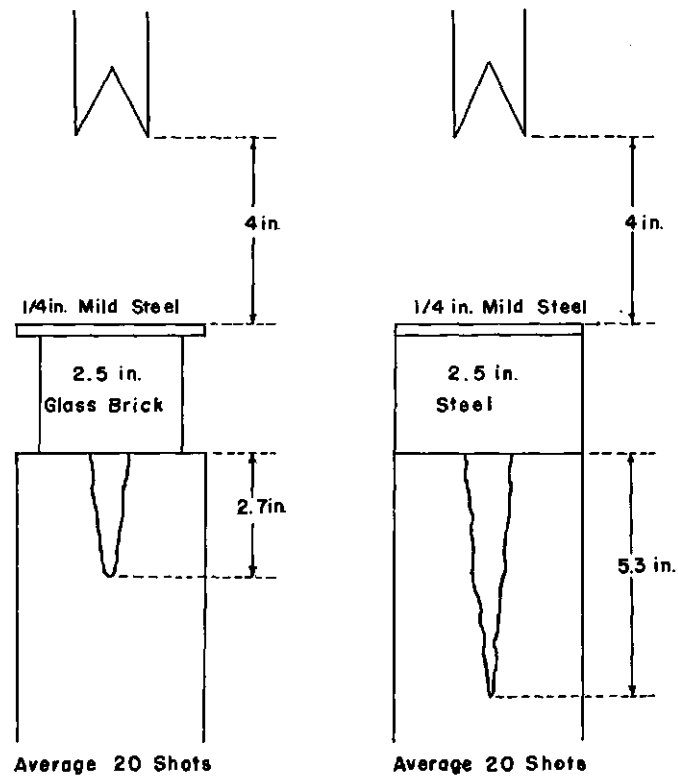
Figure 2
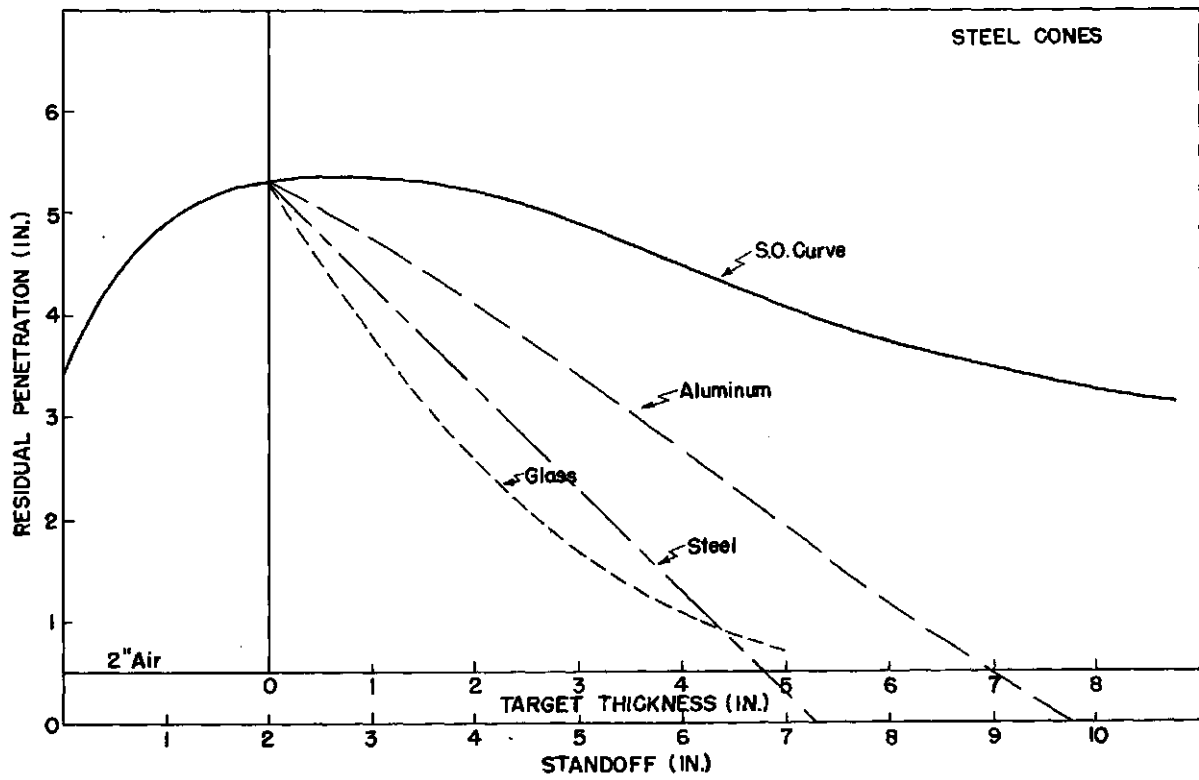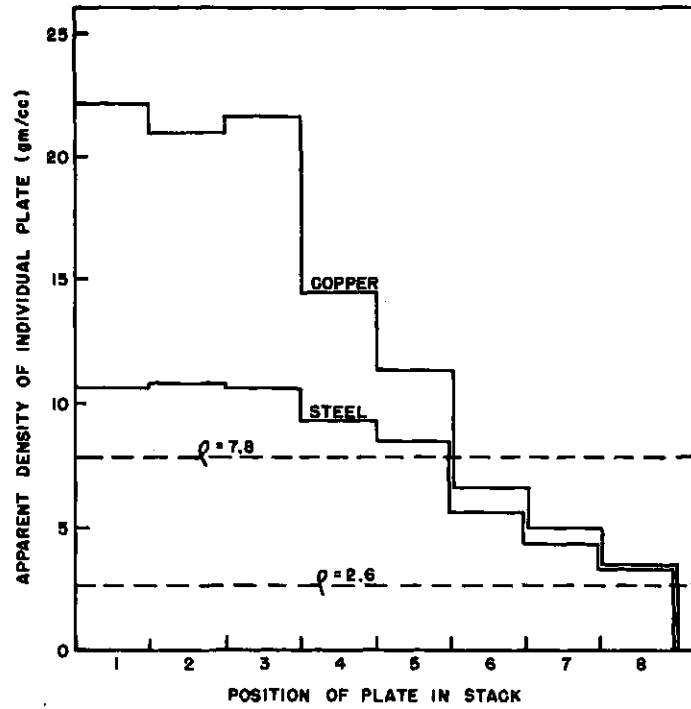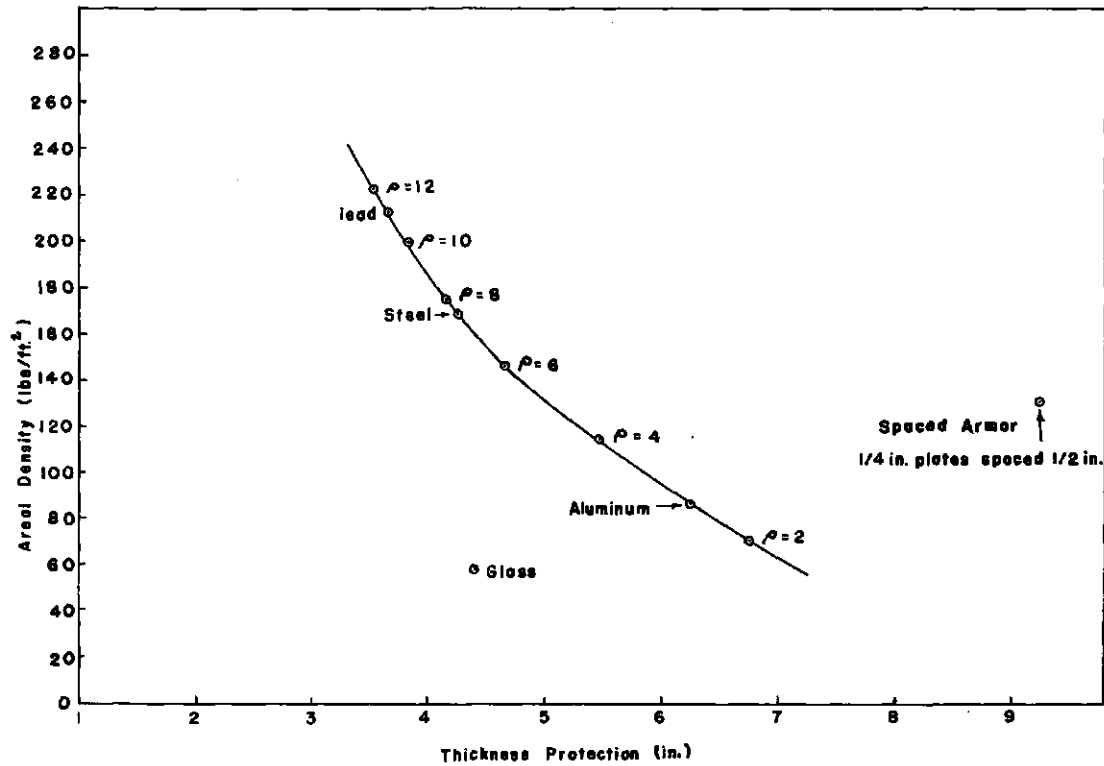

Figure 3

376

Figure 4

Figure 5

Figure 6

Figure 7

378

Furthermore, the spaced armor is under no circumstances as good protection as an equal weight of homogeneous material. In Plate III, the spaced armor has been so arranged that it is generally equal in weight to the same thickness of solid aluminum. The plot shows that the aluminum provides considerably better protection than the same weight and thickness of spaced steel armor.

It should be noted that, of the ordinary passive protections, aluminum probably constitutes the most practical compromise. It is effective against weapons other than shaped charges, presents little difficulty in application, and is not exhorbitantly expensive. In order to be efficiently used, however, it must be backed by a reasonable thickness of stell armor which will stop the relatively slow tail of the jet.

The only passive protection that has exhibited any extraordinary stopping power against shaped charge jets is glass. A typical experiment demonstrating the effectiveness of glass is illustrated in Plate IV. In the specific experiment, against copper M9A1 cones, a 2 1/2 in. brick of glass allowed only 2.7 in. average residual penetration where as the same thickness of steel allowed 5.3 inches.

A more general picture of the effectiveness of glass is shown in Plate V. According to the curve for glass, which is based on experimental data (a total of 100 shots), glass is more effective than steel on a thickness basis in thicknesses less than 4 1/4 inches. Considering its density alone, glass should provide the same degree of protection as aluminum. The plot shows how far more effective glass really is. As a matter of fact, in thicknesses less than 3 1/4 in., glass is even more effective than an equal thickness of lead.

A still more graphic illustration of the extradordinary stopping power of glass can be obtained by comparing individual layers of the protective material in the target. This has been done by using the available observations and computing from the observed reductions in residual penetration the density of a protective material of the same thickness and used in the same position in the target that would provide the same reduction in residual penetration. The result is referred to as the apparent density of the plate of glass at that position in the target. In plate VI, graphs are shown indicating the apparent density of 1/2 in. plates of glass tested against M9A1 copper and M9A1 steel cones. It is of special interest to note that the glass is considerably more effective against the copper jet than against the steel jet, and it should be remembered that previous comparisons of glass with other target materials have been made on the basis of tests with steel jets rather than copper. The plots in Plate VI show that for copper jets or steel jets the glass is much more effective at the front of the target (that is, against the front of the jet) than toward the rear. The apparent density at the front of the target when tested against a copper jet is greater than 20 and against steel the apparent density is greater than 10, as compared with the real density of only 2.6 gm/cm. It should also be noted that even the 8th plate in the test has an apparent density greater than the real density 2.6.

It must be remembered that comparisons of this sort show the advantages of glass on a thickness basis and that the disadvantages usually inherent in the use of protective materials of high density are not encountered in the case of glass. As a matter of fact, a considerable weight saving is obtained, as has been mentioned before. Weight for weight, at the front of the target a given amount of glass will provide a protection against copper jets equivalent to that of more than 5 times its weight of steel. The advantage is slightly less when used against steel jets but is still quite considerable.

The relative effectiveness of the various kinds of passive protection is illustrated in Plate VII. Here, a specific example has been considered - the protection of 1 in. of basic armor against the CIT standard laboratory charge lined with an M9A1 steel cone - and the thickness of protection plotted against the weight. The points on the curve occupied by "plastic" homogeneous materials of various densities are indicated, and points lying well off the curve illustrate the low efficiency of spaced armor and the very high efficiency of glass.

Plate VII shows clearly the need for a compromise between high density protection, of which only a relatively small thickness would be needed, and low density material which would allow a saving of weight. As a rough estimate of requirements for defense against a 3 1/2 in. Bazooka, one could multiply both thickness and weight by a factor of 3, remembering that the basic armor protected also scales and is equal to 3 inches. It is evident that, of the so-called "plastic" materials represented by the curve, aluminum represents about the most practical compromise, and that a thickness of about 18 1/2 in. weighing 255 lbs/ft^2, neglecting any necessary fastenings, would be required. Mr. F. I. Hill of BRL has estimated that about 35 to 38 tons of aluminum armor would be required to adequately protect the T42 and T43 tanks against the 3.5 Bazooka.

If glass were to be used, on the other hand, Mr. Hill has estimated that only 16 tons of added armor would be needed to protect the M42 and 17 tons to protect the T43. In other words, the use of glass in place of aluminum would permit saving of weight of more than a factor of 2.

It is evident that, in spite of practical difficulties in its application, the advantages of glass as a protective material cannot be neglected. It provides, in the example chosen, a thickness advantage equal to that of a material of density about 7 gm/cc, and the weight advantage of a material of density less than 2 gm/cc. In order to realize these potential benefits, however, certain precautions must be taken: a metal face plate must be used to detonate the charge before it damages the glass, and the glass must be used in blocks of fairly small area, with separators of shock absorbing material between, to prevent damage over a large area due to a single strike. Some of the advantage of glass is lost because of the need for these extra accoutrements, but rather detailed engineering on these aspects indicates that only a small fraction of the advantage is lost.

In practice, it is likely that only a limited thickness of glass is really desirable, since aluminum gives comparable shaped charge protection at the greater depth in the target and would provide far better protection against A.P. and similar "Kinetic energy" projectiles. It should be a simple matter to design a combination of glass and aluminum which, together with the basic steel armor, would provide complete protection against A.P. projectiles as well as against shaped charges and squash head.

It should be noted that the advantages described have been observed only in solid glass. Glass products such as fiber-glass and Doron provide only the protection to be expected from plastic materials of the same density; they exhibit none of the superiority of solid glass.

Several active means of defeating shaped charges have been tested to some extent. The one that has been most extensively tested consists of a system of heavy spikes fastened to the basic armor. Plate VIII shows a small test plate made for testing against M6 Bazookas. The spikes act by perforating the windshield of the projectile and deforming the liner before the detonation wave reaches it, thus destroying the symmetry of the jet formation process. Obviously, several factors are vital to the success of such a method. The spikes must be able to enter the windshield with a minimum of resistance and must be strong enough to resist bending or fracture during the process.

In laboratory tests with dynamically fired M6 Bazookas, the criteria for good spike shape, spacing, and length were found and, by observing the simple design "rules" so established, it was possible to achieve 100% effectiveness in protecting 1 1/2 in. of steel. The test plate of Plate VIII, after the test, is shown in Plate IX. The penetration in the plate was negligible and the damage to the spikes themselves can be seen.

The M6 Bazooka, with its low flight velocity and slow fusing, was obviously a relatively simple shell to defeat by this means. Limited field tests against a variety of larger American and German weapons indicated a surprising degree of effectiveness in defeating even such shells as the high velocity M67 and the point-detonated Racketenpanzerbuchse. Only the latter weapon failed to be consistently defeated by the spikes designed in accordance with the very simple "rules of thumb".

While it would seem that spikes could easily be defeated by the fast modern fuses, the very considerable saving in weight that might possibly be gained makes this consideration still worthwhile. Mr. Hill has estimated that the added weight needed to protect a T42 tank would be about 2 1/2 tons (compared with at least 16 tons of passive armor), or somewhat less than 4 tons for the T43 (compared with almost 17 tons).

Another means of active protection tested consists of thin layers of explosive between layers of inert material (aluminum or steel). The jet from the CIT laboratory charge is completely defeated by five layers of Pentolite 1/10 in. thick interspersed with 1/4 in. steel plates. The practicality of such protection is questionable, but its evidently general effectiveness makes it appear worthy of further consideration.

At one time, it was thought that the effectiveness of a jet could be reduced by using oxidizing agents. Thorough testing has demonstrated that there is no benefit to be gained from such materials.

The possibility of arranging small shaped charges on the surface of a tank, to be detonated by the attacking charge and destroy its performance in much the same way as spikes, has also been suggested. No tests have been made on this idea.

In general, it appears that the most certainly practical protection against shaped charges would consist of a combination of glass and aluminum, of appropriate thicknesses, together with the basic steel armor. Such armor necessarily weighs a good deal, however, and a decision is necessary as to whether the resultant loss in maneuverability of the vehicle is serious. Protection can possibly be obtained with much less added
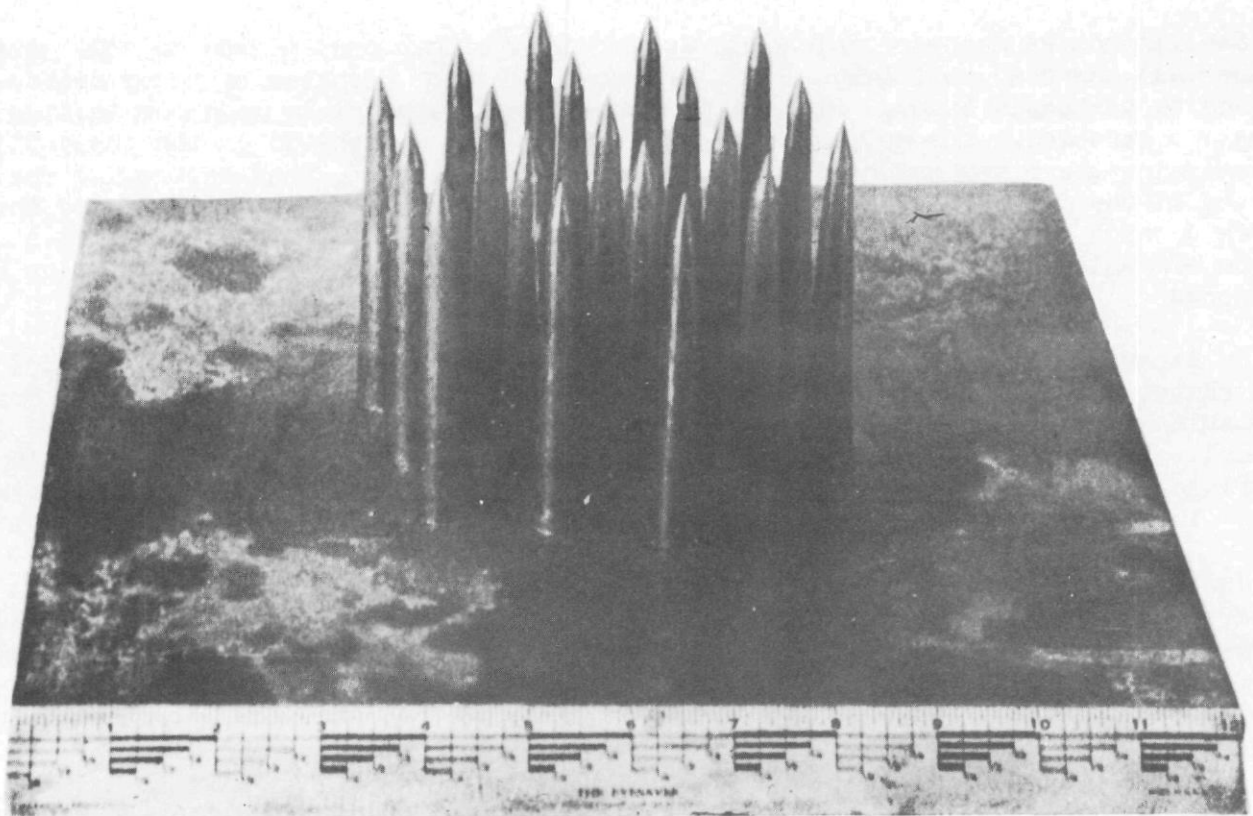
Figure 8

Figure 9

weight by using spikes, but their usefulness is evidently limited; they may be entirely ineffective against the newer fuses. Layers of explosive give generally good protection and would be effective against any type of weapon. It may be possible to devise means of making this technique practical, in which case explosive layers may well afford the lightest and thinnest defense.

BIBLIOGRAPHY

BRL Technical Note 281 by F. I. Hill, "Proposed Program for Development of Armor to Defeat HEAT and Squash-Head Projectiles", August 1950.

CIT Special Report, Contract W-36-061-ORD-2879, Emerson M. Pugh, "Survey of Devices for Protecting Armor against Shaped Charges", June 30, 1949.

OSRD No. 6384, Final Report, "Protection Against Shaped Charges", November 1945. ✓

APPENDIX I

BIBLIOGRAPHY AS DISTRIBUTED BY EMERSON M. PUGH AT THE SYMPOSIUM

BRIEF HISTORY AND BIBLIOGRAPHY OF CLASSIFIED REPORTS LEADING TO THE PRESENT
THEORY OF METALLIC JET CHARGES

A number of papers have now been released and published on the general subject of
the theory of the action of lined cavity charges. The principle applied in releasing
this information to the general public has been the desire to make fundamental in-
formation available for the use of the industries that might have need for it and to
stimulate research. It should be remembered, however, that material which has been
released in this manner is usually out of date by the time it is published and may
contain some serious omissions of material which, if published in unclassified papers,
would jeopardize national defense. It is, therefore, highly desirable that individu-
als working in this field, who are cleared for access to confidential and secret docu-
ments, consult the original classified sources.

Those who are just entering this field will find that there is a large agregate
of useful and reliable information available to them. The information is so extensive
that it is believed to be worthwhile to pick out reports that represent peaks of pro-
gress in the understanding of the phenomena, and to list them in one document for the
use of the workers in the field.

The list that follows represents a first attempt at a compilation of these peaks
of progress reports. It is recognized that this list is quite incomplete because the
time for compiling a complete list has not been available. Also, other individuals who
have worked in the field will have different ideas concerning which reports represent
the peaks of progress, and the author would greatly appreciate receiving comments and
suggestions for modification of the list. If the list can be made to represent the
views of those scientists who are most familiar with the field, it should be worthwhile
publishing it in a special classified document. Such a document should be useful not
only to new people starting in the work, but should also be useful to refresh the
memories of those of long experience.

The author has had so little access to German documents that the following list
is certain to be deficient in German references. It contains chiefly references from
workers in England and the United States and the English references are known to be
incomplete.

OTIB-1468, "Substantiating Material in Support
            of Evaluation of Compensation in
            Favor of Explosive - Experimental
            Company and F. R. Thomanek."

This report mentions a secret patent (404/39) issued August 14, 1936 to Captain
Wimmer based on work carried out from September to November 1935. This work is
summarized in a report but the author did not have access to it and therefore no
description of the patent can be given here.

The Westfalisch-Anhaltische Sprengstoff-Actien-Gesellschaft of Berlin patented in Germany an explosive charge having a cavity of conical or other suitable shape either hollow, filled with an inert material, or lined with sheet metal. The effect of the liner was probably not realized as it was not stressed.

Experiments in the CTR in 1924 showed that the lined charge produced a substantially different effect than the unlined charge. However, a basic knowledge of the penetration of lined hollow charges was not reported until February 15, 1939 by WaPruf 5.

In a German Army Ordnance Dept. (WaF) report of June 10, 1937, the value of a space or standoff between charge and target was recognized in tests using hemispherical liners. A 7.5cm aluminum lined shaped charge was ordered in November 1938 and adopted in July 1939 after trial by the troops. Hollow Charge 15 was ready by the end of 1940 and tested on the Maginot line in March 1941. On June 15, 1940 the Waf reported the superiority of sheet steel over cast iron for hemispherical liners. A report of August 3, 1940 indicates that conical liners with apex angles between 20° and 45° were investigated. Best results were obtained with 30° cones of 1 to 1.5mm wall thickness at 25 to 30mm standoff.

An evacuated cavity was suggested by F. R. Thomanek and investigations were made along these lines until May 1938, but no improvement in penetration was obtained. In 1940 Thomanek also suggested the use of a conical liner whose wall thickness increased from apex to base.

R. W. Wood, "Optical and Physical Effects
    of High Explosives," Proceedings
    of the Royal Society, London 1936,
    Band 157, S. 249. (1. Plastisches
    Fließen von Metall)

Various experiments performed with fuzes with a copper lined indentation in the bottom are reported. These fuzes upon collapse form a single slug rather than a jet and slug as do the conical lined cavity charges. Concentric rings were etched on the liners of some fuzes and their slugs collected in water or cotton. A theory for the formation of the "pellet" was developed and substantiated by firing fuzes with smaller charges to obtain various stages of formation. Wood states that the pellet has a velocity of 1800 m/sec., but he does not indicate how the velocity was measured. Although the fuzes used in this report were quite different from the metallic lined shaped charges of today, Wood's investigation is interesting and the results agree remarkably well with observations made considerably later.

AC 1591, Advisory Council on Scientific
    Research and Technical Develop-
    ment, "The Mechanism of Jet
    Formation in the Munroe Effect",
    (Phys/Ex. 216; OSRD Liaison
    Office WA-87-13) Jan. 12, 1942.

AC 1749, Advisory Council on Scientific
        Research and Technical Develop-
        ment, "Supplementary Experiments
        on Munroe Jets in Air", (Phys/Ex.
        234; OSRD Liaison Office W-156-26)
        Feb. 25, 1942.

AC 2461, Advisory Council on Scientific
        Research and Technical Develop-
        ment, "The Comparative Properties
        of Munroe Jets Formed by Various
        Lined Hollow Charges" (Phys/Ex.
        303; SC 4/25; OSRD Liaison Office
        WA-556-20B) Aug. 4, 1942.

        Above three reports by W. M. Evans and A. R. Ubbelohde.

        These reports show penetration versus standoff curves with coordinates in terms
of the diameter of the charge. Evans and Ubbelohde (probably independently) dis-
covered the increase in penetration with standoff and implied that a linear scaling law
is applicable. They made estimates of the velocities of these jets and started measure-
ments of these velocities. They also introduced the notion of optimum thickness of
the liner and made some determinations of this quantity. Spherical caps and wide angle
cones were generally used by this group. This work furnished the inspiration for the
beginning of the Explosives Research Laboratory at Bruceton, Pennsylvania in 1942.

        Work was touched off in the United States by patents of H. H. Mohaupt (a Swiss
national: U.S. Patent No. 2,419,414; applied for on October 3, 1941) and W. Blackinton
and John J. Calhoun (U.S. Patent No. 2,413,680, applied for November 21, 1942). It is
probably because these patents used conical liners having small apex angles (roughly
45°) that most of the experimental work in the United States was concentrated on
conical liners of small apex angle.

E. I. duPont de Nemours and Co.
 (OEMsr-764, W-670-ORD-4331,
and W-672-ORD-5723)

        The first research work in the United States appears to have been started by C. O.
Davis and his group at the Eastern Laboratory of the duPont Company in 1941, although
the earliest report known to the author is dated March 1942. This group furnished
most of the original information for the design of weapons. They determined optimum
values for the various parameters used in making shaped charge weapons; liner material,
liner thickness, liner apex angle, standoff, length and diameter of charge, effects of
confinement, etc.

OSRD 682, Explosives Research Laboratory
Bruceton, Pa. Set up under Div.
8 of N.D.R.C. with the joint
sponsorship of the Carnegie
Institute of Technology and the
Pittsburgh Station of the Bureau
of Mines. Hereafter simply E.R.L.
(OEMsr-202) "A Rotating Drum
Camera for the Optical Study of
Detonations," by G. H. Messerly,
Progress Report July 8, 1942
(NDRC Div. 8).

This report describes the construction and operation of a rotating drum camera designed to measure the velocities of explosive phenomena.

AC 3518, Armament Research Dept. (Great
Britain) "The Effect of Lateral
Charge Confinement on Munroe
Jets" (Part I), by W. M. Evans
(ARD Explosives report No.
60/43; SC.5; OSRD Liaison
Office WA-528-14), Feb. 22, 1943.

Linear scaling was experimentally determined for depth of penetration, entry diameter and volume of the hole. These quantities are shown to depend upon the confinement, but as the thickness of the confining wall is increased, very little change in performance was noted.

Penetration

AC 3596, Advisory Council on Scientific
Research and Technical Develop-
ment, "A Note on the Theory of
the Munroe Effect" by J. L. Tuck,
Feb. 27, 1943, Phys/Ex. 393;
SC.3; OSRD Liaison Office
WA-638-24).

A theory of jet formation based on a hydrodynamic mechanism is presented.

AC 3654, Advisory Council on Scientific
Research and Technical Develop-
ment, "Studies of Shaped Charges
by Flash Radiography 1. Pre-
liminary" by J. L. Tuck (Phys/Ex.
399; SC.6; OSRD Liaison Office
WA-693-11 or II 5-4944) March
15, 1943.

Shows flash X-rays of collapsing cones and describes the equipment and procedure used.

OSRD 1338, E.R.L. Progress Report on
"The Mechanism of Action
of Cavity Charges" to March
15, 1943, by G. B. Kistiakowsky,
D. P. MacDougall and G. H.
Messerly, Explosives Research
Laboratory, Bruceton, Pa.
(NDRC Div. 8) dated
April 12, 1943.

The most important early work on the understanding of the fundamental properties of these charges was done at the Explosives Research Laboratory, Bruceton, Pennsylvania, under D. P. MacDougall. Much of this is summarized in OSRD 1338. The experimental data furnishing the background for this report is found in Div. 8 NDRC Interim reports numbered CF-1 to 7. These reports contain the first evidence that the penetrating medium is a high velocity jet of liner material followed by a low velocity slug containing most of the liner material but having little effect upon the target. It was discovered that the front of the jet travels at high velocities and the rear at much lower velocities. Rough, but correct, values for the diameter of the jet were determined. An equation was developed for determining the velocity of penetration of jets into target materials which showed that this velocity is dependent primarily upon the density of the target materials. Experiments were performed to verify this result. It is pointed out that the process of penetration into targets consists of using up the jet from the front end and that penetration stops when the total effective length of the jet has been used up. It is postulated that the velocity gradient in the jet accounts for the improvement in penetration with standoff. The reduction in penetration of the jet after optimum standoff is reached is presumed to be due to breaking up of the jet into particles and subsequent radial spreading. This report is a remarkable source of information concerning the fundamental processes of jet penetration.

SC-1, E.R.L., "Studies of Shaped Charges"
by D. P. MacDougall, M. A.
Paul and G. H. Messerly
(NDRC Div. 8 Interim
report) Aug. 15-Sept. 15,
1943.

Conical lined charges were fired into ice blocks and liner fragments recovered for study of jet distribution in the target. The fragments recovered were not correlated with their original location in the uncollapsed liner.

It is pointed out that while the high velocity front part of the jet should penetrate practically all target materials in accordance with the simple theory of penetration, the penetration of the slower rear part of the jet should depend more upon the target material. A residual penetration theory is presented in which the reduction in penetration for a given thickness of material is shown to be approximately proportional to the square root of the density of that material. This theory is shown to hold experimentally for lead, steel, aluminum, water and many other materials. This constitutes one of the best experimental proofs of the soundness of the fundamental concepts upon which the penetration theory is based.

OSRD 4357f, Carnegie Institute of Technology (OEMsr-950 "Fundamentals of Jet Penetration; Theory of Jet Penetration", by E. M. Pugh and E. L. Fireman, Nov. 15, 1944, (Monthly Report OTB-4f, NDRC Div. 2).

OSRD 5462e, Carnegie Institute of Technology, "Fundamentals of Jet Penetration" by E. M. Pugh and E. L. Fireman, Aug. 15, 1945 (Monthly rept. OTB-13e, NDRC Div. 2).

These reports contain an integration of the penetration theory and verifies the fact that experimental penetration versus standoff curves cannot be fitted without assuming that the metals are drawn out ductilly as they travel along the axis.

AC 8355, Armament Research Dept., Fort Halstead, England, "Penetration by Munroe Jets; Secondary Penetration and the Effect of Target Strength." Part I by D. C. Pack and W. M. Evans, April 1945. (ARD Explosives rept. no. 51/45 and ARD Theoretical Research rept. no. 11/45; encl. 1 to MA London rept. R3812-45; Phys/Ex. 656; SC 151; OSRD Liaison Office WA-4586-11).

A relation for determining the effect of target strength upon penetration is derived.

OSRD 6384, Carnegie Institute of
Technology, "Protection
Against Shaped Charges",
Final Report Aug. 1,
1943, Nov. 10, 1945, by
Pugh and W. H. Bessey
rept. no. A-384 Div. 2).

This report summarizes the simple penetration theory, the integrated penetration theory and the residual penetration theory with corrections obtained by integration.

Page 64 discussed penetration theories used in England and the United States. Page 76, the anomalous behavior of glass in residual penetration experiments is ascribed to a strength effect nearly equal to the theoretical strength of the glass.

Page 85 gives theoretical and experimental proof of the detrimental effects of spaced armor for use as protection against well-made charges. It shows why spaced armor has been effective against poorly made charges. It is shown that theoretically and experimentally if a given thickness and weight can be added to a tank, it is best that the material be of uniform density rather than lumped as it would be in spaced protection.

CIT-ORD-3, Carnegie Institute of
Technology "Fundamentals
of Shaped Charges; Part E.
Theory - An Attempt at a
Theory of Hole Volume"
by E. L. Fireman and G.
H. Winslow: W-36-061-ORD-
2773, Third Bimonthly Report;
June 1, 1946.

CIT-ORD-4, Carnegie Institute of
Technology, "Fundamentals
of Shaped Charges; Part
E. Theory - Calculation
of Hole Profiles" by G.
H. Winslow, W-36-061-
ORD-2773, Fourth Bi-
monthly Report;
W-36-061-ORD-2879 First
Bimonthly Report; Aug.
31, 1946.

A theory developed by H. A. Bethe ("An Attempt at a Theory of Armor Penetration", Ordnance Lab., Frankford Arsenal, May 1941) for the penetration of armor by projectiles is adapted to metallic lined shaped charges. This adaptation states that the work per unit volume of hole is equal to the sum of the work required to penetrate a unit volume in an indefinitely long period of time (static work) plus a term proportional to the average of the squares of the velocities of penetration. Curves are calculated for the

hole volume in mild steel and armor plate as a function of standoff and compared with experimental data. A correlation between the total energy delivered by the jet and the average square penetration velocity is given by plotting each against standoff.

Jet Formation

AC 3724, Advisory Council on Scientific
        Research and Technical Develop-
        ment, "A Formulation of Mr.
        Tuck's Conception of Munroe
        Jets" by G. I. Taylor, (Phys/Ex.
        427; OSRD Liaison Office
        WA-638-32) May 27, 1943.

This report gives a fundamental hydrodynamic steady state theory of jet formation based upon the flash X-rays of AC 3654.

BRL 368, Ballistic Research
        Laboratories, "High
        Speed Radiographic
        Studies of Controlled
        Fragmentation. I. The
        Collapse of Steel
        Cavity Charge Liners"
        by L. B. Seely and J. C.
        Clark, June 16, 1943.

Excellent flash radiographs of the collapse process in conical liners are shown. These pictures are very similar to those of Tuck (AC 3596) and were probably taken about the same time.

BRL 370, Ballistics Research
        Laboratories, "Mathematical
        Jet Theory of Lined Hollow
        Charges" by Garrett Birkhoff,
        June 18, 1943.

This theory is very similar to that of AC 3724 and was formulated entirely independently. In addition it furnished a mathematical theory of the heating produced during the liner collapse and jet formation processes.

RC 193, "The Explosion of a Long
        Cylindrical Bomb" by G.
        I. Taylor.

In this paper Taylor derives his theorem showing that the motion of a liner that is struck by a constant velocity detonation wave must collapse in the direction parallel to the bisector of the angle between the original liner and the collapsing liner. This was added to his collapse theory for wedge shaped and conical liners.

BRL 623, "Hollow Charge Anti-
        Tank Projectiles" by
        Garrett Birkhoff,
        February 10, 1947

This report contains an excellent summary of the knowledge of the phenomena up to
that date. It also contains additional material on scaling effects in rotated and
non-rotated liners (some of which had previously been distributed in the form of pri-
vate letters from Dr. Birkhoff). It also contains results of some metallurgical
examinations of sectioned slugs.

CIT-ORD-21, Carnegie Institute of
        Technology (W36-061-ORD-
        2879) Eighteenth Bimonthly
        Report, Annual Summary,
        "Fundamentals of Shaped
        Charges", June 30, 1949,
        TIP C3310, by Emerson M.
        Pugh, R. J. Eichelberger
        and Norman Rostoker; Part
        II by R. v. Heine-Geldern
        S. Foner and E. C. Mutschler.

Part I presents a non-steady state hydrodynamic theory of jet formation and experi-
mental verification of this theory.

Part II contains a discussion of charge imperfections and their effects and a
description of the Kerr cell shutter and the associated circuits used to operate the
exploding wire light source and the shutter. Photographs of explosive phenomena are
shown.

CIT-ORD-31, Fourth Bimonthly Report,
        "Fundamentals of Shaped
        Charges", Feb. 28, 1951.
        Part I Theory by Emerson
        M. Pugh, R. J. Eichelberger
        and Norman Rostoker; and
        an experimental verifica-
        tion by R. J. Eichelberger
        and E. M. Pugh; Part III
        by R. v. Heine-Geldern, S.
        Foner and E. C. Mutschler.

Part I is a restatement of Part I of CIT-ORD-21, and Parts II and III summarize
much of the important work done by the Carnegie Institute of Technology group since
late 1945.

Part II contains further remarks on the generalized theory of jet formation, a
discussion of target characteristics, and a discussion of charge imperfections and
their effects.

Part III shows many photographs obtained with the Kerr cell camera setup described in Part II of CIT-ORD-21. A discussion of protection against shaped charges is also given.

396

DISTRIBUTION LIST

No. of Copies		No. of Copies	
6	Chief of Ordnance Department of the Army Washington 25, D. C. Attn: ORDTB - Bal Sec ORDTX-AR ORDTQ ORDFA - C.V. Parker ORDTA - Col. W.L. Bell,Jr.	2	Commander Naval Proving Ground Dahlgren, Virginia
10	British - ORDTB for distribution 2 cys - British Joint Services Mission, Attn: Miss Mary G. Scott 1 cy - A.R.E., Of Interest to: W. E. Soper	1	Chief, Bureau of Ordnance Department of the Navy Washington 25, D. C. Attn: Mr. H. Kimble, Re2c
		1	Director Naval Research Laboratory Washington 25, D. C. Attn: Technical Information Div.
4	Canadian Joint Staff - ORDTB for distribution Of Interest to: R. Walker R. Foster, C.A.R.D.E., ValCartier	1	Commander U.S. Naval Air Development Center Johnsville, Pennsylvania Attn: Aviation Armament Lab.
4	Chief, Bureau of Ordnance Department of the Navy Washington 25, D. C. Attn: Re3	2	Commandant U. S. Marine Corps Washington 25, D. C. Attn: Division of Aviation Plans and Policies Division Maj. W. L. Flake
2	Chief of Naval Research Technical Information Division Library of Congress Washington 25, D. C.	2	Chief of Staff U. S. Air Force Washington 25, D. C. Attn: AFDRD - AR
3	Commander Naval Ordnance Laboratory White Oak Silver Spring 19, Maryland Of Interest to: Mr. S. J. Jacobs Dr. G. K. Hartman	2	Commanding General Wright Air Development Center Wright-Patterson Air Force Base Ohio Attn: WCEGO
		2	National Advisory Committee for Aeronautics 1724 F Street, N. W. Washington 25, D. C. Of Interest to: Mr. Coleman Donaldson
3	Commander U.S. Naval Ordnance Test Station Inyokern P. O. China Lake, California Attn: Technical Library & Editorial Section Of Interest to: Mr. J.S. Rinehart Mr. G.C. Throner Mr. A.L. Bennett	2	Atomic Energy Commission Division of Military Applications Washington 25, D. C. Attn: Col. R. G. Butler

397

DISTRIBUTION LIST

No. of Copies		No. of Copies	
2	Director National Bureau of Standards Washington 25, D. C. Attn: Ordnance Development Lab.	3	Commanding Officer Office of Ordnance Research Duke University 2127 Myrtle Drive Durham, North Carolina
2	Chief of Engineers Department of the Army Washington 25, D. C. Attn: ENGNE Structure Dev. Branch	1	Commanding Officer Engineer Research & Development Laboratory Ft. Belvoir, Virginia Attn: Technical Intelligence Br.
1	Commanding General Detroit Arsenal Centerline, Michigan	1	Professor Garrett Birkhoff 21 Vanser Building Harvard University Cambridge 38, Massachusetts
3	Commanding Officer Frankford Arsenal Philadelphia 37, Pennsylvania Attn: Mr. H. S. Lipinski	1	Dr. L. H. Thomas Watson Scientific Computing Lab. 612 W. 116th Street New York 27, New York
3	Commanding Officer Picatinny Arsenal Dover, New Jersey Attn: Technical Division	1	Professor G. B. Kistiakowsky Chemistry Department Harvard University Cambridge 38, Massachusetts
1	Commanding Officer Watertown Arsenal Watertown, Massachusetts	1	Professor N. F. Ramsey, Jr. Department of Physics Harvard University Cambridge 38, Massachusetts
1	Commanding Officer Chemical Corps Chemical & Radio- logical Laboratories Army Chemical Center, Maryland	1	Professor John von Neumann Department of Mathematics The Institute for Advanced Study Princeton, New Jersey
2	Commanding General Redstone Arsenal Huntsville, Alabama Attn: Technical Library	2	Professor Richard Courant Institute for Mathematics and Mechanics New York University New York, New York
1	Los Alamos Scientific Laboratory P. O. Box 1663 Los Alamos, New Mexico Attn: D. P. MacDougall	1	Dr. A. W. Hull Research Laboratory General Electric Company Schenectady, New York
1	Commanding Officer Holston Ordnance Works Kingsport, Tennessee		

DISTRIBUTION LIST

No. of Copies		No. of Copies	

2	Dr. W. H. Prager
	Graduate Division of Applied
	  Mechanics
	Brown University
	Providence 12, Rhode Island
		2	Firestone Tire and Rubber Co.
			Akron 17, Ohio
			Attn: E. W. Ford
			      H. Winn
			THRU: District Chief
			      Cleveland Ord District
			      1367 East Sixth Street
			      Cleveland 4, Ohio

2	Chief, Explosive & Physical
	  Sciences Division
	Bureau of Mines
	4800 Forbes Street
	Pittsburgh 13, Pennsylvania
	Attn: Dr. Charles M. Mason
		1	Budd Manufacturing Co.
			Red Lion Plant
			Philadelphia, Pennsylvania
			
			THRU: District Chief
			      Philadelphia Ord District
			      1500 Chestnut Street
			      Philadelphia 21, Pa.

2	Director
	Applied Physics Laboratory
	8621 Georgia Avenue
	Silver Spring, Maryland
	Attn: Mr. H. S. Morton
	
	THRU: Naval Inspector of Ordnance
	      Applied Physics Laboratory
	      8621 Georgia Avenue
	      Silver Spring, Maryland
		1	Professor Melvin Cook
			Department of Physics
			University of Utah
			Salt Lake City, Utah
			
			THRU: Chief of Naval Research
			      Tech. Information Div.
			      Library of Congress
			      Washington 25, D. C.

1	Institute for Air Weapons Research
	University of Chicago
	Chicago 37, Illinois
	Attn: Paul E. Shanahan
	
	THRU: Commanding Officer
	      Mid Central Air Procurement
	        District
	      165 N. Canal Street
	      Chicago 15, Illinois
		1	Dr. C. O. Davis
			Eastern Laboratories
			E. I. duPont de Nemours & Co., Inc.
			Gibbstown, New Jersey
			
			THRU: District Chief
			      Philadelphia Ord District
			      1500 Chestnut Street
			      Philadelphia 21, Pa.

5	Carnegie Institute of Technology
	Pittsburgh, Pennsylvania
	Attn: Dr. E. M. Pugh
	
	THRU: District Chief
	      Pittsburgh Ord District
	      200 Fourth Avenue
	      Pittsburgh 22, Pa.
		1	Dr. T. C. Poulter
			Stanford Research Institute
			Palo Alto, California
			
			THRU: District Chief
			      San Francisco Ord District
			      P. O. Box 1829
			      Oakland, California

DISTRIBUTION LIST

No. of
Copies

1   Armour Research Foundation
Technology Center
Chicago, Illinois

THRU: District Chief
      Chicago Ordnance District
      209 W. Jackson Boulevard
      Chicago 6, Illinois

1   Arthur D. Little, Inc.
30 Memorial Drive
Cambridge 42, Massachusetts
Attn: Dr. W. C. Lothrop
THRU: District Chief
      Boston Ordnance District
      Boston Army Base
      Boston 10, Massachusetts